

# **ANNUAL REPORTS ON NMR SPECTROSCOPY**

Edited by

**G. A. WEBB**

*Department of Chemical Physics, University of Surrey, Guildford, Surrey, England*

**VOLUME 9**

1979



**ACADEMIC PRESS**

London · New York · Toronto · Sydney · San Francisco

A Subsidiary of Harcourt Brace Jovanovich, Publishers

ACADEMIC PRESS INC. (LONDON) LTD.  
24-28 Oval Road,  
London, NW1 7DX

*United States edition published by*

ACADEMIC PRESS INC.  
111 Fifth Avenue,  
New York, New York 10003

Copyright © 1979 by ACADEMIC PRESS INC. (LONDON) LTD.

*All Rights Reserved*

No part of this book may be reproduced in any form by photostat, microfilm,  
or any other means, without written permission from the publishers

*British Library Cataloguing in Publication Data*

Annual reports on NMR spectroscopy.

Vol. 9

1. Nuclear magnetic resonance spectroscopy

I. Webb, Graham Alan

541'.28 QD96.N8 68-17678

ISBN 0-12-505309-6

ISSN 0066-4103

Printed in Great Britain by  
Page Bros (Norwich) Ltd,  
Mile Cross Lane,  
Norwich

## LIST OF CONTRIBUTORS

- J. D. CARGIOLI, *General Electric Co., Corporate Research and Development Center, Schenectady, New York 12301, USA*
- W. MCFARLANE, *Department of Chemistry, City of London Polytechnic, Jewry Street, London EC3N 2EY, UK*
- K. G. ORRELL, *Department of Chemistry, University of Exeter, Exeter, Devon, UK*
- D. S. RYCROFT, *Department of Chemistry, University of Glasgow, Glasgow G12 8QQ, UK*
- FELIX W. WEHRLI, *NMR Applications Laboratory, Varian AG, CH-6300 Zug, Switzerland*  
(Present address: Spectrospin AG, Zurich-Fallanden, Switzerland)
- E. A. WILLIAMS, *General Electric Co., Corporate Research and Development Center, Schenectady, New York 12301, USA*

## PREFACE

Volume 9 of Annual Reports on NMR Spectroscopy consists of four timely reviews from different areas of NMR Spectroscopy, the literature being covered up to about mid-1978 in all cases.

Earlier reviews on NMR of paramagnetic species, in Volumes 3 and 6A of this series, are brought up to date in the present volume by Dr K. G. Orrell. The increasingly large amount of work on the less common quadrupolar nuclei is extensively covered by Dr F. W. Wehrli. The topic of  $^{29}\text{Si}$  NMR is dealt with for the first time in this series by Dr E. A. Williams and Dr J. Cargioli. Although well known for their primary publications it is the first time that these authors have reported for this series. I am very grateful to them for their reviews and look forward to working with them again on future volumes.

Finally, I am pleased to mention the review on heteronuclear magnetic double resonance by Dr W. McFarlane and Dr D. S. Rycroft which updates the thorough reviews by Dr McFarlane presented in Volumes 1 and 5A.

It is a pleasure for me to express my thanks to all of these authors for their assistance and patience in the preparation of this volume.

*University of Surrey,  
Guildford, Surrey,  
England*

G. A. WEBB  
May 1979



# Nuclear Magnetic Resonance Spectroscopy of Paramagnetic Species

K. G. ORRELL

*Department of Chemistry, University of Exeter, Exeter, Devon, England*

I. Introduction . . . . .	2
II. Theoretical background . . . . .	2
A. The paramagnetic shift . . . . .	2
B. The paramagnetic linewidth . . . . .	8
C. Spin delocalization and electronic structure . . . . .	11
III. Applications . . . . .	13
A. Electron distribution and bonding . . . . .	14
1. Four-coordinate transition metal complexes . . . . .	14
2. Five-coordinate transition metal complexes . . . . .	20
3. Six-coordinate transition metal complexes . . . . .	23
4. Complexes of the lanthanides and actinides . . . . .	35
5. Organometallic compounds . . . . .	37
6. Free radicals . . . . .	40
B. Stereochemistry and structure . . . . .	50
1. Structural equilibria . . . . .	50
2. Electronic equilibria . . . . .	54
C. Ion pairing and second sphere solvation of metal complexes . . . . .	55
D. Formation and exchange reactions of metal complexes . . . . .	59
E. Miscellaneous . . . . .	64
F. Lanthanide shift reagents . . . . .	67
1. Origin of the shifts and their interpretation . . . . .	67
2. Structure of adducts in solution . . . . .	73
3. Solution equilibria of adducts . . . . .	76
4. Chiral shift reagents . . . . .	82
5. Miscellaneous uses of shift reagents . . . . .	83
G. Biological applications . . . . .	84
1. Amino-acids, peptides, and proteins . . . . .	87
2. Paramagnetic porphyrins and heme proteins . . . . .	90
3. Iron-sulphur proteins . . . . .	99
4. Nucleic acids and related molecules . . . . .	101
5. Membranes . . . . .	103
References . . . . .	105

## I. INTRODUCTION

Previous reviews (1, 2) of NMR of paramagnetic species in this series have provided fairly exhaustive literature coverage up to the end of 1972 and more selective coverage of 1973. The present review deals with developments described in the literature between 1973 and the end of 1977. During this period there has been a dramatic growth in the applications of paramagnetic materials as chemical shift and relaxation reagents, especially in the biochemical field, and the reviewer has excluded papers that are more of biological than of chemical interest.

Literature coverage has been based on the UKCIS Macroprofile "NMR—Chemical Aspects" and, latterly, on the CA SELECTS listings of abstracts in this area.

Numerous reviews have dealt wholly or in part with NMR studies of paramagnetic systems. (3–15) Reviews specific to certain aspects of this field will be referred to later. The latest volume of the Chemical Society specialist reports on NMR is the first to include a separate chapter dealing with paramagnetic molecules. (16) The authoritative book, to which extensive reference will be made, continues to be the monograph edited by La Mar, Horrocks and Holm. (17)

In the present review isotropic shifts are reported as  $\delta$ -values, implying that  $\delta = 0$  for the diamagnetic reference; positive values denote high frequency shifts.

## II. THEORETICAL BACKGROUND

### A. The paramagnetic shift

The origin of isotropic shifts in the NMR spectra of paramagnetic species in terms of the Fermi hyperfine contact or scalar interaction and the electron–nuclear dipolar or pseudocontact interaction is now well established. The generalized theoretical treatment of these interactions by Kurland and McGarvey (18) is still valid although certain refinements have been made to the calculations of the two interactions particularly in systems involving lanthanide ions (see below). The main features of the Kurland–McGarvey treatment are summarized in the following paragraphs.

The interactions of an electron and a magnetic nucleus with an applied magnetic field and the interaction between the electron and the nucleus may be represented by the total spin Hamiltonian:

$$\mathcal{H}_s = \mu_B \mathbf{S}' \cdot \mathbf{g} \cdot \mathbf{B} - \mu_{\text{NGN}} \mathbf{B} \cdot \mathbf{I} + A_{\text{H}} \cdot \mathbf{I} \quad (1)$$

The first two terms are Zeeman terms and the third represents the hyperfine interaction of the electron and nuclear spins.  $\mu_B$  and  $\mu_N$  are the Bohr and nuclear magnetons respectively,  $S'$  is a fictitious effective spin ( $S' = \frac{1}{2}$  for a simple Kramers doublet), and  $I$  is the nuclear spin tensor. The hyperfine tensor  $A_H$  is further split into Fermi contact, dipolar, and orbital components according to:

$$\begin{aligned} A_H \cdot I &= (A_F + A_D + A_L) \cdot I \\ &= \mathcal{H}_F + \mathcal{H}_D + \mathcal{H}_L \end{aligned} \quad (2)$$

where

$$\mathcal{H}_F = (16\pi g_N \mu_N \mu_B / 3) \sum_i \delta(r_i) s_i \cdot I = a_N S \cdot I \quad (3)$$

$r_i$  defines the vector from the  $i$ th electron to the nucleus of interest, and  $S$  is the total electron spin angular momentum for a given state.

$$\mathcal{H}_D = 2g_N \mu_N \mu_B \sum_i \left\{ \frac{3(r_i \cdot s_i)(r_i \cdot I) - r_i^2 s_i \cdot I}{r_i^5} \right\} \quad (4)$$

and

$$\mathcal{H}_L = 2g_N \mu_N \mu_B \sum_i l_i \cdot I / r_i^3 \quad (5)$$

where the operators  $s_i$  and  $l_i$  represent spin and orbital angular momenta of the  $i$ th electron, respectively.

In equation (3) the Dirac delta function  $\delta(r_i)$  expresses the probability density for the electron  $i$  at the nucleus. Since

$$\langle \psi | \delta(r_i) | \psi \rangle = |\psi(0)|^2 \quad (6)$$

where  $\psi(0)$  is the wavefunction governing the distribution of the unpaired electrons evaluated at the nucleus, it follows from equation (3) that:

$$a_N = (16\pi g_N \mu_N \mu_B / 3) |\psi(0)|^2 \quad (7)$$

In equation (1) the hyperfine interaction is small compared with the Zeeman interactions. Kurland and McGarvey then developed general expressions for the nuclear-electronic interactions in both solids and freely tumbling liquids. Detailed discussion of the theory is given in the original paper and by Jesson. (19) For freely tumbling molecules, where averaging over all molecular orientations can be assumed, the general

expression for the observed isotropic shift is:

$$\begin{aligned}
 \left( \frac{\Delta B}{B} \right)_{\text{iso}} &= 3g_N\mu_N k T \sum_{\Gamma_n} \exp(-E_\Gamma/kT)^{-1} \\
 &\times \sum_{i=x,y,z} \left\{ \sum_{\Gamma_n, \Gamma_m} \exp(-E_\Gamma/kT) \langle \Gamma_n | \mu_i | \Gamma_m \rangle \langle \Gamma_m | A_{H_i} | \Gamma_n \rangle \right. \\
 &- kT \sum_{\Gamma_n, \Gamma_m} \left[ \frac{\exp(-E_\Gamma/kT) - \exp(-E_{\Gamma'}/kT)}{E_\Gamma - E_{\Gamma'}} \right] \\
 &\times \left. \langle \Gamma_n | \mu_i | \Gamma'_m \rangle \langle \Gamma'_m | A_{H_i} | \Gamma_n \rangle \right\} \quad (8)
 \end{aligned}$$

$E_\Gamma$  and  $|\Gamma_n\rangle$  represent the eigenvalues and eigenstates which are thermally accessible,  $n$  refers to the Kramers degeneracy of the levels and  $\Gamma$  to the irreducible representation of the symmetry group of the molecule to which the level belongs. This equation applies to the conditions

$$T_{1e} \ll \tau \text{ and } \frac{1}{\tau} \ll (E_{\text{max}} - E_{\text{min}})/h$$

where  $T_{1e}$  is the electron spin-lattice relaxation time,  $\tau$  is the rotational correlation time, and  $(E_{\text{max}} - E_{\text{min}})/h$  represents the magnetic anisotropy in frequency units. The general equation (8) contains many more parameters than is necessary for many paramagnetic complexes. As a result, simplified forms of equation (8) are of more practical value for many systems. Thus, for the case of an isolated multiplet in axial symmetry with no zero-field splitting, equation (8) can be simplified and split into its contact and dipolar components according to:

$$\left( \frac{\Delta B}{B} \right)_{\text{con}} = -\frac{\mu_B S'(S' + 1)}{9g_N\mu_N k T} (g_{\parallel} A + 2g_{\perp} B) \quad (9)$$

where

$$A = \frac{1}{2} a_{\text{NG} s_{\parallel}} \text{ and } B = \frac{1}{2} a_{\text{NG} s_{\perp}}.$$

$$\left( \frac{\Delta B}{B} \right)_{\text{dip}} = \frac{\mu_B^2 S'(S' + 1)}{9kTr^3} (1 - 3\cos^2 \theta) (g_{\parallel}^2 - g_{\perp}^2) \quad (10)$$

The equations for other solution averaging conditions are given in references (18) and (19). In the special case of a spin-only state with an isotropic  $g$ -tensor (i.e.  $g_{\parallel} = g_{\perp}$  and  $g_{s_{\parallel}} = g_{s_{\perp}} = 2$ ) equation (9) reduces

to:

$$\left(\frac{\Delta B}{B}\right)_{\text{con}} = -\frac{g\mu_B S(S+1)}{3g_N\mu_N kT} A \quad (11)$$

and the dipolar shift expression [equation (10)] becomes zero. Equation (11) represents the commonly used expression for the Fermi contact shift, and under these special conditions it also represents the observed isotropic shifts. It should be stressed that the large majority of paramagnetic species do *not* satisfy these special conditions and equation (11) is often not strictly valid.

During the period under review there have been few developments in methods of calculating the contact shifts arising from ions with either orbitally degenerate (i.e.  $T_1, T_2, T_{1g}, T_{2g}, E$ , or  $E_g$ ) or nondegenerate (i.e.  $A_1, A_2, A_{1g}, A_{2g}$ , or  $B_{1g}$ ) ground states. The appropriate expressions for the contact shifts in these cases are given by Jesson. (19) However, there have been a number of developments in the calculation of pseudocontact shifts. Stiles (20) has examined theoretically the contribution of molecular magnetic multipoles higher than dipole to the pseudocontact shift. He has considered the cases of shielding by a regular octahedral metal complex, a regular tetrahedral complex, and an axially symmetric metal-ion complex, and has calculated the octopolar contributions to the pseudocontact shifts. In the first two cases, the neighbour anisotropy (pseudocontact) shifts are so much smaller than the contact shifts that it is not possible to resolve the observed shifts in these particular cubic metal complexes into contact and pseudocontact components. With lanthanide ions in an axial crystal field the ratio  $K_3/(K_1 z^2)$  of octopolar to dipolar shieldings is again too small to be measured. Stiles (21) has expressed the NMR shift as:

$$\frac{\Delta B}{B} = \sum_{L=2}^K \sum_{M=0}^L (A_{LM} \cos M\phi + B_{LM} \sin M\phi) P_L^M(\cos \theta) / r^{L+1} \quad (12)$$

where  $K = 2(l+1)$  for a specific  $l$ -electron,  $P_L^M(\cos \theta)$  the associated Legendre polynomials, and the coefficients  $A_{LM}$  and  $B_{LM}$  measure the anisotropy in the multipolar magnetic susceptibilities of the molecule. This equation is a generalization of the original McConnell and Robertson (22) expression:

$$\frac{\Delta B}{B} = -\mu_B^2 \frac{S(S+1)}{3kT} \left( \frac{3 \cos^2 \theta - 1}{r^3} \right) F(g) \quad (13)$$

which was extended by Kurland and McGarvey (18) in terms of the magnetic susceptibility components,  $\chi_{xx}$ , to:

$$\Delta B/B = -(1/3r^3)[\{\chi_{zz} - \frac{1}{2}(\chi_{xx} + \chi_{yy})\}(3 \cos^2 \theta - 1) + (3/2)(\chi_{xx} - \chi_{yy})\sin^2 \theta \cos 2\phi] \quad (14)$$

In equations (13) and (14)  $r$  is the distance between the paramagnetic ion and the NMR nucleus.  $F(g)$  is a function of the principal  $g$ -values. Golding *et al.* (23) have more recently pointed out an error in Stiles's calculations using equation (12). They have calculated the pseudocontact shift for a nucleus at various distances  $r$  along the  $z$ -axis from a  $d^1$  transition metal ion in a crystal field of octahedral symmetry. They have used a multipole expansion approach involving  $r^{-5}$  and  $r^{-7}$  terms. They show that at a distance of 0.2 nm from  $Ti^{3+}$  the multipole expansion method gives rise to an error of *ca.* 3% in the shift, but if only the  $r^{-5}$  term is considered the error rises to *ca.* 12%. This contrasts sharply with Stiles's earlier conclusion that the octopolar contribution was of the order of  $-0.3$  ppm in the  $Ti^{3+}$  system and could safely be ignored. Golding *et al.* (24) have given further details of their general multipole formalism of pseudocontact shifts for the cases of a  $d^1$  transition metal in an octahedral crystal field and of a  $d^5$  transition metal ion in a strong octahedral crystal field. The results are applicable to both long-range and short-range dipolar couplings including the special case when the NMR nucleus is the transition metal ion (i.e.  $r = 0$ ). In the  $d^1$  octahedral case the extreme cases of short-range and long-range dipolar couplings are represented by the following expressions for the pseudo contact shifts.

When  $r = 0$  and the screening constant components  $\sigma_{xx} = \sigma_{yy} = \sigma_{zz}$ , then:

$$\frac{\Delta B}{B} = -\frac{8\mu_B^2 K^3}{567kT} \frac{\{(\frac{1}{5} - kT/3\zeta)\exp(-3\zeta/2kT) + kT/3\zeta\}}{\{2 + \exp(-3\zeta/2kT)\}} \quad (15)$$

When  $r$  is very large, then:

$$\begin{aligned} \frac{\Delta B}{B} = & \frac{504\mu_B^2}{K^2 r^5 kT} \{1 + 2 \exp(3\zeta/2kT)\}^{-1} \\ & + \frac{24300\mu_B^2}{K^4 r^7 kT} \frac{\{(3 + 2kT/\zeta)\exp(-3\zeta/2kT) - 2kT/\zeta\}}{\{2 + \exp(-3\zeta/2kT)\}} \end{aligned} \quad (16)$$

For the  $d^5$  octahedral case, the above expressions require a change in sign of the spin-orbit coupling constant  $\zeta$ . The authors also derived the

expressions for two cases when the crystal field has a specific tetragonal and trigonal component. They tested their theoretical expressions for the case of  $\text{Fe}(\text{CN})_6^{3-}$  and showed that the  $^{14}\text{N}$  shift arises from pseudocontact interaction involving the nitrogen p-orbitals whereas the  $^{13}\text{C}$  shift is primarily Fermi contact in nature. In a more recent contribution Golding and Stubbs (25) developed a general method for evaluating the nine hyperfine interaction tensor components  $A_{\alpha\beta}$  of the  $A_{\text{H}}$  tensor [equation (1)].

Knowing these components the degree of non-coincidence of the  $g$  and  $A_{\text{H}}$  tensors can be determined and the NMR shifts evaluated. The case of a molecule containing a  $d^1$  transition metal ion in a strong crystal field was examined in detail. Goodisman (25a) has calculated pseudocontact shifts for tetragonal high-spin  $\text{Co(II)}$  complexes using a crystal field model. The calculation involves evaluation of the anisotropy of the magnetic susceptibility tensor,  $\chi_{\parallel} - \chi_{\perp}$ . This requires firstly a knowledge of the three orbital wavefunctions of lowest energy which are deduced from the crystal field parameters  $Dq$ ,  $Ds$ ,  $Dt$ , and the Racah parameter  $B$ . Next the effect of spin-orbit coupling over the 12 states (3 orbital wavefunctions coupled with 4 spin states) is evaluated. Considering only these 12 states but allowing for thermal populations,  $\chi_{\parallel}$  and  $\chi_{\perp}$  are calculated. The theory was tested for  $\text{Co}(\text{CH}_3\text{OH})_5\text{X}^{2+}$  complexes and showed good numerical agreement with experimental results for dipole field strength and its temperature dependence. However, the calculations showed that the linearity of the pseudocontact shifts when plotted against  $T^{-1}$  is only apparent. The theoretical basis of these shifts must involve low-lying states, in which case straight-line plots of shifts versus  $T^{-1}$  are not to be expected.

Stiles (26) has developed a general multipolar susceptibility formalism (27, 28) for mapping the isotropic magnetic shielding outside axially symmetric molecules. The method, which involves an expansion of the magnetic shielding in terms of spherical harmonics about a convenient molecular origin, has been applied to molecules approximating to prolate and oblate spheroids. The theory provides accurate descriptions of magnetic shielding outside non-spherical molecules which are applicable to both paramagnetic and diamagnetic molecules.

Further developments of pseudocontact shift theory applicable to lanthanide ion systems are discussed later.

A new formulation of the theory of paramagnetic shifts particularly suited to shifts in liquid crystalline solvents has been presented. (29) The Hamiltonian expression used allows for the inclusion of effects of preferential orientational distribution of the solute molecules.

## B. The paramagnetic linewidth

Observed linewidths of NMR signals in paramagnetic systems vary enormously and the conditions that govern the observed widths are considerably more complex than in diamagnetic systems. Swift (30) reviewed the problem some years ago. Relaxation times of spin- $\frac{1}{2}$  nuclei are governed by dipolar and hyperfine exchange (Fermi contact) relaxation processes. The dipolar interaction is normally dominant except in some delocalized systems in which considerable unpaired spin density exists on nuclei far removed from the metal ions (e.g.  $\pi$ -radicals). Distinction between the two processes can be made by consideration of the different mathematical expressions involved. For dipolar relaxation when  $\omega_1^2 \tau_r \ll 1$  ( $\tau_r^{-1}$  = rate constant for rotation of the species containing the coupled pair and  $\omega_1$  = nuclear resonance frequency):

$$\frac{1}{T_1} = \frac{2S(S+1)\gamma_I^2 g^2 \mu_B^2}{15r^6} \left( 3\tau_{c1} + \frac{7\tau_{c2}}{1 + \omega_s^2 \tau_{c2}^2} \right) \quad (17)$$

and

$$\frac{1}{T_2} = \frac{S(S+1)\gamma_I^2 g^2 \mu_B^2}{15r^6} \left( 7\tau_{c1} + \frac{13\tau_{c2}}{1 + \omega_s^2 \tau_{c2}^2} \right) \quad (18)$$

In these equations  $S$  is the total electron spin of the paramagnetic ion,  $r$  is the electron-nuclear distance,  $\omega_s$  is the electron resonance frequency, and  $\tau_{c1}^{-1}$  and  $\tau_{c2}^{-1}$  are the rate constants for the reorientation of the coupled magnetic moment vectors. They are related to other rate constants by the expressions:

$$\begin{aligned} \tau_{c1}^{-1} &= T_{1e}^{-1} + \tau_r^{-1} + \tau_e^{-1} + \tau_H^{-1} \\ \tau_{c2}^{-1} &= T_{2e}^{-1} + \tau_r^{-1} + \tau_e^{-1} + \tau_H^{-1} \end{aligned}$$

$T_{1e}$  and  $T_{2e}$  are the electron spin relaxation times and  $\tau_H^{-1}$  is the rate constant for proton exchange. Thus, if this mechanism is dominant the observed linewidths,  $\Delta\nu_{\frac{1}{2}} [ = (\pi T_2)^{-1} ]$ , must reflect the  $r^{-6}$  dependence on the electron-nuclear distance. Hyperfine exchange relaxation, however, is given by the expressions:

$$\frac{1}{T_1} = \frac{2S(S+1)A^2}{3\hbar^2} \left[ \frac{\tau_{e2}}{1 + (\omega_1 - \omega_s)^2 \tau_{e2}^2} \right] \quad (19)$$

$$\frac{1}{T_2} = \frac{S(S+1)A^2}{3\hbar^2} \left[ \tau_{e1} + \frac{\tau_{e2}}{1 + (\omega_1 - \omega_s)^2 \tau_{e2}^2} \right] \quad (20)$$



Thus, in cases where contact shifts are observed the squares of the shifts must correlate with  $(\pi T_2)^{-1}$  since equation (20) involves the square of the hyperfine coupling constant  $A$ .

There have been some notable developments in the theory of dipolar relaxation. In solutions, this electron–nuclear interaction is randomly modulated by electron spin relaxation, molecular tumblings, and chemical exchange. Vega and Fiat (31) have shown that in general a fluctuating term may be decomposed into two terms, an average contribution and a remaining fluctuating term with zero average.

In the present context the former produces a nuclear resonance shift (the pseudocontact shift) whereas the latter only affects the relaxation behaviour. In the absence of chemical exchange and in cases when  $T_{1e} \ll \tau_r$ , the local field experienced by the nucleus is given by:

$$\Delta B_s \approx g\mu_B S/r^3 \quad (21)$$

This local field fluctuates with a correlation time  $T_{1e}$  about a non-vanishing average arising from the unequal populations of the electronic levels in thermal equilibrium. This average field is designated the susceptibility field,  $\Delta B_\chi$ , where:

$$\Delta B_\chi = [3\mathbf{r}(\mathbf{r} \cdot \boldsymbol{\mu}) - r^2\boldsymbol{\mu}]/r^5 \quad (22)$$

In any randomly tumbling paramagnetic species there is thus a superposition of two relaxation mechanisms, the usual  $S$ -mechanism arising from  $\Delta B_s$  and a  $\chi$ -mechanism arising from  $\Delta B_\chi$ . The relative importance of the two processes to the total NMR linewidth,  $T_2^{-1} (= T_{2s}^{-1} + T_{2\chi}^{-1})$ , is given by:

$$T_{2\chi}^{-1}/T_{2s}^{-1} = \Delta(\tau_2/T_{1e}) \quad (23)$$

where

$$\Delta \approx [g^2\mu_B^2 S(S+1)B^2]/(3kT)^2.$$

The authors derive exact expressions for  $T_{1\chi}$  and  $T_{2\chi}$  and show that the  $\chi$ -contribution is appreciable where the rotational correlation time  $\tau_2 = \tau_r/6$  is four orders of magnitude larger than the electron spin relaxation time  $T_{1e}$  but in most practical cases the  $S$ -mechanism is dominant.

The conventional approach to the theory of electron spin relaxation is to use a density matrix approach developed by Redfield. (32) However, this method is only valid when  $\tau \ll \tau_{e2}$ . Thus, cases of very fast electronic relaxation leading to sharp NMR lines, which are in general of particular interest, are strictly excluded from this theoretical approach. Doddrell *et al.* (33) have developed a more general theory for

$S = \frac{1}{2}$  and  $S > \frac{1}{2}$  systems. By working in a reference frame in which the initial density matrix is diagonal, general relaxation equations can be written in a simple analytic form without recourse to perturbation theory. In the short correlation time limit, the equations reduce to the usual Redfield equations whereas in the long correlation time limit the equations depend on the assumed ensemble distribution. The theory is tested explicitly for  $S = \frac{3}{2}$  where electron spin relaxation occurs by modulation of the quadratic zero-field splitting. For halogeno-bis-(*N,N*-diethyldithiocarbamato)iron(III) complexes the calculated  $T_1$  values are shorter than the Redfield predictions, in agreement with experiment. Doddrell *et al.* (34) have also re-examined the theory for the dependence of nuclear spin relaxation times  $T_1$  and  $T_2$  on the external magnetic flux density. Whereas current theoretical treatments using the Redfield density matrix approach (32) all predict a strong dependence, only slight (<50%) dependence is observed experimentally. The authors examine in detail the  $T_1$  values for the  $\text{CH}_3$  protons in  $\text{Cu}(\text{acac})_2$ , a complex for which  $\tau_e \gg \tau_r$  and thus falls within the Redfield limit, and the  $T_1$  values for the  $\text{CH}_2$  protons of bis-(*N,N*-diethyldithiocarbamato)iron(III) iodide,  $\text{Fe}(\text{dtc})_2\text{I}$ , a compound for which  $\tau_e \ll \tau_r$ . When  $\tau_e \gg \tau_r$ , rotational reorientation dominates the nuclear relaxation and the Redfield theory can account for the experimental results. When  $\tau_e \ll \tau_r$ ,  $T_1$  values do *not* increase with  $B_0$  as current theory predicts, and non-Redfield relaxation theory (33) has to be employed. By assuming that the spacings of the electron–nuclear spin energy levels are not dominated by  $B_0$  but depend on the value of the zero-field splitting parameter, the frequency dependence of the  $T_1$  values can be explained. Doddrell *et al.* (35) have examined the variable temperature and variable field nuclear spin–lattice relaxation times for the protons in  $\text{Cu}(\text{acac})_2$  and  $\text{Ru}(\text{acac})_3$ . These complexes were chosen since, in the former complex, rotational reorientation appears to be the dominant time-dependent process (36) whereas in the latter complex other time-dependent effects, possibly dynamic Jahn–Teller effects, may be operative. Again current theory will account for the observed  $T_1$  values when rotational reorientation dominates the electron and nuclear spin relaxation processes but is inadequate in other situations. More recent studies (37) on the temperature dependence of  $T_1$  values of protons of metal acetylacetonate complexes have led to somewhat different conclusions. If rotational reorientation dominates the nuclear and/or electron spin relaxation processes, then a plot of  $\ln(T_1^{-1})$  against  $T^{-1}$  should be linear with slope  $E_R/R$ , where  $E_R$  is the activation energy for rotational reorientation. This was found to be the case for Cu, Cr, and Fe complexes with  $E_R \approx 9.2 \text{ kJ mol}^{-1}$ . However, for V, Mn, and

Ru complexes much lower values of  $E_R$  were found, implying that a time-dependent process other than rotational reorientation is operating. Modulation of the ground state potential energy surface via a dynamic Jahn–Teller effect is suggested as the process controlling the electron spin relaxation in these compounds.

In some detailed calculations of relaxation rates due to dipolar interaction for the ruthenium(III) complex  $\text{Ru}(\text{NH}_3)_6^{3+}$ , Waysbort and Navon (285, 286) have allowed for covalency by including the distribution of unpaired spin density on the metal and ligand orbitals. They found the effect of this covalency term on the Ru d orbitals to be small but the spin delocalization to the ligands increases significantly compared with that calculated using a point dipole approximation. The new results are in better agreement with available experimental data.

A statistical method for the determination of structural and kinetic parameters of metal ion complexes in solution, based on the temperature dependences of the linear proton relaxations, has been described. (38) A study of  $T_1$  relaxation in the gas mixtures  $\text{C}_2\text{H}_4 + \text{O}_2$ ,  $\text{C}_2\text{H}_6 + \text{O}_2$ ,  $\text{CH}_2\text{CF}_2 + \text{O}_2$ ,  $\text{C}_2\text{H}_4 + \text{NO}$ , and  $\text{C}_2\text{H}_6 + \text{NO}$  has been made. (39) NO is very much less effective than  $\text{O}_2$  in paramagnetic relaxation of  $\text{C}_2\text{H}_6$  and  $\text{C}_2\text{H}_4$ . The relaxation rate depends not only on the trajectories of the interacting molecules, which are largely governed by the isotropic part of the intermolecular potential, but also on rotation of the paramagnetic molecule resulting from the anisotropy of the intermolecular potential. In the NO molecule the strong coupling of the electronic and rotational angular momenta leads to a large reduction in the effective paramagnetic moment as the anisotropy of the intermolecular potential is increased. This coupling of momenta is weak in  $\text{O}_2$  and thus this molecule is more effective in paramagnetic relaxation.

### C. Spin delocalization and electronic structure

An excellent introduction to this topic is provided by La Mar. (40) This review clearly distinguishes between the three possible spin-transfer mechanisms, namely ligand (L)  $\rightarrow$  metal (M)  $\sigma$ -spin transfer,  $\text{L} \rightarrow \text{M}$   $\pi$ -spin transfer, and  $\text{M} \rightarrow \text{L}$   $\pi$ -spin transfer. In addition to these *direct* spin delocalization mechanisms, where a fraction of unpaired electron density originally associated with the metal is actually placed into an MO that includes the ligand to some extent, there are *indirect* spin delocalization or spin polarization mechanisms. These involve essentially a redistribution of electron spin in an MO otherwise

containing paired electrons. Quantum mechanical calculations of contact shifts arising from  $\sigma$ - and/or  $\pi$ -electron delocalizations are quite commonplace. The degree of sophistication of these calculations has, however, varied enormously from the simple McLachlan–Hückel approach (41) to the all-valence electron methods of the EHMO (42) and INDO (43) approaches. INDO calculations have been the most successful to date especially for interpreting  $\sigma$ -delocalization shifts. Since spin delocalization is a fairly subtle phenomenon a fairly elaborate theoretical model is required to treat it adequately.

Unrestricted Hartree–Fock (HF) calculations are strictly required but such calculations are not realistic for the types of complexes that are usually of interest. However, Horrocks (44,45) has shown convincingly that INDO calculations can provide considerable insight into the modes of electron delocalization. For example, for complexes of the type  $\text{Ni}(\text{acac})_2\text{L}_2$  ( $\text{L}$  = pyridine,  $\alpha$ -,  $\beta$ -, or  $\gamma$ -picoline), INDO calculations can provide a semi-quantitative account of the contact shifts of the  $^1\text{H}$  and  $^{13}\text{C}$  nuclei of the pyridine-type bases. Furthermore, this shift behaviour is adequately described in terms of  $\sigma$ -spin delocalization (with concomitant spin polarization of both  $\sigma$  and  $\pi$  systems). In this case both direct delocalization and spin polarization mechanisms contribute importantly to the contact shifts, with the latter mechanism being highly variable and, in most cases, providing a low frequency contribution to the net shift. Horrocks (44) also suggests that certain qualitative distinctions can be made between  $\sigma$  and  $\pi$  delocalizations. Thus: (i)  $\sigma$ -Delocalization produces high-frequency shifts of aromatic hydrogens which attenuate in magnitude with the number of intervening bonds. This however does not necessarily apply to attached methyl protons. (ii)  $\sigma$ -Delocalization produces an alternation in sign of the  $^{13}\text{C}$  hyperfine constants around an aromatic ring. Such alternating behaviour had previously been considered diagnostic only of  $\pi$ -delocalization. (iii) The previously used (46) criterion of opposite shifts for hydrogen and methyl protons at a given position on an aromatic ring is not necessarily diagnostic of  $\pi$ -spin delocalization although it is often a useful guide.

More recently, Marcellus *et al.* (47) have questioned the usefulness of dividing spin density distributions into direct spin delocalization and spin polarization mechanisms. Both are non-observables and not uniquely defined in most calculations. The authors show that, if both unrestricted and restricted HF INDO calculations are performed, the spin densities due to spin delocalization  $\rho_d(n)$  and spin polarization  $\rho_p(n)$  may be precisely defined respectively as:

$$\rho_d(n) \equiv \rho^R(n) \quad \text{and} \quad \rho_p(n) \equiv \rho^U(n) - \rho^R(n)$$

where  $\rho^R(n)$  and  $\rho^U(n)$  represent the spin density at nucleus  $n$  obtained by the restricted HF and unrestricted HF INDO calculations respectively. The authors illustrate the use of their new formalism by considering the ethyl radical (Table I). In this table it is observed that the new formalism partitions the two mechanisms in quite different ways. In Fig. 1 the variation of the hyperfine coupling constant for the  $\beta$ -proton as a function of angle  $\theta$  is shown. The following general conclusions can be drawn: (i) the magnitude and sign of various contributions are consistent with qualitative expectations; in particular, the polarization contribution is negative at the  $\text{CH}_2$  protons and positive at the  $\text{CH}_3$  protons; (ii) the average of the hyperfine interaction for the three  $\text{CH}_3$  protons is almost independent of angle, which is consistent with a  $\cos^2 \theta$  dependence for the isotropic hyperfine splitting constant for  $\beta$ -protons; and (iii) the polarization contribution is nearly independent of angle although the  $\sigma$  and  $\pi$  parts separately exhibit a strong angular dependence. In addition, the calculations show the  $\pi$  polarization to be negative.

TABLE I  
Delocalization ( $D$ ) and polarization ( $P$ ) contributions to the  
isotropic  $\beta$ -proton hyperfine coupling constant for the ethyl radical  
(47)

$\theta^a$ (deg.)	$D$ (MHz)	$P$ (MHz)	$\pi/\sigma$
0	162.61	7.5	-9.1/16.6
20	143.40	7.5	-12.9/20.4
40	95.14	7.2	-16.6/23.9
60	40.39	7.0	-11.0/18.0
80	4.84	7.0	-1.7/8.6
90	0	7.0	0.0/7.0

<sup>a</sup> Angle between the  $2p\pi$  orbital and the  $\text{C}-\text{H}_\beta$  bond projected on a plane perpendicular to the  $\text{C}-\text{C}$  bond direction.

### III. APPLICATIONS

This major section of the review is subdivided in a manner similar to that of the previous review in the series, (1) the main difference being that Overhauser phenomena have not been included since they are regularly reviewed elsewhere. (48) The section dealing with biological systems is very much more extensive than in previous reviews and is a reflection of the enormous growth of interest in this area.

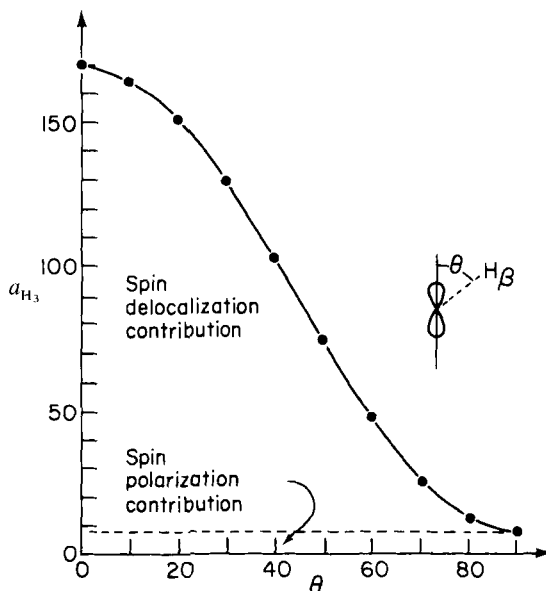


FIG. 1. Variation of the hyperfine coupling constant for the  $\beta$ -proton in the ethyl radical as a function of the angle  $\theta$ . The points are extracted from INDO calculations; the solid curve  $a_{H\beta}$  is a  $\cos^2\theta$  fit. (47)

## A. Electron distribution and bonding

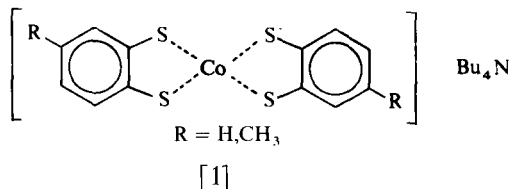
### 1. Four-coordinate transition metal complexes

Nickel(II) and cobalt(II) complexes continue to be the most widely studied first-series transition metal complexes. The well resolved NMR spectra arise from the very rapid electron-spin relaxation which occurs as a result of modulation of the zero-field splitting of these ions. In the case of 4-coordinate nickel(II), only tetrahedral complexes (ground state  $^3T_1$ ) are of interest since the square-planar complexes are invariably diamagnetic. Many complexes, however, undergo a square-planar–tetrahedral dynamic equilibrium which can be studied by standard band-shape fitting methods (Section B.1).

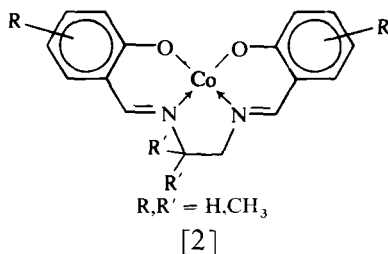
To a first approximation isotropic shifts of tetrahedral Ni(II) complexes can be treated as purely contact in origin. However, the orbital degeneracy of the ground state may be expected to result in magnetic anisotropy which leads to a significant dipolar interaction. In contrast, tetrahedral complexes of Co(II) have a non-degenerate ground state ( $^4A_2$ ). However, considerable magnetic anisotropy arises from spin–orbit coupling which mixes the ground state with split

components of excited state terms (mainly  $^4T_2$ ). This in practice produces sizeable dipolar shifts in tetrahedral Co(II) complexes. A similar situation occurs in square-planar Co(II) complexes which normally possess a  $^2A_{1g}$  ground state.

NMR (together with far-IR and magnetic susceptibility) studies have been reported (48a) for benzene- and toluene-dithiolate complexes [1]



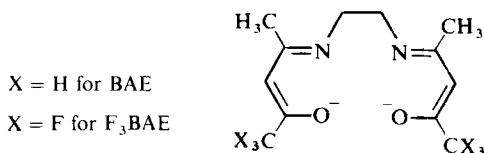
of Co(III). The results for this  $d^6$  configuration complex are consistent with a triplet ground state ( $^3B_{3g}$ ) of type  $(a_g)^1(b_{3g})^1$  in which the  $a_g$  orbital is mainly a metal-based  $d_{z^2}$  type and the  $b_{3g}$  orbital is half metal-based  $d_{yz}$  and half delocalized into the  $\pi$ -system of the aromatic ligands. The infrared results suggest that the triplet state degeneracy is lifted by a zero-field splitting of *ca.*  $35\text{ cm}^{-1}$ . The NMR shifts are predominantly contact in origin due to the low anisotropy of the  $g$ -tensors. Other square-planar complexes of cobalt to be studied (49) are the low spin complexes of Co(II) with salicylaldehyde Schiff bases (salen) [2].



Contact and dipolar interactions of comparable magnitude contribute to the observed isotropic shifts.

The appreciable contact contribution is attributed to spin delocalization involving  $L \rightarrow M$   $\pi$  charge transfer out of the highest filled  $\pi$  MO. From the mode of interaction between the cobalt ion and the ligand, the authors conclude that the complexes possess an electronic ground state with the unpaired electron in the  $d_{yz}$  orbital. Previous studies of this complex using other techniques suggest other electronic configurations. This conclusion regarding the ground state configuration of Co(salen) has more recently been brought into question. Srivnavit and Brown (50) have studied the isotropic shifts of

all six protons in this complex and argue that the results support a  $d_{z^2}$  configuration for Co(salen) in solution. From the temperature dependences of the shifts a spin equilibrium with an excited  $^4E$  state is indicated at room temperature. The same authors have studied (51) some acetylacetone ethylenediimine (BAE) complexes of Co(II) [3].

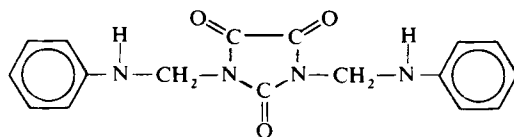


[3]

These low spin complexes produce strikingly different spectra from other low spin Co(II) systems. In the present complexes there is a dominant contact contribution to the shifts which has been interpreted with the aid of CNINDO calculations as due to  $\alpha$ -spin being delocalized into the ligand HOMO. In view of the  $\pi$ -symmetry of this orbital, in contrast to the  $\sigma$ -symmetry of the  $d_{z^2}$  orbital in which the unpaired electron is thought to reside in the ground state, the authors conclude that there must be some non-planarity of the complex in solution which will remove the orthogonality between the metal  $d_{z^2}$  and ligand  $\pi$  orbitals.

A series of pseudo-tetrahedral complexes of Co(II) of type  $[CoX_3(PPh_3)]^-$  ( $X = Cl, Br, I$ ) have been studied. (52) The magnitudes of the proton isotropic shifts of *meta* and *para* hydrogens are found to increase from  $Cl^-$  to  $I^-$  but the reverse is the case for the *ortho* H. Ion-induced magnetic anisotropy is thought to account for this reversed trend.

NMR and other spectroscopic properties have been reported (53) for pseudo-tetrahedral and pseudo-octahedral complexes of type  $MLX_2$  where  $M = Co(II), Ni(II),$  and  $Cu(II)$ ,  $X =$  halide, and  $L = N,N'$ -bis(phenylaminomethyl)parabanic acid [4]. The NMR spectra of the



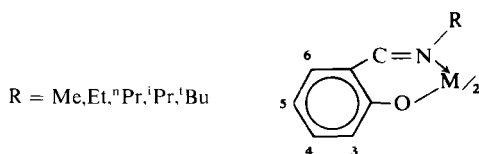
[4]

complexes in the presence of free ligand show appreciable deshielding of N-H protons which indicates that the ligand is acting as a bidentate



N-bonding species. Di-*t*-butylfluorophosphine forms stable complexes of the type  $\text{NiX}_2\text{L}_2$  and  $\text{CoX}_2\text{L}_2$  ( $\text{X} = \text{halide}$ ,  $\text{L} = {}^t\text{Bu}_2\text{PF}$ ) with metal halides. Spectroscopic measurements indicate that  $\text{NiX}_2\text{L}_2$  is a *trans* square-planar diamagnetic complex whereas  $\text{CoX}_2\text{L}_2$  is a tetrahedral paramagnetic complex. (54)

Copper(II) complexes do not usually give very useful NMR spectra owing to the unfavourable electronic relaxation times which cause excessively broad lines. However, this is not such a problem with bis-(*N*-alkylsalicylaldiminato)copper(II) complexes [5]. (55) In all cases the



[5]

4- and 5-protons give quite sharp signals whereas the 3- and 6-protons are broader and remain undetected in certain cases. The *g*-values of these complexes (Table II) were measured from the ESR spectra, and

TABLE II

*g*-Values of bis-(*N*-alkylsalicylaldiminato)copper(II) complexes (55)

Alkyl	$g_{\parallel}$	$g_{\perp}$	Alkyl	$g_{\parallel}$	$g_{\perp}$
Methyl	2.22	2.05	<i>n</i> -Propyl	2.23	2.06
Ethyl	2.21	2.06	<i>i</i> -Propyl	2.23	2.07

the isotropic shifts factorized into their dipolar and contact components (Table III). These complexes are unusual in that useful NMR and ESR spectra can be obtained from the pure complexes at

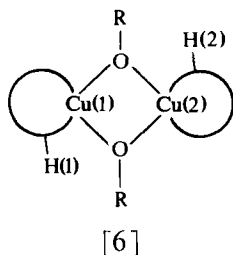
TABLE III

Contact and dipolar shifts of two complexes in Table II (55)

Proton	$\text{Cu}(\text{sal-N-}^n\text{Pr})_2$		$\text{Cu}(\text{sal-N-}^i\text{Pr})_2$	
	dipolar	contact	dipolar	contact
3	0.8		0.3	
4	0.3	-3.0	0.2	-3.4
5	0.2	2.0	0.2	3.2
6	0.4		0.3	

ambient temperature. The NMR linewidth pattern is found to increase along the series from N-Me to N-<sup>t</sup>Bu.

The main factor which allows observation of the NMR signals is the rather small magnitude of hyperfine couplings involved. Small  $A$  values will not greatly affect the transverse relaxation time  $T_2$  of the proton [equation (18)] and thus the NMR bandwidth will not be greatly increased. Byers and Williams (56) have studied some dimeric cupric complexes which are models for copper dimer units in proteins. Interest was particularly centred around the possibility that, if appreciable copper(II) interactions occur, a mechanism for mutual fast relaxation is provided which in turn may lead to much narrower linewidths and measurable paramagnetic shifts. The systems are illustrated in [6].



Weak interaction between the two metal ions results in a singlet ground state and a triplet state of slightly higher energy. This case is illustrated by cupric acetate whose magnetic moment is diminished at low temperatures. If the metal-metal interaction is large the triplet state level will possess too high an energy to be significantly populated resulting in the phenomenon of antiferromagnetism. In this instance the measured susceptibility corresponds to normal diamagnetic copper(I) complexes and no temperature dependence will be observed. The NMR signals, however, will be relatively sharp. The dimer of bis(diazoaminobenzene)copper(II) exhibits this behaviour.

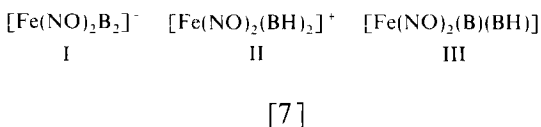
Golding's theory of temperature-dependent shifts has been extended to take into account the spin-exchange interaction of the copper atoms. The spin-exchange Hamiltonian is of the type  $-2JS_1 \cdot S_2$ . For the terminal protons H(1) and H(2) in [6] the contact shift can be shown to be given by:

$$\frac{\Delta B}{B} = -\frac{A h g \mu_B}{g_N \mu_N k T} \left[ \frac{1 + (J/kT)}{1 + 3\{1 + (J/kT)\}} \right] \quad (24)$$

This equation indicates that the contact shift of a proton associated with an interacting pair of copper ions will not have the inverse

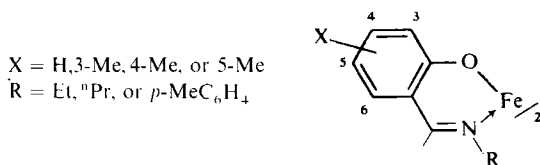
temperature dependence predicted for a monomeric complex where fast electron spin relaxation is assumed. However, the  $(1 + J/kT)$  term in equation (24) can vary only between 0.33 and 0.25, so in practice the deviation from linearity in the temperature dependence of the shifts will be difficult to observe.

Iron-nitrosyl complexes continue to attract attention. Complexes with mercaptopurines and mercaptopyrimidines have been examined by both NMR and ESR. (57) The mercapto group in mercaptopyrimidines is the preferred binding site for the Fe atom, provided that the pH value allows its ionization. At lower pH a pyrimidine nitrogen atom is the binding site. At biologically relevant pH values equilibrium between complexes of types I and III occurs [7]. In the



mercaptapurines the Fe atom is bonded to two NO molecules and two base molecules via the S atom in a type I complex. The  $\text{Fe}(\text{NO})_2$  group has been coordinated to carbazides, thiocarbazides, amino-acids, and other amino derivatives in an ESR and  $^1\text{H}/^{13}\text{C}$  NMR study. (58) Binding sites and molecular structures of the complexes were established. Carbazides bind preferentially via the  $\text{NH}_2$  groups while thiocarbazides are preferentially bonded via the  $=\text{S}$  groups.

$^{13}\text{C}$  shifts have been measured (59) for a range of paramagnetic iron salicylideneiminato complexes of the type [8]. Previous  $^1\text{H}$  studies (60)

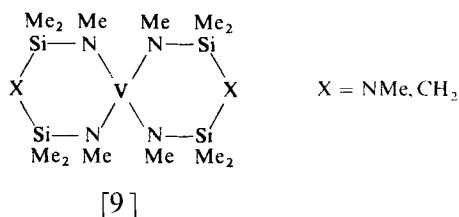


[8]

had indicated a predominant contact mechanism with  $\pi$ -delocalization causing alternation of spin density on the carbon atoms of the type 3(+), 4(-), 5(+), and 6(-). The  $^{13}\text{C}$  data added significantly to these results.  $^1\text{H}$  and  $^{13}\text{C}$  hyperfine coupling constants and  $\pi$ -spin densities

on the ring carbon atoms were calculated assuming only a contact contribution. The discrepancies between the calculated and observed hyperfine values, particularly at the 4-position, suggest that some  $\sigma$ -delocalization may also be present.

NMR spin-spin coupling and induced shifts in oxovanadium(IV) complexes have been reviewed. (61, 61a)  $^{51}\text{V}$  spectra of  $\text{VO}_2^+$  and a variety of heteropoly- and isopoly-anions (e.g.  $\text{VO}_4^{3-}$ ,  $\text{V}_{10}\text{O}_{28}^{6-}$ ) have been measured. A linear correlation is found between the measured shifts and the averaged  $g$ -factors of the reduced forms of the ions with  $^{51}\text{V}$  having an oxidation state of +4. Some spirocyclic V(IV) compounds of the type [9] have been studied by ESR and  $^1\text{H}/^{29}\text{Si}$

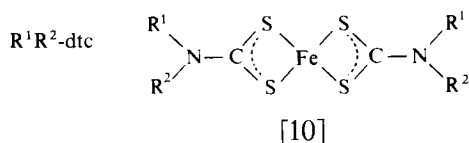


NMR methods. (63) Vanadium(V) compounds of the type  $\text{VOCl}_{3-x}(\text{OC}_2\text{H}_5)_x$ , obtained by progressive substitution of Cl by  $\text{OC}_2\text{H}_5$  groups, have been studied by magnetic and spectroscopic techniques. (64) Chemical shifts were interpreted as due to  $p\pi$ - $d\pi$  overlap from ligand to metal, the effect increasing with  $x$ , the number of  $-\text{OC}_2\text{H}_5$  groups attached.  $^{51}\text{V}$  shieldings in  $\text{VO}_3^+$  compounds (65) range from  $-432$  ppm (liq.  $\text{VOBr}_3$ ) to  $+786$  ppm ( $\text{VOF}_3\text{-CH}_3\text{CN}$ ) relative to liquid  $\text{VOCl}_3$  as reference standard. The trends can be rationalized in terms of the energy separations between HOMO and LUMO, inductive and  $\pi$ -transmission of electron density, hindered  $\sigma$ -donation, and expansion of the coordination sphere due to ligand bulkiness.

## 2. Five-coordinate transition metal complexes

The two usual limiting configurations to which 5-coordinate metal(II) complexes tend are the trigonal bipyramidal ( $D_{3h}$ ) and square pyramidal ( $C_{4v}$ ) configurations. The particular stereochemistry adopted by a complex depends mainly on the steric requirements of the ligands and crystal lattice energies.

Halogeno-bis-( $N,N$ -dialkyldithiocarbamato)iron(III) complexes,  $\text{Fe}(\text{dtc})_2\text{X}$  [10], have been extensively studied. Reference has already



been made (33) to  $T_1$  measurements on these complexes.  $^1\text{H}$  isotropic shifts have been reported (66,67) and attributed to purely contact contributions. Gregson and Doddrell (68) have reported  $^{13}\text{C}$  isotropic shifts for a series of  $\text{Fe}(\text{R}^1, \text{R}^2\text{-dte})_3$  complexes with differing alkyl ( $\text{R}^1, \text{R}^2$ ) groups. They noted that, whereas the shifts indicated dominant  $\pi$ -delocalization when the low spin state is favoured (i.e.  $t_{2g}^5$  configuration with unpaired spins only in orbitals of  $\pi$ -symmetry), the isotropic shifts of the  $\alpha$ -carbon and methyl protons are both positive for the complex in which  $\text{R}^1 = \text{R}^2 = \text{}^i\text{Pr}$ .

This is not in accord with theory for pure  $\pi$ -delocalization between metal and ligand which predicts that  $\sigma$ -contact shifts for  $^1\text{H}$  and  $^{13}\text{C}$  be of opposite sign. However, possible large pseudocontact shifts in the low spin state of these complexes complicate the issue. For a series of  $\text{Fe}(\text{dte})_2\text{X}$  complexes ( $\text{X} = \text{Cl}, \text{Br}, \text{I}$ ), however, accurate estimates of pseudocontact shifts from magnetic susceptibility data can be made.

The invariably opposite signs of the  $^{13}\text{C}$  and  $^1\text{H}$  isotropic shifts of the  $\alpha\text{-CH}_2$  nuclei (Table IV) are clear evidence of  $\pi$ -delocalization. (69) Table IV also lists proton relaxation times. The  $T_1$  values have been analysed in terms of dipolar (DD) and hyperfine contributions. For the

TABLE IV

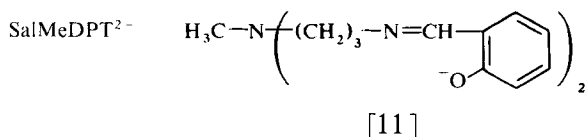
$^1\text{H}$  and  $^{13}\text{C}$  chemical shifts and relaxation times for  $\text{Fe}(\text{dte})_2\text{X}$  complexes (69)

X	Nucleus	$\sigma_{\text{iso}}$	$\sigma_{\text{pcon}}$	$\sigma_{\text{con}}$	$T_2$ (ms)	$T_1$ (ms)
Cl	$\text{CH}_2$	+186.2	-1.9	+188.1	0.63	1.4
	$\text{CH}_2$	-19.8	-1.7	-18.1		
	$\text{CH}_3$	-142.2	-1.5	-140.7	2.5	3.4
	$\text{CH}_3$	-2.0	-1.3	-0.7		
Br	$\text{CH}_2$	+193.0	-2.7	+195.7	1.0	2.5
	$\text{CH}_2$	-22.2	-2.5	-19.7		
	$\text{CH}_3$	-146.2	-2.2	-144.0	4.0	4.4
	$\text{CH}_3$	-2.4	-1.9	-0.5		

case  $\text{X} = \text{Cl}$ ,  $T_1$  for the  $\text{CH}_2$  protons is calculated to be  $1.4 \times 10^{-3}$  s for DD interaction and 4.3 s for the hyperfine interaction, clearly illustrating that dipolar coupling dominates the relaxation process. In contrast the hyperfine interaction contributes *ca.* 17% to the total  $T_2$  value.

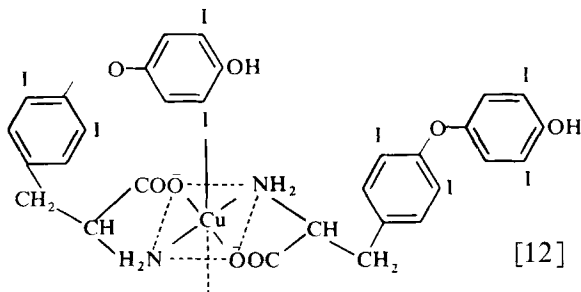
Agreement between theoretical and experimental  $T_1/T_2$  values is much poorer for  $X = \text{Br}$  and  $\text{I}$  and indicates a breakdown of the Redfield theory. (32) Isotropic proton shifts for pyridine-*N*-oxide and  $\gamma$ -picoline-*N*-oxide protons have been reported in the 5-coordinated adducts of these bases with bis(di-*p*-tolyl-dithiophosphinato)-Co(II) and -Ni(II). (70, 71) Dipolar shifts have been evaluated and indicate that the Co(II)-pyridine-*N*-oxide adducts have a bent structure in solution with Co-O-N angle of  $125^\circ$ . Results indicate that a  $\pi$ -spin delocalization mechanism is operating, and INDO calculations suggest that the highest bonding orbital is involved in the spin transfer process.

NMR and ESR studies have been carried out (72) on the  $\text{O}_2$  and CO adducts of the pentadentate Schiff base complex Co(salMeDPT) [11].



The isotropic shifts exhibit Curie behaviour. However, the authors argue that the complexes are distorted 6-coordinate complexes. The exchange  $\text{CoL.B} + \text{O}_2 \rightleftharpoons \text{CoL.B.O}_2$  is slow on the NMR time scale. The low-spin pyridine mono-adduct of *N,N'*-1,1-dimethylethylene-bis-(salicylideneiminato)cobalt(II) is 5-coordinate around Co(II) and exhibits large deviations of the shifts from the Curie law. (72a) This is interpreted in terms of the effects of a temperature-dependent ligand field arising from mixing of excited electronic states with the ground state where the unpaired electron is primarily in the  $d_{z^2}$  orbital. A series of cobalt(II) aminocarboxylates have been investigated. (73)  $\text{Co}^{\text{II}}(\text{EDTA})^{2-}$ ,  $\text{Co}^{\text{II}}(1,2\text{-PDTA})^{2-}$ , and  $\text{Co}^{\text{II}}(1,3\text{-PDTA})^{2-}$  exist in solution predominantly as 5-coordinate species and rapid racemization occurs at ambient temperatures.

Cu(II) forms a 5-coordinate complex with thyroxine which involves axial interaction with iodine at the apex of a square pyramid [12]. (559)



### 3. Six-coordinate transition metal complexes

6-Coordinate transition metal complexes are exceedingly common, with cobalt(II) and nickel(II) complexes being most suited for NMR studies. Octahedral nickel(II) complexes possess the non-degenerate ground state  ${}^3A_{2g}$  and thus are expected to experience only contact interactions in cases of regular  $O_h$  symmetry. Zero-field splittings will produce only very small dipolar shifts and in many spectra such shifts can be safely ignored. In contrast, octahedral cobalt(II) complexes possess the triply degenerate ground state  ${}^4T_{1g}$  which is expected to produce magnetic anisotropy and hence significant dipolar shifts. Differences between the NMR spectra of corresponding Co(II) and Ni(II) complexes have been attributed to the dipolar component of the isotropic shifts in the case of Co(II). Separation into contact and dipolar contributions has been accomplished by the "ratio method" of Horrocks. (74) This method is strictly valid only if the mode of spin delocalization is the same for the two series of complexes and one series is magnetically isotropic. These conditions are rarely satisfied exactly, so the method should be used with caution.

Acetylacetone (acac) and related  $\beta$ -diketones continue to be extensively used as ligands for transition metal complexes. This section deals with tris(acac) complexes followed by a discussion of the spectra of adducts of bis(acac) complexes. Cramer and Chudyk (75) have studied  $[Ni(acac)_3]2ClO_4$ . INDO calculations show that the major spin delocalization is into the highest filled ligand orbital which possesses  $\sigma$ -symmetry plus a minor contribution from delocalization into the lowest empty  $\pi$ -orbital. This is in contrast to the spin delocalization in  $Ni(acac)_3^-$  and  $Ni(acac)py_2$  where the major delocalization is into the highest filled ligand orbital of  $\pi$ -symmetry.

Furthermore, it is shown that for  $Co(acac)_2py_2$  an additional mechanism operates whereby spin is placed into the third highest filled orbital which has  $\sigma$ -symmetry. These findings have important implications on the use of the ratio method for  $M(acac)_2L_2$  complexes. Eaton and Chua (76) have reported the isotropic shifts of a variety of Co(II)  $\beta$ -diketonate complexes of the types  $Co(XCOCHCOX)_2L_2$  [ $X = CH_3, C_6H_5, C(CH_3)_3, CF_3$ ] and  $Co(XCOCHCOX)(YCOCHCOY)L_2$  [ $X = CH_3, Y = C(CH_3)_3$ ; and others] but no attempt is made to produce a quantitative separation into contact and dipolar contributions. Similar studies have been reported (77) for  $Ni(acac)_2L_2$  ( $L =$  cyclic or linear amines) and  $M(acac)_2L_2$  [ $L = py, quin, and isoquin; M = Ni(II), Co(II), Cu(II), and Mn(II)$ ]. (78) The reported  ${}^{13}C$  shifts are essentially contact in origin but the Mn(II) adduct gives anomalous results.

In contrast to pyridine adducts, those of pyridine-*N*-oxide produce isotropic shifts which support a dominant  $\pi$ -delocalization mechanism. Spin density distributions over the aromatic carbons have been determined from  $^1\text{H}$  and  $^{13}\text{C}$  spectra of several  $\text{Ni}(\text{acac})_2(\text{py-NO})_2$  complexes. (79)  $^{13}\text{C}$  relaxation measurements indicate that  $T_1$  values arise mainly from hyperfine dipolar interaction induced by spin density localized on  $\text{Ni}(\text{II})$  and on the  $^{13}\text{C}$ -centred  $2p_z$  orbital. Adducts of  $\text{Ni}(\text{acac})_2$  with aniline, (80) fluoroanilines, (80, 81) alkyanilines, (81–83) aniline derivatives, (541, 542) and nitrogen heterocycles (543) have been extensively studied. The results are consistent with a dominant  $\pi$ -spin delocalization mechanism.

INDO calculations on aniline cation radicals (80) suggest that in the complexes considered the  $\text{C}(1)\text{NH}_2$  fragment is pyramidal with an angle of  $13\text{--}15^\circ$  between the perpendicular to the  $\text{C--N}$  bond and the axis of the  $p$ -like orbital centred on nitrogen.  $^{13}\text{C}$  relaxation studies indicate a  $\text{N--Ni}$  distance of 200 pm for the aniline adduct. In the case of alkyaniline adducts, it has been shown (82) that the angular dependence of the  $\beta$ -carbon hyperfine coupling is given by:

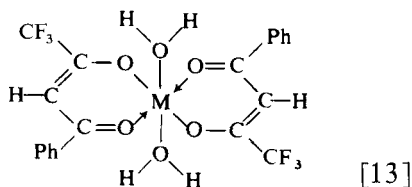
$$A_\beta^C = (B_1^C \cos^2 \theta + B_0^C) \rho_\pi^C \quad (25)$$

where  $B_1^C \approx 2.7 \text{ mT}$ ,  $B_0^C \approx -0.07 \text{ mT}$ , and  $\theta$  is the angle between the  $\text{C}(1)\text{--C}(\alpha)\text{--C}(\beta)$  plane and the perpendicular to the phenyl ring.  $^{13}\text{C}$   $T_{1\text{M}}$  measurements indicate that the  $\text{N--Ni}$  distance varies from 200 to 300 pm according to the steric hindrance of the alkyl groups in the vicinity of the  $\text{NH}_2$ . Measurements of  $T_{1\text{M}}$  and  $T_{2\text{M}}$  led to the electron relaxation time  $T_{1e}$  of  $\text{ca. } 2 \times 10^{-10} \text{ s}$  and a reorientation correlation time  $\tau_r$  of  $\text{ca. } 4 \times 10^{-11} \text{ s}$ . An alternative formulation of the angular dependence of the  $\beta$ -carbon hyperfine coupling, based on twenty 4-alkylaniline adducts of  $\text{Ni}(\text{acac})_2$ , has been given (84) as follows:

$$A_\beta^C = (23 \langle \cos^2 \theta \rangle - 1.1) \rho_\pi^C \quad (26)$$

The shifts for 4-cyclopropylanilines, however, deviate from this relationship and depend on the conformational preference of the group.

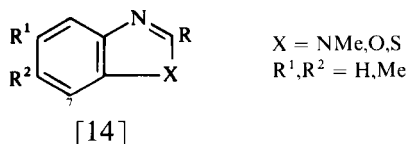
Adducts of bis(benzoyltrifluoroacetato) $\text{M}(\text{II})$  complexes have been studied by NMR methods. (84–86) Aquo complexes of stoichiometry  $\text{M}(\text{BTFA})_2(\text{H}_2\text{O})_2$  [13] were studied (84) by  $^{19}\text{F}$  and  $^1\text{H}$  NMR. Spin





density calculations show that the unpaired spin residing on the  $\text{H}_2\text{O}$  protons is  $3.7 \times 10^{-3}$  whereas at the ring protons it is  $0.6 \times 10^{-4}$  with the sign alternating for the  $\alpha$ - and  $\beta$ -positions. Spectra of  $\text{Co}(\text{BTFA})_2\text{L}_2$  ( $\text{L} = \text{py}$ , 2-Me-py, and 3-Me-py) in acetone as solvent indicate the presence of five isomeric species. (85, 86) Between  $-60$  and  $-80^\circ\text{C}$  the *cis* form predominates with 53% *cis* (*cis-cis* 17%, *cis-trans* 18%, *trans-cis* 18%), 37% *trans* (*cis-cis* 18%, *trans-trans* 18%), and the remaining 10% dissociated. The spectra of the corresponding  $\text{Ni}(\text{II})$  complexes show evidence of only two isomers.

A contact shift study (87) of various benzazole [14] adducts of



$\text{Ni}(\text{acac})_2$  has reported large high frequency shifts for the C-7 protons. These shifts have been accounted for in terms of an inter-ring spin delocalization taking place through  $\sigma$ -skeletons in a zig-zag arrangement. Pyridines continue to be widely studied as N-donor ligands. The exchange of pyridine on various bis-( $\beta$ -alkanedionato)-dipyridinenickel(II) complexes has been reported. (88) For  $\text{Ni}(\text{PhCOCHCOCH}_3)_2(\text{py})_2$  exchange with free py occurs with  $k(298\text{ K}) = (4.6 \pm 0.5) \times 10^4 \text{ s}^{-1}$ . Spin transfer mechanisms have been studied in  $\gamma$ -picoline adducts of monothio- $\beta$ -diketonates of  $\text{Ni}(\text{II})$ . (89) INDO calculations imply that the spin transfer mechanism depends on the conformational environment of the ligand molecules. For axial ligands the process involves  $\sigma$ ,  $\pi^b$ , and  $\pi^*$  molecular orbitals while for equatorial ligands the observed shifts can be explained by invoking transmission through  $\sigma$  and  $\pi^b$  orbitals only. Complexes of  $\text{Cu}(\text{acac})_2$  with N-heterocycles have been reported (90, 91) and in one case (90) both NMR and ESR data are reported.

$^1\text{H}$  and  $^{31}\text{P}$  NMR have been used to study complex formation of  $(\text{EtO})_3\text{P}$  and  $(\text{PhO})_3\text{P}$  with the  $\text{V}(\text{IV})$  ion of vanadyl acetylacetonate with  $\text{V}(\text{IV})$  in the presence of phosphites at different phosphite/hydroperoxide ratios. (92) Labile paramagnetic complexes with phosphites in the first coordination sphere are formed. Studies of the temperature dependence of the paramagnetic broadening of the NMR lines of hydroperoxide in the presence of  $\text{V}(\text{IV})$  has enabled the activation energy associated with ligand escape from the  $\text{V}(\text{IV})$  ion sphere to be estimated.

Transition metal acetylacetonates have also featured strongly in relaxation time measurements.  $^{13}\text{C}$  isotropic shifts and linewidths have

been measured and compared with the corresponding parameters of the contiguous protons. (93) Observed linewidths,  $\Delta\nu_{\frac{1}{2}} [= (\pi T_2)^{-1}]$ , are determined by dipolar (DD) and hyperfine interactions with the unpaired electrons [equations (18) and (20) respectively]. If DD relaxation is dominant for both  $^{13}\text{C}$  and  $^1\text{H}$  interactions, the relative linewidths are given by:

$$\Delta\nu_{\frac{1}{2}}^{\text{C}}/\Delta\nu_{\frac{1}{2}}^{\text{H}} = (\gamma_{\text{C}}^2/\gamma_{\text{H}}^2)(r_{\text{MH}}^6/r_{\text{MC}}^6) = 0.063(r_{\text{MH}}^6/r_{\text{MC}}^6) \quad (27)$$

If hyperfine relaxation is dominant, the expressions are:

$$\Delta\nu_{\frac{1}{2}}^{\text{C}}/\Delta\nu_{\frac{1}{2}}^{\text{H}} = A_{\text{C}}^2/A_{\text{H}}^2 = (\gamma_{\text{C}}^2/\gamma_{\text{H}}^2)(\sigma_{\text{con}}^{\text{C}}/\sigma_{\text{con}}^{\text{H}})^2 = 0.063(\sigma_{\text{con}}^{\text{C}}/\sigma_{\text{con}}^{\text{H}})^2 \quad (28)$$

Although, in general,  $r_{\text{MH}} > r_{\text{MC}}$ , it follows from equation (27) that, when DD relaxation is dominant, the  $^{13}\text{C}$  linewidth will be appreciably less than the  $^1\text{H}$  linewidth. Calculations for the olefinic and methyl positions give ratios of 0.37 and 0.08 respectively. If hyperfine relaxation is dominant, the relative linewidths of  $^{13}\text{C}$  and the contiguous  $^1\text{H}$  nuclei depend sensitively on the magnitude of the contact shifts. Assuming that  $|\sigma_{\text{con}}^{\text{C}}| \approx 10|\sigma_{\text{con}}^{\text{H}}|$ , equation (28) indicates that the  $^{13}\text{C}$  lines will not be broadened excessively relative to the  $^1\text{H}$  lines. Results on  $\text{M}(\text{acac})_3$  [ $\text{M} = \text{V(III)}, \text{Cr(III)}, \text{Mn(III)}, \text{Fe(III)}, \text{and Ru(III)}$ ] show that the hyperfine mechanism is the dominant relaxation pathway for the  $^{13}\text{C}$  spins, and in the cases where it is also the dominant mechanism for the  $^1\text{H}$  nuclei good agreement is obtained between the experimental values of  $\Delta\nu_{\frac{1}{2}}^{\text{C}}/\Delta\nu_{\frac{1}{2}}^{\text{H}}$  and those calculated on the basis of the contact shifts.

Pseudocontact interactions are thought to be important for  $\text{V}(\text{acac})_3$  and  $\text{Mn}(\text{acac})_3$ . Spin-lattice relaxation times have also been reported (94, 36) using the PRFT method (95). The  $T_1$  values are dominated by DD interactions which may be both metal- and ligand-centred. Assuming that the former are dominant, it follows that the ratio of the  $\text{CH}_3$  and  $-\text{CH}=\text{}$  carbon  $T_1$  values is related to the sixth power of the ratio of their distances from the metal, namely:

$$T_1(\text{CH}_3)/T_1(\text{CH}) = [r(\text{CH}_3)/r(\text{CH})]^6 \approx 6.2 \quad (29)$$

If hyperfine relaxation is dominant, then:

$$T_1(\text{CH}_3)/T_1(\text{CH}) \approx k[\rho(\text{CH})/\rho(\text{CH}_3)]^2 \quad (30)$$

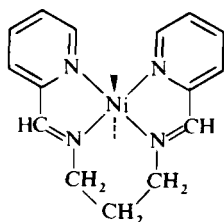
where  $\rho(\text{CH}_3)$  is the spin density in the  $p_z$  orbital on the carbonyl carbon and  $k$  is a constant ( $\sim 1-3$ ) which measures the efficiency whereby unpaired electron spins in this orbital cause relaxation of the

CH<sub>3</sub> carbon. The results indicate that ligand-centred effects are important and often dominant in controlling the relaxation of ligand nuclei. It is shown that spin density of  $\gtrsim 10^{-3}$  of an unpaired electron may be significant. This conclusion implies that calculations of geometries of paramagnetic complexes in solution based on  $T_1$  measurements should strictly allow for ligand-centred effects in addition to the metal-centred ones.

$T_2$  values and correlation times have been reported for complexes of Ni(acac)<sub>2</sub> with diethyl-, dipropyl-, and t-butyl-amines, ethylenediamine, and diaminopropane based on <sup>13</sup>C and <sup>14</sup>N studies. (96)

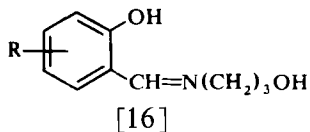
Cr(acac)<sub>3</sub> has been widely used as a relaxation reagent in <sup>13</sup>C NMR spectroscopy. It is of particular importance for studying <sup>13</sup>C=O signals which possess long  $T_1$  values. Recent studies, however, have shown that, in addition to reducing  $T_1$  values of <sup>13</sup>C signals, slight shifts (97) and increased linewidths (98) occur. The solvent CDCl<sub>3</sub> experiences a shift of 0.64 ppm in the presence of Cr(acac)<sub>3</sub>. In addition, the centre line of the triplet is broader than the outer lines whereas the opposite order of line broadening is normally expected for an  $I = \frac{1}{2}$  nucleus coupling to an  $I = 1$  nucleus. The increased linewidth effect (98) can be minimized if the Cr(acac)<sub>3</sub>/substrate mole ratio be  $\leq \frac{1}{100}$ . For accurate DNMR line-shape fitting studies it is important that this condition is satisfied.

Studies of Ni(II) complexes with the ligand *N,N'*-bis-(2-pyridylmethylene)-1,3-diaminopropane [15] and related Schiff bases

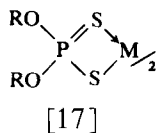


[15]

confirm the tetradentate coordination of the ligands and indicate a preferred methyl axial conformation for the central chelate ring in the complexes derived from 1,3-diaminobutane. (99) Tris-(ethylenediamine)nickel(II) complexes of the type Ni(en)<sub>3</sub>X<sub>2</sub> (X = nitrate, acetate, benzoate) exhibit a temperature dependence of the <sup>1</sup>H contact shifts which has been interpreted in terms of chelate ring conformational equilibria. (100) <sup>1</sup>H data have also been reported (101)

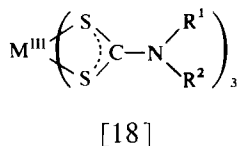


for Ni(II) complexes of *N*-hydroxypropyl-salicylaldimines [16], and various monomeric, dimeric, and trimeric complexes have been identified from the spectra. Pyridine-type bases complexed with Ni(II) and Co(II) dithiophosphates [17] and dithiophosphinates have



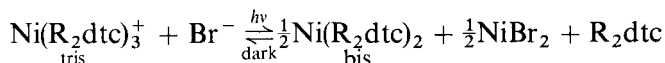
received some attention. (102–107) *A*-Values and spin densities are reported in many cases and delocalization mechanisms discussed. In the case of the isoquinoline adduct of nickel(II) dialkyldithiophosphate (102) the delocalization is primarily of the  $\sigma$ -type. For pyridine and  $\beta$ -picoline adducts,  $L \rightarrow M$  transfer of  $\beta$ -spin and delocalization of the resulting net  $\alpha$ -spin over the amino bonds is thought to occur. (103)

Dithiocarbamate complexes [18] continue to be the subjects of considerable study. For  $\text{Fe}(\text{S}_2\text{CNR}_2)_3$  and  $\text{Mn}(\text{S}_2\text{CNR}_2)_3$  the redox

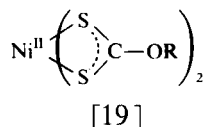


process associated with an electron spin cross-over equilibrium ( ${}^6\text{A}_1\text{--}{}^2\text{T}_2$ ) (Section B.2) is considered to occur through the nitrogen atom. (108) Detailed variable temperature studies of the  ${}^1\text{H}$  spectra of  $\text{Cr}(\text{S}_2\text{CNR}_2)_3$  reveal a double peak for the  $\text{N--CH}_n$  protons, unlike the cases of the Fe(III) and Mn(III) complexes. This is thought to arise from the high energy barriers between  $\Delta$  and  $\Lambda$  enantiomers. (109) Variable temperature studies have also been reported (110) for  $\text{Fe}(\text{S}_2\text{CNR}_2)_3$  in the range  $-60$  to  $+60^\circ\text{C}$ . Pseudocontact shifts are estimated from experimentally measured paramagnetic anisotropies. The spectra also suggest the existence of hindered rotation about the  $\text{S}_2\text{C--N}$  bond. Nickel(II) thiocarbamate complexes with amino adducts have been reported. (111) The complex  $\text{Ni}[\text{S}_2\text{CN}(\text{CH}_2\text{Ph})_2]_3^+$  has been observed

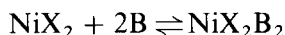
(112) to be photochromic and it undergoes a reversible redox decomposition:



The process can be followed by NMR since the tris complex is slightly paramagnetic ( $\mu_{\text{eff}} = 0.7$ ;  $\text{R} = \text{'Bu}$ ) whereas the bis complex is diamagnetic.

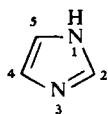


Bis(alkylxanthato)nickel(II) complexes [19] are highly suited for NMR study. Proton shifts and equilibrium constants for the equilibrium:



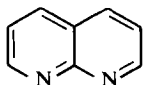
have been measured for  $\text{X} = \text{ROCS}_2$  and  $\text{B} = \text{py}$ ,  $\beta\text{-pic}$ , or  $\gamma\text{-pic}$ . (113, 114)

Imidazole [20] acts as a monodentate ligand towards transition metals, and octahedral complexes of the type  $\text{M}(\text{Im})_6^{2+}$  [ $\text{M} = \text{Fe}(\text{II})$ ,



[20]

$\text{Co}(\text{II})$ ,  $\text{Ni}(\text{II})$ ] can be isolated. The isotropic shifts for 4,5-H and 2-H are to high frequency and have been analysed (115) as approximately 95% contact and 5% dipolar in origin assuming a trigonal distortion from  $O_h$  symmetry of not more than  $2^\circ$ . Other imidazole complexes have also been reported. (116, 117) Eaton and Zaw (118, 119) have continued their studies of thiourea complexes of  $\text{Ni}(\text{II})$  and  $\text{Co}(\text{II})$ . Thiourea (tu) itself forms complexes of types  $\text{Ni}(\text{tu})_4\text{Cl}_2$ ,  $\text{Ni}(\text{tu})_6\text{Br}_2$ , and  $\text{Ni}(\text{tu})_6\text{I}_2$  but using substituted thioureas only 2 molecules of ligand are bound to each Ni atom. Complexes have tetrahedral, square-planar, and octahedral geometries in the case of  $\text{Ni}(\text{II})$  and are invariably tetrahedral in the case of  $\text{Co}(\text{II})$  with stoichiometry  $\text{CoL}_2\text{X}_2$ . Other sulphur-containing ligand complexes include alkylthiocarbonates ( $\text{ROCS}_2^-$ ) (120) and 5-thiopyrazolonates. (121)



[21]

1,8-Naphthyridine [21] acts as a stable monodentate ligand, and the contact shift data reported for Co(II) and Ni(II) complexes of this ligand (122) have been compared with those for other heterocyclic nitrogen ligands. The complexes are octahedral but in solution the following equilibrium exists:



Pyridine-*N*-oxide forms stable hexakis complexes with Co(II) and Ni(II).  $^{13}\text{C}$  studies have been carried out on  $M(\text{py-NO})_6(\text{BF}_4)_2$  ( $M = \text{Co}, \text{Ni}$ ) and the shifts compared with  $^1\text{H}$  shifts of the same complexes. Whereas the  $^1\text{H}$  contact shift patterns are the same for the two complexes, the  $^{13}\text{C}$  shifts are not and illustrate the danger of relating  $^1\text{H}$  contact shifts with carbon spin densities even in cases, like the present one, in which the alternating nature of the  $^1\text{H}$  contact shifts would suggest a substantial  $\pi$ -spin delocalization. (123)

Isotropic shift measurements of some triazene-1-oxide complexes of nickel(II) show appreciable contact shifts. (124) A detailed study of the temperature dependence of the isotropic shifts of octahedral Ni(II) complexes with a variety of amino and amide ligands reveals apparent non-Curie behaviour for most shifts. (125) The authors consider the likely causes of this anomalous behaviour, namely, pseudocontact shifts, ion-pair formation, hydrogen bonding, solvent effects, structural interconversion, and temperature independent paramagnetism.

Substituted pyridine-type complexes of Fe(II), Co(II), and Ni(II) continue to be extensively studied. (126–131) In complexes of the type  $M(4\text{-Et-py})_4\text{X}_2$  [ $\text{X} = \text{Cl}, \text{Br}, \text{I}, \text{NCO}, \text{NCS}, \text{and } \text{N}_3$ ;  $M = \text{Fe(II)} \text{ and } \text{Co(II)}$ ] appreciable dipolar effects have been measured (126) in the signals of the coordinated ligand, the solvent ( $\text{CDCl}_3$ ), and the free ligand. It is also found that the magnetic anisotropy causing these dipolar effects varies in sign with changes of the anion  $\text{X}$ .  $^1\text{H}$  and  $^{19}\text{F}$  studies of trifluoroacetate complexes of Co(II) and Ni(II) with pyridine-type ligands (127, 128) reveal distinct differences between complexes of stoichiometries  $\text{ML}_4\text{T}_2$  and  $\text{ML}_2\text{T}_2$  ( $\text{T} = \text{trifluoroacetate}$ ). *Cis-trans* isomeric exchange is detected in both series. For the  $\text{CoL}_2\text{T}_2$  complexes it becomes slow on the NMR time scale below *ca.*  $0^\circ\text{C}$  and below *ca.*  $-50^\circ\text{C}$  for the  $\text{CoL}_4\text{T}_2$  complexes. In contrast *cis-trans*

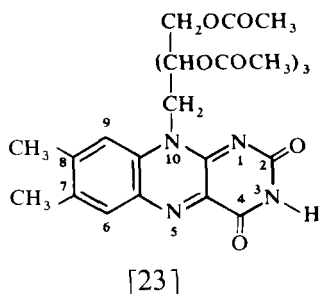
The complex formation between Ni(II) and acetate ions in aqueous solution has been studied by  $^{13}\text{C}$  NMR. Equilibrium quotients (132) and rate parameters (133) for the ligand exchange processes are reported. Complexes of hydroxy-acids (134) and iminodiacetates  $\text{RN}(\text{CH}_2\text{CO}_2^-)_2$  (135) have been the subjects of further studies. Co(II) complexes of malate, citrate, isocitrate, and monomethylcitrate all exhibit large shifts which may be accounted for by assuming a common structural unit [22] in which the ligand is tridentate. Nickel(II)



Metal complexes involving M-O bonds include ketone, alcohol, sulphoxide, and tropolone complexes. Complexes of the type  $[\text{Co}(\text{H}_2\text{O})_n\text{L}_{6-n}]\text{X}_2^-$  ( $n = 0-6$ ;  $\text{L} = \text{Me}_2\text{O}$ ,  $\text{MeOH}$ ,  $\text{MeCN}$ ,  $\text{Me}_2\text{SO}$ ,  $\text{DMF}$ ;  $\text{X} = \text{Cl}^-$ ,  $\text{ClO}_4^-$ ,  $\text{NO}_3^-$ , and others) have been studied as a function of anion, solvent, concentration, and temperature. (136) Methanol complexes of the type  $\text{Co}(\text{CH}_3\text{OH})_5\text{X}^{2+}$  ( $\text{X} = \text{py}$ , picolines,  $\text{DMF}$ ,  $\text{DMSO}$ , acetonitrile, and  $\text{H}_2\text{O}$ ) have been reported in detail. (137) *Cis* and *trans* methanol environments have been distinguished and a new procedure for separating contact and dipolar shifts is presented. Other alcohol complexes have been reported. (138, 139) Octahedral complexes of type  $\text{ML}_6(\text{ClO}_4)_2$  [ $\text{M} = \text{Co(III)}$ ,  $\text{Ni(II)}$ ;  $\text{L} = \text{Me}_2\text{SO}$ ,  $\text{EtMeSO}$ ,  $\text{Me}_2\text{CO}$ , and  $\text{EtMeCO}$ ] exhibited  $^1\text{H}$  shifts which were predominantly due to  $\sigma$ -delocalization but some  $\sigma$ - $\pi$

polarization needed to be invoked (140) to explain the low frequency shifts of the Me and CH<sub>2</sub> groups directly bonded to C=O. The equilibrium between ML<sub>2</sub> [M = Co(II), Ni(II); L = β-isopropyl tropolonate] and its octahedral adducts CoL<sub>2</sub>(L')<sub>n</sub> (L' = py, α- and γ-picoline, piperidine; n = 1 or 2) has been studied and formation constants have been calculated. (141, 142)

NMR studies have provided considerable insight into the structures and paramagnetic interactions of flavoquinone [23] complexes with



first-row transition metals. (143) Tris, bis, or mono complexes are obtained in the presence of excess flavine. Stable bidentate chelates at O(4α)–N(5) corresponding to octahedral tris complexes [for Zn(II), Cd(II), Co(II), Ni(II), and Fe(II)], tetrahedral bis complexes [for Ag(I) and Cu(I)], and square-planar bis complexes [for Cu(II)] are found. Two possible isomers for the octahedral complexes are shown in Fig. 2. Labile complexes corresponding to weak monodentate binding at the keto groups of flavine are observed with Mg(II), Mn(II), and Fe(III). The isotropic shifts of the paramagnetic complexes are analysed in terms of contact and pseudocontact interactions using relaxation and g-tensor anisotropy data. The results for the Co(II) complex are given in Table V where it will be seen that the pseudocontact shifts are appreciable unlike those observed for the Ni(II) and Fe(II) complexes. The

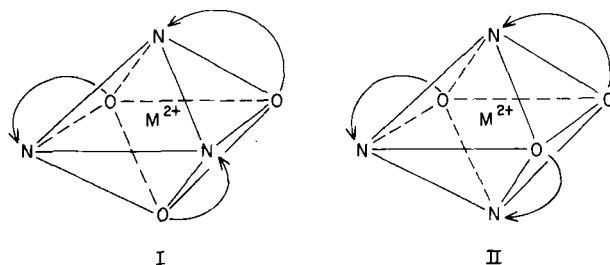


FIG. 2. The two possible isomers for the octahedral complexes M(RFl<sub>ox</sub>)<sub>3</sub><sup>2+</sup>: the *cis* form (I) and the *trans* form (II). (143)



TABLE V

Pseudocontact shifts in Co(II)-tris(flavoquinone) complexes (143)

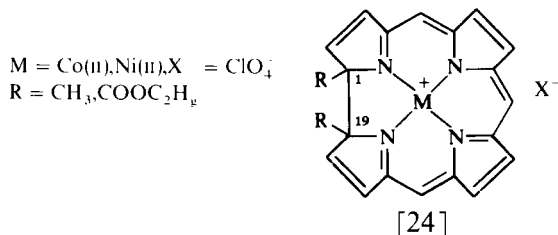
Proton	Calc. pseudocontact shifts (ppm)				Obs. isotropic shift (ppm)	Calc. contact shift (ppm)
	CH <sub>3</sub> (8)	CH <sub>3</sub> (7)	H(9)	NH(3)		
CH <sub>3</sub> (8)	—	5.2	4.9	(-5.6)	4.7	-0.3
CH <sub>3</sub> (7)	10.4	—	11.5	11.8	12.4	+1.2
H(9)	4.8	4.8	—	5.0	-5.1	-9.9
NH(3)	-14.0	-14.7	-14.9	—	-14.3	+0.2

distribution of contact shifts can be explained in terms of  $\pi$ -electron spin negatively polarized in the ligand orbitals. This appears to result from indirect  $\sigma$ - $\pi$  spin polarization at the coordination site combined with a delocalization of negatively polarized spin in the ligand  $\pi$ -bonding orbitals.

Studies of Ni(II) complexes with the potentially 8-donor ligand diethylenetriaminepentaacetic acid (DTPA) over a wide pH range have shown (144) that only some of the carboxylic groups coordinate to the nickel ion. Deuteration studies have enabled the rate constants for the exchange between coordinated and uncoordinated carboxylic groups to be evaluated.

Co(III) complexes are almost invariably of the low-spin  $d^6$  type and diamagnetic (see ref. 48a for an exception). However, there has been a report of an organocobalt(III) complex which is rendered slightly paramagnetic by possessing a thermally accessible triplet state. (145) A new range of complexes of the general formula  $\text{CapCo}(\text{dmg})_3$   $\text{Cap}^{n+}$  [Hdmg = dimethylglyoxime and Cap = diethylenetriamine-chromium(III) and similar groups] have been described. (146)  $^1\text{H}$  and  $^{59}\text{Co}$  NMR spectral data are reported. These so called metal-capped clathrochelates (Fig. 3) give magnetic susceptibility data that indicate little interaction between the unpaired electrons of the paramagnetic capping groups.

NMR data form part of a detailed spectroscopic study of Co(II) and Ni(II) complexes of 1,19-disubstituted tetrahydrocorrins [24]. (147)



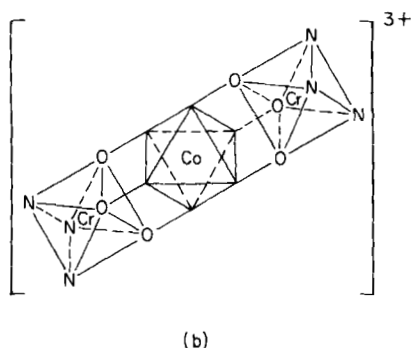
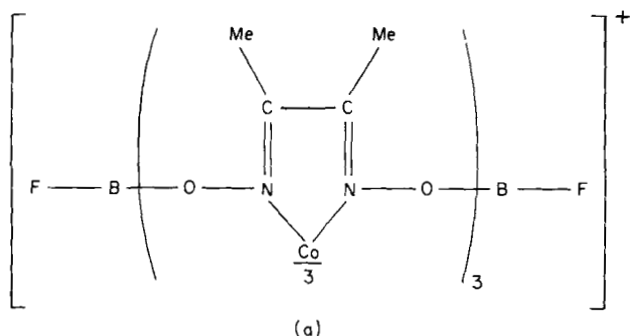


FIG. 3. (a) The clathrochelate  $[\text{Co}(\text{dmg})_3(\text{BF}_2)_2]\text{BF}_4$ . (146) (b) Suggested structure of the  $\text{Cr}(\text{dien})^{3+}$  capped metallomer (dien = diethylenetriamine).

The angular methyl groups at positions 1 and 19 show abnormally large low frequency shifts attributable to the magnetic anisotropy of the adjacent pyrrole rings.

$^1\text{H}$  and/or  $^{13}\text{C}$  data have been reported for some  $\text{Fe}(\text{II})$  complexes (148, 149) and  $\text{Fe}(\text{III})$  complexes. (150) Manganese(II) forms octahedral complexes with isocyanide ligands of types  $[\text{Mn}(\text{RCN})_6]\text{PF}_6$  and  $[\text{Mn}(\text{RCN})_6](\text{PF}_6)_2$  ( $\text{R} = \text{C}_6\text{H}_5$ ,  $p\text{-CH}_3\text{C}_6\text{H}_4$ ,  $\text{C}_6\text{H}_5\text{CH}_2$ , etc.). The first type are diamagnetic involving  $\text{Mn}(\text{I})$  while the second type are paramagnetic involving  $\text{Mn}(\text{II})$ . The shifts are found (151) to alternate in direction for *ortho* and *meta* protons indicating predominant  $\pi$ -spin delocalization and a  $^2\text{T}_{2g}$  ground state for the complexes.

NMR data for  $\text{Mo}(\text{II})$ ,  $\text{Re}(\text{III})$ , and  $\text{Cr}(\text{II})$  complexes have been reported. (152) A detailed wide-line study of  $\text{Ru}(\text{NH}_3)_6^{3+}$  at various

temperatures has revealed non-Curie behaviour of the paramagnetic shift which can be accounted for in terms of the pseudocontact interaction of Kurland and McGarvey. (18) The contact hyperfine interaction with the ammine protons is calculated to be 5.9 MHz. (153)

Magnetic susceptibility and NMR shift data have been reported for tungsten(IV) complexes of the types  $WX_4(C_3H_7CN)_2$  ( $X = Cl, Br$ ) and  $WCl_4[S(C_2H_5)_2]_2$ . (154) 8-Coordination complexes involving W(IV) and W(V) of type  $WL_4$  ( $L =$  picolinate and related ligands) have been studied. The salts  $[WL_4]X$  are paramagnetic and shift data are given. (155)

#### 4. Complexes of the lanthanides and actinides

Lanthanide ions continue to be very widely used as shift reagents for substrate molecules (Section III.F). There is, however, considerable interest in the NMR properties of the lanthanide complexes themselves. The isotropic shifts of the latter are invariably dominated by dipolar interactions between the lanthanide ion and the nucleus under question. Bleaney (156) has predicted that the dipolar shift will be dominated by a component which varies as  $T^{-2}$  around room temperature whereas Horrocks *et al.* (157, 158) predict a more complex temperature dependence. Hill *et al.* (159) have examined the temperature dependence of some tetraethylammonium tetrakis-*N,N*-diethyldithiocarbamate-lanthanate(III) salts,  $Et_4N^+Ln(dtc)_4^-$ , in an attempt to clarify the situation. The observed temperature dependences are complex and both contact and dipolar contributions had to be considered in the form:

$$\Delta B(\text{iso}) = \Delta B(\text{con}) + \Delta B(\text{dip}) = AT^{-1} + BT^{-2} \quad (31)$$

Bleaney's treatment gives a qualitative explanation of the major (i.e.  $T^{-2}$ ) contribution to the isotropic shifts (Table VI). The  $T^{-1}$  contribution is thought to arise from substantial contact interaction, particularly in the cases of the Pr and Nd complexes.

Picoline-*N*-oxide complexes have been reported in some detail. (160–162) Complexes are of the general type  $LnL_{8-n}X_3nH_2O$  ( $L =$  picoline-*N*-oxides;  $n = 0$  or  $2$ ;  $X = Br$  or  $I$ ). The isotropic shifts possess both contact and pseudocontact contributions. For  $LnL_8I_3$  a square antiprismatic geometry is assumed. Complexes of La, Nd, Er, and Lu with EDTA-type ligands are reported (163, 164) and structural differences are discussed. Aqueous solutions of dysprosium perchlorate have been examined. (165) Contact and pseudocontact shifts are separated using a least-squares method based on the different

TABLE VI  
Relative magnitudes of the  $T^{-2}$  dependent contributions to  
the isotropic shifts in the  $\text{Ln}(\text{dte})_4^-$  complexes (159)

Ln	$\text{CH}_2$	$\text{CH}_3$	Theory (156)
Pr	+5.4	+5.4	+5.0
Nd	+3	+3	+2.0
Tb	+50	+45	+40
Dy	+75	+71	+46
Ho	+35	+31	+18
Er	-17	-17	-15
Tm	-24	-24	-24
Yb	-10	-10	-10

temperature variations of the two terms somewhat analogous to the method adopted in ref. 159. Hyperfine coupling constants, electronic relaxation times, and activation energies for the relaxation processes present are also obtained.

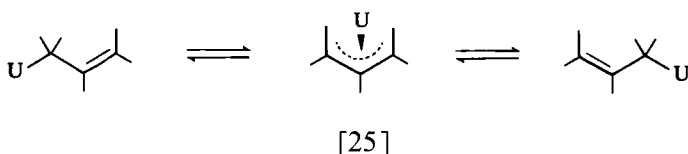
Studies of  $\text{Ln}(\text{III})$  nitrilotriacetate (539) and ethylenediamine (540) complexes have been reported. In the latter case a contact mechanism is responsible for the shifts in the lighter lanthanides (up to Ho) whereas a pseudocontact shift is dominant for the remainder of the series. Some novel lanthanide-cobalt sandwich complexes have also been reported. (587) Uranium(IV) complexes continue to be the most extensively studied of the actinide ion complexes. Appreciable dipolar interactions are expected to arise from the orbitally degenerate ground term  $^3H_4$  arising from the  $5f^2$  configuration of U(IV). However, in practice isotropic shifts of U(IV) complexes are not dominated by dipolar interactions.

Both dipolar and contact contributions are important in glycinate complexes. (166) U(IV) complexes with  $\alpha$ -alanine, (167) various amino-acids, (168) ethyl trifluoroacetoacetate, (169) tetrakis-(tetra-ethylammonium)octathiocyanatouranate  $\text{U}(\text{NCS})_8(\text{NEt}_4)_4$ , (170) and  $\beta$ -diketones (171, 172) have been examined. In studying the ligand exchange kinetics of the latter complexes (172) the mechanism is considered to involve a ninth coordination site in the U(IV) chelate.

The hydration of U(IV) in acid solutions has been followed by relaxation time ( $T_1$  and  $T_2$ ) measurements. (173) The relaxation rates observed in perchloric acid solutions at high temperature are governed by the exchange process of water molecules between the inner coordination sphere of U(IV) and the bulk water. In contrast, at low temperatures the rates are dominated by an outer sphere effect. NMR

signals are only observed from water molecules in the second coordination sphere.

Tetraallyl (174) and triscyclopentadienyl (175–178) uranium(IV) complexes have been the subjects of  $^{13}\text{C}$  and  $^1\text{H}$  shift analyses. The  $^{13}\text{C}$  contact shift of  $(\text{C}_5\text{H}_5)_3\text{UCl}$  in THF is calculated (175) to be  $-309 \pm 120$  ppm at 290 K and is approximately twice as large as the pseudocontact shift. In the complexes  $(\text{h}^5\text{-C}_5\text{H}_5)_3\text{UR}$ , when R is an allyl group, the molecule is fluxional. On cooling the sample down to 179 K the spectra change until they become characteristic of a monohapto allyl linkage. A  $\sigma \rightleftharpoons \pi \rightleftharpoons \sigma$  interconversion [25] will explain the NMR results.



### 5. Organometallic compounds

A wide variety of paramagnetic organometallic compounds are known. The large majority of these are classified as metallocenes and are of considerable NMR interest. In studying such systems Köhler (179) has suggested that  $^{13}\text{C}$  spectroscopy offers distinct advantages over  $^1\text{H}$  spectroscopy. From studies on bis- $(\text{h}^5\text{-t-butyl-cyclopentadienyl})\text{vanadium}$  he has predicted that apart from the ring carbons of metallocenes the  $^{13}\text{C}$  signals of all paramagnetic metallocenes should be observed without great difficulty. Ferricenium hexafluorophosphates,  $(\text{h}^5\text{-RC}_5\text{H}_4)_2\text{Fe}^+\text{PF}_6^-$  ( $\text{R} = \text{H}, \text{CH}_3, \text{C}_2\text{H}_5, \text{C}_4\text{H}_9$ ), have been studied (180–182) at variable temperatures. Using magnetic susceptibility and ESR  $g$ -value data, it was deduced that for the complex with  $\text{R} = \text{CH}_3$  the dipolar term contributes *ca.* 55% of the observed shift of the  $\text{CH}_3$  protons but only *ca.* 25% of the ring proton shifts.

The electron exchange kinetics between ferrocene  $(\text{h}^5\text{-C}_5\text{H}_5)_2\text{Fe(II)}$  and ferricenium ion  $(\text{h}^5\text{-C}_5\text{H}_5)_2\text{Fe}^+(\text{III})$  have been measured by the line-broadening method. (184) The rate constants are calculated to be  $(5.7 \pm 1.0) \times 10^6 \text{ M s}^{-1}$  in acetonitrile as solvent ( $25^\circ\text{C}$ ) and  $(5.4 \pm 1.0) \times 10^6 \text{ M s}^{-1}$  in methanol, with activation energies of  $21 \pm 4$  and  $13 \pm 4 \text{ kJ mol}^{-1}$  respectively. Köhler has made an extensive study of a variety of other metallocenes  $(\text{h}^5\text{-RR}'\text{C}_5\text{H}_3)_2\text{M}$  where M is V, Cr, Co, and Ni, and  $\text{R/R}'$  is H,  $\text{CH}_3$ ,  $\text{C}_2\text{H}_5$ ,  $\text{CHMe}_2$ , or Ph. (184–190) Well

resolved  $^1\text{H}$  and  $^{13}\text{C}$  spectra are obtained in most cases. The measured shifts depend greatly on the nature of the metal M. (187) In nickelocenes ( $\text{M} = \text{Ni}$ ) the spread of shifts is very large ( $\sim 3000$  ppm for  $^{13}\text{C}$  and 450 ppm for  $^1\text{H}$ ). In contrast, for cobaltocenes ( $\text{M} = \text{Co}$ ) the  $^{13}\text{C}$  shift spread is  $\sim 900$  ppm and the  $^1\text{H}$  spread  $\sim 110$  ppm. Some typical values are given in Table VII where the shifts are relative to those for the analogous diamagnetic ferrocene derivative.

TABLE VII  
 $^{13}\text{C}$  and  $^1\text{H}$  shift data for some metallocenes (187)

Compound	Nucleus	Chemical shift <sup>a</sup> (ppm)			
		1	2/5	3/4	$\text{CH}_3$
$(\text{C}_5\text{H}_5)_2\text{Ni}$	$^{13}\text{C}$	+ 1436	+ 1436	+ 1436	
	$^1\text{H}$	- 263	- 263	- 263	
$(\text{CH}_3\text{C}_5\text{H}_4)_2\text{Ni}$	$^{13}\text{C}$	+ 1285	+ 1475	+ 2695	- 640
	$^1\text{H}$		- 263	- 263	+ 210
$(\text{C}_5\text{H}_5)_2\text{Co}$	$^{13}\text{C}$	+ 577	+ 577	+ 577	
	$^1\text{H}$	- 56.2	- 56.2	- 56.2	
$(\text{CH}_3\text{C}_5\text{H}_4)_2\text{Co}$	$^{13}\text{C}$	+ 358	+ 437	+ 755	- 112
	$^1\text{H}$		- 49.0	- 73.6	+ 12.2
$(\text{C}_5\text{H}_5)_2\text{Cr}$	$^{13}\text{C}$	- 325	- 325	- 325	
	$^1\text{H}$	+ 324	+ 324	+ 324	
$(\text{CH}_3\text{C}_5\text{H}_4)_2\text{Cr}$	$^{13}\text{C}$	- 68	- 505	+ 347	+ 535
	$^1\text{H}$		+ 377	+ 318	+ 37.2
$(\text{C}_5\text{H}_5)_2\text{V}$	$^{13}\text{C}$	- 588	- 588	- 588	
	$^1\text{H}$	+ 315	+ 315	+ 315	
$(\text{CH}_3\text{C}_5\text{H}_4)_2\text{V}$	$^{13}\text{C}$	- 482	- 750	- 533	+ 915
	$^1\text{H}$		+ 326	+ 326	+ 116

<sup>a</sup> Shifts relative to analogous ferrocene derivative, with positive values denoting high frequency shifts.

Manganocene ( $\text{M} = \text{Mn}$ ) and 1,1'-dimethylmanganocene have been the subjects of detailed ESR, magnetic susceptibility, and NMR experiments, (191) the aim being to examine the electronic ground states of these molecules. Interest in manganocene centres round the fact that it is the only metallocene with a high-spin ground state ( $^6\text{A}_{1g}$ ) and crystalline samples show antiferromagnetic behaviour. Magnetic measurements show that the dimethyl derivative exhibits a subnormal and temperature dependent magnetic moment which has a maximum around 310 K whereas manganocene itself has normal magnetic behaviour. ESR results indicate that the ground state of dimethylmanganocene at 4.2 K is  $^2\text{E}_g$  whereas manganocene has the normal high-spin  $^6\text{A}_{1g}$  state. In order to account for the temperature

dependent magnetic susceptibility of the dimethyl derivative a high-spin ( $S = \frac{5}{2}$ )–low-spin ( $S = \frac{1}{2}$ ) equilibrium is suggested. The different magnetic properties of the two compounds are reflected in much larger isotropic shifts of dimethylmanganocene compared with its parent compound. The spectra suggest that the cyclopentadienyl hydrogen hyperfine coupling constant has the anomalously large value of 9 MHz for the doublet state species. This value is more reasonably rationalized by assuming thermal equilibration at higher temperatures among three states, namely,  ${}^6A_{1g}(e_{1g}^2 a_{1g}^1 e_{1g}^{*2})$ ,  ${}^2E_{2g}(e_{2g}^3 a_{1g}^2)$ , and  ${}^2A_{1g}(e_{2g}^4 a_{1g}^1)$ . A series of ring substituted nickelocenes (192) were also studied to examine the possible spin delocalization mechanisms.

The carborane analogues of the metallocenes, the so-called metallocarboranes, have been studied by Wiersema and Hawthorne. (193) The paramagnetic species that they chose to study are of the types  $(C_5H_5)M(C_2B_nH_{n+2})$  and  $M(C_2B_nH_{n+2})_2$  where  $M = Cr(III)$ ,  $Fe(III)$ ,  $Ni(III)$ , and  $Co(II)$ , and  $n = 9, 8, 7$ , and  $6$  (Fig. 4). The  ${}^{11}B$  isotropic shifts of the  $Fe(III)$  and  $Cr(III)$  complexes reflect large negative hyperfine coupling constants which are consistent with a  $\pi$ -polarization mechanism (194) or parallel spin transfer from ligand to metal (Table VIII). By contrast, the  $Co(II)$  complexes exhibit shifts that reflect

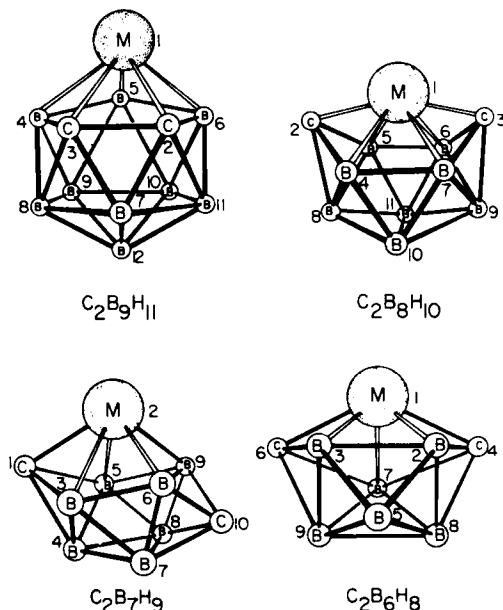


FIG. 4. Ligand geometries and numbering for various heteroboranes. (192)

positive  $A$  values which in turn are indicative of direct delocalization of metal-centred electron density into ligand orbitals. The extent of the delocalization process, whether  $L \rightarrow M$  or  $M \rightarrow L$ , is very limited and is typical of a  $\sigma$ -type of delocalization. The limited ability of the carborane cage extensively to delocalize spin density to all portions of the cage is not unexpected in view of the likely  $sp^3$  hybridization of the boron atoms. A comparison of the isotropic shifts of the metallocarboranes with those of the metallocenes shows that the  $^{13}\text{C}$ , but not the  $^1\text{H}$ , shifts are very similar. This suggests that the energetics of the metal–ligand interaction are similar, namely, that the HOMO is primarily metal-centred and non-bonding in nature.

TABLE VIII  
 $^{11}\text{B}$  data<sup>a</sup> for  $(\text{C}_5\text{H}_5)\text{M}(2,3\text{-C}_2\text{B}_9\text{H}_{11})$  (193)

Nucleus	M = Fe(III)		M = Co(II)	
	Contact shift	$A$ (mT)	Contact shift	$A$ (mT)
B-5	– 568	– 0.173	+ 485	+ 0.148
B-4, 6	– 531	– 0.162	+ 181	+ 0.055
B-7	+ 62	+ 0.019	+ 49	+ 0.015
B-8, 11	– 54	– 0.016	+ 8	+ 0.002
B-9, 10	– 40	– 0.012	+ 61	– 0.019
B-12	– 126	– 0.038	+ 4	+ 0.001

<sup>a</sup> Units of ppm. Positive values denote high frequency shifts.

## 6. Free radicals

NMR studies of free radicals are often seriously handicapped by the long electron relaxation times of these species which lead to excessively broad bands. In order to obtain useful NMR spectra one requires a sample system that involves rapid averaging of the electron spin energy levels. This is commonly achieved by promoting an intermolecular spin exchange reaction (usually between the neutral radical solute and the ligand radical di-*t*-butyl nitroxide (DBNO) which acts as a spin relaxing solvent) or an electron exchange reaction (usually between the radical and its diamagnetic precursor).

Work prior to 1973 has been comprehensively reviewed by Kreilick. (195) A review dealing with the detection of radicals by ESR, ENDOR, and NMR methods has appeared more recently. (196) Before discussing the more usual  $^1\text{H}$  and  $^{13}\text{C}$  studies of radical species mention



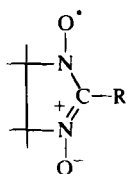
should be made of a detailed theoretical and experimental study of radical ion pairs of biphenyl and fluorenone using alkali metal NMR experiments, i.e.  $^6\text{Li}$ ,  $^7\text{Li}$ ,  $^{23}\text{Na}$ ,  $^{39}\text{K}$ ,  $^{85}\text{Rb}$ ,  $^{87}\text{Rb}$ , and  $^{133}\text{Cs}$  studies. (197,198) The alkali metal salts of biphenyl and fluorenone were examined in solutions of various ethers (e.g. tetrahydropyran, tetrahydrofuran, dimethoxyethane, diglyme). Magnitudes and signs of the hyperfine coupling constants of the alkali metals are deduced from the equations:

$$\delta_c(\text{exp}) = (B - B_0)/B_0 \approx \delta_c^0 \quad (32)$$

$$\delta_c^0 = -(|\mu_B|/\mu_N)(A/4kT) \quad (33)$$

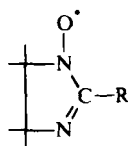
where  $\delta_c(\text{exp})$  is the shift of an alkali metal nucleus in a paramagnetic ion pair measured relative to the signal of the completely hydrated ion,  $\delta_c^0$  is the pure contact shift for a doublet radical, and  $A$  is the contact interaction constant. The influence of temperature and solvent on the  $A$  values suggested that contact interactions are dominant for the biphenyl salts. In contrast the  $A$  values for fluorenone are not appreciably temperature dependent, suggesting that the alkali metal ions in the fluorenone ion pairs are close to a site with appreciable charge and spin density, probably the oxygen atom. A detailed analysis of solvent and temperature dependences of the linewidths has enabled the contributions of various relaxation mechanisms to be assessed. For Li ion pairs magnetic dipole interactions determine the linewidths, for Na salts magnetic dipole and quadrupole interactions are important, for K and Rb salts quadrupole interactions are usually dominant, and for Cs salts the linewidths are often completely determined by the contact interaction. Spectra of the radical anions of anthracene, pyrene, and triphenylene have been analysed in detail. (199) Calculations of hyperfine interaction constants, the anisotropic electron–nucleus dipolar interaction (the  $T$ -tensor), and linewidth measurements for both  $^1\text{H}$  and  $^2\text{H}$  yield detailed information about electron spin distribution in these radicals. Electron spin and rotational correlation times ( $\tau_e$  and  $\tau_r$  respectively) are deduced from the linewidth information.

Nitroxide radicals continue to be those most widely studied by NMR. This stems from their relatively high stability, high solubility in a wide variety of solvents, and their well resolved NMR spectra when measured in concentrated solutions in which spin exchange is sufficiently rapid.  $^1\text{H}$  and/or  $^{13}\text{C}$  data have been reported for some aryl nitronyl nitroxide radicals [26], (200) imino nitroxide radicals [27], (201) *para*-substituted aryl *t*-butyl nitroxides  $\text{ArN}(\text{O}\cdot)\text{Bu}$ , (202)



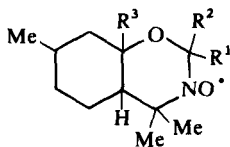
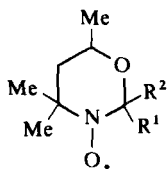
R = Ph, 2-, 3-, or 4-pyridyl

[26]

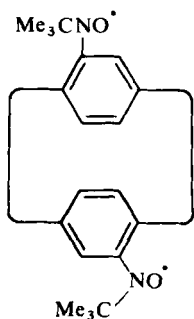


[27]

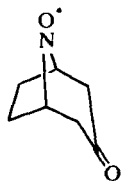
oxazinic nitroxides [28], (203) paracyclophanyl nitroxides [29], (204) di-*t*-butyl iminoxy radical  $\text{tBu}_2\text{C}=\text{NO}\cdot$ , (205) nitroxide derivatives of tropane [30], (206) 2-alkoxycarbonylphenyl nitroxide radicals [31], (207) and other miscellaneous nitroxide radicals (208, 209) and



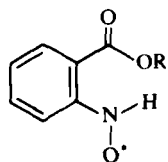
[28]



[29]



[30]



[31]

biradicals. (210–212) The nitronyl nitroxide radicals are used to measure the magnitude and signs of carbon-13 hyperfine splitting constants. Such data are not easily obtained in general. Table IX lists the shifts, splitting constants, and spin densities reported.

TABLE IX  
NMR data for aryl nitronyl nitroxide radicals (200)

Compound	Position	Shift <sup>a</sup> (ppm)	<i>A</i> (mT)	10 <sup>2</sup> <i>P</i> <sup>b</sup>
[26], R = Ph	<i>ortho</i>	342	-0.117	-1.65
	<i>meta</i>	-157	0.054	0.65
	<i>para</i>	138	-0.047	-1.41
	$\alpha$	630	-0.21	
	$\beta$	-746	0.26	

<sup>a</sup> Relative to methyl carbons of 2,2,6,6-tetramethylpiperidine.

<sup>b</sup> Calculated assuming  $Q_{CH} = -2.7$  mT.

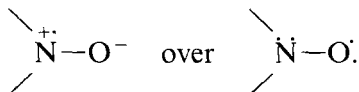
The *A* values are given by a modified version of the Karplus-Fraenkel equation: (213)

$$A_C = Q_C^C \rho^\pi + \sum_i Q_{C'-C}^C \rho_i^\pi \quad (34)$$

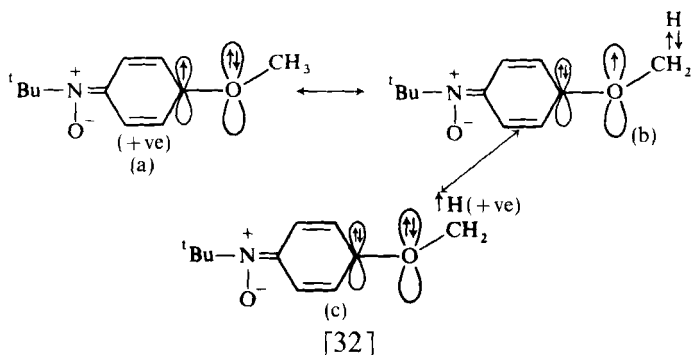
where the first term accounts for polarization of the 1s electrons and electrons in the  $sp^2$  hybrid bonds by spin in the 2p orbital of the carbon atom in question. The second term allows for unpaired spin in the 2p orbitals of adjacent carbons polarizing the  $sp^2$  electrons.  $\rho^\pi$  is the spin density at the atom in question and  $\rho_i^\pi$  the spin density of an adjacent atom. When a nitrogen atom is bonded to a carbon atom in an aromatic ring, equation (34) has to be modified to allow for the carbon-nitrogen and nitrogen-carbon spin polarization parameters,  $Q_{C-N}^C$  and  $Q_{N-C}^C$ . In order to determine the spin polarization parameters experimentally a plot of  $A_C/\rho^\pi$  against  $\sum_i \rho_i^\pi/\rho^\pi$  was made. A least-squares fitting gives a slope of  $-0.76$  mT, which equals  $Q_{C'-C}^C$ , and an intercept of  $2.4$  mT which equals  $Q_C^C$ , assuming  $Q_{CH}$  for all the radicals is  $-2.25$  mT. It is observed that the spin densities in the aromatic ring do not change appreciably when a nitrogen atom is substituted for a carbon atom, which suggests that the spin polarization parameters  $Q_{C-N}^C$  and  $Q_{N-C}^C$  are similar in magnitude to  $Q_{C'-C}^C$ . The coupling constants for the *ortho* carbons are much larger than predicted by INDO calculations. This may be due to an unexpectedly large spin density at the bridgehead carbon or to a long-range interaction with spin in the nitronyl nitroxide ring.

The imino nitroxide radicals (201) exhibit a similar spin distribution to that of the nitronyl nitroxide radicals. The methyl protons on the two sides of the imino nitroxide ring are found to have different coupling constants. This is thought to be due either to different relative geometries or to an interaction between the methyl protons on the

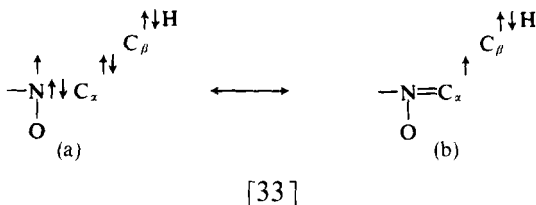
nitroxide side of the ring with spin at the oxygen atom. In the *para*-substituted aryl *t*-butyl nitroxides  $\text{ArN}(\text{O}\cdot)\text{Bu}$  (202) typical  $A$  values are (for  $\text{Ar} = p\text{-MeO}-\text{C}_6\text{H}_4$ )  $A_{\text{N}} = 1.28 \text{ mT}$ ,  $A_{\text{H}}(\text{ortho}) = 0.18 \text{ mT}$ ,  $A_{\text{H}}(\text{meta}) = 0.09 \text{ mT}$ ,  $A_{\text{H}}(\text{OMe}) = 0.019 \text{ mT}$ , and  $A_{\text{H}}(^t\text{Bu}) = -0.0102 \text{ mT}$ . These are explained in terms of the electron-donating substituent favouring the resonance structure



Electron-withdrawing groups have the reverse effect and lead to a reduced  $A_{\text{N}}$  value. The positive sign of the OMe coupling may be explained in terms of the structures [32(a)]–[32(c)] which indicate the



transfer of positive spin from the *para* carbon to the OMe hydrogen by a combination of mesomeric and hyperconjugative interactions. The small negative sign of the  $^t\text{Bu}$  coupling could arise by spin polarization of the bonds linking the nitrogen and the hydrogen atoms by the positive spin on the nitrogen and/or by hyperconjugative interaction of the unpaired electron on nitrogen with the electrons of the  $\text{C}(\alpha)\text{--}\text{C}(\beta)$  bond, the resulting spin on  $\text{C}(\beta)$  being transmitted to the adjacent hydrogen by spin polarization [33(a)]–[33(b)].



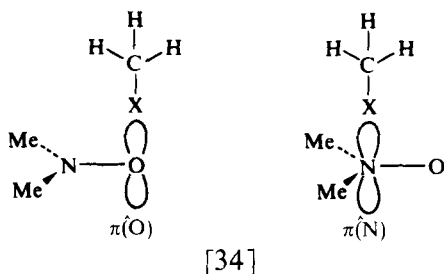
In the  $\pi$ -radical DBNO the  $^1\text{Bu}$  coupling is negative (214) whereas in the  $\sigma$ -radical  $^1\text{Bu}_2\text{C}=\text{NO}\cdot$  it has a positive value of 0.061 mT. (205) The single broad NMR signal contrasts markedly with the ESR spectra which at temperatures around  $-50^\circ\text{C}$  may be interpreted as arising from two groups of nine protons due to the *syn* and *anti* protons. At higher temperatures mutual exchange between the two groups occurs.

Nitroxide and similar radicals are being increasingly used as paramagnetic shift and relaxation probes for studying electronic structures, geometries, and association properties of diamagnetic molecules. Sysoeva *et al.* (215) have developed a method for determining lifetimes and distances between the unpaired electron and the ligand protons in the complexes formed between nitroxyl radicals and methanol, chloroform, cyclohexanol, and ethylene glycol. The method is based on the viscosity and concentration dependences of the linewidths of the complexes. Dipolar and scalar contributions to the linewidths are separated, and both isotropic and anisotropic molecular rotations of the complex assessed. Insight into the electronic structures of the complexes is based on the fact that the concentration dependences of the shifts and linewidths of two ligands in solution depend on whether these ligands form complexes with the same radical orbital or with different radical orbitals. If the latter case holds, complexation of one ligand should not influence the shift and line broadening of another ligand molecule present in solution. In the former case such an influence should exist since both ligands are in competition. Theoretical expressions for the paramagnetic shifts and linewidths for the above two cases are presented and tested experimentally.

The use of dinitrosyl-Fe(I) and -Mn(II) as relaxation probes in the above type of study has been discussed. (216) A correlation is found between the proton hyperfine splittings of  $\text{HR}\cdot$  and the  $J(\text{H}-\text{H})$  values of the parent hydrocarbons  $\text{HRH}$ , which reflects a similarity in the origins of these two parameters. (217)

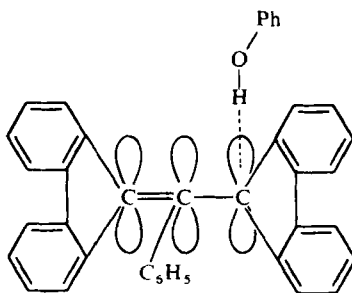
Morishima *et al.* (218–220) have continued their exhaustive study of the interactions of the nitroxide radical with a variety of closed-shell molecules. With proton donor molecules ( $\text{X}-\text{H}$ ) (e.g.  $\text{CHCl}_3$ ,  $\text{CH}_2\text{Cl}_2$ ) the low frequency shifts of the  $\text{X}-\text{H}$  proton and the high frequency  $^{13}\text{C}$  shifts of the X portion are interpreted in terms of spin polarization of electron density from DTBN to  $\text{X}-\text{H}$ . Formation constants, enthalpies, and spin densities on the  $^1\text{H}$  and  $^{13}\text{C}$  atoms for the H-bonded complex  $\text{X}-\text{H}\cdots\text{DTBN}$  have been evaluated. The spin delocalization mechanism involves positive spin density on DTBN being directly transferred on to the  $\text{C}-\text{X}$  antibonding orbital of the halogenomethane

donor molecule. Hartree–Fock MO calculations on the dimethyl nitroxide (DMNO)–halogenomethane system indicate that the high frequency  $^{13}\text{C}$  shifts are explained by a  $\pi(\text{O})$  or  $\pi(\text{N})$  model [34] for the



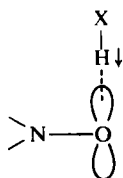
H-bonded complex rather than a  $\sigma$  model. When DTBN is H-bonded to aromatic hydrocarbons (220) substantial high frequency shifts of the aromatic  $=\text{C}-\text{H}$  carbons occur. In substituted benzenes and naphthalene similar high frequency shifts are observed but the carbons with no directly attached hydrogens experience low frequency shifts. These results suggest that the aromatic  $\text{C}-\text{H}$  proton acts as a weak proton donor in the  $\text{C}-\text{H}\cdots\text{DTBN}$  bond. As with the aliphatic complexes, both  $\sigma$  and  $\pi$  models can be suggested for the complexes. The  $\pi$  model satisfactorily accounts for the  $^{13}\text{C}$  shifts.

In order to obtain further insight into this  $\pi$ -bonding interaction the stable  $\pi$ -radical  $\alpha,\gamma$ -bisdiphenylene- $\beta$ -phenylallyl (BDPA) [35] was

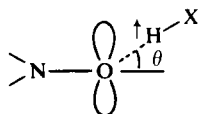


used in place of DTBN. (221) The proton of the donor molecule  $\text{XH}$  experiences a low frequency shift relative to the diamagnetic precursor of BDPA, which is attributed to the contact shift characteristic of

negative spin density on the XH proton thus vindicating the  $\pi$ -model [36] rather than the  $\sigma$ -model [37]. The experimental results are substantiated by INDO calculations on simpler model systems, e.g.  $\text{XH} \cdots \dot{\text{C}}\text{H}_2\text{CH}=\text{CH}_2$ . The dynamic nature of this hydrogen bond was investigated using proton relaxation time studies. (222) Both pulse and CW methods were performed on proton donor molecules (e.g.  $\text{CHCl}_3$ ,  $\text{C}_6\text{H}_5\text{NH}_2$ ,  $\text{CH}_3\text{OH}$ ,  $\text{CH}_3\text{CO}_2\text{H}$ ) bonded with DTBN. It is shown that the relaxation mechanism is determined chiefly by electron–nuclear dipole–dipole interaction with  $\tau_c \lesssim 10^{-10}$  s. However, exchange coupling must also be considered. Assuming  $(T_1^{-1})_{\text{DD}} \approx (T_2^{-1})_{\text{DD}}$ , the lifetime,  $\tau_e$ , of the chemical exchange process associated with the  $\text{Cl}_3\text{CH} \cdots \text{DTBN}$  H-bond is  $3.6 \times 10^{-8}$  s.



[36]



[37]

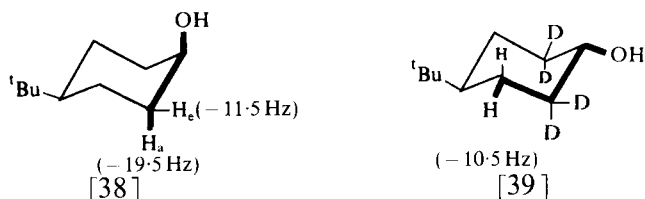
The use of aliphatic and aromatic alcohols, amines, and carboxylic acids as proton donor molecules with DTBN reveals that whereas the X–H protons are shifted to low frequency by the radical the C–H protons, other than X–H, are moved to high frequency (223) (Table X). These high frequency shifts are shown to be characteristic of protic molecules and demonstrate conformational or geometrical dependences. Thus, protons lying on a zig-zag path from the –OH or –NH

TABLE X  
DTBN-induced proton shifts in some proton donor molecules (223)

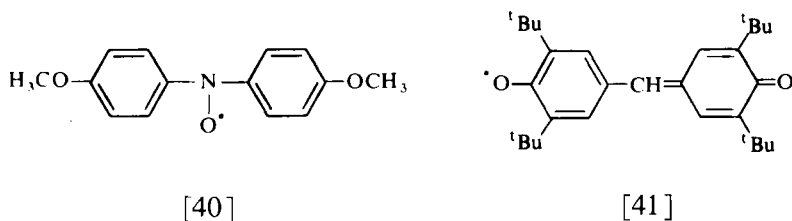
Donor	Proton	Shift <sup>a</sup> (Hz)	Donor	Proton	Shift <sup>a</sup> (Hz)
$\text{CH}_3\text{OH}$	$\text{CH}_3$	+148.8	$\text{CH}_3\text{CH}_2\text{CH}_2\text{NH}_2$	$\text{CH}_2(1)$	+24.0
$\text{CH}_3\text{CH}_2\text{OH}$	$\text{CH}_2$	+103.0	(2) (1)	$\text{CH}_2(2)$	+6.0
	$\text{CH}_3$	+15.8		$\text{CH}_3$	+4.0
$\text{CH}_3\text{CH}_2\text{CH}_2\text{OH}$	$\text{CH}_2(1)$	+121.0		$\text{NH}_2$	–89.5
(2) (1)	$\text{CH}_2(2)$	+23.8	$(\text{CH}_3\text{CH}_2)_2\text{NH}$	$\text{CH}_2$	+12.2
	$\text{CH}_3$	+10.8		$\text{CH}_3$	+1.0
				$\text{NH}$	–88.0

<sup>a</sup> Measured at 220 MHz with  $[\text{DTBN}] = 0.4 \text{ M}$  in  $\text{CCl}_4$  solution. Positive sign denotes high frequency shift.

group exhibit preferential high frequency shifts as illustrated by the cyclohexanol derivatives [38] and [39]. The potential utility of this stereospecific DTBN-induced shift for structural studies in the vicinity of the proton donor group(s) in biologically important molecules such as purine and imidazole derivatives is discussed. These authors have



recently examined a variety of halogenated molecules (halogenomethanes, alkyl halides, and dihalides) with the radicals DTBN, di-*p*-anisyl nitroxide (DANO) [40], and galvinoxyl [41]. (224) The induced high frequency  $^{13}\text{C}$  shifts are in the order  $\text{X} = \text{I} > \text{Br} > \text{Cl} > \text{F}$ . The substituted carbons exhibit anomalous low frequency shifts which are



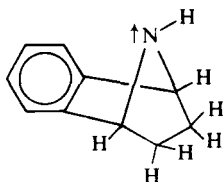
discussed in terms of hydrogen bonding,  $\pi$ -stacking, and charge-transfer interactions. MO calculations show that the charge-transfer interaction involves intermolecular spin delocalization while spin polarization is the essential feature in the hydrogen-bonding interaction. The use of the DTBN radical to study the affinity of hydrogen-bonding in the nucleic acid base pairs adenosine(A)-uracil(U) and guanine(G)-cytosine(C) has recently been reported. (225) The radical induces broadening of the imino N-H proton signal of free uracil derivatives but in the case of  $\text{U} \cdots \text{A}$  or  $\text{G} \cdots \text{C}$  base pairing no broadening is detected even at high DTBN concentrations. This insensitivity to broadening reflects the strength of the  $\text{U} \cdots \text{A}$  association.

Various nitroxide radicals, including 2,2,6,6-tetramethylpiperidine-*N*-oxide, have been used to investigate interactions with water, (226) Lewis acids, (227) and various organic solutes. (228) The contact shifts



induced in the Lewis acids show a non-Curie law behaviour which is ascribed to a temperature dependence of the  $A$  values arising from varying populations of thermally excited vibrational states.

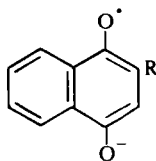
NMR studies have also been reported on a wide variety of other radicals, namely monosubstituted benzyl radicals ( $^{19}\text{F}$  data), (229) 7-norbornenyl-type radicals [42], (230) hydrazyl radicals, (231) cation



[42]

radicals of 4,4'-bipyridylium derivatives, (232) triarylaminium cation radicals ( $p\text{-RC}_6\text{H}_4$ ) $_3\text{N}^{+\cdot}$ , (233, 234) and cation radicals of 9,9-dialkylthioxanthenes. (235) The studies on the ( $p\text{-RC}_6\text{H}_4$ ) $_3\text{N}^{+\cdot}$  radicals used a side-band deconvolution technique (236) which generates a normal absorption spectrum from a side-band spectrum containing up to seven overlapping side-bands. The technique is employed to cope with the combination of broad and narrow lines produced by these paramagnetic samples. The results are in general agreement with available ESR data with the exception of the Cl-substituted radical. For the  $p\text{-MeO}$ -substituted radical the hyperfine coupling constants were  $A(\text{ortho}) = -0.176 \text{ mT}$ ,  $A(\text{meta}) = 0.061 \text{ mT}$ , and  $A(\text{Me}) = 0.065 \text{ mT}$ .

Sanders *et al* (237, 238) have developed a method first introduced by de Boer and Maclean (239) for determining the site of free electron density in organic compounds based on the selective line broadenings observed in the NMR spectra of stable free radicals undergoing fast exchange with their related molecular species. This was first demonstrated by adding increasing amounts of *t*-butylamine to solutions of naphthoquinone derivatives. The quinonoid protons exhibit greater broadening than the aromatic protons, indicating the presence of the naphthosemiquinone radical anion [43] in rapid



[43]

exchange with the large excess of neutral naphthoquinone. The method has been applied to some metalloporphyrin radicals (238) and to chlorophyll-a radical cation. (240) When the radical cations are in fast exchange with their related neutral species, line broadenings ( $\Delta T_2^{-1}$ ) are induced in the latter according to:

$$\Delta T_2^{-1} = \frac{1}{4}([P]/[D])^2 A_H^2 k^{-1} \quad (35)$$

where  $[P]$  and  $[D]$  are the respective concentrations of the radical and neutral species, and  $k$  is the bimolecular rate constant for the electron exchange. Hyperfine coupling constants for all protons (except those of the phytol side-chain) are determined with *ca.* 15 % accuracy. Dipolar broadenings are assumed to be very small and no contact shifts are observed. The rate of electron transfer is estimated to be between  $2 \times 10^8$  and  $2 \times 10^{10} \text{ dm}^3 \text{ mol}^{-1} \text{ s}^{-1}$ , values that indicate a very efficient transfer process.

## B. Stereochemistry and structure

The high sensitivity of the isotropic shifts of paramagnetic species to very slight changes in structure makes the NMR technique particularly useful for studying dynamic, stereochemical, and conformational problems.

### 1. Structural equilibria

Under this heading both structural and conformational equilibria are discussed. Perhaps the most well known case of a diamagnetic-paramagnetic equilibrium is the square-planar-tetrahedral equilibrium exhibited by 4-coordinate Ni(II) complexes to which reference has already been made. Such an equilibrium exists for dihalogenobis(tertiary phosphine)nickel(II) complexes. (241) Complexes of the type  $\text{NiL}_2\text{X}_2$  ( $\text{L} = \text{PR}_3$ ,  $\text{PR}_2\text{Ph}$ , and  $\text{PRPh}_2$ ;  $\text{R} = \text{cyclopropyl}$ ,  $\text{cyclohexyl}$ , or  $\text{Ph}$ ) were prepared and their variable temperature spectra studied. The spectra show linear Curie behaviour for the 'frozen-out' tetrahedral species but at higher temperatures exhibit the usual non-Curie behaviour, which is expressed as:

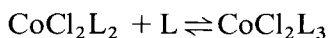
$$\frac{\Delta B_i}{B} = -A_i \frac{\gamma_e}{\gamma_N} \frac{g\mu_B S(S+1)}{6SkT} x_1 + C \quad (36)$$

where  $x_1$  is the mole fraction of the tetrahedral species,  $C$  is a temperature independent term, and the other symbols have their usual meanings. The change in Gibbs function  $\Delta G$  for the planar-tetrahedral

interconversion is calculated from:

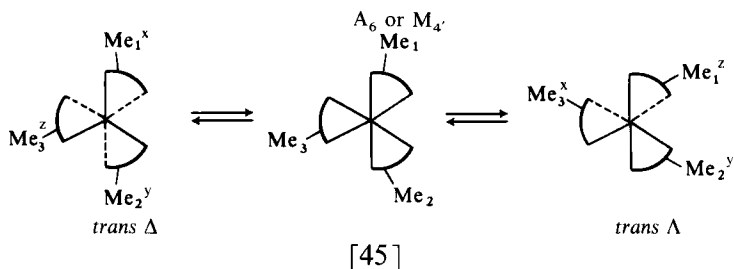
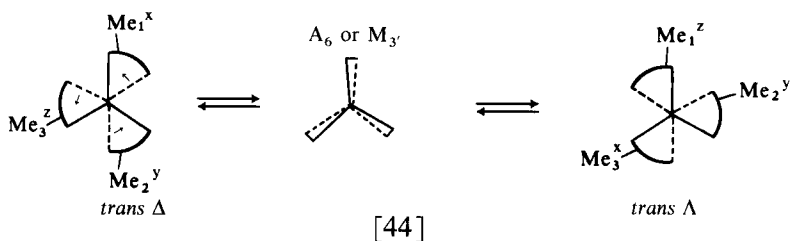
$$\Delta G = -RT \ln [x_i / (1 - x_i)] \quad (37)$$

Calculated  $\Delta G(-50^\circ\text{C})$  values are in the range 38.6 to 43.7 kJ mol<sup>-1</sup> and rate constants in the range  $1.1 \times 10^3$  to  $4.9 \times 10^3$  s<sup>-1</sup>. Similar studies on other Ni(II) complexes are reported (54, 242, 243, 252). Co(II) complexes with ethyl phosphite, phosphonite, and phosphinite ligands (L) may be high spin complexes of the type  $\text{CoCl}_2\text{L}_2$  or low spin, 5-coordinate complexes of the type  $\text{CoCl}_2\text{L}_3$ . In organic solvents the equilibrium:



exists. (253) Equilibrium constants and thermodynamic data are deduced by an adaptation of the Evans shift method. (254)

Tris(dithiocarbamato) complexes of M(III) and M(IV) have been studied (244, 245) in order to reveal the primary rearrangement pathway of these stereochemically non-rigid tris-chelate complexes. Kinetic parameters have been deduced for the intramolecular metal-centred rearrangement by line-broadening techniques. The spectral changes strongly suggest that the rearrangement results in optical inversion, and permutational analysis (246) indicates that two pathways [44] and [45] are possible. Both of these pathways are non-bond-rupture trigonal twists with a trigonal-prismatic transition state.



The degree of non-rigidity of these complexes depends greatly on the nature of the metal. For example, the  $\text{Rh}(\text{R},\text{R}'\text{-dte})_3$  complex is rigid up to  $+200^\circ\text{C}$ , the  $\text{Cr}(\text{R},\text{R}'\text{-dte})_3$  complex up to  $84^\circ\text{C}$ , whereas vanadium(III) and manganese(III) complexes show averaged spectra by  $-20$  and  $-45^\circ\text{C}$  respectively. Typical kinetic parameters are given in Table XI. The overall metal ion dependence on the rate of optical inversion is  $\text{In}, \text{Ga}, \text{V} > \text{Mn} > \text{Fe} > \text{Ru} > \text{Co} > \text{Rh}$ , with Cr at least less than Ru. The values for  $\text{Fe}(\text{III})$  complexes depend also on the position of the spin equilibrium:  $S = \frac{1}{2} \rightleftharpoons S = \frac{5}{2}$  (see below).

TABLE XI  
Kinetic parameters for metal-centred inversion for  $\text{M}(\text{dte})_3$  complexes (245)

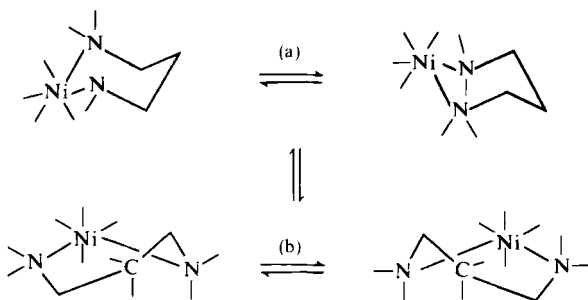
$\text{M}(\text{III})^a$	$\Delta H^\ddagger (\text{kJ mol}^{-1})$	$\Delta S^\ddagger (\text{J K}^{-1} \text{mol}^{-1})$	$\Delta G^\ddagger (\text{kJ mol}^{-1})$
V	$< 34$		$< 32.2$
Mn	$46 \pm 4$	$6.3 \pm 21$	$44.4 \pm 0.8$
Ga	$< 36$		$< 33.9$
In	$< 36$		$< 33.9$
$\text{Cr}^b$	$> 71.5$		$> 67$
Fe	$43 \pm 4$	$17.2 \pm 21$	$38.9 \pm 0.8$
Co	$106.7 \pm 4$	$17.2 \pm 21$	$98.7 \pm 0.8$
Rh	$> 113$		$> 105.9$

<sup>a</sup>  $\text{M}[\text{BzBz}(\text{dte})]_3$  complexes.

<sup>b</sup>  $\text{Cr}[\text{EtEt}(\text{dte})]_3$  complex.

<sup>c</sup> Values refer to widely ranging temperatures. See full paper for details.

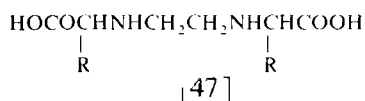
Pseudo-octahedral complexes of  $\text{Ni}(\text{II})$  with 1,3-diamine chelates have been shown (247) to undergo a rapid conformational inter-conversion [46]. In the diagram, (a) refers to the chair-chair equilibrium and (b) to the twist-twist equilibrium. The results indicate that



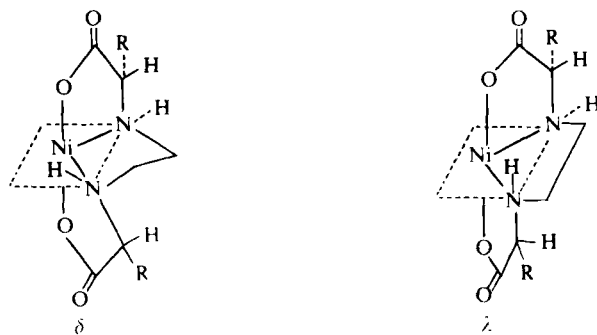
[46]

the chair conformation is the most stable but that the presence of alkyl groups in axial positions of the chair conformers can introduce significant amounts of twist conformer in the equilibrium distribution. Reilley *et al.* (248, 249) have also examined octahedral complexes of Ni(II) with bidentate donors (e.g. ethylene glycol, ethanolamine, etc.) and tridentate donors (e.g. iminodiethanol, diethylenetriamine, 2,2'-diamino-diethyl ether). In the case of the bidentate donor complexes the complex formation constant rapidly decreases with increasing alkyl substitution on a coordinating oxygen atom. Oxygen inversion is fast in the ethanolamine complex  $\text{Ni}(\text{ea})(\text{H}_2\text{O})_4^{2+}$  and takes place via an intermolecular proton exchange reaction involving H-bonded water molecules. The diethylenetriamine complex  $\text{Ni}(\text{dien})(\text{H}_2\text{O})_3^{2+}$  exists as a mixture of *fac* and *mer* forms with interconversion fast on the NMR time scale.  $\delta \rightleftharpoons \lambda$  conversion (250) is rapid for *fac* coordination but slow for *mer* coordination since the latter requires inversion of the central coordinating atom of the ligand.

The conformations of Ni(II) complexes with ethylenediamine-*N,N'*-diacetic acid type quadridentate ligands [47] have been examined by



NMR and CD methods. (251) From the spectral data it is concluded that these complexes stereospecifically adopt the  $\Delta$ -*s-cis* form(s) in solution [48]. The solution structures of a variety of EDTA-type complexes have been deduced from variable temperature studies. (306) Racemization of  $\text{Ni}(\text{EDTA})^{2-}$  and  $\text{Ni}(\text{1,3-DDTA})^{2-}$  is rapid at 80°C but is slow for the other complexes studied. The kinetic data indicate predominant 5-coordination by EDTA and 1,3-PDTA. The suggested racemization mechanism (Fig. 5) involves a 7-coordinate intermediate.



[48]

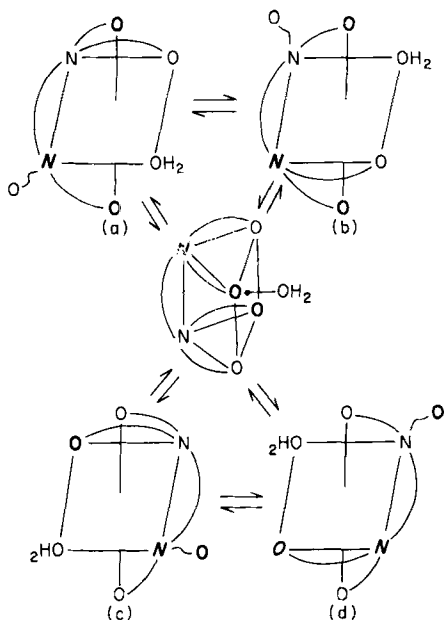
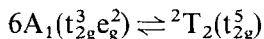


FIG. 5. Suggested solution structure and racemization mechanism of the Ni-EDTA complex in aqueous solution. (306)

## 2. Electronic equilibria

Numerous complexes are known to possess electronic structures that are thermal averages over states with different spin multiplicities. The study of such equilibria is commonly based on magnetic susceptibility measurements. However, the NMR isotropic shift method is of comparable importance and has already provided considerable insight into the spin equilibria of Fe(II) and Fe(III) systems. The latter system has been further studied recently by way of Fe(III) dithiocarbamate complexes. (68, 255) The spin equilibrium is of the form:



A series of complexes that possessed a wide range of magnetic moments ( $\mu_{\text{eff}} = 2.41\text{--}5.83$  B.M.) were chosen. Since the low-spin state ( ${}^2T_2$ ) is favoured there is an increase in metal-ligand  $\pi$ -bonding. Whereas the NMR technique is very useful for studying spin equilibria it has been shown (255) that a combination of electronic spectral and magnetic data can yield reliable values of ligand field parameters for this high-spin ( $S = \frac{5}{2}$ )-low-spin ( $S = \frac{1}{2}$ )  $d^5$  system. Mention has already been

made of such a spin equilibrium in the case of dimethylmanganocene. (191) Manganocene itself possesses a normal high-spin ground state, so it must be concluded that the electron-releasing  $\text{CH}_3$  groups must significantly increase the donor character of the ligands and cause spin pairing. A similar spin equilibrium has been reported for the  $\text{Mn(II)}$  complex of fluorescein (L),  $\text{Mn}_2\text{L}_2(\text{OH})_4(\text{H}_2\text{O})_3 \cdot$  (256)

### C. Ion pairing and second sphere solvation of metal complexes

The presence of paramagnetic anions in dilute solutions of diamagnetic cations manifests itself in the NMR spectra of the latter as resonance shifts and/or line broadenings. Such effects have been attributed to ion pair formation. Isotropic shifts due to ion pair formation are often, but not invariably (see below), predominantly dipolar in origin. Walker *et al* (257, 258) have measured such shifts for some penta- and hexa-nitratolanthanate(III) complexes of formulae  $[\text{R}_4\text{N}]_2\text{Ln}(\text{NO}_3)_5$ ,  $[\text{R}'\text{-py-R}]_2\text{Ln}(\text{NO}_3)_5$ , and  $[\text{R}_4\text{N}]_2\text{Ln}(\text{NO}_3)_6$ . The shifts are to high frequency for all complexes except Tm and Yb complexes which show strong low frequency shifts.

To account for these shifts the ion pair structure model shown in Fig. 6 is suggested. Two variants of this model are considered, a static model in which the cation nitrogen is at a fixed distance  $A$  from the central

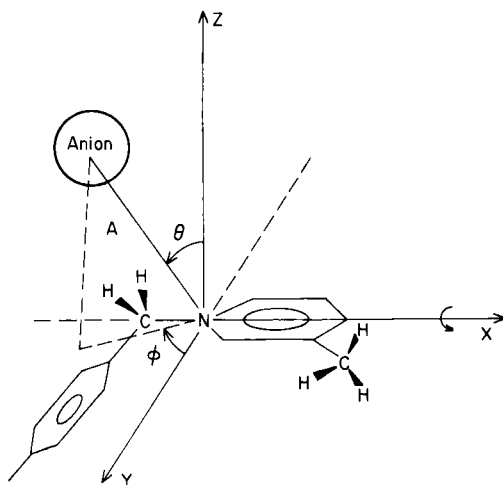


FIG. 6. Cation-based coordinate system showing relative orientation of counterions in the ion-paired complex. The principal susceptibility axis of the anion is assumed to lie along the vector  $\text{Ln}-\text{N}$ . (258)

lanthanide cation, and a rotating model which permits the cation to rotate about the  $x$ -axis of the coordinate system. In this case angle  $\theta$  is set at  $90^\circ$  and both distance  $A$  and angle  $\phi$  are varied until the calculated and observed shift ratios are in agreement. Furthermore a distribution function may also be introduced to give greater weighting to certain preferred orientations of the cation with respect to the anion. Some selected results for Er, Tb, Tm, and Yb complexes are in Table XII. The shifts indicate that the pyridine ring is in rapid rotation with respect to the anion and the lanthanide ion is sited at approximately  $90^\circ$  to the  $C_2$  axis of the pyridine ring. An interionic distance of 70 pm is thus obtained which suggests that the NMR technique is detecting predominantly contact ion pairs with no intervening layer of solvent molecules. This work has more recently (259) been extended to  $N$ -alkyl-lutidinium cations. In this case the NMR data indicate that 3,5-methyl substitution on the pyridine ring restricts the motion of the pyridine ring in contrast to the 4-substituted rings although the interionic distance is unaffected.

TABLE XII  
Best fit structural parameters for  $[\text{oct-py-Ph}]_2\text{Ln}(\text{NO}_3)_5$  complexes<sup>a</sup> (258)

Anion	Concn. (M)	$\phi$ (deg.)	Arithmetic $R$ -factor (%)
$\text{Tb}(\text{NO}_3)_5^{2-}$	0.052	$-8.5$	9.6
$\text{Er}(\text{NO}_3)_5^{2-}$	0.050	$1.5$	7.1
$\text{Er}(\text{NO}_3)_5^{2-}$	0.010	$3.5$	3.7
$\text{Tm}(\text{NO}_3)_5^{2-}$	0.050	$-7.5$	9.5
$\text{Yb}(\text{NO}_3)_5^{2-}$	0.050	$-5.0$	8.6

<sup>a</sup> Distance  $A = 700$  pm and angle  $\theta = 90^\circ$  in all cases.

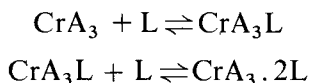
All the above studies have assumed a predominantly axial dipolar origin to the shifts. This assumption, while probably valid for the above lanthanide complexes, is not valid in the case of ion pairs involving the anions  $\text{CoX}_4^{2-}$  and  $\text{NiX}_4^{2-}$  ( $X = \text{halide}$ ). (260) Such anions induce very different shift patterns on substituted ammonium and phosphonium cations. The data suggest that the proton isotropic shifts in the  $\text{CoX}_4^{2-}$  complexes contain a sizeable axial dipolar term in contrast to an earlier conclusion of a dominant contact term. (261) This most likely arises from the influence of the cations in producing a low symmetry ligand field. Ion pairs involving tribromo(triphenylphosphine)cobalt(II) with tetraalkylammonium cations have been investigated. (262, 263) The complex  $[\text{NMeBu}_3][\text{CoBr}_3(\text{PPh}_3)]$  in non-aqueous solutions exhibits a signal due to the  $N$ -methyl protons which is broader and more greatly



shifted than the *N*-methylene signal. Furthermore, the shift difference between these signals increases with decreasing dielectric constant of the solvent. This is explained in terms of a reduction in interionic distance with decreasing dielectric constant and a preferred orientation of the asymmetrical quaternary ammonium ion with respect to the magnetic axis of the anion. This conclusion has been confirmed by studying the complex  $[\text{NMe}(\text{C}_8\text{H}_{17})_3][\text{CoBr}(\text{PPh}_3)]$ . (263) The linear correlation of shift difference with solvent dielectric constant is found to be only valid for solvents of low dielectric constant ( $\epsilon \leq 10$ ). From a study of chemical shifts, relaxation times, and ESR counterion signals, it is possible to distinguish between site-bound, atmospherically bound, and free counterions in polyelectrolyte trimethylammonium salt solutions containing varying concentrations of divalent counterions. (281)

The study of the structure of the weak second coordination sphere around a metal complex in solution using NMR methods is now well established. (264) Second sphere effects are due primarily (but not solely) to dipolar interactions with unpaired electrons. Such interactions lead to an enhanced relaxation rate in the second sphere (usually measured by  $T_{2M}^{-1}$ ) and, in many cases, dipolar shifts [equation (13)].

Transition metal tris(acetylacetonato) complexes have been chosen by numerous workers (265–270, 282) for investigating second sphere phenomena.  $\text{Cr}(\text{acac})_3$  with solvents (L) such as  $\text{CHCl}_3$ ,  $\text{CH}_2\text{Cl}_2$ , and  $\text{C}_6\text{H}_6$  is involved in the equilibria: (266)

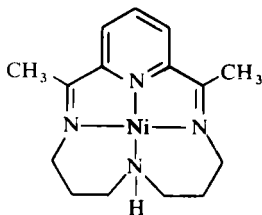
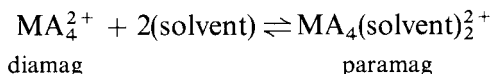


Measurements of  $T_1$  have been made (269, 270) to probe the structure of the second coordination sphere around  $\text{Cr}(\text{acac})_3$ . Acetone, chloroform, and methylene chloride were chosen as second sphere ligands. The shortening of their  $T_1$  values is found to be independent of solute concentration, and the value measured is determined by the diffusional correlation time of the solute molecule. No detectable second coordination sphere therefore exists in these solvents. However, methanol forms a discrete second sphere, and above a certain concentration the measured  $T_1$  values vary linearly with solute concentration. The observed  $T_1$  values are compatible with a model having a coordination number of 8, a  $\text{Cr}-\text{CH}_3$  separation of 700 pm, and an equilibrium constant for displacing solvent ( $\text{CHCl}_3$ ) of *ca.* 10. This equilibrium constant value is consistent with values previously

reported for the Co(II) pyrazylborate system. (271) The enthalpy of activation,  $\Delta H^\ddagger$ , for the formation of the second coordination sphere around Cr(acac)<sub>3</sub> is 14.3 kJ mol<sup>-1</sup> for DMSO as solvent.

A variety of organic solvents (including acetone, methanol, ethanol, methylene dichloride, ether, benzene) have been added to solutions of various salts of Co(II) and Ni(II) and the structures of the resulting outer sphere complexes studied by <sup>1</sup>H, <sup>13</sup>C, <sup>14</sup>N, and <sup>35</sup>Cl NMR methods. (272–275) From the variations of shifts with solute concentrations the structures of the second coordination spheres are postulated. In the case of Co(ClO<sub>4</sub>)<sub>2</sub> in the presence of aqueous acetone, mono-, bis-, and tris-acetone complexes are suggested. (272) In contrast Co(NO<sub>3</sub>)<sub>2</sub> solutions behave quite differently. Knowledge of the temperature dependences of the shifts has enabled the hyperfine interaction constants to be calculated in some cases.

Solvent NMR studies of some Co(II), Ni(II), and Cu(II) complexes with the Schiff base [49] have been performed. (276, 277) The complex is involved in the equilibrium:



[49]

Kinetic studies were performed with allowance being made for both first- and second-sphere dipolar relaxation mechanisms such that:

$$(T_{2p}P_M)^{-1} = T_{2M}^{-1} + T_{2O}^{-1} \quad (38)$$

where  $T_{2M}$  refers to the first (or inner) coordination sphere and  $T_{2O}$  to the second (or outer) coordination sphere. The linewidth and shift variations with solute concentration and temperature can only be rationalized in terms of a sum of both inner sphere and outer sphere dipolar relaxation mechanisms.

The existence of a second solvation sphere around iron(III) perchlorate has been deduced from proton relaxation times ( $T_{1M}$  and  $T_{2M}$ ) of dimethyl sulphoxide molecules. (278) The results imply that

electronic relaxation is the predominant mechanism at low temperatures, such a mechanism being controlled by the modulation of the quadratic zero-field splitting. The average distance between the protons of DMSO and  $\text{Fe}^{3+}$  is computed to be 452 pm at 125°C.

Manganese(II) forms both inner- and outer-sphere complexes in hydrochloric acid solutions. (279) For 1.5 M HCl, the species  $\text{Mn}(\text{H}_2\text{O})_6^{2+}$  and  $\text{Mn}(\text{H}_2\text{O})_6^{2+}\text{Cl}^-$  are present in solution in relative amounts 3:2. An outer sphere complex has been suggested by the spectral data for the binding of  $\text{Mn}^{2+}$  with the polymeric humic acid, fulvic acid. (280) This is in contrast to the corresponding  $\text{Fe}^{3+}$  complex which is of the inner sphere type.

#### D. Formation and exchange reactions of metal complexes

This section is concerned with the complexation of ligands in the first coordination sphere of the metal ion. By observing the isotropic shifts and line broadenings induced in ligand molecules by the presence of paramagnetic metal ions it is possible to examine the structure, stability, and exchange kinetics of the metal complex(es) formed in solution. When the rate of exchange between free and complexed ligand molecules is slow on the NMR time scale, separate signals for the two types of ligand molecules are detected. Measurement of their relative intensities gives the coordination numbers and provides insight into competitive solvation phenomena.

It is, however, more usual for rapid exchange to occur between the free and coordinated ligand molecules giving rise to a single averaged signal such that:

$$\Delta\nu = P_M \Delta\nu_M \quad (39)$$

where  $\Delta\nu$  is the observed isotropic shift measured relative to the pure free ligand and  $P_M$  is the fraction of ligand molecules coordinated to the metal ion. Swift and Connick (283, 284) have shown that a careful analysis of the linewidths of the exchange averaged signals can give valuable information on the kinetics of the ligand exchanges.

The various limiting equations on which the analysis is based are given in the previous review. (2) The majority of the reported kinetic data are based on the appropriate form of the Swift-Connick theory. A development of NMR exchange theory by Granot and Fiat (287) has examined the condition under which the absorption signal of nuclei undergoing chemical exchange between diamagnetic and paramagnetic sites is exactly Lorentzian in shape. They have shown that the usual requirement that the solution should be very dilute in the

paramagnetic species, i.e.  $P_M \ll 1$ , is insufficient and that when chemical exchange is occurring the requirements are that:

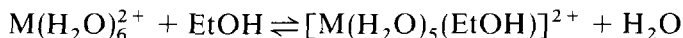
$$P_M \ll T_2/T_{2P} = T_{2A}/(T_{2A} + T_{2P}) \quad (40)$$

This implies that the larger the contribution to the relaxation rate, the more dilute the solution needs to be.

Metal ion hydration studies continue to attract particular attention. Bound and unbound  $H_2O$  and  $D_2O$  molecules in aqueous nickel(II) perchlorate exhibit two clearly distinguishable although overlapping signals at low temperatures. (288) Curve fitting analysis yields hyperfine coupling constants of  $(1.3 \pm 0.1) \times 10^5$  and  $(2.0 \pm 0.2) \times 10^4$  Hz respectively. The rate constant for exchange at 298 K is  $3 \times 10^4 \text{ s}^{-1}$  and the activation energy is  $50.4 \text{ kJ mol}^{-1}$ . Similar studies were performed on chromium(III) perchlorate. (289) Koenig and Epstein (290) have investigated the problem of evaluating an accurate value for  $\tau_M$ , the lifetime of a proton in the first hydration sphere of a paramagnetic ion, from relaxation data. For ions where the scalar (contact) term is negligible, the commonly made assumption that  $\tau_M \ll T_{1M}$  is reported to be questionable. In an attempt to resolve this problem these authors measured proton  $T_1$  values in aqueous solutions of  $Gd^{3+}$  ions. The data are obtained for different solution pH and as a function of applied magnetic field, and are found to fit the theory for both the case when  $\tau_M \approx T_{1M}$  and also when  $\tau_M \ll T_{1M}$ ; thus a value of  $\tau_M$  from an independent experiment is required to resolve the ambiguity.

Reuben (291) has latterly suggested that the way round this problem is to investigate both proton and deuteron relaxation rates. In the Solomon expression for  $T_1$  [equation (17)] the deuterons are less susceptible than protons to the dipolar relaxation by a factor  $(\gamma_H/\gamma_D)^2$  which equals 42.4. Thus if  $\tau_M \gg T_{1M}$  the ratio of the induced relaxation of protons to that of deuterons is unity, but this ratio increases with increasing  $T_{1M}/\tau_M$  values until it reaches a value of 42.4 for the case when  $\tau_M \ll T_{1M}^H$ . When applied to the  $Gd^{3+}$  system it is found that  $\tau_M \leq 0.03 T_{1M} = 3.3 \times 10^{-7} \text{ s}$ .

Miscellaneous kinetic data for water exchange reactions are given in Table XIII. Equilibrium constants for deaquation of  $M(H_2O)_6^{2+}$  [ $M = Co(II), Ni(II)$ ] have been obtained for complexes involving nitrate ions (294) and ethyl alcohol molecules. (295) For the equilibrium:



when  $M = Co(II)$  and  $Ni(II)$ ,  $K$  is calculated to be  $\sim 6$  and  $1.4$  respectively.

Kinetic parameters for alcohol exchange have been deduced from  $^1\text{H}$  and  $^{13}\text{C}$  studies on  $\text{Co(II)}$ , (296)  $\text{Ni(II)}$ , (297) and  $\text{Mn(II)}$  (298) systems. The complex  $[\text{Co}(\text{CH}_3\text{OH})_5\text{py}]^{2+}$  (296) provides a clear example of the operation of the *trans* effect in a labile octahedral complex, in that the exchange rate constants for *cis* and *trans* methanol sites with respect to pyridine are  $410\text{ s}^{-1}$  and  $1200\text{ s}^{-1}$  respectively.

Ethylenediamine (en), diethylenetriamine (dien), triethylenetetramine (trien), and tetraethylenepentamine (tetren) form well characterized complexes with  $\text{M(II)}$  ions. Such complexes have been the subjects of a number of NMR exchange studies. (299–303)  $^1\text{H}$  studies have established the identities of  $[\text{Cu}(\text{en})(\text{H}_2\text{O})_4]^{2+}$ ,  $[\text{Cu}(\text{en})_2(\text{H}_2\text{O})_2]^{2+}$ , and complexes involving both en and sulphosalicylic acid ligands. (299–301)  $^{17}\text{O}$  NMR studies have been made on aqueous solutions of  $[\text{Ni}(\text{dien})(\text{H}_2\text{O})_3]^{2+}$ ,  $[\text{Ni}(\text{tren})(\text{H}_2\text{O})_2]^{2+}$ , and  $[\text{Ni}(\text{tetren})(\text{H}_2\text{O})]^{2+}$ . The Ni–dien system shows at least two water exchange rates which are not well resolved whereas the other systems show only a single rate process (Table XIII).

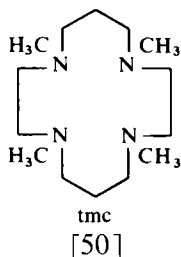
Solvation parameters for dimethyl sulphoxide have been measured for  $\text{Cu(II)}$  and  $\text{Ni(II)}$  en complexes (303) and solutions of  $\text{Co(II)}$  and  $\text{Ni(II)}$

TABLE XIII  
Kinetic data<sup>a</sup> for water exchange with transition metal complexes

Complex	$k\text{ (s}^{-1}\text{)}$	$\Delta H^\ddagger\text{ (kJ mol}^{-1}\text{)}$	$\Delta S^\ddagger\text{ (J K}^{-1}\text{ mol}^{-1}\text{)}$	Ref.
$[\text{Ni}(\text{H}_2\text{O})_6]^{2+}$	$3 \times 10^4$			289
$[\text{Ni}(\text{dien})(\text{H}_2\text{O})_3]^{2+}$	$3 \times 10^6$	38	8	302
	$4 \times 10^5$	46	12.5	302
$[\text{Ni}(\text{trien})(\text{H}_2\text{O})_2]^{2+}$	$(5.7 \pm 1.6) \times 10^5$	$34.3 \pm 3.8$	$-19.2 \pm 15$	302
$[\text{Ni}(\text{tetren})(\text{H}_2\text{O})]^{2+}$	$(1.12 \pm 0.22) \times 10^7$	$36.0 \pm 2.9$	$10.5 \pm 10.5$	302
$[\text{Co}(\text{tmc})\text{H}_2\text{O}]^{2+ b}$	$4.2 \times 10^4$	$36.5 \pm 1.4$	$-34 \pm 4$	292
$[\text{Mn}(\text{PhDTA})\text{H}_2\text{O}]^{2-}$	$3.5 \times 10^8$	33.9	31.8	293

<sup>a</sup> Data at 298 K.

<sup>b</sup> tmc = 1,4,8,11-tetramethyl-1,4,8,11-tetraazacyclotetradecane [50].



perchlorates. (304, 305) At low temperatures axially coordinated DMSO molecules of  $[\text{Cu}(\text{DMSO})_6]^{2+}$  exchange with a rate constant of  $4.7 \times 10^3 \text{ s}^{-1}$ . In contrast, in  $\text{Cu}(\text{en})_2^{2+}$  the DMSO exchange is too fast to be measured. The average rates of exchange for DMSO in the  $\text{Ni}(\text{II})$  system follow the order  $\text{Ni}^{2+} < \text{Ni}(\text{en})^{2+} < \text{Ni}(\text{en})_2^{2+}$ , implying an amine *trans* effect. For  $[\text{Ni}(\text{DMSO})_6]^{2+}$  the authors have calculated a rate constant at 298 K for DMSO exchange of  $69 \times 10^3 \text{ s}^{-1}$ . The difference is probably due to the influence of the different anions in the two cases.

Complexes with EDTA-type ligands have been extensively studied recently, particularly by Russian workers. (307–317) Exchange of  $\text{EDTA}^{4-}$  with  $\text{Cu}(\text{EDTA})^{2-}$  was studied (307) by the line broadening technique and yields an activation energy for the ligand exchange reaction of  $45.1 \text{ kJ mol}^{-1}$  and a rate constant at  $25^\circ\text{C}$  of  $45 \text{ M}^{-1} \text{ s}^{-1}$ . This value for the unprotonated EDTA is surprisingly very similar to the value for monoprotonated EDTA.

The papers cited above include studies of  $\text{La}^{3+}$  and  $\text{Lu}^{3+}$  EDTA-type complexes, (308, 309, 311, 312)  $\text{Cu}^{2+}$  complexes, (314, 315)  $\text{Fe}^{3+}$  complexes, (310) and  $\text{Sm}^{3+}$  complexes. (316, 317) Kinetic parameters and stability constants have been calculated in many cases. In one study (315) the variation in the relaxation time of  $[\text{Cu}(\text{EDTA})(\text{H}_2\text{O})]^{2-}$  was followed on gradual addition of ammonia at pH 9. Values were found to shorten and then remain constant after addition of a ten-fold excess of ammonia. This is due to the formation of  $[\text{Cu}(\text{EDTA})(\text{NH}_3)_2]^{2-}$  with a formation constant of 18.8.

$^{14}\text{N}$  NMR has been particularly useful in the measurement of kinetic parameters for acetonitrile exchange. (318–323) Some data are listed in Table XIV. From the  $^{14}\text{N}$  contact shifts the  $^{14}\text{N}$  hyperfine coupling constants are found to vary appreciably in magnitude and sign depending on whether the spin density resides in  $\sigma$  and/or  $\pi$  orbitals. (318) The data quoted here for  $[\text{Ni}(\text{CH}_3\text{CN})_6]^{2+}$ , however, differ substantially from those of Lincoln and West (319) who have examined a variety of  $\text{CH}_3\text{CN}$  complexes with multidentate ligands. The acetonitrile lability is found to depend greatly on the nature of ligand.  $\text{NH}_2$ -coordinating groups in the latter considerably labilize acetonitrile whereas OH groups reduce the lability. The data suggest that the exchange processes of the  $\text{Ni}(\text{II})$  complexes are predominantly dissociative in nature but in the other cases it is not as clear-cut. The rapid exchange of  $[\text{Cu}(\text{CH}_3\text{CN})_6]^{2+}$  (323) is explained in terms of a dynamic Jahn–Teller effect.

There have been several reports of ligand exchange studies involving oxovanadium(IV) complexes. (324–327).  $^{31}\text{P}$  NMR was used to study

TABLE XIV  
Kinetic data for acetonitrile exchange with transition metal complexes

Complex	$k$ (s <sup>-1</sup> )	$\Delta H^\ddagger$ (kJ mol <sup>-1</sup> )	$\Delta S^\ddagger$ (J K <sup>-1</sup> mol <sup>-1</sup> )	Ref.
[Ni(CH <sub>3</sub> CN) <sub>6</sub> ] <sup>2+</sup>	1.45 × 10 <sup>4</sup>	39.5	-32.6	318
	(2.0 ± 0.3) × 10 <sup>3</sup>	68.6 ± 2	50.2	319
[Ni(triol)(CH <sub>3</sub> CN) <sub>3</sub> ] <sup>2+</sup>	(1.0 ± 0.2) × 10 <sup>3</sup>	66.5 ± 3	36.4 ± 10.5	321
[Ni(triam)(CH <sub>3</sub> CN) <sub>3</sub> ] <sup>2+</sup>	(555 ± 60) × 10 <sup>3</sup>	38.9 ± 4	-3.8 ± 14.6	321
[Co(CH <sub>3</sub> CN) <sub>6</sub> ] <sup>2+</sup>	2.7 × 10 <sup>5</sup>	36.8	-17.6	318
[Co(triol)(CH <sub>3</sub> CN) <sub>3</sub> ] <sup>2+</sup>	(23 ± 2) × 10 <sup>4</sup>	40 ± 2	-9.6 ± 6.2	322
[Co(tren)(CH <sub>3</sub> CN) <sub>3</sub> ] <sup>2+</sup>	≥ 2 × 10 <sup>6</sup>	—	—	319
[Cu(CH <sub>3</sub> CN) <sub>6</sub> ] <sup>2+</sup>	≥ 1.6 × 10 <sup>7</sup>	—	—	323
[Cu(tren)(CH <sub>3</sub> CN) <sub>3</sub> ] <sup>2+</sup>	(1.7 ± 0.2) × 10 <sup>6</sup>	45 ± 4	26 ± 16	323
	(5.1 ± 0.7) × 10 <sup>3</sup>			

triol = 2-hydroxymethyl-2-methylpropane-1,3-diol

triam = 2,2-di(aminomethyl)-1-propylamine

tren = 2,2',2''-triaminotriethylamine

the rate of loss of phosphate from VO(H<sub>2</sub>PO<sub>4</sub>)<sub>2</sub> (326) and <sup>1</sup>H, <sup>2</sup>D, and <sup>17</sup>O NMR techniques were used to study deuterium exchange between VO(OD)<sub>3</sub>(D<sub>2</sub>O)<sub>2</sub><sup>-</sup> and solvent water. The rate constant is 8.4 × 10<sup>6</sup> s<sup>-1</sup> with  $\Delta H^\ddagger = 40 \pm 2$  kJ mol<sup>-1</sup> and  $\Delta S^\ddagger = 22 \pm 7$  J K<sup>-1</sup> mol<sup>-1</sup>. A mechanism involving deuterium transfer from an equatorial aquo ligand to hydroxide ion is suggested. Oxygen exchange between VO(OH)<sub>3</sub>(H<sub>2</sub>O)<sub>2</sub><sup>-</sup> and solvent water is slow on the <sup>17</sup>O NMR time scale.

The rate of electron transfer between the tris(dithiocarbamate) complexes Fe(Me<sub>2</sub>dtc)<sub>3</sub> and [Fe(Me<sub>2</sub>dtc)<sub>3</sub>]BF<sub>4</sub> has been measured by the line-broadening technique to be (1.5 ± 0.4) × 10<sup>8</sup> dm<sup>3</sup> mol<sup>-1</sup> s<sup>-1</sup> at -57°C. (328) A similar electron transfer study involving tris-phenanthroline-iron(II) and -iron(III) complexes has been performed. (329) The exchange kinetics of Ni(di-R,R'-dtc)<sub>2</sub> with various nitrogen bases yield rate constants at 5°C of 12.5 × 10<sup>4</sup> s<sup>-1</sup> and 6.2 × 10<sup>4</sup> s<sup>-1</sup> for 3-picoline and 4-picoline respectively. (330)

Other exchange studies involve bis-(2,4-pentanedionato) complexes of Co(II) and Ni(II), (331) α-dioximates of Ni(II), (332) thiosemicarbazide-type complexes, (333) aquomethyl-*N,N'*-ethylene-bis-(salicylideneiminato)cobalt with metal cations, (334) nickel(II) acetate complexes, (133) and chromium(II) formate complexes. (335)

The exchange kinetics of monoacetatonicel(II) with bulk acetate were followed by variable temperature <sup>13</sup>C studies of [1-<sup>13</sup>C]acetate

species. The acetate (Ac) dissociation rate from  $\text{NiAc}^+$  is  $(3.9 \pm 0.3) \times 10^3 \text{ s}^{-1}$ , and the rate of formation of  $\text{NiAc}_2$  is  $(2.1 \pm 0.4) \times 10^4 \text{ M}^{-1} \text{ s}^{-1}$ , both measured at 300 K. The results are consistent with acetate exchange controlled by loss of acetate and water respectively from  $\text{Ni}(\text{H}_2\text{O})_5\text{Ac}^+$ . In the latter case loss of water is followed by acetate entry and subsequent rapid dissociation of the diacetato species. (133) Equilibrium studies of  $\text{Cr(II)}$  with formate ions in aqueous solution indicate the formation of a binuclear complex, analogous to the quadruply metal-metal bonded dichromium tetraacetate:



The equilibrium constant is  $2.1 \pm 0.2 \text{ M}^{-2}$  but at the highest formate ion concentrations the binuclear complex dissociates to mononuclear high-spin complexes. (335)

Copper(II) complexes have been the subject of numerous NMR exchange and relaxation studies.  $\text{Cu}^{2+}$  ions have been extensively used to locate binding sites in ligands by the differential line broadenings produced in the ligand spectra. Dillon and Rossotti (336) have used this method to study  $\text{Cu(II)}$  binding in 35 carboxylate ligands. They found that 2- and 3-hydroxy- and 2-alkoxy-carboxylates are predominantly bidentate towards  $\text{Cu(II)}$  whereas 4-hydroxy- and 3-alkoxy-carboxylates are predominantly unidentate. Dipolar and scalar contributions to the proton relaxation rates in the bis(acetato) complex are calculated to be 25 % and 75 % respectively. This result supports the observation made by Espersen *et al.* (337) that induced broadenings of ligand absorptions by  $\text{Cu(II)}$  are generally far from being determined by dipolar interactions, and therefore any conclusions concerning the site of  $\text{Cu(II)}$  attachment, based on an assumed  $r^{-6}$  dependence [equations (17) and (18)], need to be reconsidered. For ligands undergoing fast or intermediate exchange the only reliable way to invoke the  $r^{-6}$  dependence, in order to establish binding sites, is to measure  $T_{1\rho}$  rather than  $T_{2\rho}$ .

Reports of other  $\text{Cu(II)}$  complexes include complexes with citrulline, (338) glutathione, (339) amino-acids, (340) amines such as ammonia, asparagine, and serine, (341) and dibutyl sulphide. (342)

## E. Miscellaneous

This section includes three topics not easily classified elsewhere, namely the use of relaxation reagents, the measurement of magnetic moments in solution, and the use of paramagnetic ions for studying surface phenomena.



Chromium(III) and other paramagnetic ions have been frequently used to enhance the spin-lattice relaxation pathways of  $^{13}\text{C}$  nuclei. Levy *et al.* (343–345) have assessed the efficiency of  $\text{Cr}(\text{acac})_3$  to enhance the relaxation rates of different solute nuclei using the specific electron-nuclear relaxation rate parameter,  $R_1^e = (T_1^e)^{-1}$ . The value of  $R_1^e$  increases significantly when intermolecular interactions or other weak interactions, which result in ordering of the chromium complex-substrate, are present. For medium or large organic substrates the  $^{13}\text{C}$ -H nuclear Overhauser effect suppression becomes incomplete and variable when efficient  $^{13}\text{C}$ -H dipole-dipole relaxation competes successfully with electron-nuclear relaxation to  $\text{Cr}(\text{acac})_3$ . In such cases  $\text{Cr}(\text{acac})_3$  can actually degrade the quality of the spectra by producing extensive line-broadenings.

The complex  $\text{Cr}(\text{dpm})_3$  is in many cases preferable to  $\text{Cr}(\text{acac})_3$  as a leveller of  $T_1$  values since it is more inert to physical interactions with organic substrate molecules. (345) It has been shown that  $\text{Gd}(\text{dpm})_3$  is also a useful relaxation reagent. When added to 4-picoline, the relaxation due to  $\text{Gd}(\text{dpm})_3$  shows a close correlation with  $r^{-6}$ ,  $r$  being the distance from the metal to the  $^{13}\text{C}$  nucleus being relaxed. (515)

In contrast to  $\text{Cr}(\text{acac})_3$ ,  $\text{Cu}(\text{acac})_3$  is an efficient differential line-broadening agent. Electron relaxation is relatively long, and the broadening operates through the electron-nuclear hyperfine interaction, i.e.  $(T_{1e})^{-1} \ll (\gamma_e/2\pi)A_i$ . Such broadenings are found to be strongly dependent on the relative geometrical arrangement of the interacting centres in the case of complexes with aliphatic amines. (346) Relaxation reagents have provided conformational information on thioproline and related molecules. (516)

The measurement of paramagnetic susceptibilities in solution by the NMR method of Evans (347) has been very extensively employed for many years. More recently the same author (348) has developed the method for magnetic titrations. Such titrations of a metal complex are expressed by the equation:

$$\Delta\chi_A = [3(\Delta v_1 - \Delta v_0)M]/2\pi\nu m_1 \quad (41)$$

where  $\Delta\chi_A$  represents the change in magnetic susceptibility of the dissolved substances,  $(\Delta v_1 - \Delta v_0)$  represents the difference in the two intercepts on the typical titration curve (Fig. 7),  $M$  is the atomic mass of the metal, and  $m_1$  is the mass of metal in  $1\text{ cm}^3$  of the initial solution being titrated. The method has been tested by the titrations of  $\text{K}_4\text{Fe}(\text{CN})_6$  with  $\text{KBrO}_3$  and  $\text{Ni}(\text{H}_2\text{O})_6^{2+}$  with  $\text{C}_2\text{O}_4^{2-}$ . (348)

Engel *et al.* (349) have suggested a modification to the standard Evans technique. The latter involves placing the paramagnetic

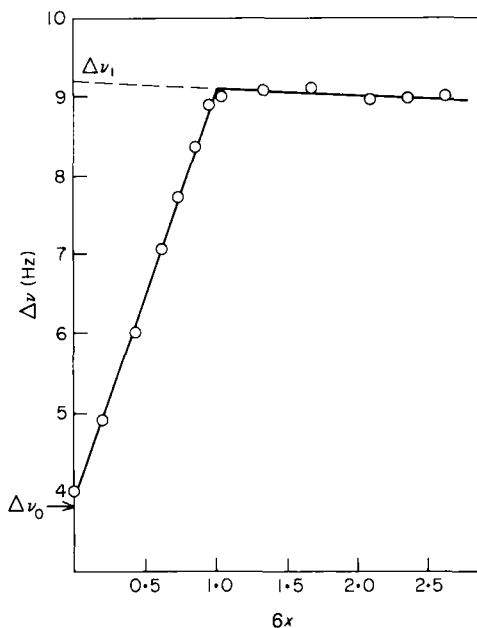


FIG. 7. Magnetic titration of  $1.03 \times 10^{-2}$  M  $\text{K}_4\text{Fe}(\text{CN})_6$  in  $0.3$  M  $\text{HCl}$  with  $6 \times 10^{-2}$  M  $\text{KBrO}_3$ .  $\Delta\nu$  is the difference in chemical shifts of the internal and external references;  $x$  is the molar ratio of  $\text{BrO}_3^-$  added to  $\text{Fe}(\text{CN})_6^{4-}$  taken. (348)

substance with solvent and a reference material in the outer cavity of a concentric cavity tube and having the solvent and reference material above in the inner cavity. The new method in contrast involves the reference material being placed in the outer cavity and the solution of the paramagnetic substance in the inner cavity. If the sample tube is *stationary* in the probe, the reference material is in an inhomogeneous magnetic field and its signal is split into a doublet according to:

$$\Delta\nu = 4\pi\nu_0[(\chi_1 - \chi_2)(a^2/r^2) + (\chi_2 - \chi_3)(b^2/r^2)] \quad (42)$$

where  $\chi_1$ ,  $\chi_2$ , and  $\chi_3$  are the magnetic susceptibilities of the paramagnetic solution, the glass, and the reference material respectively, and  $a$ ,  $b$ , and  $r$  are geometric shape factors of the concentric NMR tube. Measurement of this splitting ( $\Delta\nu$ ) for different solute concentrations ( $c$ ) enables  $\chi_p$ , the molar susceptibility of the solute, to be calculated from:

$$\chi_p = (\Delta\Delta\nu/\Delta c)(r^2/4\pi\nu_0 a^2) \quad (43)$$

However, the shape factor  $r$  is mistakenly referred to as "the mean radius of the annulus" both in the above paper (349) and in the original

publication of equation (42) by Reilly, McConnell, and Meisenheimer. (349a) This parameter  $r$  should refer to "the inner radius of the outer tube" for the method to work successfully (349b) and it is not clear how the  $\chi_p$  values quoted by Engel *et al.* were calculated.

Paramagnetic ions are now being used quite extensively to study adsorption phenomena.  $\text{Mn}^{2+}$  ions have been used as probes for studying molecular motion in synthetic zeolites, (350)  $\text{Co}^{2+}$  and  $\text{Ni}^{2+}$  ions have been used for studying the complexation of molecular hydrogen on the surface of zeolites, (351) and these same ions have been used in a variety of studies of adsorption on Aerosil surfaces. (352–358) Adsorbed molecules studied include olefins, saturated hydrocarbons, alcohols, and benzene. From the measured line-shifts the number of active surface sites can be deduced in favourable cases. (357, 358)

## F. Lanthanide shift reagents

The use of lanthanide shift reagents in NMR spectroscopy is now very widespread. On the one hand they are used in a routine manner for simplifying strongly coupled spectra and aiding the assignment of bands. On the other hand they are employed in a much more exact and specific manner for deducing the average solution geometries of adduct molecules which may vary in size from simple monomer molecules to highly complex biopolymers. The literature of lanthanide shift reagents (LSR) is nowadays very extensive and it is not possible, or indeed desirable, in this review to attempt any kind of comprehensive coverage. Instead, mention will be made of review articles and a selection of papers which describe either basic developments in theoretical aspects of the subject or rigorous quantitative uses of LSR.

During the period covered by this review two books have appeared devoted to the principles, methodology, and applications of LSR. (359, 360) Some major reviews (361–364) and a variety of shorter reviews have appeared. (365–377) The latter two references (376, 377) refer specifically to biological systems, a topic that is dealt with in more detail in Section G.

### 1. Origin of the shifts and their interpretation

Induced shifts of ligand atoms adjacent to rare earth ions are usually attributed to the contact interaction whereas shifts of more remote ligand atoms are generally considered to arise from a dipolar term. McGarvey (378, 379) has described a reformulated covalent model which can account for the observed  $^{19}\text{F}$  hyperfine interactions for  $\text{Yb}^{3+}$  and  $\text{Tm}^{2+}$  in cubic and tetragonal sites of alkaline earth

fluorides. On the other hand the model cannot explain the data for  $\text{Ce}^{3+}$ ,  $\text{Gd}^{3+}$ , or  $\text{Eu}^{2+}$ , suggesting that in the first part of the rare earth series the dominant mechanism is spin polarization whereas the covalent model becomes dominant in the latter half of the series. Further study of the  $^{19}\text{F}$  shifts of the  $\text{Yb}^{3+}$  system has revealed that the main contribution to the isotropic shift is *not* from a contact interaction, as previously assumed, but from a second-order Zeeman term due to a spin-orbit interaction between the nuclear spin and the orbital motion of unpaired electrons in the ligand p orbitals.

The induced shifts of nuclei not directly adjacent to lanthanide ions have been known for many years to be predominantly dipolar in nature. However, a fully satisfactory theory to account for the variation in these induced shifts across the lanthanide series has been difficult to achieve. Theoretical treatments have been developed independently by Bleaney, (380) Golding and Pyykkö, (381) and Horrocks *et al.* (382) Bleaney's approach involves the following power series expansion in temperature for the susceptibility anisotropy, assuming axial symmetry:

$$\Delta\chi = \chi_{\parallel} - \chi_{\perp} = N(g_{\parallel}^2 - g_{\perp}^2)\mu_B^2 J(J+1)/3kT \\ - N(2g_{\parallel}^2 + g_{\perp}^2)\mu_B^2 DJ(J+1)(2J-1)(2J+3)/90(kT)^2 \quad (44)$$

where  $J$  is the total angular momentum quantum number,  $D$  is the zero-field splitting tensor, and the other symbols have their usual significance. This equation implies that if the first term dominates (e.g. if there is considerable anisotropy in the  $g$  tensor) the shift will have a  $T^{-1}$  dependence. On the other hand, if the second term dominates (as it is expected to do for all lanthanides other than  $\text{Eu}^{3+}$  and  $\text{Sm}^{3+}$ ) a  $T^{-2}$  dependence of the induced shift is predicted. This was confirmed experimentally in the case of the induced high frequency shifts in acetone by  $\text{Yb}(\text{fod})_3$ . (383, 439)

Horrocks *et al.* (382) have attempted to refine Bleaney's theory by using a more general field model including all the  $J$  multiplets of the ground term as a basis. There are two principal differences between the two approaches. Firstly, Bleaney's ligand field model is restricted to ligand field parameters of the second degree whilst the Horrocks method employs a general ligand field expansion. Secondly, Bleaney's equations are based on a thermodynamic approach and a high-temperature approximation whereas the high-temperature approximation of Horrocks is implicit in the Van Vleck formula he uses. The different natures of these high-temperature approximations can be expected to become important at lower temperatures, with the Horrocks approach being more correct.

Stout and Gutowsky (384) have examined this point and found that the method of Horrocks agrees with an exact calculation of the susceptibility anisotropy for a  $J = \frac{3}{2}$  state to within 0.1% at temperatures down to 200 K, whereas Bleaney's equation gives a deviation of 1.49%. However, inclusion of a term linear in  $T^{-3}$  brings the agreement to within 0.27% of the exact result. This deviation from  $T^{-2}$  dependence of the magnetic susceptibility has been further studied by Horrocks (385) for two axially symmetric Yb(III) complexes and a non-axial Yb(III) shift reagent. The appreciable deviations from  $T^{-2}$  dependence can be accounted for by the Horrocks approach but not by the simpler Bleaney approach.

The use of LSR as structural probes depends on the following conditions (386) being satisfied. (1) The shifts used in the analysis are purely dipolar in origin. (2) Only a single stoichiometric complex species exists in solution in equilibrium with uncomplexed substrate. (3) Only a single geometric isomer of this complex is present. (4) This isomer is magnetically axially symmetric so that the shifts are proportional to the geometric factor  $\langle (3 \cos^2 \theta - 1)/r^3 \rangle$ . (5) The principal magnetic axis has a particular, known orientation with respect to the substrate ligand(s). (6) The substrate ligand exists in a single conformation or an appropriate averaging over internal motion is performed.

If one or more of these conditions is not met, then the results of a particular analysis must be treated with considerable caution. Condition (1) is generally valid for nuclei more than three bonds removed from the lanthanide nucleus. Even if there are both dipolar and contact contributions to the observed shifts, methods have been developed for separating the two. Reilley *et al.* (387, 388) have made extensive studies of this problem. Their method is based on the fact that the experimental shift can be expressed as a summation of contact and dipolar terms according to:

$$(\Delta\nu^E/\nu)_{ij} = F_i \langle S_z \rangle_j + G_i C_j^D \quad (45)$$

where  $F_i$  is a factor that depends upon the nucleus  $i$  being observed and is independent of the lanthanide ion employed,  $\langle S_z \rangle_j$  values have been computed by Golding and Halton (389) and found to depend only on the lanthanide ion,  $G_i$  is the geometric factor term, and  $C_j^D$  depends only on the lanthanide being employed.

It is seen from equation (45) that if experimentally observed shifts  $(\Delta\nu^E/\nu)_{ij}$  are measured for a given nucleus  $i$  using a variety of lanthanides  $j$  it is possible to set up and solve the appropriate number of simultaneous equations in order to evaluate the terms  $F_i$  and  $G_i$  for this

nucleus. The method is valid only for cases of effective axial symmetry and has been tested for a variety of lanthanide tris-complexes of pyridine-2,6-dicarboxylic acid (DPA) and its *para*-substituted methyl analogue (MDPA). Some typical results are given in Table XV. The agreement factor, AF, is defined as:

$$(\text{AF})^2 = \left\{ \sum_i [v_i(\text{obs.}) - v_i(\text{calc.})]^2 \right\} / \sum_i [v_i(\text{obs.})]^2 \quad (46)$$

TABLE XV

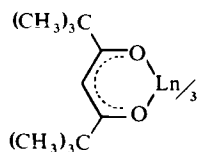
Experimental shifts<sup>a</sup> for Ln(DPA)<sub>3</sub> and Ln(MDPA)<sub>3</sub> complexes and the corresponding computed values for contact and dipolar contributions (387)

Nucleus	Shift	Pr	Tb	Ho	Yb	AF	$F_i$	$G_i$
$C_\alpha$	$\nu^{\text{tot}}$	-10.9	-133.0	-75.0	39.0	0.09	-0.022	1.575
	$\nu^C$	0.0	0.7	0.4	0.1			
	$\nu^D$	-10.9	12.0	-75.4	38.9			
$C_\beta$	$\nu^{\text{tot}}$	-19.9	41.3	27.4	17.5	0.17	-2.623	0.554
	$\nu^C$	-11.2	86.9	51.8	6.3			
	$\nu^D$	-8.7	-45.8	-24.4	11.2			
$H_\beta$	$\nu^{\text{tot}}$	—	-29.2	-16.5	7.3	0.09	0.009	0.339
	$\nu^C$	—	-0.3	-0.3	0.0			
	$\nu^D$	—	-28.9	-16.2	7.3			
$H_\gamma$	$\nu^{\text{tot}}$	—	-26.4	-14.1	6.5	0.08	0.013	0.299
	$\nu^C$	—	-0.9	-0.7	-0.1			
	$\nu^D$	—	-26.0	-13.7	6.5			

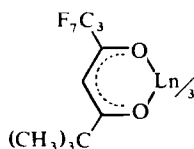
<sup>a</sup> Values in ppm relative to the diamagnetic La complex.

It is noted that the magnitude of the contact contribution varies considerably between the  $^1\text{H}$  and  $^{13}\text{C}$  resonances. In order to obtain structural information on the lanthanide complexes at least six  $G_i$  values are, in general, required (three polar coordinates to fix the position of the lanthanide ion relative to the molecule, two additional angles to define the main magnetic axis orientation, and one signed value for the proportionality constant). The six nuclei used to provide these  $G_i$  values need not necessarily be protons. In a later paper Reilley *et al.* (388) discuss certain refinements of their method and apply it to a wide variety of LSR complexes including those of water, pyridines, alcohols, anilines, aliphatic amines, and ketones. The contact contributions of the  $^{13}\text{C}$  shifts of Ln(DPA)<sub>3</sub> and Ln(MDPA)<sub>3</sub> complexes are found to be important even for carbons five bonds removed from the lanthanide ion. (390)

Separation of contact and dipolar terms using the different temperature dependences of the shifts has been reported. (391) The LSR  $\text{Gd}(\text{dpm})_3$  and  $\text{Gd}(\text{fod})_3$  are known to induce shifts that are essentially contact in origin since the  $g$ -tensor of  $\text{Gd}^{3+}$  is predicted to be isotropic. They can therefore be used to assess the contact contributions for shifts induced by other  $\text{Ln}(\text{dpm})_3$  [51] and  $\text{Ln}(\text{fod})_3$  [52] reagents. This method has been tested on quinoline (392) and a variety of aliphatic and aromatic compounds. (393)



[51]



[52]

A sizeable complex formation shift contribution is noted for aromatic adducts. Sizeable complex formation  $^{13}\text{C}$  shifts are also observed (394) for the diamagnetic LSR  $\text{La}(\text{dpm})_3$ . The shifts induced by paramagnetic complexes such as  $\text{Eu}(\text{dpm})_3$  and  $\text{Pr}(\text{dpm})_3$  are accordingly corrected for this factor. In this work it is found that contact contributions to the  $^{13}\text{C}$  shifts are generally larger in amines than in alcohols or ketones. For quantitative structural work  $\text{Yb}(\text{dpm})_3$  is found to be particularly useful since it produces minimal contact shifts without any adverse line-broadening.

Quantitative separation of the  $\pi$  contact and pseudocontact contributions to the lanthanide induced shifts (LIS) in aniline and *m*- and *p*-toluidines has been reported. (395, 396) The contact shift patterns are estimated from the  $\pi$ -spin density distribution of the appropriate cation radical or from the  $\text{Ni}(\text{acac})_2$  induced shifts. The separation of the shifts was checked by comparing the relative contact shift contribution with the  $\langle S_z \rangle$  value of Golding and Halton (389) and the remaining pseudocontact contribution with the calculated values of Bleaney's theory. (380)

Separation of contact and dipolar terms of isotropic  $^{31}\text{P}$  shifts has been achieved for  $\text{Ln}(\text{III})$  complexes of cytidine-5'-monophosphate. (397) Contact contributions to LIS in the spectra of isoquinoline and *endo*-norbornenol were estimated from the differences between the calculated and observed behaviour of the LSR  $\text{Ln}(\text{dpm})_3$ . (398)

Condition (2) (above) can often be satisfied by using the appropriate experimental conditions such as having a large excess of adduct present, but conditions (3), (4), and (5) are far more difficult to achieve in

practice. The question of an assumed axial symmetry of the LSR adduct complex has caused considerable comment. The general expression for dipolar shifts is given by:

$$\Delta B(\text{dip})/B = (1/3N)[\chi_{zz} - \frac{1}{2}(\chi_{xx} + \chi_{yy})][\langle 3 \cos 2\theta - 1 \rangle / r^3] \\ - (1/2N)[\chi_{xx} - \chi_{yy}][\langle \sin^2 \theta \cos 2\phi \rangle / r^3] \quad (47)$$

where the  $\chi_{\alpha\alpha}$  are the principal molecular magnetic susceptibilities, and  $r$ ,  $\theta$ , and  $\phi$  are the usual spherical polar coordinates of the nucleus in question in the coordinate system of the principal magnetic axes. The assumption of axial symmetry presupposes that the second term of equation (47) can be neglected. This assumption appears to work in practice, enabling many workers to calculate very reasonable lanthanide substrate bond distances although the lanthanide adducts are definitely known *not* to possess axial symmetry in the solid state. Horrocks (399) has explained this situation as arising from a dynamic equilibrium between a number of interconnecting forms (30 or more). Such a process leads to shift ratios that will approximate but not exactly equal those derived from the axial model.

Cramer *et al.* (400, 401) have made a detailed study of the adducts  $\text{Eu}(\text{dpm})_3(\text{py})_2$  and  $\text{Eu}(\text{dpm})_3(3\text{-pic})_2$  and have demonstrated that the LIS of all protons can only be accounted for by using the full form of equation (47). These workers were able to slow down the rate of exchange between the free and coordinated adduct molecules such that at *ca.*  $-105^\circ\text{C}$  separate signals were observed which when integrated showed that a 1:2 adduct was present. Cooling to  $-120^\circ\text{C}$  in carbon disulphide reveals two signals each for the *ortho* hydrogen and methyl groups, indicating that rotation about the Eu–N bond is slow. The rotation barrier was estimated to be at least  $29 \text{ kJ mol}^{-1}$ . (424)

The agreement between calculated and measured LIS for 2:1 adducts of substituted pyridines with  $\text{Eu}(\text{thd})_3$  (thd = 2,2,6,6-tetramethyl-3,5-heptanedionato) using the full form of equation (47) is found (402, 423) to be fairly insensitive to the Ln–N distance. This brings into question the validity of Ln–substrate distances determined exclusively from the single-term McConnell–Robertson equation [equation (13)]. The importance of non-axial symmetry has been shown in the study of LIS for ketones. (403) The importance of *not* assuming axial symmetry when using  $\text{Gd}(\text{dpm})_3$  or  $\text{Gd}(\text{fod})_3$  as relaxation reagents has been stressed; (404) otherwise the induced broadenings will not reflect the true geometry of the complex.

Line-broadenings by shift reagents of the  $\text{Ln}(\text{fod})_3$  type have been examined as a function of concentration, frequency, and temperature.



(405) Pinacolone was chosen as the substrate molecule. The main finding is that a term containing the modulation by chemical exchange of the chemical shift difference between coordinated and free substrate molecules makes a significant contribution to the observed line-broadenings and this produces a non-linear dependence of linewidth on the fraction of complexed substrate. Simultaneous application of both shift and relaxation data gives a much more definitive description of the solution geometry of an adduct that can be achieved if only one kind of data is used. (422)

A large number of papers have appeared describing computational methods, usually based on the McConnell–Robertson equation [equation (13)], for calculating the solution geometry of an LSR adduct which can best account for the measured LIS ratios. These programs vary greatly in their sophistication, firstly in the size of adducts that they can handle, secondly in the conformational averaging procedures that are used, and thirdly in the error analyses of the fitting procedures. Space prevents any detailed discussion of these methods. (406–420) Suffice it to say that a computer program of this type, LISCA, developed by Lienard (421) is available to U.K. users in the S.R.C. NMR computer program library at the S.R.C. Daresbury Laboratory. The program examines the solution conformations of semi-flexible molecules of considerable complexity. It incorporates a non-linear, least-squares fitting of a set of calculated LIS ratios to an experimentally observed set supplied as input data. Weightings can be assigned to the LIS ratios. The best fit is achieved by altering the values of a preselected set of conformational degrees of freedom in a computer-generated model of the lanthanide–substrate complex.

Despite the fact that correlations of LIS ratios with the solution geometry of the LSR–substrate adduct are now well established and very widely employed, warnings have been given (425, 426) that predictions of conformations of non-rigid molecules must be made with extreme caution.

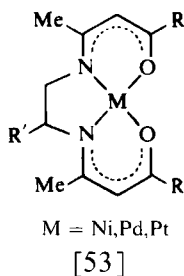
## *2. Structure of adducts in solution*

This section reviews a selection of the more quantitative uses of LSR for substrate structure determinations. The substrates are grouped according to their donor properties.

Oxygen donor substrates continue to be extensively studied. Conformations of esters, (427) aldehydes and ketones, (428, 429) ketones, (430, 431) cyclohexanones, (432, 433) carboxylates, (434) benzene-1,2-dioxydiacetate, (435) borneols, (436) troponeiron tricarbonyl, (437) and nitrosopiperidines (438) have been deduced. It is

generally found that LIS of  $^{13}\text{C}$  nuclei contain significant contact contributions whereas such contributions are often negligibly small for proton shifts. In the studies on 2-alkylcyclohexanones (432, 433) equations are derived relating the induced shift ratios to the conformational equilibrium constants for the complexes. The nature of the  $\text{Ln(III)}$  binding to indol-3-yl acetate (434) is found to vary over the lanthanide series. For members of the series before  $\text{Gd(III)}$  the shift ratios are compatible with bidentate binding of the carboxylate but this changes to monodentate binding in the case of  $\text{Tm(III)}$ .

LSR have recently been used to study the structures of coordination complexes. (440–442) Diamagnetic coordination complexes of quadridentate ligands containing oxygen and nitrogen donor atoms of the general type [53] were studied. The two oxygen atoms coordinate with  $\text{Eu(fod)}_3$  and other LSR to give 1:1 adducts. LIS studies have shown that the backbone methyl group in the complex with  $\text{R}' = \text{CH}_3$  occupies an axial position. The kinetics of the adduct formation and dissociation have also been studied, yielding  $k_f$  and  $k_d$  values of  $7.7 \times 10^7 \text{ M}^{-1} \text{ s}^{-1}$  and  $(7.7 \pm 0.6) \times 10^4 \text{ s}^{-1}$ , respectively. (440)



A theoretical calculation has been made (443) of the structures of mono-adducts of tris-( $\beta$ -diketonato) LSR of the type  $[\text{Ln}(\text{bidentate})_3(\text{unidentate})]^{x+}$ . Three favoured structures having similar potential energies are suggested. These are a capped octahedron ( $C_{3v}$ ), an irregular polyhedron ( $C_1$ ), and a structure intermediate between a pentagonal bipyramid and a capped trigonal prism. The first two structures have been observed experimentally when the unidentate ligand is water or a carbonyl function.

Nitrogen-donor substrates that have been studied in some detail include pyridines and piperidines, (444, 446) pyrroles, (447) quinoline and isoquinoline, (448) naphthylamine, (449) and nitriles. (450) The study of 1- and 2-naphthylamine (449) involved the use of the paramagnetic reagents  $\text{Gd(dpm)}_3$ ,  $\text{Ni(acac)}_2$ , and  $\text{Pr(fod)}_3$  which induced predominant relaxation, contact shift, and pseudocontact shift

effects respectively. The coordination of nitriles with lanthanide ions (450) is thought to occur with the lanthanide ion collinear with the nitrile group. Lanthanide induced  $^{14}\text{N}$  shifts are particularly useful in studying structures of N-donor substrates. (538)

The application of LSR to amino-acids has received some attention. (451–456, 498) Such studies are an essential preliminary to the use of LSR for amino-acid sequence determination in simple peptides and proteins. The latter are discussed more comprehensively in Section G. A detailed study has been made (453) of the interaction of Eu(III), Pr(III), Gd(III), and La(III) with *N*-acetyl-L-3-nitrotyrosine in order to characterize the nitrotyrosine residue as a potential specific lanthanide binding site in proteins. The parameters of the dipolar interaction indicate a significant contribution from non axially symmetric terms. The conformations of the nucleotides cyclic  $\beta$ -adenosine 3',5'-phosphate (3',5'-AMP) (457, 458) and adenosine triphosphate (ATP) (459) have been deduced using LSR. In the former case the conformation of the ribose and phosphate groups is consistent with the solid state structure. A combination of lanthanide shift and relaxation reagents was used to deduce the most favoured family of conformations for ATP in aqueous solution. One of these conformations corresponds closely to one of the crystal structure forms.

The interactions of LSR with various organophosphorus substrates have been reported (460–463).  $\text{Yb}(\text{fod})_3$  and  $\text{Pr}(\text{fod})_3$  are considered to be the best LSR for organophosphorus compounds. Proton shifts are, as usual, dominated by pseudocontact interactions.  $^{13}\text{C}$  shifts are predominantly pseudocontact in nature but have sizeable contact contributions for phosphine and phosphoryl compounds. In contrast  $^{31}\text{P}$  shifts have large contact components where direct phosphoryl–oxygen or phosphorus–lanthanide interactions occur. Large pseudocontact  $^{31}\text{P}$  shifts for triethyl phosphite indicate little or no direct phosphorus–lanthanide interaction.

Conformational analysis of substituted 1,3,2-dioxaphosphorinanes has been achieved using a topological approach (429) rather than the more elaborate random search method. This simplified approach only considers chemically and physically accessible positions for the lanthanide. Using this approach the LIS calculations are found to predict the conformational equilibrium for complexed *cis* conformers which is in good agreement with that based on the response of the coupling constants  $J(\text{H}–\text{H})$  and  $J(\text{P}–\text{H})$  to lanthanide addition. For the *trans* conformers the two approaches are not in agreement.

The binding of lanthanides to sugars and related molecules has received some attention. (464–467) Methyl  $\alpha$ -D-gulopyranoside forms a

1:1 complex with Eu(III) and Pr(III) (464) whereas the sodium salt of methyl  $\alpha$ -D-galactopyranoside forms essentially a 1:3 complex which shows a high-degree of axial symmetry. (465)

Some new lanthanide porphyrin complexes of general formula  $\text{Ln(III)TAP}(\beta\text{-diketonate})$ , where TAP = tetraarylporphine, have been prepared (468, 469) and their shift reagent capabilities assessed. The complexes of the early lanthanides (Pr, Nd, Sm, Eu) induce very small shifts whereas the complexes of Tb, Dy, and Ho produce quite large low frequency shifts in  $\gamma$ -picoline. Analogous shift reagents based on silicon, germanium, low-spin iron, (517, 518) and cobalt (519) have been reported.

These complexes, like the majority of LSR, are soluble only in organic solvents. However, LSR probes for biological systems need to be water-soluble. Aquo-lanthanides can be used but these are stable only in acid solutions. Water-soluble chelates of lanthanides that can be used at higher pH values are therefore desirable. The anionic chelates  $\text{Ln(EDTA)}^-$  have been examined as suitable aqueous LSR. (470–472) The induced shifts, which are pseudocontact in origin, are to low frequency for  $\text{Pr(EDTA)}^-$  and to high frequency for  $\text{Yb(EDTA)}^-$ .  $\text{Gd(EDTA)}^-$  causes line-broadenings. The practical pH range is 6–10. At higher pH values there is effective competition due to the formation of hydroxo complexes. There is evidence that the lighter lanthanides are pentachelated whereas the heavier ones are hexachelated. However,  $\text{Pr(EDTA)}^-$  and  $\text{Yb(EDTA)}^-$  are isostructural. The complexes form ion pairs with organic cations such as substituted ammonium ions (472) and can thereby act as aqueous shift and relaxation reagents in these systems.

Lanthanide chlorides (473) and nitrates (474, 475) have been used as aqueous LSR for investigating the structures of a number of carbohydrates. Shifts induced by  $\text{Ln}^{3+}$  ions in the proton spectrum of methoxyacetate have been discussed. (476) The water-soluble Eu complexes of pyridoxalideneaspartic acid and *o*-vanillideneaspartic acid have been suggested as suitable shift reagents. They have been tested with aqueous solutions of amino-acids and peptides. (477)

### 3. *Solution equilibria of adducts*

The use of lanthanide shift reagents as structural probes depends firstly on a knowledge of the stoichiometry and equilibria of interaction between the LSR and the substrate, and secondly on being able to separate the dipolar contribution from the total averaged isotropic shift. This latter aspect has already been considered. The accurate study of the binding modes of substrates to LSR is often not straightforward. Early

studies tended to support 1:1 adduct formation in most cases but it is now becoming evident that it is not uncommon for more than one binding mode to occur. A two-step mechanism is now usually considered:



$K_{m1}$  ( $= [\text{RS}]/[\text{R}][\text{S}]$ ) and  $K_{m2}$  ( $= [\text{RS}_2]/[\text{RS}][\text{S}]$ ) are the two equilibrium constants involved. Reuben (478) has shown that the complex formation between  $\text{Eu}(\text{fod})_3$  and acetone, dimethylsulphoxide, 2-propanol, and  $\beta$ -picoline involves a total stoichiometry of LSR-substrate adduct of 1:2 with complexes of the type RS and  $\text{RS}_2$  present in equilibrium. For acetone and dimethyl sulphoxide  $K_{m1} > 4K_{m2}$  whereas for 2-propanol and  $\beta$ -picoline  $K_{m1} < 4K_{m2}$ .

Similar results are found (479) for the equilibria of  $\text{Eu}(\text{fod})_3$  with the basic substrate  $(\pi\text{-C}_5\text{H}_5)\text{Fe}(\text{CO})_2(\text{CN})$ . In the case of  $\text{Pr}(\text{fod})_3$  1:3 adduct formation is also observed. These results are confirmed by vapour pressure osmometry. Evans and Wyatt (480, 481) have utilized low-temperature NMR conditions to deduce solvation numbers of the shift reagent. They have demonstrated that at temperatures around  $-60^\circ\text{C}$  or lower the exchange rate between substrates such as dimethyl sulphoxide, hexamethylphosphoramide, tetramethylurea, and triethylamine and the reagents  $\text{Ln}(\text{dpm})_3$  [ $\text{Ln} = \text{Eu}(\text{III}), \text{Pr}(\text{III})$ ] becomes slow on the NMR time scale. Accurate measurement of the areas enclosed by the free and complexed substrate peaks yields the solvation numbers of the adducts. Accurate line-shape studies in the higher temperature range enable the kinetics of the substrate exchange to be measured [Fig. 8(a)]. It is found that 1:1 complexes are more favoured with  $\text{Ln}(\text{dpm})_3$  than  $\text{Ln}(\text{fod})_3$  where 1:2 complexes are the norm.

Evans and Wyatt (481) have suggested an energy profile [Fig. 8(b)] for substrate exchange. The species  $\text{RS}_2^*$  is considered to be an unstable isomer of  $\text{RS}_2$  in which the configuration of the  $\beta$ -diketone ligands is similar to that in the 7-coordinate RS. Other equilibrium studies involving  $\text{Ln}(\text{dpm})_3$  have been reported. (482–485)

$\text{Eu}(\text{NO}_3)_3$  has been shown to form essentially 1:1 adducts with L-azetidine-2-carboxylic acid (480) and  $\text{Eu}(\text{fod})_3$  forms similar adducts with dialkyl nitrosamines. (487) 1:1 Stoichiometry between  $\text{Eu}(\text{fod})_3$  and various cyclic 6-membered sulphites has been assumed. (488) Both 1:1 and 1:2 adducts have been reported for  $\text{Eu}(\text{fod})_3$  bound to cyclohexanones and cyclohexanols, (489) n-hexylamine, (490) hexamethylphosphoramide, (491, 492) and methyl dimethylcarbamate. (493)

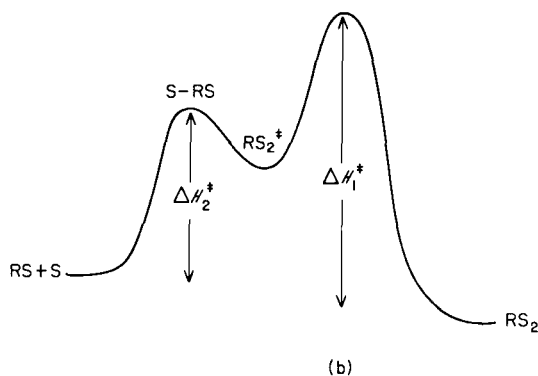
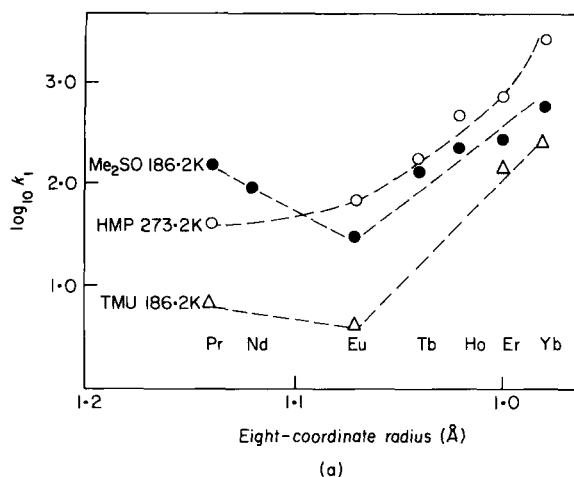
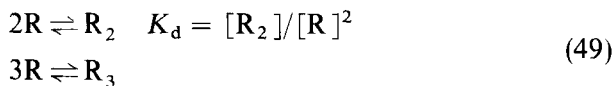


FIG. 8. (a) Plot of  $\log_{10} k_1$  against the 8-coordinate ionic radius of the lanthanide ion for  $\text{Ln}(\text{fod-d}_9)$  complexes.  $k_1$  is the first-order rate constant for substrate exchange; HMP = 1,2-hexamethylphosphoramidate; TMU = tetramethylurea. (b) Suggested energy profile for substrate exchange. (481)

In some of these studies allowance has been made for the self-association of the LSR. Thus in addition to considering the two equilibria [equations (48)] other equilibria such as:



need to be considered. No self-association of  $\text{Eu}(\text{fod})_3$  in  $\text{CCl}_4$  was found in one study (489) whereas in another study self-association of both

$\text{Pr}(\text{fod})_3$  and  $\text{Eu}(\text{fod})_3$  in non-polar solvents such as carbon tetrachloride was found to be appreciable. The equilibrium constants for dimer and trimer formation are  $140 \pm 8 \text{ M}^{-1}$  and  $45 \pm 5 \text{ M}^{-1}$  for  $\text{Pr}(\text{fod})_3$  and  $367 \pm 22 \text{ M}^{-1}$  and  $12 \pm 2 \text{ M}^{-1}$  for  $\text{Eu}(\text{fod})_3$ . These species are thought to involve 7- and 8-coordination of the Ln ion respectively.  $\text{Eu}(\text{thd})_3$  and  $\text{Pr}(\text{thd})_3$  were not associated in non-polar solvents.

More recently, de Boer *et al.* (494, 495) have presented a detailed discussion of the binding modes of various mono- and bi-functional ethers with  $\text{Pr}(\text{fod})_3$  and other  $\text{Ln}(\text{fod})_3$  reagents. They specifically chose systems where a single type of adduct species predominates in solution. This circumvents having to perform the detailed statistical analysis of the shifts for systems containing appreciable amounts of species  $\text{RS}$  and  $\text{RS}_2$  which was found by Johnston *et al.* (489) to be necessary in order to obtain reliable association equilibrium constants  $K_{m1}$  and  $K_{m2}$  and bound shifts  $\delta_1$  and  $\delta_2$ . The binding scheme considered by de Boer *et al.* (494) is shown in Fig. 9 (where  $\text{L} \equiv \text{R}$ ). It is noted that in addition to the

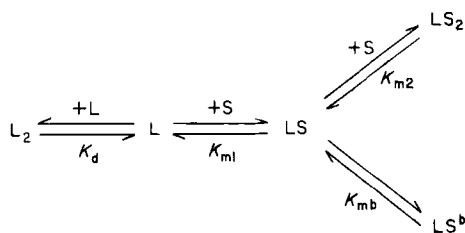


FIG. 9. Reaction scheme for the binding of a bidentate substrate S to the shift reagent L. The equilibrium constants shown are association constants. (494)

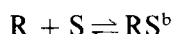
equilibria [equations (48) and (49)] a fourth equilibrium which allows for the bidentate binding of the substrate is considered:

$$\text{RS} \rightleftharpoons \text{RS}^b \quad K_{mb} = [\text{RS}^b]/[\text{RS}] \quad (50)$$

The bifunctional ethers predominantly bind in a bidentate manner and thus the spectra of these substrates in the presence of  $\text{Ln}(\text{fod})_3$  are governed by the  $\text{RS}^b$  complexes. In such a case the measured shift  $\delta$  is given by:

$$\begin{aligned}
 \delta = \frac{[\text{R}]_0}{[\text{S}]_0} & \left\{ \delta_{\text{RS}^b} \left( 1 - \frac{1}{K_b[\text{S}]_0} - \frac{2K_d[\text{R}]_0}{(K_b[\text{S}]_0)^2} \right) + \frac{(\delta_{\text{RS}} - \delta_{\text{RS}^b})}{K_{mb}} \right. \\
 & \left. + \frac{K_{m2}[\text{S}]_0(2\delta_{\text{RS}_2} - \delta_{\text{RS}^b})}{K_{mb}} \right\} \quad (51)
 \end{aligned}$$

where  $K_b$  relates to the possible equilibrium:



and is therefore given by the expression  $[RS^b]/[R][S]$  which in turn equals  $K_{m1}K_{mb}$ . For bidentate binding a plot of  $\delta$  versus  $[R]_0/[S]_0$  will yield an initial slope of  $\delta_{RS^b}$ , the bound shift of the species  $RS$ . 1,2-Dimethoxyethane (DME), 1-methoxy-2-n-octyloxyethane (MOE), and 1,2-dimethoxy-4,5-dimethylbenzene (DMV) behave in this manner, and values of  $K_{m1}$ ,  $K_{m2}$ ,  $K_{mb}$ , and  $K_b$  have been accurately determined (Table XVI). On the other hand the monofunctional ethers methyl n-butyl ether (MBE) and anisole produce less tractable equilibria data. Attempts to separate the contact and pseudocontact contributions to the observed shifts of the bifunctional ethers using the temperature dependence method have proved unsuccessful. A  $T^{-1}$  temperature dependence is observed which is not in accord with Bleaney's theory. (380) This is thought likely to result from the assumption that the ligand splittings are small compared with  $kT$  not being valid. The measured shifts for the  $\text{Ln}(\text{fod})_3$ -DMV complexes indicate a definite lack of axial symmetry around the z-axis. The same authors have more recently considered the chemical exchange effects that occur in the  $\text{Ln}(\text{fod})_3$ -DME system. (496) In addition to substrate exchange, (fod) ligand exchange may also occur from one complex to another.  $\text{La}(\text{fod})_3$ ,  $\text{Pr}(\text{fod})_3$ , and DME in molar ratio 1:1:2 were used. Substrate exchange involves both first-order and second-order kinetics depending on the free substrate concentration. A mixed dimer model is suggested to explain qualitatively the fod exchange.

TABLE XVI  
Equilibrium constants (31°C) for the binding of ethers to  $\text{Pr}(\text{fod})_3$  in  $\text{CCl}_4$  solution (494)

Substrate	$K_{m1} (\text{M}^{-1})$	$K_{m2} (\text{M}^{-1})$	$K_{mb} (\text{M}^{-1})$	$K_b (\text{M}^{-1})$
MBE	30	8	—	—
DME	60	16	$3.5 \times 10^3$	$2 \times 10^5$
MOE	60	16	$1.1 \times 10^3$	$6.6 \times 10^4$
Anisole	2.5	0.7	—	—
DMV	5.0	1.3	$6 \times 10^3$	$3 \times 10^4$

The distinction between enantiomeric species is normally made by the use of a chiral shift reagent (Section F.4). However, it has been reported that in certain circumstances such a distinction can be achieved with an achiral shift reagent. (497) Enantiomeric shift differences  $\Delta\Delta\delta$  are induced by  $\text{Ln}(\text{fod})_3$  for partly resolved alkylamines (Fig. 10). The values



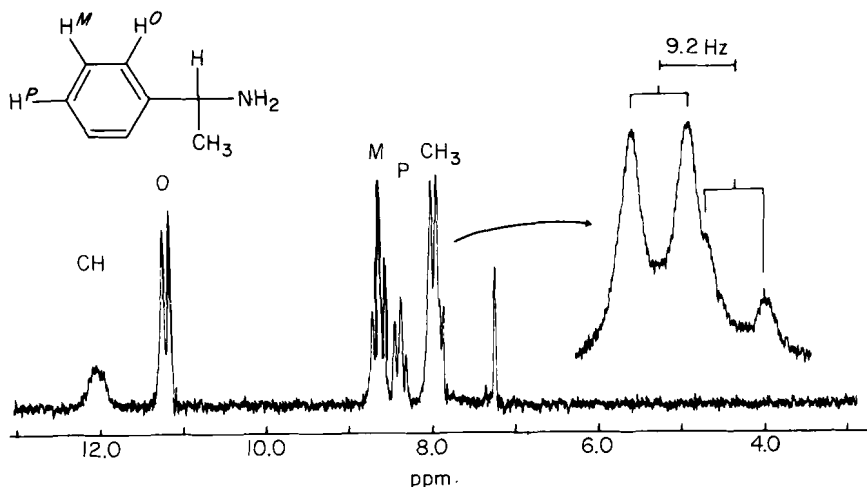


FIG. 10. 100 MHz spectrum of partly resolved  $\alpha$ -phenylethylamine in  $\text{CDCl}_3$  (total [amine] = 0.1 M; enantiomeric ratio S/R = 0.2) in the presence of 0.05 M  $\text{Eu}(\text{fod})_3$ . (497)

of  $\Delta\Delta\delta$  depend not only on the ratio of the enantiomers but also on the relative concentrations of substrate and LSR. A series of equilibria are invoked (Fig. 11) involving 1:1 and 1:2 adducts. In this scheme R and S

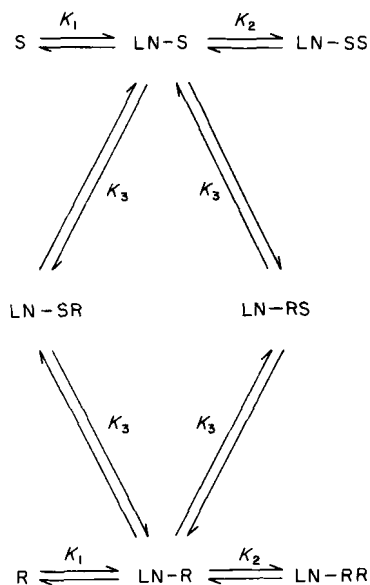


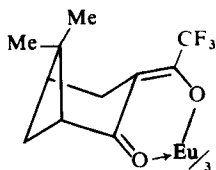
FIG. 11. Series of equilibria from which enantiomeric shift differences arise. (497)

are the two enantiomers, Ln-RR and Ln-SS constitute the *dl* pair, and Ln-RS and Ln-SR are the *meso* forms of the diastereoisomeric set of complexes. For such an equilibrium scheme the expression for  $\Delta\Delta\delta$  has the following properties. (1) In a racemic mixture (i.e.  $[S] = [R]$ )  $\Delta\Delta\delta = 0$ . (2) Even if the induced chemical shifts of the diastereoisomeric forms are identical  $\Delta\Delta\delta$  may be non-zero if  $K_2 \neq K_3$ . (3) Even if  $K_2 = K_3$ ,  $\Delta\Delta\delta$  will be non-zero if there is a difference in induced shift between the *meso* form and the *dl* pair.

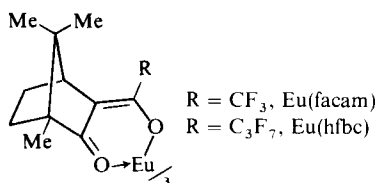
#### 4. Chiral shift reagents

The use of chiral shift reagents to determine enantiomeric purity is now well established and continues to be widely exploited. Some recent developments in the technique are mentioned here.

Whitesides *et al.* (499) have synthesized a wide range of chiral tris-( $\beta$ -diketonato)europium(III) chelates and tested their effectiveness as chiral shift reagents. They conclude that the most effective are tris-(*d,d*-dicampholylmethanato)europium(III), tris-(3-trifluoroacetyl-*d*-nopinonato)europium(III) [54], and tris-(3-trifluoroacetyl-*d*-camphorato)europium(III), Eu(facam) [55]. It is not at present possible to



[54]



[55]

predict with any accuracy the effectiveness of a particular chiral shift reagent on a mixture of enantiomers. To achieve the best resolution between enantiotopic protons in complex polyfunctional structures it is normally necessary to test several shift reagents and vary both sample concentration and temperature.

The reagent Eu(facam), its derivative Eu(hfbc), and their Pr(III) analogues have been used in the resolution of a wide variety of enantiotopic protons. (500–503) A variety of other Eu(III), Pr(III), and Yb(III) chiral shift reagents have been used to resolve optically active 2-methyl-substituted acids, (504) 1-phenylalkanols PhCHROH, (505) PhCHXMe (X = OH, NH<sub>2</sub>), (506) bianthrone, (507) and derivatives of cyclopentadienyliron. (508) The reagents tris-[3-*t*-butylhydroxymethylene-(+)-camphorato]Ln(III) (Ln = Pr, Nd, and Sm) have been

reported (509) to be dimeric in dry carbon tetrachloride unlike the later members of the series. The use of chiral shift reagents for the study of rates of certain intramolecular motions in chiral and prochiral molecules has been discussed. (510–512) In particular the partial rotation about the aniline bond in (*RS*)-2,6-MeCl-C<sub>6</sub>H<sub>3</sub>N(NO)CH<sub>2</sub>Ph was studied in the presence of ( $\pm$ )- and (+)-Eu(hfbc) and in the absence of these shift reagents. The activation parameters for the rotation process are identical, within experimental error, in all three cases.

Enantiomeric distinction can also be achieved using chiral solvents without shift reagents. The determination of enantiomeric purity and the assignment of absolute configuration of cyclic and acyclic sulphinate esters has recently been achieved (573) using chiral 1-aryl-2,2,2-trifluoroethanols as solvents. Enhanced enantiomeric distinction has been demonstrated using a combination of both a chiral solvent and an achiral LSR. (514)

### 5. Miscellaneous uses of shift reagents

It has been suggested that, as an alternative to lanthanide shift reagents, titanium tetrachloride (520) and the Lewis acids BCl<sub>3</sub> and SnCl<sub>4</sub> (521) be seriously considered as shift reagents for substrates containing oxygen functions. The main advantages of these materials are that they are cheaper and more readily available than most LSR but the induced shifts tend to be rather smaller.

The presence of a paramagnetic centre can produce chemical exchange spin decoupling which shows up as a decrease in or complete removal of spin–spin splitting in NMR signals of substrate nuclei. This has been demonstrated for the pyridine substrate. (522) The addition of Gd(fod)<sub>3</sub> to a solution of pyridine and Eu(fod)<sub>3</sub> causes rapid relaxation of the C-2 protons and effective spin-decoupling from the C-3 protons. Mixtures of Gd(fod)<sub>3</sub> and Eu(fod)<sub>3</sub> are superior to other lanthanides which broaden and decouple because the amount of broadening associated with a given shift can be controlled. Ni(acac)<sub>2</sub> has been used (523) to remove spin–spin coupling in the proton spectrum of *N*-vinylpyrazole.

Two rather less common uses of Ln(fod)<sub>3</sub> reagents have been reported. Eu(fod)<sub>3</sub> has been used instead of Cr(acac)<sub>3</sub> to suppress nuclear Overhauser enhancements in <sup>13</sup>C signals (524) and CIDNP spectra have been simplified. (525) Eu(fod)<sub>3</sub> and Pr(fod)<sub>3</sub> selectively shift certain enhanced lines although CIDNP intensities are reduced somewhat on adding LSR.

The techniques of gas chromatography (526) and fluorescence spectroscopy (527) have been employed to examine the nature of the

LSR–substrate interaction and the conformations of LSR and their adducts.

There have been a number of reports of LSR being used for DNMR studies of intramolecular rate processes. Whereas most DNMR experiments involve varying the rate(s) of the observed process by changing the temperature or concentration of reactants while keeping constant  $\Delta\nu_{\infty}$  (the chemical shift difference of the exchanging nuclei in the absence of exchange), the same information is obtained by keeping the rate of the dynamic process constant and varying  $\Delta\nu_{\infty}$ . This can be achieved quite conveniently using LSR. The method was demonstrated for restricted C–N bond rotation in trimethylcarbamate (528) and gave a value of  $\Delta G^{\ddagger}$  in excellent agreement with a literature value obtained by the conventional method.

Other rate processes studied include isopropyl group rotation, (529) restricted rotations in phosphine derivatives of cyclopentadienyl complexes of iron and nickel, (530) and ring and nitrogen inversion in (en) complexes of praseodymium. (531) Molecular geometries of molecules in solution can be accurately determined from NMR spectra of the molecules oriented in a nematic phase of a liquid crystalline solvent. The effect of  $\text{Eu}(\text{dpm})_3$  on the nematic phase spectrum of pyridine has been examined. The pyridine geometry is unaffected by the LSR. The observed LIS values can be separated into isotropic and anisotropic components. (532)

Paramagnetic ion probes have been successfully used to study the binding characteristics and solution conformations of a number of biochemically important molecules. These include vitamin D, (533) penicillins, (534) and the antibiotics tetracycline, (535–537) vancomycin, (632) and bacitracin. (633) Antibodies and antibody fragments (immunoglobulins, IgG) have been studied by proton relaxation enhancement methods when lanthanide ions, particularly  $\text{Gd(III)}$ , are bound to the proteins. (746–748).

### G. Biological applications

The upsurge in research activity in this area during the past 4–5 years has been most striking. The range of studies is now so wide that three books (544–546) and numerous review articles (547–556) have appeared. The present author has been selective; papers have been chosen for their particular chemical as opposed to biological interest and emphasis has been given to pulse FT rather than to pulse relaxation studies.

The growth in biological applications of NMR stems undoubtedly from the wide variety of paramagnetic probes whose binding properties

are now well characterized. The probes fall essentially into two classes, namely, shift perturbation probes and relaxation perturbation probes. They have recently been summarized (554) as in Table XVII. The different behaviours of these probes arise from the different dominant mechanisms of spin-lattice relaxation. The reorientational correlation time  $\tau_c$  of nuclei bound to paramagnetic ions is given by:

$$1/\tau_c = 1/\tau_r + 1/\tau_s + 1/\tau_M \quad (52)$$

where  $\tau_M$  is the lifetime of a nucleus in the bound site and  $\tau_s$  is the electron spin relaxation time. When the rotational correlation time  $\tau_r$  is the shortest time,  $\tau_c^{-1}$  is dominated by  $\tau_r^{-1}$ . This is the case (Case 1) for Mn(II), Gd(III), Eu(II), Cu(II), and V(II), and usually  $\tau_c \approx 10^{-10}$ – $10^{-11}$  s. When electron spin relaxation is the dominant relaxation process,  $\tau_c^{-1}$  is dominated by  $\tau_s^{-1}$ , and this usually results in  $\tau_c \approx 10^{-12}$ – $10^{-13}$  s. Metal ions that induce this situation (Case 2) include Co(II), Ni(II), Fe(II), Fe(III), and most Ln(III) ions. The resultant values of  $T_{1M}^{-1}$  [from equation (17)] in this latter case (Case 2) are about two orders of magnitude less than in Case 1. The ions included in Case 1 are therefore essentially relaxation probes. The relative inefficiency of the Case 2 metal ions in causing relaxation causes the linewidth to remain relatively sharp, thus enabling chemical shift effects to be measured. Hence they are essentially shift probes.

The enhanced proton relaxation rates are normally assumed to vary with  $r^{-6}$  [equation (17)] where  $r$  is the distance from the metal to the nucleus under study. This, however, is only the case when the dipolar term [equation (18)] is the dominant contributor to the line-broadening. It has been pointed out that this may not be the case when using Mn(II) and Cu(II) particularly at high ligand to M(II) molar ratios. (557, 558) In such cases binding sites and distances may be estimated from selective  $T_1$  measurements, provided that it is established that the predominant dipolar interaction contributing to relaxation is that between the paramagnetic ion and the affected nucleus, and other, closer, interactions from unpaired spin density on the ligand do not contribute to any great extent. Whereas the effectiveness of the relaxation probes varies as  $r^{-6}$  and is *not* direction dependent, the shift probes induce shifts that are direction dependent and vary as  $r^{-3}$  [equation (13)] (assuming no appreciable contact interaction). Using a combination of relaxation and shift probes, a detailed three-dimensional mapping of the substrate conformation(s) can be built up. This has been impressively demonstrated in the case of protein conformations (see below).

A different approach to the study of the solution conformation of proteins, involving measurements of  $^{139}\text{La}$  relaxation rates, has been

TABLE XVII

Paramagnetic NMR perturbation probes (554)

Site of binding	Probe	Example of use	Ref.
(a) <i>Relaxation probes</i>			
General cation binding site	Gd(III), Mn(II), Fe(III), Cr(III), Cu(II), VO(II)	Transferrin, phospholipase A.2	
General anion binding site	[Gd(dipic) <sub>3</sub> ] <sup>3-</sup> , [Cr(CN) <sub>6</sub> ] <sup>3-</sup> , [Cr(oxalate) <sub>3</sub> ] <sup>3-</sup> , and EDTA complexes of above cations	Cytochrome-c	663-668
General neutral binding sites	[Cr(acac) <sub>3</sub> ]	Membranes	778-782
Neutral organic grouping	Nitroxide radicals	Lysozyme inhibitors	
(b) <i>Shift probes</i>			
General negatively charged site	Ln(III) [excluding Gd(III), La(III), and Lu(III)]	Lysozyme Ribonuclease Membranes	564, 583  778-782
General positively charged site	[Ln(III)EDTA] <sup>-</sup> [Fe(III)(CN) <sub>6</sub> ] <sup>3-</sup>	Membranes Lysozyme	778-782 564, 583
Intrinsic site	Fe(III)haem	Cytochrome-c	663-668
Neutral site	Organic shift reagents	Interior of membranes	

developed theoretically and experimentally. Reuben and Luz (634) have shown that a protein will induce frequency dependent enhancements in the  $^{139}\text{La}$  relaxation rates. In the case of bovine serum albumin (BSA) this occurs through the rapid exchange of  $\text{La}^{3+}$  between its aquo and BSA complexes.

In solutions of biologically important molecules proton relaxation measurements are normally made on the solvent water molecules, and the extent to which the relaxation is enhanced when paramagnetic ions are present is measured. This proton relaxation enhancement (PRE) technique is most valuable when used as a titration indicator to obtain metal-protein binding data but less useful for molecular dynamics studies since a large number of variable parameters are involved in the best fitting procedure. It has been suggested (655) that a more suitable and simpler method is one based on solvent proton-deuteron comparative relaxation measurements made at a limited number of different magnetic fields. The method, which is based on a suggestion of Reuben, (636) was applied to the protein immunoglobulin G (IgG) in the presence of  $\text{Gd}^{3+}$  ions, and yielded reliable values of the ion hydration number, the residence lifetime of water molecules in the hydration sphere of the ion, and a correlation time for a portion of the IgG molecule.

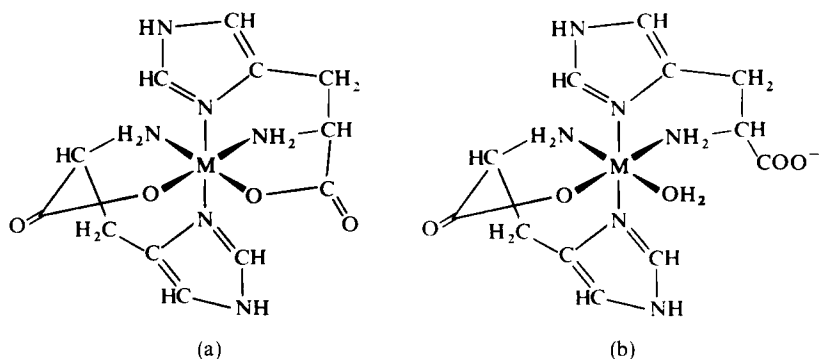
### *1. Amino-acids, peptides, and proteins*

A number of review articles have appeared. (560–564) One of these (563) discusses the problems of using computerized searches for the most likely conformations of flexible molecules. Generally, a single conformation is not preferred but rather a set or family of conformations. Conformational studies of a variety of Ln(III) complexes of amino-acids and peptides have been discussed. The lanthanides La(III) to Dy(III) are bound to carboxylate ligands in a bidentate manner whereas the other lanthanides, typified by Tm(III), are bound through a single oxygen.

The conformations and binding sites, usually based on the selective broadening of Cu(II) ions, have been measured for a wide range of amino-acid and peptide complexes. (565–573, 600–602) Some of these results must be questionable in view of the above-mentioned (557) limitations of Cu(II) as a relaxation probe. Beattie *et al.* (574) have also expressed serious doubts as to the usefulness of Cu(II) as a preferential broadening agent. They claim that: (i) the Cu(II) species involved in the broadening are not normally properly characterized, (ii) exchange lifetime broadening is not normally distinguished from other relaxation effects, and (iii) the relative contributions of scalar and dipolar interactions to the relaxation mechanisms are not normally established. They have

tested these three points on the Cu(II)–glycine (G) system and found firstly that, in addition to the species  $\text{CuG}^+$  and  $\text{CuG}_2$ ,  $\text{CuHG}^+$ ,  $\text{CuHG}_2^+$ , and  $\text{CuG}_3^-$  are also present. Secondly, these species undergo slow exchange over several pH units, contrary to the usual assumption of fast exchange in such systems. Thirdly, proton  $T_1$  and  $T_2$  measurements show that dipolar interactions make negligible contributions to the observed line-broadenings. Thus for  $^1\text{H}$  studies on glycine, Cu(II) fails on all three counts as a suitable line-broadening agent for structural purposes.

The advantages of using line-broadening probes for inducing  $^{13}\text{C}$  rather than  $^1\text{H}$  relaxation have been pointed out (575) and the technique applied to a Mn(II) complex (575) and Ni(II) complexes (576) of histidine. The spin–lattice relaxation of the  $^{13}\text{C}$  nuclei is dominated by the dipolar interaction whereas the paramagnetic contribution to the spin–spin relaxation is controlled by scalar interaction. Distances between the M(II) ion and the individual carbon atoms are evaluated from the dipolar relaxation terms and indicate octahedral bis(histidino)metal(II) complexes as shown in [56(a), (b)]. The  $\text{Mn}^{2+}$  complex exists as [56(a)]



[56]

whereas the  $\text{Ni}^{2+}$  ions produce two complexes in abundance ratio 1:0.08 at 298 K with the more abundant species being of type [56(a)]. Complexes of Mn(II) with peptides and amino-acids have been examined by both NMR and ESR, and dynamic aspects of their equilibria in aqueous solution reported. (577, 578) Both  $^1\text{H}$  and  $^{13}\text{C}$  LIS values are reported for alanine. (579) The values suggest monodentate coordination geometry for the lanthanides  $\text{Pr}^{3+}$  to  $\text{Tb}^{3+}$  and a bidentate carboxyl coordination for  $\text{Dy}^{3+}$  to  $\text{Yb}^{3+}$ . Various lanthanide probes have been used for studying the conformations of linear and cyclic peptides. (580–582)



The transition from amino-acids and peptides to proteins represents a major jump in complexity from the point of view of NMR spectroscopy. Nevertheless, considerable progress has been made during the past 5 years both in the U.K. and the United States in interpreting both the  $^1\text{H}$  and  $^{13}\text{C}$  spectra of proteins and obtaining conformational information. The Oxford Enzyme Group have placed their emphasis on  $^1\text{H}$  spectral studies whereas natural abundance  $^{13}\text{C}$  spectroscopy of proteins has been pioneered by Allerhand *et al.* (696–698) Great strides have been made in trying to unravel the spectral complexities of the protein enzyme lysozyme. (564, 583, 584) This protein, consisting of a chain of 129 amino-acids, presents a daunting problem. Nevertheless by utilizing many established assignment methods (e.g. double resonance, multiplet splittings, pH titrations, site-specific paramagnetic probes) and the resolution enhancement technique of convolution difference spectroscopy (585) more than forty  $^1\text{H}$  signals have now been assigned to specific amino-acid residues. It has also been established that the fold of the protein is the same in solution as in the crystalline state. More recently the assumption of axial symmetry for the lanthanide ion complexes with lysozyme has been seriously questioned (588) since the shifts induced by  $\text{Nd}^{3+}$  and  $\text{Ce}^{3+}$  exhibit considerable non-axial character.

The plant lectin concanavalin A, a metalloprotein isolated from the jack bean, has also received considerable attention. (588–590, 630, 631) Using the stopped flow NMR technique three distinct conformational states of the protein, when it is bound to  $\text{Mn}^{2+}$ ,  $\text{Ca}^{2+}$ , and  $\alpha$ -methyl-D-mannoside, (630) have been deduced.

The copper proteins, plastocyanins, which play a key role in electron transfer processes associated with photosynthesis, have been examined using high frequency (i.e. 250 and 270 MHz) NMR methods. (591, 592) The copper binding stabilizes the organic structure but does not cause any major reorganization of it. (591) Exchange between the paramagnetic  $\text{Cu(II)}$  form and the diamagnetic  $\text{Cu(I)}$  form is slow on the NMR time scale. (592) The copper protein azurin and its cobalt analogue have been examined by  $^1\text{H}$  NMR. (593, 594)

The vitamin  $\text{B}_{12}$  and related coenzymes (cobalamins, cobinamides, and corrinoids) have been studied in detail using  $^1\text{H}$  and  $^{13}\text{C}$  shift and relaxation studies. (595–598) With the aid of lanthanide probes the conformations of cobalamins in solution are shown to be very similar to those in the crystalline state. The appreciable temperature dependences of the electronic and  $^1\text{H}$  NMR spectra are attributed to a conformational change rather than to a 6-coordinate–5-coordinate equilibrium as previously suggested. (599) The binding of 5'-ATP to the respiratory protein hemocyanin has been studied by  $^1\text{H}$  and  $^{31}\text{P}$  NMR.

The results suggest that the copper at the oxygen-binding site is at least partly Cu(II) but no Cu(II) ESR signal has been detected. (728)

The use of paramagnetic probes for investigating the active sites of enzymes has greatly increased of late, and only a representative set of references is reported here. The usual aims of these studies include establishing the number, the nature, and the configurations of the active sites, deducing the environment of the bound metal ion, and calculating the binding constant(s). Such studies have been carried out on ribulose 1,5-diphosphate carboxylase, (603) D-xylose isomerase, (604) galactose oxidase, (605) bovine pancreatic trypsin inhibitor, (606–608) carbonic anhydrase, (609–611) pyruvate kinase, (612–616) glutamine synthetase, (617–620) carboxypeptidase B, (621) arginine kinase, (622) and other miscellaneous enzymes. (623–629)

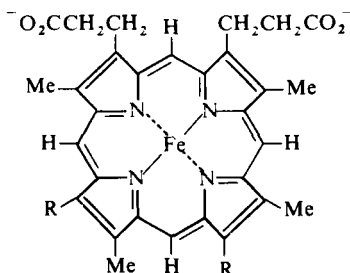
## *2. Paramagnetic porphyrins and heme proteins*

This section firstly includes discussion of the NMR properties of certain paramagnetic porphyrins and is then concerned with recent developments in the study of the heme proteins cytochrome c and myoglobin, both of which comprise single polypeptide chains to which a protoporphyrin IX is bound, and hemoglobin which consists of four subunit heme polypeptides.

A book including a survey of NMR studies of porphyrins and metalloporphyrins has appeared. (637) Iron porphyrins may involve Fe(II) and Fe(III) with both high and low spin states of iron. All are paramagnetic except those of low-spin Fe(II).

Low-spin Fe(III) porphyrins have been the subject of a number of studies. (638–650) The favourably short electronic spin–lattice relaxation time and appreciable anisotropic magnetic properties of low-spin Fe(III) make it highly suited for NMR studies. Horrocks and Greenberg (638) have shown that both contact and dipolar shifts vary linearly with inverse temperature and have assessed the importance of second-order Zeeman (SOZ) effects and thermal population of excited states when evaluating the dipolar shifts in such systems. Estimation of dipolar shifts directly from *g*-tensor anisotropy without allowing for SOZ effects can lead to errors of up to 30% in either direction. Appreciable population of the excited orbital state(s) produces temperature dependent hyperfine splitting parameters. Such an explanation has been used to explain deviations between the measured and calculated shifts in bis-(1-methylimidazole) (641) and pyridine complexes (642) of ferriporphyrins. In the former complexes the contact shifts are considered to involve directly delocalized  $\pi$ -spin density

arising from  $\text{Fe(II)} \rightarrow \text{imidazole } \pi^*$  charge transfer. Such  $\pi$  bonding suggests a possible role for axial histidylimidazole in electron transfer in cytochromes. (644) Bis-(4-substituted pyridine) complexes of tetraphenylporphyrin and octaethylporphyrin are exclusively in the low-spin ( $S = \frac{1}{2}$ ) state. The shifts for both the porphyrin and axial ligand protons are very sensitive to the basicity of the substituted pyridine. The contact shifts reflect a decrease in porphyrin  $\rightarrow$  iron  $\pi$  charge transfer as the ligand basicity is lowered. The solvent dependence of the shifts (648) indicates that increased hydrogen bonding significantly decreases the magnetic anisotropy of the iron and diminishes porphyrin  $\rightarrow$  Fe  $\pi$  bonding. A detailed analysis of  $^{13}\text{C}$  shifts in protoporphyrin IX iron(III) dicyanide [57] has led to evaluation of the parameters  $Q_{\text{CCH}_3}^{\text{H}}$ ,  $Q_{\text{CCH}}^{\text{H}}$ , and



R = H, Deuterioporphyrin IX iron (III)

R =  $-\text{CH}=\text{CH}_2$ , Protoporphyrin IX iron (III)

[57]

$Q_{\text{CCH}}^{\text{C}}$  characterizing the coupling, via hyperconjugation, between  $^1\text{H}$  and  $^{13}\text{C}$  nuclei of the porphyrin side-chains and the unpaired spin density on the aromatic carbons. (646)

The high-spin  $\text{Fe(III)}$  porphyrins typically yield poorly resolved spectra. This arises indirectly from the fact that such complexes involve 5-coordinate iron with the latter out of the porphyrin plane. On addition of a sixth ligand a low-spin  $\text{Fe(II)}$  ( $S = 0$ ) or  $\text{Fe(III)}$  ( $S = \frac{1}{2}$ ) complex results with the iron sited in the porphyrin plane again. The broadened lines for certain porphyrin protons arise from shorter  $T_2$  values which reflect the motion of the iron atoms relative to the heme plane. A possible mechanism for this inversion process, involving halogen exchange, is illustrated in Fig. 12. (651) The high-spin  $\text{FeX}_3$  ( $\text{X} = \text{halogen}$ ) complexes of tetra-*p*-tolylporphyrins show concentration-dependent line-widths and chemical shifts indicating significant aggregation in solution. (652)

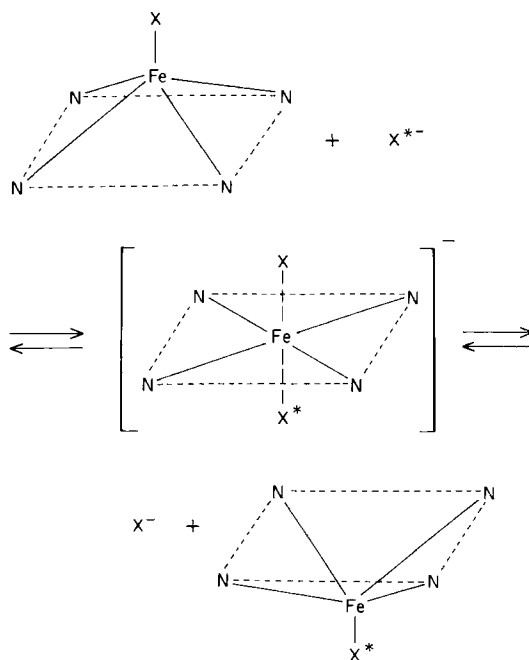


FIG. 12. Mechanism for porphyrin inversion via halogen exchange. (651)

The magnetic, electronic, and spectroscopic properties of Fe(II) porphyrins are less well known. The low spin complexes are diamagnetic whereas the paramagnetic Fe(II) complexes may exist in either high spin ( $S = 2$ ) or intermediate spin ( $S = 1$ ) states. Rigorously anaerobic conditions are necessary in order to study ferrous porphyrins. Octaethylporphyrin iron(II), deuteroporphyrin IX iron(II) dimethyl ester, and other ferrous porphyrins have been shown (653) to exist in the  $S = 1$  spin state in non-polar solvents. The isotropic shifts have been analysed using fluorine-substituted tetraphenylporphins as probes. The proton contact shifts arise from a predominant  $\pi$ -spin delocalization mechanism, and the dipolar shifts are large compared with other metalloporphyrins. This is thought to arise from the absence of orbital quenching in these square-planar complexes which results in a large anisotropy of the magnetic susceptibility tensor. Similar conclusions are reached in the case of tetraphenylporphyrin iron(II) and derivatives. (654) The NMR shifts are only compatible with an  $S = 1$  ground state. Large  $\pi$  contact shifts strongly support the ground state configuration  $(d_{xy})^2(d_z^2)(d_{xy}, d_{yz})^2$ . In contrast, the isotropic shifts for a variety of high spin ( $S = 2$ ) complexes are predominantly of a  $\sigma$ -contact nature. (654a)

Other paramagnetic ions that can be incorporated in the porphyrin ring include Mn(III), Fe(III), Co(II), Ni(II), Cu(II), and Ag(II). Of these ions Co(II) is the best shift probe, and Fe(III) and Mn(III) the best relaxation probes. This whole series of ion probes was used to study a variety of porphyrin-caffeine complexes. (655) Shift and line-broadening data suggest that the solution structures are of the plane-to-plane type with the metal situated above nitrogen-9 of the caffeine ring.

Manganese(III) complexes of the general type  $[\text{Mn}(\text{Por})\text{ClH}_2\text{O}]$ , where Por is etioporphyrin I, mesoporphyrin IX dimethyl ester, and others, have been shown (656) to be present as high spin ( $S = 2$ ) complexes in  $\text{CDCl}_3$  solution. Methyl protons attached to the porphyrin rings are shifted *ca.* 30 ppm to high frequency and methine-bridge protons *ca.* 20 ppm to low frequency of their diamagnetic positions. Isotropic shifts of protons in high spin Mn(III) porphyrin complexes are predominantly contact in origin, reflecting extensive porphyrin-to-metal  $\pi$  bonding, and are similar to the shifts of low spin Fe(III) complexes. (657) There have been several reports on Co(II) porphyrin complexes. (658–662) Weak molecular complexes of Co(II) porphyrins are formed with 1,3,5-trinitrobenzene (TNB), (658, 661) various quinones, (659) and 2,4,7-trinitrofluorenone. (662) The formation of these  $\pi$  complexes causes sizeable changes in dipolar shifts, the magnetic anisotropy increasing markedly in the presence of  $\pi$ -acceptors such as TNB and decreasing in the presence of a donor (e.g. *N,N,N',N'*-tetramethyl-*p*-phenylenediamine). The solution structure of the TNB was uniquely determined (661) and found to be that of a peripheral complex (arising from pure  $\pi$ - $\pi$  interaction) with an interplane spacing of  $320 \pm 20$  pm and with TNB centred approximately over a pyrrole. Analogous Ni(II) porphyrin complexes have been examined. (659, 662)

The globular protein cytochrome c has been the subject of extensive NMR study for many years. The protein exhibits stable oxidized and reduced forms. The oxidized form, ferricytochrome c, involves low spin Fe(III) ( $S = \frac{1}{2}$ ), whereas the reduced form, ferrocytochrome c, has low spin Fe(II) ( $S = 0$ ) and is diamagnetic. By 1973 partial analyses had been made of the  $^1\text{H}$  (663) and  $^{13}\text{C}$  spectra (664) of the oxidized and reduced forms of the horse heart protein. In the 220 MHz  $^1\text{H}$  spectrum of ferrocytochrome c signals of His-18, Met-80 (heme iron ligands), and porphyrin meso protons were firmly assigned. The  $^1\text{H}$  spectrum of ferricytochrome c revealed 15 contact shifted signals outside the central region of which 14 were tentatively assigned. Natural abundance  $^{13}\text{C}$  spectral studies of ferrocytochrome c showed 22 narrow single-carbon signals and 6 narrow two-carbon signals. A mixture of the oxidized and

reduced forms of the protein indicates fast electron transfer since many of the signals thought to be due to the carbons near the iron atom exhibit exchange broadening. Other  $^{13}\text{C}$  studies (665, 665a) have shown that the  $[2-^{13}\text{C}]$ carboxymethylcytochrome c is markedly different in structure from the starting cytochrome c.

A detailed  $^1\text{H}$  study of *P. aeruginosa* cytochrome c-557 has been made (666) with the aid of the convolution difference technique. (585) A partial analysis has been reported and the structure of this cytochrome is shown to have many features in common with the mammalian cytochromes c despite having 20–25 fewer amino-acids.

From the addition of *ca.* 1 % of ferricytochrome c-551 to a solution of ferrocytochrome c-551 appreciable broadening of the heme meso, heme methyl, Met-61, and His-16 signals occurs, from which a bimolecular rate constant for the electron exchange process of  $1.2 \times 10^7 \text{ M}^{-1} \text{ s}^{-1}$  is calculated. (667) Such electron exchange is enhanced by having the iron hexacyanides  $\text{K}_3\text{Fe}(\text{CN})_6$  and  $\text{K}_4\text{Fe}(\text{CN})_6$  present. (668) In aqueous solution the  $^1\text{H}$  spectrum reveals 12 well resolved resonances due to exchangeable peptide protons in reduced cytochrome c and a smaller number of resonances due to partial exchange in the oxidized protein. (731) Proton relaxation studies of  $\text{H}_2\text{O}$  protons in aqueous solutions of acid ferricytochrome c suggest that concomitantly with the low-spin–high-spin transition the His-18 and Met-80 Fe(III) bonds break simultaneously. (669)  $^{15}\text{N}$  studies have recently been made (670, 671) in order to study cyanide binding to various hemoproteins (cytochrome c, myoglobin, hemoglobins). The  $^{15}\text{N}$  isotropic shift of  $-\text{C}^{15}\text{N}$  is a most sensitive probe for characterizing the ligand binding or the environmental structure of the prosthetic groups.

Detailed investigations of the oxidized and reduced forms of cytochromes  $\text{b}_2$  and  $\text{b}_5$  have been made. (672, 673) Quite striking structural similarities between the two proteins are revealed. Cytochrome  $\text{b}_5$  appears to exist in aqueous solution as two different molecular species. (673)

Myoglobin (Mb) is a protein consisting of a single polypeptide chain of amino-acid residues to which a protoporphyrin IX heme group is coordinatively bound by a histidine residue. The iron atom can be present as *either* Fe(II) with  $S = 2$  (Mb) or  $S = 0$  (oxymyoglobin) *or* Fe(III) with  $S = \frac{5}{2}$  (metmyoglobin,  $\text{Mb.H}_2\text{O}$ ) or  $S = \frac{1}{2}$  (cyanoferri-myoglobin,  $\text{MbCN}$ ).

Deoxymyoglobin is a high spin ferrous hemoprotein and its  $^1\text{H}$  100 and 220 MHz spectra exhibit a large number of hyperfine shifted lines. Comparison of the two spectra shows that the widths increase

markedly with increasing applied magnetic field. (674) This is explained in terms of a Curie spin relaxation process. (675)

In the case of Fe(III) myoglobins, the low spin protein cyanoferrimyoglobin has been most studied. Horrocks and Greenberg (676) have presented a general method for evaluating principal magnetic susceptibilities and dipolar shifts in  $d^5$  low spin hemin systems and have applied the method to cyanoferrimyoglobin and ferricytochrome. Selective deuteration techniques have enabled three of the four hyperfine shifted heme methyl signals of cyanoferrimyoglobin to be assigned with certainty. (677) Other  $^1\text{H}$  studies have been directed towards studying acid-base transitions, (678) pH-dependent spin state changes, (679) and restricted rotation of heme side-chain methyl groups. (680) Ionic additives such as sodium chloride caused a release of this restricted motion which may therefore be due to the salt bridge around the heme side-chain environment. It is suggested that monitoring of this rotation barrier may serve as a sensitive probe for detecting van der Waals contacts or steric interactions between the heme side-chain and the apoprotein.

A number of  $^{13}\text{C}$  studies of cyanoferrimyoglobins have been reported. (681–684, 697) In one study (682) using  $^{13}\text{C}$  enriched methionine methyl groups, the signals due to Met-55 and Met-131 are assigned with some certainty. Spin-lattice relaxation time measurements of the methionine carbon signals show that the two methionine side-chains undergo continuous variations in environment, which are controlled by events at a distance within the protein structure. Allerhand *et al.* have examined the titration behaviour of histidine residues (683) and *N*-terminal glycine residues. (684) In horse cyanoferrimyoglobin (Fig. 13) eight of the eleven histidine residues exhibit titration behaviour with  $pK$  values in the range 4.4–6.6. (683)

Histidine titrations have also been performed on the high spin protein metmyoglobin. (685) Four proton resonances were examined as a function of pH and ionization constants evaluated. The addition of azide ions causes extensive changes in the spectra indicating conformational changes affecting several imidazole side-chains.

Leghemoglobins, monomeric heme proteins containing one heme per molecule, qualitatively resemble myoglobins in their oxygen and ligand binding properties. NMR studies on ferric soybean leghemoglobin a, its cyanide complex, and the oxygen and carbon monoxide complexes of the ferrous protein have been discussed. (730)

The NMR technique is continuing to probe the profound complexities of the structure of hemoglobin (Hb) and a review of recent work has appeared. (686) High field  $^1\text{H}$  studies have usually been aimed

(a)

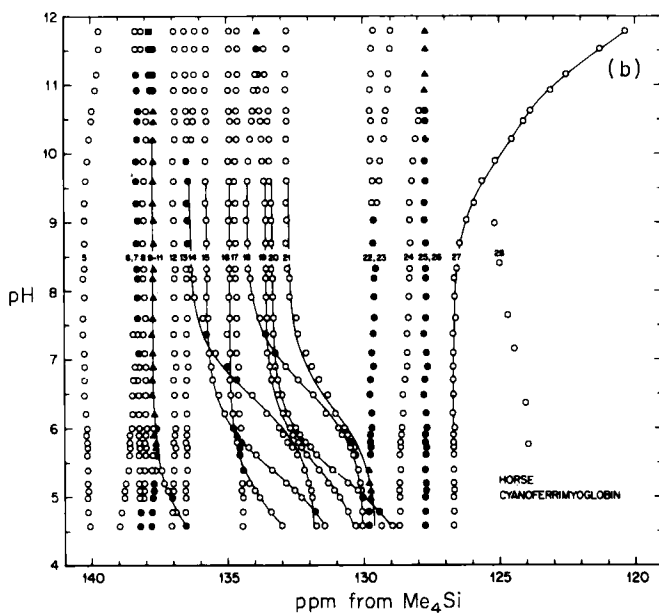
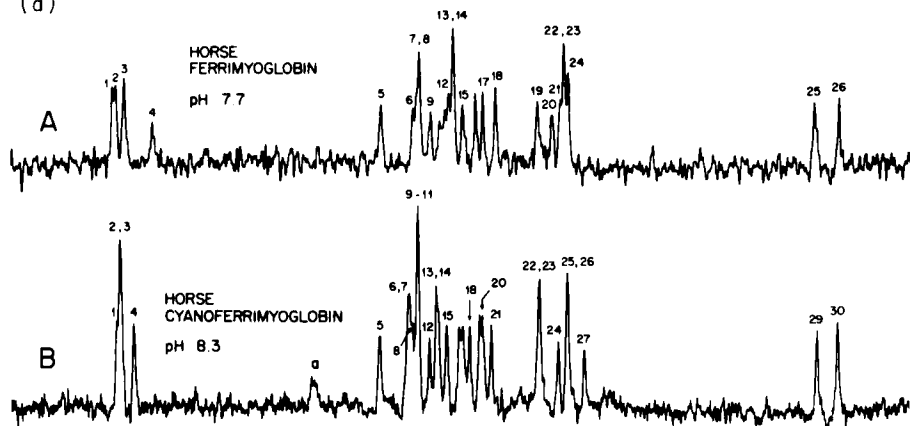


FIG. 13. (a) Aromatic carbon region in the convolution-difference natural abundance  $^{13}\text{C}$  spectra of myoglobins recorded at 15-18 MHz, under conditions of noise-modulated off-resonance decoupling and 32 768 accumulations per spectrum. See ref. 683 for line assignments. (b) The eight titratable carbons of the histidine residues (plus  $\text{C}^\gamma$  of Tyr-103, peak 27) of horse cyanoferrimyoglobin at  $38^\circ\text{C}$ .



at investigating the conformational properties of the  $\alpha$  and  $\beta$  chains of amino-acid residues, the magnetic properties of the protein in solution, and the role of oxygen binding. Progress has been made with the assignment of the proximal histidine proton signals in hemoglobin and deoxymyoglobin. (687) Various cyanide, azide, imidazole, and deuterioxide complexes of myoglobin and hemoglobin were studied by variable temperature  $^1\text{H}$  NMR methods. Most of the complexes exhibit abnormal temperature dependence of the hyperfine shifted lines which can be explained by invoking a spin equilibrium between low ( $S = \frac{1}{2}$ ) and high ( $S = \frac{5}{2}$ ) spin states of iron. (688, 689) The dicyanide complexes of deuterio-Hb are low spin. In aqueous solution a slow exchange is shown to occur between such complexes and high spin dihydroxy aquo complexes. (690, 691)

Cooperative oxygen binding in hemoglobin is thought to depend on the existence of two conformational states associated with distinct quaternary structures of deoxy and ligated hemoglobins. These two states are labelled T and R respectively. The switch between the two states has been studied in des-Arg-Hb. A distinct spectral change occurs around pH 9 from which it is inferred that the  $\text{T} \rightleftharpoons \text{R}$  interconversion rate may be as slow as  $10^4 \text{ s}^{-1}$ . (692) Oxy-deoxy titrations are commonly followed by the titration behaviours of histidine signals. However, sometimes the signal movements are discontinuous and correlations of the signals due to the oxy and deoxy forms are not possible. A method that is based on a simple chemical exchange model and requires that the rate of exchange between ligated and unligated hemoglobin be faster than  $T_1^{-1}$  has been developed. (714) A study of the relative oxygen binding to the  $\alpha$  and  $\beta$  subunits of human adult Hb has revealed no large affinity difference. (693) However, in the presence of organic phosphates preferential oxygen binding to the  $\alpha$ -hemes is indicated. (694) Oxygen binding of Co(II)-porphyrin complexes, which are models for the active site in Co-substituted Hb, was measured and compared with other porphyrins and the protein. Negligible enhancement of the oxygen affinity of a Co(II)-porphyrin is found when an axial base is covalently attached. (695)

$^{13}\text{C}$  studies of hemoglobins have been primarily concerned with the diamagnetic carbon monoxide hemoglobins. (698–701) Paramagnetic ferrihemoglobins give less well resolved spectra with heme carbon resonances not being detected. (698) Separate  $^{13}\text{C}$  signals can be resolved for  $^{13}\text{CO}$  bound to the hemes of the  $\alpha$  and  $\beta$  hemoglobin chains although the dependence of the bound  $^{13}\text{CO}$  shift on variations in heme environment is rather small. (699) A more sensitive  $^{13}\text{C}$  labelled ligand is ethyl isocyanide ( $\text{C}_2\text{H}_5\text{N}^{13}\text{C}$ ). (702) Three separate  $^{13}\text{C}$

signals of the ligand can be assigned to the ligand bound to  $\alpha$ ,  $\beta$ , and  $\gamma$  subunits of the protein.

A development in the theory of nuclear relaxation in macromolecules by paramagnetic ions has been suggested by Guéron. (675) In the case of heme proteins there is a net polarization of the iron electronic spin magnetic moment which is oriented along the direction of the magnetic field. Modulation of this dipolar field due to the spin polarization (Curie spin) by rotational diffusion introduces an additional term into the expression for transverse relaxation [equation (18)] giving:

$$1/T_2 = (4/5)\Delta^2 S_c^2 \tau_r + (7/15)\Delta^2 S(S+1)T_{1e} + 1/T_2(\text{diamag}) \quad (53)$$

where

$$\Delta = \gamma_I g \mu_B / r^3, \quad S_c = g \mu_B S(S+1) B_0 / 3kT.$$

The first term is the Curie spin term and the second term the usual dipolar expression. It follows that the Curie spin linewidth contribution should exhibit a field dependence of  $B_0^2$  and a temperature dependence of  $\tau_r/T^2$ . Since for Brownian diffusion:

$$\tau_r = (4\pi a^3 / 3kT) \eta \quad (54)$$

where  $a$  is the molecular radius and  $\eta$  is the solvent viscosity, the Curie spin term should have a temperature dependence of  $\eta/T^3$ . This theory has been tested on deoxymyoglobin ( $S = 2$ ), deoxyhemoglobin ( $S = 2$ ), azidometmyoglobin ( $S = \frac{5}{2}, \frac{1}{2}$  mixture), and cyanomethemoglobin ( $S = \frac{1}{2}$ ) and found to account adequately for the field and temperature dependences of the heme methyl signals of the  $\alpha$  and  $\beta$  chains. (703) The spin-lattice relaxation time  $T_{1e}$  is calculated to be  $\sim 6.1 \times 10^{-12}$  s for deoxy-Mb and deoxy-Hb. Other proton relaxation studies of hemoglobin solutions have provided data on the frequency, field, temperature, and protein concentration dependences of the  $T_1$  and  $T_2$  values. (704–707) In one of these studies (707) an attempt was made to calculate the distance of the bound  $H_2O$  protons from the sixth coordination site of the heme Fe atom. The binding of other solvents, and in particular inositol hexaphosphate, to human hemoglobins has been reported. (708–711) In a study of the temperature dependence of the solvent  $T_1$  values it was concluded (712) that the  $\beta$ -heme pocket is tighter than the  $\alpha$ -heme pocket. Nitric oxide is a powerful relaxation probe which binds to the heme Fe(II) atom and causes a widening of the heme pocket. (713) The measurement of the magnetic susceptibilities of weakly paramagnetic heme proteins has been considered by comparing the NMR and Gouy methods. For methemoglobin the NMR method is

definitely preferable but for other heme proteins it is insensitive and rather inaccurate. (729)

Comparisons of NMR spectra of normal and mutant hemoglobins can often throw light on the line assignments particularly when the structural difference between the two forms is well established. Two mutant hemoglobins HbM Iwate and Hb Kansas have been examined (715, 716) in order to obtain information on the ligand-binding properties of the deoxy quaternary state since the existence of this state has been established by X-ray crystallography. Comparisons of spectra of normal Hb with a variety of mutant Hbs having single amino-acid substitutions have enabled progress to be made in explaining the changes in the tertiary structure around the heme groups during the cooperative oxygenation process. (717)

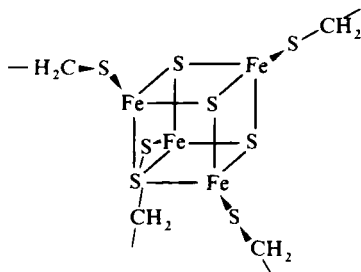
The well known mutant hemoglobin sickle cell hemoglobin HbS differs from normal adult hemoglobin only in the replacement of a glutamic acid residue by a valine residue in the  $\beta$ -chain of the protein. NMR studies have been directed towards finding conformational or other structural differences between HbS and Hb which might explain the low oxygen affinity of the mutant species.  $^1\text{H}$  and  $^{31}\text{P}$  studies (718–720) have revealed small but distinct differences in the histidyl residues of the two species. Addition of 2,3-diphosphoglycerate to both Hb and HbS produced distinct differences in the spectra of both proteins. The results suggest that some of the surface residues of HbS differ from Hb in being in a more hydrophobic environment and this may be related to the gelation properties of HbS. Distinction between Hb and HbS is achieved from  $T_{1\rho}$  measurements of the proteins. (721) Other mutant Hb species to be studied include HbM Milwaukee (722, 723) and Friend leukemic cell Hb-CO. (724, 725) In the latter case  $^{15}\text{N}$  studies were carried out on the mutant Hb specifically  $^{15}\text{N}$ -enriched in the glycyl residues. Numerous  $^{15}\text{N}$  resonances due to such residues with different conformations and modes of hydrogen binding were detected.

The dramatic progress of the NMR technique in the study of living tissues is reflected here by  $^1\text{H}$  studies of living tunicate blood cells (726) and  $^{31}\text{P}$  studies of the binding of 2,3-diphosphoglycerate to Hb in intact human erythrocytes. (727) In the first mentioned study a broad high frequency signal is observed which disappears on cell disruption. This is thought to be due to a labile V(III) aquo complex contained in the cell vacuoles.

### 3. Iron-sulphur proteins

Members of this important class of proteins play key roles in

photosynthesis, nitrogen fixation, and hormone biosynthesis. A number of review articles dealing with NMR investigations of iron-sulphur proteins up to around 1973 are available. (732–735) NMR studies have been most concerned with bacterial and plant ferredoxins. The former contains two ‘cages’ of four iron atoms and four inorganic sulphur atoms [58] whereas the latter is thought to



[58]

involve two iron atoms linked by two sulphurs and coordinatively bound to the apoprotein via the sulphurs of four cysteine residues.

Magnetic susceptibility and  $^1\text{H}$  NMR studies (736) of ferredoxin I from *Bacillus polymyxa* indicate that in the oxidized protein antiferromagnetic coupling occurs between component iron atoms which is similar to that observed for clostridial ferredoxins. Contact shifted resonances of the oxidized and reduced forms of the *B. polymyxa* protein have been correlated with those of the clostridial ferredoxins. A study of a partly reduced *B. polymyxa* ferredoxin indicates a slow electron exchange between redox forms which suggests that fast electron exchange previously observed in the clostridial ferredoxins may be due to an intramolecular process. A study of the exchange rates for slowly exchangeable amide protons of algal ferredoxin yields data consistent with an  $\alpha$ -helical and  $\beta$ -pleated sheet conformation for the secondary protein structure. (737)

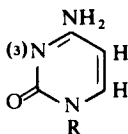
$^{13}\text{C}$  spectral studies of *Clostridium acid-urici* and *Clostridium pasteurianum* ferredoxins have enabled the two  $\text{Fe}_4\text{S}_4^*$  clusters within each protein to be distinguished. The  $^{13}\text{C}$  results suggest that the midpoint oxidation–reduction potentials of the two  $\text{Fe}_4\text{S}_4^*$  clusters in *C. pasteurianum* and *C. acid-urici* differ by  $10 \pm 5$  mV and  $<10$  mV respectively. (738) This is thought to be due to different conformational changes in the vicinity of at least one of the  $\text{Fe}_4\text{S}_4^*$  clusters. The same authors (739) have used  $^1\text{H}$  NMR spectra to detect the cysteinyl protons, the slowly exchangeable protons, and the aromatic protons of

*C. acidu-urici* ferredoxin and several other ferredoxins. NMR has also been used to characterize three forms of ferredoxin from the sulphate reducing bacteria of *Desulfovibrio gigas*. (740) One of these ferredoxins is tetrameric and its interaction with cytochrome  $c_3$  has been followed. (741)

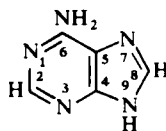
Laboratory syntheses have been achieved for a variety of tetranuclear clusters  $[\text{Fe}_4\text{S}_4(\text{SR})_4]^{2-}$  ( $\text{R} = \text{alkyl or aryl}$ ) which are close representations of the active sites of iron-sulphur proteins. Proton NMR studies of these species (742, 743) have revealed that the magnitudes and temperature dependences of the  $-\text{CH}_2-\text{S}-$  shifts are very similar to those of the high frequency shifted resonances of the proteins. The isotropic shifts are predominantly contact in nature, their temperature dependences being related to the antiferromagnetic properties of the clusters. (744) A recent report of a molybdenum-iron-sulphur species  $[\text{Fe}_6\text{Mo}_2\text{S}_8(\text{SPh})_9]^{3-}$  mentions that its NMR spectrum suggests the absence of antiferromagnetic coupling. (745)

#### 4. Nucleic acids and related molecules

The use of paramagnetic ions to examine the binding sites and solution conformations of nucleosides and nucleotides is becoming very widespread. Studies that describe the complexing of a variety of nucleosides and nucleotides with paramagnetic ions involve the use of  $\text{Mn(II)}$ , (749–751)  $\text{Cu(II)}$ , (750, 752–754) and lanthanide ions. (755)  $\text{Mn}^{2+}$  ions appear to bind to multiple sites on purine and pyrimidine nucleosides (749) whereas the phosphate group is the primary binding site on monophosphate nucleotides. (750)  $^{13}\text{C}$  relaxation studies indicate that  $\text{Cu}^{2+}$  ions bind to N-3 of 5'-cytidine monophosphate (5'-CMP). In contrast to cytidine [59], adenosine [60] appears to have



[59]



[60]

two metal binding sites at N-1 and N-7 with the latter favoured by a factor of about 2. (753) Lanthanide ions are invariably bound to phosphate or pyrophosphate groups of nucleotides. (755)

Numerous studies have been made on the metal binding properties of adenosine-5'-monophosphate (5'-AMP), (756–761) cyclic 3',5'-

AMP, (762) and cytidine-5'-monophosphate (5'-CMP). (763)  $^{13}\text{C}$  spectra indicate that  $\text{Cu}^{2+}$  binds to N-7 of 5'-AMP and 2'-AMP. (756,760) Lanthanide shift and relaxation probes have been used to show that the family of conformations of 5'-AMP in solution which most closely fits the NMR data is very similar to that of the crystal structure of AMP. This work (758) includes a description of the computer program used for the conformational searches. A subsequent study of cyclic 3',5'-AMP (762) (Fig. 14) produced families of solution conformations with the pucker of the phosphate and ribose rings similar to that in an approximate X-ray study of the nucleotide. The solution conformation of 5'-CMP is found (763) to be similar to that of 5'-AMP.

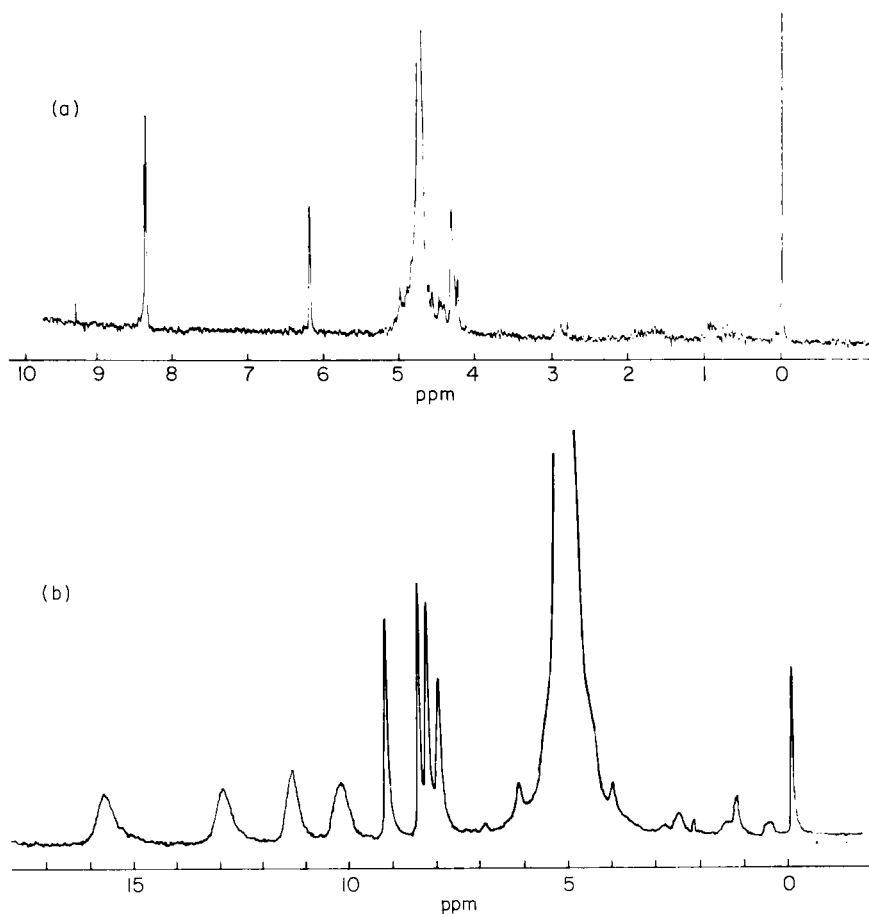


FIG. 14.  $^1\text{H}$  FT spectrum of cyclic 3',5'-AMP (25 mM, pH 2.0) recorded (a) without and (b) with  $\text{Dy}^{3+}$  (43 mM) present when all eight proton signals of cAMP are revealed. (762)

The binding of  $\text{Co}^{2+}$  ions to the adenine nucleotides 5'-AMP, adenosine-5'-diphosphate (5'-ADP), and adenosine-5'-triphosphate (5'-ATP) is found (764) to take place both at the 5'-phosphate and N-7 of the adenine ring. There have been a number of studies (765–768) of the interaction of  $\text{Mn}^{2+}$  ions with ATP using  $^1\text{H}$ ,  $^{13}\text{C}$  and  $^{31}\text{P}$  techniques.  $^{31}\text{P}$  relaxation data (765) are consistent with  $\text{Mn}^{2+}$  forming a complex with ATP which has an average lifetime of  $6.5\ \mu\text{s}$  at  $25^\circ\text{C}$  and where the ion is closer to the  $\beta$  and  $\gamma$  phosphorus atoms than the  $\alpha$  atom.  $^{13}\text{C}$  relaxation data (766) indicate a consecutive binding mechanism involving initial binding to the phosphate groups followed by interaction with N-7 of the adenine ring. The rate constant for the latter interaction is  $2.7 \times 10^7\ \text{s}^{-1}$  at  $27^\circ\text{C}$ .  $^1\text{H}$  NMR data (768) are consistent with an equilibrium between  $\text{MnATP}^{2-}$  ( $>25\%$ ) and  $\text{Mn(ATP)}_2^{6-}$  ( $<75\%$ ). In the 1:2 complex, both adenine H-8 protons are approximately equidistant from the  $\text{Mn}^{2+}$  ion. Both 1:1 and 1:2 complexes of ATP with  $\text{Cu}^{2+}$  ions are found to exist in  $\text{D}_2\text{O}$  solvent. The hydrolysed species  $\text{CuATP(OD)}^{3-}$  and  $\text{CuATP(OD)}_2^{4-}$  are also detected. (769) In another study, ATP and ADP are shown to associate with cytochrome c but no such association occurs with AMP. (770) The nucleotide inosine-5'-triphosphate forms 1:1 complexes with  $\text{Mn}^{2+}$ , the binding occurring at the  $\text{C}=\text{O}$  and N-7 positions. (771)

The structure of tRNA molecules in aqueous solution is being actively pursued by NMR methods. (772) Lanthanide ions ( $\text{Eu}^{3+}$ ,  $\text{Pr}^{3+}$ , and  $\text{Dy}^{3+}$ ) have been used as structural probes for tRNA. The highest frequency resonance (14.4 ppm) is unambiguously assigned to the Watson–Crick base pair  $\text{AU}_6$ . Since this is one of the signals most shifted by the lanthanide ions it is concluded that the strongest metal binding site is close to  $\text{AU}_6$ . (773) A subsequent study (774) using  $\text{Eu}^{3+}$  ions shows that there are at least four strong binding sites. The metal binding is in the fast exchange limit and the binding to different sites is sequential rather than cooperative. More recently, the binding of  $\text{Mn}^{2+}$  ions to tRNA and poly-A has been examined. (775–777) Trace amounts of  $\text{Mn}^{2+}$  cause selective broadening of the tRNA resonances which is thought to be due to specific tertiary interactions. Three of the strong binding sites are the same for both  $\text{Mn}^{2+}$  and  $\text{Mg}^{2+}$  and these sites are located close to the tertiary interactions which are stabilized by the strongly bound metal ions. Poly-A is reported to have one  $\text{Mn}^{2+}$  binding site for every two phosphate groups. (777)

## 5. Membranes

Paramagnetic shift and relaxation probes are proving of great benefit in studying the structures, dynamics, and permeabilities of

phospholipid membranes. A number of reviews, which include reference to paramagnetic probes, have appeared. (778–782)

Lanthanide shift and relaxation probes have been used to distinguish strikingly between protons on the inside and outside of closed bilayers of phosphatidylcholine (lecithin) vesicles. (783) The  $\text{Ln}^{3+}$  ions coordinate to the phosphate head groups and produce appreciable shifts and/or broadenings of the  $-\text{NMe}_3$  signals due to the outer choline resonances (Table XVIII). The data shown imply a dominant dipolar

TABLE XVIII

Isotropic shifts and line broadenings effected by  $\text{Ln}^{3+}$  ions in phospholipid bilayers<sup>a</sup> (783)

$\text{Ln}^b$	Rel. shift, $\Delta^c$	$\Delta\nu_{\frac{1}{2}}$ (Hz)( $-\text{NMe}_3$ ) <sub>outer</sub>	$\chi_{\text{anis}}^d$	Obs. shift, $\Delta$ (ppm)
Pr	-1.0	6.0	-3180	-0.14
Eu			1502	$\leq 0.05$
Tb	-5.8	23.5	-15830	-0.81
Dy	-7.9	( $\geq 30$ )	-24600	( $\sim -1.1$ )
Tm	3.7	17.0	1823	0.52
La	0.0	6.0	0	0.00

<sup>a</sup> Phospholipid concentration 36 mM.

<sup>b</sup>  $[\text{Ln}^{3+}] = 1.1$  to  $1.2$  mM.

<sup>c</sup> Relative to Pr = -1.0.

<sup>d</sup>  $\chi_{\text{anis}} = [\chi_{zz} - \frac{1}{2}(\chi_{xx} + \chi_{yy})]$ .

interaction since the observed shifts correlate well with the solid state magnetic susceptibility anisotropies. It is known that a certain antibiotic X-537A transports alkali metal and alkaline earth cations across membranes. The possibility of its transporting paramagnetic cations was explored (784) using  $\text{Pr}^{3+}$ . Only one signal due to  $-\text{NMe}_3$  protons is observed when  $\text{Pr}^{3+}$  is added to lecithin liposomes containing the ionophore X-537A, implying that the antibiotic allows diffusion of the lanthanide into the interior of the vesicle. The transport rate has been expressed as  $0.221 \text{ Hz min}^{-1}$ . (785)

$^{13}\text{C}$  NMR has been used to study the effects of  $\text{Pr}^{3+}$  on phospholipid membranes, (786) and a combination of  $^1\text{H}$ ,  $^{13}\text{C}$ , and  $^{31}\text{P}$  techniques has provided information on the average distances of paramagnetic ions within the polar head groups of the phospholipid molecules. (787) The effect of bound  $\text{Mn}^{2+}$  on  $T_1$  values of the solvent water protons was studied. (788)

The rotation of the  $\text{Mn}^{2+}$  aquo complex is considered to dominate the relaxation of water protons in bulk solvent when phospholipids are present. In addition to lanthanide ions  $\text{Fe}(\text{CN})_6^{3-}$  is shown to



distinguish between the inner and outer layers of lecithin vesicles by producing low frequency shifts of the outer layer  $-\text{NMe}_3$  groups. (789)  $^1\text{H}$  NMR has recently been applied to the problem of determining the transmembrane asymmetry (the charge difference between external and internal sides of a membrane) of a liposome. (790) The method is found to be more sensitive than the  $^{31}\text{P}$  method.

Proton relaxation studies on chloroplast membranes have been presented. (791) Chloroplasts are the sites for the photosynthetic process, many details of which are still unknown. Manganese is known to be essential for oxygen evolution and thus it is important to be able to monitor manganese in its bound state. Water proton  $T_1$  values in chloroplast thylakoid membrane suspensions were used to monitor membrane-bound manganese. The results indicate that there may be a mixture of manganese oxidation states in the dark-adapted chloroplasts, with  $\text{Mn(II)}$  and  $\text{Mn(III)}$  being the most likely states.

#### REFERENCES

1. G. A. Webb, in "Annual Reports on NMR Spectroscopy", Vol. 3, E. F. Mooney (ed.), Academic Press, London, 1970, pp. 211–259.
2. G. A. Webb, in "Annual Reports on NMR Spectroscopy", Vol. 6, E. F. Mooney (ed.), Academic Press, London, 1975, pp. 1–145.
3. J. R. Wasson and D. K. Johnson, *Analyt. Chem.*, 1974, **46**, 314R.
4. I. H. Sadler, *Ann. Reports Chem. Soc. (B)*, 1972, **69**, 19; 1973, **70**, 22.
5. I. Bertini and L. Sacconi, *J. Mol. Struct.*, 1973, **19**, 371.
6. K. Jackowski and Z. Kecki, *Adv. Mol. Relax. Proc.*, 1973, **5**, 269.
7. H. J. Keller and K. E. Schwarzhans, *Method Chim.*, Vol. 1A, F. Korte (ed.), Academic Press, 1974, p. 395.
8. G. A. Webb, in "NMR of Nuclei Other than Protons", T. Axenrod and G. A. Webb, (eds.), Wiley-Interscience, 1974, pp. 127–142.
9. A. M. Achlama and D. Fiat, in ref. 8, pp. 143–152.
10. R. S. Drago and J. I. Zink, *J. Chem. Educ.*, 1974, **6**, 371–376; **7**, 464–467.
11. L. M. Jackman and F. A. Cotton (eds.), "Dynamic NMR Spectroscopy", Academic Press, New York, 1975. Ch. 9.
12. A. A. Shklyayev and V. F. Anufrienko, *Zh. Strukt. Khim.*, 1975, **16**, 1082.
13. O. A. Gansow and W. D. Vernon, *Topics in C-13 NMR Spectroscopy*, 1976, **2**, 269.
14. L. M. Venanzi, *Chimia*, 1976, **30**, 277.
15. R. B. Jones and L. Phillips, *Ann. Reports Chem. Soc. (B)*, 1974, **71**, 17.
16. C. L. Honeybourne, in "Nuclear Magnetic Resonance", R. J. Abraham (ed.), Specialist Periodical Reports, The Chemical Society, London, 1977, Vol. 6, pp. 122–140.
17. G. N. La Mar, W. de W. Horrocks and R. H. Holm, "NMR of Paramagnetic Molecules: Principles and Applications", Academic Press, New York, 1973.
18. R. J. Kurland and B. R. McGarvey, *J. Magn. Resonance*, 1970, **2**, 286.
19. J. P. Jesson, in ref. 17, Ch. 1, pp. 1–52.
20. P. J. Stiles, *Mol. Phys.*, 1974, **27**, 501.
21. P. J. Stiles, *Mol. Phys.*, 1975, **29**, 1271.

22. H. M. McConnell and R. E. Robertson, *J. Chem. Phys.*, 1958, **27**, 1361.
23. R. M. Golding, R. O. Pascual and L. C. Stubbs, *Mol. Phys.*, 1976, **31**, 1933.
24. R. M. Golding, R. O. Pascual and J. Vrbancich, *Mol. Phys.*, 1976, **31**, 731.
25. R. M. Golding and L. C. Stubbs, *Proc. Roy. Soc. (A)*, 1977, **354**, 223.
- 25a. J. Goodisman, *J. Phys. Chem.*, 1975, **79**, 1206.
26. P. J. Stiles, *Proc. Roy. Soc. (A)*, 1975, **346**, 209.
27. A. D. Buckingham and P. J. Stiles, *Mol. Phys.*, 1972, **24**, 99.
28. P. J. Stiles, *Proc. Roy. Soc. (A)*, 1974, **336**, 251.
29. G. Giacometti, P. L. Nordio, G. Rigatti and U. Segre, *J. Chem. Soc., Faraday II*, 1973, **69**, 1815.
30. T. J. Swift, in ref. 17, Ch. 2, pp. 53–83.
31. A. J. Vega and D. Fiat, *Mol. Phys.*, 1976, **31**, 347.
32. A. G. Redfield, *I.B.M.J. Res. Dev.*, 1957, **1**, 19.
33. D. T. Pegg and D. M. Doddrell, *Austral. J. Chem.*, 1976, **29**, 1869.
34. D. T. Pegg, D. M. Doddrell, M. R. Bendall and A. K. Gregson, *Austral. J. Chem.*, 1976, **29**, 1885.
35. D. M. Doddrell, D. T. Pegg, M. R. Bendall and A. K. Gregson, *Austral. J. Chem.*, 1977, **30**, 1635.
36. D. M. Doddrell, D. T. Pegg, M. R. Bendall and A. K. Gregson, *Chem. Phys. Lett.*, **40**, 142.
37. D. M. Doddrell, M. R. Bendall, D. T. Pegg, P. C. Healy and A. K. Gregson, *J. Amer. Chem. Soc.*, 1977, **99**, 1281.
38. V. A. Glebov, Yu. D. Knyazev and T. M. Nikitina, *Koord. Khim.*, 1976, **2**, 700.
39. M. Lipsicas, M. Siegel, J. Piott, T. Higgins and J. A. Gerber, *J. Magn. Resonance*, 1976, **22**, 303.
40. G. N. La Mar, in ref. 17, Ch. 3, pp. 85–126.
41. A. D. McLachlan, *Mol. Phys.*, 1960, **3**, 233.
42. R. Hoffman, *J. Chem. Phys.*, 1964, **40**, 2745.
43. J. A. Pople, D. L. Beveridge and P. A. Dobosh, *J. Chem. Phys.*, 1967, **47**, 2026.
44. W. de W. Horrocks, in ref. 17, Ch. 4, pp. 127–177.
45. W. de W. Horrocks, *Inorg. Chem.*, 1973, **12**, 1211.
46. J. A. Happe and R. L. Ward, *J. Chem. Phys.*, 1963, **39**, 1211.
47. D. H. Marcellus, E. R. Davidson and A. L. Kwiram, *Chem. Phys. Lett.*, 1975, **33**, 522.
48. The Chemical Society Specialist Periodical Reports, "Nuclear Magnetic Resonance", Volumes 1–7.
- 48a. P. J. van der Put and J. Reedijk, *Proc. 16th Int. Conf. Coord. Chem.*, 1974, R78; P. J. van der Put and A. A. Schilperoord, *Inorg. Chem.*, 1974, **13**, 2476.
49. K. Migita, M. Iwaizumi and T. Isobe, *J. Amer. Chem. Soc.*, 1975, **97**, 4228.
50. C. Srivanavit and D. G. Brown, *J. Amer. Chem. Soc.*, 1976, **98**, 4447.
51. C. Srivanavit and D. G. Brown, *Inorg. Chem.*, 1975, **14**, 2950.
52. L. Y. Yan, *J. Chem. Soc., Faraday II*, 1977, **73**, 446.
53. A. C. Fabretti, G. C. Franchini, C. Preti and G. Tosi, *Canad. J. Chem.*, 1977, **55**, 344.
54. O. Stelzer and E. Unger, *J. Chem. Soc., Dalton*, 1973, 1783.
55. I. Bertini, A. Dei and A. Scozzafava, *Inorg. Chem.*, 1975, **14**, 1526.
56. W. Byers and R. J. P. Williams, *J. Chem. Soc., Dalton*, 1973, 555.
57. R. Basosi, E. Gaggelli, E. Tiezzi and G. Valensin, *J. Chem. Soc., Perkin II*, 1975, 423.
58. G. Martini, N. Niccolai and E. Tiezzi, *J. Phys. Chem.*, 1975, **79**, 1721.
59. K. S. Murray, *J. Chem. Soc., Dalton*, 1975, 1538.
60. P. D. W. Boyd and K. S. Murray, *J. Chem. Soc. (A)*, 1971, 2711.
61. A. Syamal, *Coord. Chem. Rev.*, 1975, **16**, 309.
- 61a. A. P. Gulya, N. V. Gerbeleu, E. P. Obrezha and V. M. Buzash, *Zh. Neorg. Khim.*, 1977, **22**, 128.
62. L. P. Kazanskii and V. I. Sintsyn, *Dokl. Akad. Nauk SSSR*, 1975, **223**, 381.
63. K. Wiegel and H. Buerger, *J. Organometal. Chem.*, 1977, **129**, 309.
64. D. Gervais and J. Choukroun, *J. Inorg. Nuclear Chem.*, 1974, **36**, 3679.
65. D. Rehder, *Z. Naturforsch.*, 1977, **32b**, 771.

66. G. E. Chapps, S. W. McCann, H. H. Wickman and R. C. Sherwood, *J. Chem. Phys.*, 1974, **60**, 990.
67. M. M. Dhingra, P. Ganguli and S. Mitra, *Chem. Phys. Lett.*, 1974, **27**, 579.
68. A. K. Gregson and D. Doddrell, *Chem. Phys. Lett.*, 1975, **31**, 125.
69. D. M. Doddrell, M. R. Bendall and A. K. Gregson, *Austral. J. Chem.*, 1976, **29**, 55.
70. M. M. Dhingra, M. D. Zingde and R. N. Mukherjee, *Chem. Phys. Lett.*, 1975, **35**, 540.
71. R. N. Mukherjee, M. S. Venkateshan and M. D. Zingde, *J. Inorg. Nuclear Chem.*, 1976, **38**, 689.
72. B. S. Tovrog and R. S. Drago, *J. Amer. Chem. Soc.*, 1974, **96**, 6765.
- 72a. K. Migita, M. Iwaizumi and T. Isobe, *J. Chem. Soc., Dalton*, 1977, 532.
73. D. S. Everhart and R. F. Evilia, *Inorg. Chem.*, 1977, **16**, 120.
74. W. de W. Horrocks, *Inorg. Chem.*, 1970, **9**, 690.
75. R. E. Cramer and M. Chudyk, *J. Magn. Resonance*, 1973, **12**, 168.
76. D. R. Eaton and K. L. Chua, *Canad. J. Chem.*, 1973, **51**, 2632.
77. A. A. Obynochnyi, R. Z. Sagdeev, Yu. N. Molin and A. I. Razvukhin, *Koord. Khim.*, 1975, **1**, 817.
78. K. Hayamizu, M. Murata and O. Yamamoto, *Bull. Chem. Soc. Japan*, 1975, **48**, 1842.
79. J. C. Ronfard-Haret and C. Chachaty, *Chem. Phys.*, 1976, **18**, 345.
80. C. Chachaty, A. Forchioni and J. Virlet, *Canad. J. Chem.*, 1975, **53**, 648.
81. E. I. Berus, P. V. Schastnev, V. A. Barkhash and Yu. N. Molin, *Zh. Strukt. Khim.*, 1973, **14**, 34.
82. C. Chachaty, A. Forchioni and J. C. Ronfard-Haret, *Mol. Phys.*, 1976, **31**, 325.
- 82a. C. Chachaty, A. Forchioni, J. Virlet and J. C. Ronfard-Haret, *Chem. Phys. Lett.*, 1974, **29**, 436.
83. L. M. Stock and M. R. Wasielewski, *J. Amer. Chem. Soc.*, 1977, **99**, 50.
84. A. P. Gulya, D. G. Batyr and V. A. Shcherbakov, *Zh. Neorg. Khim.*, 1973, **18**, 553 (English trans.).
85. D. G. Batyr, V. T. Balan and A. P. Gulya, *Izv. Akad. Nauk Mold. SSR Biol. Khim. Nauk*, 1973, **2**, 64.
86. A. P. Gulya, D. G. Batyr and E. U. Iorga, *Zh. Neorg. Khim.*, 1976, **21**, 1038.
87. K. Tori, T. Fujii, Y. Yoshimura and M. Ueyama, *Chem. Lett.*, 1973, 11.
88. J. Crea and S. F. Lincoln, *Austral. J. Chem.*, 1975, **28**, 1523.
89. M. M. Dhingra, B. Maiti and R. M. Sathe, *Indian J. Chem.*, 1975, **13**, 359.
90. V. P. Tatarskii, V. B. Leont'ev and G. Sh. Talipov, *Teor. Eksp. Khim.*, 1973, **9**, 224.
91. M. Kondo, *Bull. Chem. Soc. Japan*, 1977, **50**, 2185.
92. D. G. Pobedimskii, Sh. A. Nasybullin, P. A. Kirpichnikov, R. B. Svitych, O. P. Yoblonskii and A. L. Buchachenko, *Org. Magn. Resonance*, 1977, **9**, 61.
93. D. M. Doddrell and A. K. Gregson, *Chem. Phys. Lett.*, 1974, **29**, 512.
94. D. M. Doddrell, D. T. Pegg, M. R. Bendall, H. P. W. Gottlieb, A. K. Gregson and M. Anker, *Chem. Phys. Lett.*, 1976, **39**, 65.
95. A. Allerhand, D. Doddrell and R. Komoroski, *J. Chem. Phys.*, 1971, **55**, 189.
96. R. Z. Sagdeev, A. A. Obynochnyi and Yu. N. Molin, *Koord. Khim.*, 1975, **1**, 897.
97. P. M. Heinrichs and S. Gross, *J. Magn. Resonance*, 1975, **17**, 399.
98. F. A. Cotton, D. L. Hunter and A. J. White, *Inorg. Chem.*, 1975, **14**, 703.
99. T. G. Campbell and F. L. Urbach, *Inorg. Chem.*, 1973, **12**, 1840.
100. R. E. Cramer and R. L. Harris, *Inorg. Chem.*, 1974, **13**, 2208.
101. H. A. O. Hill and N. Zarb-Adami, *J. Inorg. Nuclear Chem.*, 1976, **38**, 2189.
102. A. T. Pilipenko, N. V. Mel'nikova and A. L. Rozenfel'd, *Zh. Neorg. Khim.*, 1973, **18**, 1430 (English trans.).
103. A. T. Pilipenko, N. V. Mel'nikova and A. L. Rozenfel'd, *Zh. Neorg. Khim.*, 1974, **19**, 721 (English trans.).
104. N. V. Mel'nikova and A. T. Pilipenko, *Koord. Khim.*, 1975, **1**, 1703.
105. A. T. Pilipenko, N. V. Mel'nikova and A. L. Rozenfel'd, *Zh. Neorg. Khim.*, 1976, **21**, 1019.

106. M. M. Dhingra, M. D. Zingde and R. N. Mukherjee, *Chem. Phys. Lett.*, 1973, **23**, 131.
107. A. T. Pilipenko, N. V. Mel'nikova and A. L. Rozenfel'd, *Ukr. Khim. Zh.*, 1976, **42**, 981.
108. R. M. Golding and K. Lehtonen, *Austral. J. Chem.*, 1974, **27**, 2083.
109. R. M. Golding, P. C. Healy, P. Colombero and A. H. White, *Austral. J. Chem.*, 1974, **27**, 2089.
110. M. M. Dhingra, P. Ganguli, V. R. Marathe, S. Mitra and R. L. Martin, *J. Magn. Resonance*, 1975, **20**, 133.
111. B. J. McCormick and D. L. Greene, *J. Coord. Chem.*, 1974, **4**, 125.
112. D. P. Schwendiman and J. I. Zink, *J. Amer. Chem. Soc.*, 1976, **98**, 1248.
113. L. Y. Yan, *Austral. J. Chem.*, 1974, **27**, 213.
114. A. T. Pilipenko, N. V. Mel'nikova and N. M. Pashkova, *Zh. Neorg. Khim.*, 1975, **20**, 155.
115. M. Wicholas, R. Mustacich, B. Johnson, T. Smedley and J. May, *J. Amer. Chem. Soc.*, 1975, **97**, 2113.
116. V. K. Voronov, E. S. Domnina, N. P. Glazkova and G. G. Skvortsova, *Izv. Akad. Nauk SSSR, Ser. Khim.*, 1974, **11**, 2598.
117. S.-M. Wang and J.-T. Chen, *J. Chin. Chem. Soc.*, 1975, **22**, 179.
118. D. R. Eaton and K. Zaw, *Canad. J. Chem.*, 1975, **53**, 633.
119. D. R. Eaton and K. Zaw, *Inorg. Chim. Acta*, 1976, **16**, 61.
120. Y. Y. Lim and K. L. Chua, *J. Chem. Soc., Dalton*, 1975, 1917.
121. L. E. Nivorozhkin, L. E. Konstantinovskii, V. I. Minkin, O. A. Osipov, A. D. Garnovskii, V. P. Kurbatov and I. Ya. Kvitko, *Zh. Neorg. Khim.*, 1975, **20**, 3012.
122. I. Bertini and D. Gatteschi, *Inorg. Chem.*, 1973, **12**, 2740.
123. I. Bertini, C. Luchinat and A. Scozzafava, *Inorg. Chim. Acta*, 1976, **19**, 201.
124. P. S. Zacharias and A. Chakravorty, *Inorg. Chim. Acta*, 1974, **11**, 133.
125. J. E. Jentoft and W. L. Reynolds, *Inorg. Chim. Acta*, 1973, **7**, 187.
126. D. Forster, *Inorg. Chem.*, 1973, **12**, 4.
127. P. Anstey and K. G. Orrell, *J. Chem. Soc., Dalton*, 1974, 870.
128. P. Anstey and K. G. Orrell, *J. Chem. Soc., Dalton*, 1974, 1711.
- 128a. K. G. Orrell, *Inorg. Chim. Acta*, 1975, **12**, 255.
129. P. Mignot and J. P. Grivet, *Chem. Phys.*, 1976, **15**, 261.
130. V. M. Nekipelov, A. N. Shupik and K. I. Zamaraev, *Koord. Khim.*, 1975, **1**, 956.
131. M. Iwaizumi, K. Migita and T. Isobe, *Bull. Chem. Soc. Japan*, 1976, **49**, 3325.
132. R. Fuentes, L. O. Morgan and N. A. Matwiyoff, *Inorg. Chem.*, 1975, **14**, 1837.
133. R. Fuentes, L. O. Morgan and N. A. Matwiyoff, *Inorg. Chem.*, 1975, **14**, 2774.
134. G. Occupati and L. Pratt, *J. Inorg. Nuclear Chem.*, 1974, **36**, 1731.
135. M. B. Jones and L. Pratt, *J. Chem. Soc., Dalton*, 1976, 1207.
136. A. P. Gulya and V. A. Shcherbakov, *Fiz. Mat. Metody. Koord. Khim., Tezisy Dokl. Vses. Soveshch.*, 5th, 1974, 106.
137. J. R. Vriesenga and J. Goodisman, *J. Magn. Resonance*, 1975, **20**, 102.
138. M. Olczak-Kobza and R. Soloniewicz, *J. Inorg. Nuclear Chem.*, 1977, **39**, 697.
139. R. B. Svitych, A. L. Buchachenko, O. P. Yablonskii, A. A. Petukhov, V. A. Belyaev and A. K. Kobaykov, *Kinet. Katal.*, 1974, **15**, 1300.
140. K. Jackowski and Z. Kecki, *J. Inorg. Nuclear Chem.*, 1977, **39**, 1073.
141. B. Maiti and R. M. Sathe, *J. Inorg. Nuclear Chem.*, 1976, **38**, 1748.
142. B. Maiti and R. M. Sathe, *J. Inorg. Nuclear Chem.*, 1977, **39**, 1244.
143. J. Lauterwein, P. Hemmerich and J.-M. Lhoste, *Inorg. Chem.*, 1975, **14**, 2152, 2161.
144. B. Jezowska-Trzebiatowska, L. Latos-Grazynski and H. Kozlowski, *Inorg. Chim. Acta*, 1977, **21**, 145.
145. V. L. Goedken and S.-M. Peng, *Chem. Comm.*, 1975, 258.
146. R. S. Drago and J. H. Elias, *J. Amer. Chem. Soc.*, 1977, **99**, 6570.
147. Y. Murakami, K. Sakata, Y. Tanaka and T. Matsuo, *Bull. Chem. Soc. Japan*, 1975, **48**, 3622.

148. J. Strouse, *J. Amer. Chem. Soc.*, 1977, **99**, 572.
149. J. W. Schindler, J. R. Luoma and J. P. Cusick, *Inorg. Chim. Acta*, 1974, **10**, 203.
150. W. M. Reiff and R. E. DeSimone, *Inorg. Chem.*, 1973, **12**, 1793.
151. P. Fantucci, L. Naldini and F. Cariati, *J. Organometal. Chem.*, 1974, **64**, 109.
152. A. P. Sattelberger and J. P. Fackler, *J. Amer. Chem. Soc.*, 1977, **99**, 1258.
153. D. Waysbort and G. Navon, *J. Chem. Phys.*, 1973, **59**, 5585.
154. M. A. King and M. R. E. Schaefer, *Inorg. Chem.*, 1973, **12**, 1972.
155. C. J. Donahue and R. D. Archer, *Inorg. Chem.*, 1977, **16**, 2903.
156. B. Bleaney, *J. Magn. Resonance*, 1972, **8**, 91.
157. W. de W. Horrocks, Jr. and J. P. Sipe III, *Science*, 1972, **177**, 994.
158. W. de W. Horrocks, Jr., J. P. Sipe III and D. Sudnick, in "NMR Shift Reagents", R. E. Sievers (ed.), Academic Press, 1973.
159. H. A. O. Hill, D. Williams and N. Zarb-Adami, *J. Chem. Soc., Faraday II*, 1976, **72**, 1494.
160. P. V. Sivapullaiah and S. Soundararajan, *Monatsh. Chem.*, 1976, **107**, 871.
161. P. V. Sivapullaiah and S. Soundararajan, *Inorg. Nuclear Chem. Lett.*, 1977, **13**, 291.
162. L. Ramakrishnan and S. Soundararajan, *Proc. Indian Acad. Sci.*, 1977, **86A**, 59.
163. N. A. Kostromina, *Zh. Neorg. Khim.*, 1974, **19**, 665.
164. N. A. Kostromina and N. N. Tananaeva, *Zh. Neorg. Khim.*, 1975, **20**, 2343.
165. J. Granot and D. Fiat, *J. Magn. Resonance*, 1975, **19**, 372.
166. C. Miyake and S. Imoto, *Chem. Phys. Lett.*, 1974, **24**, 606.
167. G. Folcher, C. Neveu and P. Rigny, *J. Inorg. Nuclear Chem.*, 1975, **37**, 1537.
168. C. Neveu, G. Folcher and A. M. Laurent, *J. Inorg. Nuclear Chem.*, 1976, **38**, 1223.
169. J. Paris and G. Folcher, *Canad. J. Chem.*, 1976, **54**, 1433.
170. G. Folcher, H. Marquet-Ellis, P. Rigny, E. Soulie and G. Goodman, *J. Inorg. Nuclear Chem.*, 1976, **38**, 747.
171. C. Miyake, H. Sakurai and S. Imoto, *Chem. Phys. Lett.*, 1975, **30**, 273.
172. G. Folcher, N. Keller, C. Kiener and J. Paris, *Canad. J. Chem.*, 1977, **55**, 3559.
173. C. Kiener, G. Folcher, P. Rigny and J. Virlet, *Canad. J. Chem.*, 1976, **54**, 303.
174. M. Brunelli, G. Lugli and G. Giacometti, *J. Magn. Resonance*, 1973, **9**, 247.
175. E. Fukushima and S. D. Larsen, *Chem. Phys. Lett.*, 1976, **44**, 285.
176. H. Marquet-Ellis and G. Folcher, *J. Organometal. Chem.*, 1977, **131**, 257.
177. H. D. Amberger, *J. Organometal. Chem.*, 1976, **116**, 219.
178. T. J. Marks, A. M. Seyam and J. R. Kolb, *J. Amer. Chem. Soc.*, 1973, **95**, 5529.
179. F. H. Köhler, *Z. Naturforsch.*, 1974, **29b**, 708.
180. F. H. Köhler, *J. Organometal. Chem.*, 1974, **64**, C27.
181. F. H. Köhler, *J. Organometal. Chem.*, 1974, **69**, 145.
182. S. E. Anderson and R. Rai, *Chem. Phys.*, 1973, **2**, 216.
183. E. S. Yang, M-S. Chan and A. C. Wahl, *J. Phys. Chem.*, 1975, **79**, 2049.
184. F. H. Köhler, *J. Organometal. Chem.*, 1975, **91**, 57.
185. F. H. Köhler and G. Matsubayashi, *Chem. Ber.*, 1976, **109**, 329.
186. J. H. Mueller, W. Holzinger and F. H. Köhler, *Chem. Ber.*, 1976, **109**, 1222.
187. F. H. Köhler, *J. Organometal. Chem.*, 1976, **110**, 235.
188. K. Eberl, F. H. Köhler and L. Mayring, *Angew. Chem.*, 1976, **88**, 575.
189. F. H. Köhler and G. Matsubayashi, *Z. Naturforsch.*, 1976, **31b**, 1153.
190. F. H. Köhler, *J. Organometal. Chem.*, 1976, **121**, C61.
191. M. E. Switzer, R. Wang, M. F. Rettig and A. H. Maki, *J. Amer. Chem. Soc.*, 1974, **96**, 7669.
192. W. T. Scroggins, M. F. Rettig and R. M. Wing, *Inorg. Chem.*, 1976, **15**, 1381.
193. R. J. Wiersema and M. F. Hawthorne, *J. Amer. Chem. Soc.*, 1974, **96**, 761.
194. D. A. Levy and L. E. Orgel, *Mol. Phys.*, 1961, **3**, 583.
195. R. W. Kreilick, in ref. 17, Ch. 15, pp. 595-626.

196. K. H. Hausser and K. Moebius, *Method. Chim.*, 1974, **1A**, 379.
197. G. W. Canters and E. de Boer, *Mol. Phys.*, 1973, **26**, 1185.
198. G. W. Canters and E. de Boer, *Mol. Phys.*, 1974, **27**, 665.
199. B. M. P. Hendriks and E. de Boer, *Mol. Phys.*, 1975, **29**, 129.
200. J. W. Neely, G. F. Hatch and R. W. Kreilick, *J. Amer. Chem. Soc.*, 1974, **96**, 652.
201. J. W. Neely, C. H. Lam and R. W. Kreilick, *Mol. Phys.*, 1975, **29**, 1663.
202. A. R. Forrester, S. P. Hepburn and G. McConnachie, *J. Chem. Soc., Perkin I*, 1974, 2213.
203. A. Rassat and P. Rey, *Tetrahedron*, 1974, **30**, 3315.
204. A. R. Forrester and R. Ramasseul, *J. Chem. Soc., Perkin I*, 1975, 1753.
205. K. U. Ingold and S. Brownstein, *J. Amer. Chem. Soc.*, 1975, **97**, 1817.
206. A. Rassat and J. Ronzaud, *Tetrahedron*, 1976, **32**, 239.
207. B. G. Cox, R. J. Gillespie, R. S. Hay and A. E. A. Porter, *J. Chem. Soc., Perkin II*, 1977, 904.
208. T. D. Lee and J. F. W. Keana, *J. Org. Chem.*, 1975, **40**, 3145.
209. R. A. Sadykov, R. Z. Sagdeev, Yu. N. Molin, V. I. Ovcharenko, S. V. Larionov and L. B. Volodarskii, *Koord. Khim.*, 1977, **3**, 71.
210. V. N. Parmon, A. I. Kokorin and G. M. Zhidomirov, *Zh. Strukt. Khim.*, 1977, **18**, 132.
211. R. A. Sadykov, R. Z. Sagdeev, Yu. N. Molin and L. B. Volodarskii, *Sib. Otd. Akad. Nauk SSSR, Ser. Khim. Nauk.*, 1974, **1**, 63.
212. P. Michon and A. Rassat, *J. Amer. Chem. Soc.*, 1975, **97**, 696.
213. M. Karplus and G. K. Fraenkel, *J. Chem. Phys.*, 1961, **35**, 1312.
214. R. W. Kreilick, *J. Chem. Phys.*, 1966, **45**, 1922; 1967, **46**, 4260.
215. N. A. Sysoeva, A. Yu. Karmilov and A. L. Buchachenko, *Chem. Phys.*, 1975, **7**, 123; 1976, **15**, 313; 1976, **15**, 321.
216. F. Laschi, E. Tiezzi and G. Valensin, *Gazz. Chim. Ital.*, 1976, **106**, 359.
217. T. Kawamura, M. Matsunaga and T. Yonezawa, *Chem. Lett.*, 1975, 867.
218. I. Morishima, K. Endo and T. Yonezawa, *J. Chem. Phys.*, 1973, **58**, 3146.
219. I. Morishima, T. Inubushi, K. Endo, T. Yonezawa and K. Goto, *J. Amer. Chem. Soc.*, 1972, **94**, 4812.
220. I. Morishima, K. Kawakami, T. Yonezawa, K. Goto and M. Imanari, *J. Amer. Chem. Soc.*, 1972, **94**, 6555.
221. I. Morishima, K. Toyoda and K. Yoshikawa, *J. Amer. Chem. Soc.*, 1973, **95**, 8627.
222. K. Endo, B. Knuettel, I. Morishima, T. Inubushi and T. Yonezawa, *Chem. Phys. Lett.*, 1975, **31**, 387.
223. I. Morishima, K. Ishihara, K. Tomishima, T. Inubushi and T. Yonezawa, *J. Amer. Chem. Soc.*, 1975, **97**, 2749.
224. I. Morishima, T. Inubushi and T. Yonezawa, *J. Amer. Chem. Soc.*, 1976, **98**, 3808.
225. I. Morishima, T. Inubushi, T. Yonezawa and Y. Kyogoku, *J. Amer. Chem. Soc.*, 1977, **99**, 4299.
226. K. Meise, W. Mueller-Warmuth and H. W. Nientiedt, *Ber. Bunsenges. Phys. Chem.*, 1976, **80**, 584.
227. R. E. Cramer, P. L. Dahlstrom and H. Heya, *J. Phys. Chem.*, 1975, **79**, 376.
228. C. Jolicœur, P. Bernier, E. Firkins and J. K. Saunders, *J. Phys. Chem.*, 1976, **80**, 1908.
229. J. Bargon and K. G. Seifert, *J. Phys. Chem.*, 1973, **77**, 2877.
230. G. R. Underwood and H. S. Friedman, *J. Amer. Chem. Soc.*, 1974, **96**, 4989.
231. V. A. Gubanov, V. I. Koryakov and A. K. Chirkov, *J. Magn. Resonance*, 1973, **11**, 326.
232. B. I. Shapiro, V. V. Minin and Ya. K. Syrkin, *Zh. Strukt. Khim.*, 1973, **14**, 642.
233. G. A. Pearson and R. I. Walter, *J. Amer. Chem. Soc.*, 1977, **99**, 5262.
234. S. J. G. Linkletter, G. A. Pearson and R. I. Walter, *J. Amer. Chem. Soc.*, 1977, **99**, 5269.
235. D. Deavenport, J. T. Edwards, A. L. Ternay, E. T. Strom and S. A. Evans, *J. Org. Chem.*, 1975, **40**, 103.
236. G. A. Pearson and R. I. Walter, *J. Magn. Resonance*, 1974, **16**, 348.

237. I. S. Baxter and J. K. M. Sanders, *Chem. Comm.*, 1974, **7**, 255.
238. J. K. M. Sanders and I. Baxter, *Tetrahedron Lett.*, 1974, 4543.
239. E. de Boer and C. Maclean, *J. Chem. Phys.*, 1966, **44**, 1334.
240. J. K. M. Sanders and J. C. Waterton, *Chem. Comm.*, 1976, 247.
241. L. Que and L. H. Pignolet, *Inorg. Chem.*, 1973, **12**, 156.
242. S. O. Grim and L. C. Satek, *Z. Naturforsch.*, 1973, **28b**, 683.
243. J. Csaszar, T. Szabo and G. Dombi, *Acta. Chim. Acad. Sci. Hung.*, 1976, **88**, 1.
244. M. C. Palazzotto, D. J. Duffy, B. L. Edgar, L. Que and L. H. Pignolet, *J. Amer. Chem. Soc.*, 1973, **95**, 4537.
245. L. Que and L. H. Pignolet, *Inorg. Chem.*, 1974, **13**, 351.
- 245a. D. J. Duffy and L. H. Pignolet, *Inorg. Chem.*, 1974, **13**, 2045.
246. S. S. Eaton and G. R. Eaton, *J. Amer. Chem. Soc.*, 1973, **95**, 1825.
247. J. E. Sarneski and C. N. Reilley, *Inorg. Chem.*, 1974, **13**, 977.
248. R. F. Evilia and C. N. Reilley, *J. Coord. Chem.*, 1973, **3**, 7.
249. R. F. Evilia, D. C. Young and C. N. Reilley, *J. Coord. Chem.*, 1973, **3**, 17.
250. R. H. Holm and C. J. Hawkins, in ref. 17, Ch. 7.
251. T. Murakami, I. Hirako and M. Hatano, *Bull. Chem. Soc. Japan*, 1977, **50**, 164.
252. L. E. Nivorozhkin, L. E. Konstantinovskii, M. A. Voronov, V. I. Minkin, O. A. Osipov, V. P. Kurbatov and L. S. Minkina, *Zh. Neorg. Khim.*, 1973, **18**, 1300 (English trans.).
253. I. B. Joedicke, H. V. Studer and J. T. Yoke, *Inorg. Chem.*, 1976, **15**, 1352.
254. D. F. Evans, *J. Chem. Soc.*, 1959, 2003.
255. C. A. Tsipis, C. C. Hadjikostas and G. E. Manoussakis, *Inorg. Chim. Acta*, 1977, **23**, 163.
256. R. A. Bhobe, *J. Indian Chem. Soc.*, 1977, **54**, 344.
257. I. M. Walker and D. H. Weeden, *Inorg. Chem.*, 1973, **12**, 772.
258. M. S. Quereshi and I. M. Walker, *Inorg. Chem.*, 1974, **13**, 2896.
259. M. S. Quereshi and I. M. Walker, *Inorg. Chem.*, 1975, **14**, 2187.
260. M. S. Quereshi, L. Rosenthal and I. M. Walker, *J. Coord. Chem.*, 1976, **5**, 77.
261. I. M. Walker, L. Rosenthal and M. S. Quereshi, *Inorg. Chem.*, 1971, **10**, 2463.
262. T-C. Tan and Y-Y. Lim, *Inorg. Chem.*, 1973, **12**, 2203.
263. T-C. Tan, K-L. Chua and Y-Y. Lim, *J. Chem. Soc., Dalton*, 1976, 863.
264. C. H. Cooper and T. R. Stengle, in ref. 17, Ch. 9, pp. 372-385.
265. V. M. Nekipelov, A. M. Shupik and K. I. Zamaraev, *Zh. Fiz. Khim.*, 1975, **49**, 1061.
266. A. N. Shupik, V. P. Lezina and V. M. Nekipelov, *Zh. Fiz. Khim.*, 1975, **49**, 1063.
267. V. M. Nekipelov, A. N. Shupik and K. I. Zamaraev, *Zh. Fiz. Khim.*, 1975, **49**, 1028.
268. R. B. Svitych, A. L. Buchachenko, O. P. Yablonskii, N. N. Rzhetskaya, V. A. Belyaev and A. A. Petukhov, *Kinet. Katal.*, 1976, **17**, 73.
269. S. O. Chan and D. R. Eaton, *Canad. J. Chem.*, 1976, **54**, 1332.
270. G. S. Vigee and C. L. Watkins, *Inorg. Chem.*, 1977, **16**, 709.
271. D. R. Eaton and K. L. Chua, *Canad. J. Chem.*, 1973, **51**, 4137.
272. A. P. Gulya, V. A. Shcherbakov and A. V. Ablov, *Dokl. Akad. Nauk SSSR*, 1973, **209**, 854.
273. V. V. Matveev and A. S. Balashov, *Koord. Khim.*, 1976, **2**, 424.
274. M. Olczak-Kobza and Z. Kecki, *Rocz. Chem.*, 1974, **48**, 2225.
275. A. V. Ablov, A. P. Gulya, V. M. Vdovenko, V. A. Shcherbakov, N. V. Morkovin and I. I. Chepurnykh, *Zh. Neorg. Khim.*, 1973, **18**, 381 (English trans.).
276. L. L. Rusnak and R. B. Jordan, *Inorg. Chem.*, 1975, **14**, 988.
277. L. L. Rusnak and R. B. Jordan, *Inorg. Chem.*, 1976, **15**, 709.
278. J. C. Boubel, J. J. Delpuech and G. Mathis, *Mol. Phys.*, 1977, **33**, 1729.
279. V. A. Glebov and T. M. Nikitina, *Koord. Khim.*, 1975, **1**, 1106.
280. D. S. Gamble, C. H. Langford and J. P. K. Tong, *Canad. J. Chem.*, 1976, **54**, 1239.
281. P. Spegt and G. Weill, *Biophys. Chem.*, 1976, **4**, 143.

282. A. N. Kitaigorodskii, V. M. Nekipelov and K. I. Zamaraev, *Dokl. Akad. Nauk SSSR*, 1977, **235**, 622.
283. T. J. Swift and R. E. Connick, *J. Chem. Phys.*, 1962, **37**, 307.
284. T. J. Swift and R. E. Connick, *J. Chem. Phys.*, 1964, **41**, 2553.
285. D. Waysbort and G. Navon, *J. Chem. Phys.*, 1973, **59**, 5585.
286. D. Waysbort and G. Navon, *J. Chem. Phys.*, 1975, **62**, 1021.
287. J. Granot and D. Fiat, *J. Magn. Resonance*, 1974, **15**, 540.
288. A. M. Achlama and D. Fiat, *J. Chem. Phys.*, 1973, **59**, 5197.
289. J. Granot, A. M. Achlama and D. Fiat, *J. Chem. Phys.*, 1974, **61**, 3043.
290. S. H. Koenig and M. Epstein, *J. Chem. Phys.*, 1975, **63**, 2279.
291. J. Reuben, *J. Chem. Phys.*, 1975, **63**, 5063.
292. P. Meier, A. Merbach, S. Buerki and T. A. Kaden, *Chem. Comm.*, 1977, 36.
293. G. Liu, H. W. Dodgen and J. P. Hunt, *Inorg. Chem.*, 1977, **16**, 2652.
294. V. V. Matveev, Yu. G. Gladkii, G. I. Skubnevskaya and Yu. N. Molin, *Zh. Strukt. Khim.*, 1974, **15**, 931.
295. V. V. Matveev, *Zh. Fiz. Khim.*, 1976, **50**, 220.
296. K. Plotkin, J. Copes and J. R. Vriesenga, *Inorg. Chem.*, 1973, **12**, 1494.
297. A. A. Obynochnyi, O. I. Bel'chenko, P. V. Schastnev, R. Z. Sagdeev, A. V. Dushkin, Yu. N. Molin and A. I. Rezvukhin, *Zh. Strukt. Khim.*, 1976, **17**, 620.
298. E. Tiezzi and G. Valensin, *Org. Magn. Resonance*, 1975, **7**, 602.
299. M. S. Shapnik, A. N. Gil'manov, V. E. Ermakova and I. Kh. Muzeev, *Zh. Neorg. Khim.*, 1974, **19**, 436.
300. M. S. Shapnik, A. N. Gil'manov, V. E. Ermakova and I. Kh. Muzeev, *Zh. Neorg. Khim.*, 1975, **20**, 3117.
301. A. A. Popel and A. V. Zakharov, *Zh. Neorg. Khim.*, 1974, **19**, 1345.
302. D. P. Rablen, H. W. Dodgen and J. P. Hunt, *Inorg. Chem.*, 1976, **15**, 931.
303. C. L. Watkins and G. S. Vigee, *J. Phys. Chem.*, 1976, **80**, 83.
304. J. C. Boubel and J. J. Delpuech, *Mol. Phys.*, 1974, **27**, 113.
305. J. C. Boubel, K. Bouatouch and J. J. Delpuech, *Compt. rend., B*, 1977, **284**, 393.
306. D. S. Everhart and R. F. Evilia, *Inorg. Chem.*, 1975, **14**, 2755.
307. R. K. Force, R. S. Marianelli and J. D. Carr, *Inorg. Chem.*, 1976, **15**, 2653.
308. N. A. Kostromina, L. B. Novikova and I. P. Gorelov, *Koord. Khim.*, 1975, **1**, 901.
309. N. A. Kostromina and N. N. Tananaeva, *Koord. Khim.*, 1976, **2**, 910.
310. N. A. Kostromina, N. V. Beloshitskii and I. A. Sheka, *Zh. Neorg. Khim.*, 1973, **18**, 1563 (English trans.).
311. N. A. Kostromina and L. B. Novikova, *Zh. Neorg. Khim.*, 1975, **20**, 1793.
312. N. A. Kostromina and T. V. Ternovaya, *Zh. Neorg. Khim.*, 1976, **21**, 366.
313. K. I. Popov, V. F. Chuvaev, L. I. Martynenko and V. I. Spitsyn, *Izv. Akad. Nauk SSSR*, 1975, **8**, 1710.
314. M. S. Shapnik, A. N. Gil'manov, T. P. Petrova and F. F. Gubaidullin, *Zh. Neorg. Khim.*, 1975, **20**, 2148.
315. M. S. Shapnik, A. N. Gil'manov, T. P. Petrova and F. F. Gubaidullin, *Zh. Neorg. Khim.*, 1977, **22**, 1289.
316. E. D. Romanenko, L. I. Budarin and K. B. Yatsimirskii, *Teor. Eksp. Khim.*, 1976, **12**, 26.
317. E. D. Romanenko and L. I. Budarin, *Teor. Eksp. Khim.*, 1976, **12**, 379.
318. V. K. Kapur and B. B. Wayland, *J. Phys. Chem.*, 1973, **77**, 634.
319. R. J. West and S. F. Lincoln, *Inorg. Chem.*, 1973, **12**, 494.
320. S. F. Lincoln and R. J. West, *Austral. J. Chem.*, 1973, **26**, 255.
321. S. F. Lincoln and R. J. West, *J. Amer. Chem. Soc.*, 1974, **96**, 400.
322. S. F. Lincoln and R. J. West, *Austral. J. Chem.*, 1974, **27**, 97.



323. R. J. West and S. F. Lincoln, *J. Chem. Soc., Dalton*, 1974, 281.
324. H. Tomiyasu, S. Ito and S. Tagami, *Bull. Chem. Soc. Japan*, 1974, **47**, 2843.
325. E. Kwiatkowski and J. Trojanowski, *J. Inorg. Nuclear Chem.*, 1975, **37**, 979.
326. M. W. Kendig and P. H. Riegger, *Inorg. Chim. Acta*, 1976, **17**, 175.
327. W. C. Copenhafer and P. H. Rieger, *Inorg. Chem.*, 1977, **16**, 2431.
328. M. C. Palazzotto and L. H. Pignolet, *Inorg. Chem.*, 1974, **13**, 1781.
329. N-S. Chan and J. B. Deroos, *J. Phys. Chem.*, 1973, **77**, 2163.
330. G. S. Vigee and C. L. Watkins, *J. Inorg. Nuclear Chem.*, 1975, **37**, 1739.
331. S. F. Lincoln, *J. Chem. Soc., Dalton*, 1973, 1896.
332. I. N. Marov, A. T. Panfilov, E. K. Ivanova and N. A. Plekhanov, *Koord. Khim.*, 1975, **1**, 1516.
333. A. P. Gulya and V. B. Kolokol'tsov, *Zh. Neorg. Khim.*, 1975, **20**, 1906.
334. G. R. Tauszik, G. Pellizer and G. Costa, *Inorg. Nuclear Chem. Lett.*, 1973, **9**, 717.
335. E. H. Abbott and J. M. Mayer, *J. Coord. Chem.*, 1977, **6**, 135.
336. K. B. Dillon and F. J. C. Rossotti, *J. Chem. Soc., Dalton*, 1973, **10**, 1005.
337. W. G. Espersen, W. C. Hutton, S. T. Chow and R. B. Martin, *J. Amer. Chem. Soc.*, 1974, **96**, 8111.
338. B. Jezowska-Trzebiatowska, E. Matczak and H. Kozlowski, *Bull. Acad. Pol. Sci.*, 1976, **24**, 981.
339. B. Jezowska-Trzebiatowska, L. Latos-Grazynski, G. Formicka-Kozlowska and T. Kowalik, *Bull. Acad. Pol. Sci.*, 1974, **22**, 1075.
340. I. Nagypal, E. Farkas and A. Gergely, *Magy. Kem. Foly.*, 1974, **80**, 545.
341. A. A. Popel, A. V. Zakharov and I. I. Evgen'eva, *Kinet. Katal*, 1977, **18**, 1061.
342. V. M. Mastikhin, L. B. Avdeeva and M. A. Fedotov, *Izv. Akad. Nauk SSSR, Ser. Khim.*, 1977, **2**, 266.
343. G. C. Levy and J. D. Cargioli, *J. Magn. Resonance*, 1973, **10**, 231.
- 343a. G. C. Levy and R. A. Komoroski, *J. Amer. Chem. Soc.*, 1974, **96**, 678.
344. G. C. Levy and U. Edlund, *J. Amer. Chem. Soc.*, 1975, **97**, 4482.
345. G. C. Levy, U. Edlund and J. G. Hexem, *J. Magn. Resonance*, 1975, **19**, 259.
346. D. Doddrell, I. Burfitt and N. U. Riggs, *Austral. J. Chem.*, 1975, **28**, 369.
347. D. F. Evans, *J. Chem. Soc.*, 1959, 2003.
348. D. F. Evans, *J. Chem. Soc., Dalton*, 1973, 2587.
349. R. Engel, D. Halpern and S. Bienenfeld, *Analyt. Chem.*, 1973, **45**, 367.
- 349a. C. A. Reilly, H. M. McConnell and R. E. Meisenheimer, *Phys. Rev.*, 1955, **98**, 264.
- 349b. K. G. Orrell, V. Šik and A. J. Wybrow, unpublished results.
350. O. M. Taranukha, P. N. Galich and Ya. S. Lebedev, *Teor. Eksp. Khim.*, 1974, **10**, 697.
351. V. Yu. Borovkov, A. D. Shuklov, S. A. Surin and V. B. Kazanskii, *Kinet. Katal.*, 1973, **14**, 1081.
352. V. Yu. Borovkov, G. M. Zhidomirov and V. B. Kazanskii, *Zh. Strukt. Khim.*, 1974, **15**, 547.
353. V. B. Kazanskii, V. Yu. Borovkov and G. M. Zhidomirov, *J. Catal.*, 1975, **39**, 205.
354. V. Yu. Borovkov and V. B. Kazanskii, *Kinet. Katal.*, 1974, **15**, 1283.
355. N. N. Mozharovskii, V. Yu. Borovkov and V. B. Kazanskii, *Kinet. Katal.*, 1976, **17**, 1341.
356. W. D. Hoffmann, *Z. Phys. Chem. (Leipzig)*, 1976, **257**, 817.
357. W. D. Hoffmann, *Kinet. Katal.*, 1976, **17**, 718.
358. D. Deininger, V. Yu. Borovkov and V. B. Kazanskii, *J. Catal.*, 1977, **48**, 35.
359. J. Reuben, in "Progress in Nuclear Magnetic Resonance Spectroscopy", Vol. 9, Pt. 1, 'Lanthanide Shift Reagents in NMR Spectroscopy: Principles, Methodology and Applications', Pergamon Press, Oxford, 1973.
360. R. E. Sievers (ed.), "Nuclear Magnetic Resonance Shift Reagents", Academic Press, New York and London, 1973.
361. A. F. Cockerill and G. L. O. Davies, *Chem. Rev.*, 1973, **73**, 553.
362. B. C. Mayo, *Chem. Soc. Rev.*, 1973, **2**, 49.

363. B. D. Flockhart, *CRC Crit. Rev. Anal. Chem.*, 1976, **6**, 69.  
364. O. Hofer, *Topics Stereochem.*, 1976, **9**, 111.  
365. F. Lefevre and M. L. Martin, *Org. Magn. Resonance*, 1972, **4**, 737.  
366. C. C. Hinckley, *Proc. Rare Earth Res. Conf. 10th*, 1973, 362.  
367. M. R. Willcott and R. E. Davis, *Proc. Rare Earth Res. Conf. 10th*, 1973, 405.  
368. R. E. Rondeau and R. E. Sievers, *Analyt. Chem.*, 1973, **45**, 2145.  
369. C. C. Hinckley, *Mod. Methods Steroid Anal.*, 1973, 265.  
370. S. P. Sinha, *J. Mol. Struct.*, 1973, **19**, 387.  
371. I. Ya. Slonim and A. Kh. Bulai, *Usp. Khim.*, 1973, **42**, 1976.  
372. V. K. Voronov, *Usp. Khim.*, 1974, **43**, 432.  
373. Z. Ksandr and M. Hajek, *Czech. Chem. Listy*, 1974, **68**, 129.  
374. D. H. Williams, *Pure Appl. Chem.*, 1974, **40**, 25.  
375. S. Rebuffat, D. Davoust, M. Giraud and D. Molho, *Bull. Mus. Natl. Hist. Nat. Sci. Phys.-Chim.*, 1976, **8**, 17.  
376. J. A. Glasel, *Progr. Inorg. Chem.*, 1973, **18**, 383.  
377. J. Reuben, *Naturwiss.*, 1975, **62**, 172.  
378. B. R. McGarvey, *J. Chem. Phys.*, 1976, **65**, 955.  
379. B. R. McGarvey, *J. Chem. Phys.*, 1976, **65**, 962.  
380. B. Bleaney, *J. Magn. Resonance*, 1972, **8**, 91.  
381. R. M. Golding and P. Pyykkö, *Mol. Phys.*, 1973, **26**, 1389.  
382. W. de W. Horrocks, J. P. Sipe III and D. R. Sudnick in ref. 360.  
383. G. A. Elgavish and J. Reuben, *J. Magn. Resonance*, 1974, **16**, 360.  
384. E. W. Stout and H. S. Gutowsky, *J. Magn. Resonance*, 1976, **24**, 389.  
385. W. de W. Horrocks, *J. Magn. Resonance*, 1977, **26**, 333.  
386. W. de W. Horrocks, in ref. 17, Ch. 12, pp. 479-519.  
387. C. N. Reilley, B. W. Good and J. F. Desreux, *Analyt. Chem.*, 1975, **47**, 2110.  
388. C. N. Reilley, B. W. Good and R. D. Allendoerfer, *Analyt. Chem.*, 1976, **48**, 1446.  
389. R. M. Golding and M. P. Halton, *Austral. J. Chem.*, 1972, **25**, 2577.  
390. J. F. Desreux and C. N. Reilley, *J. Amer. Chem. Soc.*, 1976, **98**, 2105.  
391. A. M. Grotens, J. J. M. Backus and E. de Boer, *Tetrahedron Lett.*, 1973, 4343.  
392. A. A. Chalmers and K. G. R. Pachler, *J. Chem. Soc., Perkin II*, 1974, 748.  
393. K. Ajisaka and M. Kainosho, *J. Amer. Chem. Soc.*, 1975, **97**, 330.  
394. D. J. Chadwick and D. H. Williams, *J. Chem. Soc., Perkin II*, 1974, 1202.  
395. M. Hirayama and M. Sato, *Chem. Lett.*, 1974, 725.  
396. M. Hirayama and M. Sato, *Bull. Chem. Soc. Japan*, 1975, **48**, 2690.  
397. C. M. Dobson, R. J. P. Williams and A. V. Xavier, *J. Chem. Soc., Dalton*, 1973, 2662.  
398. O. A. Gansow, P. A. Loeffler, R. E. Davis, R. E. Lenkinski and M. R. Willcott, *J. Amer. Chem. Soc.*, 1976, **98**, 4250.  
399. W. de W. Horrocks, *J. Amer. Chem. Soc.*, 1974, **96**, 3022.  
400. R. E. Cramer and R. Dubois, *J. Amer. Chem. Soc.*, 1973, **95**, 3801.  
401. R. E. Cramer, R. Dubois and K. Seff, *J. Amer. Chem. Soc.*, 1974, **96**, 4125.  
402. R. E. Cramer, C. K. Furuike and R. Dubois, *J. Magn. Resonance*, 1975, **19**, 382.  
403. R. H. Newman, *Tetrahedron*, 1974, **30**, 969.  
404. G. N. La Mar and E. A. Metz, *J. Amer. Chem. Soc.*, 1974, **96**, 5611.  
405. R. E. Lenkinski and J. Reuben, *J. Magn. Resonance*, 1976, **21**, 47.  
406. G. Montaudo, S. Caccamese, V. Librando and P. Maravigna, *Tetrahedron*, 1973, **29**, 3915.  
407. R. M. Wing, J. J. Uebel and K. K. Andersen, *J. Amer. Chem. Soc.*, 1973, **95**, 6046.  
408. A. J. Rafalski and J. Barciszewski, *J. Mol. Struct.*, 1973, **19**, 223.  
409. A. Recca and P. Finocchiaro, *Tetrahedron Lett.*, 1974, 4185.  
410. J. W. ApSimon and H. Beierbeck, *Tetrahedron Lett.*, 1973, 581.

411. B. L. Shapiro and M. D. Johnston, *Org. Magn. Resonance*, 1973, **5**, 21.
412. B. L. Shapiro, M. J. Shapiro, A. D. Godwin and M. D. Johnston, *J. Magn. Resonance*, 1972, **8**, 402.
413. D. J. Chadwick, *Tetrahedron Lett.*, 1974, 1375.
414. J. J. Cawley and D. V. Petrocine, *Org. Magn. Resonance*, 1974, **6**, 544.
415. M. R. Willcott, R. E. Davis and R. W. Holder, *J. Org. Chem.*, 1975, **40**, 1952.
416. H. J. Schneider and E. F. Weigand, *Tetrahedron*, 1975, **31**, 2125.
417. P. Stilbs, *Chem. Scripta*, 1975, **7**, 59.
418. M. D. Johnston, D. J. Raber and N. K. De Gennaro, A. D'Angelo and J. W. Perry, *J. Amer. Chem. Soc.*, 1976, **98**, 6042.
419. C. C. Hinckley and W. C. Brumley, *J. Magn. Resonance*, 1976, **24**, 239.
420. C. C. Hinckley and W. C. Brumley, *J. Amer. Chem. Soc.*, 1976, **98**, 1331.
421. B. H. S. Lienard, Ph.D. thesis, University of East Anglia.
422. R. E. Lenkinski and J. Reuben, *J. Amer. Chem. Soc.*, 1976, **98**, 4065.
423. R. E. Cramer, R. Dubois and C. K. Furuike, *Inorg. Chem.*, 1975, **14**, 1005.
424. R. E. Cramer and R. Dubois, *Chem. Comm.*, 1973, 936.
425. J. D. Roberts, G. E. Hawkes, J. Husar, A. W. Roberts and D. W. Roberts, *Tetrahedron*, 1974, **30**, 1833.
426. G. R. Sullivan, *J. Amer. Chem. Soc.*, 1976, **98**, 7162.
427. K. Sakamoto and M. Oki, *Bull. Chem. Soc. Japan*, 1974, **47**, 2623.
428. G. Montaudo, V. Librando, S. Caccamese and P. Maravigna, *J. Amer. Chem. Soc.*, 1973, **95**, 6365.
429. P. Finocchiaro, A. Recca, P. Maravigna and G. Montaudo, *Tetrahedron*, 1974, **30**, 4159.
430. H. Kessler and M. Molter, *Angew. Chem.*, 1974, **86**, 552.
431. D. J. Chadwick and D. H. Williams, *Chem. Comm.*, 1974, 128.
432. K. L. Servis, D. J. Bowler and C. Ishii, *J. Amer. Chem. Soc.*, 1975, **97**, 73.
433. K. L. Servis and D. J. Bowler, *J. Amer. Chem. Soc.*, 1975, **97**, 80.
434. B. A. Levine, J. M. Thornton and R. J. P. Williams, *Chem. Comm.*, 1974, 669.
435. L. Kullberg and G. R. Choppin, *Inorg. Chem.*, 1977, **16**, 2926.
436. F. Inagaki, M. Tasumi and T. Miyazawa, *J. Magn. Resonance*, 1977, **27**, 91.
437. B. F. G. Johnson, J. Lewis and P. McArdle, *J. Chem. Soc., Dalton*, 1974, 1253.
438. T. P. Forrest, D. L. Hooper and S. Ray, *J. Amer. Chem. Soc.*, 1974, **96**, 4286.
439. G. A. Elgavish, R. E. Lenkinski and J. Reuben, *Proc. Rare Earth Res. Conf. 11th*, 1974, 885.
440. L. F. Lindoy and W. E. Moody, *J. Amer. Chem. Soc.*, 1975, **97**, 2275.
441. J. K. Beattie, L. F. Lindoy and W. E. Moody, *Inorg. Chem.*, 1976, **15**, 3170.
442. L. F. Lindoy and W. E. Moody, *J. Amer. Chem. Soc.*, 1977, **99**, 5863.
443. D. L. Kepert, *J. Chem. Soc., Dalton*, 1974, 617.
444. R. Z. Sagdeev, A. A. Obynochnyi, Yu. N. Molin and A. I. Rezvukhin, *Izv. Sib. Otd. Akad. Nauk SSSR, Ser. Khim. Nauk*, 1975, **5**, 106.
445. G. Beech and R. J. Morgan, *Tetrahedron Lett.*, 1974, 973.
446. K. Tori, Y. Yoshimura, M. Kainosho and K. Ajisaka, *Tetrahedron Lett.*, 1973, 3127.
447. G. Gacel, M. C. Fournie-Zaluski and B. P. Roques, *Org. Magn. Resonance*, 1976, **8**, 525.
448. M. Hirayama and Y. Hanyu, *Bull. Chem. Soc. Japan*, 1973, **46**, 2687.
449. J. C. Ronfard-Haret and C. Chachaty, *J. Chim. Phys. Phys.-Chim. Biol.*, 1977, **74**, 552.
450. R. E. Davis, M. R. Willcott, R. E. Lenkinski, W. von E. Doering and L. Birladeann, *J. Amer. Chem. Soc.*, 1973, **95**, 6846.
451. E. Nieboer, W. P. Flora, F. M. Podolski and H. Falter, *Proc. Rare Earth Res. Conf. 10th*, 1973, 388.
452. A. D. Sherry, *Proc. Rare Earth Res. Conf. 12th*, 1976, 250.
453. T. D. Marinetti, G. H. Snyder and B. D. Sykes, *J. Amer. Chem. Soc.*, 1975, **97**, 6562.

454. D. L. Howland and R. L. Flurry, *J. Inorg. Nuclear Chem.*, 1976, **38**, 1568.
455. H. Kessler and M. Molter, *J. Amer. Chem. Soc.*, 1976, **98**, 5969.
456. F. Inagaki, M. Tasumi and T. Miyazawa, *J. Chem. Soc., Perkin II*, 1976, 167.
457. D. K. Lavalley and A. H. Zeltmann, *J. Amer. Chem. Soc.*, 1974, **96**, 5552.
458. M. Kainosho and K. Ajisaka, *J. Amer. Chem. Soc.*, 1975, **97**, 6839.
459. P. Tanswell, J. M. Thornton, V. Korda and R. J. P. Williams, *Eur. J. Biochem.*, 1975, **57**, 135.
460. F. S. Mandel, R. H. Cox and R. C. Taylor, *J. Magn. Resonance*, 1974, **14**, 235.
461. T. A. Gerken and W. M. Ritchey, *J. Magn. Resonance*, 1976, **24**, 155.
462. P. Finocchiaro, A. Recca, W. G. Bentrude, H-W. Tan and K. C. Yee, *J. Amer. Chem. Soc.*, 1976, **98**, 3537.
463. P. A. J. Gorin and M. Mazurek, *Canad. J. Chem.*, 1974, **52**, 3070.
464. H. Grasdalen, T. Anthonsen, B. Larsen and O. Smidsroed, *Acta Chem. Scand., B.*, 1975, **29**, 17.
465. H. Grasdalen, T. Anthonsen and B. Larsen, *Acta Chem. Scand., B.*, 1975, **29**, 99.
466. L. D. Hall and C. M. Preston, *Carbohydrate Res.*, 1975, **41**, 53.
467. G. Montaudo, S. Caccamese, V. Librando and A. Recca, *J. Mol. Struct.*, 1975, **27**, 303.
468. C-P. Wong, R. F. Venteicher and W. de W. Horrocks, *J. Amer. Chem. Soc.*, 1974, **96**, 7149.
469. W. de W. Horrocks and C-P. Wong, *J. Amer. Chem. Soc.*, 1976, **98**, 7157.
470. G. A. Elgavish and J. Reuben, *J. Amer. Chem. Soc.*, 1976, **98**, 4755.
471. J. Reuben, *J. Amer. Chem. Soc.*, 1976, **98**, 3726.
472. G. A. Elgavish and J. Reuben, *J. Amer. Chem. Soc.*, 1977, **99**, 1762.
473. J. Reuben, *J. Amer. Chem. Soc.*, 1977, **99**, 1765.
474. A. P. G. Kieboom, T. Spoormaker, A. Sinnema, J. M. van der Toorn and H. van Bekkum, *Rec. Trav. Chim.*, 1975, **94**, 53.
475. A. P. G. Kieboom, A. Sinnema, J. M. van der Toorn and H. van Bekkum, *Rec. Trav. Chim.*, 1977, **96**, 35.
476. G. A. Elgavish and J. Reuben, *J. Amer. Chem. Soc.*, 1977, **99**, 5590.
477. L. M. Vainer, V. F. Zolin, L. G. Koreneva and R. Z. Sagdeev, *Koord. Khim.*, 1975, **1**, 1512.
478. J. Reuben, *J. Amer. Chem. Soc.*, 1973, **95**, 3534.
479. R. Porter, T. J. Marks and D. F. Shriver, *J. Amer. Chem. Soc.*, 1973, **95**, 3548.
480. D. F. Evans and M. Wyatt, *Chem. Comm.*, 1972, 312; 1973, 339.
481. D. F. Evans and M. Wyatt, *J. Chem. Soc., Dalton*, 1974, 765.
482. J. S. Ghotra, F. A. Hart, G. P. Moss and M. L. Staniforth, *Chem. Comm.*, 1973, 113.
483. R. Radeaglia, *Z. Chem.*, 1974, **14**, 72.
484. A. Arduini and I. M. Armitage, *Carbohydrate Res.*, 1973, **31**, 255.
485. J. Bouquant and J. Chucho, *Tetrahedron Lett.*, 1973, 493.
486. F. Inagaki, S. Takahashi, M. Tasumi and T. Miyazawa, *Bull. Chem. Soc. Japan*, 1975, **48**, 853.
487. R. A. Perry and Y. L. Chow, *Canad. J. Chem.*, 1974, **52**, 315.
488. L. Cazaux, G. Chassaing and P. Maroni, *Org. Magn. Resonance*, 1976, **8**, 461.
489. M. D. Johnston, B. L. Shapiro, M. J. Shapiro, T. W. Proulx, A. D. Godwin and H. L. Pearce, *J. Amer. Chem. Soc.*, 1975, **97**, 542.
490. F. Inagaki, M. Tasumi and T. Miyazawa, *Bull. Chem. Soc. Japan*, 1975, **48**, 1427.
491. K. B. Yatsimirskii, V. A. Bidzilya, N. K. Davidenko and L. P. Golovkova, *Teor. Eksp. Khim.*, 1974, **10**, 115.
492. V. A. Bidzilya, N. K. Davidenko and L. P. Golovka, *Teor. Eksp. Khim.*, 1975, **11**, 687.
493. A. H. Bruder and S. R. Tanny, *Inorg. Chem.*, 1974, **13**, 880.
494. J. W. M. de Boer, C. W. Hilbers and E. de Boer, *J. Magn. Resonance*, 1977, **25**, 437.
495. J. W. M. de Boer, P. J. D. Sakkers, C. W. Hilbers and E. de Boer, *J. Magn. Resonance*, 1977, **25**, 455.
496. J. W. M. de Boer, P. J. D. Sakkers, C. W. Hilbers and E. de Boer, *J. Magn. Resonance*, 1977, **26**, 253.

497. K. Ajisaka and M. Kainosho, *J. Amer. Chem. Soc.*, 1975, **97**, 1761.  
498. A. D. Sherry and C. Yoshida, *J. Amer. Chem. Soc.*, 1973, **95**, 3011.  
499. M. D. McCreary, D. W. Lewis, D. L. Wernick and G. M. Whitesides, *J. Amer. Chem. Soc.*, 1974, **96**, 1038.  
500. H. L. Goering, J. N. Eikenberry, G. S. Koermer and C. J. Lattimer, *J. Amer. Chem. Soc.*, 1974, **96**, 1493.  
501. G. R. Sullivan, D. Ciavarella and H. S. Mosher, *J. Org. Chem.*, 1974, **39**, 2411.  
502. N. J. Cranbury, *J. Pharm. Sci.*, 1976, **65**, 592.  
503. A. F. Cockerill and G. L. O. Davies, *Org. Magn. Resonance*, 1974, **6**, 669.  
504. O. Korver and M. van Gorkom, *Tetrahedron*, 1974, **30**, 4041.  
505. K. Yamamoto, T. Hayashi and M. Kumada, *Bull. Chem. Soc. Japan*, 1974, **47**, 1555.  
506. R. R. Fraser, J. B. Stothers and C. T. Tan, *J. Magn. Resonance*, 1973, **10**, 95.  
507. D. W. Cameron, J. S. Edmonds, G. I. Feutrill and E. A. Hoy, *Austral. J. Chem.*, 1976, **29**, 2257.  
508. D. L. Reger, *Inorg. Chem.*, 1975, **14**, 660.  
509. R. G. Denning, F. J. C. Rossotti and P. J. Sellars, *Chem. Comm.*, 1973, 381.  
510. A. Mannschreck, V. Jonas, H-O. Bödecker and G. Köbrich, *Tetrahedron Lett.*, 1974, 2153.  
511. A. Mannschreck, V. Jonas and B. Kolb, *Angew. Chem. Internat. Edn.*, 1973, **12**, 583909.  
512. L. Lefevre, T. Burgemeister and A. Mannschreck, *Tetrahedron Lett.*, 1977, 1125.  
513. W. H. Pirkle and M. S. Hoekstra, *J. Amer. Chem. Soc.*, 1976, **98**, 1832.  
514. C. P. R. Jennison and D. Mackay, *Canad. J. Chem.*, 1973, **51**, 3726.  
515. J. W. Faller, M. A. Adams and G. N. La Mar, *Tetrahedron Lett.*, 1974, 699.  
516. G. V. Fazakerley and G. E. Jackson, *J. Chem. Soc., Perkin II*, 1975, 567.  
517. J. R. Mooney, C. K. Choy, K. Knox and M. E. Kenney, *J. Amer. Chem. Soc.*, 1975, **97**, 3033.  
518. J. E. Maskasky and M. E. Kenney, *J. Amer. Chem. Soc.*, 1973, **95**, 1443.  
519. M. Gouedard, F. Gaudemer and A. Gaudemer, *Tetrahedron Lett.*, 1973, 2257.  
520. A. K. Bose, P. R. Srinivasan and G. Trainor, *J. Amer. Chem. Soc.*, 1974, **96**, 3670.  
521. J. Brunn and C. Beck, *Z. Chem.*, 1977, **17**, 296.  
522. J. W. Faller and G. N. La Mar, *Tetrahedron Lett.*, 1973, 1381.  
523. V. K. Voronov, L. A. Shestova, E. S. Domnina and G. G. Skvortsova, *Izv. Akad. Nauk SSSR, Ser. Khim.*, 1976, **2**, 412.  
524. G. L. Blackmer and R. L. Roberts, *J. Magn. Resonance*, 1973, **10**, 380.  
525. J. Bargon, *J. Amer. Chem. Soc.*, 1973, **95**, 941.  
526. J. J. Brooks and R. E. Sievers, *J. Chromat. Sci.*, 1973, **11**, 303.  
527. G. A. Catton, F. A. Hart and G. P. Moss, *J. Chem. Soc., Dalton*, 1975, 221.  
528. S. R. Tanny, M. Pickering and C. S. Springer, *J. Amer. Chem. Soc.*, 1973, **95**, 6227.  
529. K. Yamada and S. Ishihara, *Chem. Lett.*, 1973, 549.  
530. J. W. Faller and B. V. Johnson, *J. Organometal. Chem.*, 1975, **96**, 99.  
531. D. F. Evans and G. C. de Villardi, *Chem. Comm.*, 1976, 7.  
532. I. M. Armitage, E. E. Burnell and M. B. Dunn, *J. Magn. Resonance*, 1974, **13**, 167.  
533. G. N. La Mar and D. L. Budd, *J. Amer. Chem. Soc.*, 1974, **96**, 7317.  
534. C. M. Dobson, L. O. Ford and S. E. Summers, *J. Chem. Soc., Faraday II*, 1975, **71**, 1145.  
535. D. E. Williamson and G. W. Everett, *J. Amer. Chem. Soc.*, 1975, **97**, 2397.  
536. J. Gulbis and G. W. Everett, *Tetrahedron*, 1976, **32**, 913.  
537. J. Gulbis, G. W. Everett and C. W. Frank, *J. Amer. Chem. Soc.*, 1976, **98**, 1280.  
538. M. Witanowski, L. Stefaniak, H. Januszewski and G. A. Webb, *J. Cryst. Mol. Struct.*, 1975, **5**, 141.  
539. Y. Moriguchi, *Chem. Lett.*, 1974, 47.  
540. E. R. Birnbaum and S. Stratton, *Inorg. Chem.*, 1973, **12**, 379.  
541. L. M. Stock and M. R. Wasielewski, *J. Amer. Chem. Soc.*, 1974, **96**, 583.  
542. G. P. Underwood and H. S. Friedman, *J. Amer. Chem. Soc.*, 1974, **96**, 4089.

543. K. Yoshikawa, M. Hashimoto, H. Masuda and I. Morishima, *J. Chem. Soc., Perkin II*, 1977, 809.
544. R. A. Dwek, "Nuclear Magnetic Resonance in Biochemistry: Applications to Enzyme Systems", Oxford University Clarendon Press, 1973.
545. T. L. James, "NMR in Biochemistry: Principles and Applications", Academic Press, New York, 1975.
546. R. A. Dwek, I. D. Campbell, R. E. Richards and R. J. P. Williams (eds.), "NMR in Biology", Academic Press, 1977.
547. K. Wuethrich, *Naturwiss*, 1973, **60**, 221.
548. W. D. Phillips, *Methods Enzymol.*, 1973, 825.
549. K. Wuethrich, *Experientia*, 1974, **30**, 577.
550. R. A. Dwek, R. J. P. Williams and A. V. Xavier, in "Metal Ions in Biological Systems", Vol. 4, H. Sigel (ed.), Marcel Dekker, New York, 1974, pp. 61–210.
551. S. J. Ferguson, *Tech. Top. Bioinorg. Chem.*, 1975, 305.
552. J. Feeney, in "New Techniques in Biophysics and Cell Biology", Vol. 2, R. H. Pain and B. J. Smith (eds.), Wiley, 1975, pp. 287–340.
553. S. N. Rosenthal and J. H. Fendler, *Adv. Phys. Org. Chem.*, 1976, **13**, 279.
554. R. J. P. Williams, *Chem. Brit.*, 1978, **14**, 25.
555. S. Förster and B. Lindman, *Chem. Brit.*, 1978, **14**, 29.
556. C. M. Dobson and B. A. Levine, in "New Techniques in Biophysics and Cell Biology", Vol. 3, R. H. Pain and B. J. Smith (eds.), Wiley, 1976, p. 19.
557. W. G. Espersen and M. R. Bruce, *J. Amer. Chem. Soc.*, 1976, **98**, 40.
558. W. G. Espersen and M. R. Bruce, *J. Phys. Chem.*, 1976, **80**, 161.
559. W. R. Walker, Y-H. L. Shaw and N. C. Li, *J. Amer. Chem. Soc.*, 1973, **95**, 3015.
560. P. J. Quilley and G. A. Webb, *Coord. Chem. Rev.*, 1974, **12**, 407.
561. J. J. Villafranca, in ref. 550, pp. 29–59.
562. J. H. Griffin and B. Furie, *Biochemie*, 1975, **57**, 453.
563. B. A. Levine and R. J. P. Williams, *Proc. Roy. Soc. (A)*, 1975, **345**, 5.
564. I. D. Campbell and C. M. Dobson, *Proc. Roy. Soc. (A)*, 1975, **345**, 23.
565. D. F. S. Natusch, *J. Amer. Chem. Soc.*, 1973, **95**, 1688.
566. R. V. Snyder and R. J. Angelici, *Inorg. Chem.*, 1974, **13**, 14.
567. L. Gelbaum and R. Engel, *J. Inorg. Nuclear Chem.*, 1975, **37**, 793.
568. G. V. Fazakerley and G. E. Jackson, *J. Chem. Soc., Perkin II*, 1975, 567.
569. I. Nagypal, E. Farkas and A. Gergely, *J. Inorg. Nuclear Chem.*, 1975, **37**, 2145.
570. W. R. Walker, J. M. Guo and N. C. Li, *Austral. J. Chem.*, 1973, **26**, 2391.
571. W. Voelter, G. Sokolowski, U. Weber and U. Weser, *Eur. J. Biochem.*, 1975, **58**, 159.
572. R. E. Wasylshen and J. S. Cohen, *J. Amer. Chem. Soc.*, 1977, **99**, 2480.
573. H. Kozłowski and B. Jezowska-Trzebiatowska, *J. Inorg. Nuclear Chem.*, 1977, **39**, 1275.
574. J. K. Beattie and D. J. Fensom, *J. Amer. Chem. Soc.*, 1976, **98**, 500.
575. J. J. Led and D. M. Grant, *J. Amer. Chem. Soc.*, 1975, **97**, 6962.
576. J. J. Led and D. M. Grant, *J. Amer. Chem. Soc.*, 1977, **99**, 5845.
577. H. J. Grande, R. L. Houghton and C. Veeger, *Eur. J. Biochem.*, 1973, **37**, 563.
- 577a. R. Basosi, E. Tiezzi and G. Valensin, *J. Phys. Chem.*, 1975, **79**, 1725.
578. E. Tiezzi, *J. Chem. Soc., Perkin II*, 1975, 769.
579. A. D. Sherry and E. Pascual, *J. Amer. Chem. Soc.*, 1977, **99**, 5871.
580. B. Warren and J. H. Bradbury, *Austral. Polym. Symp.*, 1974, 65.
581. P. E. Young, V. Madison and E. R. Blout, *J. Amer. Chem. Soc.*, 1973, **95**, 6142.
582. P. E. Young, V. Madison and E. R. Blout, *J. Amer. Chem. Soc.*, 1976, **98**, 5365.
583. I. D. Campbell, C. M. Dobson and R. J. P. Williams, *Proc. Roy. Soc. (A)*, 1975, **345**, 41.
584. C. M. Dobson, in ref. 546, pp. 63–94.

585. I. D. Campbell, C. M. Dobson, R. J. P. Williams and A. V. Xavier, *J. Magn. Resonance*, 1973, **11**, 172.
586. D. G. Agresti, R. E. Lenkinski and J. D. Glickson, *Biochem. Biophys. Res. Commun.*, 1977, **76**, 711.
587. W. Klaeui, *Helv. Chim. Acta.*, 1977, **60**, 1296.
588. B. H. Barber and J. P. Carver, *Canad. J. Biochem.*, 1975, **53**, 371.
589. B. H. Barber, B. J. Fuhr and J. P. Carver, *Biochemistry*, 1975, **14**, 4075.
590. J. P. Carver, B. H. Barber and B. J. Fuhr, *J. Biol. Chem.*, 1977, **252**, 314.
591. J. L. Markley, E. L. Ulrich, S. P. Berg and D. W. Krogmann, *Biochemistry*, 1975, **14**, 4428.
592. J. K. Beattie, D. J. Fensom, H. C. Freeman, E. Woodcock, H. A. O. Hill and A. M. Stokes, *Biochim. Biophys. Acta*, 1975, **405**, 109.
593. H. A. O. Hill, J. C. Leer, B. E. Smith, C. B. Storm and R. P. Ambler, *Biochem. Biophys. Res. Commun.*, 1976, **70**, 331.
594. H. A. O. Hill, B. E. Smith, C. B. Storm and R. P. Ambler, *Biochem. Biophys. Res. Commun.*, 1976, **70**, 783.
595. H. P. C. Hogenkamp, R. D. Tkachuck, M. E. Grant, R. Fuentes and N. A. Matwiyoff, *Biochemistry*, 1975, **14**, 3707.
596. H. P. C. Hogenkamp, P. J. Vergamini and N. A. Matwiyoff, *J. Chem. Soc., Dalton*, 1975, 2628.
597. S. A. Cockle, O. D. Hensens, H. A. O. Hill and R. J. P. Williams, *J. Chem. Soc., Dalton*, 1975, 2633.
598. O. D. Hensens, H. A. O. Hill, J. Thornton, A. M. Turner and R. J. P. Williams, *Phil. Trans. Roy. Soc. (B)*, 1976, **273**, 353.
599. R. A. Firth, H. A. O. Hill, B. E. Mann, J. M. Pratt, R. G. Thorp and R. J. P. Williams, *J. Chem. Soc. (A)*, 1968, 2419.
600. B. Jezowska-Trzebiatowska, G. Formicka-Kozłowska and H. Kozłowski, *Chem. Phys. Lett.*, 1976, **42**, 242.
601. B. Jezowska-Trzebiatowska, G. Formicka-Kozłowska and H. Kozłowski, *Bull. Acad. Pol. Sci., Ser. Sci. Chim.*, 1976, **24**, 987.
602. B. Jezowska-Trzebiatowska, G. Formicka-Kozłowska and H. Kozłowski, *J. Inorg. Nuclear Chem.*, 1977, **39**, 1265.
603. H. M. Mizioro and A. S. Mildvan, *J. Biol. Chem.*, 1974, **249**, 2743.
604. J. M. Young and K. J. Schray, *J. Biol. Chem.*, 1975, **250**, 9021.
605. B. J. Marwedel, R. J. Kurland, D. J. Kosman and M. J. Ettinger, *Biochem. Biophys. Res. Commun.*, 1975, **63**, 773.
606. T. D. Marinetti, G. H. Snyder and B. D. Sykes, *Biochemistry*, 1976, **15**, 4600.
607. M. Epstein and J. Reuben, *Biochim. Biophys. Acta*, 1977, **481**, 164.
608. J. P. Cohen-Addan and J. C. Leyssieux, *J. Phys. (Paris), Colloq.*, 1973, 53.
609. A. Lanir and G. Navon, *Biochim. Biophys. Acta*, 1974, **341**, 75.
610. A. Lanir, S. Gradstajn and G. Navon, *Biochemistry*, 1975, **14**, 242.
611. I. Bertini, C. Luchinat, A. Scozzafava, *J. Amer. Chem. Soc.*, 1977, **99**, 581.
612. E. Melamud and A. S. Mildvan, *J. Biol. Chem.*, 1975, **250**, 8193.
613. G. L. Cottam and R. L. Ward, *Biochem. Biophys. Res. Commun.*, 1975, **64**, 797.
614. T. L. James, J. Reuben and M. Cohn, *J. Biol. Chem.*, 1973, **248**, 6443.
615. K. M. Valentine and G. L. Cottam, *Proc. Rare Earth Res. Conf. 10th*, 1973, 127.
616. R. K. Gupta, *J. Biol. Chem.*, 1977, **252**, 5183.
617. J. J. Villafranca and F. C. Wedler, *Biochemistry*, 1974, **13**, 3286.
618. J. J. Villafranca, D. E. Ash and F. C. Wedler, *Biochemistry*, 1976, **15**, 536.
619. J. J. Villafranca and D. E. Ash, *Biochemistry*, 1976, **15**, 544.
620. J. J. Villafranca, D. E. Ash and F. C. Wedler, *Biochem. Biophys. Res. Commun.*, 1975, **66**, 1003.
621. N. Zisapel, G. Navon and M. Sokolovsky, *Eur. J. Biochem.*, 1975, **52**, 487.

622. D. H. Buttlair and M. Cohn, *J. Biol. Chem.*, 1974, **249**, 5733.
623. D. L. Sloan, J. M. Young and A. S. Mildvan, *Biochemistry*, 1975, **14**, 1998.
624. S. Fan, L. W. Harrison and G. G. Hammes, *Biochemistry*, 1975, **14**, 2219.
625. R. D. Hershberg, G. H. Reed, A. J. Slotboom and G. H. de Haas, *Biochemistry*, 1976, **15**, 2268.
626. Y-F. Lam, W. A. Bridger and G. Kotowycz, *Biochemistry*, 1976, **15**, 4742.
627. J. F. Chlebowski, I. M. Armitage, P. P. Tusa and J. E. Coleman, *J. Biol. Chem.*, 1976, **251**, 1207.
628. D. H. Buttlair, G. H. Reed and R. Himes, *J. Biol. Chem.*, 1975, **250**, 261.
629. D. H. Buttlair, M. Cohn and W. A. Bridger, *J. Biol. Chem.*, 1977, **252**, 1957.
630. J. J. Grimaldi and B. D. Sykes, *J. Biol. Chem.*, 1975, **250**, 1618.
631. J. J. Villafranca and R. E. Viola, *Arch. Biochem. Biophys.*, 1974, **165**, 51.
632. D. H. Williams and J. R. Kalman, *J. Amer. Chem. Soc.*, 1977, **99**, 2768.
633. R. E. Wasylishen and M. R. Graham, *Canad. J. Biochem.*, 1975, **53**, 1250.
634. J. Reuben and Z. Luz, *J. Phys. Chem.*, 1976, **80**, 1357.
635. D. R. Burton, R. A. Dwek, S. Forsén and G. Karlstrom, *Biochemistry*, 1977, **16**, 250.
636. J. Reuben, *J. Chem. Phys.*, 1975, **63**, 5063.
637. H. Scheer and J. J. Katz, in "Porphyrins and Metalloporphyrins", 1975, pp. 399-524.
638. W. de W. Horrocks and E. S. Greenberg, *Mol. Phys.*, 1974, **27**, 993.
639. K. Wuethrich and R. Baumann, *Ann. New York Acad. Sci.*, 1973, **222**, 709.
640. E. von Goldammer, H. Zorn and A. Daniels, *Eur. J. Biochem.*, 1975, **57**, 291.
641. E. von Goldammer and H. Zorn, *Mol. Phys.*, 1976, **32**, 1423.
642. E. von Goldammer, H. Zorn and A. Daniels, *J. Magn. Resonance*, 1976, **23**, 199.
643. G. N. La Mar, J. S. Frye and J. D. Satterlee, *Biochim. Biophys. Acta*, 1976, **428**, 78.
644. J. D. Satterlee and G. N. La Mar, *J. Amer. Chem. Soc.*, 1976, **98**, 2804.
645. J. T. Wang, J. C. Herman and D. F. Johnson, *J. Amer. Chem. Soc.*, 1975, **97**, 1968.
646. K. Wuethrich and R. Baumann, *Helv. Chim. Acta*, 1974, **57**, 336.
647. G. N. La Mar, T. J. Bold and J. D. Satterlee, *Biochim. Biophys. Acta*, 1977, **498**, 189.
648. G. N. La Mar, J. Del Gaudio and J. S. Frye, *Biochim. Biophys. Acta*, 1977, **498**, 422.
649. G. N. La Mar and J. Del Gaudio, *Adv. Chem. Ser.*, 1977, 162.
650. J. G. Brassington, R. J. P. Williams and P. E. Wright, *Chem. Comm.*, 1975, 338.
651. G. N. La Mar, *Pure Appl. Chem.*, 1974, **40**, 13.
652. R. V. Snyder and G. N. La Mar, *J. Amer. Chem. Soc.*, 1977, **99**, 7178.
653. J. Mispelter, M. Momenteau and J. M. Lhoste, *Mol. Phys.*, 1977, **33**, 1715.
654. H. Goff, G. N. La Mar and C. A. Reed, *J. Amer. Chem. Soc.*, 1977, **99**, 3641.
- 654a. H. Goff and G. N. La Mar, *J. Amer. Chem. Soc.*, 1977, **99**, 6599.
655. C. D. Barry, H. A. O. Hill, P. J. Sadler and R. J. P. Williams, *Proc. Roy. Soc. (A)*, 1973, **334**, 493.
656. T. R. Janson, L. J. Boucher and J. J. Katz, *Inorg. Chem.*, 1973, **12**, 940.
657. G. N. La Mar and F. A. Walker, *J. Amer. Chem. Soc.*, 1975, **97**, 5103.
658. H. A. O. Hill, P. J. Sadler and R. J. P. Williams, *J. Chem. Soc., Dalton*, 1973, 1663.
659. L. Ford, H. A. O. Hill, B. E. Mann, P. J. Sadler and R. J. P. Williams, *Biochim. Biophys. Acta*, 1976, **430**, 413.
660. G. P. Fulton and G. N. La Mar, *J. Amer. Chem. Soc.*, 1976, **98**, 2119.
661. G. P. Fulton and G. N. La Mar, *J. Amer. Chem. Soc.*, 1976, **98**, 2124.
662. C. D. Barry, H. A. O. Hill, B. E. Mann, P. J. Sadler and R. J. P. Williams, *J. Amer. Chem. Soc.*, 1973, **95**, 4545.
663. C. C. McDonald and W. D. Phillips, *Biochemistry*, 1973, **12**, 3170.
664. E. Oldfield and A. Allerhand, *Proc. Nat. Acad. Sci. USA*, 1973, **70**, 3531.
665. R. T. Eakin, L. O. Morgan and N. A. Matwiyoff, *Biochemistry*, 1975, **14**, 4538.
- 665a. L. O. Morgan, R. T. Eakin, P. J. Vergamini and N. A. Matwiyoff, *Biochemistry*, 1976, **15**, 2203.



666. G. R. Moore, R. C. Pitt and R. J. P. Williams, *Eur. J. Biochem.*, 1977, **77**, 53.
667. R. M. Keller, K. Wuethrich and I. Pecht., *FEBS Lett.*, 1976, **70**, 180.
668. E. Stellwagen and R. G. Shulman, *J. Mol. Biol.*, 1973, **80**, 559.
669. A. Lanir and I. Aviram, *Arch. Biochem. Biophys.*, 1975, **166**, 439.
670. I. Morishima and T. Inubushi, *FEBS Lett.*, 1977, **81**, 57.
671. I. Morishima, T. Inubushi, S. Neya, S. Satoshi and T. Yonezawa, *Biochem. Biophys. Res. Commun.*, 1977, **78**, 739.
672. R. Keller, O. Groudinsky and K. Wuethrich, *Biochim. Biophys. Acta*, 1973, **328**, 233.
673. R. Keller, O. Groudinsky and K. Wuethrich, *Biochim. Biophys. Acta*, 1976, **427**, 497.
674. K. Wuethrich, J. Hochmann, R. M. Keller, G. Wagner, M. Brunori and C. Giacometti, *J. Magn. Resonance*, 1975, **19**, 111.
675. M. Guéron, *J. Magn. Resonance*, 1975, **19**, 58.
676. W. de W. Horrocks and E. S. Greenberg, *Biochim. Biophys. Acta*, 1973, **322**, 38.
677. A. Mayer, S. Ogawa, R. G. Shulman, T. Yamane, J. A. S. Cavaleiro, A. M. d'A. Rocha Gonsalves, G. W. Kenner and K. M. Smith, *J. Mol. Biol.*, 1974, **86**, 749.
678. T. Iizuka and I. Morishima, *Biochim. Biophys. Acta*, 1975, **400**, 143.
679. T. Iizuka, S. Ogawa, T. Inubushi, T. Yonezawa and I. Morishima, *FEBS Lett.*, 1976, **64**, 156.
680. I. Morishima and T. Iizuka, *J. Amer. Chem. Soc.*, 1974, **96**, 7365.
681. R. B. Visscher and F. R. N. Gurd, *J. Biol. Chem.*, 1975, **250**, 2238.
682. W. C. Jones, T. M. Rothgeb and F. R. N. Gurd, *J. Biol. Chem.*, 1976, **251**, 7452.
683. D. J. Wilbur and A. Allerhand, *J. Biol. Chem.*, 1977, **252**, 4968.
684. D. J. Wilbur and A. Allerhand, *FEBS Lett.*, 1977, **79**, 144.
685. M. B. Hayes, H. Hagenmaier and J. S. Cohen, *J. Biol. Chem.*, 1975, **250**, 7461.
686. J. S. Morrow and F. R. N. Gurd, *C. R. C. Crit. Rev. Biochem.*, 1975, **3**, 221.
687. G. N. La Mar, D. L. Budd and H. Goff, *Biochem. Biophys. Res. Commun.*, 1977, **77**, 104.
688. I. Morishima and T. Iizuka, *J. Amer. Chem. Soc.*, 1974, **96**, 5279.
689. T. Iizuka and I. Morishima, *Biochim. Biophys. Acta*, 1974, **371**, 1.
690. W. Schoessler, R. Hintsche, K. Pommerening and P. Mohr, *Stud. Biophys.*, 1973, **39**, 25.
691. W. Schoessler, K. Gerisch, R. Hintsche, K. Pommerening and P. Mohr, *Acta Biol. Med. Ger.*, 1975, **34**, 345.
692. S. Ogawa, D. J. Patel and S. R. Simon, *Biochemistry*, 1974, **13**, 2001.
693. T.-H. Huang and A. G. Redfield, *J. Biol. Chem.*, 1976, **251**, 7114.
694. J. J. Breen, D. A. Bertoli and J. Dadok, *Biophys. Chem.*, 1974, **2**, 49.
695. F. S. Molinaro, R. G. Little and J. A. Ibers, *J. Amer. Chem. Soc.*, 1977, **99**, 5628.
696. E. Oldfield, R. S. Norton and A. Allerhand, *J. Biol. Chem.*, 1975, **250**, 6368.
697. E. Oldfield, R. S. Norton and A. Allerhand, *J. Biol. Chem.*, 1975, **250**, 6381.
698. E. Oldfield and A. Allerhand, *J. Biol. Chem.*, 1975, **250**, 6403.
699. R. B. Moon and J. H. Richards, *Biochemistry*, 1974, **13**, 3437.
700. R. B. Moon, K. Dill and J. H. Richards, *Biochemistry*, 1977, **16**, 221.
701. J. S. Morrow, J. B. Matthew, R. J. Wittebort and F. R. N. Gurd, *J. Biol. Chem.*, 1976, **251**, 477.
702. D. Mansuy, J. Y. Lallemand, J. C. Chottard, B. Cendrier, G. Gacon and H. Wajcman, *Biochem. Biophys. Res. Commun.*, 1976, **70**, 595.
703. M. E. Johnson and L. W. M. Fung, *J. Amer. Chem. Soc.*, 1977, **99**, 1245.
704. B. Blicharska and J. I. Dimitriew, *Mag. Res. Relat. Phenom.*, *Proc. Congr. Ampère 18th*, 1974, 281.
705. G. Lahajnar, I. Zupancic, R. Blinc, G. Pifat and S. Maricic, *Biopolymers*, 1974, **13**, 1187.
706. T. D. Lindstrom and S. H. Koenig, *J. Magn. Resonance*, 1974, **15**, 344.
707. G. Pifat, S. Maricic and S. Grandja, *Biopolymers*, 1973, **12**, 905.
708. S. Vuk-Pavlovic, *Biophys. Chem.*, 1976, **5**, 395.
709. S. Vuk-Pavlovic, B. Benko, S. Maricic, B. Markovska and G. D. Efremov, *Internat. J. Biochem.*, 1976, **7**, 367.

710. S. Vuk-Pavlovic, V. Bracika, B. Benko and S. Maricic, *Biochim. Biophys. Acta*, 1977, **491**, 447.
711. B. Benko, S. Vuk-Pavlovic and S. Maricic, *Biochim. Biophys. Acta*, 1977, **491**, 457.
712. B. Markovska, G. D. Efremov, S. Vuk-Pavlovich, B. Benko and S. Maricic, *Arch. Biochem. Biophys.*, 1975, **171**, 337.
713. B. Benko and S. Vuk-Pavlovich, *Biochem. Biophys. Res. Commun.*, 1976, **71**, 1303.
714. F. F. Brown and I. D. Campbell, *FEBS Lett.*, 1976, **65**, 322.
715. R. G. Shulman, S. Ogawa, A. Mayer and C. L. Castillo, *Ann. New York Acad. Sci.*, 1973, **222**, 9.
716. A. Mayer, S. Ogawa, R. G. Shulman and K. Gersonde, *J. Mol. Biol.*, 1973, **81**, 187.
717. C. Ho, T. R. Lindstrom, J. J. Baldassare and J. J. Breen, *Ann. New York Acad. Sci.*, 1973, **222**, 21.
718. L. W. M. Fung, K-L. C. Lin and C. Ho, *Biochemistry*, 1975, **14**, 3424.
719. C. Ho, L. W. M. Fung, K-L. C. Lin, G. S. Supinski and K. J. Wiechelmann, *Proc. Symp. Mol. Cell. Aspects Sickle Cell Dis.*, 1975, 65.
720. R. J. Gupta, *J. Biol. Chem.*, 1976, **251**, 6815.
721. A. Zipp, I. D. Kuntz and T. L. James, *Arch. Biochem. Biophys.*, 1977, **178**, 435.
722. L. W. M. Fung, A. P. Minton and C. Ho, *Proc. Nat. Acad. Sci. USA*, 1976, **73**, 1581.
723. L. W. M. Fung, A. P. Minton, T. R. Lindstrom, A. V. Pisciotta and C. Ho, *Biochemistry*, 1977, **16**, 1452.
724. A. Lapidot, C. S. Irving and Z. Malik, *J. Amer. Chem. Soc.*, 1976, **98**, 632.
725. A. Lapidot and C. S. Irving, *J. Amer. Chem. Soc.*, 1977, **99**, 5488.
726. R. M. K. Carlson, *Proc. Nat. Acad. Sci. USA*, 1975, **72**, 2217.
727. W. E. Marshall, A. J. R. Costello and T. O. Henderson, *Biochim. Biophys. Acta*, 1977, **490**, 290.
728. J-M. Gwo, R. E. Specher and N. C. Li, *J. Magn. Resonance*, 1975, **18**, 427.
729. K. D. Bartle, B. J. Dale and D. W. Jones, *J. Magn. Resonance*, 1973, **12**, 286.
730. P. E. Wright and C. A. Appleby, *FEBS Lett.*, 1977, **78**, 61.
731. D. J. Patel and L. L. Canuel, *Proc. Nat. Acad. Sci. USA*, 1976, **73**, 1398.
732. W. D. Phillips and M. Poe, *Methods Enzymol.*, 1972, **24B**, 304.
733. C. C. McDonald, W. D. Phillips, W. Lovenberg and R. H. Holm, *Ann. New York Acad. Sci.*, 1973, **222**, 789.
734. W. D. Phillips, in ref. 17, Ch. 11, pp. 458-475.
735. W. D. Phillips and M. Poe, in "Iron-Sulphur Proteins, Vol. 2", W. Lovenberg (ed.), Academic Press, New York, 1973, pp. 255-284.
736. W. D. Phillips and C. C. McDonald, *Proc. Nat. Acad. Sci. USA*, 1974, **71**, 140.
737. H. L. Crespi, A. G. Kostka and U. H. Smith, *Biochem. Biophys. Res. Commun.*, 1974, **61**, 1407.
738. E. L. Packer, H. Sternlicht, E. T. Lode and J. C. Rabinowitz, *J. Biol. Chem.*, 1975, **250**, 2062.
739. E. L. Packer, W. V. Sweeney, J. C. Rabinowitz, H. Sternlicht and E. N. Shaw, *J. Biol. Chem.*, 1977, **252**, 2245.
740. J. J. G. Moura, A. V. Xavier, M. Bruschi and J. Le Gall, *Biochim. Biophys. Acta*, 1977, **459**, 278.
741. J. J. G. Moura, A. V. Xavier, D. J. Cookson, G. R. Moore, R. J. P. Williams, M. Bruschi and J. Le Gall, *FEBS Lett.*, 1977, **81**, 275.
742. R. H. Holm, W. D. Phillips, B. A. Averill, J. J. Mayerle and T. Herskovitz, *J. Amer. Chem. Soc.*, 1974, **96**, 2109.
743. L. Que, M. A. Bobrik, J. A. Ibers and R. H. Holm, *J. Amer. Chem. Soc.*, 1974, **96**, 4168.
744. G. N. La Mar, G. R. Eaton, R. H. Holm and F. A. Walker, *J. Amer. Chem. Soc.*, 1973, **95**, 63.
745. G. Christou, C. D. Garner and F. E. Mabbs, *Inorg. Chim. Acta*, 1978, **28**, L189.
746. R. A. Dwek, J. A. Knott, A. C. McLaughlin, R. W. Myatt, E. M. Press, N. C. Price and R. E. Richards, *Proc. Rare Earth Res. Conf. 11th*, 1974, 184.

747. D. R. Burton, S. Forsén, G. Karlstrom, R. A. Dwek and A. C. McLaughlin, *Eur. J. Biochem.*, 1976, **71**, 519.
748. D. R. Burton, S. Forsén, G. Karlstrom, R. A. Dwek, A. C. McLaughlin and S. Wain-Hobson, *Eur. J. Biochem.*, 1977, **75**, 445.
749. G. Kotowycz and O. Suzuki, *Biochemistry*, 1973, **12**, 3434.
750. H. Fritzsche, K. Arnold and R. Krusche, *Stud. Biophys.*, 1974, **45**, 131.
751. R. Basosi, F. Laschi, E. Tiezzi and G. Valensin, *J. Chem. Soc., Faraday I*, 1976, **72**, 1505.
752. G. Kotowycz, *Canad. J. Chem.*, 1974, **52**, 924.
753. L. G. Marzilli, W. C. Trogler, D. P. Hollis, T. J. Kistenmacher, C-H. Chang and B. E. Hanson, *Inorg. Chem.*, 1975, **14**, 2568.
754. Y-Y. H. Chao and D. R. Kearns, *J. Amer. Chem. Soc.*, 1977, **99**, 6425.
755. C-Y. Lee and M. J. Raska, *J. Magn. Resonance*, 1975, **17**, 151.
756. G. Kotowycz and O. Suzuki, *Biochemistry*, 1973, **12**, 5325.
757. C. M. Dobson, R. J. P. Williams and A. V. Xavier, *J. Chem. Soc., Dalton*, 1974, 1762.
758. C. D. Barry, T. A. Glasel and R. J. P. Williams, *J. Mol. Biol.*, 1974, **84**, 471.
759. U. Weser, G. J. Strobel, H. Rupp and W. Voelter, *Eur. J. Biochem.*, 1974, **50**, 91.
760. U. Weser, G. J. Strobel and W. Voelter, *FEBS Lett.*, 1974, **41**, 243.
761. G. V. Fazakerley and M. A. Wolfe, *Eur. J. Biochem.*, 1977, **74**, 337.
762. C. D. Barry, D. R. Martin and R. J. P. Williams, *J. Mol. Biol.*, 1974, **84**, 491.
763. C. D. Barry, C. M. Dobson, R. J. P. Williams and A. V. Xavier, *J. Chem. Soc., Dalton*, 1974, 1765.
764. J. Torrelles and A. C. de Paulet, *Biochemie*, 1973, **55**, 845.
765. F. F. Brown, I. D. Campbell, R. Henson, C. W. J. Hirst and R. E. Richards, *Eur. J. Biochem.*, 1973, **38**, 54.
766. Y-F. Lam, G. P. P. Kuntz and G. Kotowycz, *J. Amer. Chem. Soc.*, 1974, **96**, 1834.
767. G. P. P. Kuntz, Y-F. Lam and G. Kotowycz, *Canad. J. Chem.*, 1975, **53**, 926.
768. V. Wee, I. Feldman, P. Rose and S. Gross, *J. Amer. Chem. Soc.*, 1974, **96**, 103.
769. I. Feldman and V. Wee, *Biochemistry*, 1974, **13**, 1836.
770. L. A. Sibeld'dina, L. P. Kayushin, M. S. Okon and A. U. Stepanyants, *Stud. Biophys.*, 1973, **38**, 177.
771. G. P. P. Kuntz and G. Kotowycz, *Biochemistry*, 1975, **14**, 4144.
772. G. T. Robillard, in ref. 546, pp. 201-230.
773. C. R. Jones and D. R. Kearns, *J. Amer. Chem. Soc.*, 1974, **96**, 3651.
774. C. R. Jones and D. R. Kearns, *Proc. Nat. Acad. Sci. USA*, 1974, **71**, 4237.
775. Y-Y. H. Chao and D. R. Kearns, *Biochim. Biophys. Acta*, 1977, **477**, 20.
776. L. M. Weiner, S. V. Vossel, J. M. Backer, Yu. N. Molin and A. I. Rezvukhin, *Izv. Sib. Otd. Akad. Nauk SSSR, Ser. Khim. Nauk*, 1975, 111.
777. A. Yamada, K. Akasaka and H. Hatano, *Biopolymers*, 1976, **15**, 1315.
778. A. G. Lee, N. J. M. Birdsall and J. C. Metcalfe, in "Methods in Membrane Biology, Vol. 2", E. D. Korn (ed.), Plenum Press, New York, 1974, pp. 1-156.
779. J. Seelig, *Pathol. Microbiol.*, 1974, **41**, 151.
780. L. D. Bergel'son and V. F. Bystrov, Fed. Eur. Biochem. Soc. Meeting Proceedings, Biomembranes: Struct. Funct., 1975, 33.
781. L. W. Reeves, *Int. Rev. Sci., Phys. Chem. Ser. 2*, 1975, 139.
782. V. F. Bystrov, *Int. Biophys. Congr.* 4th, 1973, 113.
783. S. B. Andrews, J. W. Faller, J. M. Gilliam and R. J. Barnett, *Proc. Nat. Acad. Sci. USA*, 1973, **70**, 1814.
784. M. S. Fernandez, H. Celis and M. Montal, *Biochim. Biophys. Acta*, 1973, **323**, 600.
785. G. R. A. Hunt, *FEBS Lett.*, 1975, **58**, 194.

- 786. Yu E. Shapiro, A. V. Viktorov, V. I. Volkova, L. I. Barsukov, V. F. Bystrov and L. D. Bergel'son, *Chem. Phys. Lipids*, 1975, **14**, 227.
- 787. P. W. Nolden and T. Ackermann, *Biophys. Chem.*, 1976, **4**, 297.
- 788. P. W. Nolden and T. Ackermann, *Biophys. Chem.*, 1975, **3**, 183.
- 789. K. Arnold, J. Frenzel and R. Pausch, *Stud. Biophys.*, 1976, **54**, 163.
- 790. A. V. Viktorov, I. A. Vasilenko, L. I. Barsukov, R. P. Evstigneeva and L. D. Bergel'son, *Dokl. Akad. Nauk SSSR*, 1977, **234**, 207.
- 791. T. Wydrzynski, N. Zumbulyadis, P. G. Schmidt and Govindjee, *Biochim. Biophys. Acta*, 1975, **408**, 349.

# Nuclear Magnetic Resonance of the Less Common Quadrupolar Nuclei

FELIX W. WEHRLI\*

*NMR Applications Laboratory, Varian AG,  
CH-6300 Zug, Switzerland*

I. Background, scope, and objectives . . . . .	126
II. Instrumental requirements . . . . .	128
III. The alkali metal nuclei . . . . .	130
A. Nuclear properties: experimental aspects . . . . .	130
B. Mechanisms of relaxation . . . . .	132
C. Quadrupolar relaxation of ionic nuclei in aqueous and organic media . . . . .	134
D. Ionic solvation . . . . .	137
E. Alkali metal ion complexation . . . . .	142
F. Covalent compounds . . . . .	149
IV. The alkaline earth nuclei . . . . .	153
A. Nuclear properties and experimental aspects . . . . .	153
B. Ionic relaxation in aqueous solution . . . . .	154
C. Complexation studies . . . . .	156
D. Structural studies of covalent compounds . . . . .	159
V. The main Groups III and IV . . . . .	161
A. Nuclear properties . . . . .	161
B. Quadrupole relaxation of the hydrated ion . . . . .	162
C. Solvation and complexation studies . . . . .	164
D. Covalent compounds . . . . .	174
E. Germanium-73 . . . . .	176
VI. The main Groups V and VI . . . . .	177
A. Arsenic-75, antimony-121,123, and bismuth-209 . . . . .	177
B. Sulphur-33 . . . . .	181

\* Present address: Spectrospin AG, Zurich-Fallanden, Switzerland.

VII. The transition metals . . . . .	182
A. Group IIIb . . . . .	183
B. Group IVb . . . . .	187
C. Group Vb . . . . .	188
D. Group VIb . . . . .	196
E. Group VIIb . . . . .	198
F. Group VIIIb . . . . .	201
G. Groups Ib and IIb . . . . .	209
VIII. Conclusions and outlook . . . . .	212
Acknowledgements . . . . .	214
References . . . . .	214

## I. BACKGROUND, SCOPE, AND OBJECTIVES

Although three-quarters of the naturally occurring magnetic nuclei are quadrupolar, NMR studies on them have until recently been unduly sparse. This is probably because some of the widely occurring elements in organic molecules have spin- $\frac{1}{2}$  isotopes ( $^1\text{H}$ ,  $^{13}\text{C}$ ,  $^{31}\text{P}$ ,  $^{19}\text{F}$ ,  $^{15}\text{N}$ ), and thus are more suitable as structural probes. Noteworthy exceptions are oxygen and sulphur, as well as the halogens (chlorine, bromine, and iodine), whose only magnetic isotopes are quadrupolar. The limited success of NMR on the latter group of nuclei ( $^{17}\text{O}$ ,  $^{33}\text{S}$ ,  $^{35}\text{Cl}$ ,  $^{37}\text{Cl}$ ,  $^{79}\text{Br}$ ,  $^{81}\text{Br}$ ,  $^{127}\text{I}$ ) for the study of organic molecules may have deterred many researchers from pursuing these resonances further. In cases where atoms having a quadrupolar nucleus enter into covalent bonding, quadrupolar relaxation may in fact assume such proportions that their nuclear resonances broaden beyond observability. Moderately narrow lines ( $0.1 \text{ Hz} \leq \Delta\nu_1 \leq 100 \text{ Hz}$ ) are observed for  $^2\text{H}$ ,  $^6\text{Li}$ ,  $^7\text{Li}$ ,  $^9\text{Be}$ ,  $^{11}\text{B}$ , and  $^{51}\text{V}$ , even in situations where the electronic symmetry around the nucleus is lower than cubic. This is because these isotopes are characterized by comparatively weak quadrupole moments. For most other quadrupolar nuclei, however, the observation of NMR signals requires either high valence electron symmetry or, alternatively, that there be chemical exchange involving at least one sufficiently populated high-symmetry site.

In their ionic state most simple cations and anions possess a solvation sheath with the degree of orientational order of the coordinating solvent molecules depending on the specific solvation abilities of the ion in question. The electric field gradient (e.f.g.) at the site of the nucleus may cancel for strong solvation in a cubically symmetric solvation shell. However, any perturbation causing a distortion of the coordination symmetry produces a resultant e.f.g. at the nuclear site and thus quadrupole relaxation. Apart from inherent coordination

disorder in the case of weak solvation an e.f.g. may be engendered at higher solute concentrations by the electric monopoles of counter-ions. The e.f.g. in such systems is therefore not an intrinsic molecular or ionic property; it is rather a function of the medium. This looks like an unwelcome complication, but it offers a potential probe for the study of medium effects and weak interactions of various kinds. Owing to the dependence of the relaxation rate on the square of the local e.f.g. an amplification effect ensues, i.e. a small perturbation can lead to a sizeable enhancement of the relaxation rate. It is therefore not surprising that NMR of the alkali metals and halogens, which both have a largely ionic chemistry, has very extensively been applied especially in view of the key role that some of these elements play in biology. Lindman and Fors  n have published a comprehensive review on physico-chemical and biological applications of halogen NMR, (1) and more recently also on NMR of the alkali metals and alkaline earths. (2)

The greatest opportunities for magnetic resonance of quadrupolar nuclei undoubtedly lie in the domain of inorganic solution chemistry. This field is still largely unexploited, and for many of the more 'exotic' nuclei the existing literature provides not much more than a precision measurement of the magnetic moment. The nuclei that have been studied more widely have, in most cases, been observed with obsolete instrumentation which very much limits the scope. New instrumentation meeting the requirements outlined above will give a tremendous impetus to the study of these nuclei. Straightforward applications comprise the study of weak interactions, such as solvation, ion pairing, complexation, etc. Apart from the qualitative characterization of the species occurring in solution, kinetic and thermodynamic information may be retrieved from concentration and temperature dependence experiments. Because of its sensitivity to minor environmental alterations it is again the relaxation rate that offers itself as a further experimental observable.

The basics of quadrupolar relaxation will not be provided here. For an introduction the reader is referred to Chapters 1 and 2 of ref. 1.

The main objective of the present chapter is to review the solution NMR of the less common quadrupolar nuclei, with particular emphasis on chemical applications. The main review period covers the years 1976 through the summer of 1978. Earlier literature will partly be cited for reference purposes. A more thorough discussion of earlier data and concepts is provided where it appears essential to an understanding of newer papers, and also in those cases where recent work is particularly sparse or nonexistent.

The following nuclei are not considered here:  $^2\text{H}$ ,  $^{10}\text{B}$ ,  $^{11}\text{B}$ ,  $^{14}\text{N}$ ,  $^{17}\text{O}$ , and the halogens.

Deuteron NMR was recently treated by Mantsch *et al.* (3) and the halogens, with particular emphasis on chlorine, by Lindman and Forsén. (1) Some of the more specialized applications of alkali metal NMR, such as those that involve large biomolecules, paramagnetic systems, and liquid crystals, will be ignored. Besides the already cited review on alkali metal and alkaline earth NMR, (2) a brief but comprehensive summary on sodium NMR has recently appeared. (4) Nitrogen-14 NMR has been thoroughly discussed in a text edited by Witanowski and Webb. (5) Oxygen-17 NMR and its chemical applications has been reviewed by Klemperer (6) and will also be the subject of a chapter in volume 11 of this series.

## II. INSTRUMENTAL REQUIREMENTS

Some of the nuclei discussed in this text suffer from low intrinsic sensitivity caused either by their low magnetogyric ratios and/or low natural abundances. In spite of such potential natural deficiencies, nuclei with extremely small natural abundances such as  $^2\text{H}$  or  $^{17}\text{O}$  were measured in favourable cases without enrichment 20 years ago. The quadrupolar nature of the latter two nuclei turned out to be advantageous in that the concomitant rapid relaxation permitted the application of much larger rf power levels than are admissible for the observation of spin- $\frac{1}{2}$  nuclei. Nonetheless NMR studies of such nuclei have been the privilege of a few physicists, and it was not before the advent of pulse FT NMR techniques in the early 1970s that 'other' nuclei magnetic resonance became more readily amenable to the chemist. However, in spite of these very significant instrumental advances there remained further obstacles which prevented these nuclei from becoming popular. The so-called multinuclear spectrometers provided by commercial manufacturers were typically based on dedicated frequencies in the sense that narrow-band transmitters, preamplifiers, and probes were utilized. In practice this meant that every nucleus required a separate transmitter, pulse power amplifier, and preamplifier. It was thus cost and the complexity of changeover that deterred many scientists from the study of some of the more 'exotic' nuclei.

A major innovation in spectrometer design involved modification of instruments by, in essence, broad-banding the rf source by use of a frequency synthesizer as an input to a broad-band transmitter. (7-11) Nevertheless these instruments remained hybrids in that they only



partly satisfied the requirements. An essential further step was the replacement of narrow-band preamplifiers by an appropriate wide-band unit, thus obviating preamplifier exchange and tuning. It was not until 1977 that a commercial instrument became available that permitted observation of all nuclei resonating between 5.7 and 32 MHz (i.e. from  $^{14}\text{N}$  to  $^{31}\text{P}$ , at 1.8 T) with a single tunable probe, reportedly without any sensitivity loss. Apart from setting the synthesizer frequency, the operator establishes probe matching with the aid of a multi-turn capacitor and a diode detector indicator. However, no exchange of inserts or of tunable components is required. The nuclear frequency is typically selected by way of a keyboard or equivalent operator interface. Similar wide-band observing systems have recently also become available in the 4.7 T field range using single tunable probes covering a typical range of 20–80 MHz ( $^{15}\text{N}$  to  $^{31}\text{P}$ ). Other instrument manufacturers prefer octave-type probes (for example ranging from 10 to 20, 20 to 40, and 40 to 80 MHz at the last-mentioned field strength).

A further design criterion, which is particularly stringent when quadrupolar resonances are observed, concerns the recovery time following a short rf pulse, since the broader a resonance line is the more rapidly its free precession signal decays. Hence the necessary receiver blanking pulse should be far shorter than the time constant for the FID decay if the signal is to be recovered at all. Critical for the prevention of pulse breakthrough (i.e. an unwanted residual transmitter signal) is a suitable gating scheme assuring fast pulse rise and fall times and efficient receiver protection over a wide band of frequencies. Ackerman and Maciel (12) have described a gating scheme in which the local oscillator frequency is gated prior to entering the mixer. The scheme employed by these authors is claimed to provide better than 60 dB attenuation over the frequency range from 51.9 MHz ( $^{205}\text{Tl}$ ) to 4.19 MHz ( $^{109}\text{Ag}$ ). In extreme cases this requirement may not always be met (e.g. liquid crystal resonances) and recourse to refocussing techniques becomes mandatory. Instead of recording the FID following the pulse, a solid echo is formed by a  $90_x-90_y$  sequence, followed by sampling of the second half-echo.

In order to assure adequate receiver gain dynamic range modern spectrometers utilize multiple conversion in the receiver stage with two or more intermediate frequencies. Santini and Grutzner (13) have pointed out the advantages of adding to rather than subtracting the nuclear frequency from the local oscillator frequency. They claim to achieve improved spectral purity (absence of spurious resonances) in this manner.

The large spectral widths required by some of the applications also put more severe demands on pulse power, if uniform excitation is to be achieved across the full width of the spectrum. If both components of the complex magnetization are detected (quadrature phase detection) the carrier can be placed at the centre of the spectrum without any rf carrier folding occurring as in single-channel detection; better uniformity of excitation is thus achieved at a given transmitter power.

The final consideration concerns the magnet generating the external field. All available multinuclear spectrometers use either electromagnets (1.9 or 2.1 T) or cryomagnets operating between 3.5 and 9.2 T. The criterion of the field as a factor governing signal separation is less important for the heteronuclear resonances than for protons although there are nuclei that are characterized by either a small shielding range or intrinsically broad lines, both limiting signal separation. In such cases the benefits of increased field are obvious. However, it is probably the sensitivity advantage that calls for fields above 2.3 T. At field strengths around 4.7 T a sensitivity roughly 3–4 times that obtainable at electromagnet fields can generally be expected. This, coupled with bore sizes permitting acceptance of sample tubes up to 25 mm diameter, leads to a further increase in sensitivity by a factor of 3–4 compared with the 10 mm samples used at present. As regards cost, cryomagnets that have recently appeared on the market guarantee a liquid helium autonomy of several months and are thus less expensive to operate than electromagnets. Over the years ahead the electromagnet will probably be entirely superseded by the superconducting magnet even for fields as low as 2.3 T, while permanent magnets are likely to replace the electromagnet at fields below 2.3 T.

### III. THE ALKALI METAL NUCLEI

#### A. Nuclear properties: experimental aspects

With the exception of lithium, which has a comparatively strong tendency to form covalent bonds, the chemistry of the alkali metals is essentially ionic. In spite of this common property there are many dissimilarities which result from differences in the ionic radii and the concomitant different solvation abilities. While in aqueous solution at least  $\text{Li}^+$ , and to a lesser extent also  $\text{Na}^+$ , has a kinetically comparatively inert solvation sphere, i.e. exchange between solvated and bulk solvent is slow, this is not at all the case for the larger cations  $\text{K}^+$ ,  $\text{Rb}^+$ , and  $\text{Cs}^+$  where, owing to the larger radius of the ion,

electrostatic interactions between solvent and cation are weaker. Apart from the intrinsically different nuclear properties of the magnetic nuclei of the alkali metals, in terms of nuclear spin and quadrupole moment, it is largely the above-stated chemical differences that are responsible for the differing relaxation behaviour.

Concerning the shielding range there are also discriminating features; however, these occur with respect to the absolute magnitudes rather than to the relative trends. Since the number of electrons increases from 2 ( $\text{Li}^+$ ) to 54 ( $\text{Cs}^+$ ) the shielding range is predicted to increase greatly within the group. Whereas for lithium the dominating contribution to the chemical shift undoubtedly arises from the diamagnetic screening term, the paramagnetic term should be dominant for all other Group I elements, thus giving rise to progressively larger shielding ranges. For illustrative purposes the relative shieldings are compiled in Table I, as the cation at infinite dilution, in the cryptate ( $\text{M}^+\text{C}$ ), and as the anion.

Unfortunately the data in Table I are incomplete in that potassium is missing and the lithium shift in the anion is not known. Nevertheless, it is seen that caesium shieldings are 5–10 times more sensitive to alterations in the electronic environment of the nucleus. The total shielding range  $\Delta\nu$  is an important criterion, but at least as important is the width of a typical line,  $\delta\nu$ , since it is the chemical shift dispersion expressed as the ratio  $\Delta\nu/\delta\nu$  which determines the accuracy of the chemical shift measurement. The relative line width, however, is given by the fundamental nuclear parameters, i.e. the quadrupole moment  $Q$ , the spin number  $I$ , and, for ionic nuclei, the Sternheimer antishielding factor  $(1 + \gamma_\infty)$  which describes the distortion of the ion's electron shell, as a result of polarization due to the electric field generated by neighbouring nuclei. These quantities are listed in Table II. With the exception of  $^6\text{Li}$  and  $^{39}\text{K}$  the alkali metal nuclei listed have sufficient

TABLE I

Experimental alkali metal shieldings (14, 15)<sup>a</sup>

Sample	$^7\text{Li}$	$^{23}\text{Na}$	$^{87}\text{Rb}$	$^{133}\text{Cs}$
$\text{M}^+/\text{H}_2\text{O}$ , inf. dilution	0	0	0	0
$\text{M}^+\text{C}^b$	-0.4 <sup>c</sup>	+10	+50	+132
$\text{M}^-$	—	-62	-185	-292

<sup>a</sup> A positive sign denotes relative deshielding.

<sup>b</sup> C = 2,2,2-cryptand.

<sup>c</sup> Measured in 2,2,1-cryptand.

TABLE II

Alkali metal nuclear properties

Nucleus	Spin <i>I</i>	Abund. (%)	Mag. moment <sup>a</sup>	<i>Q</i> (barns)	1 + $\gamma_x$
<sup>6</sup> Li	1	7.4	0.822	$4.6 \times 10^{-4}$	0.74
<sup>7</sup> Li	3/2	92.6	3.256	-0.042	0.74
<sup>23</sup> Na	3/2	100	2.216	0.10	5.1
<sup>39</sup> K <sup>b</sup>	3/2	93.1	0.391	0.049	18.3
<sup>85</sup> Rb	5/2	72.2	1.348	0.26	48.2
<sup>87</sup> Rb	3/2	27.8	2.741	0.13	48.2
<sup>133</sup> Cs	7/2	100	2.564	-0.003	111

<sup>a</sup> In multiples of the nuclear magneton  $\mu_N$ .<sup>b</sup> Because of their low abundances and weak magnetic moments <sup>40</sup>K (0.012%) and <sup>41</sup>K (6.88%) are ignored.

magnetic moments and abundances to provide good sensitivity. With standard pulse FT instrumentation the practical lower concentration limit for <sup>7</sup>Li, <sup>23</sup>Na, and <sup>133</sup>Cs is definitely below 1 millimole per litre.

With the exception of <sup>6</sup>Li (16, 17) and <sup>7</sup>Li (18), which have weak quadrupole moments, the prevalent source of relaxation in electrolyte solution is quadrupolar interaction with residual electric field gradients. It may at first sight be surprising that this also holds true for <sup>133</sup>Cs with its quadrupole moment of only -0.004 barn. A more detailed discussion on this is in the following section. As regards <sup>6</sup>Li, according to recent findings (17) this nucleus seems to have promising applications in organolithium chemistry. In aqueous solution, however, its applicability may be hampered by extraordinarily long spin-lattice relaxation times. (16)

## B. Mechanism of relaxation

Since the effects of a perturbation on the relaxation rate are mechanism-specific, clarity about the active spin relaxation mechanism is essential. While there is no doubt about the overwhelming dominance of quadrupolar relaxation for <sup>23</sup>Na, <sup>39</sup>K, <sup>85</sup>Rb, and <sup>87</sup>Rb, <sup>7</sup>Li in aqueous solution is found to be relaxed by dipole relaxation involving hydrate protons to about the same extent as quadrupolar relaxation. (18) For <sup>133</sup>Cs the absence of dipole-dipole relaxation has been inferred on the basis of a 20% increase in the relaxation rate upon changing the solvent from H<sub>2</sub>O to D<sub>2</sub>O. (18) This is explained in terms

of an increase in the solution viscosity. If there were substantial proton-induced dipole-dipole relaxation the reverse behaviour would be observed. The absence of  $^1\text{H}$ - $^{133}\text{Cs}$  dipole-dipole interaction was later corroborated on the basis of the lack of a detectable NOE. (20) Since the relaxation time of  $^{133}\text{Cs}$  in aqueous solutions of  $\text{CsCl}$  is as long as 13 s at  $25^\circ\text{C}$  (0.1 M) spin-rotation cannot *a priori* be excluded. However, an Arrhenius plot affords a straight line between 25 and  $100^\circ\text{C}$ , clearly proving the absence of this mechanism in the temperature interval studied. (20) Essentially the same temperature dependence is found in DMF solution.

A recent mechanistic study on  $^6\text{Li}$  in aqueous lithium chloride (16) shows that in light water at  $40^\circ\text{C}$  84 % of the relaxation is dipolar, 8 % is spin-rotation, while quadrupole relaxation accounts for less than 0.1 %. The separation of the dipolar portion was accomplished on the basis of NOE experiments. Figure 1 shows an Arrhenius plot for the experimental  $^6\text{Li}$  relaxation time,  $T_1^{\text{tot}}$ , as well as for  $T_1^{\text{DD}}$ , the dipolar portion. The non-linearity of the plot of  $\log T_1$  against inverse absolute temperature clearly reveals the presence of spin-rotation whilst the corresponding plot for  $T_1^{\text{DD}}$  is linear. The latter confirms that the non-linearity arises from spin-rotation and not for example from a chemical exchange process. Other mechanisms such as  $^6\text{Li}$ - $^7\text{Li}$  dipole-dipole interaction are also evaluated but found to be insignificant; 7 % of the experimental relaxation rate has not been assigned. This portion probably arises from a small concentration of paramagnetic substances. While in  $\text{H}_2\text{O}$  the relaxation time reaches a maximum of *ca.* 300 s, it rises to a value of over 1000 s in  $\text{D}_2\text{O}$ , which is probably the longest  $T_1$  observed so far in the liquid phase. Because of the smaller magnetic moment of the deuteron the  $^6\text{Li}$ - $^2\text{H}$  dipolar interaction is only *ca.* 7.5 % of that in  $\text{H}_2\text{O}$ .

It is well known that in organolithium compounds  $^7\text{Li}$  relaxation is surprisingly inefficient (17) with relaxation times typically occurring in the range 50–500 ms. On the assumption of the dominance of the quadrupolar mechanism for  $^7\text{Li}$  the corresponding  $^6\text{Li}$  quadrupolar relaxation contributions can readily be predicted. In  $\text{MeLi}$ ,  $^n\text{BuLi}$ , and  $\text{PhLi}$  the respective quadrupolar contributions to  $^6\text{Li}$  relaxation are found to be only .3, 17, and 15 % with a sizeable portion being of dipole-dipole origin (20, 35, and 17 %, respectively) as again evidenced by the NOE. (17) Experimental  $^6\text{Li}$   $T_1$  values in organolithium compounds are typically of the order of seconds or even tens of seconds. True high-resolution spectra, comparable to those observed for spin- $\frac{1}{2}$  nuclei, are therefore obtained for this nucleus and it is predicted that  $^7\text{Li}$  will eventually be superseded by  $^6\text{Li}$  NMR.

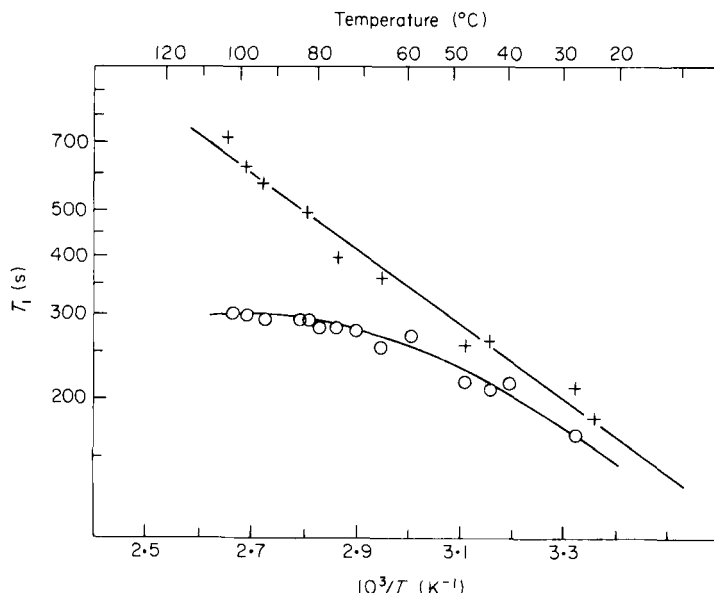


FIG. 1. Spin-lattice relaxation time of  $^6\text{Li}$  in 3.9 M LiCl in  $\text{H}_2\text{O}$  as a function of inverse absolute temperature. Circles: experimental relaxation time,  $T_1^{\text{tot}}$ ; crosses: dipolar contribution,  $T_1^{\text{dp}}$ , obtained from  $T_1^{\text{tot}}$  and the nuclear Overhauser enhancement factor  $\eta$ . The linear least-squares fit for the latter yields an activation energy of  $3.6 \text{ kcal mol}^{-1}$ . (16)

### C. Quadrupolar relaxation of ionic nuclei in aqueous and organic media

There are two conceptually different theories for quadrupolar relaxation of ionic nuclei in solution. Deverell (22) rationalized the electric field gradients at the site of the nucleus as arising from distortions of the closed-shell orbitals in the ion due to collisions with solvent molecules and, at higher concentrations, also counter-ions. In another theory developed by Valiev (23) and by Hertz and his coworkers (24) it is assumed that the electric field gradients are caused by the electric dipoles of the surrounding solvate molecules. It is certainly Hertz to whom we owe the detailed understanding of ionic quadrupole relaxation, and because of the fundamental implications that his work has on ionic solvation the important results are briefly summarized here.

It is well known that, depending upon net charge and size of an ion, the solvent-ion electrostatic interactions vary. In its most recent form the theory therefore distinguishes three different states of solvation:

(25) (a) fully random distribution (FRD); (b) non-oriented solvation; and (c) fully oriented solvation (FOS).

At infinite dilution the relaxation rate for a solvated ionic nucleus can be expressed as:

$$\frac{1}{T_1} = \frac{6\pi(2I + 3)}{5I^2(2I - 1)} \left( \frac{PeQ(1 + \gamma_{\infty})}{\hbar} \right)^2 \cdot d \quad (1)$$

in which  $P$  represents a polarization factor defined by:

$$P = (2\varepsilon + 3)/5\varepsilon$$

where  $\varepsilon$  is the dielectric constant of the medium. The factor  $d$  is related to the electric dipole moment  $m$  of the solvent dipoles, the solvent concentration  $c'_{\text{solv}}$ , the rotational correlation time  $\tau_{\text{solv}}$  of the solvent molecules, and the distance of closest approach  $r_0$  between solvent dipole and the nucleus.

*Model (a).* It may be assumed that no distinct solvation sphere exists owing to the weakness of the electrostatic interactions, i.e. the solvent dipoles surround the ion in a totally random fashion as far as both their orientation and distribution are concerned. In this case:

$$d = d_1 = m^2 c'_{\text{solv}} \tau_{\text{solv}} r_0^{-5} \quad (2)$$

holds.

*Model (b).* This model implies a distinct first solvation sphere, built up of  $n_{\text{solv}}$  solvent molecules, but random orientation of their dipoles. For this situation the  $d$ -factor is given by:

$$d = d_2 = (5/4\pi)m^2 n_{\text{solv}} \tau_{\text{solv}} r_0^{-8} + d_1(r_0^*) \quad (3)$$

$d_1(r_0^*)$  is an expression analogous to equation (2) except that the radius of the second solvation sphere,  $r_0^*$ , has to be inserted.  $d_1(r_0^*)$  is a correction that accounts for outer-sphere contributions to the field gradient. The latter, however, has been shown to be negligible in many cases. (24) This model is predicted to be applicable to ions intermediate between  $\text{Li}^+$  and  $\text{Cs}^+$ .

*Model (c).* The assumption is made in this model that the solvent dipoles in the first solvation sphere are radially oriented:

$$d = d_3 = (9/4\pi)m^2 n_{\text{solv}} \tau_{\text{solv}} r_0^{-8} (1 - e^{-6\lambda}) + d_1(r_0^*) \quad (4)$$

In equation (4)  $\lambda$  denotes a distribution width parameter that describes the occurrence probability for angular distortions of the solvation complex from cubic symmetry ( $n_{\text{solv}} = 4, 6, 8$ ). For a sharp lateral geometry  $\lambda \rightarrow 0$ , i.e. the first term in equation (4) vanishes. This means

that the whole contribution to quadrupole relaxation arises from outer-sphere solvent dipole fluctuation and is precisely what one would predict for a strongly solvating ion, such as  $\text{Li}^+$ . The other extreme is random lateral distribution, i.e.  $\lambda \rightarrow \infty$  which converts equation (4) back into equation (3).

The procedure for determining  $\tau_{\text{solv}}$ , the correlation time for overall reorientation of the solvent molecules, consists of measuring proton or deuteron relaxation times in the pure solvent and in electrolyte solution. All the parameters, with the exception of  $\lambda$  which is adjustable, are known. Excellent agreement between experimental and computed relaxation rates is obtained for both aqueous (24) and non-aqueous (25) solutions.

Interesting data have recently been reported by Geiger and Hertz (26) who studied the temperature and field dependence of the  $^7\text{Li}^+$  and  $^{133}\text{Cs}^+$  relaxation rate in glycerol. For either nucleus a distinct maximum was observed, which was explained as arising from the rate of reorientation ( $1/\tau_c$ ) being of the same order of magnitude as the Larmor frequency. The analysis of the data, taking into consideration the non-exponentiality of the magnetization recovery outside the motional narrowing limit, permitted the correlation times to be deduced. These are found to be the same for the two ions in spite of the fact that  $\text{Cs}^+$  is a structure-breaking or weakly solvating ion whereas  $\text{Li}^+$  is structure-forming. The field gradients derived are in accordance with the fully oriented solvation model.

Some Russian workers (27, 28) have established a correlation between the  $^7\text{Li}^+$ , (27)  $^{23}\text{Na}^+$  and  $^{133}\text{Cs}^+$  (28) relaxation rates, measured in a number of solvents, and Gutmann donor numbers for the respective solvent. This relationship is well established for the alkali metal ion chemical shifts (see above).

These findings lend support to Deverell's electronic distortion theory (22) which conveys the idea that orbital distortion affects both the electric field gradient and the paramagnetic shielding term according to:

$$\frac{1}{T_1} = \frac{1}{T_2} = \frac{3\pi^2(2I + 3)}{1000I^2(2I - 1)} \left( \frac{e^2 Q}{h} \right)^2 \frac{\sigma_p \Delta E}{\alpha^2} \tau_c \quad (5)$$

where  $\sigma_p$  and  $\Delta E$  represent the paramagnetic shielding term and the average excitation energy, respectively, and  $\alpha \equiv e^2/\hbar c$ .

Ion-ion interactions, which become operative at increased solute concentrations, tremendously complicate the description of quadrupolar relaxation. This aspect, albeit important, would break the scope



of the present review. For a survey on the phenomenology and theory the reader is referred to Chapter 5 of ref. 1.

#### D. Ionic solvation

Both the shielding of an alkali metal nucleus and its relaxation rate depend sensitively on the coordinating solvent. It is therefore not surprising that a great many studies of this kind have been conducted, since the method bears the potential for gaining an understanding of the nature of solvent-solute and solute-solute interactions such as ion pairing. Mixed solvation experiments may further afford information on preferential solvation. However, whereas a rather clear picture exists on the mechanism underlying the quadrupolar relaxation of ionic nuclei, the effects on the shielding of these nuclei are less well understood. In spite of this the bulk of available data has been obtained from chemical shift studies, probably because this parameter is more easily obtainable. However, in order to be meaningful as a criterion for ion solvation, both chemical shifts and relaxation rates have to be extrapolated to infinite dilution. This in itself represents a problem since in solvents of low dielectric constant contact ion-pair formation may already occur at very low concentrations. Qualitatively the effect can usually be verified by varying the counter-ion.

A general result of chemical shift studies is that the ionic shieldings increase with increasing electron-donating ability of the solvent molecule's coordinating group. From Bloor and Kidd's (29) early work on  $^{23}\text{Na}$  chemical shifts, measured in a variety of solvents, one finds that nitrogen-coordinating basic solvents deshield while oxygen-coordinating solvents, whose corresponding protonated species are strong acids, have a tendency to shield. Calculations show that donation of an electron to a  $\text{Na}^+$  ion increases  $\sigma_a$  by 9.7 ppm, clearly confirming that the effect must be due to the paramagnetic term. A simple calculation yields  $\sigma_p = -270$  ppm as the result of donating a solvent electron to a sodium 3p orbital.

The shielding and solvent donor ability relationship can be illustrated by plotting the alkali metal shieldings either against the pK of the corresponding acid of the solvent (29) or against the Gutmann donor numbers, as has been done for correlating  $^{23}\text{Na}^+$ , (30, 31)  $^{39}\text{K}^+$ , (32) and  $^{133}\text{Cs}^+$  (33) shieldings. The latter type of plot is illustrated in Fig. 2 which also gives an idea about the range of shieldings encountered, in particular for the heavier isotopes. Noticeable exceptions are methanol, DMSO, and acetonitrile, which have also been found to fall off the line in the  $^{39}\text{K}^+$  plots with the sign and relative magnitude of the deviation being of the same order for both nuclei. It is

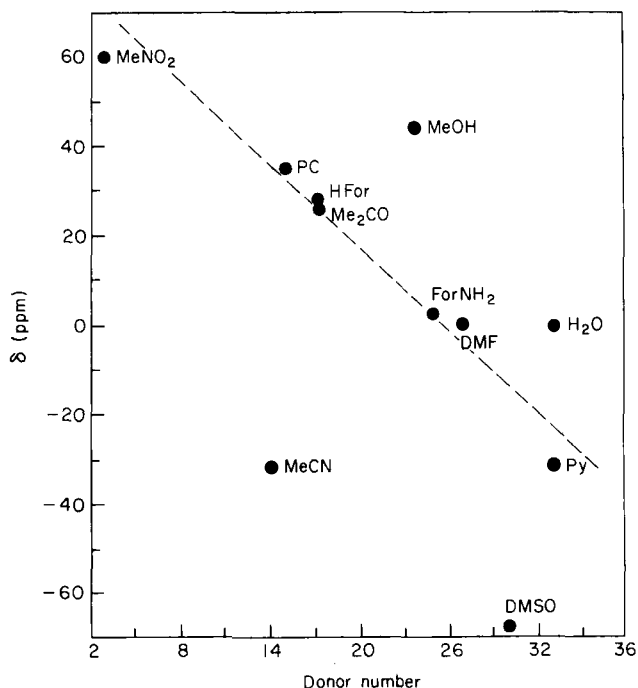


FIG. 2. Plot of infinite dilution  $^{133}\text{Cs}$  shieldings against Gutmann donor numbers for the respective solvents. (33)

interesting that for  $^7\text{Li}^+$  no such correlation is found, (34) clearly pointing to a different shielding mechanism which is probably due entirely to the diamagnetic term.

Qualitative evidence for ion-pairing is usually provided by the concentration dependence of the shieldings, with decreasing dielectric constant of the medium favouring the formation of contact ion-pairs. Evidently the nature of the counter-ion will play an important role too. So it is found that iodide has a much greater tendency towards ion-pairing than tetraphenylborate. Whereas with increasing solute concentration the  $^{23}\text{Na}$  resonance in  $\text{NaI}$  moves to high frequency, it remains almost invariant for  $\text{NaBPh}_4$  in both acetone and acetonitrile. (30) A qualitative indication for ion-pairing is the initial rapid change in chemical shift and levelling off at higher concentration. (33)

Quantitative information can be derived by considering that the observed shift represents a weighted average between those for the free ( $\delta_f$ ) and ion-paired ( $\delta_{ip}$ ) species:

$$\delta_{\text{obs}} = x_f \delta_f + x_{ip} \delta_{ip} = x_f + (1 - x_f) \delta_{ip} \quad (6)$$

with  $x_f$  and  $x_{ip}$  denoting the respective mole fractions.  $x_f$  can be expressed by:

$$x_f = c_f^M / c_t^M \quad (7)$$

with  $c_f^M$  and  $c_t^M$  representing the free and total metal concentration respectively. The ion-pairing stability constant can now be formulated as:

$$K_{ip} = \frac{[M^+, X^-]}{[M^+][X^-]} = \frac{c_t^M - c_f^M}{(c_f^M)^2} \quad (8)$$

From equations (6) and (8) one then obtains:

$$\delta_{obs} = \frac{-1 \pm (1 + 4K_{ip}c_t^M)^{1/2}}{2K_{ip}c_t^M}(\delta_f - \delta_{ip}) + \delta_{ip} \quad (9)$$

By fitting  $\delta_{obs} = f(c_t^M)$  to equation (9) the two unknowns  $K_{ip}$  and  $\delta_{ip}$  can be extracted. Since dissociation of the ion-pair involves charge separation, activities rather than concentrations ought to be inserted. In this manner ion-pairing formation constants can be evaluated for sodium (35) and caesium (33) salts. Some data obtained from  $^{133}\text{Cs}$  shieldings are listed in Table III. The magnitudes of the derived ion-pairing formation constants do not seem to be related in a straightforward manner to either solvent donor ability or dielectric constant.

There has recently been increasing interest in mixed solvation using either the chemical shift (29, 36–43) or the relaxation (27, 44–49) as an experimental variable. Either method bears the potential to provide information on preferential solvation as a function of solvent composition. The chemical shift method is based on the assumptions (a) that the shielding of the solvated ionic nucleus varies linearly with the composition of the solvation sheath and (b) that outer-sphere

TABLE III  
Ion-pair formation constants for  $\text{CsBPh}_4$  in various solvents  
(33)

Solvent	$K_{ip} \text{ (M}^{-1}\text{)}$
Pyridine	$(3.7 \pm 0.2) \times 10^2$
Acetonitrile	$40 \pm 10$
Acetone	$22 \pm 3$
Dimethylformamide	$\sim 0$
Dimethyl sulphoxide	$\sim 0$

contributions to the shielding are negligible. If assumption (a) is correct, then for random solvation the observed shift should vary linearly with bulk solvent composition. While there is good experimental evidence for the validity of assumption (b), hypothesis (a) has recently been disputed. (43)

Qualitative and quantitative information can in essence be derived from the non-linearity of the shielding *vs.* solvent composition plots. It has therefore become common practice (35,40) to define an isosolvation point which corresponds to the solvent composition at which the chemical shift is midway between the extrema observed for the pure solvents. A noticeable result of Greenberg and Popov's (40) studies on  $\text{Na}^+$  solvation competition in binary solvent mixtures is that preference is generally given to the solvent with higher donor ability. These workers also derived equilibrium constants for preferential solvation by making use of a solvation model derived by Covington *et al.* (38) In addition to the previously stated assumptions this model assumes that individual equilibrium constants for successive replacement of one solvent molecule A in the solvation sphere of the cation by a molecule of solvent B is purely governed by statistics. If  $n$  solvent molecules (irrespective of solvent composition) occupy the cation's solvation shell, an equilibrium constant  $K^{1/n}$  can be defined, which is related to the observed chemical shift  $\delta$  and the total range of chemical shifts  $\Delta\delta$  by: (38)

$$1/\delta = (1/\Delta\delta) \{1 + (K^{1/n} x_A/x_B)^{-1}\} \quad (10)$$

where  $x_A$  and  $x_B$  denote the respective mole fractions of the two solvents A and B.

Recently the  $^{133}\text{Cs}$  experiments of Gustavsson *et al.* (43) aimed at studying solvation competition between DMF and water have cast doubt on the assumption of linearity between chemical shift and the composition of the solvation sheath. It is reported that the  $^{133}\text{Cs}$  chemical shift range extends far beyond the extrema observed in the pure solvents. In order to circumvent this problem an interesting idea was put forward which consists in measuring the chemical shift in  $\text{H}_2\text{O}$ –DMF as well as in  $\text{D}_2\text{O}$ –DMF. The magnitude of the isotope shift should then be a direct measure of the extent of ion–water contact and thus provide information on preferential solvation. Figure 3(a) and (b) show the shielding dependence on solvent composition for both  $\text{H}_2\text{O}$ –DMF and  $\text{D}_2\text{O}$ –DMF solvent mixtures [Fig. 3(a)] as well as for the difference  $\delta(\text{H}_2\text{O}) - \delta(\text{D}_2\text{O})$  [Fig. 3(b)]. The latter plot reveals a slight preference for water solvation. From the Covington plot in Fig. 3(c) an equilibrium constant  $K^{1/n} = 1.6$  can be evaluated.

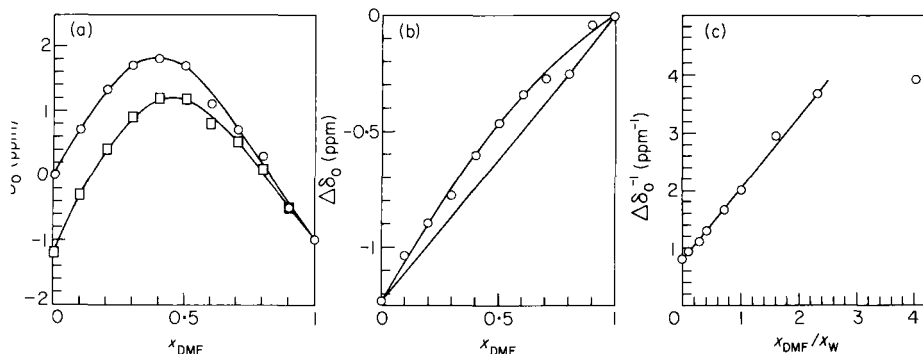


FIG. 3. (a)  $^{133}\text{Cs}^+$  chemical shifts at infinite dilution in  $\text{H}_2\text{O}$ -DMF (O) and  $\text{D}_2\text{O}$ -DMF (□) plotted against mole fraction of DMF,  $x_{DMF}$ .

(b) Water isotope effect on the  $^{133}\text{Cs}^+$  shielding,  $\Delta\delta_0 = \delta(\text{D}_2\text{O-DMF}) - \delta(\text{H}_2\text{O-DMF})$ , plotted against  $x_{DMF}$ .

(c) Covington plot for the above system obtained by plotting  $\Delta\delta_0^{-1}$  against  $x_{DMF}/x_W$ . (43)

Holz *et al.* (47) have recently presented a relaxation model for mixed ionic solvation in binary solvent mixtures. The model, which is an extension of the Hertz electrostatic relaxation theory for ionic quadrupole relaxation at infinite dilution, is based on partial field gradients produced by a single solvent dipole. In a single solvent the quadrupole relaxation rate may be formulated as:

$$1/T_1 = An\bar{V}_{zz}^2 g_Q \Lambda \tau_c^* \quad (11)$$

where  $A$  is a constant for given nuclear species,  $\bar{V}_{zz}^2$  is the mean square electric field gradient caused by a *single* solvent dipole,  $\Lambda$  is a field gradient quenching factor correcting for symmetry effects,  $g_Q$  is a measure for the sharpness of the radial part of the ion-solvent pair distribution function, (48) and  $\tau_c^*$  is the correlation time for the reorientation of the field gradient.

For a binary solvent mixture equation (11) can be extended to:

$$1/T_1 = A\{n_1(\bar{V}_{zz}^2)_1 g_{Q1} \Lambda_1 \tau_{c1}^* + n_2(\bar{V}_{zz}^2)_2 g_{Q2} \Lambda_2 \tau_{c2}^*\} + \Lambda^* \quad (12)$$

The subscripts in equation (12) refer to solvents 1 and 2.  $\Lambda^*$  accounts for the non-additivity of symmetry quenching.

On the assumptions that  $(\bar{V}_{zz}^2)_1$  and  $(\bar{V}_{zz}^2)_2$  differ insignificantly from the respective values in the pure solvents and that the coordination number remains unaltered, the relaxation rate was calculated for several binary solvent mixtures. (48, 49). In the numerical results it was further assumed that the solvent composition in the solvation sheath is

equal to the bulk solvent composition (non-preferential solvation). Excellent agreement between computed and experimental relaxation rates is obtained for  $^{23}\text{Na}^+$  in  $\text{H}_2\text{O}$ -formamide and  $\text{H}_2\text{O}$ -*N*-methylformamide solvent mixtures (Fig. 4), indicating the statistical nature of the solvent distribution in the first coordination shell. (49) However, a slight deviation from the theoretical curve is observed for  $\text{H}_2\text{O}$ -dimethylformamide, which is believed to be due to a slight preference for  $\text{H}_2\text{O}$  solvation.

### E. Alkali metal ion complexation

Alkali metal NMR enjoys increasing popularity as a tool in the study of complexation between alkali metal ions and a variety of biomolecules

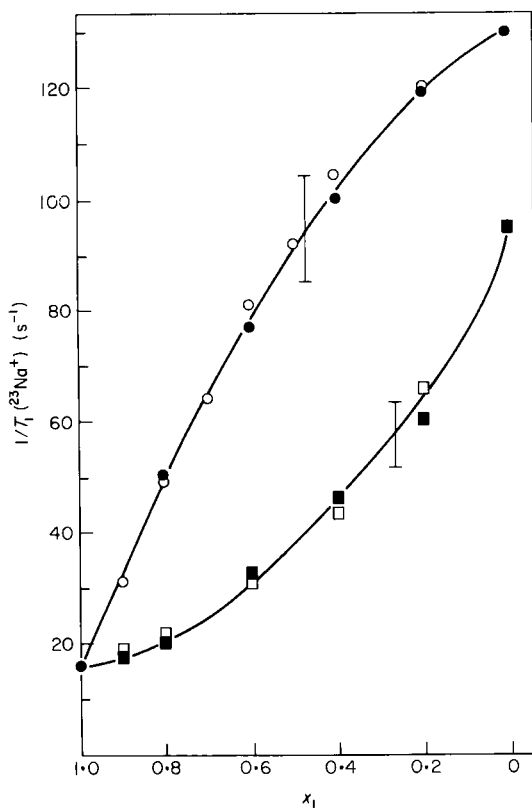


FIG. 4. Infinite dilution  $^{23}\text{Na}^+$  spin-lattice relaxation rate in NaBr dissolved in formamide-water (squares) and *N*-methylformamide-water (circles), both as a function of water mole fraction,  $x_1$ . (49) The solid lines are computed on the basis of the theory outlined in the text.

such as amino-acids, (50) nucleosides and nucleotides, (51, 52) sugars, (53–55) and for a number of organic acids (50, 56) and synthetic drug molecules. (57, 58) All these molecules form comparatively weak complexes. Generally complex formation manifests in line displacements and relaxation effects. The complexes formed are further characterized by being kinetically labile to the extent that exchange between the solvated and complexed ion is fast on the NMR time scale.

Entirely different behaviour is shown by molecules that can trap the ion in two- or three-dimensional cavities. Synthetic molecules having this property are the macrocyclic polyethers (also called crown ethers) and the so-called cryptands. The chemistry and ion-binding properties of these molecules have been reviewed by Lehn. (59) This category of molecules, designated ionophores, form complexes that are orders of magnitude more stable than those of the previously discussed group, in both the thermodynamic and the kinetic sense. This group of molecules has naturally occurring representatives, namely cyclic peptides and lactones. (60) The tremendous interest in ionophores is primarily due to their biological ramifications since they play a key role in ion transport through membranes.

Alkali metal NMR has greatly contributed to a better understanding of the complexing behaviour of ionophores. The kind of information that the technique is capable of providing primarily concerns the dynamics and partly the stability of the complexes.

Crown ether and cryptand complexation has been studied by  $^7\text{Li}$ , (15, 61)  $^{23}\text{Na}$ , (62–66)  $^{39}\text{K}$ , (67)  $^{87}\text{Rb}$ , (67) and  $^{133}\text{Cs}$  (20, 65, 68–72) NMR. Naturally occurring ionophores and their interactions with sodium and lithium ions were investigated by means of several physico-chemical methods including  $^7\text{Li}$  (71) and  $^{23}\text{Na}$  (71, 72) NMR.

The methodology in processing the spectral information depends on the level of sophistication of the model to be used. Usually simplifying assumptions have to be made. Ideally both thermodynamic and kinetic information is to be obtained. As regards the cryptates (complexes between cations and cryptands) typical stability constants are of the order of  $10^5$ – $10^8$  and are therefore not accessible by NMR. The study of the kinetics of decomplexation, on the other hand, is facilitated by the availability of slow-exchange spectra. The limiting chemical shifts in the two species are thus known. The data evaluation is complicated by the fact that the intrinsic line-width (i.e. the contribution not arising from site exchange) is, in contrast to studies with spin- $\frac{1}{2}$  nuclei, not a negligible quantity. Since the experiments are conducted as a function of temperature,  $T_1$  varies and it may well have a different temperature dependence in the solvated ion and in the complex. Thanks to the high

stability of the complexes at 1:1 ion to ionophore ratio, the assumption of all ionophore being bound is a good approximation (most ionophores and cations form 1:1 complexes). In order to determine  $T_{2f}$ ,  $T_{2b}$ ,  $\omega_f$ ,  $\omega_b$  ( $f$  = free,  $b$  = bound) the temperature dependence of the line-width and Larmor frequency is initially studied for the free cation in the absence of ionophore and for an equimolar solution. The actual exchange experiments are then performed at excess ion concentration and the observed line-shape is fitted to the theoretical band-shape:

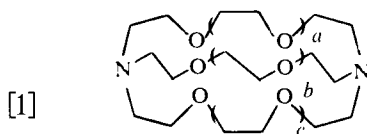
$$G(\omega) = K \{ I \cos(\theta_0 + \theta') - R \sin(\theta_0 + \theta') \} + C \quad (13)$$

In equation (13)  $I$  and  $R$  are given by the exchange-modified Bloch equations. They are functions of the exchange lifetime  $\tau = \tau_f \tau_b / (\tau_f + \tau_b)$ , the populations  $p_f = \tau_f / (\tau_f + \tau_b)$  and  $p_b = \tau_b / (\tau_f + \tau_b)$ , the relaxation times  $T_{2f}$  and  $T_{2b}$ , and the Larmor frequencies  $\omega_f$  and  $\omega_b$ . The quantities  $\theta_0$  and  $\theta'$  refer to the zero-order and first-order phase corrections respectively.

From the temperature dependence of the rate of decomplexation  $k_{-1} = 1/\tau$  the activation parameters  $\Delta G^\ddagger$  and  $\Delta S^\ddagger$  can finally be determined. Figure 5 displays some temperature-dependent  $^{23}\text{Na}$  spectra for complexation between  $\text{Na}^+$  and cryptand C222. (64) Free enthalpies and entropies of activation for complexation between  $\text{Li}^+$  and cryptands C211 and C221 as well as between  $\text{Na}^+$  and cryptands C222 are in Table IV. While for the lithium cryptates the enthalpies of

TABLE IV  
Kinetic parameters for lithium and sodium cryptate [1] decomplexation (61, 64)

Metal ion	Cryptand	Solvent	$\Delta G_b^\ddagger$ (kcal mol $^{-1}$ )	$\Delta S_b^\ddagger$ (cal K $^{-1}$ mol $^{-1}$ )
$\text{Li}^+$	C211	pyridine	22.7	-12.5
$\text{Li}^+$	C211	$\text{H}_2\text{O}$	20.6	+ 0.4
$\text{Li}^+$	C211	DMSO	19.7	-13.8
$\text{Li}^+$	C211	DMF	20.0	-15.5
$\text{Li}^+$	C211	formamide	20.8	-22.8
$\text{Li}^+$	C221	pyridine	17.9	-14.9
$\text{Na}^+$	C222	pyridine	17.4	-12.6
$\text{Na}^+$	C222	THF	16.2	-8.1
$\text{Na}^+$	C222	$\text{H}_2\text{O}$	14.5	+5.3
$\text{Na}^+$	C222	ethylenediamine	14.4	-7.6





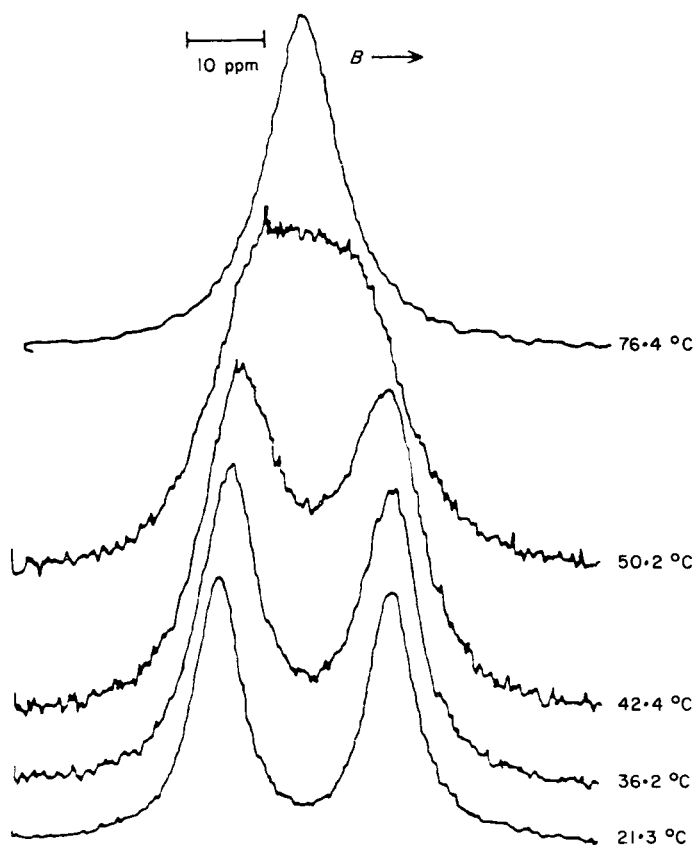


FIG. 5. Temperature-dependent  $^{23}\text{Na}$  NMR spectra recorded in the pulsed mode at 15.9 MHz for a sample consisting of 0.3 M cryptand C222 and 0.6 M NaBr in ethylenediamine. (64)

activation  $\Delta H_0^\ddagger$  are found to increase with increasing solvent donor ability, no such trend is observed for the sodium cryptates.

For crown ether complexation the procedure for obtaining the kinetic parameters is entirely different. Because of the lack of a three-dimensional cavity the ion remains in close contact with the solvent, and as a consequence of this the chemical shifts for the two sites differ only insignificantly. The starting point for the analysis is again the exchange-modified Bloch equations. However, since the exchange is rapid on the NMR time scale, only a single resonance is observed whose width is a function of the relaxation times  $T_{2f}$  and  $T_{2b}$  as well as of the lifetime of the ion in its uncomplexed form,  $\tau_f$ . Under these limiting conditions

Shchori *et al.* (62, 63) obtained the following expression for the reciprocal mean life-time:

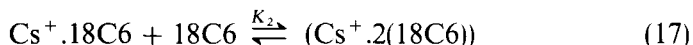
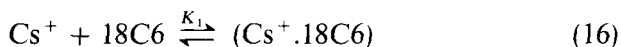
$$\frac{1}{\tau_f} = \frac{(1/T_{2b} - 1/T_2)(1/T_2 - 1/T_{2f})p_b}{(1/T_{2av} - 1/T_2)} \quad (14)$$

where  $1/T_{2av} = p_f/T_{2f} + p_b/T_{2b}$ .

Alkali metal NMR has also furnished qualitative and partly quantitative information on structure and bonding as well as on relative and absolute thermodynamic stability. The preferred experimental variable in this case is the chemical shift which is measured as a function of temperature and ligand concentration. (15, 65, 68–70) Additionally qualitative information has been obtained from quadrupole coupling constants (66) and  $T_1$  measurements. (20)

A most significant result of these studies is the solvent independence of the alkali metal chemical shifts for those cryptates in which the ion is closely packed in the ligand cavity. This is generally the case when the ion perfectly matches the cryptand cavity (15) and it unambiguously demonstrates that long-range shielding effects are negligible. This has important ramifications in solvation studies where recourse is made to the chemical shift as an observable (see below).

The chemical shift behaviour of  $^{133}\text{Cs}$  in the 18-crown-6 (18C6) complexation with  $\text{CsBPh}_4$  (68) indicates a two-step reaction whose analysis requires the following processes to be considered:



The observed chemical shift  $\delta_{\text{obs}}$  is a weighted average and can be formulated as:

$$\delta_{\text{obs}} = x_f \delta_f + x_{ip} \delta_{ip} + x_1 \delta_1 + x_2 \delta_2 \quad (18)$$

An iterative fitting procedure thus permits the experimental plot  $\delta_{\text{obs}}$  against  $[18\text{C6}]/[\text{Cs}^+]$  to be fitted to equation (18) thereby extracting the unknowns  $K_1$  and  $K_2$  as well as the limiting chemical shifts  $\delta_1$  and  $\delta_2$ . However, since  $K_1 \gg K_2$  only an approximate value can be determined for the former. The data obtained are  $K_1 \approx 10^6$  and  $K_2 = 44$  at  $25^\circ\text{C}$ .

An interesting result reported recently by the same group of workers (70) relates to the discovery of two types of 1:1 caesium cryptates for cryptand C222. The possibility for the existence of an exclusive complex

$\text{Cs}^+ \cdot \text{C222}$  was postulated on the basis of the fact that the diameter of the caesium ion is slightly larger than the cavity size of C222. Evidence for an exclusive complex is provided by the solvent dependence of the limiting chemical shift at high mole ratios  $[\text{C222}]/[\text{Cs}^+]$ . Figure 6 displays a plot of limiting chemical shifts as a function of temperature for three different solvents. It is interesting that at low temperatures the chemical shifts, which are very different from those at room temperature, converge to a single, solvent-independent value of 245 ppm to high frequency of aqueous  $\text{Cs}^+$ . This behaviour suggests an equilibrium between an inclusive and an exclusive complex. Further arguments in favour of such an equilibrium are provided by the rate data in that Arrhenius plots for the exchange time, which was derived from total line-shape analysis, show marked curvature. While in acetone solution the line-width for the complex progressively decreases towards lower temperature, in propylene carbonate it first sharpens and then broadens again as the temperature is lowered, showing that the inclusive-exclusive interchange starts affecting the line-width in the low-temperature region.

Relative thermodynamic stabilities of crown ether complexes with several cations can also be evaluated by means of  $T_1$  competition experiments. (20) Addition of 18C6 to a solution of caesium iodide affects

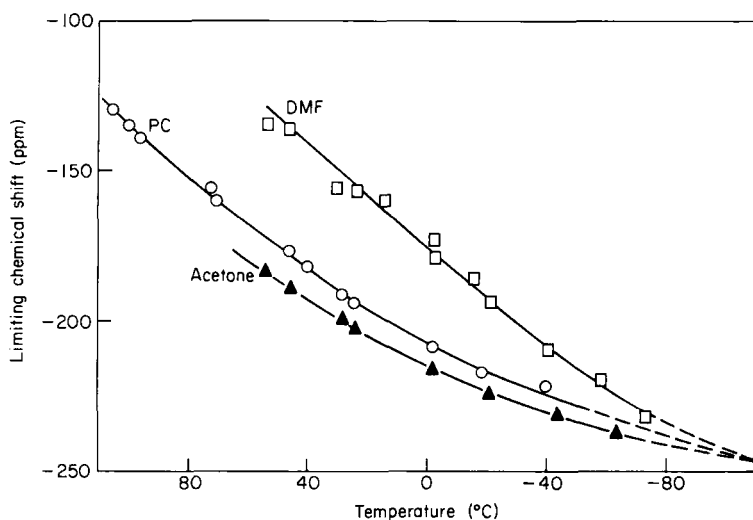


FIG. 6. Limiting  $^{133}\text{Cs}^+$  chemical shifts in  $^{133}\text{Cs}^+ \cdot \text{C222}$  complex at high mole ratios  $[\text{C222}]/[\text{Cs}^+]$  as a function of temperature, in dimethylformamide (DMF), propylene carbonate (PC), and acetone. (70)

$T_1$  leading to either a maximum or a minimum at equimolar ratios of 18C6 and  $\text{Cs}^+$ , depending on solvent. In the presence of equal concentrations of  $\text{Cs}^+$  and  $\text{K}^+$  in DMF the minimum is shifted to  $[\text{18C6}]/[\text{Cs}^+] = 2$  with the  $^{133}\text{Cs}$  relaxation time remaining constant in the interval  $0 < [\text{18C6}]/[\text{Cs}^+] < 1$ . This indicates that the potassium complex is preferentially formed. In the presence of  $\text{Rb}^+$  as a competitor, however, the relaxation rate decreases gradually between  $[\text{18C6}]/[\text{Cs}^+] = 0$  and 2 and then rises again, thus showing the simultaneous formation of either complex (Fig. 7).

Alkali metal NMR in conjunction with cryptand complexation finally led to the sensational discovery of alkali metal anions by Dye and coworkers. (14) The complexing power of the cryptands is such that the ionophore is capable of extracting the cation from alkali metal in solutions of THF, methylamine, and ethylamine. The electron left behind is conclusively proved to form the anion  $\text{M}^-$  ( $\text{M} = \text{Na}, \text{Rb}, \text{Cs}$ ) leading to a separate resonance line at low temperature. The corresponding shielding is close to the theoretical value computed for the metal anion. A most striking feature of this resonance is its solvent independence. The absence of solvent-induced chemical shifts for  $\text{Na}^-$

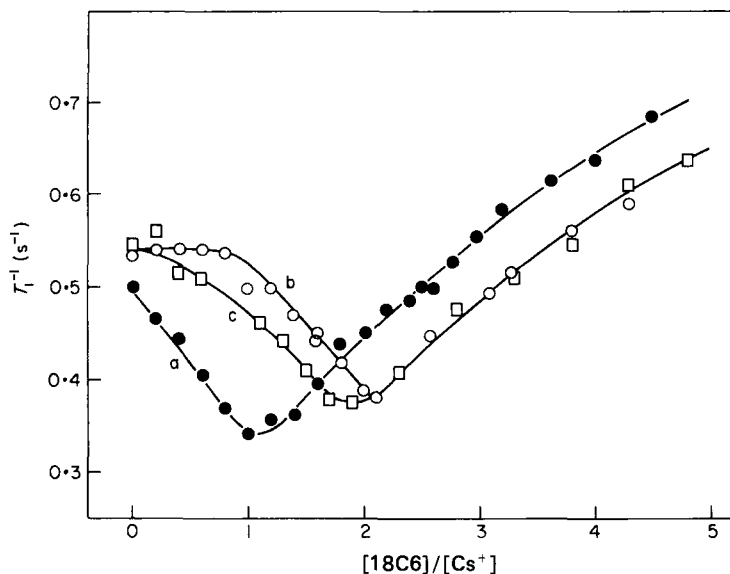


FIG. 7.  $^{133}\text{Cs}$  spin-lattice relaxation rate,  $T_1^{-1}$ , in the complex  $\text{Cs}^+ \cdot 18\text{C6}$  as a function of the 18C6 to  $\text{Cs}^+$  molar ratio, in dimethylformamide solvent, with (a) 0.1 M CsI, (b) 0.1 M CsI + 0.1 M KI, and (c) 0.1 M CsI + 0.1 M RbI. (20)

shows that the 2p orbitals are effectively shielded from the solvent by the filled 3s orbital.

### F. Covalent compounds

The least electropositive alkali metal, lithium, has a marked tendency toward covalency. We owe it not least to NMR studies of this metal that a rather complete picture exists today of the structure, bonding, and dynamic behaviour of organolithium compounds in solution. (73–78) One conspicuous feature of organolithium compounds is their oligomeric nature. In the polyhedral aggregates that generally form in apolar solvents the individual monomer units are held together by multicentre bonds, the most common forms being dimers, tetramers, and hexamers whose presumed structures are schematically illustrated in Fig. 8. The organometallic compounds of the remaining alkali metals are primarily ionic, forming ion-pairs in solution.

$^7\text{Li}$  is probably the first metal nucleus whose magnetic resonance has afforded important chemical information. In spite of a sizeable quadrupole moment of 0.04 barn, surprisingly narrow lines are observed for most organolithium compounds. Lucken (79) has estimated an upper limit of 16 kHz for the quadrupole coupling constant in methyl-lithium and a value of 98 kHz for ethyl-lithium, the latter possessing the substantial asymmetry parameter of 0.62. These surprisingly small quadrupole coupling constants explain the observed  $^7\text{Li}$  relaxation times which are of the order of 10–1000 ms in typical alkyl-lithium compounds. (17, 21) However, in view of the small chemical shift range of less than 2 ppm ( $< 80$  Hz at 2.3 T) for alkyl-lithium compounds, a line-width of 30 Hz may still be prohibitive. The recently reported  $^6\text{Li}$  relaxation data which indicate an order of magnitude of 10–20 s in

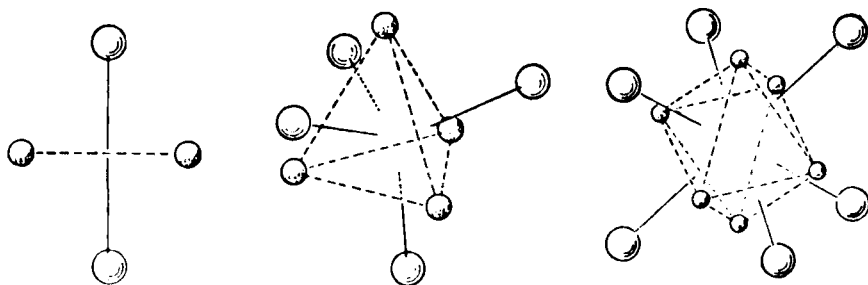


FIG. 8. Structures of dimeric, tetrameric, and hexameric organolithium compounds. Small spheres indicate lithium atoms; large spheres represent the carbon atoms of the organic groups. (74)

typical organolithium compounds (17) point to the superior NMR properties of the minor lithium isotope. An enhanced chemical shift dispersion is therefore expected for this nucleus in spite of its lower resonance frequency (14.1 *vs.* 38.8 MHz at 2.3 T).

The chief limitation of lithium NMR is undoubtedly the relatively small chemical shift range which only slightly exceeds 2 ppm in covalent organolithium compounds. The principal shielding mechanism is definitely not field-induced mixing between ground and excited states (paramagnetic shielding) which governs the shielding of most nuclei. Local contributions such as neighbour anisotropy effects need therefore to be considered. In fact recent calculations (80) show that the diamagnetic and paramagnetic terms largely cancel one another and that the relative shieldings can best be rationalized in terms of McConnell's model for anisotropic substituent susceptibility. The small shielding range also requires special care in the choice of the standard. For most of the data reported an external aqueous LiBr standard was used but no special attention was paid either to concentration or to susceptibility corrections. Recently a number of shifts were re-measured relative to internal TMS as a secondary standard; the data, referenced to aqueous LiBr (0.7 g/ml) as an arbitrary shift chart, are in Fig. 9. A considerably larger chemical shift range was found in aryl-lithium compounds (81, 82) where the aryl moiety is a di-anion. In such systems lithium is largely ionic, its shift being determined by its location relative to the induced ring currents. In cyclooctatetraenyl-lithium, for example, the  $^7\text{Li}$  resonance is at 8.5 ppm to low frequency of aqueous LiCl, suggesting that the lithium ion is associated with the  $\pi$ -cloud of the  $10\pi$ -electron ring and therefore experiencing a large diamagnetic ring current. In those cases where the organic moiety is a resonance-stabilized anion a pronounced solvent dependence of the  $^7\text{Li}$  shielding is observed. (83–85) This may be exemplified with benzyl-lithium (85) where the  $^7\text{Li}$  chemical shift moves to low frequency with change in solvent from THF to benzene ( $\Delta\delta$  1 ppm), reflecting a transfer of electron density from the benzyl moiety to lithium.

The most significant contribution of  $^7\text{Li}$  NMR has been in the elucidation of the structure of the alkyl-lithium oligomers in solution.  $^{13}\text{C}$  enrichment resulted in  $^{13}\text{C}$ -coupled  $^7\text{Li}$  spectra for MeLi, (86)  $^i\text{BuLi}$  and  $^n\text{BuLi}$  (87) thus providing definite proof for the tetrameric structure of these compounds. The lithium atoms are situated at opposite corners of a cube with the  $\alpha$ -carbons occupying the other corners so that each lithium atom interacts with three neighbouring carbons. Because of incomplete enrichment the observed  $^7\text{Li}$  spectra are superpositions of the sub-spectra of the following isotopomers:  $^7\text{Li}_4^{12}\text{C}_4$  (singlet),

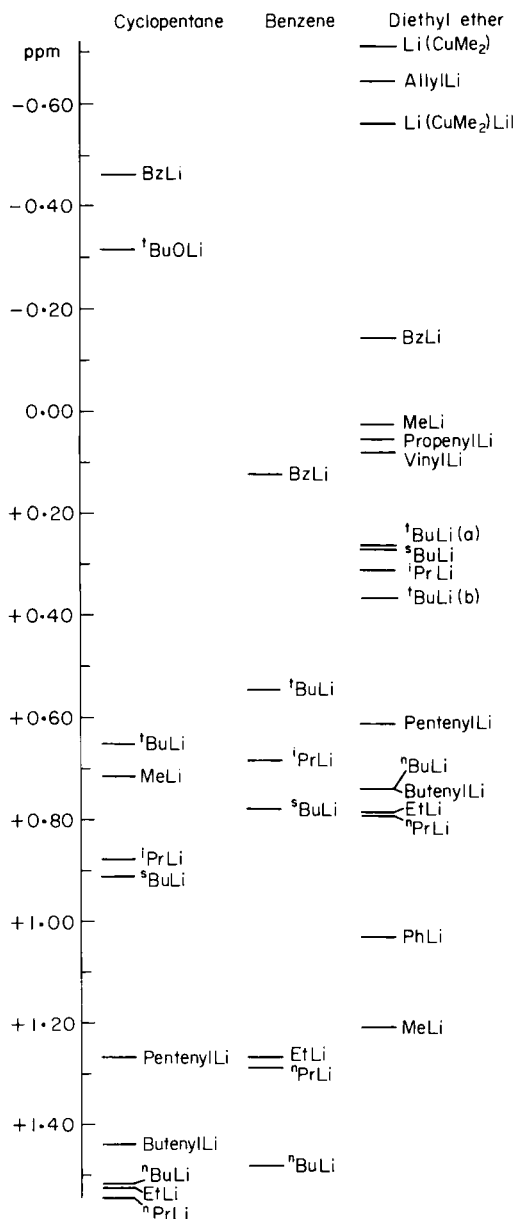


FIG. 9.  $^7\text{Li}$  chemical shifts in organolithium compounds, measured in three different solvents. The shieldings were originally determined relative to the proton frequency of tetramethylsilane which served as an internal lock signal, and subsequently referenced to external LiBr (0.7 g/ml). (80)

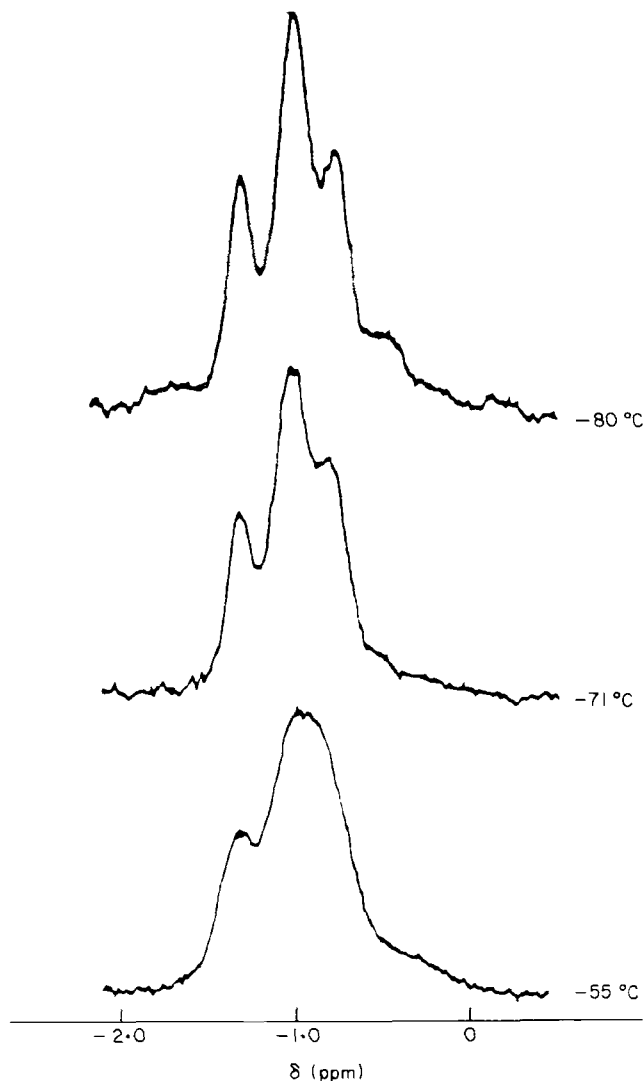


FIG. 10. Temperature-dependent  ${}^7\text{Li}$  NMR spectra of a mixture of ethyl-lithium and methyl-lithium in ether ( $\text{EtLi}:\text{MeLi} = 1:1.55$ ). The least shielded lithium is the one having three adjacent methyls. (89)

${}^7\text{Li}_4 {}^{13}\text{C}^{12}\text{C}_3$  (doublet),  ${}^7\text{Li}_4 {}^{13}\text{C}_2 {}^{12}\text{C}_2$  (triplet), and  ${}^7\text{Li}_4 {}^{13}\text{C}_3 {}^{12}\text{C}$  and  ${}^7\text{Li}_4 {}^{13}\text{C}_4$  (quartet each) ignoring  ${}^6\text{Li}$ -containing isotopomers.

From the absence of any observable  ${}^6\text{Li}$ - ${}^7\text{Li}$  spin-spin coupling in  ${}^6\text{Li}$ -enriched methyl-lithium it is inferred that the Li-Li bond order in these compounds is small. (88)



Cross-association resulting from mixing of two organolithium compounds  $\text{LiR}$  and  $\text{LiR}'$  can be observed in the  $^7\text{Li}$  spectra with the mixed forms  $\text{Li}_x\text{R}_x\text{R}'_{n-x}$  giving rise to separate peaks. In the  $\text{LiMe-LiEt}$  system in ether (89) four distinct peaks are seen in the  $^7\text{Li}$  spectrum indicating slow intra- and inter-aggregate exchange (Fig. 10). This is expected on the assumption of the validity of the local environment approximation which states that the  $^7\text{Li}$  chemical shift is determined by the three adjacent alkyl groups. The four observationally distinguishable environments are then:  $3\text{R}$ ;  $2\text{R}, \text{R}'$ ;  $\text{R}, 2\text{R}'$ ;  $3\text{R}'$ . Mixed aggregation is also known to occur between dimethyl compounds of divalent metals such as  $\text{Mg}$ ,  $\text{Cd}$ , and  $\text{Zn}$  on the one hand and  $\text{LiCH}_3$  on the other, forming dimers, trimers, and tetramers. (90, 91) The stoichiometry of  $\text{Li}_2\text{Mg}(\text{CH}_3)_4$  and  $\text{Li}_3(\text{CH}_3)_5$  is established on the basis of the low-temperature  $^7\text{Li}$  spectrum and the known  $\text{Li/Mg}$  ratio. (90) Further mixed complexes whose solution structures have been studied by  $^7\text{Li}$  NMR include those involving Group III and IV alkyl and aryl compounds. (92-94)

Temperature-dependent  $^7\text{Li}$  NMR providing qualitative information on the dissociation kinetics has been reported for  $\text{Li}_4(\text{CH}_3)_4$ , (95)  $\text{Li}_4^t\text{Bu}_4$ , (75) and for methyl and lithium exchange in the  $\text{LiCH}_3\text{-M}(\text{CH}_3)_2$  ( $\text{M} = \text{Mg}, \text{Zn}, \text{Cd}$ ) systems. (91) Two general types of exchange can be distinguished in the latter systems. At  $[\text{Li}]/[\text{M}] < 2$  methyl group exchange occurs between  $\text{M}(\text{CH}_3)_2$  and  $\text{Li}_2\text{M}(\text{CH}_3)_4$ , whereas the condition  $[\text{Li}]/[\text{M}] > 2$  results in methyl and lithium exchange between methyl-lithium and the 2:1 and 3:1 complexes, demonstrating the complexity of the exchange phenomena in these systems.

#### IV. THE ALKALINE EARTH NUCLEI

##### A. Nuclear properties and experimental aspects

The alkaline earths are chemically rather similar, and with the exception of beryllium and, to some extent, magnesium which have a pronounced tendency towards covalency, they form essentially ionic compounds. Both calcium and magnesium ions play a key role in various physiological processes by acting as cofactors in many enzymic reactions. In contrast beryllium is characterized by its extreme toxicity. (96)

From an NMR point of view the alkaline earths are distinguished by generally lower receptivities, arising from weak magnetic moments coupled in some instances with low abundances ( $^{43}\text{Ca}$ ,  $^{87}\text{Sr}$ ). Their measurement therefore puts more stringent demands on spectrometer

sensitivity. This is undoubtedly the reason for the small number of papers that have appeared on alkaline earth NMR. The physical properties of the relevant nuclei, which have in common a quadrupolar nature, are summarized in Table V. High precision measurements of the magnetic moments have recently been reported for  $^{25}\text{Mg}$ , (97)  $^{43}\text{Ca}$ , (98)  $^{87}\text{Sr}$ , (99)  $^{135}\text{Ba}$  and  $^{137}\text{Ba}$ . (100) For the latter two isotopes the ratio of the quadrupole moments  $Q_{135}/Q_{137} = 0.67$  was reported. (100)

TABLE V  
Alkaline earth nuclear properties

Nucleus	Spin $I$	Abund. (%)	Mag. moment ( $\mu_N$ )	$Q$ (barns)
$^9\text{Be}$	3	100	-1.177	0.052
$^{25}\text{Mg}$	5/2	10.1	-0.855	0.22
$^{43}\text{Ca}$	7/2	0.13	-1.315	$\pm 0.02$
$^{87}\text{Sr}$	9/2	7.0	-1.089	0.36
$^{135}\text{Ba}$	7/2	6.6	0.832	0.18
$^{137}\text{Ba}$	11/2	11.3	0.931	0.28

## B. Ionic relaxation in aqueous solution

Except for  $^9\text{Be}$  and possibly  $^{43}\text{Ca}$  which owing to the weakness of their quadrupole moments are likely candidates for other than quadrupolar relaxation contributions, quadrupole relaxation seems to prevail. While in aqueous solution the relaxation times for  $^{87}\text{Sr}^{2+}$ ,  $^{135}\text{Ba}^{2+}$  and  $^{137}\text{Ba}^{2+}$  are in the millisecond range [ $^{87}\text{Sr}^{2+}$  4.9 ms at infinite dilution; (99)  $^{135}\text{Ba}^{2+}$  0.5 ms at 0.5 M;  $^{137}\text{Ba}^{2+}$  0.26 ms (100)], the comparison between the  $^{25}\text{Mg}^{2+}$  linewidth in  $\text{H}_2\text{O}$  and  $\text{D}_2\text{O}$  shows the absence of dipolar relaxation by solvent protons. (101) A mechanistic relaxation study on  $^9\text{Be}$  in aqueous beryllium nitrate (102) has unambiguously demonstrated the importance of other relaxation mechanisms. A separation of the experimentally observed relaxation rate is accomplished by means of NOE experiments and the temperature dependence of  $T_1$ . Simultaneous irradiation of the water protons affords a signal intensity reduction of 50% at room temperature, corresponding to an Overhauser enhancement factor  $\eta = -0.5$  or a 14% dipolar contribution. This value gradually decreases with increasing temperature thus pointing to the onset of spin-rotation as a third mechanism. An Arrhenius plot for the experimental relaxation time as well as its dipolar and non-dipolar portion is in Fig. 11 which shows that  $T_1^{\text{exp}}$  reaches a sharp maximum at 40°C at which  $T_1^{\text{SR}}$  is equal to all of

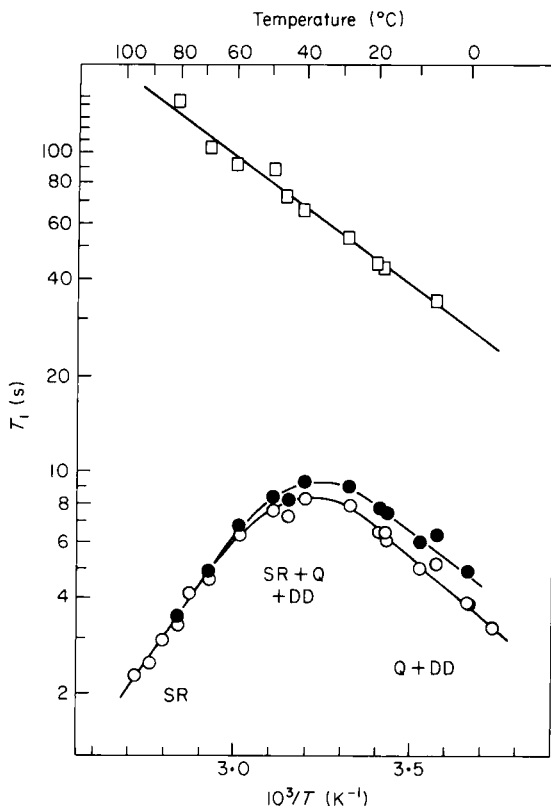


FIG. 11.  $^9\text{Be}$  spin-lattice relaxation time in 1 M aqueous  $\text{Be}(\text{NO}_3)_2$  as a function of temperature. Open circles: experimental relaxation time; squares: dipolar relaxation time,  $T_1^{\text{DD}}$ , obtained from  $T_1^{\text{exp}}$  and the nuclear Overhauser enhancement factor,  $\eta$ ; filled circles: nondipolar relaxation time,  $(1/T_1^{\text{exp}} - 1/T_1^{\text{DD}})^{-1}$ . (102)

the other relaxation contributions (quadrupolar and dipolar). By contrast a straight line is obtained for the dipolar  $T_1$ , the slope of which corresponds to an activation energy of 3.7 kcal/mol, which is typical of a structure-forming ion.

For  $^{43}\text{Ca}^{2+}$  no detailed study of this kind is yet available. While a dipolar contribution due to the larger size of the ion and also because of the shorter experimental relaxation time is unlikely, spin-rotation thus cannot be ruled out.

The alkaline earth nuclei in their ionic solvated state are expected to follow the quadrupolar relaxation pattern established for their Group I counterparts. However, there is one predictable distinguishing feature. Owing to their larger effective charge the alkaline earths are more

strongly hydrated, leading to a symmetry-induced quenching of the electric field gradient due to the more perfect order of the solvent dipoles in the first hydration sphere. It can therefore be expected that the main contribution to quadrupolar relaxation of at least the smaller cations ( $\text{Be}^{2+}$ ,  $\text{Mg}^{2+}$ ,  $\text{Ca}^{2+}$ ) has its origin in outer-sphere contributions. Lindman and coworkers (103) have recently examined this question for  $^9\text{Be}^{2+}$ ,  $^{25}\text{Mg}^{2+}$ ,  $^{43}\text{Ca}^{2+}$ ,  $^{87}\text{Sr}^{2+}$ , and  $^{135}\text{Ba}^{2+}$  by computing the infinite dilution quadrupolar relaxation rates on the basis of the Hertz electrostatic model. The models tested were that for "fully random distribution" (FRD) and its direct counterpart the "fully oriented solvation" model (FOS). Excellent agreement is generally obtained except for  $^{43}\text{Ca}^{2+}$  for which the model gives too large a value for the relaxation rate. This discrepancy is likely to arise from the uncertainty in the  $^{43}\text{Ca}$  quadrupole moment. The paper also reports the first infinite dilution relaxation time for  $^{25}\text{Mg}^{2+}$  and  $^{43}\text{Ca}^{2+}$  obtained from pulse experiments.

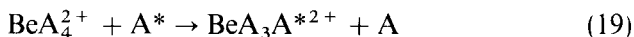
The concentration dependence of the line-width has been reported for  $^{25}\text{Mg}^{2+}$  (97, 101) and  $^{87}\text{Sr}^{2+}$  (99) and a variety of counter-ions, but only Simeral and Maciel (101) attempted to rationalize the effects observed. The latter workers plotted  $\Delta\nu_{\frac{1}{2}}/\eta$  ( $\eta$  is the bulk viscosity) against concentration and found that  $\Delta\nu_{\frac{1}{2}}/\eta$  remains nearly constant over the concentration range 0–3 M. From this observation it was inferred that specific cation–anion interactions, which could affect the local e.f.g., are absent and that the increase in the relaxation rate is a purely dynamic effect. This is probably too simple a view, however; the tight binding of the hydrate water in the long-lived magnesium hydration complex will effectively insulate the magnesium ion from ion–ion encounters.

### C. Complexation studies

Both the chemical shift and the relaxation rate may serve as an experimental observable in studies directed towards obtaining structural and thermodynamic information on cation binding. There are very few such studies in the literature making use of direct observation of alkaline earth resonances. The choice of the two possible experimental parameters depends on the sensitivity of either quantity to environmental changes. From early studies of the concentration dependence of  $^{25}\text{Mg}^{2+}$  shieldings in aqueous magnesium salts (104) which show that  $\delta(^{25}\text{Mg})$  varies by no more than 2 ppm over the concentration range 0–4 M, magnesium chemical shifts do not seem to meet the requirements for this type of experiment. For  $^{43}\text{Ca}^{2+}$ , as expected, the shift range is larger as concluded from the data of Lutz *et al.*

(97) where the  $^{43}\text{Ca}$  chemical shift varies typically by 10 ppm over the concentration range 0–5 M. For  $^{87}\text{Sr}^{2+}$  the shieldings are considerably more sensitive to concentration (99) but the accuracy of the measurement is impaired by the large inherent line-widths. No such data are available for  $^9\text{Be}^{2+}$  but the shift range is small as evidenced by the data of Kovar and Morgan (105) for organoberyllium compounds. Some shielding studies have been reported for  $^{135,137}\text{Ba}$ , but the experiment is hampered by the very broad lines observed for this nucleus. (100)

Delpuech *et al.* (106) examined the tetrahedral solvates of the beryllium cation with trimethyl phosphate (TMPA), dimethyl methyl phosphonate (DMMP), *N,N*-dimethylamido-*O,O'*-dimethyl phosphate (DMADMP), bis-*N,N*-dimethylamido-*O*-methyl phosphate (TMDAMP), and hexamethylphosphorotriamide (HMPT) by NMR including that of  $^9\text{Be}$ . The kinetics of ligand exchange:



are evaluated from total line-shape analysis of the temperature-dependent  $^9\text{Be}$  spectra by observing the gradual collapse of the multiplet pattern due to  $^{31}\text{P}$  spin coupling applying the Kubo–Sack–Anderson procedure for multiple-site exchange. Tetrahedral coordination of the complexes can readily be inferred from the 1:4:6:4:1 intensity pattern of the  $^9\text{Be}$  spectrum. Figure 12 shows the experimental and simulated spectra for  $^9\text{Be}(\text{TMPA})_4^{2+}$  for a set of temperatures. Because of the different time scale the proton and  $^9\text{Be}$  exchange experiments complement one another by extending the rate scale. The rate constant obtained from the  $^9\text{Be}$  spectra is four times that from the  $^1\text{H}$  experiments. From the concentration dependence of the rate constant  $k_1$ , defined for the exchange between free and bound ligand, it was inferred that both TMPA and DMMP obey an associative  $\text{S}_{\text{N}}2$ -type mechanism with probably a pentacoordinated transition state. By contrast a rate constant independent of concentration is found for the remaining ligands, suggesting a dissociative  $\text{S}_{\text{N}}1$  mechanism with a trigonal transition state. This behaviour mirrors the more severe steric congestion exerted by the bulkier ligands.

Exchange rates have been derived by Bryant (107) for ATP binding to  $\text{Mg}^{2+}$  from the temperature dependence of the  $^{25}\text{Mg}$  line-width monitored in a large excess of magnesium chloride. The rapid exchange limit is shown to hold, and the exchange rate derived from fitting the data to a theoretical equation for two-site exchange was  $2 \times 10^4 \text{ s}^{-1}$ . Somewhat surprising is the very large chemical shift difference of 260 ppm, which is calculated between free and bound  $\text{Mg}^{2+}$ . Because of

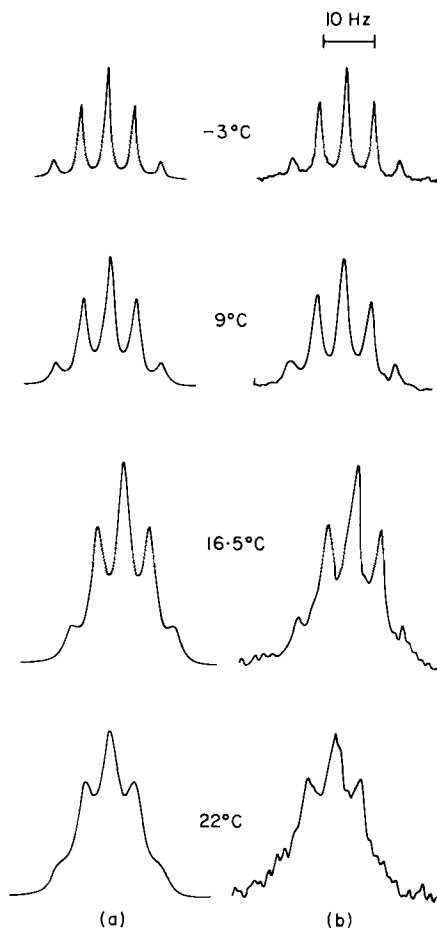


FIG. 12. Temperature-dependent  $^9\text{Be}$  NMR spectra in  $^9\text{Be}(\text{TMPA})_4^{2+}$ , recorded in the pulsed mode at 12.2 MHz in trimethyl phosphate (TMPA); (a) simulated, (b) experimental spectrum. (106)

the inaccuracy of the data this value should certainly be used with caution.

A very recent paper by Robertson *et al.* (108) explores the utilization of  $^{27}\text{Mg}$  NMR for the study of  $\text{Mg}^{2+}$  binding to  $\gamma$ -carboxyglutamic acid-containing peptides. These are taken as a model for prothrombin, an enzyme possessing 10  $\gamma$ -carboxyglutamic acid residues and which is known to interact with  $\text{Mg}^{2+}$  and  $\text{Ca}^{2+}$ . Whereas the addition of the peptide to an aqueous solution of  $\text{Mg}^{2+}$  affects the line-width rather than the shift, the  $^{43}\text{Ca}$  line-widths remain almost invariant in the

corresponding calcium binding experiment. From the line-width and chemical shift variation a binding constant of  $K = 1.6 \times 10^3$  is obtained for either cation and the dipeptide Z-D-Gla-D-Gla-OMe (Z = benzyloxycarbonyl), assuming a 1:1 complex and rapid exchange conditions. The  $^{43}\text{Ca}$  chemical shift titration curve is shown in Fig. 13. These experiments were performed in the Fourier transform mode using large sample-diameter probes and enriched materials. Although the exact ion concentrations are not indicated, Fig. 13 suggests a concentration of *ca.* 20 mM, which shows that experiments at rather low concentration have now become feasible on these nuclei.

#### D. Structural studies of covalent compounds

Beryllium and magnesium have a rather extensive covalent chemistry, and both  $^9\text{Be}$  and  $^{25}\text{Mg}$  seem to be useful NMR nuclei for the study of structure and bonding. Thanks to its small quadrupole moment  $^9\text{Be}$  has the potential to provide rather high-resolution spectra even for a lower than cubic coordination geometry. (105) For magnesium this seems doubtful although experimental evidence is missing.

Kovar and Morgan (105) have studied a wide range of organoberyllium compounds whose  $^9\text{Be}$  shieldings are in Table VI

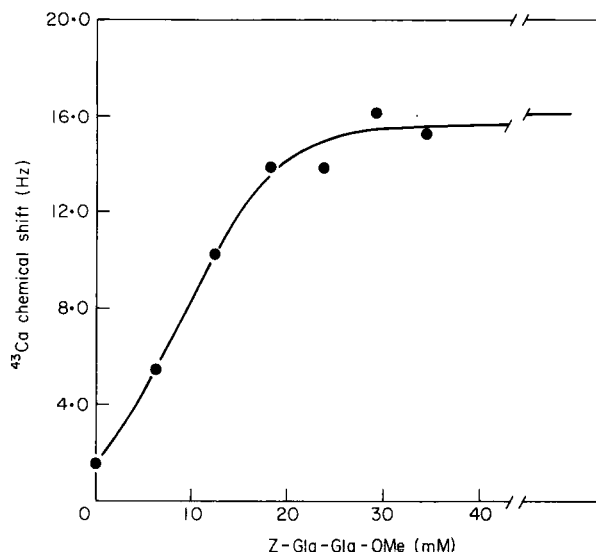
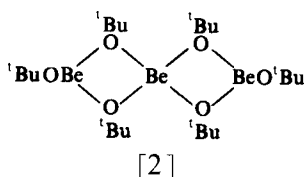


FIG. 13.  $^{43}\text{Ca}^{2+}$  chemical shifts plotted against concentration of Z-D-Gla-D-Gla-OMe (Z = benzyloxycarbonyl, Gla =  $\gamma$ -carboxyglutamic acid) relative to an arbitrary standard in  $\text{H}_2\text{O}$  at pH 6.6. Initial calcium concentration was 19.5 mM. (108)

along with some more recent data. (106, 109) Noteworthy features of these data are: (a) tetracoordination generally gives rise to a higher shielding than tricoordination (7–8 ppm); (b) increasing the substituent electronegativity progressively deshields  $^9\text{Be}$ . In the trimer [2] the line-widths observed are 64 Hz for the terminal and 5 Hz for the central quasi-tetrahedral beryllium, thus reflecting the very different field gradients at the two sites.



Spin-spin coupling has been observed between  $^9\text{Be}$  and both  $^{19}\text{F}$  (110, 111) and  $^{31}\text{P}$ . (106) In the  $\text{BeF}_4^{2-}$  anion, for example,  $^1J(\text{F}-\text{Be}) = 34 \pm 2$  Hz is found, and in the tetrahedral organophos-

TABLE VI

$^9\text{Be}$  chemical shifts in some inorganic and organometallic compounds  
(105, 106, 109)

Species	Solvent	$\delta(^9\text{Be})^a$	Ref.
$\text{Be}(\text{HMPT})_2^{2+ b}$	$\text{MeNO}_2$	-3.3	11
$\text{Be}(\text{TPMA})_2^{2+ c}$	$\text{MeNO}_2$	-3.2	11
$\text{Be}(\text{DMMP})_2^{2+ d}$	$\text{MeNO}_2$	-2.9	11
$\text{BeF}_2(\text{H}_2\text{O})_2$	$\text{H}_2\text{O}$	-0.8	10
$\text{Be}(\text{H}_2\text{O})_4^{2+}$	$\text{H}_2\text{O}$	0	—
$\text{Be}(\text{NH}_3)_4^{2+}$	$\text{NH}_3$	+1.7	10
$\text{Be}(\text{OH})_4^{2-}$	$\text{H}_2\text{O}-\text{NaOH}$	+1.4	14
$\text{BeCl}_2 \cdot 2\text{OEt}_2$	$\text{Et}_2\text{O}$	+3.1	10
$[\text{Be}(\text{NMe}_2)_2]_3$	$\text{C}_6\text{H}_6$		
central		+3.0	10
terminal		+9.8	10
$\text{BeCl}_2 \cdot 2\text{SMe}_2$	$\text{Me}_2\text{S}$	+5.5	10
$\text{MeBeCl}_2 \cdot 2\text{SMe}_2$	$\text{Me}_2\text{S}$	+4.2	10
$\text{Me}_2\text{Be} \cdot \text{SMe}_2$	$\text{Me}_2\text{S}$	+11.6	10
$\text{Me}_2\text{Be} \cdot 2\text{PMe}_3$	$\text{Me}_3\text{P}$	+3.6	10
$\text{Me}_2\text{Be} \cdot 2\text{NMe}_3$	$\text{Me}_3\text{N}$	+12.0	10
$\text{Me}_2\text{Be} \cdot \text{NMe}_3$	$\text{C}_6\text{H}_{12}$	+19.9	10
$\text{Me}_2\text{Be} \cdot \text{OEt}_2$	$\text{Et}_2\text{O}$	+20.8	10

<sup>a</sup> A positive sign indicates relative deshielding.

<sup>b</sup> HMPT = hexamethylphosphorotriamide.

<sup>c</sup> TPA = trimethyl phosphate.

<sup>d</sup> DMMP = dimethyl methylphosphonate



phorus complexes values ranging between 4 and 6 Hz are reported for  $^2J(\text{P}-\text{Be})$ . (106) The small values are taken as evidence for the predominantly ionic character of the metal-ligand bonds in these systems. The broadened 1:2:1 triplet [ $^1J(\text{F}-\text{Be}) = 28 \text{ Hz}$ ] lends support to the presence of a tetrahedral species  $\text{BeF}_2(\text{H}_2\text{O})_2$  (105) rather than a mixture of  $\text{BeF}_n^{2-n}$  ( $n = 1, 2, 3, 4$ ) complexes. The second multiplet in the low-temperature  $^{19}\text{F}$  spectrum of aqueous  $(\text{NH}_4)_2\text{BeF}_4$  is tentatively assigned to a species  $\text{BeF}_3(\text{H}_2\text{O})^-$ . Conclusive evidence for the occurrence of such an ion was provided recently. (111) The high-resolution  $^9\text{Be}$  spectrum of ammonium tetrafluoroberyllate at  $-9^\circ\text{C}$  reveals two partly overlapping multiplets, a quintet [ $^1J(\text{F}-\text{Be}) = 34 \text{ Hz}$ ] and a quartet [ $^1J(\text{F}-\text{Be}) = 38 \text{ Hz}$ ]. The two species also exhibit different  $^9\text{Be}$  relaxation times (660 and 85 ms respectively). While  $^9\text{BeF}_4^{2-}$  is probably predominantly relaxed by  $^9\text{Be}-^{19}\text{F}$  dipolar relaxation, in the less symmetric minor species quadrupolar relaxation is definitely prevalent.

In bis(acetylacetonato)beryllium,  $\text{Be}(\text{acac})_2$ , the  $^9\text{Be}$  quadrupole coupling constant can be determined from a combined  $^{13}\text{C}$  and  $^9\text{Be}$  relaxation experiment, which is favoured in this molecule of  $D_{2d}$  symmetry, by the fact that the C-H bond vector for the olefinic carbon is coincident with the z principal axis of the e.f.g. tensor. Hence it is the same diffusion constant which modulates  $V_{zz}$  and  $r_{\text{C-H}}$ . For the quadrupole coupling constant a value of 350 kHz was derived. (111)

## V. THE MAIN GROUPS III AND IV

### A. Nuclear properties

The chemical and technological significance of the Group III metals, in particular of aluminium but also of gallium and indium, need not be particularly stressed. Because of its widespread occurrence in nature and importance as a metal, the chemistry of aluminium has been very well investigated. Besides its extensive solution chemistry, which is predominantly ionic, aluminium has a remarkable tendency to form covalent bonds. In both domains  $^{27}\text{Al}$  NMR has proved suitable as a structural and dynamic probe. Gallium and indium attracted the interest of solid-state physicists at an early stage and both elements are now widely used as a doping material for pnp-type semiconductors.

Besides their chemical similarity the three elements also have rather similar NMR properties; large magnetic moments make them easy to measure, and all the magnetic isotopes have sizeable quadrupole moments. The receptivity of  $^{27}\text{Al}$  is only five times lower than that of the proton, which enables experiments to be performed on a

submillimole concentration level, at least for reasonably symmetric species. The gallium line-widths are more sensitive to coordination geometry although the quadrupole moments (at least for  $^{71}\text{Ga}$ ) are comparable. However, the lower spin quantum number of both gallium isotopes accounts for a fourfold increase of the relaxation rate relative to that of a spin- $\frac{5}{2}$  nucleus. Both indium isotopes are handicapped by their very large quadrupole moments, and the observation of any species of lower than cubic coordination geometry is probably impracticable.

Because of its very different chemistry the only quadrupolar Group IV nucleus,  $^{73}\text{Ge}$ , is treated in a separate section. The nuclear properties of the six quadrupolar nuclides pertaining to main Groups III and IV are in Table VII.

### B. Quadrupole relaxation of the hydrated ion

Both  $\text{Al}^{3+}$  and  $\text{Ga}^{3+}$  have a tightly bound hydrate shell in aqueous solution and both are prone to hydrolysis. In terms of the Hertz electrostatic model for quadrupolar relaxation of ionic nuclei in electrolyte solution (see Section III.C) one therefore expects effective quenching of the electric field gradient caused by the surrounding water dipoles, due to a nearly perfect  $O_h$  coordination symmetry. Any contribution to the e.f.g. should therefore arise from outer-sphere solvent dipoles. In terms of the "fully orientated solvation" (FOS) model this would correspond to a distribution width parameter approaching zero ( $\lambda \rightarrow 0$ ) with the first term in equation (4) vanishing. This is indeed what Hertz (24) found for both  $^{27}\text{Al}^{3+}$  and  $^{69}\text{Ga}^{3+}$ , and the experimental infinite dilution relaxation rates ( $^{27}\text{Al}^{3+}$   $7.5\text{ s}^{-1}$ ;  $^{69}\text{Ga}^{3+}$   $\sim 350\text{ s}^{-1}$ ) are remarkably well matched by the computed ones ( $4.0$  and  $216\text{ s}^{-1}$  respectively). Tarasov and Buslaev (112) have looked

TABLE VII  
Physical constants of main-Group III and IV quadrupolar nuclei<sup>a</sup>

Nucleus	Spin $I$	Abund. (%)	Mag. moment ( $\mu_N$ )	$Q$ (barns)
$^{27}\text{Al}$	$\frac{5}{2}$	100	3.368	0.149
$^{69}\text{Ga}$	$\frac{3}{2}$	39.8	2.011	0.232
$^{71}\text{Ga}$	$\frac{3}{2}$	60.2	2.555	0.146
$^{113}\text{In}$	$\frac{9}{2}$	4.3	5.495	1.144
$^{115}\text{In}$	$\frac{9}{2}$	95.7	5.507	1.161
$^{73}\text{Ge}$	$\frac{9}{2}$	7.6	-0.877	-0.29

<sup>a</sup> The two boron isotopes are not listed.

into the relaxation behaviour of  $^{69}\text{Ga}^{3+}$  and  $^{71}\text{Ga}^{3+}$  in both  $\text{H}_2\text{O}$  and  $\text{D}_2\text{O}$  solutions with the aim of verifying the quadrupolar nature of the relaxation mechanism. The only mechanism considered besides the quadrupolar was proton-induced dipole-dipole interaction. Since the ratio of the relaxation rates  $1/T_2(^{69}\text{Ga})/1/T_2(^{71}\text{Ga})$  is less than  $Q^2(^{69}\text{Ga})/Q^2(^{71}\text{Ga})$ , the discrepancy is suggested to arise from dipole-dipole relaxation involving hydrate protons. This, however, is very unlikely since the derived correlation time for reorientation of the hydration complex is  $2 \times 10^{-9}$  s which is two orders longer than the correlation time of neat water! Further contradictions are the decrease of the calculated dipolar relaxation time with increasing solute concentration as well as the enhanced relaxation rate in  $\text{D}_2\text{O}$ .

More recently Takahashi (113, 114) has approached the problem on the hypothesis that the electric field gradient at the  $\text{Al}^{3+}$  cation is engendered by rotation of the solvate water molecules around their twofold axis, i.e. parallel to the electric field of the spherical ion. The six water molecules in the innermost solvation shell give rise to  $T_h$  overall symmetry as long as the O-H bonds situated at opposite corners of the octahedron lie in the same plane. However, a  $90^\circ$  rotation of one of the hydrate water molecules lowers the symmetry to  $C_{2v}$  leading to an e.f.g. at the site of the Al nucleus.

With the aid of a point-charge model for the  $\text{H}_2\text{O}$  molecule the electrostatic energies for the various configurations can be calculated. This ultimately yields the transition probabilities  $W_0$  and  $W$  per unit

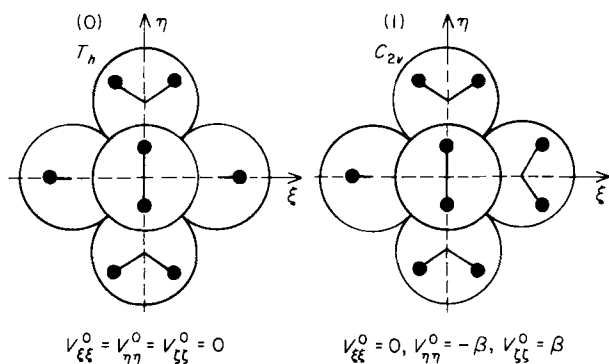


FIG. 14. Two possible configurations of the orientation of water molecules in the first hydration sphere of  $\text{Al}(\text{H}_2\text{O})_6^{3+}$ . The rotation of one of the equatorial water molecules in configuration (0) by an angle of  $\pi/2$  radians around the Al-O axis lowers the symmetry from  $T_h$  to  $C_{2v}$ , simultaneously introducing field gradients  $V_{\eta\eta}$  and  $V_{\zeta\zeta}$ . (113)

time for the symmetry transitions  $T_h \rightarrow C_{2v}$  and  $C_{2v} \rightarrow T_h$ , respectively, resulting in the following simple formulae:

$$\frac{1}{T_1^Q} = \frac{(2I + 3)}{10I^2(2I - 1)} \left( \frac{e^2 q Q}{\hbar} \right)^2 \frac{W\bar{\tau}_c}{(3W_0 + W)} \quad (20)$$

$$1/\bar{\tau}_c = W + 1/\tau_c \quad (21)$$

where  $\tau_c$  is the rotational correlation time for overall reorientation of the solvation complex. The transition probabilities  $W_0$  and  $W$  can be derived from reaction rate theory by calculating the partition functions in the ground state and in the activated form. The weakest part of the theory probably concerns the correlation time which is simply obtained from the Stokes–Debye formula. Nevertheless excellent agreement with experimental relaxation rates is obtained at a concentration of 1.6 M  $\text{AlCl}_3$  in  $\text{H}_2\text{O}$  (e.g.  $28 \text{ s}^{-1}$  calculated *vs.*  $29.7 \text{ s}^{-1}$  experimental at  $23^\circ\text{C}$ ). Extrapolating to infinite dilution is achieved by means of a viscosity correction using the same values of  $W_0$  and  $W$ . The value of  $18 \text{ s}^{-1}$  (at  $23^\circ\text{C}$ ) obtained in this way, however, is too large by a factor of 2.5. (24)

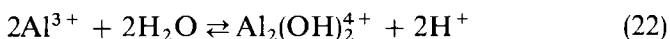
Takahashi's approach is diametrically opposed to Hertz's electrostatic model in that it assumes the source of the transient electric field gradients to arise from symmetry distortions in the first solvation shell. Moreover, the theory is of less general applicability since it requires a well defined solvation complex hence confining it to strongly hydrating cations.

One aspect that nobody appears to have taken into consideration is the effect of hydrolysis. Low-symmetry hydrolysates such as  $\text{Al}(\text{H}_2\text{O})_5\text{OH}^{2+}$  or its dimer (115–117) could in fact substantially contribute to the relaxation rate unless the various species are in mutually slow exchange.

### C. Solvation and complexation studies

The solvating abilities of the cations  $\text{Al}^{3+}$ ,  $\text{Ga}^{3+}$ , and  $\text{In}^{3+}$  differ much from their Group I and II analogues. This is primarily due to the smaller size and greater effective charge of the trivalent cation. The resulting increased electrostatic attraction leads to very tightly bound solvates which makes them ideal objects for study by NMR. The solvation sheath of such species is generally kinetically inert, i.e. the exchange between bulk and solvate molecules is usually slow on the NMR time scale.

A century-old problem which has been investigated by a variety of techniques concerns the hydrolysis of aluminium salts.  $^{27}\text{Al}$  NMR has undoubtedly provided a significant contribution to the understanding of this complicated process. (115–117) Akitt and coworkers (117) have provided convincing evidence for the presence of the  $\text{Al}_2(\text{OH})_2(\text{H}_2\text{O})_8^{4+}$  dimer as well as for a species  $\text{Al}_{13}\text{O}_4(\text{OH})_{24}(\text{H}_2\text{O})_{12}^{7+}$  in aqueous solutions of aluminium trichloride. The latter contains at its centre a tetrahedrally coordinated aluminium which resonates at 62.5 ppm to high frequency of  $\text{Al}(\text{H}_2\text{O})_6^{3+}$ . Owing to the greater field gradients at the surrounding, less symmetric, aluminium moieties these cannot be detected. Evidence for the earlier suggested dimeric nature of  $\text{Al}(\text{OH})(\text{H}_2\text{O})_5^{2+}$  was obtained from  $^{27}\text{Al}$  line intensity measurements. Ignoring hydrate water and defining an apparent formation constant  $K$  for an equilibrium:



or

$$\log[\text{Al}_2(\text{OH})_2^{4+}] = \log K + 2\log[\text{Al}^{3+}] + 2\text{pH} \quad (23)$$

a plot of  $\log[\text{Al}_2(\text{OH})_2^{4+}]$  vs.  $(\text{pH} + \log[\text{Al}^{3+}])$  should afford a straight line of slope  $m = 2$ , which is in fact observed. At the pH values used for these experiments the dimer concentration is calculated from the difference  $([\text{Al}_{\text{tot}}] - [\text{Al}^{3+}])$  since the dimer cannot be directly observed (except at high rf power levels where a broad resonance slightly to high frequency of  $^{27}\text{Al}(\text{H}_2\text{O})_6^{3+}$  is detected).

Solvation of aluminium salts in a host of pure (118–123) as well as mixed solvents (124–127) has been reported. Analogous experiments have been conducted on gallium salts using  $^{69}\text{Ga}$  and  $^{71}\text{Ga}$  NMR. (128) The most significant result of these studies is the occurrence and coexistence of tetra- and hexa-coordinated species. The first report by Hon, (118) who investigated the solvates of aluminium trichloride in acetonitrile, points to the formation of  $\text{Al}(\text{CH}_3\text{CN})_6^{3+}$  and  $\text{AlCl}_4^-$  in a ratio of 1:3 according to the equilibrium:



This explanation has received further support from  $^1\text{H}$  NMR data. The solid adduct is known to consist of  $[\text{AlCl}(\text{CH}_3\text{CN})_5]^{2+} [\text{AlCl}_4]_2^{2-}$ . Under the higher resolution achievable in the absorption mode spectra, Akitt and Duncan (123) detected a broad resonance in the region of octahedrally coordinated aluminium, apparently due to the presence of several species. The changes in the relative intensities observed upon addition of chloride or perchlorate permitted assignment of the peaks

to  $\text{Al}(\text{CH}_3\text{CN})_6^{3+}$  and the halogeno species  $\text{AlCl}(\text{CH}_3\text{CN})_5^{2+}$  and  $\text{AlCl}_2(\text{CH}_3\text{CN})_4^+$  or their bromine counterparts in the case of  $\text{AlBr}_3$ .

Buslaev *et al.* (128) examined the solution properties of the corresponding  $\text{GaX}_3$  ( $\text{X} = \text{Cl}, \text{Br}, \text{I}$ ) compounds in acetonitrile, benzene, and nitromethane as well as in the corresponding binary mixtures. Two signals are generally observed and these are assigned to  $\text{GaX}_4^-$  and  $\text{GaS}_6^{3+}$  ( $\text{S} = \text{solvent}$ ) with the following shifts:  $\text{GaCl}_4^-$  252 ppm,  $\text{GaBr}_4^-$  63 ppm,  $\text{GaI}_4^-$  -505 ppm, and  $\text{Ga}(\text{CH}_3\text{CN})_6^{3+}$  -72 ppm, all relative to external  $\text{Ga}(\text{H}_2\text{O})_6^{3+}$ . The shielding sequence for the tetrahalogenogallates is thus the same as that reported for the corresponding aluminates  $^{27}\text{AlX}_4^-$  (119) with the absolute shieldings of course being smaller for  $^{27}\text{Al}$  (102, 80, and -28 ppm respectively). This shielding sequence seems to be common to all main-group halides or halide complexes (see above) and has been rationalized in terms of the nephelauxetic effect of the halide ions. (129)

Instead of the observed 3:1 ratio between anionic and cationic species of  $\text{Al}_2\text{Cl}_6$  in acetonitrile, the corresponding solutions of  $\text{GaCl}_3$  furnished a 10:1 population ratio. In the light of the recent re-interpretation of the data for the aluminium solvates (123) this may be explained as arising from the formation of the corresponding asymmetric hexacoordinated mixed solvates which, owing to enhanced quadrupole relaxation, may be unobservable. For the bromide and iodide complexes this ratio is even larger and moreover dependent upon which isotope,  $^{69}\text{Ga}$  or  $^{71}\text{Ga}$ , is observed. This observation further lends support to the previously made interpretation.

Addition of a small amount of water to a solution of  $\text{GaCl}_3$  in acetonitrile sharpens the resonance assignable to  $\text{GaCl}_4^-$  (131) probably as a result of the increased dielectric constant of the medium (the electronic distortion due to ion pairing is alleviated!). In addition new resonances appear in the region of the hexacoordinated species. Besides that at -72 ppm further peaks develop at 40 and 10 ppm, which are attributed to species of the type  $[\text{Ga}(\text{CH}_3\text{CN})_{6-n}(\text{H}_2\text{O})_n]^{3+}$ . In aqueous solution the ratios of peak intensities and line-widths are a function of the solute concentration. At concentrations below 1.7 M no  $\text{GaCl}_4^-$  is found, species of the type  $[\text{GaCl}_{4-n}(\text{H}_2\text{O})_n]^{n-1}$  probably being unobservable.

Octahedral and tetrahedral solvates  $(\text{AlS}_n)(\text{ClO}_4)_3$  [ $n = 4, 6$ ;  $\text{S} = \text{trimethyl phosphate (TMPA), hexamethylphosphorotriamide (HMPT), triethyl phosphate (TEPA), dimethyl methylphosphonate (DMMP), diethyl ethylphosphonate (DEEP), and dimethyl hydrogen phosphite (DMHP)}$ ] are shown by  $^{27}\text{Al}$  NMR to have tetrahedral and octahedral structures which are retained in nitromethane solution.

(125) All except  $\text{Al}(\text{HMPT})_4^{3+}$  can be assigned a hexacoordination on the basis of the observed multiplicities due to  $^{27}\text{Al}$ – $^{31}\text{P}$  spin coupling. The spin couplings are markedly different in the two types of coordination geometry reflecting the different hybridization ( $d^2sp^3$  versus  $sp^3$  for  $n = 6$  and 4 respectively).

Mixed solvation was first studied by Canet *et al.* (124) who observed separate partly overlapping  $^{27}\text{Al}$  resonances from  $\text{Al}(\text{ClO}_4)_3$  dissolved in a  $\text{TMPA}$ – $\text{H}_2\text{O}$  solvent mixture. The four peaks can be assigned to  $\text{Al}(\text{H}_2\text{O})_6^{3+}$ ,  $\text{Al}(\text{H}_2\text{O})_5(\text{TMPA})^{3+}$ ,  $\text{Al}(\text{H}_2\text{O})_4(\text{TMPA})_2^{3+}$ , and probably  $\text{Al}(\text{H}_2\text{O})_3(\text{TMPA})_3^{3+}$ . It is noteworthy that proton,  $^{13}\text{C}$ , and  $^{31}\text{P}$  NMR have failed to detect the individual species as separate resonances.

More recently the solvation of  $\text{Al}^{3+}$  in binary mixtures of DMF and DMSO (126) and nitromethane and DMF (127) was investigated. For the former solvent system all possible mixed solvates  $\text{Al}(\text{DMF})_n(\text{DMSO})_{6-n}^{3+}$  were found to give rise to separate  $^{27}\text{Al}$  resonances. In the presence of nitromethane as a diluent the distribution of solvates follows the bulk solvent composition, and the coordination number is retained at all mixing ratios. In the undiluted binary system, however,  $\text{Al}^{3+}$  is preferentially solvated by DMSO.

Besides solvation, which presupposes a reaction between an inorganic salt and the organic (or inorganic) solvent,  $^{27}\text{Al}$  NMR (125, 129–142) as well as  $^{69}\text{Ga}$  and  $^{71}\text{Ga}$  NMR (143–147) have rather extensively been applied to the study of complex formation in solution.  $^{27}\text{Al}$  data have provided conclusive evidence for the occurrence of a sulphato complex (116, 138, 139) in sulphate-containing solutions of aluminium salts. This was established on the basis of the appearance of a second peak 3.3 ppm to low frequency of  $\text{Al}(\text{H}_2\text{O})_6^{3+}$  with a relative intensity related to the total sulphate concentration. Upon addition of sulphuric acid a third peak emerges to even lower frequencies which is attributed to a sulphuric acid or bisulphato complex. (139) The former species is also present in aqueous solution of  $\text{KAl}(\text{SO}_4)_2$ . (148)  $^{27}\text{Al}$  spin–lattice relaxation measurements in 0.1 M  $\text{KAl}(\text{SO}_4)_2$  at 28°C yield 44 and 130 ms for the major and minor species respectively, pointing to a lower-symmetry moiety for the sulphato complex. (148) The two spectra in light and heavy water exhibit different relative areas for the two peaks, revealing a remarkable isotope effect on the formation constant for the sulphato complex. For a 1:1 complex as assumed in ref. 139,

$$K = [\text{Al}(\text{SO}_4)^+]/[\text{SO}_4^{2-}][\text{Al}^{3+}]$$

ignoring hydrate water. At 0.1 M concentration of  $\text{KAl}(\text{SO}_4)_2$  and 28°C values of 0.88 and 0.60 were obtained in  $\text{D}_2\text{O}$  and  $\text{H}_2\text{O}$ , respectively.

Figure 15 shows the  $^{27}\text{Al}$  spectra in the two solvents. (148)

Haraguchi and Fujiwara (119) have studied the complexes formed upon dissolution of the dimeric halides  $\text{Al}_2\text{X}_6$  ( $\text{X} = \text{Cl}, \text{Br}, \text{I}$ ) in a broad range of solvents and in the presence of complexing anions. This work has revealed a notable property of  $^{27}\text{Al}$  shieldings which is diagnostically useful and seems to be of general validity, namely the considerably lower shielding of tetrahedrally compared with octahedrally coordinated  $^{27}\text{Al}$ . This rule has been found to hold true for  $^{69}\text{Ga}$  and  $^{71}\text{Ga}$  shieldings. (128)

$^{27}\text{Al}$  NMR turned out to be an excellent tool for the characterization of mixed tetrahalogenoaluminates of the type  $\text{AlX}_n\text{Y}_{4-n}^-$  ( $n = 0-4$ ) (129, 130) which coexist in solution and are kinetically inert so as to furnish separate peaks for the various species. Recently Tarasov *et al.* (145) examined the formation of mixed tetrahalogenogallates of the type  $[\text{GaBr}_n\text{Cl}_{4-n}]^-$  by combined  $^{69}\text{Ga}$  and  $^{71}\text{Ga}$  relaxation and chemical shift experiments. Separate resonances are observed for all theoretically possible anions as is seen from the inversion-recovery  $T_1$  spectra in Fig. 16. The  $^{69}\text{Ga}$  and  $^{71}\text{Ga}$  relaxation times, both obtained

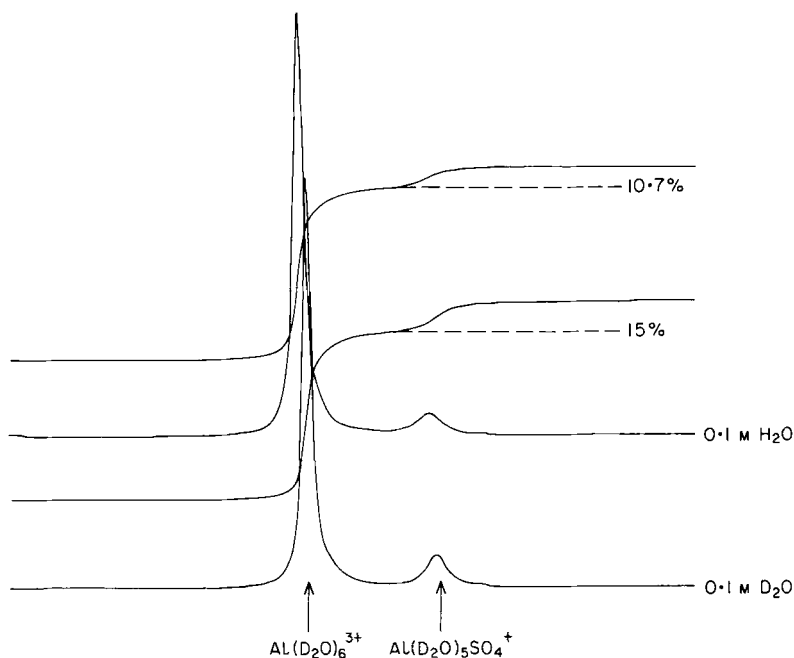


FIG. 15.  $^{27}\text{Al}$  spectra of aqueous  $\text{KAl}(\text{SO}_4)_2$ , 0.1 M in  $\text{D}_2\text{O}$  and  $\text{H}_2\text{O}$ , respectively. (148)



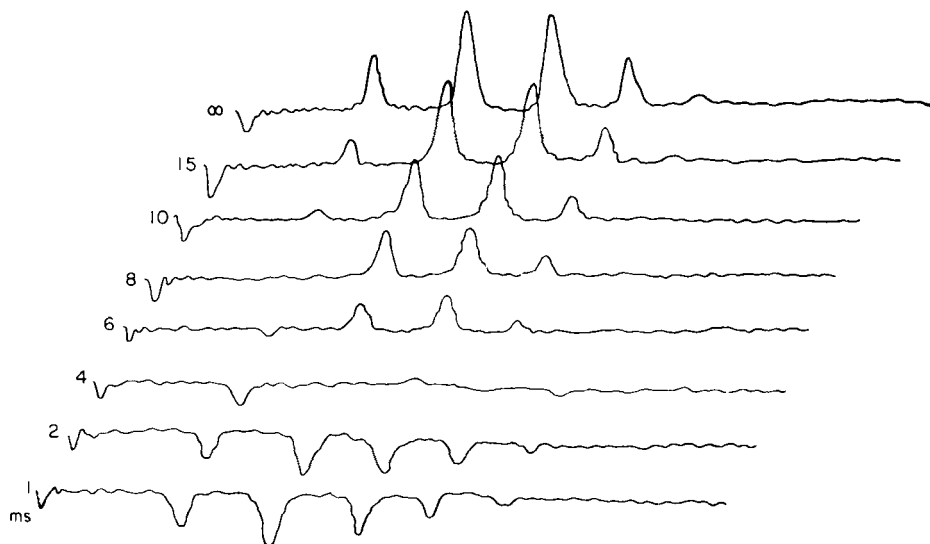


FIG. 16.  $^{71}\text{Ga}$  inversion-recovery spectra, recorded at 12.3 MHz from a solution of  $\text{GaBr}$  and  $\text{NbCl}_5$  in acetonitrile. Peak assignments from high to low frequency are as follows:  $\text{GaCl}_4^-$ ,  $\text{GaCl}_3\text{Br}^-$ ,  $\text{GaCl}_2\text{Br}_2^-$ ,  $\text{GaClBr}_3^-$ ,  $\text{GaBr}_4^-$ . (145)

at the same frequency but at different field strengths, are summarized in Table VIII along with the respective chemical shifts.

Three observations can be made from these data: (a) the relative magnitudes of both  $T_1$  and  $T_2$  are clearly related to the symmetry of the complex with the cubically symmetric environments giving the longest  $T_1$  in accordance with expectation for quadrupolar relaxation; (b)  $T_2 < T_1$ ; and (c)  $T_1(^{69}\text{Ga})$  and  $T_1(^{71}\text{Ga})$  do not behave as the squares of the quadrupole moments ( $Q_{69}^2/Q_{71}^2 = 2.52$ ) as one would predict for

TABLE VIII

Chemical shifts and relaxation times<sup>a</sup> of  $^{69}\text{Ga}$  and  $^{71}\text{Ga}$  in  $\text{GaCl}_n\text{Br}_{4-n}$  ( $n = 0-4$ ) anions (145)

Anion	Symmetry	$\delta(\text{Ga})$	$T_1$ (ms)		$T_2$ (ms)	
			$^{69}\text{Ga}$	$^{71}\text{Ga}$	$^{69}\text{Ga}$	$^{71}\text{Ga}$
$\text{GaCl}_4^-$	$T_d$	0	9.5	15.0	2.4	3.5
$\text{GaCl}_3\text{Br}^-$	$C_{3v}$	-40	3.0	6.6	1.9	2.9
$\text{GaCl}_2\text{Br}_2^-$	$C_{2v}$	-84	2.9	5.5	1.6	2.7
$\text{GaClBr}_3^-$	$C_{3v}$	-133	2.8	6.1	1.6	2.8
$\text{GaBr}_4^-$	$T_d$	-184	5.0	12.0	2.5	3.2

<sup>a</sup> All measured at 12.3 MHz by the inversion-recovery technique ( $T_1$ ) or from line-widths ( $T_2$ ).

quadrupolar relaxation. Observation (b) points to a second relaxation mechanism which affects  $T_2$  but not (or to a lesser extent)  $T_1$ . This is either scalar relaxation or chemical exchange. Observation (c) finally allows the conclusion that even  $T_1$  is not entirely governed by quadrupolar relaxation. On the assumption that the additional  $T_1$  mechanism is of the scalar type, an estimate can be made for the coupling constant between  $^{71}\text{Ga}$  and  $^{35}\text{Cl}$ . The four unknowns  $^{69}R_1^Q$ ,  $^{71}R_1^Q$ ,  $^{69}R_1^{\text{SC}}$ , and  $^{71}R_1^{\text{SC}}$  ( $R_1 \equiv 1/T_1$ ) are calculated from the equations:

$$\frac{^{69}R_1^{\text{SC}}}{^{71}R_1^{\text{C}}} = \left( \frac{^{69}\gamma}{^{71}\gamma} \right)^2 \left\{ \frac{\omega_{71}}{\omega_{69}} \left( \frac{1 - \omega_{35}/\omega_{71}}{1 - \omega_{35}/\omega_{69}} \right) \right\} \quad (25)$$

$$^{69}R_1 = ^{69}R_1^Q + ^{69}R_1^{\text{SC}} \quad (26)$$

$$^{71}R_1 = ^{71}R_1^Q + ^{71}R_1^{\text{SC}} \quad (27)$$

$$^{69}R_1^Q / ^{71}R_1^Q = (^{69}Q / ^{71}Q)^2 \quad (28)$$

Using  $T_1(^{35}\text{Cl}) \approx 10^{-6} \text{ s}$ ,  $^1J(^{71}\text{Ga}-^{35}\text{Cl}) \approx 3000 \text{ Hz}$  is obtained from the equation for scalar spin-lattice relaxation.

More recently Tarasov *et al.* provided unambiguous evidence for the superposition of scalar and quadrupolar spin-lattice relaxation mechanisms in the case of  $^{27}\text{Al}$  in the corresponding mixed tetrahalogenoaluminates  $\text{AlCl}_n\text{Br}_{4-n}^-$  (244). From the temperature dependence of  $T_1(^{27}\text{Al})$  in  $^{27}\text{AlCl}_4^-$  and  $^{27}\text{AlBr}_4^-$  the scalar contributions to the  $^{27}\text{Al}$  relaxation rates are determined, providing the following estimates for the respective scalar coupling constants:  $^1J(^{27}\text{Al}-^{37}\text{Cl}) = 650 \text{ Hz}$  and  $^1J(^{27}\text{Al}-^{81}\text{Br}) = 750 \text{ Hz}$ .

The same group of workers have also studied mixed complexation involving aluminium and gallium halides on the one hand and isocyanate and isothiocyanate on the other in acetonitrile solution, resulting in kinetically stable complexes of the types  $\text{MX}_n(\text{NCO})_{4-n}^-$  and  $\text{MX}_n(\text{NCS})_{4-n}^-$  with  $\text{M} = \text{Al}^{3+}$ ,  $\text{Ga}^{3+}$ , and  $\text{X} = \text{Cl}^-$ ,  $\text{Br}^-$ ,  $\text{I}^-$ . (245, 246) In this case unambiguous identification of the mixed species was accomplished on the basis of the observed spin-spin coupling constants between the metal nucleus and nitrogen-14. The observability of this coupling constant stipulates a sufficiently long lifetime of the nitrogen spin states. This is only possible owing to a redistribution of electronic charge leading to species with high positive charge density at the nitrogen atom. The relative magnitudes are found to be 40 Hz ( $^{27}\text{AlCl}_3\text{NCO}^-$ ) and 95 Hz ( $^{71}\text{GaCl}_3\text{NCO}^-$ ) suggesting dominance of the Fermi contact term and nitrogen coordination. A typical spectrum exhibiting separate signals for  $^{27}\text{AlCl}_4^-$ ,  $^{27}\text{AlCl}_3\text{NCS}^-$ , and  $^{27}\text{AlCl}_2(\text{NCS})_2^-$  is shown in Fig. 17.

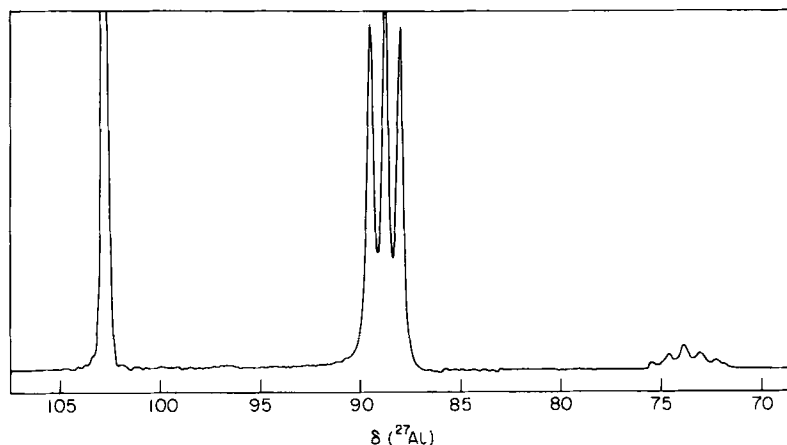


FIG. 17. 52.2 MHz  $^{27}\text{Al}$  NMR spectrum of  $\text{AlCl}_3$  in  $\text{CH}_3\text{CN}$  in the presence of  $\text{KNCS}$  ( $[\text{Al}^{3+}]/[\text{NCS}^-] = 1.4$ ) showing from high to low frequency the signals due to  $^{27}\text{AlCl}_4^-$ ,  $^{27}\text{AlCl}_3\text{NCS}^-$ , and  $^{27}\text{AlCl}_2(\text{NCS})_2^-$ .

Mixed complexes are also obtained upon substitution of hydride by  $^-\text{OR}$  or  $^-\text{SR}$  ( $\text{R} = \text{alkyl}$ ) in  $\text{LiAlH}_4$ , resulting in species that are identified as  $\text{LiAlH}(\text{YR})_3$  with  $\text{Y} = \text{O}$  or  $\text{S}$ . (142) In this study  $^{27}\text{Al}$  NMR data are reported for  $\text{LiAlH}_4$  and what is believed to be " $\text{AlH}_3$ ". The chemical shift and line-width of the latter depend on the sample preparation made. The spectrum obtained upon treatment of  $\text{LiAlH}_4$  with sulphuric acid affords an exceedingly broad line ( $\Delta\nu_{\frac{1}{2}} \approx 3 \text{ G}$ ) at 65 ppm to high frequency of  $\text{Al}(\text{H}_2\text{O})_6^{3+}$ . If, on the other hand, the hydride is prepared by interaction of  $\text{LiAlH}_4$  with  $\text{AlCl}_3$  a much narrower line at 115 ppm is observed. It has been suggested that in the former case the species in solution is the true aluminium hydride whereas the latter reaction leads to a quasi-tetrahedral ion  $\text{AlH}_3\text{Cl}^-$ . It is reported that  $[\text{AlH}(\text{SR})_3]^-$  is less shielded (131–146 ppm) than  $[\text{AlH}(\text{OR})_3]^-$  (51–98 ppm).

The aluminium ion is well known to form chelates with bidentate ligands such as dicarboxylic acids or hydroxy-carboxylic acids. However, a single resonance line is observed in the presence of chelating agents such as tartaric acid, mandelic acid, etc. with a pH-dependence typical of tetra- and hexa-coordination. (140) At low pH the signal gradually diminishes and eventually disappears probably owing to the formation of polynuclear chelates. In a spectroscopic study of the aluminium complexes with oxalate as a ligand,  $^{27}\text{Al}$  NMR has confirmed the successive formation of the complexes  $\text{Al}(\text{C}_2\text{O}_4)^+$ ,  $\text{Al}(\text{C}_2\text{O}_4)_2^-$ , and  $\text{Al}(\text{C}_2\text{O}_4)_3^{3-}$ . (141) Analogous experiments have

recently been reported for  $\text{Ga}^{3+}$ . (147) In an attempt to determine the stoichiometry of a family of gallium complexes with ligands such as morpholinopropanesulphonic acid (MOPS), tris(hydroxymethyl)-aminomethane (TRIS), ethylenediaminetetraacetic acid (EDTA), nitrilotriacetic acid (NTA), and lactate, the  $^{71}\text{Ga}$  resonance was measured in acidic and alkaline media. The complex stoichiometry can be derived from plots of the line intensity of the signal due to  $^{71}\text{Ga}(\text{H}_2\text{O})_6^{3+}$ , which gradually disappears upon addition of the ligand. The disappearance of the signal is attributed to a large quadrupole coupling constant in the chelated gallium preventing its observation. While for EDTA and NTA 1:1 complexes are formed, the plots indicate a 1:3 complex with lactate and no complexation with other ligands. At high pH there appears to be competition between the formation of the complex and the gallate ion  $\text{Ga}(\text{OH})_4^-$ . In the presence of equimolar amounts of EDTA and  $\text{Ga}^{3+}$  37% of gallium occurs as  $\text{Ga}(\text{OH})_4^-$  whose gallium resonance is shifted to high frequency by *ca.* 220 ppm.

In analogy to Be(II) and Al(III), also gallium(III) and indium(III) form stable complexes with organophosphorus ligands. Illustrative examples are the hexakis(trimethyl phosphate)-gallium(III) and -indium(III) complexes which have been recently examined. (146)

In contrast to the  $^{27}\text{Al}$  NMR spectra in the analogous  $\text{Al}(\text{TMPA})_6^{3+}$  (125) neither the  $^{71}\text{Ga}$  nor the  $^{31}\text{P}$  spectrum exhibits fully resolved P-Ga spin-spin couplings, which mirrors the faster relaxation of the gallium and indium isotopes. Nevertheless total line-shape analysis of the quadrupole relaxation-broadened  $^{31}\text{P}$  signals permits the determination of the  $^{71}\text{Ga}$  and  $^{115}\text{In}$  quadrupole coupling constants, one of which has subsequently been used for fitting the  $^{71}\text{Ga}$  line as a superposition of Lorentzians. Whereas on the basis of spin quantum numbers and quadrupole moments the ratio of the relaxation rates in the three complexes should be 1:2.4:14 ( $^{27}\text{Al}$ ,  $^{71}\text{Ga}$ ,  $^{115}\text{In}$ ), a ratio of 1:28:85 is observed. Differences in the reorientational correlation times cannot account for the discrepancies. The authors suggest that for the aluminium complex the small  $\text{Al}^{3+}$  cation forces the P-O-Al bond angle to assume a value of nearly  $180^\circ$  in order to allow for sufficient space for the six substituents. This lowers the electric field gradient at the Al nucleus. On the other hand the space requirements for coordination of the bigger  $\text{Ga}^{3+}$  and  $\text{In}^{3+}$  ions are less stringent, thus allowing a deviation of the P-O-Me bond angle from  $180^\circ$ .

Almost nothing is known about the NMR properties of the fourth element in Group III which has two magnetic isotopes,  $^{113}\text{In}$  and  $^{115}\text{In}$ , both having spin  $I = \frac{9}{2}$ . The adverse effect of the very large quadrupole moments of 1.144 and 1.161 barns respectively is somewhat

compensated for by the large spin number. A peculiarity of the two nuclei is the closeness of their magnetogyric ratios which allows simultaneous observation ( $\Delta\nu = 45$  kHz at 2.3 T). The line-widths observed by Buslaev and coworkers (150) are large for both  $\text{In}(\text{NO}_3)_3$  and  $\text{In}(\text{ClO}_4)_3$  in aqueous solution. This is explained in terms of the formation of the species  $[\text{In}(\text{NO}_3)_n(\text{H}_2\text{O})_m]^{3-n}$  and  $[\text{In}(\text{OH})_n(\text{H}_2\text{O})_m]^{3-n}$  respectively. In perchlorate solution a line-width of 2000 Hz is observed even at low pH where hydrolysis is minimal. Extremely large concentration shifts are observed for both solutions. In the concentration interval between 1.2 and 3.5 M the  $^{115}\text{In}$  shielding in aqueous perchlorate solution increases by more than 900 ppm. (150)

TABLE IX  
 $^{27}\text{Al}$  chemical shifts in selected aluminium complexes<sup>a</sup>

Species	Solvent	$\delta(^{27}\text{Al})^b$	Ref.
$\text{Al}(\text{C}_6\text{H}_5\text{CN})_6^{3+}$	$\text{C}_6\text{H}_5\text{CN}$	-46	119
$\text{Al}(\text{CH}_3\text{CN})_6^{3+}$	$\text{CH}_3\text{CN}$	-34	119
$\text{AlI}_4^-$	$\text{CH}_3\text{CN}$	-28	119
$\text{Al}(\text{OPCl}_2)_3^{3+}$	$\text{POCl}_3$	-22.4	122
$\text{Al}(\text{TMPA})_5\text{H}_2\text{O}^{3+}$	$\text{H}_2\text{O}$	-17.5	125
$\text{Al}(\text{TMPA})_4(\text{H}_2\text{O})_2^{3+}$	$\text{H}_2\text{O}$	-14	125
$\text{Al}(\text{TMPA})_3(\text{H}_2\text{O})_3^{3+}$	$\text{H}_2\text{O}$	-10	125
$\text{Al}(\text{TMPA})_2(\text{H}_2\text{O})_4^{3+}$	$\text{H}_2\text{O}$	-6.7	125
$\text{Al}(\text{TMPA})(\text{H}_2\text{O})_5^{3+}$	$\text{H}_2\text{O}$	-3.7	125
$\text{Al}(\text{H}_2\text{O})_5\text{SO}_4^+$	$\text{H}_2\text{O}$	-3.3	139
$\text{Al}(\text{H}_2\text{O})_6^{3+}$	$\text{H}_2\text{O}$	0	—
$\text{Al}(\text{acac})_3$	$\text{C}_6\text{H}_6$	0	119
$\text{Al}(\text{C}_2\text{O}_4)_3^{3-}$	$\text{H}_2\text{O}$	0	119
$\text{Al}(\text{C}_3\text{H}_7\text{OH})_6^{3+}$	$\text{C}_3\text{H}_7\text{OH}$	0	119
$\text{AlI}_3\text{Cl}^-$	$\text{CH}_2\text{Cl}_2$	+21.7	129
$\text{Al}(\text{HMPT})_4^{3+}$	HMPT	+34.1	125
$\text{AlI}_2\text{Cl}_2^-$	$\text{CH}_2\text{Cl}_2$	+59.4	129
$\text{Al}(\text{OH})_4^-$	$\text{H}_2\text{O}$ -alk.	+80	119
$\text{AlBr}_4^-$	$\text{CH}_3\text{CN}$	+80	119
$\text{AlCl}_3^-$	$\text{CH}_2\text{Cl}_2$	+86.2	129
$\text{LiAlH}_4$	$\text{Et}_2\text{O}$	+100	119
$\text{AlCl}_4^-$	$\text{CH}_3\text{CN}$	+102	119
$\text{AlCl}_3\text{NCO}^-$	$\text{CH}_3\text{CN}$	+88.7	246
$\text{AlCl}_3\text{NCS}^-$	$\text{CH}_3\text{CN}$	+89.8	246
$\text{LiAlH}_4$	$\text{Et}_2\text{O}$	+100	246
$\text{AlCl}_4^-$	$\text{CH}_3\text{CN}$	+102.8	246

<sup>a</sup> Abbreviations: TMPA = trimethyl phosphite; acac = acetylacetonate; HMPT = hexamethylphosphorotriamide.

<sup>b</sup> A positive sign indicates relative deshielding

**TABLE X**  
Ga chemical shifts in simple complexes

Compound	Solvent	$\delta\text{Ga}^a$	Ref.
$\text{GaCl}_4^-$	$\text{CH}_3\text{CN}$	+251	146
$\text{GaCl}_3\text{NCS}^-$	$\text{CH}_3\text{CN}$	+225	146
$\text{Ga}(\text{OD})_4$	$\text{D}_2\text{O}$	+220	152
$\text{GaCl}_3\text{Br}^-$	$\text{CH}_3\text{CN}$	+212	148
$\text{GaCl}_2(\text{NCS})_2^-$	$\text{CH}_3\text{CN}$	+194	146
$\text{GaCl}_2\text{Br}_2^-$	$\text{CH}_3\text{CN}$	+168	148
$\text{GaCl}(\text{NCS})_3^-$	$\text{CH}_3\text{CN}$	+157	146
$\text{GaClBr}_3^-$	$\text{CH}_3\text{CN}$	+119	148
$\text{GaI}(\text{NCS})_3^-$	$\text{CH}_3\text{CN}$	+72	146
$\text{GaBr}_4^-$	$\text{CH}_3\text{CN}$	+68	148
$\text{Ga}(\text{H}_2\text{O})_6^{3+}$	$\text{H}_2\text{O}$	0	—
$\text{Ga}(\text{DMF})_6^{3+}$	DMF	-25	152
$\text{GaI}_2(\text{NCS})_2^-$	$\text{CH}_3\text{CN}$	-50	146
$\text{Ga}(\text{CH}_3\text{CN})_6^{3+}$	$\text{CH}_3\text{CN}$	-72	128
$\text{GaI}_3(\text{NCS})_3^-$	$\text{CH}_3\text{CN}$	-234	146
$\text{GaI}_4^-$	$\text{CH}_3\text{CN}$	-500	146

<sup>a</sup> A positive sign indicates relative deshielding.

Rather little is known about the chemical nature of fused salts. Because of the high temperatures required, such studies are usually inaccessible to NMR. The exceptionally low-melting ternary system  $\text{AlCl}_3\text{--NaCl--KCl}$  has recently been investigated by combined  $^1\text{H}$ ,  $^{23}\text{Na}$ ,  $^{27}\text{Al}$ , and  $^{35}\text{Cl}$  NMR. (151) Whereas the proton and sodium line-widths show no composition dependence, both the  $^{27}\text{Al}$  and  $^{35}\text{Cl}$  line-widths depend sensitively on the relative populations. The data permit the conclusion that the  $\text{Al}_2\text{Cl}_7^-$  ion exists in rapid equilibrium with  $\text{AlCl}_4^-$ .

From the discussion in this section it is obvious that  $^{27}\text{Al}$ ,  $^{69}\text{Ga}$ , and  $^{71}\text{Ga}$  NMR can be used to investigate the solution chemistry of the two elements; however, the exact nature of many of the complexes remains to be clarified. The chemical shift data in Tables IX and X for  $^{27}\text{Al}$ ,  $^{69}\text{Ga}$ , and  $^{71}\text{Ga}$  in some selected solution complexes should therefore be used with the utmost care. It is interesting that there is only one exception each to the rule that the nucleus is less shielded in tetra- than in hexa-coordinated compounds. The exceptions are  $^{27}\text{AlI}_4^-$ , and  $^{69}\text{Ga}$  and  $^{71}\text{Ga}$  in  $\text{GaI}_4^-$ .

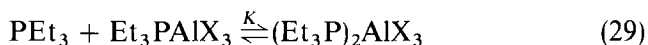
#### D. Covalent compounds

Trialkylaluminium compounds are Lewis acids and as such have a strong tendency to form adducts with donor molecules. The oligomeric nature of the parent compounds is well known. They usually occur as dimers but trimers and tetramers have also been reported. (152) Because

of the valence orbital asymmetry  $^{27}\text{Al}$  relaxation is usually enhanced to the point that line-widths of several hundred Hz result. Quadrupole coupling constants determined on the basis of line-width measurements and either the Debye equation or a microviscosity model give values of 13 and 27 MHz respectively in triethylaluminium. (153, 154) The  $^{27}\text{Al}$  resonance typically occurs at around 150 ppm to high frequency of  $^{27}\text{Al}(\text{H}_2\text{O})_6^{3+}$ .

Upon addition of a base three effects can generally be observed: (155) (a) the resonance moves to high frequency with the relative shielding following the sequence  $\text{N} > \text{O} > \text{S}$ ; (b) disruption of the dimeric structure introduces an additional field gradient which invokes line-broadening, increasing with increasing size of the donor molecule; and (c) the adduct rapidly exchanges with the substrate giving rise to a single  $^{27}\text{Al}$  line also in the case of non-stoichiometric ratios of substrate and base. Vinogradova *et al.* (156) deduced the relative stability of various adducts of triisobutylaluminium with esters and nitriles from competition experiments using the  $^{27}\text{Al}$  line-width as a parameter. Aluminium triisopropoxide, which is a tetramer, reacts with trimethylaluminium to yield mixed polynuclear compounds. (157) However, no signals other than those assignable to the centre aluminium of  $\text{Al}[\text{OCH}(\text{CH}_3)_2]_3$  and  $\text{Al}(\text{CH}_3)_3$  are observed at various molar ratios of the two constituents. Earlier, Akitt and Duncan (123) observed both types of aluminium in the former parent compound, a narrow line near the resonance of  $^{27}\text{Al}(\text{H}_2\text{O})_6^{3+}$  which is assigned to the central hexacoordinated Al and a broad line which could only be determined at elevated temperature at around 100 ppm, i.e. at the position of  $^{27}\text{Al}(\text{OH})_4^-$ . This line is assigned to the peripheral tetracoordinated aluminium atoms.

Aluminium halides which, like the alkides, are strong Lewis acids are also well known to form stable adducts with nitrogen, oxygen, and phosphorus bases.  $^{27}\text{Al}$  titration shifts lead to the remarkable conclusion that in some instances two base molecules are added, resulting in pentacoordination. (160) Stepwise formation of  $\text{R}_3\text{PAIX}_3$  and  $(\text{R}_3\text{P})_2\text{AlX}_3$  ( $\text{X} = \text{Cl}, \text{Br}$ ) occurs with small alkyl substituents ( $\text{R} = \text{CH}_3, \text{C}_2\text{H}_5$ ) but not with  $\text{R} = \text{C}_6\text{H}_5$ . Titration of  $\text{AlCl}_3$  with  $\text{PEt}_3$  for example displaces the  $^{27}\text{Al}$  resonance, reaching a maximum of 109.9 ppm at  $[\text{PEt}_3]/[\text{AlCl}_3] = 1$ , subsequently sharply falling off towards  $[\text{PEt}_3]/[\text{AlCl}_3] = 2$ , and attaining a limiting value of 55.9 ppm, all to high frequency of  $^{27}\text{Al}(\text{H}_2\text{O})_6^{3+}$ . The shielding difference of over 50 ppm clearly points to a change in hybridization. From the titration curves the equilibrium constants for the process:



can be derived: 14.5 and 41.5 in benzene, for X = Cl and Br respectively. The coupling constants  $^1J(^{27}\text{Al}-^{31}\text{P})$  which are 260 and 240 Hz in the respective mono-adducts reduce to zero upon formation of the di-adduct.

A further interesting category of aluminium compounds are the aluminium tetrahydroborates for which mixed species of the type  $\text{Al}(\text{BH}_4)_n\text{R}_{3-n}$  ( $n = 1, 2$ ; R = alkyl) have been reported. (161) While in the parent compound  $\text{Al}(\text{BH}_4)_3$  the  $^{27}\text{Al}$  resonance is found at 97 ppm (162) the mixed forms lead to resonances between this and those of the alanes. Like the parent compound the mixed species show a tendency towards adduct formation. The ether and amine adduct exhibits  $^{27}\text{Al}$  resonances in the region 100–150 ppm with excessively broad lines ( $\sim 2$  kHz). (161)

### E. Germanium-73

The only magnetic isotope of germanium is  $^{73}\text{Ge}$  which has  $I = \frac{9}{2}$  and a magnetic moment of  $-0.877 \mu_N$ . The small magnetic moment along with the low abundance of 7.6% is probably the main reason for the scarcity of high-resolution NMR data on this technologically important element. High-resolution measurements are further hampered by the sizeable quadrupole moment of  $-0.18$  barn. Kaufmann *et al.* (163) utilizing a home-built pulsed spectrometer were the first to obtain high-resolution  $^{73}\text{Ge}$  data. Table XI contains chemical shifts and spin-spin

TABLE XI  
 $^{73}\text{Ge}$  chemical shifts and spin-spin relaxation times in  
compounds  $\text{GeR}_4$  (163)

R	Solvent	$\delta$ (Ge) <sup>a</sup>	$T_2$ (ms) <sup>b</sup>
Cl	neat	0	$163 \pm 20$
Br	neat	-343	$196 \pm 30$
I	$\text{C}_6\text{H}_6$	-1139	
		-852 <sup>c</sup>	
I	$\text{CS}_2$	-1112	
		-831 <sup>c</sup>	
OMe	neat	-67	$30 \pm 3$
Me	neat	-31	$740 \pm 80$
Et	neat	-13	$140 \pm 20$
<sup>n</sup> Pr	neat	-29	$100 \pm 12$
<sup>n</sup> Bu	neat	-25	$65 \pm 7$

<sup>a</sup> The negative sign indicates relative shielding.

<sup>b</sup> Obtained from spin-echo measurements.

<sup>c</sup> Two resonances are observed.



relaxation times obtained from a variety of symmetric  $\text{GeR}_4$  compounds. Surprisingly,  $\text{GeI}_4$  affords two separate resonances. The second peak is tentatively ascribed to a species containing less iodine. This is concluded from the fact that iodine is evolved from the solution.

Kidd and Spinney (164) obtained all twelve theoretically possible mixed halides upon mixing the neat halogenogermenes  $\text{GeX}_3$  ( $\text{X} = \text{Cl}, \text{Br}, \text{I}$ ).  $^{73}\text{Ge}$  NMR in this case turned out to be a unique method for identifying and characterizing these compounds. The chemical shifts, which follow the pattern already established for  $^{27}\text{Al}$ ,  $^{69}\text{Ga}$ , and  $^{71}\text{Ga}$  in the tetrahalogeno complexes, i.e.  $\text{I} > \text{Br} > \text{Cl}$ , can be rationalized in terms of a pairwise additivity model by fitting the shifts to the following empirical equation:

$$\delta(^{73}\text{Ge}) = a + \sum_i b_i \delta_i + \sum_{ij} c_{ij} \delta_{ij} \quad (30)$$

In equation (30)  $\delta_i$  represents the direct shielding effect of halogen  $i$  ( $i = \text{Cl}, \text{Br}, \text{I}$ ),  $\delta_{ij}$  accounts for a pair interaction between halogen  $i$  and  $j$ , and  $b_i$  and  $c_{ij}$  denote the number of halogens  $i$  and the number of pair interactions  $ij$ .

Recently some Belgian workers (165) have calculated the germanium atomic charges in the pure halides using a modified CNDO/2 model and established linearity with the experimentally observed chemical shifts.

## VI. THE MAIN GROUPS V AND VI

### A. Arsenic-75, antimony-121,123, and bismuth-209

All the Group V quadrupolar nuclei ( $^{14}\text{N}$  is not considered here) have so far received only little attention. The first systematic study of  $^{75}\text{As}$  chemical shifts was reported in 1977. (166, 167)  $^{75}\text{As}$  has spin  $I = \frac{3}{2}$ , a magnetic moment of  $1.435 \mu_N$ , and a natural abundance of 100%. It can thus be considered an "easy" nucleus except for the fact that the quadrupole moment of 0.29 barn prevents non-symmetric species from being observed, notably compounds in the trivalent state. All the compounds studied (166, 167) are thus of the tetra- or hexa-coordinated pentavalent type. The total established shift range in this category of compounds is *ca.* 700 ppm, with  $^{75}\text{AsH}_4^+$  the most shielded and  $^{75}\text{AsO}_4^{3-}$  the least shielded species. A chemical shift stick diagram for a number of arsonium compounds is provided in Fig. 18. From the shieldings observed in the tetraalkylarsonium salts the  $\alpha$ ,  $\beta$ , and  $\gamma$  substituent effects can be determined:

$$\Delta\delta_\alpha = 124 \text{ ppm}; \Delta\delta_\beta = 10\text{--}11 \text{ ppm}; \Delta\delta_\gamma = -4 \text{ to } -5 \text{ ppm}$$

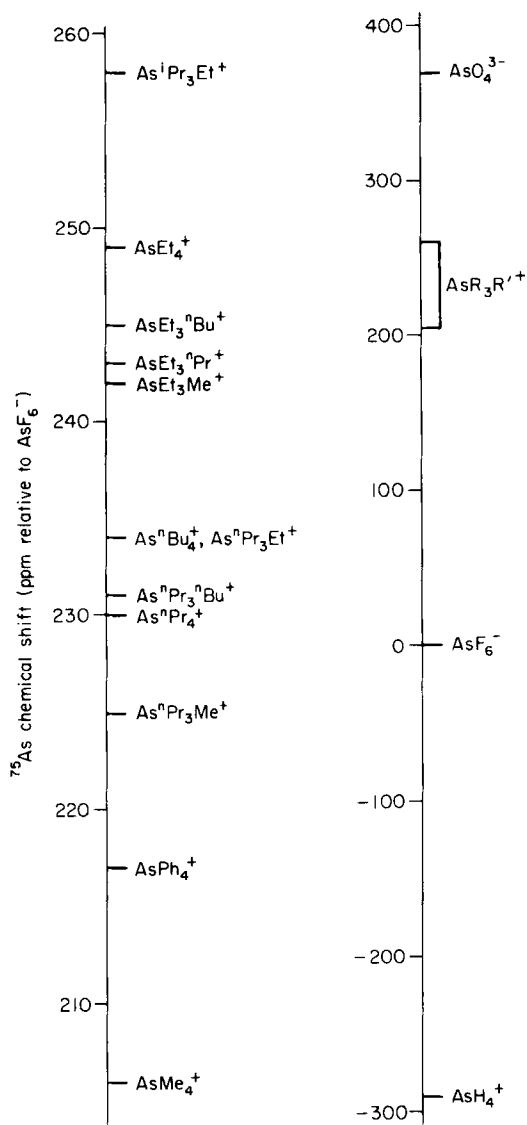


FIG. 18.  $^{75}\text{As}$  chemical shift chart: the left-hand section shows the region of alkyl and aryl arsonium salts. (166) A positive sign indicates relative deshielding.

Compared with phosphorus  $^{75}\text{As}$  substituent effects are approximately 2.5 times larger.

The only systems in which spin-spin couplings can be detected are  $(\text{AsH}_4)(\text{Ta}_2\text{F}_{11})$  [ $^1\text{J}(\text{As-H}) = 555 \text{ Hz}$ ] and  $\text{KAsF}_6$  [ $^1\text{J}(\text{As-F}) = 930 \text{ Hz}$ ]. The latter value is in agreement with earlier data determined from  $^{19}\text{F}$  spectra.

Quadrupole coupling constants were derived from the temperature dependence of the line-widths. With the aid of the Debye relationship, which should be a reasonable model for these symmetric compounds, the quadrupole coupling constant was derived from plots of the line-width against the ratio  $\eta/T$  where  $\eta$  and  $T$  represent bulk solvent viscosity and absolute temperature. Some representative values of  $e^2qQ/h$  obtained in this manner are in Table XII. The considerably larger value found for  $\text{AsPh}_4^+$  appears to reflect the increased steric strain exerted by the bulkier phenyl substituents causing more severe angular distortions from tetrahedral symmetry.

Reinarsson *et al.* (168) have investigated the feasibility of using the  $\text{AsF}_6^-$  ion for probing anion sites in proteins. Similarly to the approach chosen by Rodehüser *et al.* (146) they analysed the band shape of the  $^{19}\text{F}$  multiplet in terms of the transition probabilities for  $^{75}\text{As}$  relaxation. Outside the motional narrowing limit the transition probabilities  $P_{m,m+1}$  and  $P_{m,m+2}$  for  $^{75}\text{As}$  relaxation become unequal. The actual transition probabilities, however, dominating the line-shape, are weighted averages of those in the free and bound states, since binding usually occurs under fast exchange limit conditions. The authors have faithfully reproduced the experimental  $^{19}\text{F}$  line-shape for the binding of  $\text{AsF}_6^-$  to human serum albumin, and a mean correlation time derived in this way equals that found for chloride binding.

Both naturally occurring isotopes of antimony possess a spin angular momentum:  $^{121}\text{Sb}$  ( $I = \frac{5}{2}$ , 57.2%) and  $^{123}\text{Sb}$  ( $I = \frac{7}{2}$ , 43.8%). With magnetic moments of 3.342 and 2.533  $\mu_N$  sensitivity poses no problem. However, the magnitudes of their quadrupole moments ( $-0.53$  and  $-0.68$  barn) impair the observation of species in which the coordination symmetry around the metal atom is lower than cubic.

TABLE XII  
Quadrupole coupling constants for some simple  
arsenic salts (167)

Compound <sup>a</sup>	$e^2qQ/h$ (MHz)
KAsF <sub>6</sub>	1.6
AsMe <sub>4</sub> Br	1.1
AsEt <sub>4</sub> Br	1.1
AsPh <sub>4</sub> Cl	1.9

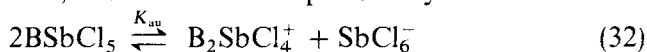
<sup>a</sup> All 0.1 M in H<sub>2</sub>O.

Kidd and Matthews (169) were the first to provide chemical shift data for a series of simple antimony compounds. The narrowest line was observed for the  $\text{SbCl}_6^-$  ion (300 Hz) and the total span of established shieldings is *ca.* 3500 ppm. Some representative chemical shifts and line-widths are in Table XIII.

Antimony pentachloride is well known to be a strong Lewis acid, therefore forming adducts with bases B which leads to species  $\text{BSbCl}_5$ . Auto-ionization may produce ion-pairs of the type  $\text{B}_2\text{SbCl}_4^+ \text{SbCl}_6^-$  in solvents of high dielectric constant.  $^{121}\text{Sb}$  NMR lends itself as a probe for distinguishing the two types of adduct. (170) While the reaction:



is usually quantitative, auto-ionization expressed by:



usually is not. The measurement of the degree of auto-ionization from monitoring the narrow resonance of the octahedral  $^{121}\text{SbCl}_6^-$  is thus straightforward. In this manner  $K_{\text{au}} = 0.023$  can be derived for the tetramethylurea– $\text{SbCl}_5$  system in methylene chloride. (170)

The last member of the quadrupolar Group V nuclei,  $^{209}\text{Bi}$ , represents another potentially useful nucleus although, surprisingly, the literature seems to be devoid of any chemical applications of its resonance.  $^{209}\text{Bi}$  is the only stable bismuth isotope. It has a spin of  $\frac{9}{2}$ , a magnetic moment of  $4.039 \mu_{\text{N}}$ , and is only six times less sensitive than the proton. Its quadrupolar moment of  $-0.38$  barn definitely confines applications to symmetric moieties.

Although solid-state work is generally omitted from this review a report by Fukushima and Mastin (171) who measured the  $^{19}\text{F}$  spectrum in polycrystalline  $\text{KBiF}_6$  is also relevant to the potential use

TABLE XIII  
 $^{121}\text{Sb}$  chemical shifts<sup>a</sup> and line-widths (169)

Compound	Solvent	$\delta(\text{Sb})$	$\Delta\nu_1$ (Hz)
$\text{Na}_3\text{SbS}_4 \cdot 9\text{H}_2\text{O}$	$\text{H}_2\text{O}$	$+1032 \pm 10$	550
$(\text{CH}_3)_4\text{SbI}$	$\text{H}_2\text{O}$	+780	
$\text{KSb}(\text{OH})_6$	$\text{H}_2\text{O}$	$+296 \pm 15$	1800
$\text{SbCl}_5$	neat	$+509 \pm 20$	8000
$\text{AgSbF}_6$	$\text{CH}_3\text{CN}$	+88	300
$(\text{C}_2\text{H}_5)_4\text{NSbCl}_6$	$\text{CH}_3\text{CN}$	0	300
$(\text{C}_2\text{H}_5)_4\text{NSbBr}_6$	$\text{CH}_3\text{CN}$	$-2436 \pm 10$	300

<sup>a</sup> A positive sign indicates relative deshielding.

of  $^{209}\text{Bi}$  in liquid-phase NMR. The spectrum affords a well separated doublet corresponding to  $^1J(^{209}\text{Bi}-^{19}\text{F}) = 2.7 \pm 0.3 \text{ kHz}$  which implies a rather small quadrupole coupling constant and probably a fairly narrow line in the  $^{209}\text{Bi}$  spectrum of dissolved  $\text{KBiF}_6$ .

### B. Sulphur-33

Apart from  $^{17}\text{O}$  which is not reviewed here,  $^{33}\text{S}$  is the only quadrupole nucleus in Group VI.  $^{33}\text{S}$  has spin  $I = \frac{3}{2}$ , a magnetic moment of only  $0.643\mu_N$ , and a natural abundance of  $0.74\%$ . These properties render  $^{33}\text{S}$  a low-sensitivity nucleus. In spite of the small quadrupole moment of  $-5.5 \times 10^{-2}$  barn, the lines are typically several hundred Hz wide in all but the most symmetric compounds with tetracoordinated hexavalent sulphur. Earlier  $^{33}\text{S}$  NMR data were obtained in the dispersion model. (171–174) A few years ago Lutz *et al.* (175) reported the first natural-abundance  $^{33}\text{S}$  FT NMR spectra along with an accurate determination of the magnetic moment relative to that of  $^{85}\text{Rb}$ . Instead of  $\text{CS}_2$ , used earlier as a chemical shift reference, (174) the sulphate ion is suggested by Lutz *et al.* (175) since it affords a particularly narrow resonance which is nearly concentration-invariant. In a more recent report some additional  $^{33}\text{S}$  data became available (176) including those for thiosulphate which provides only a single resonance  $34.5 \text{ ppm}$  to high frequency of  $^{33}\text{SO}_4^{2-}$  with a narrow line ( $\Delta\nu_{\frac{1}{2}} = 36 \text{ Hz}$ ) attributed to the coordinating rather than to the central sulphur(VI). Lutz *et al.* found support for this assignment by comparing the chemical shift measured in  $\text{S}_2\text{O}_3^{2-}$  with that in the tetrathiomolybdate ion for which  $\delta^{33}\text{S} = 33.4 \text{ ppm}$  is determined. (176) More recent experiments, however, afforded for the latter a shift of  $344 \text{ ppm}$  to high frequency from 4-molar aqueous  $\text{Cs}_2\text{SO}_4$ . (251) The similarity of both line width and shielding in  $\text{S}_2\text{O}_3^{2-}$  with that in the sulphate ion, in the reporter's view, strongly favour assignment to the central sulphur atom.

While pulsed experiments have failed to detect any  $^{33}\text{S}$  signals in other systems, dispersion-mode spectra have been obtained on a number of simple organic compounds. (174)  $^{33}\text{S}$  chemical shifts referenced to  $\text{CS}_2$  along with line-widths are in Table XIV. (174–176)

TABLE XIV

<sup>33</sup>S chemical shifts and line-widths in simple compounds

Compound	Sample state	$\delta(^{33}\text{S})^a$	$\Delta\nu_{1/2}^b$	Ref.
Na <sub>2</sub> S	H <sub>2</sub> O	-592	0.5	174
S <sub>2</sub> (C <sub>2</sub> H <sub>5</sub> ) <sub>2</sub>	neat	-499	1.6	174
Tetrahydrothiophen	neat	-420	0.8	174
CS <sub>2</sub>	neat	-331	0.05	174
3-Bromothiophen	neat	-197	0.5	174
2-Methylthiophen	neat	-153	0.4	174
3-Methylthiophen	neat	-134	0.5	174
Thiophen	neat	-111	0.19	174
H <sub>2</sub> SO <sub>4</sub> (conc.)	--	-106	0.7	174
Dimethyl sulphoxide	neat	-98	0.8	174
H <sub>2</sub> SO <sub>4</sub>	10 M/H <sub>2</sub> O	-17	500	176
H <sub>2</sub> SO <sub>4</sub>	4 M/H <sub>2</sub> O	-8	340	176
Rb <sub>2</sub> SO <sub>4</sub>	0.5, 1.5 M/D <sub>2</sub> O	0	70	176
Cs <sub>2</sub> SO <sub>4</sub>	0.5, 1.5 M/D <sub>2</sub> O	0	70	176
CdSO <sub>4</sub>	2.2 M/D <sub>2</sub> O	0	130	176
(NH <sub>4</sub> ) <sub>2</sub> S <sub>2</sub> O <sub>3</sub> <sup>c</sup>	4 M/H <sub>2</sub> O	+34.5	36	176

<sup>a</sup> A positive sign indicates relative deshielding.<sup>b</sup> In mT from ref. 174; in Hz from ref. 176.<sup>c</sup> Only one resonance observed.

## VII. THE TRANSITION METALS

Transition elements are strictly defined as those having partly filled d or f shells. For practical purposes the range is widened in this review to include the Group IIB elements (zinc, cadmium, mercury) in spite of their possessing a d<sup>10</sup> shell in all their oxidation states.

The often paramagnetic nature of many transition metal compounds imposes a severe limitation on the applicability of NMR. Typical representatives of paramagnetic oxidation states are V(III, IV), Cr(III), Mn(II), Cr(III), and Co(II). By contrast d<sup>0</sup>, f<sup>0</sup>, d<sup>10</sup>, and f<sup>14</sup> states of course give rise to diamagnetism, but also many other oxidation states with even numbers of d or f electrons may, but need not, result in diamagnetic compounds. By contrast the lanthanides generally afford paramagnetic compounds, notable exceptions being La(III) and Lu(III). NMR is thus practically confined to elements 21 (Sc) to 30 (Zn), 39(Y) to 48(Cd), 72(Hf) to 80(Hg), and 57(La).

It is interesting that among the 29 naturally occurring elements belonging to this category 20 have only isotopes with  $I > \frac{1}{2}$  (besides of

TABLE XV  
Physical properties of some transition element nuclei

Nucleus	Spin	Abund. (%)	Mag. moment ( $\mu_N$ )	$Q$ (barns)
$^{45}\text{Sc}$	$\frac{7}{2}$	100	4.7492	-0.22
$^{138}\text{La}$	5	0.089	3.684	0.51
$^{139}\text{La}$	$\frac{7}{2}$	99.9	2.7614	0.22
$^{47}\text{Ti}$	$\frac{5}{2}$	7.3	-0.78710	$\pm 0.02$
$^{49}\text{Ti}$	$\frac{7}{2}$	5.5	-1.1022	0.29
$^{51}\text{V}$	$\frac{7}{2}$	99.8	5.1392	-0.05
$^{93}\text{Nb}$	$\frac{9}{2}$	100	6.144	-0.22
$^{53}\text{Cr}$	$\frac{3}{2}$	9.6	-0.47354	0.03
$^{95}\text{Mo}$	$\frac{5}{2}$	15.7	-0.9099	-0.015
$^{97}\text{Mo}$	$\frac{5}{2}$	9.5	-0.9289	0.17
$^{55}\text{Mn}$	$\frac{5}{2}$	100	3.4610	0.4
$^{185}\text{Re}$	$\frac{5}{2}$	37.1	3.1437	2.3
$^{187}\text{Re}$	$\frac{5}{2}$	62.9	3.1760	2.2
$^{59}\text{Co}$	$\frac{7}{2}$	100	4.6163	0.38
$^{63}\text{Cu}$	$\frac{3}{2}$	69.1	2.2206	-0.211
$^{65}\text{Cu}$	$\frac{3}{2}$	30.9	2.3789	-0.195
$^{67}\text{Zn}$	$\frac{5}{2}$	4.1	0.8733	0.16

course those that are magnetically inactive) whereas only 6 possess  $I = \frac{1}{2}$ . Two of the transition elements have one representative of either type (Os and Hg).

Table XV lists the physical properties of those nuclei that have been studied in the liquid phase beyond simply a report of their magnetic moments.

### A. Group IIIb

Scandium is a congener of aluminium and is trivalent in all its chemistry. The only stable isotope,  $^{45}\text{Sc}$ , has a sizeable magnetic moment and is therefore a very sensitive NMR nucleus. Lutz (178) determined the magnetic moment with high accuracy and referred it to that of the deuteron. In the same paper an isotope shift of  $-6.2$  ppm is reported for the  $^{45}\text{Sc}$  resonance of aqueous  $\text{ScCl}_3$  in light and heavy water.

Pfadenhauer and McCain (179) and Tarasov and Buslaev (180) studied the hexafluoroscandate ion in terms of two dynamic processes affecting the line-shape of the  $^{19}\text{F}$  resonance, namely chemical exchange involving fluoride ions on the one hand and  $^{45}\text{Sc}$  relaxation on the other hand. The latter two authors tackled the problem by solving the Kubo-Sack master equation for chemical exchange using

the known scalar coupling constant  $^1J(^{45}\text{Sc}-^{19}\text{F}) = 180 \text{ Hz}$ . This yields, in terms of Aksnes formalism [ref. 6 of (180)], the  $\alpha$  parameter which is defined as:

$$\alpha \equiv \tau_c \overline{\text{QCC}} / 2\pi J \quad (33)$$

in which  $\tau_c$  represents the reorientational correlation time, and  $\overline{\text{QCC}}$  and  $J$  are the averaged quadrupole coupling constant and scalar coupling constant. Combined with viscosity data this affords an estimate for the quadrupole coupling constant of 9.5 MHz in  $^{45}\text{ScF}_6^{3-}$ .

Buslaev *et al.* (181) have studied the  $^{45}\text{Sc}$  resonance of a variety of salts in aqueous and non-aqueous media. The range of chemical shifts established by these experiments is 126 ppm. Since the experimental conditions in ref. 181 are not well defined no shielding data are reproduced here as these turn out to be sensitive to concentration. (182) Nelson *et al.* (182) showed that  $^{45}\text{Sc}$  shieldings and line-widths are suited for monitoring the complex formation of cationic scandium, and have reported the concentration dependence of both the chemical shift and the line-width of the  $^{45}\text{Sc}$  resonance for  $\text{ScCl}_3$ ,  $\text{ScBr}_3$ ,  $\text{Sc}(\text{ClO}_4)_3$ ,  $\text{Sc}(\text{NO}_3)_3$ ,  $\text{Sc}_2(\text{SO}_4)_3$ , and  $\text{ScI}_3$  in aqueous solution and partly also in tetrahydrofuran. Although the observed effects cannot be quantified, they provide qualitative evidence for complexation confirming some earlier results. The  $^{45}\text{Sc}$  data are consistent with the formation of species of the type  $\text{ScX}^{2+}$  and  $\text{ScX}_2^+$  ( $\text{X} = \text{Cl}, \text{Br}$ ). Quantification of the effects is complicated by the scandium ion's extreme tendency towards hydrolysis. It can be assumed that the unhydrolysed ion  $\text{Sc}(\text{H}_2\text{O})_6^{3+}$  exists only at very low pH. It was earlier suggested [ref. 31 of (182)] that upon addition of hydrochloric acid to an aqueous solution of  $\text{ScCl}_3$  stepwise chloride complexation takes place, leading ultimately to  $\text{ScCl}_4^-$ . The plot of  $\delta(^{45}\text{Sc})$  and  $^{45}\text{Sc}$  line-width as a function of added HCl furnishes corroborative evidence for such a process (Fig. 19). From this it is seen that both chemical shift and line-width essentially follow the same general trend except at low HCl concentration. The transition to the symmetric  $\text{ScCl}_4^-$  complex between  $[\text{HCl}]/[\text{ScCl}_3] = 8$  and 12 should actually result in a decrease in line-width. That this does not occur could be due to rapid exchange involving a less symmetric species. Moreover it should be noted that no viscosity corrections are made. The shift to high frequency (144 ppm at  $[\text{HCl}]/[\text{Sc}^{3+}] = 12$ ) is a further indication that tetracoordination is taking place.

Large high frequency shifts are observed for  $\text{ScCl}_3$  and  $\text{ScBr}_3$  in tetrahydrofuran (202 and 273 ppm at 0.02 and 0.007 M scandium concentration) whereas for  $\text{Sc}(\text{NO}_3)_3$  and  $\text{Sc}(\text{ClO}_4)_3$  the observed shifts are an order of magnitude smaller. This behaviour is interpreted in



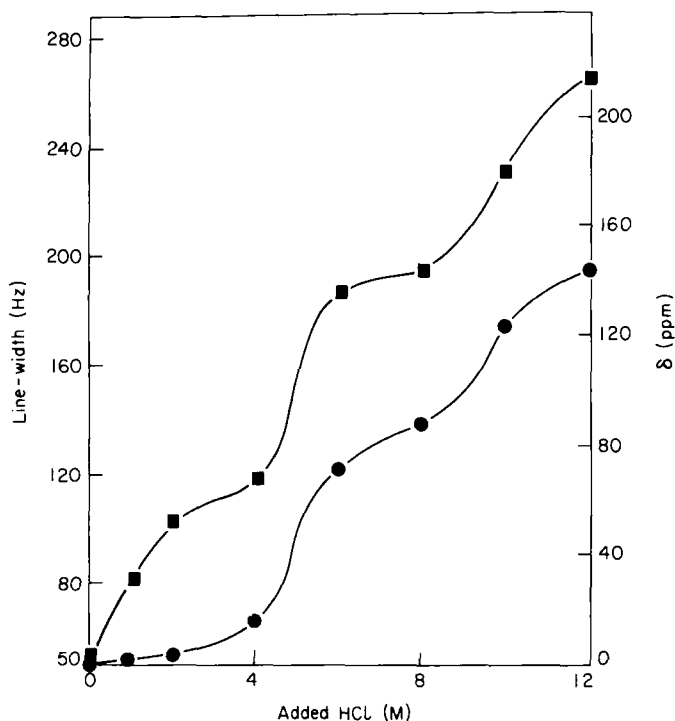


FIG. 19.  $^{45}\text{Sc}$  chemical shifts and line-widths measured at 55.1 MHz in an aqueous solution of  $\text{ScCl}_3$  as a function of added hydrochloric acid. (182)

terms of the formation of contact ion-pairs for the former two compounds.

The NMR of  $^{139}\text{La}$  has recently aroused the interest of biophysicists in view of the specific binding abilities of  $\text{La}^{3+}$  to certain proteins and nucleic acids.  $^{139}\text{La}$  is in fact a rather favourable magnetic resonance nucleus, comparable in receptivity to  $^{31}\text{P}$ .

An accurate determination of the magnetic moment of  $^{139}\text{La}$  and also of the minor isotope  $^{138}\text{La}$  has only very recently (100) been reported, along with the ratio of the quadrupole moments for which  $Q(^{138}\text{La})/Q(^{139}\text{La}) = 2.15$  is calculated from the respective line-widths, assuming quadrupolar relaxation for either isotope. The latter is confirmed on the basis of the relative line-widths in  $\text{H}_2\text{O}$  and  $\text{D}_2\text{O}$ . In a 0.6 M solution of  $\text{LaCl}_3$  in  $\text{H}_2\text{O}$ ,  $\Delta\nu_{\frac{1}{2}}(^{139}\text{La}) = 157 \text{ Hz}$  or  $T_2 = 2.03 \text{ ms}$ , somewhat less than what Reuben (183) reported from pulsed studies (2.73 ms for  $\text{LaCl}_3$ , 0.18 M in  $\text{H}_2\text{O}$ ,  $23^\circ\text{C}$ ).

The potential of field-dependent  $^{139}\text{La}^{3+}$  relaxation experiments for probing binding to macromolecules has recently been outlined (183, 184) and the theory developed for quadrupole relaxation of an  $I = \frac{7}{2}$  spin outside the white spectrum limit. Under slow motion conditions relaxation of a quadrupolar nucleus is well known to be field-dependent with non-exponential magnetization recovery (cf. Ch. 7 of ref. 1). An interesting result of the Reuben and Luz calculations is the near-exponentiality of signal recovery, which makes it appear appropriate to treat relaxation by an averaged relaxation rate  $\langle 1/T_1 \rangle$  for which the following explicit expression can be derived: (184)

$$\langle 1/T_1 \rangle = \frac{C\tau_c}{1 + B(\omega_0\tau_c)^2} \quad (34)$$

with  $B = 2.67$ , valid over the region  $0.1 < \omega_0\tau_c < 2$ , and  $C$  containing the quadrupole coupling constant and asymmetry parameters, i.e.

$$C = \frac{1}{98} \left( \frac{e^2qQ}{\hbar} \right)^2 \left( 1 + \frac{\eta^2}{3} \right) \quad (35)$$

It is readily seen that in the motional narrowing limit equation (34) assumes the familiar form for quadrupole relaxation in that the frequency-dependent term vanishes.

Addition of bovine serum albumin (BSA) to a solution of  $\text{LaCl}_3$  results in a linear increase of the relaxation rate, the slope of the thus obtained straight lines being frequency-dependent. This is illustrated in Fig. 20 where the excess relaxation rate,  $1/T_{1p} = 1/T_1 - 1/T_1^0$ , is plotted against BSA concentration. For the former quantity

$$1/T_{1p} = p_b/T_{1b} \quad (36)$$

holds, with  $p_b$  and  $T_{1b}$  representing the population of bound lanthanum and the relaxation time in the bound state. Combining equations (34) and (36) yields:

$$T_{1p} = \frac{2.67\omega_0^2\tau_cp_b}{C} + \frac{p_b}{C\tau_c} \quad (37)$$

i.e. a plot of  $T_{1p}$  vs.  $\omega_0^2$  should be linear and should afford  $\tau_c$  from its slope and intercept. In this way  $\tau_c = 3.7 \times 10^{-8}$  s can be calculated in good agreement with values obtained from other sources.

The quadrupole coupling constant for  $^{139}\text{La}^{3+}$  bound to a single acetate moiety as well as the dissociation constant  $K_D$  can be derived from the concentration dependence of the excess relaxation rate,  $1/T_{1p}$ , when plotted against  $[\text{La}^{3+}]/[\text{CH}_3\text{CO}_2^-]$ . The values obtained are  $K_D = 14$  mM and  $e^2qQ/\hbar = 7.5$  MHz. (184)

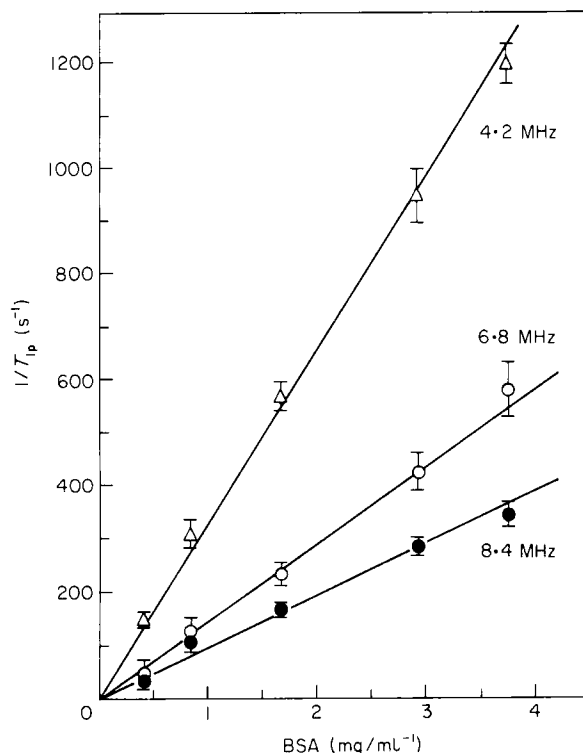


FIG. 20. Excess longitudinal relaxation rate,  $1/T_{1p}$ , for  $^{139}\text{La}$  in 0.4M aqueous solutions of  $\text{LaCl}_3$  as a function of added bovine serum albumin (BSA) at three different field strengths. (184)

The Reuben and Luz treatment was recently applied to the study of cation binding to prothrombin. (185) Instead of  $T_1$  experiments the  $^{139}\text{La}^{3+}$  line-width is monitored as a function of added prothrombin or of fragment - 1. In either case  $\Delta\nu_{\frac{1}{2}}$  increases linearly with increasing protein concentration. From plots of the  $^{139}\text{La}^{3+}$  line-width *vs.*  $[\text{La}_{\text{tot}}^{3+}]$  at fixed protein concentration, the apparent dissociation constant is evaluated as  $K_D = 8.9 \text{ mM}$ . This again permits calculation of the line-width in the bound state using the earlier determined quadrupole coupling constant of 7.5 MHz by inserting this value into the simple equation for quadrupole relaxation in the motional narrowing limit. For fragment - 1 this gives  $1.3 \times 10^{-8} \text{ s}$ .

## B. Group IVB

Titanium has two magnetic isotopes,  $^{47}\text{Ti}$  ( $I = \frac{5}{2}, 7.3\%$ ) and  $^{49}\text{Ti}$  ( $I = \frac{7}{2}, 5.5\%$ ). Their weak magnetic moments of  $-0.787$  and

$-1.103 \mu_N$  severely hamper observation of these nuclei. A peculiar feature of the two nuclei is the similarity of their resonance frequencies which differ by only 271 ppm. (186) The only chemically significant Ti NMR data are those by Kidd *et al.* (186) in which the tetrahalides were studied. While the analogous compounds for aluminium, gallium, and germanium all exhibit the same trends in their chemical shifts (shielding sequence:  $I > Br > Cl$ ), the titanium shieldings in the tetrahalides reveal contrasting behaviour. A further distinguishing feature concerns the kinetic lability of the mixed species. In mixtures of  $TiCl_4$  and  $TiBr_4$  only a single line is found with its frequency varying linearly with mole fraction. Most surprisingly the titanium resonances in  $TiBr_4$  are located at 498 ppm to high frequency of  $TiCl_4$  whereas no signal at all is detected for  $TiI_4$ . Although  $TiCl_4$  and  $TiI_4$  are only partly miscible, a displacement of the line towards higher frequencies is found in a  $TiCl_4$ - $TiI_4$  mixture, which permits the conclusion that the shielding sequence is in fact  $Br, I < Cl$  ( $TiI_4$  is insoluble in  $TiBr_4$  so the relative shieldings in these compound mixtures cannot be verified). This anomalous behaviour can be explained with the aid of the longest wavelength electronic transitions which are  $34\,840\text{ cm}^{-1}$  ( $TiCl_4$ ),  $28\,680\text{ cm}^{-1}$  ( $TiBr_4$ ), and  $19\,400\text{ cm}^{-1}$  ( $TiI_4$ ). Although this sequence is the same for the main-group metal halides the transition energies are at least  $10\,000\text{ cm}^{-1}$  higher and the dominating effect in the paramagnetic shielding term of the main-group metal halides is  $\langle r^{-3} \rangle$ . The latter decreases in the order  $Cl > Br > I$ . (It is to be noted that the sign of the paramagnetic shielding term,  $\sigma_p$ , is negative.)

From the fact that the chemical shift in  $TiCl_4$  and  $TiBr_4$  is concentration-invariant it is inferred that the two halides exist as monomers in the neat liquid. This is also confirmed by the line-widths which vary only insignificantly.

### C. Group VB

NMR studies of the Group VB nuclei are particularly plentiful. Both  $^{51}V$  and  $^{93}Nb$  are sensitive nuclei exhibiting large chemical shift ranges.

Vanadium has two magnetic isotopes,  $^{51}V$  (99.75%,  $I = \frac{7}{2}$ ) and  $^{50}V$  (0.25%,  $I = 6$ ). Because of its much larger abundance all liquid-phase NMR studies have been devoted to  $^{51}V$ . With its strong magnetic moment and almost 100% natural abundance,  $^{51}V$  is only a factor of 2.5 less sensitive than the proton. The experiment is further favoured by the very weak quadrupole moment of  $7.3 \times 10^{-3}$  barn which, together with a large shielding range, makes  $^{51}V$  a unique metal NMR nucleus

in that it allows the experimentalist to study virtually any compound irrespective of the electronic symmetry around the nucleus, still giving rise to reasonably narrow lines. These favourable properties probably explain why  $^{51}\text{V}$  NMR has been in use for almost 15 years. Howarth and Richards (187) proved  $^{51}\text{V}$  NMR to be an excellent tool for the characterization of the pH-dependent species that occur in aqueous solutions of vanadate ions. More recently  $^{51}\text{V}$  chemical shifts have been systematically studied in a host of derivatives of  $\text{VO}^{3+}$ , (188, 189) iso- and hetero-polyanions of  $\text{V}(\text{v})$ , (190, 191) and for a family of vanadium-(+1) and  $-(-1)$  carbonyl complexes. (192–194) The established range of  $^{51}\text{V}$  shieldings is *ca.* 2500 ppm with external  $\text{VOCl}_3$  appearing to be the generally accepted reference compound. A chemical shift correlation chart for some representative compounds is provided in Fig. 21.

The relative shieldings in the simple oxohalides  $\text{VOX}_3$  ( $\text{X} = \text{F}, \text{Cl}, \text{Br}$ ) reflect variations of the paramagnetic shielding constant. As for the titanium halides, shielding increases with increasing electronegativity of the halogen substituent. This is rationalized on the basis of the energy separation between the highest occupied and lowest unoccupied molecular orbitals relevant for electronic transitions. The shifts of the simple halides turn out to be solvent-dependent. This effect is particularly striking for  $\text{VOBr}_3$  where a low frequency displacement of 680 ppm occurs upon dissolution in THF! The suggestion was made (189) that the weak  $\text{V}-\text{Br}$  bond is disrupted and species that are coordinated directly to the solvent molecules are formed. In the case of  $\text{VOCl}_3$  the spectrum in THF affords a second resonance which, it is suggested, arises from a moiety of the type  $\text{VOCl}_n(\text{THF})_m\text{Cl}_{3-n}$  being in equilibrium with a solvated species  $\text{VOCl}_{3-n}\text{THF}_m$ . The same shielding trend with substituent electronegativity is observed when oxygen and nitrogen substituents are compared. The shielding order established is  $\text{Br} \ll \text{Cl} < \text{N} < \text{O} < \text{F}$ .

From the relative line-widths observed in vanadyl complexes such as  $\text{VO}_2(\text{O}_4\text{C}_2)_2^{3-}$ ,  $\text{VO}_2(\text{edta})^{3-}$ , etc. it is inferred that these possess a *cis*-dioxo structure since their line-widths are considerably larger than those in the pseudo-tetrahedral ions  $\text{VCl}_2\text{O}_2^-$ ,  $\text{VF}_2\text{O}_2^-$ , or metavanadate. (191) Support for this view is provided by the very different chemical shifts observed in the two groups of compounds, the hexacoordinated species exhibiting generally higher shieldings.

Vanadium- $(-1)$  and  $-(+1)$  carbonyl complexes whose  $^{51}\text{V}$  NMR data have recently been published (194) display interesting shielding trends which suggest  $^{51}\text{V}$  NMR to be diagnostically useful for the characterization of these compounds. For example in systems of the

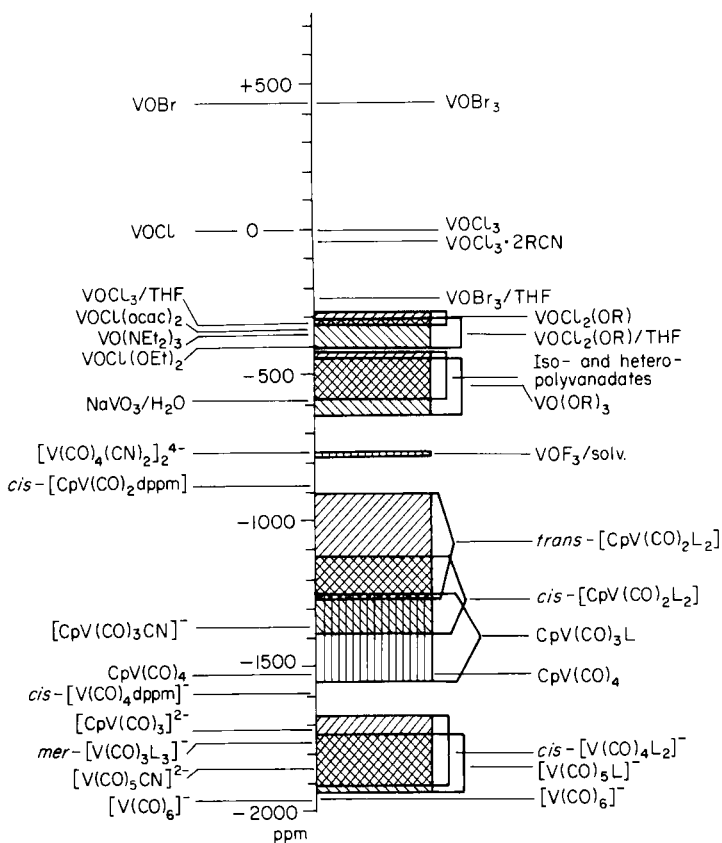


FIG. 21.  $^{51}\text{V}$  chemical shift chart for diamagnetic  $\text{V}(-\text{I})$ ,  $\text{V}(0)$ ,  $\text{V}(+\text{I})$ , and  $\text{V}(+\text{V})$  compounds relative to external  $\text{VOCl}_3$ , positive values indicating relative deshielding. Abbreviations: Cp = cyclopentadienyl, L = Group V donor ligand. (189)

type  $\text{CpV}(\text{CO})_n(\text{PR}_3)_{5-n}$  (Cp = cyclopentadienyl;  $n = 2, 3$ )  $^{51}\text{V}$  is more heavily shielded in compounds with  $n = 2$ . For those with  $n = 2$  that allow for *cis-trans* isomerism,  $^{51}\text{V}$  seems to be generally less shielded in the *trans* isomer.

Scalar coupling between  $^{51}\text{V}$  and  $^{31}\text{P}$  has been reported for phosphine and trialkyl phosphite coordinated vanadium carbonyl complexes.  $(194) \ ^1J(^{51}\text{V}-^{31}\text{P})$  typically ranges from 150 to 350 Hz. No stereochemical specificity was found, however.

A problem that has recently aroused considerable interest concerns the site of protonation in complex transition metal oxyanions. Klemperer and coworkers have employed  $^{17}\text{O}$  NMR for studying the

problem in  $V_{10}O_{28}^{6-}$  (195) and more recently in the mixed-metal polyoxovanadate  $cis-V_2W_4O_{19}^{4-}$ . (196) High-resolution  $^{51}V$  NMR confirms the existence of three non-equivalent vanadium sites with a population ratio of 4:4:2 in solution. (197) From the stereostructure of  $V_{10}O_{28}^{6-}$  (Fig. 22) it is recognized that the ion possesses eight apical sites which are generally believed to be the sites for protonation. In an attempt to shed some light on this complex problem  $^{51}V$  chemical shift titrations were carried out for the three distinguishable resonances (198) as illustrated in Fig. 23. Only two of the peaks exhibit appreciable pH dependence [V(1) and V(2) in Fig. 22]. This is taken as supporting evidence for protonation at the apical oxygens. If it occurred at the bridging oxygens, it is argued that it should also affect the shielding of V(3). The observed low frequency shift upon protonation is explained as arising from an increase in the ligand-to-metal charge transfer which lowers the magnitude of the paramagnetic shielding contribution. The individual  $pK_a$  values for mono- and di-protonation at the eight apical sites were determined on the basis of an analysis of the protonation curves in Fig. 23. By contrast Klemperer and Shum (195) have concluded from the shielding behaviour of  $^{17}O$  that the preferred sites of protonation are the bridging oxygens b rather than the apical oxygens f and g. Experimentally they find that oxygens b and, to a lesser extent, c shift to low frequency between pH 6 and 4.5. Since protonation

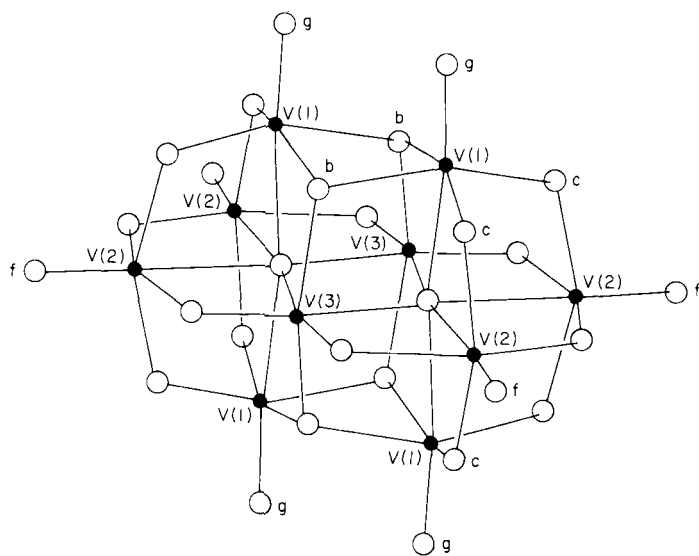


FIG. 22. Crystal structure of  $V_{10}O_{28}^{6-}$ .

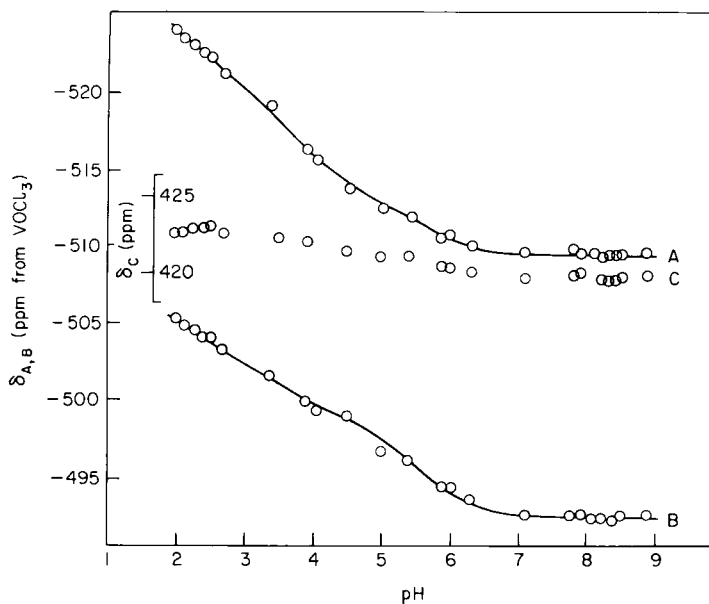


FIG. 23. pH dependence of  $^{51}\text{V}$  shieldings in aqueous  $\text{V}_{10}\text{O}_{28}^{6-}$ . Shifts designated A, B, and C correspond to the three non-equivalent vanadium sites. Chemical shifts are relative to  $\text{VOCl}_3$  with the minus sign indicating relative shielding. (198)

weakens a V–O bond this should effect a low frequency shift. It is further argued that the greater covalency of the apical oxygens (which is also rejected by the  $^{17}\text{O}$  shifts and V–O bond lengths) makes these less basic and hence less likely for protonation. Further experiments are probably necessary to settle this controversy.

The second Group VB transition metal nucleus,  $^{93}\text{Nb}$ , has also been fairly extensively studied.  $^{93}\text{Nb}$  has spin  $I = \frac{9}{2}$  (100%), a magnetic moment of  $6.144 \mu_N$ , and a quadrupolar moment of  $-0.22$  barn.

The first high-resolution  $^{93}\text{Nb}$  spectrum was reported for the hexafluoronioabate ion in 1963. (199)  $^{93}\text{Nb}$  NMR studies were performed on the mixed hexahalogenoniobates, (200–202) on solvent adducts of pentahalogenoniobium, (200, 201) and on niobium oxide halides and related species. (203, 204) A compilation of the few chemical shifts reported is in Table XVI. A comparison of the relative shieldings in the  $\text{NbX}_6^-$  ion ( $\text{X} = \text{F}, \text{Cl}, \text{Br}$ ) indicates the same trend as for the  $^{49}\text{Ti}$  and  $^{51}\text{V}$  shieldings in the respective  $\text{TiX}_4$  and  $\text{VOX}_3$  compounds, in that the shielding decreases with decreasing electronegativity of the halogen substituents as opposed to the behaviour found for the halides of main-group elements (see below).



TABLE XVI

<sup>93</sup>Nb chemical shifts<sup>a</sup> for some representative niobium compounds

Compound	Solvent/Conditions	$\delta(^{93}\text{Nb})$	Ref.
NbF <sub>6</sub> <sup>-</sup>	NbCl <sub>5</sub> :HF = 1:5	-1620 <sup>b</sup>	207
NbF <sub>5</sub> /HF	—	-1560	207
NbF <sub>5</sub> Cl <sup>-</sup>	NbCl <sub>5</sub> :HF = 1:5/CH <sub>3</sub> CN	-1270	247
[NbOF <sub>4</sub> ·H <sub>2</sub> O] <sup>-</sup>	(NH <sub>4</sub> ) <sub>3</sub> Nb <sub>2</sub> O <sub>2</sub> F <sub>9</sub>	-1270 <sup>c</sup>	206
NbF <sub>5</sub> Br <sup>-</sup>	NbX <sub>5</sub> :HF = 1:5/CH <sub>3</sub> CN	-1230	247
NbF <sub>4</sub> Cl <sub>2</sub> <sup>-</sup>	NbX <sub>5</sub> :HF = 1:5/CH <sub>3</sub> CN	-1080	247
NbF <sub>3</sub> Cl <sub>3</sub> <sup>d</sup>	NbX <sub>5</sub> :HF = 1:5/CH <sub>3</sub> CN	-780	247
NbF <sub>4</sub> Br <sub>2</sub> <sup>-</sup>	NbX <sub>5</sub> :HF = 1:5/CH <sub>3</sub> CN	-755	247
NbF <sub>3</sub> Cl <sub>4</sub> <sup>-</sup>	NbX <sub>5</sub> :HF = 1:5/CH <sub>3</sub> CN	-530	247
NbCl <sub>4</sub> (CH <sub>3</sub> CN) <sub>2</sub> <sup>+</sup>	NbX <sub>5</sub> /CH <sub>3</sub> CN	-500	247
NbF <sub>3</sub> Br <sub>3</sub> <sup>-</sup>	NbX <sub>5</sub> :HF = 1:5/CH <sub>3</sub> CN	-405	247
NbBr <sub>4</sub> (CH <sub>3</sub> CN) <sub>2</sub> <sup>+</sup>	NbX <sub>5</sub> /CH <sub>3</sub> CN	-350	247
NbFCl <sub>5</sub> <sup>-</sup>	NbX <sub>5</sub> :HF = 1:5/CH <sub>3</sub> CN	-250	247
NbCl <sub>6</sub> <sup>-</sup>	CH <sub>3</sub> CN	0	202
NbF <sub>2</sub> Br <sub>4</sub> <sup>-</sup>	NbX <sub>5</sub> :HF = 1:5/CH <sub>3</sub> CN	+5	247
NbCl <sub>5</sub> ·CH <sub>3</sub> CN	CH <sub>3</sub> CN	+49	204
NbCl <sub>5</sub> Br <sup>-</sup>	CH <sub>3</sub> CN	+126	202
<i>trans</i> -NbCl <sub>4</sub> Br <sub>2</sub> <sup>-</sup>	CH <sub>3</sub> CN	+246	202
<i>cis</i> -NbCl <sub>4</sub> Br <sub>2</sub> <sup>-</sup>	CH <sub>3</sub> CN	+253	202
<i>trans</i> -NbCl <sub>3</sub> Br <sub>3</sub> <sup>-</sup>	CH <sub>3</sub> CN	+371	202
NbFBr <sub>5</sub> <sup>-</sup>	NbX <sub>5</sub> :HF = 1:5/CH <sub>3</sub> CN	+375	247
<i>cis</i> -NbCl <sub>3</sub> Br <sub>3</sub> <sup>-</sup>	CH <sub>3</sub> CN	+378	202
<i>trans</i> -NbCl <sub>2</sub> Br <sub>4</sub> <sup>-</sup>	CH <sub>3</sub> CN	+492	202
<i>cis</i> -NbCl <sub>2</sub> Br <sub>4</sub> <sup>-</sup>	CH <sub>3</sub> CN	+497	202
NbClBr <sub>5</sub> <sup>-</sup>	CH <sub>3</sub> CN	+616	202
NbBr <sub>5</sub> CH <sub>3</sub> CN	NbX <sub>5</sub> /CH <sub>3</sub> CN	+633	247
NbBr <sub>6</sub> <sup>-</sup>	CH <sub>3</sub> CN	+735	202

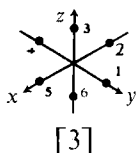
<sup>a</sup> A positive sign indicates relative deshielding.<sup>b</sup> <sup>1</sup>J(<sup>93</sup>Nb-<sup>19</sup>F) = 334 Hz.<sup>c</sup> <sup>1</sup>J(<sup>93</sup>Nb-<sup>19</sup>F) = 410 Hz.<sup>d</sup> <sup>1</sup>J(<sup>93</sup>Nb-<sup>19</sup>F) = 281 Hz; quartet observed at -10°C assigned to *cis* isomer.

Kidd and Spinney (201) ascribed the fact that only seven chemically shifted <sup>93</sup>Nb resonances are detected for the [NbCl<sub>n</sub>Br<sub>6-n</sub>]<sup>-</sup> system to the non-statistical formation of the mixed halogenoniobates by concluding that only the *cis* isomer is formed for those constituents where geometric isomerism is conceivable. This view has recently been challenged (202) and definitive proof is given for the statistical coexistence of all ten possible isomers. The failure to observe the remaining isomers is definitely due to instrumental limitations, i.e. the

limited resolution achievable in the dispersion mode and the low field strength at which the spectra were recorded. Tarasov *et al.* (202) very recently succeeded in detecting and assigning all ten resonances. An unequivocal designation is obtained by calculating the relative linewidths with the aid of a point charge model. (205) The basic idea behind this is to express the e.f.g. tensor invariant in terms of independent components. Since the method is generally practicable for the prediction of quadrupole relaxation of the central nucleus in simple molecular ions it is outlined here in some detail. According to Valiev and Zaripov (205) the e.f.g. tensor invariant,  $g_\phi^2$ , is related to the independent components  $\phi_{ij}$  of the e.f.g. tensor through the equation:

$$g_\phi^2 = \frac{1}{2}\{(\phi_{xx} - \phi_{yy})^2 + (\phi_{yy} - \phi_{zz})^2 + (\phi_{zz} - \phi_{xx})^2 + 6(\phi_{xy}^2 + \phi_{yz}^2 + \phi_{zx}^2)\} \quad (38)$$

In the case of the hexahalogenoniobate ions the negative charges represented by the halide ions lie on the axes of a Cartesian coordinate system [3]. The ligand coordinates may then be defined in the



following way:  $\vec{R}_1(0, R_1, 0)$ ,  $\vec{R}_2(-R_2, 0, 0)$ ,  $\vec{R}_3(0, 0, R_3)$ , etc. and independent components are calculated on this basis from the equation:

$$\phi_{ij}^{(n)} = e_n R_n^{-5} (3R_i^{(n)} R_j^{(n)} - R_n^2 \delta_{ij}) \quad (39)$$

where  $n$  represents the  $n$ th ligand atom and  $\delta_{ij} = 0$  or  $1$  depending on whether  $i \neq j$  or  $i = j$ .

Table XVII lists the e.f.g. tensor invariant  $g_\phi^2$  calculated on the basis of equations (38) and (39) and of the interatomic distances  $a (=r_{\text{Nb}-\text{Cl}})$  and  $b (=r_{\text{Nb}-\text{Br}})$  and the  $\text{Cl}^-$  and  $\text{Br}^-$  charges,  $e_1$  and  $e_2$ . Since the transverse relaxation rates are proportional to both  $g_\phi^2$  and the correlation time  $\tau_c$ , and since this latter is proportional to the molecular volume, numerical values are given for the product  $g_\phi^2 \cdot r^3$ . From Table XVII it is seen that excellent agreement is obtained between the experimentally observed relaxation rate  $R_1^Q$  and  $g_\phi^2 \cdot r^3$  (both normalized).

The 24.5 MHz  $^{93}\text{Nb}$  NMR spectrum in Fig. 24 reveals peak asymmetry which is due to partly overlapping signals of very different

TABLE XVII

Invariants of the e.f.g. tensor  $g_\phi^2$ , normalized theoretical values of  $g_\phi^2 \cdot r^3$ , and normalized experimental values of the  $^{93}\text{Nb}$  relaxation rate for the  $[\text{NbCl}_n\text{Br}_{6-n}]^-$  anions (202)

Anion	Symmetry	$g_\phi^2$	$g_\phi^2 \cdot r^3$	$R_1^0$ at $-44^\circ\text{C}$
$[\text{NbCl}_6]^-$	$O_h$	0	0.00	0.04
$[\text{NbCl}_5\text{Br}]^-$	$C_{4v}$	$9(e_2/b^3 - e_1/a^3)^2$	1.00	1.00
<i>trans</i> - $[\text{NbCl}_4\text{Br}_2]$	$D_{4h}$	$36(e_2/b^3 - e_1/a^3)^2$	4.10	$\sim 3.3$
<i>cis</i> - $[\text{NbCl}_4\text{Br}_2]^-$	$C_{2v}$	$\sim 16(e_2/b^3 - e_1/a^3)^2$	1.81	1.40
<i>trans</i> - $[\text{NbCl}_3\text{Br}_3]^-$	$C_{2v}$	$27(e_2/b^3 - e_1/a^3)^2$	3.21	3.00
<i>cis</i> - $[\text{NbCl}_3\text{Br}_3]^-$	$C_{3v}$	0	0.00	0.05
<i>trans</i> - $[\text{NbCl}_2\text{Br}_4]^-$	$D_{4h}$	$36(e_2/b^3 - e_1/a^3)^2$	4.40	$\sim 3.5$
<i>cis</i> - $[\text{NbCl}_2\text{Br}_4]^-$	$C_{2v}$	$\sim 16(e_2/b^3 - e_1/a^3)^2$	1.95	1.60
$[\text{NbClBr}_5]^-$	$C_{4v}$	$9(e_2/b^3 - e_1/a^3)^2$	1.15	1.45
$[\text{NbBr}_6]^-$	$O_h$	0	0.00	0.06

line-widths assignable to the three *cis-trans* pairs. It is interesting that the *trans* configuration consistently gives rise to far larger field gradients and thus far broader lines. The data of Tarasov *et al.* clearly establish the statistical nature of the formation of all mixed hexahalogenoniobates. Arrhenius plots for  $R_1$  and  $R_2$  afford straight lines except for *cis*- $\text{NbCl}_3\text{Br}_3^-$  where a minimum is observed. Spin-

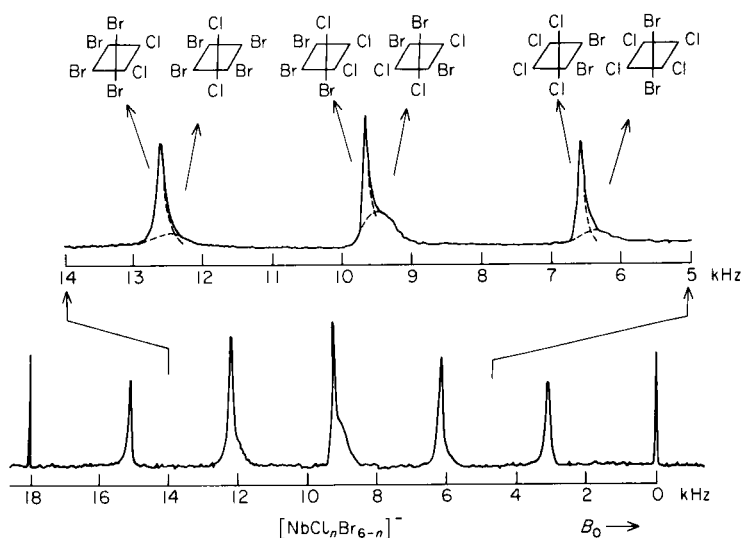


FIG. 24. 24.5 MHz  $^{93}\text{Nb}$  spectrum of a mixture containing mixed hexahalogenoniobates ( $[\text{NbCl}_n\text{Br}_{6-n}]^-$ ) in acetone.

rotation and scalar relaxation can be excluded since there is no indication for such processes in the case of the  $\text{NbCl}_6^-$  and  $\text{NbBr}_6^-$  species. The effect is thus ascribed to an intramolecular exchange.

Very recently Il'in *et al.* (247) complemented the study of mixed hexahalogenoniobates by including fluorine as a ligand. For this purpose acetonitrile solutions containing  $\text{NbX}_5$  ( $\text{X} = \text{Cl}, \text{Br}$ ) and hydrofluoric acid at a molar ratio of 1:5 were found to contain all possible mixed species except that no geometric isomers were detected for  $\text{NbF}_2\text{X}_4^-$ ,  $\text{NbF}_3\text{X}_3^-$ , and  $\text{NbF}_4\text{X}_2^-$ . This may probably be ascribed to too fast isomerization relative to the  $^{93}\text{Nb}$  chemical shift differences. At  $-10^\circ\text{C}$  the  $^{93}\text{Nb}$  resonance at 770 ppm in  $\text{NbCl}_5\text{--HF}$  sharpens to a quartet, thus clearly assigning it to *cis*- $\text{NbCl}_3\text{F}_3^-$  where the three fluorines are magnetically equivalent, in contrast to the *trans* isomer. The remaining signals are assigned on the assumption that successive replacement of X ( $\text{X} = \text{Cl}, \text{Br}$ ) by fluorine invokes relative shielding.

Dissolution of  $\text{NbX}_5$  in acetonitrile affords three separate  $^{93}\text{Nb}$  resonances at 0,  $-49$ , and  $-500$  ppm ( $\text{X} = \text{Cl}$ ) and  $+725$ ,  $+633$ , and  $-350$  ppm ( $\text{X} = \text{Br}$ ) which are ascribed to  $\text{NbX}_6^-$ ,  $\text{NbX}_5\text{CH}_3\text{CN}$ , and  $\text{NbX}_4(\text{CH}_3\text{CN})_2^+$ , respectively, on the basis of their chemical shifts and line-widths.

Mixed complexation involving isocyanate was also studied and the various resonances are assigned by varying the  $\text{NbX}_5/\text{KNCO}$  ratio as well as on the basis of line-width considerations. Successive replacement of X ( $\text{X} = \text{Cl}, \text{Br}$ ) generally result in low frequency shifts.

#### D. Group VIb

The only magnetic isotope of chromium,  $^{53}\text{Cr}$  ( $I = \frac{3}{2}$ , 9.5%), has the very weak magnetic moment of only  $-0.474\mu_N$  and is thus one of the least receptive nuclei. This definitely explains the scarcity of NMR data for this nucleus.

The first study of  $^{53}\text{Cr}$  in natural abundance and in the liquid phase was reported by Egozy and Loewenstein (206) in 1969 from which the rate constant for the chromate–dichromate equilibrium was derived. Although the quadrupole moment of  $^{53}\text{Cr}$  is small (0.03 barn) no chromium signal could be detected for the dichromate anion in which the valence electron symmetry is only slightly perturbed relative to the tetrahedral  $\text{CrO}_4^{2-}$ .

The first, and so far only, experiments in the pulsed mode are those by Epperlein *et al.* (207) who provide shielding data for the chromate ion as a function of counter-ion and concentration. The deuterium induced isotope effect for the chromate system is 1.3 ppm with a higher

shielding observed in  $D_2O$  than in  $H_2O$  solution. The same workers also reported the first shielding for a Cr(0) compound,  $Cr(CO)_6$ , in which  $^{53}Cr$  is shielded by 1795 ppm relative to the chromate. It is therefore expected that the total shielding range for  $^{53}Cr$  is comparable to that for other first-row transition metals.

More is known about the second Group VIB transition element, molybdenum, which possesses two magnetic isotopes of largely differing quadrupole moments:  $^{95}Mo$  ( $I = \frac{5}{2}$ , 15.7%,  $Q = -0.015$  barn) and  $^{97}Mo$  ( $I = \frac{5}{2}$ , 9.5%,  $Q = 0.17$  barn). The magnetic moment of each nucleus is weak ( $-0.910$  and  $-0.929 \mu_N$ ).

The exceptionally large difference between the quadrupole moments of the two nuclides has interesting implications in chemical exchange. These have recently been outlined in detail by Lindman and Forsén (1) in connection with chlorine NMR in biological systems. In order to control the exchange rate in a dynamic process the temperature is usually varied, which is always accompanied by a change in the relaxation rate. Whereas for spin- $\frac{1}{2}$  nuclei the contribution of the relaxation rate to the line-width is negligible, it is of course not so for quadrupolar nuclei. The existence of two isotopes with intrinsically different relaxation rates thus obviates the variation of temperature. This property was recently exploited by Vold and Vold (208) in order to determine the rate constant for protonation of the molybdate ion  $MoO_4^{2-}$  and the, not directly observable, Mo relaxation rate in  $Mo_7O_{24}^{6-}$ . Their result of  $4.8 \times 10^9 \text{ l mol}^{-1} \text{ s}^{-1}$  for  $k_H$  is in excellent agreement with earlier reported values obtained from ultrasonic relaxation. From a measurement of the nuclear frequencies for  $^{39}K$ ,  $^{95}Mo$ , and  $^{97}Mo$ , all performed on the same sample of potassium molybdate, the magnetic moment for the two molybdenum isotopes can be determined with great accuracy. (209)

More recently Buckler *et al.* (210) and Lutz *et al.* (211) have studied the isotope effect on  $^{95}Mo$  shielding in molybdate ( $^{18}O/^{16}O$ ) and tetrathiomolybdate ( $^{34}S/^{32}S$ ). In the latter case the isotope peak can be observed at the natural abundance of  $^{34}S$  (4.2%) on the species  $^{95}Mo^{32}S_3^{34}S^{2-}$  (14%). An isotope effect of 0.25 ppm towards lower frequencies is observed upon exchange of one  $^{16}O$  by  $^{18}O$ . The isotope shift induced by  $^{34}S$  (relative to  $^{32}S$ ) in  $MoS_4^{2-}$  was found to be 0.09 ppm to low frequency. This represents a rare case where the shielding isotope effects are known for two isotope pairs and identical molecular geometries since both ions are tetrahedrally coordinated. As a first approximation the isotope effect on the shielding should be proportional to  $(m_1^{-\frac{1}{2}} - m_2^{-\frac{1}{2}})$  with  $m_1$  and  $m_2$  representing the mass numbers of the isotope pairs [ref. 10 in (211)]. A value of 2.7 is predicted

for the ratio  $\Delta\sigma_{16,18}/\Delta\sigma_{32,34}$  which is in good agreement with the observed one of 2.8.

The chemical shift range for molybdenum is enormous. This is not surprising for a heavy element and in particular in view of the different valence states that may occur in diamagnetic compounds (0, +4, +6). But even within the group of hexavalent compounds the spread of chemical shifts observed is excessively large. Successive replacement of oxygen by sulphur in molybdate displaces the  $^{95}\text{Mo}$  resonance to low frequency by *ca.* 500–600 ppm. (212) As for other transition metals, a lowering of the substituent electronegativity deshields. Whereas a freshly prepared solution of  $\text{K}_2\text{MoS}_4$  affords a single signal assignable to the tetrathiomolybdate ion, further peaks appear upon standing the solution for a longer time. The additional signals are assigned to the mixed species  $\text{MoO}_{4-n}\text{S}_n^{2-}$  ( $n = 0, 1, 2, 3, 4$ ). The chemical shift of 496.1 ppm reported earlier by the same group (213) was erroneously assigned to  $\text{MoS}_4^{2-}$  whereas it is due to  $\text{MoO}_3\text{S}^{2-}$ . From the few known shielding data it can be concluded that the shielding range is in excess of 4000 ppm. A compilation of molybdenum shieldings is in Table XVIII.

TABLE XVIII

$^{95}\text{Mo}$  chemical shifts in some simple molybdenum compounds

Compound	Solvent	$\delta(\text{Mo})^a$	Ref.
$\text{MoS}_4^{2-}$	$\text{H}_2\text{O}$	2259	212
$\text{MoOS}_3^{2-}$	$\text{H}_2\text{O}$	1654	212
$\text{MoO}_2\text{S}_2^{2-}$	$\text{H}_2\text{O}$	1067	212
$\text{MoO}_3\text{S}^{2-}$	$\text{H}_2\text{O}$	497	212
$\text{MoO}_4^{2-}$	$\text{H}_2\text{O}$	0	212
$\text{Mo}(\text{CN})_8^{4-}$	$\text{H}_2\text{O}$	–1309	213
$\text{Mo}(\text{CO})_6$	THF	–1856	213

<sup>a</sup> A positive sign indicates relative deshielding.

### E. Group VIIb

There has not been much recent work on  $^{55}\text{Mn}$  NMR, probably because of the fairly large quadrupole moment of 0.4 barn which impairs measurements on compounds of low intrinsic Mn symmetry. From a sensitivity point of view, however,  $^{55}\text{Mn}$  can be considered a favourable nucleus. It has spin  $I = \frac{5}{2}$  (100%) and a magnetic moment of  $3.461 \mu_N$ . The total shift range known today is about 2300 ppm with

manganese in all compounds resonating to low frequency of  $^{55}\text{MnO}_4^-$  the generally accepted reference standard. (214, 215) Calderazzo *et al.* (214) and more recently Nakano (216) have reported  $^{55}\text{Mn}$  shifts for carbonyl compounds which span a range of *ca.* 1600 ppm.  $^{55}\text{Mn}$  chemical shifts for some representative  $^{55}\text{Mn}$  carbonyl complexes are in Table XIX. (214, 216) Molecular orbital theory correctly predicts the shielding order in  $\text{Mn}(\text{CO})_5\text{X}$  ( $\text{X} = \text{I}, \text{Br}, \text{Cl}$ ),  $\text{I} > \text{Br} > \text{Cl}$ . (216)

Lutz and Steinkilberg (217) were the first to provide an accurate value of the  $^{55}\text{Mn}$  magnetic moment. They also reported the concentration dependence of the chemical shift in permanganate for a variety of counter-ions and found a deuterium-induced isotope shift  $[\sigma(\text{D}_2\text{O}) - \sigma(\text{H}_2\text{O})]$  of 0.76 ppm, which is surprisingly large in view of the fact that the solvent molecules around  $^{55}\text{MnO}_4^-$  are physically insulated from the manganese ion. The shielding isotope effect has also been the subject of a more recent study (218) in which permanganate is dissolved in  $\text{H}_2^{18}\text{O}$ . The experiment, which also permits the oxygen exchange rate to be determined, affords spectra showing the presence of all five isotopomers  $^{55}\text{Mn}^{16}\text{O}_{4-n}^{18}\text{O}_n^-$  ( $n = 0, 1, 2, 3, 4$ ). The total isotope effect upon complete exchange of all four oxygens amounts to 2.25 ppm, corresponding to a higher shielding for the heavier isotopomer. The time constant for the exchange of a single oxygen is reported as 7 days.

Ireland *et al.* (219) have found that by plotting the quadrupole coupling constant against the liquid-phase line-width a straight line is obtained whose slope is proportional to the reorientational correlation time  $\tau_c$ . Such a plot is displayed in Fig. 25 for some Mn(II) carbonyl complexes. The result is surprising in showing that (a) molecular reorientation is the same for all the compounds and (b) the quadrupole coupling constant in the solid is the same as that governing relaxation in the liquid. The correlation time of 1.3 ps has subsequently been compared with the correlation time obtained by other workers from infrared absorption line-shapes yielding values in the region 3.5–4 ps. Considering the well known relationship:

$$\tau_c(\text{infrared}) = 3\tau_c(\text{nuclear}) \quad (40)$$

the agreement is satisfactory. However, if  $\tau_c$  is derived from the Debye equation a value too large by an order of magnitude is obtained. This discrepancy clearly shows that the use of a microviscosity scaling factor is obligatory if satisfactory correlation times are to be derived in this manner. Recourse is therefore made to a modified Debye equation:

$$\tau_c(\text{microviscosity}) = \eta V_m f / kT \quad (41)$$

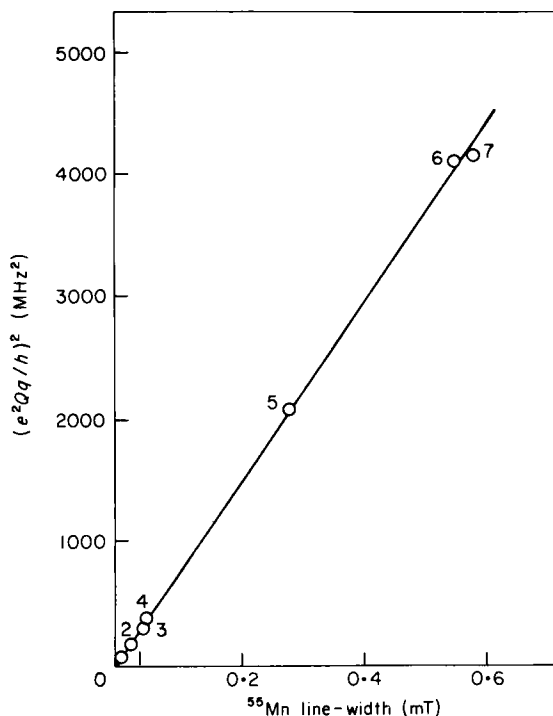


FIG. 25. Square of the  $^{55}\text{Mn}$  quadrupole coupling constant in the solid state plotted against the  $^{55}\text{Mn}$  line-width in tetrahydrofuran solution. (1)  $\text{Mn}_2(\text{CO})_{10}$ ; (2)  $\text{Mn}(\text{CO})_5\text{Cl}$ ; (3)  $\text{Mn}(\text{CO})_5\text{Br}$ ; (4)  $\text{Mn}(\text{CO})_5\text{I}$ ; (5)  $\text{Mn}(\text{CO})_5\text{D}$ ; (6)  $\eta^5\text{-C}_5\text{H}_5\text{Mn}(\text{CO})_3$ ; (7)  $\text{Mn}(\text{CO})_5^-$ . (219)

in which  $\eta$  and  $V_m$  represent the solution viscosity and solute molecular volume, and  $f$  is the microviscosity scaling factor defined as:

$$f = a/6a_s \quad (42)$$

with  $a$  and  $a_s$  being the solute and solvent molecular radii. In this manner  $\tau_c = 4.3$  ps is obtained in qualitative agreement with the value derived from line-width measurements.

The other stable element in Group VIIb, rhenium, has been the subject of a single study (220) aimed at deriving the quadrupole coupling constant in  $\text{ReO}_4^-$ . Both magnetic isotopes of rhenium,  $^{185}\text{Re}$  ( $I = \frac{5}{2}$ , 37.1%) and  $^{187}\text{Re}$  ( $I = \frac{5}{2}$ , 62.9%), are characterized by the exceedingly large quadrupole moments of 2.3 and 2.2 barns. It is therefore expected that even in cubically symmetric rhenium compounds minute perturbations will give rise to a large quadrupole coupling constant. This prediction is confirmed by the line-widths



reported by Dwek and coworkers (220) who found 14 kHz in aqueous  $^{187}\text{ReO}_4^-$ . Along with an estimated correlation time based on the Debye equation,  $e^2qQ/h = 60$  MHz was derived for the  $^{187}\text{Re}$  quadrupole coupling constant. Various mechanisms were tested which could explain this extraordinarily large value. Ion-ion effects could be ruled out on the basis of the insensitivity of the line-width to concentration. Solvation and exchange effects are excluded as a result of the insensitivity to pH changes and the observation of a single  $^{17}\text{O}$  line. Since optical spectroscopy data do not provide evidence for any permanent angular distortions from tetrahedral symmetry the strong quadrupole interaction is suggested to arise from short-lived collision complexes causing a transient distortion of the tetrahedron.

TABLE XIX  
 $^{55}\text{Mn}$  chemical shifts in carbonyl compounds<sup>a</sup>

Compound	$\delta(^{55}\text{Mn})$	Ref.
$\text{HMn}(\text{CO})_5$	-2560% (neat)	214
$\text{NaMn}(\text{CO})_5$	-2780	214
$\text{Mn}_2(\text{CO})_8(\text{PPh}_3)_2$	-2325	214
$\text{Mn}_2(\text{CO})_{10}$	-2325	214
$\text{CH}_3\text{Mn}(\text{CO})_5$	-2265	214
$\text{C}_5\text{H}_5\text{Mn}(\text{CO})_3$	-2225	214
$\text{CH}_2\text{FMn}(\text{CO})_5$	-2130	214
$\text{C}_6\text{H}_5\text{CH}_2\text{COMn}(\text{CO})_5$	-2035	214
$\text{CH}_2\text{FCOMn}(\text{CO})_5$	-2010	214
$\text{CH}_2\text{FMn}(\text{CO})_5$	-1970	214
$^n\text{PrCOMn}(\text{CO})_5$	-1900	214
$\text{CH}_3\text{COMn}(\text{CO})_5$	-1895	214
$\text{CHF}_2\text{COMn}(\text{CO})_5$	-1885	214
$^i\text{PrCOMn}(\text{CO})_5$	-1885	214
$\text{CH}_2\text{ClCOMn}(\text{CO})_5$	-1855	214
$\text{CF}_3\text{Mn}(\text{CO})_5$	-1850	214
$\text{CH}_3\text{COMn}(\text{CO})_5$	-1720	214
$\text{IMn}(\text{CO})_5$	-1520	216
$\text{BrMn}(\text{CO})_5$	-1200	216
$\text{SCNMn}(\text{CO})_5$	-1130	216
$\text{Mn}(\text{CO})_6^+$	-935 (in acetone)	216

<sup>a</sup> In tetrahydrofuran to low frequency of aqueous  $\text{KMnO}_4$ .

## F. Group VIIIb

$^{59}\text{Co}$  is the only naturally occurring cobalt isotope. With its magnetic moment of  $4.639 \mu_N$  it is less sensitive than the proton by a factor of 3. The handicap of the large quadrupole moment of 0.38 barn

is alleviated by the spin quantum of  $\frac{7}{2}$  but even more so by the extremely large range of shieldings of *ca.* 20 000 ppm and the comparatively high resonance frequency (23.7 MHz at 2.3 T). Hence, in spite of broad lines (several kHz for asymmetric coordination), an extraordinarily large chemical shift dispersion results. It is thanks to this property, but also because of the well established chemistry of diamagnetic Co(III), that a large body of shielding data for  $^{59}\text{Co}$  is available. The frequency dependence of the  $^{59}\text{Co}$  resonance in cobalt(III) complexes was detected in the course of the initial determination of the magnetic moment by Proctor and Yu as early as 1951. (221) The first systematic  $^{59}\text{Co}$  chemical shift studies were subsequently reported by Freeman *et al.* (222) who rationalized the shieldings in terms of Ramsey's formalism for field-induced paramagnetic shielding. This was probably the first manifestation of what is now commonly referred to as paramagnetic shielding. The treatment by Griffith and Orgel (223) in essence implies that the most significant contribution to the shielding is due to the first d-d transition with an increased ligand  $\sigma$  donation and/or  $\pi$  back-bonding resulting in an increased energy separation between the ground and excited electronic states and hence a lowered paramagnetic contribution to the shielding. Experimental verification is provided by a correlation of the shift with the wavenumbers of the first electronic absorption maxima. (222)

Lucken *et al.* (224) have calculated the paramagnetic shielding term for the cobalticenium ion  $\text{Co}(\text{C}_5\text{H}_5)_2^+$  in terms of ligand field theory and obtained a value of  $-1.15\%$ , whereas for  $\text{Co}(\text{CN})_6^{3-}$   $-1.39\%$  is computed. On the assumption that the diamagnetic contribution remains invariant, a low frequency shift of  $0.24\%$  is thus predicted for  $\text{Co}(\text{C}_5\text{H}_5)_2^+$  relative to  $\text{Co}(\text{CN})_6^{3-}$ , in excellent agreement with an observed shift of  $-2410$  ppm. A similar calculation for the  $\text{Co}(\text{CO})_4^-$  anion yields  $\sigma_p = -1.08\%$  corresponding to a shielding of  $0.31\%$  relative to the reference while the observed shielding change is  $-3100$  ppm. These examples illustrate the feasibility of chemical shift calculations for  $^{59}\text{Co}$ .

There are also reports on substantial deviations from proportionality between chemical shifts and the inverse of the longest wavelength. Yamasaki *et al.* (225) have found that sulphur-coordinated cobalt complexes do not obey this linear relation. Tris(ethylxanthato)-cobalt(III) as well as other  $\text{CoS}_6$ -type complexes are far more shielded than one would expect on the basis of the UV absorption maxima, clearly showing the importance of the radial parameter in the paramagnetic shielding term (which has been considered in the Lucken

*et al.* ligand-field-based calculations). Deviations from the simple  $(\Delta E)^{-1}$  vs.  $\sigma$  correlation were also predicted by Betteridge and Golding (226) who pointed out that low-symmetry crystal fields might result in additional deshielding and also that the paramagnetic shielding term should decrease in the case of 3d electron delocalization into the ligands. The latter is precisely what is found in unsymmetrical complexes of the type  $\text{Co}(\text{CN})_5\text{X}$  and  $\text{Co}(\text{NH}_3)_5\text{X}$  ( $\text{X} = \text{I}, \text{Br}, \text{Cl}, \text{F}, \text{OH}, \text{OH}_2$ ) where higher shieldings are observed throughout. (227) The deviation from the correlation line follows the order  $\text{Cl} < \text{Br} < \text{I}$ , consistent with the trend in electron delocalization predicted by the nephelauxetic series of ligands. A further unique aspect of transition metal shieldings, especially pronounced for  $^{59}\text{Co}$ , is their temperature dependence, arising from the temperature dependence of the ligand field splitting. For  $^{59}\text{Co}$  shieldings the temperature coefficient may be as large as  $3 \text{ ppm } ^\circ\text{C}^{-1}$ . (221)

Some representative  $^{59}\text{Co}$  chemical shifts are collated in Table XX. Although the generally accepted shielding reference appears to be  $\text{Co}(\text{CN})_6^{3-}$ ,  $\text{Co}(\text{NH}_3)_6^{3+}$  unfortunately is still in use even in the most recent work. In Table XX the  $^{59}\text{Co}$  shieldings, if not already reported as such in the original papers, have been recalculated to the former standard using  $\delta(\text{Co}(\text{CN})_6^{3-}) = \delta(\text{Co}(\text{NH}_3)_6^{3+}) + 8100$  (assuming that positive values reflect deshielding in either case).

TABLE XX

 $^{59}\text{Co}$  chemical shifts in some representative  $\text{Co(III)}$  complexes

Compound <sup>a</sup>	$\delta(^{59}\text{Co})^b$	Ref.
$\text{K}[\text{Co}(\text{PF}_3)_4]$	-4220	224
$\text{HCo}(\text{PF}_3)_4$	-3910	224
$\text{Na}[\text{Co}(\text{CO})_4]$	-3100	224
$\text{C}_5\text{H}_5\text{Co}(\text{CO})_2$	-2675	224
$\text{HgCo}_2(\text{CO})_8$	-2520	224
$\text{Co}_2(\text{CO})_8$	-2100	224
$\text{Co}_4(\text{CO})_{12}$	-1960, -810	224
$\text{Co}(\text{CO})_3\text{NO}$	-1365	224
$\text{Co}[\text{P}(\text{OCH}_3)_3]_6^{3+}$	-304	238
$\text{K}_3[\text{Co}(\text{CN})_6]$	0	—
$\text{Co}(\text{CN})_5\text{I}^{3-}$	+780	227
$\text{Co}(\text{CN})_5\text{Br}^{3-}$	+1220	227
$\text{Co}(\text{CN})_5\text{NO}_2^{3-}$	+1400	225
$\text{Co}(\text{CN})_5\text{OH}^{3-}$	+1840	227
$\text{Co}(\text{CN})_5\text{OH}_2^{3-}$	+1822	227
$\text{Co}(\text{dmg})_3[\text{Co}(\text{dien})]_2^{3+}$	+4610	228
$\text{Co}(\text{dmg})_3[\text{Zn}(\text{dien})]_2^{+}$	+4800	228
$[\text{Co}(\text{dmg})_3(\text{BF}_3)_2]^{+}$	+4970	228

TABLE XX (cont)

Compound <sup>a</sup>	$\delta(^{59}\text{Co})^b$	Ref.
$\text{Co}(\text{dmg})_3^{3-}$	+ 5160	228
$\text{Co}(\text{C}_2\text{H}_5\text{CSS})_3$	+ 6360	225
$\text{Co}(\frac{1}{2}\text{C}_3\text{H}_7\text{SS})_3$	+ 6360	225
$\text{Co}[(\text{C}_2\text{H}_5)_2\text{NCSS}]$	+ 6450	225
$[\text{Co}(\text{NH}_2\text{OH})_6]\text{Cl}_3$	+ 6500	225
$\text{Li}[\text{Co}(\text{NH}_3)_2(\text{NO}_2)_4]$	+ 6860	225
$[\text{Co}(\text{phen})_3]\text{Cl}_3$	+ 7080	225
<i>trans</i> - $[\text{Co}(\text{NH}_3)_4(\text{NO}_2)_2]\text{Cl}$	+ 7080	225
<i>cis</i> - $[\text{Co}(\text{NH}_3)_4(\text{NO}_2)_2]\text{Cl}$	+ 7080	225
<i>cis</i> - $[\text{Co}(\text{en})_2(\text{NH}_3)_2]\text{I}_3$	+ 7300	225
$\text{Na}_3[\text{Co}(\text{NO}_2)_6]$	+ 7440	225
$[\text{Co}(\text{NH}_3)_5\text{NO}_2]\text{Cl}_2$	+ 7440	225
<i>trans</i> - $[\text{Co}(\text{en})(\text{NH}_3)_2]\text{I}_3$	+ 7510	225
$\text{Co}(\text{NH}_3)_5\text{NO}_2^{2+}$	+ 7630	227
$[\text{Co}(\text{NH}_3)_6]\text{Cl}_3$	+ 8100	225
$\text{Co}(\text{NH}_3)_5\text{I}^{2+}$	+ 8760	227
$\text{Co}(\text{NH}_3)_5\text{Br}^{2+}$	+ 8820	227
$\text{Co}(\text{NH}_3)_5\text{Cl}^{2+}$	+ 8850	227
$[\text{Co}(\text{NH}_3)_5\text{N}_3](\text{N}_3)_2$	+ 9100	225
$\text{Co}(\text{NH}_3)_5\text{OH}^{2+}$	+ 9117	227
<i>trans</i> - $\text{Co}(\text{NH}_3)_4(\text{N}_3)_2^+$	+ 9170	225
$\text{Co}(\text{en})_2\text{CO}_3^-$	+ 9180	225
<i>cis</i> - $\text{Co}(\text{NH}_3)_4(\text{N}_3)_2^+$	+ 9400	225
$\text{Co}(\text{NH}_3)_5\text{F}^{2+}$	+ 9520	227
$\text{Co}(\text{NH}_3)_4\text{CO}_3^+$	+ 9680	225
<i>cis</i> - $\text{Co}(\text{NH}_3)_4(\text{OH}_2)_2^{3+}$	+ 9820	225
$\text{Co}(\text{edta})$	+ 10 300	225
$\text{Co}(\text{NH}_3)_2(\text{CO}_3)_2$	+ 11 500	225
$\text{Co}(\text{bzac})_3$	+ 12 400	225
$\text{Co}(\text{dbzm})_3$	+ 12 400	225
$\text{Co}(\text{acac})_3$	+ 12 500	225
$\text{Co}(\text{tfac})_3$	+ 12 500	225
$\text{Co}(\text{C}_2\text{O}_4)_3$	+ 13 000	225
$\text{Co}(\text{CO}_3)_3$	+ 13 900	225

<sup>a</sup> Abbreviations: en = ethylenediamine; phen = *o*-phenanthroline;

edta = ethylenediaminetetraacetate; bzac = benzoylacetate;

dbzm = dibenzoylmethanate; acac = acetylacetate;

tfac = trifluoroacetylacetate; dmg = dimethylglyoximate;

dien = diethylenetriamine.

<sup>b</sup> A positive sign indicates relative deshielding.

A further diagnostically useful aspect of  $^{59}\text{Co}$  shieldings is their sensitivity to stereochemistry. As an example we may compare the shieldings in *cis*- and *trans*- $\text{Co}(\text{en})_2(\text{NH}_3)_2^{3+}$ : + 7300 and + 7510 ppm respectively. (225) If there is intrinsic ligand configurational

asymmetry, optical as well as geometric isomerism may occur in the resulting cobalt complexes. Tris( $\pm$ )-propylenediamine)cobalt(III), for example, forms eight optical isomers (229) with the possibility of *cis-trans* isomerism in each of them, resulting in a total of 24 distinguishable species. Whereas the optical isomers could be separated chromatographically the geometrical isomers turned out not to be resolvable in this manner. However,  $^{59}\text{Co}$  NMR, along with fractionation techniques, has enabled full assignment of all the peaks in the spectrum of the mixture and has afforded the equilibrium populations of the various species. (230) The  $^{59}\text{Co}$  spectra of various fractions of the stereoisomeric mixtures of tris(propylenediamine)cobalt(III) are in Fig. 26.

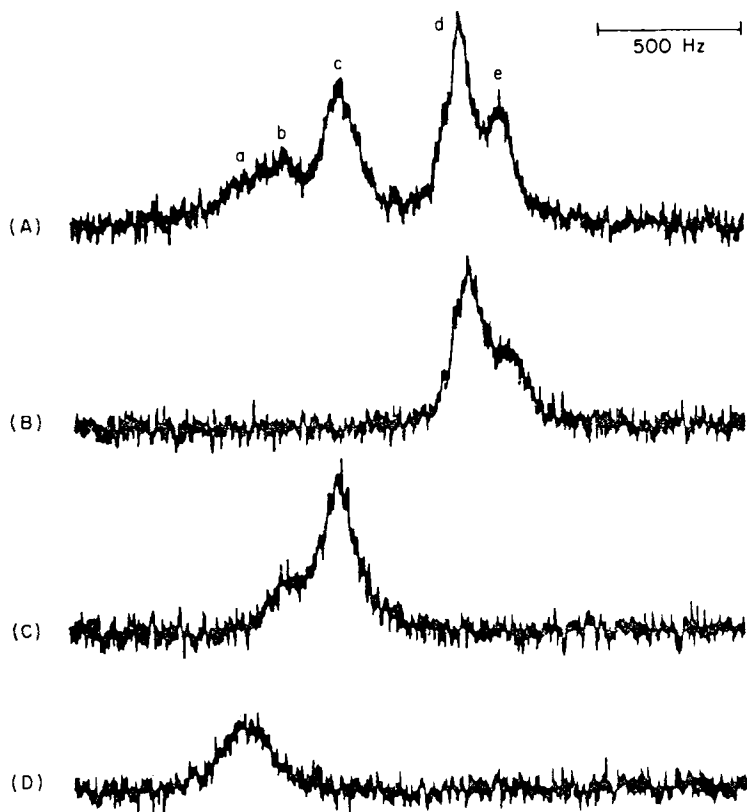
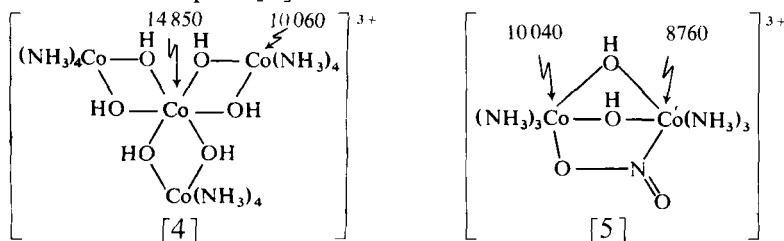


FIG. 26.  $^{59}\text{Co}$  NMR spectra of various fractions containing stereoisomers of aqueous  $\text{Co}(\text{pn})_3^{3+}$  (pn = propylenediamine). (A) 0.4 M  $[\text{Co}((\pm)\text{pn})_3]\text{Cl}_3$ ; (B) fraction containing  $\Delta\text{-Co}((-)\text{pn})_3^{3+}$  and  $\Lambda\text{-Co}(+)\text{pn})_3^{3+}$ ; (C)  $\Delta\text{-Co}((-)\text{pn})_2((+)\text{pn})_3^{3+}$  and  $\Lambda\text{-Co}(+)\text{pn})_2((-)\text{pn})_3^{3+}$ ; (D) fraction containing remaining four racemic pairs. (230)

The effects of geometric and ligand stereoisomerism on  $^{59}\text{Co}$  shielding are reported for a series of tris(bidentate)cobalt complexes involving chiral and achiral  $\beta$ -diketones. (231) Owing to the broad lines in some of the asymmetrically coordinated systems separate resonances are not always resolved.

The extreme sensitivity of the shieldings to ligand field strength is convincingly documented by the  $^{59}\text{Co}$  spectra of polynuclear complexes where enormous shielding differences are observed within the same cluster. (232) Illustrative examples are the tetranuclear [4] and binuclear complex [5] whose  $^{59}\text{Co}$  chemical shifts are indicated in



ppm relative to  $\text{Co}(\text{CN})_6^{3+}$ . In [4] the central oxygen-coordinated cobalt is less shielded by 4800 ppm than the peripheral cobalt nuclei. The former is probably the least shielded cobalt observed so far, resulting from the weakness of the ligand field produced by the six hydroxyl substituents. In [5] the two chemically distinguishable cobalt nuclei still differ in their shieldings by 1300 ppm in spite of their very similar coordinative environments.

Besides shielding it is the nuclear quadrupole coupling constant and asymmetry parameter that provide a more profound understanding of bonding in terms of charge distribution. It is therefore not surprising that several workers have addressed themselves to this problem, in particular since NQR data, because of the inherent sensitivity of  $^{59}\text{Co}$ , can be obtained fairly easily. A comprehensive body of data has been collected by Rossa and Brown (233) who reported both quadrupole coupling constants and asymmetry parameters for a number of cobaloximes of the type  $\text{XCo}(\text{dh})_2\text{L}$  (dh = dimethylglyoxime mono-anion;  $\text{X} = \text{CH}_3^-$ ,  $\text{CH}_2\text{Cl}^-$ ,  $\text{Br}^-$ ;  $\text{L} =$  a Lewis base). In these systems the quadrupole coupling constant and the asymmetry parameter can be rationalized in terms of partial field gradients produced by the planar nitrogens and by the substituents  $\text{L}$  and  $\text{X}$  located on the  $\text{C}_2$  axis of the molecular ion. The ratio of the respective quantities, denoted by  $L_{\text{eq}}$  and  $L_{\text{ax}}$ , can be calculated and correlated with  $eq_{zz}$  and  $\eta$ . Some of the experimental quadrupole coupling data from ref. 233 are in Table XXI in order of increasing magnitude of  $e^2qQ/h$ . It is surprising that,

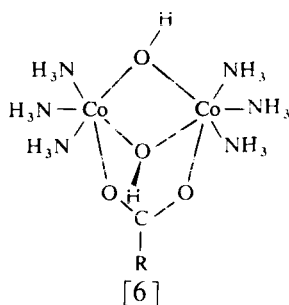
TABLE XXI

<sup>59</sup>Co quadrupole coupling constants and asymmetry parameters (233)<sup>a</sup>

Compound	$e^2q_{zz}Q/h$ (MHz)	$\eta$
CH <sub>3</sub> Co(dh) <sub>2</sub> L		
L = PPh <sub>3</sub>	28.12	0.77
NC <sub>5</sub> H <sub>5</sub>	29.52	0.22
S(CH <sub>3</sub> ) <sub>2</sub>	30.30	0.58
AsPh <sub>3</sub>	30.59	0.35
N(CH <sub>3</sub> ) <sub>3</sub>	30.55	0.16
CH <sub>3</sub> OH	41.62	0.30
P(OCH <sub>3</sub> ) <sub>3</sub>	43.33	0.57
P(n-C <sub>4</sub> H <sub>9</sub> ) <sub>3</sub>	46.20	0.55
ClCo(dh) <sub>2</sub> P(n-C <sub>4</sub> H <sub>9</sub> ) <sub>3</sub>	40.91	0.35
ClCo(dh) <sub>2</sub> PPh <sub>3</sub>	60.45	0.81
ClCo(dh) <sub>2</sub> NC <sub>5</sub> H <sub>5</sub>	64.82	0.63
N(C <sub>2</sub> H <sub>5</sub> ) <sub>4</sub> [Cl <sub>2</sub> Co(dh) <sub>2</sub> ]	73.15	0.72
N(C <sub>2</sub> H <sub>5</sub> ) <sub>4</sub> [Br <sub>2</sub> Co(dh) <sub>2</sub> ]	75.88	0.68

<sup>a</sup> Taken from NQR data.

although all four central planar ligands contain nitrogen, the asymmetry parameters are substantial. Determinations of  $e^2qQ/h$  from liquid spectra with the aid of line-width measurements and extraction of the correlation time from the Debye equation are therefore suspect. The absence of shielding variations but the presence of sizeable differentials in line-widths prompted Hackbusch *et al.* (234) to estimate the electric field gradient in some closely related binuclear cobalt(III) complexes of the type [6] with R = H, Me, CH<sub>2</sub>F, CHF<sub>2</sub>, etc. On the



assumption of no angular distortions of the metal–ligand bonds, and equal contributions of all oxygens to the electric field gradients,  $V_{xx} = V_{yy} \neq V_{zz}$ , i.e.  $\eta = 0$ . On this simplifying assumption the principal electric field gradient was determined from line-width measurements

and a reorientational correlation time estimated on the basis of different models. The authors established a fair linear correlation between the basicity of  $\text{RCOO}^-$  and the relative field gradient, showing that the small charge differences at the carboxy group, caused by the nature of the substituent R, are essentially responsible for the field gradient at the cobalt nucleus.

$^{59}\text{Co}$  NMR finally provided insight into binding of anions and cations in the second coordination sphere of cobalt(III) complexes. In particular phosphate appears to bind rather strongly to cations such as  $\text{Co(en)}_3^{3+}$  (235, 236) and also  $\text{Co(pn)}_3^{3+}$ . (136) Outer-sphere association constants for the former systems have been reported and the NMR data were corroborated by optical spectroscopy. However, in spite of substantial  $^{59}\text{Co}$  shielding variations ( $>100$  ppm between  $[\text{PO}_4^{3-}]/[\text{Co(en)}_3^{3+}] = 0$  and 5), the quadrupole coupling constant remains unaffected. This was ascertained with the aid of  $^{13}\text{C}$  relaxation measurements which show that the increase of the  $^{59}\text{Co}$  line-width is entirely due to the lengthened correlation time. (237)

Scalar couplings between  $^{59}\text{Co}$  and  $^{13}\text{C}$ ,  $^{31}\text{P}$ , and  $^{19}\text{F}$  have occasionally been observed in  $^{59}\text{Co}$  spectra of octahedral and tetrahedral complexes (224, 238) (Table XXII).

TABLE XXII

$^{59}\text{Co}$  spin-spin coupling constants in Co(III) complexes (228, 242)

Compound	$^1J(^{59}\text{Co}-\text{X})$ (Hz)	
$\text{Na}[\text{Co}(\text{CO})_4]$	287	(X = $^{13}\text{C}$ )
$\text{K}_3[\text{Co}(\text{CN})_6]$	127	(X = $^{13}\text{C}$ )
$\text{K}[\text{Co}(\text{PF}_3)_4]$	1222	(X = $^{31}\text{P}$ )
	57	(X = $^{19}\text{F}$ )
$[\text{Co}(\text{P}(\text{OCH}_3)_3)_6](\text{BF}_4)_3$	414	(X = $^{31}\text{P}$ )

Although the coordinating character of trifluorophosphine and trialkyl phosphite can be assumed to be very similar, the observed coupling constants  $^1J(^{59}\text{Co}-^{31}\text{P})$  differ substantially from one another. The smaller value found in the octahedral complex has therefore been accounted for by the larger fractional s-character of the Co-P bond in the trimethyl phosphite complex. (238)

Although Group VIIIb comprises further quadrupolar nuclei (e.g.  $^{61}\text{Ni}$ ,  $^{99,101}\text{Ru}$ ,  $^{105}\text{Pd}$ ,  $^{191,193}\text{Ir}$ ) their resonances remain to be studied in the liquid phase.



### G. Groups Ib and IIb

Liquid-state NMR data, to the best of the reporter's knowledge, are available only for copper and zinc within the above groups of elements.

Copper has two magnetic isotopes,  $^{63}\text{Cu}$  (69%,  $I = \frac{3}{2}$ ) and  $^{65}\text{Cu}$  (31%,  $I = \frac{3}{2}$ ), with similar magnetic moments of 2.221 and 2.379  $\mu_N$  and quadrupole moments of  $-0.211$  and  $-0.195$  barn. NMR studies are confined to diamagnetic copper(I) complexes. Only very recently Lutz *et al.* (248) provided high-precision values for the magnetic moments of the two isotopes based on measurements in  $[\text{Cu}^{\text{I}}(\text{CH}_3\text{CN})_4]\text{BF}_4$  dissolved in acetonitrile. These workers also established an atomic reference scale for copper shieldings and reported chemical shifts for some tetracoordinated Cu(I) complexes with nitrogen- and phosphorus-coordinating ligands. (249) Including the data reported earlier (250) the thus far established shift range is *ca.* 1000 ppm.

Yamamoto *et al.* (239) were the first to study  $^{63}\text{Cu}$  with the objective of extracting chemical information. In an aqueous solution of copper(I) cyanide they found the line-width of the  $^{63}\text{Cu}$  resonance to be markedly affected by the relative amount of cyanide added. Below the critical ratio  $[\text{Cu}^+]/[\text{CN}^-] = 4$  no signal at all could be detected. This behaviour was interpreted in terms of chemical exchange between  $\text{Cu}(\text{CN})_4^{3-}$  and lower populations of the less symmetric species  $\text{Cu}(\text{CN})_3^{2-}$  and  $\text{Cu}(\text{CN})_2^-$  whose formation is well known. At excess cyanide concentration the population of the minor species should be small and the line-width entirely governed by the quadrupole coupling constant in  $\text{Cu}(\text{CN})_4^{3-}$ , which was estimated to be of the order of 0.4 MHz on the basis of a correlation time derived from the Stokes-Debye equation. The above value is also in fair agreement with that observed in the solid.

In a preliminary study aimed at assessing the feasibility of copper NMR for probing copper(I) complexation, von Zelewsky *et al.* (240) recorded the  $^{69}\text{Cu}$  spectrum of  $[\text{Cu}(\text{CH}_3\text{CN})_4]\text{ClO}_4$  in acetonitrile as a function of temperature. The spectra at 30°C and 60°C (Fig. 27) clearly point to fast exchange between  $\text{Cu}(\text{CH}_3\text{CN})_4^+$  and species of lower coordination symmetry. Such behaviour manifests itself in the 22 ppm shift to low frequency that occurs upon increasing the temperature. Further to this the line-width is found to increase. Since  $T_2$  increases with temperature the observed change in line-width must be attributed to the growing population of at least one low-symmetry species appreciably contributing to transverse relaxation. The temperature dependence of the copper chemical shift in  $\text{Cu}(\text{CH}_3\text{CN})_4^+$  hampers its usefulness as a shielding reference compound.

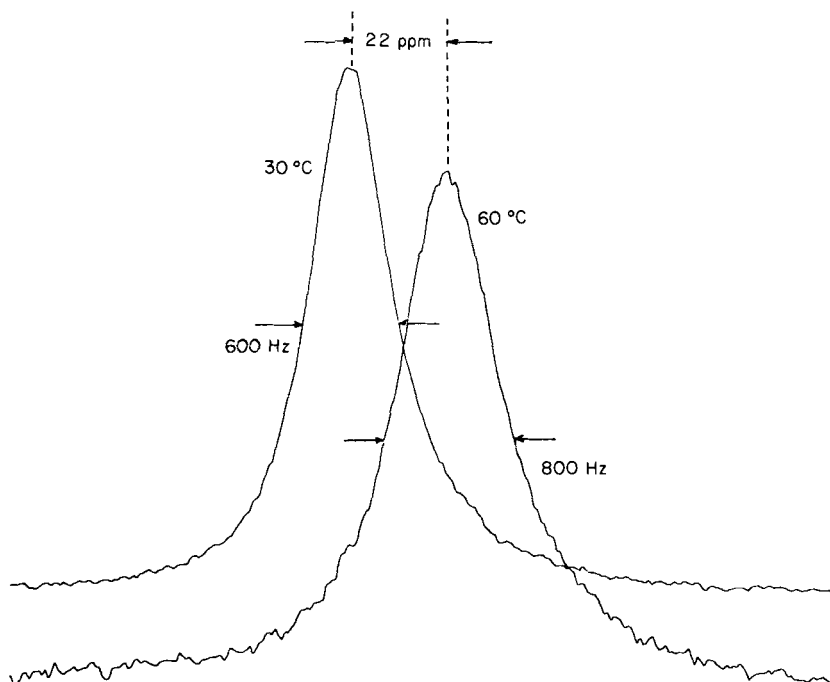


FIG. 27. 26.5 MHz  $^{63}\text{Cu}$  NMR spectra of 0.15 M  $[\text{Cu}(\text{CH}_3\text{CN})_4]\text{ClO}_4$  in acetonitrile at two different temperatures. (240)

McFarlane and Rycroft (241) have determined the spin-spin coupling constant in the  $\text{Cu}[\text{P}(\text{OCH}_3)_3]_4^+$  ion on the basis of the  $^1\text{H}-\{^{31}\text{P}\}$  INDOR spectrum which is found to be a faithful reproduction of the direct  $^{31}\text{P}$  spectrum, consisting of two partly overlapping 1:1:1:1 quartets whose splittings of 1210 Hz and 1290 Hz correspond to  $^1J(^{63}\text{Cu}-^{31}\text{P})$  and  $^1J(^{65}\text{Cu}-^{31}\text{P})$ . By simultaneously irradiating one of the components of the  $^{63}\text{Cu}$  quintet a triple resonance spectrum referred to as MINDOR (modified INDOR) is obtained from which the  $^{63}\text{Cu}$  resonance frequency can be determined.

So far no copper chemical shifts seem to have been reported; however, the shielding range will definitely be lower than for the previous transition metals since Cu(I) has a  $d^{10}$  electron shell.

$^{67}\text{Zn}$  ( $I = \frac{5}{2}$ ,  $Q = 0.16$  barn, 4.1%) has a magnetic moment of  $0.784 \mu_N$  and therefore can be considered a low-receptivity nucleus. This together with the not very extensive chemistry of this element, is primarily responsible for the little interest that this nucleus has attracted so far.

The first systematic study of  $^{67}\text{Zn}$  shieldings by high-resolution pulse FT methods is that by Epperlein *et al.* (242). The non-linearity of the shift dependence on concentration for a variety of zinc salts is taken as evidence for complexation with the counter-ion through displacement of water molecules from the hexacoordinated hydration sphere. Generally the concentration shifts for the halides follow the order  $\text{Cl} > \text{Br} > \text{I}$  whereas nitrate, perchlorate, and sulphate do not show any concentration dependence.

Maciel *et al.* (243) have determined the shifts for the halide complexes  $\text{ZnX}_n^{2-n}$  ( $n = 0, 1, 2, 3, 4$ ;  $\text{X} = \text{Cl}^-, \text{Br}^-$ ) on the basis of the observed dependence of  $^{67}\text{Zn}^{2+}$  shieldings on halide concentration and individual formation constants available from other sources. For this purpose they developed a least-squares treatment which has permitted them to fit the experimental shieldings to:

$$\delta_{\text{obs}} = \delta_0 x_0 + \delta_1 x_1 + \delta_2 x_2 + \delta_3 x_3 + \delta_4 x_4 \quad (43)$$

in which  $x_0, x_1$ , etc. represent the respective mole fractions of free and halide-bound zinc, and  $\delta_0, \delta_1$ , etc. are the respective chemical shifts in  $\text{Zn}^{2+}$ ,  $\text{ZnX}^+$ , etc. This procedure has led to the chemical shifts of the individual species listed in Table XXIII.

TABLE XXIII

$^{67}\text{Zn}$  chemical shifts in halide complexes, obtained by the procedure outlined in the text or by direct observation (243)

Complex	$\delta(^{67}\text{Zn})$
$\text{Zn}^{2+}$	0 calculated
$\text{ZnCl}^+$	+ 30 calculated
$\text{ZnCl}_2$	+ 295 calculated
$\text{ZnCl}_3^-$	+ 119 calculated
$\text{ZnCl}_4^{2-}$	+ 253 calculated
$\text{ZnBr}^+$	+ 10 calculated
$\text{ZnBr}_2$	+ 511 calculated
$\text{ZnBr}_3^-$	- 230 calculated
$\text{ZnBr}_4^{2-}$	+ 136 calculated
$\text{Zn}(\text{NH}_3)_4^{2+}$	+ 288.2 1.0 M $\text{Zn}(\text{NO}_3)_2$ in 11 M $\text{NH}_3/\text{H}_2\text{O}$
$\text{Zn}(\text{CN})_4^{2-}$	+ 283.6 $\text{Zn}(\text{CN})_2$ in 3 M $\text{NaCN}/\text{H}_2\text{O}$

Figure 28 shows the mole fractions of the various chloride complexes, computed as a function of chloride concentration, on the basis of known formation constants. The experimental and computed chemical shift dependence of  $^{67}\text{Zn}$  in  $\text{ZnClO}_4$  as a function of chloride concentration is given in Fig. 29.

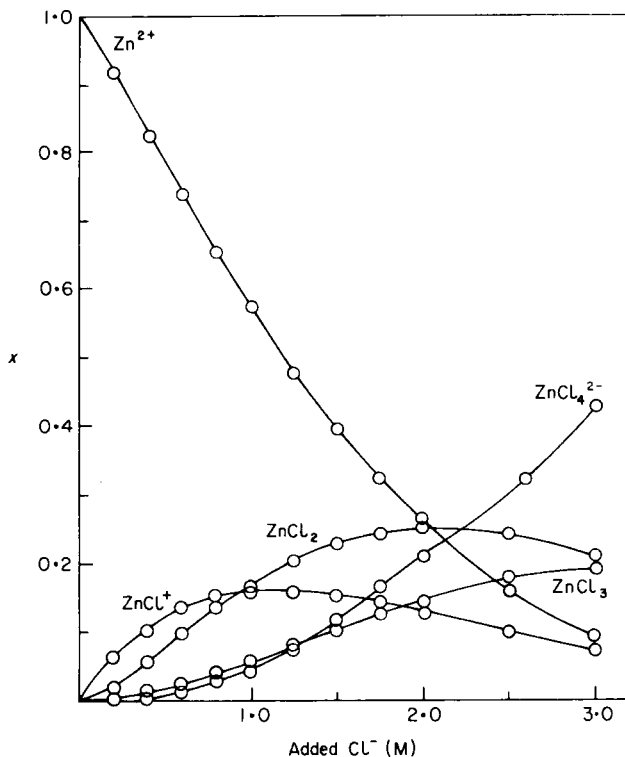


FIG. 28. Dependence of the various mole fractions present in aqueous solutions of  $\text{Zn}^{2+}$  on added chloride, all at constant zinc concentration ( $[\text{Zn}_{\text{tot}}] = 0.5 \text{ M}$ ). Mole fractions are calculated from known formation constants. (243)

## VIII. CONCLUSIONS AND OUTLOOK

Quadrupolar nuclei constitute most of the magnetic nuclei within the Periodic Table of the elements. However, the lack of suitable instrumentation as well as the misconception of the deleterious nature of these nuclei have impeded a more widespread utilization of their resonances. Quadrupolar relaxation resulting from the interaction of the nuclear quadrupolar moment with finite electric field gradients is the principal source of nuclear relaxation in nearly all compounds. However, albeit generally considered a nuisance, the phenomenon may as well be exploited to the experimenter's advantage. In contrast to spin- $\frac{1}{2}$  nuclei whose relaxation behaviour is principally dictated by the dynamics of the molecules in solution, structural and electronic effects play the key role in the relaxation process of quadrupolar nuclei.

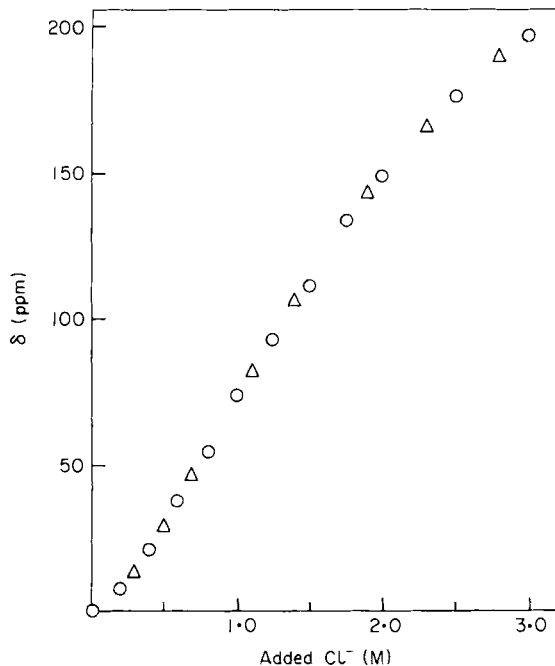


FIG. 29.  $^{67}\text{Zn}$  chemical shift in a 0.50 M solution of  $\text{Zn}(\text{ClO}_4)_2$  as a function of added NaCl. Experimental data are represented by circles; triangles correspond to computed values obtained from best fits to equation (43). (243)

Because of the square dependence of the relaxation rate on the electric field gradient tensor invariant minor alterations of valence electron symmetry may give rise to sizeable relaxation differentials. Thanks to this amplification effect the binding of ions can be studied at low substrate concentration provided that the resulting complex is kinetically labile. The relaxation rate thus emerges as a complementary experimental observable, at least as informative as the chemical shift.

Concentration-, temperature-, and frequency-dependent experiments on ionic nuclei have been shown to be very successful in evaluating complexation and solvation equilibria. In slowly exchanging systems chemical shift and relaxation data have often provided unique information on the nature of the species present in solution. We certainly face the beginning of a new era of NMR, and significant new applications in the field of inorganic, organometallic, and bioinorganic chemistry are expected. From a NMR point of view these areas are still largely unexplored and it is hoped that the present review will stimulate researchers to utilize the technique as a problem-solving tool.

## Acknowledgements

The author is very much indebted to the following ladies and gentlemen for their generosity in providing data prior to publication: Prof. Yu. A. Buslaev and Dr. V. P. Tarasov; Profs. S. Forsén and B. Lindman; Dr. M. Holz; Prof. W. G. Klemperer and Dr. W. Shum; Prof. K. A. Koehler and Drs. D. L. Harris, H. C. Harsh, R. G. Hiskey, P. Robertson, and M. E. Scott; and Prof. A. von Zelewsky. The provision of a copy of Dr. P. Balimann's Ph.D. thesis by Dr. P. S. Pregosin is gratefully acknowledged. Further, the author thanks Mrs E. Hubbeling and Miss K. Santschi for typing the manuscript, and Mr. R. Leibundgut for part of the artwork.

## REFERENCES

1. B. Lindman and S. Forsén, Chlorine, bromine and iodine NMR: physicochemical and biological applications, in "NMR Basic Principles and Progress", Vol. 12, P. Diehl, E. Fluck and R. Kosfeld (eds.), Springer, 1976.
2. B. Lindman and S. Forsén, NMR of the alkalis; NMR of the alkaline earths, in "NMR and the Periodic Table", B. Mann and R. K. Harris (eds.), Academic Press, 1978.
3. H. H. Mantsch, H. Saitô and I. C. P. Smith, Deuterium magnetic resonance applications in chemistry, physics and biology, in "Progress in NMR Spectroscopy", J. Emsley, J. Feeney and L. Sutcliffe (eds.), Pergamon Press, 1976.
4. P. Laszlo, *Angew. Chem.*, 1978, **90**, 271.
5. M. Witanowski and G. A. Webb, "Nitrogen NMR", Plenum Press, 1973.
6. W. G. Klemperer, *Angew. Chem. Internat. Edn.*, 1978, **17**, 246.
7. P. D. Ellis, H. C. Walsh and C. S. Peters, *J. Magn. Resonance*, 1973, **11**, 426.
8. C. S. Peters, R. S. Codrington, H. C. Walsh and P. D. Ellis, *J. Magn. Resonance*, 1973, **11**, 431.
9. D. D. Traficante, J. A. Simms and M. Mulcahy, *J. Magn. Resonance*, 1974, **15**, 484.
10. H. C. Dorn, L. Simeral, J. J. Natterstad and G. E. Maciel, *J. Magn. Resonance*, 1975, **18**, 1.
11. A. G. Marshall, L. D. Hall, M. Hutton and J. Sallos, *J. Magn. Resonance*, 1974, **13**, 392.
12. J. J. H. Ackerman and G. E. Maciel, *J. Magn. Resonance*, 1976, **23**, 67.
13. R. E. Santini and J. B. Grutzner, *J. Magn. Resonance*, 1976, **22**, 155.
14. J. L. Dye, C. W. Andrews and J. M. Ceraso, *J. Phys. Chem.*, 1975, **79**, 3076.
15. Y. M. Cahen, J. L. Dye and A. I. Popov, *J. Phys. Chem.*, 1975, **79**, 1289.
16. F. W. Wehrli, *J. Magn. Resonance*, 1976, **23**, 527.
17. F. W. Wehrli, *Org. Magn. Resonance*, 1978, **11**, 106.
18. H. G. Hertz, R. Tutsch and H. Versmold, *Ber. Bunsenges. Phys. Chem.*, 1971, **75**, 1177.
19. H. G. Hertz, M. Holz, G. Keller, H. Versmold and C. Yoon, *Ber. Bunsenges. Phys. Chem.*, 1974, **78**, 493.
20. F. W. Wehrli, *J. Magn. Resonance*, 1977, **25**, 575.
21. G. E. Hartwell and A. Allerhand, *J. Amer. Chem. Soc.*, 1971, **93**, 4415.
22. C. Deverell, in "Progress in NMR Spectroscopy", J. Emsley, J. Feeney and L. Sutcliffe (eds.), Vol. 6, 1969.
23. Refs. 240-243 in ref. 1.
24. See e.g. H. G. Hertz, *Ber. Bunsenges. Phys. Chem.*, 1973, **77**, 531.
25. C. A. Melendres and H. G. Hertz, *J. Chem. Phys.*, 1974, **61**, 4156.
26. A. Geiger and H. G. Hertz, *Adv. Mol. Relax. Proc.*, 1976, **9**, 293.
27. A. I. Mishustin and Yu. M. Kessler, *J. Solution Chem.*, 1975, **4**, 779.

28. Y. M. Kessler, A. I. Mishustin and A. I. Podkovyrin, *J. Solution Chem.*, 1977, **6**, 111.
29. E. G. Bloor and R. G. Kidd, *Canad. J. Chem.*, 1968, **46**, 3425.
30. R. E. Erlich and A. I. Popov, *J. Amer. Chem. Soc.*, 1971, **93**, 5620.
31. M. Herlem and A. I. Popov, *J. Amer. Chem. Soc.*, 1972, **94**, 1431.
32. J. S. Shih and A. I. Popov, *Inorg. Nuclear Chem. Lett.*, 1977, **13**, 105.
33. W. J. de Witte, L. Liu, E. Mei, J. L. Dye and A. I. Popov, *J. Solution Chem.*, 1977, **6**, 337.
34. Y. M. Cahen, P. R. Handy, E. T. Roach and A. I. Popov, *J. Phys. Chem.*, 1975, **79**, 80.
35. M. S. Greenberg, D. M. Wied and A. I. Popov, *Spectrochim. Acta*, 1973, **29A**, 1927.
36. A. L. van Geel, *J. Amer. Chem. Soc.*, 1972, **94**, 5583.
37. C. Detellier and P. Laszlo, *Helv. Chim. Acta*, 1976, **59**, 1333.
38. A. K. Covington, T. H. Lilley, K. E. Newman and G. A. Porthouse, *J. Chem. Soc., Faraday I*, 1973, **69**, 963.
39. A. K. Covington, K. E. Newman and T. H. Lilley, *J. Chem. Soc., Faraday I*, 1973, **69**, 973.
40. M. S. Greenberg and A. I. Popov, *Spectrochim. Acta*, 1975, **31A**, 697.
41. R. G. Baum and A. I. Popov, *J. Solution Chem.*, 1975, **4**, 441.
42. A. K. Covington, I. R. Lantzke and J. M. Thain, *J. Chem. Soc., Faraday I*, 1974, **70**, 1869.
43. H. Gustavsson, T. Ericsson and B. Lindman, *Inorg. Nuclear Chem. Lett.*, 1978, **14**, 37.
44. R. D. Green and J. S. Martin, *Canad. J. Chem.*, 1972, **50**, 3935.
45. P. Neggia, M. Holz and H. G. Hertz, *J. Chim. Phys.*, 1974, **71**, 56.
46. M. Goldsmith, D. Hor and R. Damadian, *J. Chem. Phys.*, 1976, **65**, 1708.
47. M. Holz, H. Weingärtner and H. G. Hertz, *J. Chem. Soc., Faraday I*, 1977, **73**, 71.
48. M. Holz, *J. Chem. Soc., Faraday I*, 1978, **74**, 644.
49. M. Holz, H. Weingärtner and H. G. Hertz, *J. Solution Chem.*, 1978, **7**.
50. T. L. James and J. H. Noggle, *J. Amer. Chem. Soc.*, 1969, **91**, 3424; *Bioinorg. Chem.*, 1972, **2**, 69.
51. R. G. Bryant, *Biochem. Biophys. Res. Commun.*, 1970, **40**, 1162.
52. A. C. Plausch and R. R. Sharp, *J. Amer. Chem. Soc.*, 1976, **98**, 7973.
53. C. Detellier, J. Grandjean and P. Laszlo, *J. Amer. Chem. Soc.*, 1976, **98**, 3375.
54. J. Grandjean and P. Laszlo, *Helv. Chim. Acta*, 1977, **60**, 259.
55. J. Andrasko and S. Forsén, *Biochem. Biophys. Res. Commun.*, 1974, **52**, 233.
56. J. W. Akitt and M. Parekh, *J. Chem. Soc. (A)*, 1968, 2195.
57. R. L. Bodner, M. S. Greenberg and A. I. Popov, *Spectroscopy Lett.*, 1972, **5**, 489.
58. Y. M. Cahen, R. F. Beisel and A. I. Popov, *J. Inorg. Nuclear Chem. Suppl.*, 1976, 209.
59. J. M. Lehn, *Struct. Bonding (Berlin)*, 1973, **16**, 1.
60. W. Simon, W. E. Morph and P. Ch. Meier, *Struct. Bonding (Berlin)*, 1973, **16**, 113.
61. Y. M. Cahen, J. L. Dye and A. I. Popov, *J. Phys. Chem.*, 1975, **79**, 1292.
62. E. Shchori, J. Jagur-Grodzinski, Z. Luz and M. Shporer, *J. Amer. Chem. Soc.*, 1971, **93**, 7133.
63. E. Shchori, J. Jagur-Grodzinski and M. Shporer, *J. Amer. Chem. Soc.*, 1973, **95**, 3842.
64. J. M. Ceraso, P. B. Smith, J. S. Landers and J. L. Dye, *J. Phys. Chem.*, 1977, **81**, 760.
65. A. Hourdakis and A. I. Popov, *J. Solution Chem.*, 1977, **6**, 299.
66. J. P. Kintzinger and J. M. Lehn, *J. Amer. Chem. Soc.*, 1974, **96**, 3313.
67. M. Shporer and Z. Luz, *J. Amer. Chem. Soc.*, 1975, **97**, 665.
68. E. Mei, J. L. Dye and A. I. Popov, *J. Amer. Chem. Soc.*, 1977, **99**, 5308.
69. E. Mei, L. Liu, J. L. Dye and A. I. Popov, *J. Solution Chem.*, 1977, **6**, 771.
70. E. Mei, A. I. Popov and J. L. Dye, *J. Amer. Chem. Soc.*, 1977, **99**, 6532.
71. P. G. Gertenbach and A. I. Popov, *J. Amer. Chem. Soc.*, 1975, **97**, 4738.
72. D. H. Haynes, B. C. Pressman and A. Kowalsky, *Biochemistry*, 1971, **10**, 852.
73. T. L. Brown, *Adv. Organometal. Chem.*, 1966, **3**, 365.
74. T. L. Brown, *Accounts Chem. Res.*, 1968, **1**, 23.
75. T. L. Brown, *J. Pure Appl. Chem.*, 1970, **23**, 447.

76. L. D. McKeever, in "Ions and Ion Pairs in Organic Reactions", Vol. I, M. Swarc (ed.), Wiley-Interscience, New York, 1972.
77. P. West, *Int. Rev. Sci., Med. Tech. Publ. Co.*, 1972.
78. W. H. Glaze, *J. Organometal. Chem.*, 1973, **48**, 1.
79. E. A. C. Lucken, *J. Organometal. Chem.*, 1965, **4**, 252.
80. P. A. Scherr, R. J. Hogan and J. P. Oliver, *J. Amer. Chem. Soc.*, 1974, **96**, 6055.
81. R. H. Cox, H. W. Terry, Jr. and L. W. Harrison, *J. Amer. Chem. Soc.*, 1971, **93**, 3297.
82. R. H. Cox, H. W. Terry, Jr. and L. W. Harrison, *Tetrahedron Lett.*, 1971, 4815.
83. J. A. Ladd and J. Parker, *J. Chem. Soc., Dalton*, 1972, 930.
84. R. H. Cox and H. W. Terry, Jr., *J. Magn. Resonance*, 1974, **14**, 317.
85. R. Waack, L. D. McKeever and M. A. Doran, *Chem. Comm.*, 1969, 117.
86. L. D. McKeever, R. Waack, M. A. Doran and E. B. Baker, *J. Amer. Chem. Soc.*, 1968, **90**, 3244; 1969, **91**, 1057.
87. L. D. McKeever and R. Waack, *Chem. Comm.*, 1969, 750.
88. T. L. Brown, L. M. Seitz and B. Y. Kimura, *J. Amer. Chem. Soc.*, 1968, **90**, 3245.
89. L. M. Seitz and T. L. Brown, *J. Amer. Chem. Soc.*, 1966, **88**, 2174.
90. L. M. Seitz and T. L. Brown, *J. Amer. Chem. Soc.*, 1960, **88**, 4140.
91. L. M. Seitz and B. F. Little, *J. Organometal. Chem.*, 1969, **18**, 227.
92. R. L. Gerteis, R. E. Dickinson and T. L. Brown, *Inorg. Chem.*, 1964, **3**, 872.
93. R. J. Hogan, P. A. Scherr, A. T. Weibel and J. P. Oliver, *J. Organometal. Chem.*, 1975, **85**, 265.
94. W. L. Wells and T. L. Brown, *J. Organometal. Chem.*, 1968, **11**, 271.
95. K. C. Williams and T. L. Brown, *J. Amer. Chem. Soc.*, 1966, **88**, 4134.
96. D. A. Everest, "The Chemistry of Beryllium", Elsevier, New York, 1964.
97. O. Lutz, A. Schwenk and A. Uhl, *Z. Naturforsch.*, 1975, **30a**, 1122.
98. O. Lutz, A. Schwenk and A. Uhl, *Z. Naturforsch.*, 1973, **28a**, 1534.
99. J. Banck and A. Schwenk, *Z. Physik*, 1973, **265**, 165.
100. H. Krüger, O. Lutz and H. Oehler, *Phys. Lett.*, 1977, **62a**, 131; O. Lutz, H. Oehler, *Z. Phys.* (1978) **A288**, 11.
101. L. Simeral and G. E. Maciel, *J. Phys. Chem.*, 1976, **80**, 552.
102. F. W. Wehrli, *J. Magn. Resonance*, 1976, **23**, 181.
103. B. Lindman, S. Forsén and H. Lilja, *Chem. Scripta*, 1977, **11**, 91.
104. M. Ellenberg and M. Villemin, *Compt. rend., B*, 1968, **266**, 1430.
105. R. A. Kovar and G. L. Morgan, *J. Amer. Chem. Soc.*, 1970, **92**, 5067.
106. J. J. Delpuech, A. Péguy, P. Rubini and J. Steinmetz, *Nouv. J. Chim.*, 1976, **1**, 133.
107. R. G. Bryant, *J. Magn. Resonance*, 1972, **6**, 159.
108. P. Robertson, Jr., R. G. Hiskey and K. A. Koehler, *J. Biol. Chem.*, 1978.
109. F. W. Wehrli, unpublished.
110. J. C. Kotz, R. Schaeffer and A. Clouse, *Inorg. Chem.*, 1967, **6**, 620.
111. F. W. Wehrli, *J. Magn. Resonance*, 1978, **30**, 193.
112. V. P. Tarasov and Yu. A. Buslaev, *Mol. Phys.*, 1972, **24**, 665.
113. A. Takahashi, *J. Phys. Soc. Japan*, 1977, **43**, 968.
114. A. Takahashi, *J. Phys. Soc. Japan*, 1977, **43**, 976.
115. J. W. Akitt, N. N. Greenwood and G. D. Lester, *Chem. Comm.*, 1969, 988.
116. J. W. Akitt, N. N. Greenwood and G. D. Lester, *Inorg. Phys. Theor.*, 1969, 803.
117. J. W. Akitt, N. N. Greenwood, B. L. Khandelwal and G. D. Lester, *J. Chem. Soc., Dalton*, 1971, 604.
118. J. F. Hon, *Mol. Phys.*, 1968, **15**, 57.
119. H. Haraguchi and S. Fujiwara, *J. Phys. Chem.*, 1969, **73**, 3467.
120. W. G. Movius and N. A. Matwiyoff, *Inorg. Chem.*, 1967, **6**, 847.
121. W. H. N. Vriezen and F. Jellinek, *Rec. Trav. Chim.*, 1970, **89**, 1306.
122. R. G. Kidd and D. R. Truauux, *Chem. Comm.*, 1969, 160.



123. J. W. Akitt and R. H. Duncan, *J. Magn. Resonance*, 1977, **25**, 391.
124. D. Canet, J. J. Delpuech, M. R. Khaddar and P. Rubini, *J. Magn. Resonance*, 1973, **9**, 329.
125. J. J. Delpuech, M. R. Khaddar, A. A. Péguy and P. R. Rubini, *J. Amer. Chem. Soc.*, 1975, **97**, 3373.
126. H. Schneider, *Electrochim. Acta*, 1976, **21**, 711.
127. E. Schippert, *Adv. Mol. Relax. Proc.*, 1976, **9**, 167.
128. Yu. A. Buslaev, V. P. Tarasov, S. P. Petrosyants and N. N. Melnikov, *Zh. Strukt. Khim.*, 1974, **15**, 617.
129. R. G. Kidd and D. R. Truax, *J. Amer. Chem. Soc.*, 1968, **90**, 6867.
130. R. G. Kidd and D. R. Truax, *Canad. Spectr.*, 1969, **14**, 1.
131. Yu. A. Buslaev, V. P. Tarasov and S. P. Petrosyants, *Koord. Khim.*, 1975, **1**, 1435.
132. R. F. Cormick and R. E. Poulsen, *J. Amer. Chem. Soc.*, 1957, **79**, 5153.
133. D. E. O'Reilly, *J. Chem. Phys.*, 1960, **32**, 1007.
134. E. M. Delarco and H. E. Swift, *J. Phys. Chem.*, 1964, **68**, 551.
135. W. G. Movius and N. A. Matwiyoff, *Inorg. Chem.*, 1967, **6**, 847.
136. T. Thomas and W. L. Reynolds, *J. Chem. Phys.*, 1966, **44**, 3148.
137. A. Fratiello, R. E. Lee, V. M. Nishida and R. E. Shuster, *J. Chem. Phys.*, 1967, **47**, 4951.
138. J. W. Akitt, N. N. Greenwood and G. O. Lester, *J. Chem. Soc. (A)*, 1971, 2450.
139. J. W. Akitt, N. N. Greenwood and B. L. Khandelwal, *J. Chem. Soc., Dalton*, 1972, 1226.
140. A. D. Toy, T. D. Smith and J. R. Pilbrow, *Austral. J. Chem.*, 1973, **26**, 1889.
141. M. Jaber, F. Bertin and G. Thomas-David, *Canad. J. Chem.*, 1977, **55**, 3689.
142. J. Huet, J. Durand and Y. Infarnet, *Org. Magn. Resonance*, 1976, **8**, 382.
143. J. W. Akitt, N. N. Greenwood and A. Storr, *J. Chem. Soc. (A)*, 1965, 4410.
144. W. G. Movius and N. A. Matwiyoff, *Inorg. Chem.*, 1969, **9**, 925.
145. V. P. Tarasov, V. I. Privalov, Yu. A. Buslaev and I. A. Kuzmin, *Dokl. Akad. Nauk SSSR*, 1977, **234**, 636.
146. L. Rodehüser, P. L. Rubini and J. J. Delpuech, *Inorg. Chem.*, 1977, **16**, 2837.
147. C. H. F. Chang, T. P. Pitner, R. E. Lenkinski and J. D. Glickson, *Bioinorg. Chem.*, 1978, **8**, 11.
148. F. W. Wehrli, unpublished data.
149. W. G. Movius and N. A. Matwiyoff, *Inorg. Chem.*, 1969, **8**, 925.
150. Yu. A. Buslaev, V. P. Tarasov, M. N. Buslaeva and S. P. Petrosyants, *Dokl. Akad. Nauk SSSR*, 1973, **209**, 882.
151. U. Anders and J. A. Plambeck, *J. Inorg. Nuclear Chem.*, 1978, **40**, 387.
152. See e.g. G. E. Coates and K. Wade, "Organometallic Compounds", Methuen, London, 1967, Ch. 3.
153. L. Petrakis, *J. Phys. Chem.*, 1968, **72**, 4182.
154. C. P. Poole, Jr., H. E. Swift and J. F. Itzel, Jr., *J. Phys. Chem.*, 1965, **69**, 3663.
155. H. E. Swift, C. P. Poole, Jr. and J. F. Itzel, Jr., *J. Phys. Chem.*, 1964, **68**, 2509.
156. S. I. Vinogradova, V. M. Denisov and A. I. Koltsov, *Zh. Obshch. Khim.*, 1972, **42**, 1031.
157. M. Uetsuki and Y. Fujiwara, *Bull. Chem. Soc. Japan*, 1977, **50**, 673.
158. J. W. Akitt and R. H. Duncan, *J. Magn. Resonance*, 1974, **15**, 162.
159. W. H. N. Vriezen and F. Jellinek, *Chem. Phys. Lett.*, 1967, **1**, 284.
160. W. H. N. Vriezen and F. Jellinek, *Rec. Trav. Chim.*, 1970, **89**, 1306.
161. P. R. Oddy and M. G. H. Wallbridge, *J. Chem. Soc., Dalton*, 1976, 2076.
162. P. C. Lauterbur, R. C. Hopkins, R. W. King, O. V. Ziebarth and C. W. Heitsch, *Inorg. Chem.*, 1968, **7**, 1025.
163. J. Kaufmann, W. Sahm and A. Schwenk, *Z. Naturforsch.*, 1971, **26a**, 1384.
164. R. G. Kidd and H. G. Spinney, *J. Amer. Chem. Soc.*, 1973, **95**, 88.
165. P. Geerlings and Ch. v. Alsenoy, *J. Organometal. Chem.*, 1976, **117**, 13.

166. G. Balimann and P. S. Pregosin, *J. Magn. Resonance*, 1977, **26**, 283.
167. G. Balimann, Ph.D. Thesis No 6020, ETH Zürich, 1977.
168. P. Reinarrsson, T. Drakenberg and B. Lindman, *J. Magn. Resonance*, 1978, **29**, 169.
169. R. G. Kidd and R. W. Matthews, *J. Inorg. Nuclear Chem.*, 1975, **37**, 661.
170. P. Stilbs and G. Olofsson, *Acta Chem. Scand.*, 1974, **A28**, 647.
171. E. Fukushima and S. H. Mastin, *J. Magn. Resonance*, 1969, **1**, 648.
172. H. L. Retcofsky and R. A. Friedel, *Appl. Spectroscopy*, 1970, **24**, 379.
173. H. D. Schultz, C. Karr, Jr. and G. D. Vickers, *Appl. Spectroscopy*, 1971, **25**, 363.
174. H. L. Retcofsky and R. A. Friedel, *J. Amer. Chem. Soc.*, 1972, **94**, 6579.
175. O. Lutz, A. Nolle and A. Schwenk, *Z. Naturforsch.*, 1973, **28a**, 1370.
176. O. Lutz, W. Nepple and A. Nolle, *Z. Naturforsch.*, 1976, **31a**, 978.
177. R. R. Vold and R. L. Vold, *J. Chem. Phys.*, 1974, **61**, 4360.
178. O. Lutz, *Phys. Lett.*, 1969, **29A**, 58.
179. E. H. Pfadenhauer and D. C. McCain, *J. Phys. Chem.*, 1970, **74**, 3291.
180. V. P. Tarasov and Yu. A. Buslaev, *J. Magn. Resonance*, 1977, **25**, 197.
181. Yu. A. Buslaev, S. P. Petrosyants, V. P. Tarasov and V. I. Chagin, *Zh. Neorg. Khim.*, 1974, **19**, 1790.
182. G. A. Nelson, D. J. Olszanski and A. K. Rahimi, *Spectrochim. Acta*, 1977, **33A**, 301.
183. J. Reuben, *J. Amer. Chem. Soc.*, 1975, **17**, 3823.
184. J. Reuben and Z. Luz, *J. Phys. Chem.*, 1976, **80**, 1357.
185. M. E. Scott, H. C. Marsh, D. L. Harris, R. G. Hiskey and K. A. Koehler, *J. Biol. Chem.*, in press.
186. R. G. Kidd, R. W. Matthews and H. G. Spinney, *J. Amer. Chem. Soc.*, 1972, **94**, 6686.
187. O. W. Howarth and R. E. Richards, *J. Chem. Soc.*, 1965, 864.
188. J. A. S. Howell and K. C. Moss, *J. Chem. Soc. (A)*, 1971, 270.
189. D. Rehder, *Z. Naturforsch.*, 1977, **32b**, 771.
190. L. P. Kazanskii and V. I. Spitsyn, *Dokl. Akad. Nauk SSSR*, 1975, **223**, 381.
191. S. E. O'Donnell and M. T. Pope, *J. Chem. Soc., Dalton*, 1976 2290.
192. D. Rehder and J. Schmidt, *J. Inorg. Nuclear Chem.*, 1974, **36**, 333.
193. D. Rehder, W. L. Dorn and J. Schmidt, *Transition Met. Chem.*, 1976, **1**, 74.
194. D. Rehder, *J. Magn. Resonance*, 1977, **25**, 177.
195. W. G. Klemperer and W. Shum, *J. Amer. Chem. Soc.*, 1977, **99**, 3544.
196. W. G. Klemperer and W. Shum, *J. Amer. Chem. Soc.*, 1978, **100**.
197. L. P. Kazanskii and V. I. Spitsyn, *Dokl. Akad. Nauk SSSR*, 1975, **223**, 1798.
198. O. W. Howard and M. Jarrold, *J. Chem. Soc., Dalton*, 1978, 503.
199. K. J. Packer and E. L. Muetterties, *J. Amer. Chem. Soc.*, 1963, **85**, 3035.
200. Yu. A. Buslaev, V. D. Kopanev and V. P. Tarasov, *Chem. Comm.*, 1971, 1175.
201. R. G. Kidd and H. G. Spinney, *Inorg. Chem.*, 1973, **12**, 1967.
202. V. P. Tarasov, V. I. Privalov and Yu. A. Buslaev, *Mol. Phys.*, 1978, **35**, 1047.
203. Yu. A. Buslaev, E. G. Il'in and V. D. Kopanev, *Dokl. Akad. Nauk SSSR*, 1971, **196**, 829.
204. Yu. A. Buslaev, V. D. Kopanev, S. M. Sinitsyna and V. G. Khlebodarov, *Russ. J. Inorg. Chem.*, 1973, **18**, 1362.
205. K. A. Valiev and M. M. Zaripov, *Zh. Strukt. Khim.*, 1966, **7**, 494.
206. Y. Egozy and A. Loewenstein, *J. Magn. Resonance*, 1969, **1**, 494.
207. B. W. Epperlein, H. Krüger, O. Lutz and A. Nolle, *Z. Naturforsch.*, 1975, **30a**, 1237.
208. R. R. Vold and R. L. Vold, *J. Magn. Resonance*, 1975, **19**, 365.
209. O. Lutz, A. Nolle and P. Kroneck, *Z. Naturforsch.*, 1976, **31a**, 454.
210. K. U. Buckler, A. R. Haase, O. Lutz, M. Müller and A. Nolle, *Z. Naturforsch.*, 1977, **32a**, 126.
211. O. Lutz, A. Nolle and P. Kroneck, *Z. Physik*, 1977, **A282**, 157.
212. O. Lutz, A. Nolle and P. Kroneck, *Z. Naturforsch.*, 1977, **32a**, 505.

213. W. D. Kantt, H. Krüger, O. Lutz, H. Maier and A. Nolle, *Z. Naturforsch.*, 1976, **31a**, 351.
214. F. Calderazzo, E. A. C. Lucken and D. F. Williams, *J. Chem. Soc. (A)*, 1967, 154.
215. W. J. Miles, Jr., B. B. Garrett and R. J. Clark, *Inorg. Chem.*, 1967, **8**, 2817.
216. T. Nakano, *Bull. Chem. Soc. Japan*, 1977, **50**, 661.
217. O. Lutz and W. Steinkilberg, *Z. Naturforsch.*, 1974, **29a**, 1467.
218. A. R. Haase, O. Lutz, M. Müller and A. Nolle, *Z. Naturforsch.*, 1976, **31a**, 1427.
219. P. S. Ireland, C. A. Deckert and T. L. Brown, *J. Magn. Resonance*, 1976, **23**, 485.
220. R. A. Dwek, Z. Luz and M. Shporer, *J. Phys. Chem.*, 1970, **74**, 2232.
221. W. G. Proctor and F. C. Yu, *Phys. Rev.*, 1951, **81**, 20.
222. R. Freeman, G. R. Murray and R. E. Richards, *Proc. Roy. Soc.*, 1957, **A242**, 455.
223. J. S. Griffith and L. E. Orgel, *Trans. Faraday Soc.*, 1957, **53**, 601.
224. E. A. C. Lucken, K. Noack and D. F. Williams, *J. Chem. Soc. (A)*, 1967, 601.
225. A. Yamasaki, F. Yajima and S. Fujiwara, *Inorg. Chim. Acta*, 1968, **2**, 39.
226. G. P. Betteridge and R. M. Golding, *J. Chem. Phys.*, 1969, **51**, 2497.
227. N. A. Matwiyoff and W. E. Wageman, *Inorg. Chim. Acta*, 1970, **4**, 460.
228. R. S. Drago and J. H. Elias, *J. Amer. Chem. Soc.*, 1977, **99**, 6570.
229. F. P. Dwyer, A. M. Sargeson and L. P. James, *J. Amer. Chem. Soc.*, 1964, **86**, 590.
230. K. L. Craighead, *J. Amer. Chem. Soc.*, 1973, **95**, 4434.
231. A. Johnson and G. W. Everett, *Inorg. Chem.*, 1973, **12**, 2801.
232. W. Hackbusch, H. H. Rupp and K. Wiegardt, *J. Chem. Soc., Dalton*, 1975, 1015.
233. R. A. Rossa and T. L. Brown, *J. Amer. Chem. Soc.*, 1976, **96**, 2072.
234. W. Hackbusch, H. H. Rupp and K. Wiegardt, *J. Chem. Soc., Dalton*, 1975, 2364.
235. T. H. Martin and B. M. Fung, *J. Phys. Chem.*, 1973, **77**, 637.
236. K. L. Craighead, P. Jones and R. G. Bryant, *J. Phys. Chem.*, 1975, **79**, 1868.
237. K. L. Craighead and R. G. Bryant, *J. Phys. Chem.*, 1975, **79**, 1602.
238. A. Yamasaki, T. Ayoma, S. Fujiwara and K. Nakamura, *Bull. Chem. Soc. Japan*, 1978, **51**, 643.
239. T. Yamamoto, H. Haraguchi and S. Fujiwara, *J. Phys. Chem.*, 1970, **74**, 4369.
240. A. v. Zelewsky, W. Schläpfer and F. W. Wehrli, unpublished.
241. W. McFarlane and D. S. Rycroft, *J. Magn. Resonance*, 1976, **24**, 95.
242. B. W. Epperlein, H. Krüger, O. Lutz and A. Schwenk, *Z. Naturforsch.*, 1974, **29a**, 1553.
243. G. E. Maciel, L. Simeral and J. Ackerman, *J. Phys. Chem.*, 1977, **81**, 263.
244. V. P. Tarasov, V. I. Privalov and Yu. A. Buslaev, 20th Ampère Congress, Tallinn, 1978, Paper D2507.
245. V. P. Tarasov, S. P. Petrosyants, G. A. Kirakosyan and Yu. A. Buslaev, 20th Ampère Congress, Tallinn, 1978, Paper D2504.
246. V. P. Tarasov, S. P. Petrosyants, G. A. Kirakosyan and Yu. A. Buslaev, *Dokl. Akad. Nauk SSSR*, 1978, **242**, 156.
247. E. G. Il'in, V. P. Tarasov, M. M. Ershova, V. A. Ermakov, M. A. Glushkova and Yu. A. Buslaev, *Koord. Khim.*, 1978, **4**, 1370.
248. O. Lutz, H. Oehler and P. Kroneck, *Z. Physik*, 1978, **A288**, 17.
249. O. Lutz, H. Oehler and P. Kroneck, *Z. Naturforsch.*, 1978, **33a**, 1021.
250. H. M. McConnell and H. E. Weaver, *J. Chem. Phys.*, 1956, **25**, 307.
251. O. Lutz, personal communication.

# Silicon-29 NMR Spectroscopy

E. A. WILLIAMS AND J. D. CARGIOLI

*General Electric Co., Corporate Research and Development Center, Schenectady,  
New York 12301, USA*

I. Introduction . . . . .	221
II. Chemical shifts . . . . .	223
A. Theoretical background . . . . .	223
B. Reference compounds . . . . .	227
C. Substituted methylsilanes . . . . .	229
D. Arylsilanes . . . . .	236
E. Halogenosilanes . . . . .	237
F. Silicon hydrides and alkylsilanes . . . . .	238
G. Cyclic and polysilanes . . . . .	240
H. Organosilicones . . . . .	245
I. Silicates . . . . .	258
J. Silatranes . . . . .	261
K. Extracoordinate silicon compounds . . . . .	262
L. Solvent effects . . . . .	266
M. Steric effects . . . . .	268
N. Applications . . . . .	270
III. Coupling constants . . . . .	271
A. Theoretical considerations . . . . .	271
B. Calculations of silicon coupling constants . . . . .	272
C. One-bond coupling . . . . .	276
D. Longer range coupling . . . . .	282
IV. Relaxation phenomena and the nuclear Overhauser effect . . . . .	283
Appendix . . . . .	287
Acknowledgements . . . . .	312
References . . . . .	312

## I. INTRODUCTION

State-of-the-art in high resolution NMR has advanced to the point where many nuclei that have a spin can be observed with relative ease. The single most important contribution to the observation of dilute

nuclei of low sensitivity has been the discovery and development of the pulsed Fourier transform NMR method. (1) Multinuclei FT NMR instrumentation incorporating solid state electronics coupled with dedicated minicomputers has become a practical reality offered by many analytical instrument manufacturers.

For many years high resolution proton NMR satisfied the needs of most chemists to solve many complex characterization problems. As new techniques and instrumentation became available the desire to observe other nuclei by NMR increased. In organic chemistry, for example,  $^{13}\text{C}$  NMR has become one of the most powerful structure elucidation tools used, and in many laboratories it has surpassed proton NMR for routine product identification. The advantages are clear; there is more information to be gathered by studying the backbone of organic molecules than there is by studying the appendages. The same is true in inorganic chemistry.  $^{31}\text{P}$  and  $^{19}\text{F}$  have been studied by NMR for many years because of their high sensitivity and high natural abundance; the less abundant nuclei, however, are now becoming more popular because of the availability of multinuclei NMR spectrometers.

One nucleus that has become increasingly important from an NMR point of view is  $^{29}\text{Si}$ . Nearly seven-eighths of the earth's surface is made up of silicon compounds of one type or another. Silicones and silicates are finding their way into our life styles in the form of rubber, glues, additives, and consumer products. Silanes are important to the chemical industry as catalysts or additives in catalyst systems. New and better ways to characterize these compounds are urgently needed.

The  $^{29}\text{Si}$  isotope is a very difficult nucleus to observe because of its low natural abundance (4.7%) and low NMR sensitivity at constant field ( $7.84 \times 10^{-3}$ ) relative to  $^1\text{H}$ . To make matters worse, the magnetogyric ratio ( $\gamma$ ) is negative which means that under proton decoupling conditions the nuclear Overhauser effect enhancement (NOE) is negative. This can result in greatly reduced signal intensity, signals nulled into the base-line, or negative peaks. A further complication is that spin-lattice relaxation times ( $T_1$ ) for most  $^{29}\text{Si}$  nuclei are greater than 20 s, which makes time-averaged experiments very time-consuming. Fortunately, the addition of a small amount (0.01 M) of a relaxation reagent (2) to each sample is sufficient to shorten  $T_1$  to a few seconds by replacing all other relaxation mechanisms with a much more efficient electron-nuclear dipole-dipole interaction which dominates the spin-lattice relaxation. Since the proton-nuclear dipole-dipole relaxation mechanism becomes unimportant, under proton decoupling conditions the NOE is eliminated.

Short  $^{29}\text{Si}$   $T_1$  values and the absence of any NOE produces an absorption spectrum similar to that obtained for  $^{13}\text{C}$  and with the same relative ease. The result is that much more chemical shift information has been gathered (3-6) in addition to a substantial amount of data concerning  $^{29}\text{Si}$  relaxation times, coupling constants, and Overhauser effects.

## II. CHEMICAL SHIFTS

### A. Theoretical background

Although the theory of nuclear shielding is well established, it is apparent that the relationship between  $^{29}\text{Si}$  chemical shifts and theoretical concepts is not straightforward. The shielding constant of a nucleus can be presented as a sum of local and long range effects: (7)

$$\sigma = \sigma_d + \sigma_p + \sigma' \quad (1)$$

where the local contribution is further divided into a diamagnetic term  $\sigma_d$  and a paramagnetic term  $\sigma_p$ . The long range effects ( $\sigma'$ ) are contributions from other atoms in the molecule and include such factors as magnetic anisotropy and electric field effects. It is usually assumed that local effects dominate  $^{29}\text{Si}$  nuclear shielding. The diamagnetic term depends on the electron density at the nucleus and is given by Lamb's formula: (8)

$$\sigma_d = (\mu_0 e^2 / 12m\pi) \sum_i P_{ii} \langle r_i^{-1} \rangle \quad (2)$$

where  $P_{ii}$  is the charge density in the atomic orbital  $i$  which is at an average distance of  $r_i$  from the nucleus. The paramagnetic term may be written: (9)

$$\sigma_p = (-\mu_0 e^2 \hbar^2 / 6\pi m^2 \Delta E) [\langle r^{-3} \rangle_p P_u + \langle r^{-3} \rangle_d D_u] \quad (3)$$

where  $\Delta E$  is a mean excitation energy,  $\langle r^{-3} \rangle_p$  and  $\langle r^{-3} \rangle_d$  are the mean inverse cubes of the distances of the valence p and d electrons from the nucleus, and  $P_u$  and  $D_u$  represent the unbalance of the p and d electron populations. These last terms include elements of the charge density and bond order matrix. Although changes in  $\sigma_p$  are generally accepted as dominant for heavier nuclei, this assumption has been strongly challenged. (10)

Problems in theoretical calculations of  $^{29}\text{Si}$  chemical shifts arise because of uncertainties regarding the magnitude of substituent effects on the values of the  $\Delta E$ ,  $\langle r^{-3} \rangle$ , and  $P_u$  terms in equation (3). Furthermore, it is not clear if the d-orbital term may be neglected, and

whether or not  $(p-d)\pi$  bonding is significant. In one of the earliest discussions of  $^{29}\text{Si}$  shieldings, Lauterbur (3) graphically demonstrated the "sagging" pattern exhibited by compounds of the type  $(\text{CH}_3)_n\text{SiX}_{4-n}$  as  $n$  is varied from 0 to 4 and when X is an electronegative group (Fig. 1). The comparison of  $^{13}\text{C}$  and  $^{29}\text{Si}$  shieldings in the series  $(\text{CH}_3)_n\text{M}(\text{OR})_{4-n}$  presented by Lauterbur also shows the significant differences in substituent effects for the two nuclei, a phenomenon which is attributed to  $(p-d)\pi$  bonding effects in the silanes (in addition to the inductive effects which should be similar for both nuclei). Since Hunter and Reeves published their collection of chemical shift data, (4) and the subsequent explosion of papers in the field, several attempts to explain silicon shieldings have been made.

Ernst *et al.* (11) found that plots of  $\delta_{\text{Si}}$  vs. Hammett  $\sigma$  constants for a series of aryl silanes  $\text{ArSiY}_3$  give different slopes of both positive and negative sign depending upon the nature of Y (Fig. 2). In order to explain these changes in sign, the approach used by Letcher and Van Wazer (12) for  $^{31}\text{P}$  chemical shifts was adopted. This theory considers only changes in  $\sigma_p$  and derives chemical shift contributions from p electrons as a function of substituent electronegativities. The value of  $\langle r^{-3} \rangle_p / \Delta E$  is assumed to be constant. Their calculations of  $\delta_{\text{Si}}$  reproduce the experimentally found reversal in slope. However, the theoretically determined electronegativity of Y at which the slope of the Hammett plot changes sign is in disagreement with the experimental

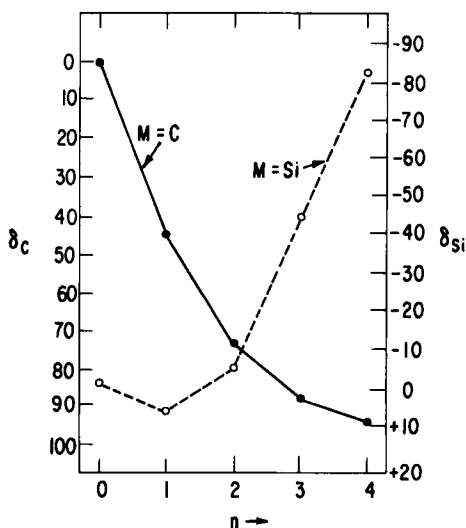


FIG. 1.  $^{13}\text{C}$  and  $^{29}\text{Si}$  chemical shifts in the series  $\text{Me}_n\text{Si}(\text{OR})_{4-n}$ . (3) Shifts in ppm relative to  $\text{Me}_4\text{Si}$ .

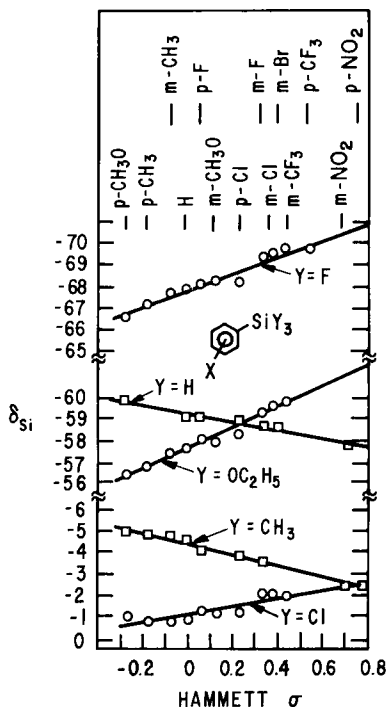


FIG. 2. Hammett plots of  $^{29}\text{Si}$  chemical shifts (in ppm from  $\text{Me}_4\text{Si}$ ) of arylsilanes. (11)

observations, and the results must be considered qualitative. A single electronegativity summation over all the silicon substituents was used by the same authors to generate the U-shaped relationship with silicon shielding shown in Fig. 3. (11) Although this relationship is quite rough, it nonetheless predicts the appropriate trends for many silanes with substituents of vastly different electronic properties. In another empirical approach, pairwise interaction parameters were found to be useful for predicting silicon chemical shifts in a number of silanes. (251) Deviations from pairwise additivity are significant, however, for fluorine or oxygen substituents on silicon.

Earlier, Engelhardt *et al.* (13) presented a semi-empirical theory which achieved qualitative success in predicting  $^{29}\text{Si}$  chemical shifts for compounds of the structure  $(\text{CH}_3)_{4-n}\text{SiX}_n$ . They used only the local paramagnetic contribution to the chemical shift, the average excitation energy approximation with a constant value of  $\Delta E$ , and neglected  $(p-d)\pi$  contributions. The  $\sigma$  bonding structure is described by four localized orbitals and assumed tetrahedral bond angles on silicon. A single empirical correction factor is found to be necessary in



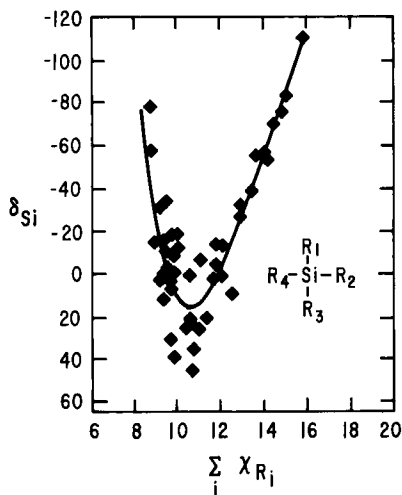


FIG. 3. Plot of  $^{29}\text{Si}$  chemical shifts of substituted silanes in ppm relative to  $\text{Me}_4\text{Si}$  vs. the sum of the substituent electronegativities. (11)

addition to the Si and substituent electronegativities. This approach is able to account for the "sagging" pattern (13) as well as the Hammett plots in ref. 11. (14) An angular correction factor was later introduced (15) for silanes with substituents of highly different electronegativity (e.g.  $\text{Si}_2\text{F}_6$ ) to account for rehybridization of the silicon atom. This model is qualitatively confirmed by CNDO/2 calculations for which the best results are found by neglecting d-orbitals. (16)

Although reasonable success has been achieved employing only changes in  $\sigma_p$ , van den Berghe and van der Kelen (17) have suggested that electric field and magnetic anisotropy interactions as well as changes in  $\sigma_d$  may be major contributors to  $^{29}\text{Si}$  shielding variations in halogenosilanes. Furthermore, the assumption of a constant value of  $\Delta E$  in the paramagnetic term has been shown to be invalid (18) according to CNDO/2 calculations for compounds of the type  $\text{Me}_{4-n}\text{SiX}_n$  ( $X = \text{F}, \text{OMe}, \text{NMe}_2, \text{Cl}$ ). Lyubimov and Ionov (19) previously demonstrated that variations in  $\Delta E$  are sufficient to account for deviations in additivity of two series of substituted silanes. Using calculated values of  $\Delta E$  they are able to reproduce the observed shielding trends for the systems  $\text{F}_{4-n}\text{SiX}_n$  where  $X = \text{Br}$  or  $\text{Cl}$ .

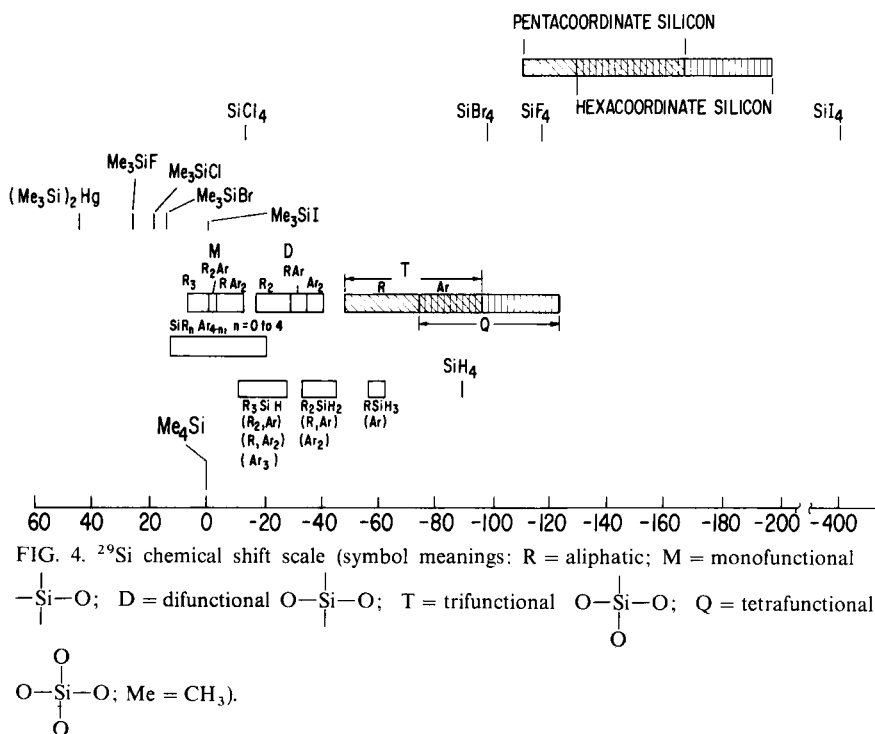
Thus it becomes apparent that a comprehensive and quantitative theoretical treatment may require a revision of some of the simplifying assumptions that have provided qualitative explanations for silicon shieldings. Meanwhile, the qualitative interpretations are sufficient for many of the structural problems to which  $^{29}\text{Si}$  NMR is applied.

## B. Reference compounds

The present practical  $^{29}\text{Si}$  chemical shift range is about 250 ppm, with trimethylhalogenosilanes appearing at the high frequency end of the spectrum and extravalent (6) silicon compounds occurring at the low frequency end. As in  $^{13}\text{C}$  NMR, the tetraiodo derivative ( $\text{SiI}_4$ ) is the most shielded resonance (20) found to date, and if included it would extend the  $^{29}\text{Si}$  chemical shift range to about 400 ppm (Fig. 4). With the large amount of chemical shift data appearing in the literature it is becoming increasingly important to define the  $^{29}\text{Si}$  chemical shift scale relative to an accepted reference standard.

The convention for selecting a standard reference compound for most nuclei has been to use a compound that: (a) has a single resonance line, (b) has good solubility in most solvents yet remains unreactive, and (c) appears at the low frequency end of the spectrum so that all other resonance lines can then be reported in ppm as positive numbers to the high frequency side of the standard. (21)

Several reference compounds have been suggested for  $^{29}\text{Si}$  NMR. Early studies reported  $^{29}\text{Si}$  chemical shifts for organosilicone



compounds relative to polydimethylsiloxane. (1,3) More recently, tetramethylsilane ( $\text{Me}_4\text{Si}$ ), (22–31) tetramethoxysilane  $[(\text{MeO})_4\text{Si}]$ , (32) and tetraethoxysilane  $[(\text{EtO})_4\text{Si}]$  (33) have been suggested. Tetrafluorosilane (34, 35) and octamethylcyclotetrasiloxane  $[(\text{Me}_2\text{SiO})_4]$  (33) have also been suggested. Several workers (33, 36) have examined the effect of solvent on internal  $^{29}\text{Si}$  chemical shifts in a mixture of  $\text{Me}_4\text{Si}$ , hexamethyldisiloxane  $[(\text{Me}_3\text{Si})_2\text{O}]$ , and  $(\text{EtO})_4\text{Si}$  (33) in different solvent systems. Levy *et al.* (33) determined the internal chemical shifts of  $(\text{Me}_2\text{SiO})_4$ ,  $(\text{Me}_2\text{SiO})_x$ , and  $(\text{MeO})_4\text{Si}$  in carbon tetrachloride, and compared  $(\text{Me}_3\text{Si})_2\text{O}$  and  $\text{Me}_4\text{Si}$  shifts in six solvent systems (Table I) in an attempt to find a suitable reference compound. The ranges of observed  $^{29}\text{Si}$  shifts for  $\text{Me}_4\text{Si}$  (0.8 ppm) and  $(\text{Me}_3\text{Si})_2\text{O}$  (0.3 ppm) are both somewhat smaller than analogous solvent-induced  $^{13}\text{C}$  shifts. (37) For both  $\text{Me}_4\text{Si}$  and  $(\text{Me}_3\text{Si})_2\text{O}$  the resonances in carbon tetrachloride are at the high frequency end of these ranges.

The original suggestion was to use the  $(\text{EtO})_4\text{Si}$  resonance line as a standard because it is located at the low frequency end of the spectral range, is reasonably stable, and is commercially available.  $(\text{EtO})_4\text{Si}$  has, however, one of the slowest relaxing silicon nuclei (38) with a  $T_1 \approx 135$  at  $38^\circ\text{C}$ . In  $^{29}\text{Si}$  NMR studies not utilizing effective

TABLE I  
 $^{29}\text{Si}$  chemical shifts for some reference compounds (33)<sup>a</sup>

Compound	Solvent	$^{29}\text{Si}$ (ppm)	
$[(\text{CH}_3)_3\text{Si}]_2\text{O}$ (MM)		6.87	
$(\text{CH}_3)_4\text{Si}$ (TMS)	$\text{CCl}_4$	0.00	
$[(\text{CH}_3)_2\text{SiO}]_4$	$\text{CCl}_4$	-19.54	
$(\text{CH}_3)_3\text{SiO}[(\text{CH}_3)_2\text{SiO}]_x\text{Si}(\text{CH}_3)_3$ ( $\bar{x} \approx 50$ )	$\text{CCl}_4$	-22.22	
$(\text{CH}_3\text{O})_4\text{Si}$	$\text{CCl}_4$	-79.22	
TMS, MM <sup>b</sup>		TMS	MM
	cyclohexane	82.4	89.2
	acetone	82.1	89.2
	benzene	81.7	89.1
	methylene chloride	82.2	89.3
	dioxan	82.3	89.4
	carbon tetrachloride		
	$2 \times 10^{-2}$ M $\text{Cr}(\text{acac})_3$	82.5	89.4
	$5 \times 10^{-2}$ M $\text{Cr}(\text{acac})_3$	82.5	89.4
	$5 \times 10^{-2}$ M $\text{Fe}(\text{acac})_3$	82.5	89.4

<sup>a</sup> At  $\sim 30^\circ$ . Chemical shifts determined  $\pm 0.07$  ppm relative to internal  $\text{Me}_4\text{Si}$  unless otherwise noted. Positive shifts are to high frequency.

<sup>b</sup> Chemical shifts relative to internal  $(\text{EtO})_4\text{Si}$ : solute and  $(\text{EtO})_4\text{Si}$  concn. 15%, v/v.

paramagnetic relaxation reagents such as  $\text{Cr}(\text{acac})_3$  (2, 38, 39) or  $\text{Fe}(\text{acac})_3$  (40) (e.g. for  $T_1$  or NOE studies) the resonance of  $(\text{EtO})_4\text{Si}$  will be difficult to observe; high concentrations ( $>10\%$ ) of the standard are required.  $\text{Me}_4\text{Si}$  has a short  $T_1$  near room temperature (4, 41) and can be used as a reference at lower concentrations ( $<5\%$ ). Unfortunately, the  $\text{Me}_4\text{Si}$  resonance lies in the middle of the range of common  $^{29}\text{Si}$  chemical shifts. It does, however, seem to be the most widely accepted  $^{29}\text{Si}$  standard despite some inherent problems. (42) In this review all chemical shifts, unless otherwise noted, are reported relative to  $\text{Me}_4\text{Si}$  with positive shifts to high frequency.

### C. Substituted methylsilanes

The largest body of data on  $^{29}\text{Si}$  chemical shifts has been collected for substituted methylsilanes,  $\text{Me}_{4-n}\text{SiX}_n$  and  $\text{Me}_{3-n}\text{X}_n\text{Si}(\text{CH}_2)_m\text{Y}$ . Substituent effects are probably most clearly examined by starting with the monosubstituted trimethylsilyl derivatives,  $\text{Me}_3\text{SiX}$ . (3, 4, 22, 26, 32, 42, 43) Early workers (4) noted a dependence of the  $^{29}\text{Si}$  chemical shift on the electronegativity of the substituent ( $\chi_x$ ), with the least shielded silicon nuclei appearing in the compounds with the most electronegative substituents. Harris *et al.* (42, 43) conducted an extensive study of fourteen trimethylsilyl compounds in which they noted that the correlation of  $\delta_{\text{Si}}$  and  $\chi_x$  is actually quite poor (Fig. 5), whereas a good linear correlation is obtained for  $^1J(\text{Si}-\text{C})$  vs.  $\chi_x$  (Section III). This suggests that factors other than simple inductive effects are operating in these compounds. They found no correlation between the  $^{29}\text{Si}$  and  $^{13}\text{C}$  chemical shifts in the series. Comparison of the  $^{29}\text{Si}$  data for the trimethylsilyl derivatives with the  $^{13}\text{C}$  data of the

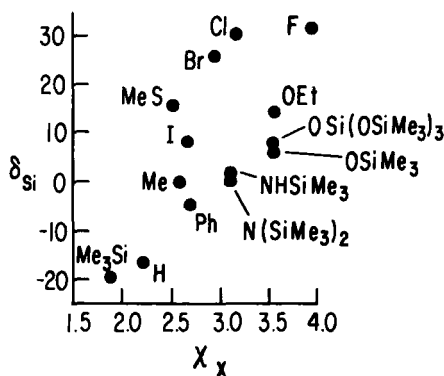


FIG. 5. Plot of  $^{29}\text{Si}$  chemical shifts vs. substituent electronegativity,  $\chi_x$ , for trimethylsilyl compounds,  $\text{Me}_3\text{SiX}$ . (42)

analogous *t*-butyl derivatives (26) shows that the trend with  $\chi_x$  predicted by Engelhardt's approach, which excludes (p-d) $\pi$  interactions (Section II.A), is followed in the  $^{13}\text{C}$  series but not in the  $^{29}\text{Si}$  series. The most serious deviations from the predicted order occur in the  $\text{X} = \text{OR}$  and  $\text{X} = \text{F}$  derivatives. Since these are the substituents most likely to  $\pi$  bond, the authors suggest that this might lead to the poor correlation between  $\delta_{\text{Si}}$  and  $\chi_x$ . It was pointed out, however, that there is no definitive evidence for this.

Linear correlations between the  $\text{pK}_a$  of acids and the  $^{29}\text{Si}$  chemical shift of the corresponding trimethylsilyl esters were found by McFarlane and Seaby (24) and Marsmann and Horn. (44) In the study conducted by the former authors, a series of substituted methylsilyl carboxylates  $\text{Me}_{4-n}\text{Si}(\text{O}_2\text{CR})_n$  were examined. Although a smaller chemical shift range was covered in this series than in the inorganic and organic acids examined by Marsmann and Horn, the advantage is that the structural changes are three bonds removed from silicon. This eliminates variations in the silicon shielding from factors other than the electronic effect of the R group. A good linear correlation (Fig. 6) with the  $\text{pK}_a$  of the acids is obtained for the mono-, di-, and tri-carboxylates for R groups of varying electronegativity. The slope of the lines for  $n = 1, 2$ , and 3 decreases from 1.0 to 0.88 and 0.42 respectively. As is the case for many of the trends in  $^{29}\text{Si}$  shieldings, several alternative

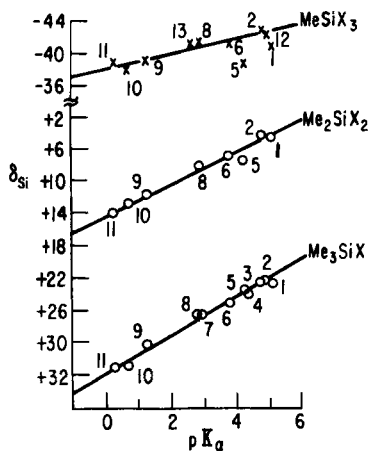


FIG. 6. Plot of  $^{29}\text{Si}$  chemical shifts (in ppm relative to  $\text{Me}_4\text{Si}$ ) of the methylsilyl carboxylates  $\text{Me}_3\text{SiX}$ ,  $\text{Me}_2\text{SiX}_2$ , and  $\text{MeSiX}_3$  vs. the  $\text{pK}_a$  of the corresponding acid  $\text{HX}$ : (24)  $\text{X} = \text{RCOO}$  where  $\text{R} =$  (1)  $^t\text{Bu}$ , (2)  $\text{Me}$ , (3)  $\text{CH}=\text{CHMe}$ , (4)  $\text{CH}_2\text{Ph}$ , (5)  $\text{Ph}$ , (6)  $\text{H}$ , (7)  $\text{CH}_2\text{Br}$ , (8)  $\text{CH}_2\text{Cl}$ , (9)  $\text{CHCl}_2$ , (10),  $\text{CCl}_3$ , and (11)  $\text{CF}_3$ .

explanations are possible, and concepts such as (p-d) $\pi$  bonding,  $\sigma$ - $\pi$  conjugation, (45) and bond polarization by electronegative substituents may be invoked. For example, an increase in the electronegativity of R, and therefore of the carboxylate group, increases the electron unbalance of the Si-O bond by giving more electron withdrawing character to the oxygen atom. When two or three carboxylate groups are substituted on silicon, the silicon electron density is reduced and the net change in  $P_u$ , and therefore  $\sigma_p$ , is smaller. Alternatively, if (p-d) $\pi$  bonding occurs between oxygen and silicon in these systems, the electron withdrawing effect is mitigated by the presence of other carboxylate groups and the net change in electron density at silicon is small.

Data showing the effect of multiple  $\alpha$ -substitution at silicon are presented graphically in Figs. 7 and 8. Figure 7 shows the "sagging" pattern observed for the electronegative substituents OMe, NMe<sub>2</sub>, Br, F, and Cl. The exceptional behaviour exhibited by the series Me<sub>4-n</sub>Si(SMe)<sub>n</sub> is attributed to van der Waals interactions and the diamagnetic anisotropy of the C-S bond. (46) In contrast to Fig. 7, no "sagging" pattern is observed for the substituents presented in Fig. 8. It was suggested that this is due to the absence of opposing inductive and (p-d) $\pi$  bonding effects for these derivatives. Clearly this explanation is not necessary since reasonable quantitative results can be obtained without including d-orbitals in the theoretical treatment. (26) In either case, it is obvious that the substituent effect is not a constant value.

Several studies have been conducted by Schraml *et al.* (31, 47-52) on the effect of  $\beta$ -substituents on the trends observed for silicon shielding with multiple  $\alpha$ -substitution. A series of derivatives of general structure Me<sub>3-n</sub>X<sub>n</sub>Si(CH<sub>2</sub>)<sub>m</sub>Y was examined in which X = F, Cl, O<sup>i</sup>Bu, OSiMe<sub>3</sub>, OEt, OAc, or Et, and Y = OAc, NH<sub>2</sub>, Ph, Cl, or CH=CH<sub>2</sub> ( $m = 1$ ). In addition, the vinyl and phenyl silanes ( $m = 0$ ) have also been examined.

In most cases the results were compared with those for the corresponding methyl derivatives Me<sub>4-n</sub>SiX<sub>n</sub>. In all cases in which a  $\beta$ -substituent was added ( $m = 1$ ) the general trend of the shielding for the same X substituent with increasing  $n$  is maintained. This is not surprising since it would be expected that the more remote  $\beta$ -substituent would have less effect on the silicon shielding than the groups directly attached to silicon. For comparative purposes, a substituent chemical shift (SCS) increment,  $\Delta\delta$ , is defined by:

$$\Delta\delta = \delta_{\text{Si}}[\text{Me}_{3-n}\text{X}_n\text{Si}(\text{CH}_2)_m\text{Y}] - \delta_{\text{Si}}[\text{Me}_{3-n}\text{X}_n\text{Si}(\text{CH}_2)_m\text{H}] \quad (4)$$

If this is plotted as a function of  $n$  for the series when  $m = 1$ , the relationships shown in Fig. 9 are obtained. If  $n = 0$ , the effect of

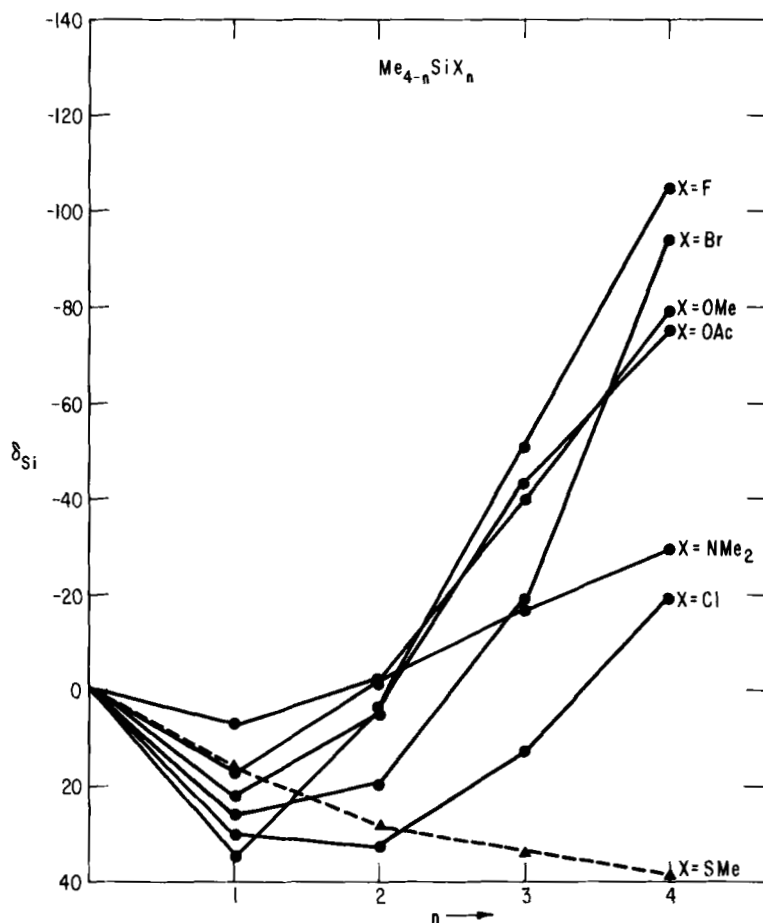


FIG. 7.  $^{29}\text{Si}$  chemical shifts (in ppm relative to  $\text{Me}_4\text{Si}$ ) for the methylsilanes  $\text{Me}_{4-n}\text{SiX}_n$ . Data are from ref. 6 and references therein; data for  $\text{X} = \text{SMe}$ ,  $\text{OMe}$ ,  $\text{NMe}_2$  are from ref. 46.

replacing a methyl group with a  $\text{CH}_2\text{Y}$  substituent ( $\text{Me}_4\text{Si} \rightarrow \text{Me}_3\text{SiCH}_2\text{Y}$  where  $\text{Y}$  is electronegative) is a small high frequency shift in the silicon resonance. Each subsequent increase in  $n$  ( $n > 0$ ), however, leads to a low frequency shift relative to the corresponding methyl derivative and the absolute value of  $\Delta\delta$  increases with  $n$ .

If the substituent  $(\text{CH}_2)_m\text{Y}$  is changed from methyl to allyl to vinyl ( $\text{Y} = \text{H}$ ,  $m = 1$ ;  $\text{Y} = \text{CH}=\text{CH}_2$ ,  $m = 1$ ;  $\text{Y} = \text{CH}=\text{CH}_2$ ,  $m = 0$ , respectively) the shielding trends for the same  $\text{X}$  substituent are not appreciably affected, although the vinyl derivatives are in all cases more

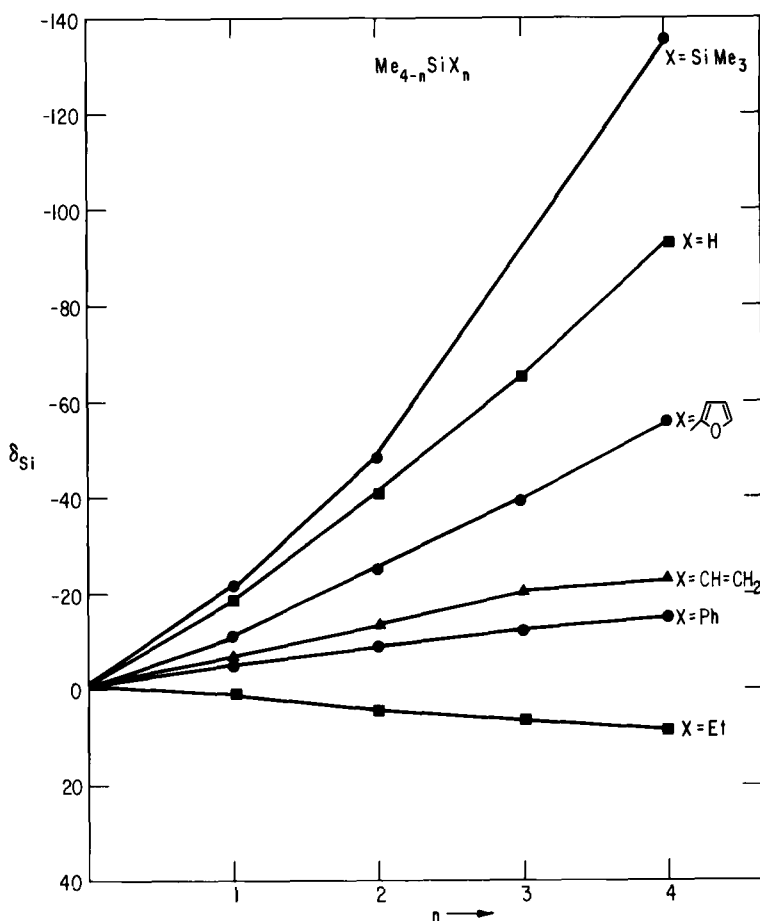


FIG. 8.  $^{29}\text{Si}$  chemical shifts for the methylsilanes  $\text{Me}_{4-n}\text{SiX}_n$ . Data are from ref. 6 and references therein; data for  $\text{X} = \text{furyl}$  are from ref. 96; data for  $\text{X} = \text{SiMe}_3$  are from refs. 32 and 73.

shielded than the allyl derivatives, which are more shielded than the methyl derivatives. (49) Similarly, very little change in trend is observed in the sequence from methyl to benzyl to phenyl ( $\text{Y} = \text{H}$ ,  $m = 1$ ;  $\text{Y} = \text{Ph}$ ,  $m = 1$ ;  $\text{Y} = \text{Ph}$ ,  $m = 0$ , respectively; Fig. 10), although the shifts are to low frequency relative to the corresponding methyl derivative and the absolute value of  $\Delta\delta$  increases with  $n$ .

The effects of introduction of an electronegative  $\beta$ -substituent in ethoxysilanes  $\text{Me}_{3-n}(\text{EtO})_n\text{SiCH}_2\text{Y}$  were compared with compounds of "inverted" structure  $\text{Me}_{4-n}\text{Si}(\text{OCH}_2\text{CH}_2\text{Y})_n$  by Schraml *et al.* (52) In



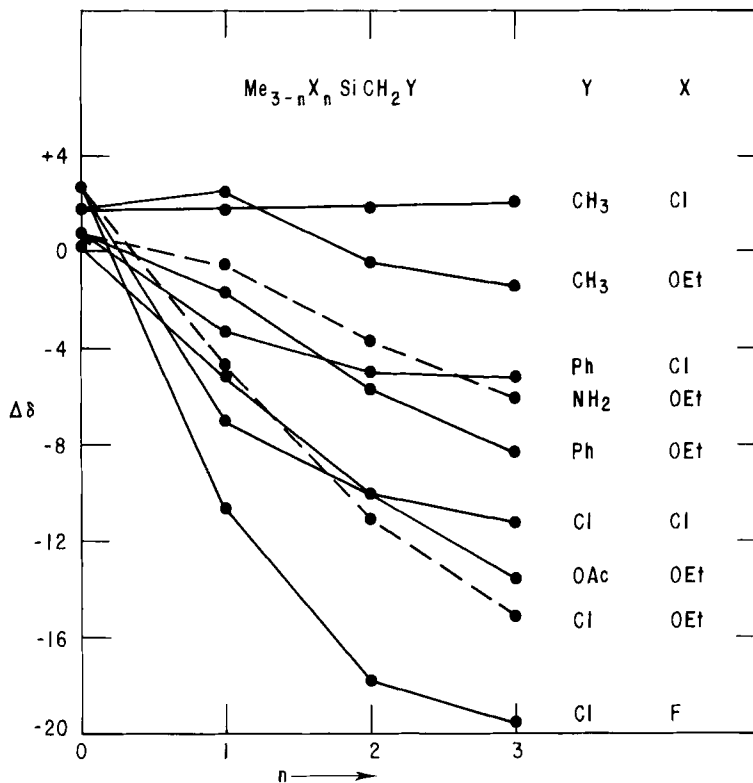


FIG. 9. Plot of  $\Delta\delta$  vs.  $n$  for the methylsilanes  $\text{Me}_{3-n}\text{X}_n\text{SiCH}_2\text{Y}$ . Data are from refs. 31, 47-49, and 52.

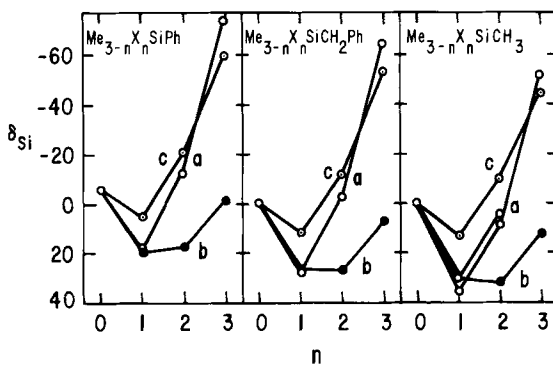


FIG. 10. Chemical shift trends in the series  $\text{Me}_{3-n}\text{X}_n\text{SiR}$  where  $\text{R} = \text{Ph}, \text{CH}_2\text{Ph},$  and  $\text{CH}_3$ ;  $\text{X} = (\text{a}) \text{F}, (\text{b}) \text{Cl}, (\text{c}) \text{OE}_t$ . (49)

the former case the change from  $Y = H$  to  $Y = NH_2$  ( $n = 1$  to 3) leads to a low frequency shift in the silicon resonance, whereas in the latter case an introduction of an electronegative substituent ( $Y = H$  to  $Y = NH_2$  or  $Cl$ ) leads to a high frequency shift for all values of  $n$ . These results are consistent with the concept of  $(p \rightarrow d)\pi$  bonding in these compounds. In the former case ( $X-Si \cdots Y$ ) the electronegative substituent  $Y$  enhances the  $X \rightarrow Si$  backbonding and a net shielding effect is observed. In the inverted compounds ( $Si-X \cdots Y$ ) the effect is to decrease the efficiency of  $X \rightarrow Si$  backbonding and inductively remove electron density from silicon as well; both effects result in a deshielding of the silicon nucleus. The authors attributed the chemical shift changes in these systems to four factors: (1) the electron withdrawing ability of  $Y$ ; (2) the efficiency of the saturated chain at transmitting inductive effects (if the substituent  $Y$  is placed further from silicon on a longer alkyl chain the effect is severely reduced); (3) the backbonding ability of  $X$ ; and (4) the electron withdrawing ability of  $X$ . The influence of the first factor is illustrated by the fact that the slopes of the  $\Delta\delta$  vs.  $n$  plots for  $Y = NH_2$ ,  $OAc$ ,  $Cl$  in the ethoxy derivatives (Fig. 11) correspond roughly to the substituent inductive effects of  $Y$ .

Much larger effects, of course, are observed if the substituent  $Y$  is directly attached to silicon. In a recent paper (53) silicon chemical shifts of several  $N$ -silylated triorganophosphinimines are reported. A comparison similar to those shown above is made between derivatives for  $X = Cl$ ,  $OMe$  (Table II). The results obtained in this investigation are explained preferentially on the basis of hyperconjugation rather than  $(p \rightarrow d)\pi$  bonding. If this is assumed to be the dominant

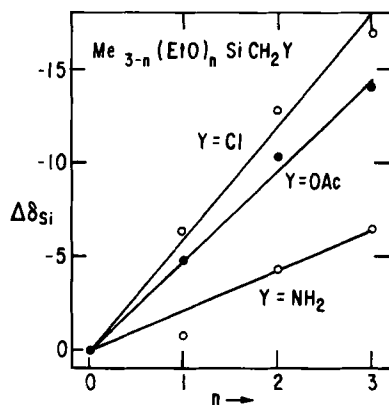


FIG. 11. Plot of  $\Delta\delta$  vs.  $n$  for the ethoxy-substituted methylsilanes  $Me_{3-n}(EtO)_nSiCH_2Y$ , where  $X = (a) F, (b) Cl, (c) OEt$ . (49)

TABLE II

Substituent effect of the  $\text{Et}_3\text{P}=\text{N}$  group in substituted methylsilanes  $\text{Et}_3\text{PNSiX}_n\text{Me}_{3-n}$ <sup>a</sup>

Compound	$\delta(^{29}\text{Si})$ (53)	Compound	$\delta(^{29}\text{Si})$ (13)	$\Delta\delta$
$\text{Et}_3\text{PNSiMe}_3$	-15.73	$\text{Me}_4\text{Si}$	0.0	-15.7
$\text{Et}_3\text{PNSiMe}_2\text{Cl}$	-7.87	$\text{Me}_3\text{SiCl}$	29.5	-37.4
$\text{Et}_3\text{PNSiMeCl}_2$	-25.29	$\text{Me}_2\text{SiCl}_2$	32.0	-57.3
$\text{Et}_3\text{PNSiCl}_3$	-54.35	$\text{MeSiCl}_3$	12.1	-66.5
		$\text{SiCl}_4$	-18.5	
$\text{Et}_3\text{PNSiMe}_3$	-15.73	$\text{Me}_4\text{Si}$	0.0	-15.7
$\text{Et}_3\text{PNSiMe}_2(\text{OMe})$	-17.26	$\text{Me}_3\text{Si}(\text{OMe})$	17.2	-34.5
$\text{Et}_3\text{PNSiMe}(\text{OMe})_2$	-40.07	$\text{Me}_2\text{Si}(\text{OMe})_2$	-2.5	-37.6
$\text{Et}_3\text{PNSi}(\text{OMe})_3$	-69.94	$\text{MeSi}(\text{OMe})_3$	-41.1	-28.5
		$\text{Si}(\text{OMe})_4$	-79.2	

<sup>a</sup>Chemical shifts in ppm relative to  $\text{Me}_4\text{Si}$ .

mechanism by which the silicon acts as an acceptor, the chemical shifts will be dependent upon: (1) the influence of the substituent electronegativity on the  $\sigma$  framework; (2) the  $\pi$  donor ability of the substituents; (3) the availability of the  $\sigma^*$  orbital as a  $\pi$  acceptor (this is again dependent on substituent electronegativity); and (4) repression of  $\pi$  bonding of one substituent by the presence of other  $\pi$  donors. The significance of items 1 and 3 is demonstrated by the monotonic change in  $\Delta\delta$  for the chloro derivatives, whereas the maximum which occurs at  $n = 2$  for the methoxy derivative is attributed to item 4.

#### D. Arylsilanes

The linear correlation between silicon chemical shifts and Hammett  $\sigma$  constants in trimethylsilyl substituted benzenes was first pointed out by Scholl *et al.* (32) Subsequent studies (54, 55) demonstrated that, although a high degree of linearity existed between  $\sigma$  and  $\delta_{\text{Si}}$  of the silanes  $\text{XC}_6\text{H}_4\text{SiY}_3$  where  $\text{Y} = \text{F}, \text{OEt}, \text{CH}_3, \text{H}, \text{and Cl}$  (Fig. 2), the magnitude and signs of the slopes of these lines are not necessarily the same. Thus, for the electronegative substituents  $\text{Y} = \text{F}, \text{Cl}, \text{and OEt}$ , an increase in the electron withdrawing ability of  $\text{X}$  leads to a shielding effect at silicon, and the opposite is observed for  $\text{Y} = \text{CH}_3$  and  $\text{H}$ . Unfortunately, data for an intermediate series such as  $\text{ArSiF}_2\text{Me}$  or  $\text{ArSiFMe}_2$  are not available.

An oxygen link between the phenyl ring and silicon has been found to enhance the substituent effect. (56, 252) Both phenyltrimethylsilanes and phenoxytrimethylsilanes give reasonable linear correlations

between  $\delta_{\text{Si}}$  and Hammett  $\sigma$  constants but the slope for the phenoxytrimethylsilanes is greater even though the silicon is one bond further removed from the substituents. (56)

### E. Halogenosilanes

Most studies of halogenosilanes have been concerned with the methylsilanes (Section II.C). The data that have been collected for the mixed silicon halides  $\text{Y}_{4-n}\text{SiX}_n$  (26, 57) are presented graphically in Fig. 12. In contrast to the methylhalogenosilanes ( $\text{Me}_{4-n}\text{SiF}_n$  is shown in Fig. 12 for comparison), the "sagging" pattern, which is apparently

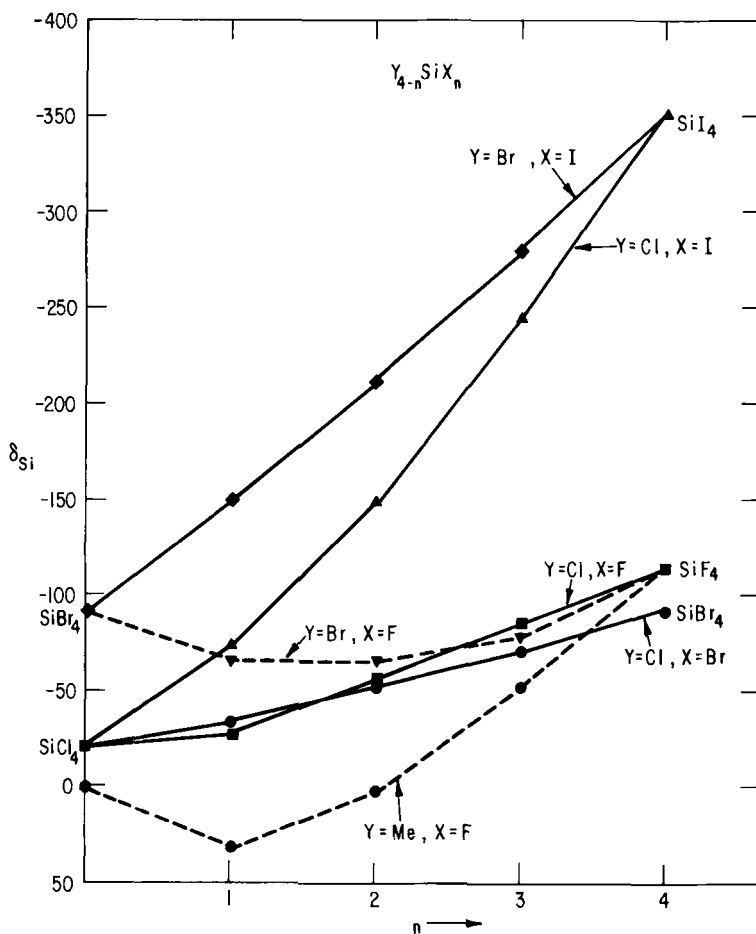


FIG. 12. Chemical shift trends for the mixed halogenosilanes  $\text{Y}_{4-n}\text{SiX}_n$ . (26, 57) Shifts are in ppm relative to  $\text{Me}_4\text{Si}$ .

dependent upon an electronegativity difference between X and Y, is not characteristic of these compounds. As mentioned above, the tetraiodo derivative appears well above other silicon resonances and at  $-346.2$  ppm (58) defines the present low frequency limit for  $^{29}\text{Si}$  chemical shifts. The pronounced shielding effect of iodine and, to a lesser degree, bromine is similar to that observed for the analogous carbon derivatives—the “heavy-atom effect”. (59)

## F. Silicon hydrides and alkylsilanes

Most silicon hydride shifts appear beyond  $\text{Me}_4\text{Si}$  at relatively low frequencies. Replacement of each subsequent methyl group with a hydride ( $\text{Me}_4\text{Si} \rightarrow \text{SiH}_4$ ) leads to consistently lower frequency shifts, and silane itself appears at  $-91.9$  ppm from  $\text{Me}_4\text{Si}$ . (57) Although the silicon trihydrides ( $\text{RSiH}_3$ ) generally contain the most shielded silicon atoms ( $\sim -30$  to  $-70$  ppm) followed by the dihydrides ( $\sim -20$  to  $-40$  ppm) and monohydrides ( $\sim 0$  to  $-30$  ppm), there are many exceptions. The nature of the other substituents is obviously of major importance, e.g. when the shifts for triethylsilane ( $+0.15$  ppm) (60) and tris(trimethylsilyl)silane [ $(\text{Me}_3\text{Si})_3\text{Si}^*\text{H}$ ,  $-117.40$  ppm] (6) are compared. It is interesting to note that the anion  $\text{H}_3\text{Si}^-$  has a chemical shift of  $-165$  ppm which corresponds to a shielding effect of  $73$  ppm relative to silane. Data for some representative silanes are collected in Table III.

A series of homologous silanes  $\text{R}_3\text{SiH}$ , where  $\text{R} = \text{Me}$ , Et,  $^n\text{Pr}$ ,  $^n\text{Bu}$ , and  $n$ -hexyl, were reported by Harris and Kimber. (60) The silicon chemical shifts do not vary monotonically with increasing chain length (Fig. 13) which implies that long range  $\alpha$ ,  $\beta$ ,  $\gamma$ , etc. effects are operative similar to those observed for  $^{13}\text{C}$  shieldings of alkyl groups. Accordingly, the approach of Grant and Paul (61) was taken to evaluate the additivity of alkyl substituent effects in these silanes. The silicon chemical shift is thought to be represented by:

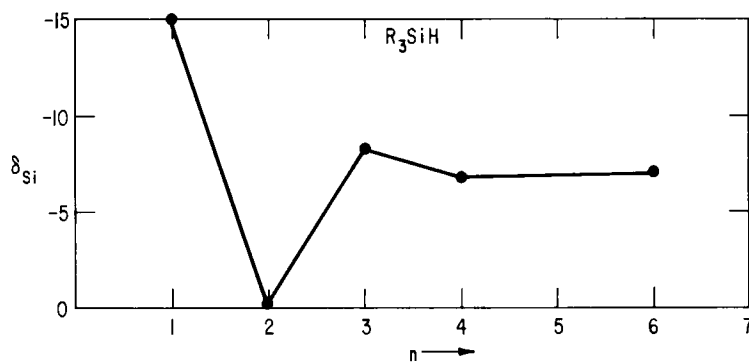
$$\delta_{\text{Si}} = B + \sum_i A_i n_i \quad (5)$$

where  $B$  is the chemical shift of silane,  $n_i$  is the number of carbon atoms at the  $i$ th substituent position from silicon, and  $A_i$  are constants. (60) The relationships found for these alkylsilanes and for the series  $\text{Me}_{4-n}\text{SiH}_n$  ( $n = 0$  to  $4$ ) lead to the following values for the parameters:  $A_\alpha = +25.2$  ( $+9.1$ ) ppm,  $A_\beta = +5.50$  ( $+5.75$ ) ppm,  $A_\gamma = -2.75$  ( $-2.49$ ) ppm,  $A_\delta = +0.51$  ( $+0.31$ ) ppm, and  $4^\circ$  ( $1^\circ$ ) =  $-2.2$  ( $-1.50$ ) ppm, where the numbers in parentheses correspond to the  $^{13}\text{C}$  parameters and  $A_\beta^*$  includes branching corrections. (61) The similarity

TABLE III

<sup>29</sup>Si chemical shifts for some silicon hydrides<sup>a</sup>

	Compound	$\delta_{\text{Si}}$	Ref.
SiH	(H <sub>3</sub> Si) <sub>3</sub> Si*H	-96.0	230
	Me <sub>3</sub> SiSi*Me <sub>2</sub> H	-39.1	73
	Ph <sub>3</sub> SiH	-21.1	231
	Ph <sub>2</sub> MeSiH	-19.5	4
	PhMe <sub>2</sub> SiH	-17.15	32
	(EtO) <sub>2</sub> MeSiH	-16.1	55
	Me <sub>3</sub> SiH	-16.34	42
	<sup>n</sup> Pr <sub>3</sub> SiH	-8.11	60
	<sup>n</sup> Bu <sub>3</sub> SiH	-6.58	60
	(PhCH <sub>2</sub> ) <sub>3</sub> SiH	-3.83	60
	Et <sub>3</sub> SiH	0.15	60
SiH <sub>2</sub>	(H <sub>3</sub> Si) <sub>2</sub> Si*H <sub>2</sub>	-116.5	230
	PhMeSiH <sub>2</sub>	-36.80	3
	Ph <sub>2</sub> SiH <sub>2</sub>	-34.5	4
	(H <sub>3</sub> SiCH <sub>2</sub> ) <sub>2</sub> Si*H <sub>2</sub>	-30.44	6
	(H <sub>3</sub> SiCCl <sub>2</sub> ) <sub>2</sub> Si*H <sub>2</sub>	-5.09	6
SiH <sub>3</sub>	H <sub>3</sub> SiSiH <sub>3</sub>	-104.8	230
	PhSiH <sub>3</sub>	-59.9	232
	PhCH <sub>2</sub> SiH <sub>3</sub>	-56.0	232
	N(SiH <sub>3</sub> ) <sub>3</sub>	-39.92	233
	SiH <sub>4</sub> <sup>n</sup>	-91.9	57

<sup>a</sup> Chemical shifts in ppm relative to Me<sub>4</sub>Si.FIG. 13. <sup>29</sup>Si chemical shifts in ppm relative to Me<sub>4</sub>Si for the trialkylsilanes R<sub>3</sub>SiH vs. the number (*n*) of carbons in the alkyl chain. (60)

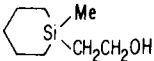
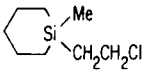
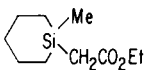
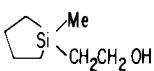
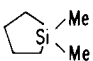
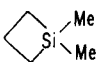
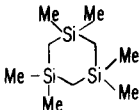
of the  $^{29}\text{Si}$  and  $^{13}\text{C}$  values for  $A_\beta^*$ ,  $A_\gamma$ ,  $A_\delta$ , and  $4^\circ$  ( $1^\circ$ ) suggest a common origin for the effects. It is interesting that the estimated value of  $B$  ( $-91.9$  ppm) is identical to the value found by Niemann and Marsmann. (57) The large difference in  $A_\gamma$  for  $^{13}\text{C}$  and  $^{29}\text{Si}$  indicates that other factors, possibly d-orbital effects, may be operative for silicon. A wider variety of molecules must still be examined before this approach can be validated. In the earlier work of Scholl *et al.* (32) the parameters were estimated to be  $A_\gamma \approx 14$  ppm,  $A_\beta = 2$  ppm, and  $A_\gamma = -2$  ppm, based on a number of tetraalkylsilanes and excluding the effects of chain branching.

### G. Cyclic and polysilanes

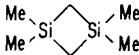
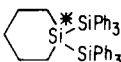
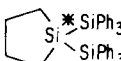
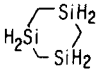
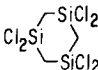
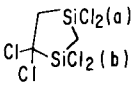
The chemical shift data available for cyclic silanes (32, 62–71) show definite trends with the size of the ring into which the silicon atom is incorporated. Compounds [1]–[6] in Table IV show the deshielding

TABLE IV

$^{29}\text{Si}$  chemical shifts for some silacyclic compounds<sup>a</sup>

	Compound	$\delta_{\text{Si}}$	Ref.
[1]		$-4.11$	32
[2]		$-1.31$	32
[3]		$-1.25$	32
[4]		$16.33$	32
[5]		$16.77$	32
[6]		$18.90$	32
[7]		$0.3$	68

effect of *ca.* 20 ppm for a five-membered ring relative to a six-membered ring (compare [1] and [4]). (32) Another 2 ppm deshielding occurs when the silicon is incorporated into a four-membered ring (compare [5] and [6]). (32) The six-membered cyclic silane is shielded by about 4 ppm relative to  $\text{Me}_4\text{Si}$ . This trend is repeated for the linear and five- and six-membered cyclic species [9]–[11] where the methyl substituents at silicon in [5] and [6] have been replaced by triphenylsilyl groups. Two other points should be noted from these data: (1) this generalization appears to be valid only for the monosilacyclic compounds (the chemical shifts of [7] and [8] and [13] and [14a], for example, are within 3 and 4.5 ppm, respectively, of each other and clearly do not follow this trend); and (2) the influence of  $\alpha$ - and  $\beta$ -substituents is similar to that in the analogous open chain

	Compound	$\delta_{\text{Si}}$	Ref.
[8]		2.73	32
[9]		-48.6	74
[10]		-34.8	74
[11]	$(\text{Ph}_3\text{Si})_2\text{Si}^*\text{Me}_2$	-45.9	74
[12]		-34.1	68
[13]		19.5	68
[14]		(a) 15.1 (b) 7.3	6

\* In ppm relative to  $\text{Me}_4\text{Si}$ . Data from ref. 32 converted using  $\delta_{\text{Si}}[(\text{MeO})_4\text{Si}] = -78.5$  ppm. Data from ref. 68 converted using  $\delta_{\text{Si}}[(\text{Me}_2\text{SiO})_4] = -19.51$  ppm.



compounds. The latter point is most clearly demonstrated for the  $\alpha$ -substituents by the similarity of the chemical shift difference ( $\Delta\delta$ ) between [5] and [10] (51 ppm) to  $\Delta\delta$  for the corresponding linear compounds  $\text{Me}_4\text{Si}$  and [11] (46 ppm).

The silacyclopropanes form a unique class of compounds whose silicon resonances are unusually shielded. (62–65) Although cyclic and acyclic tetraalkylsilanes usually appear within a chemical shift range of +5 to –20 ppm relative to  $\text{Me}_4\text{Si}$ , the tetraalkylsilacyclopropane resonances occur at about 50–60 ppm to low frequency of  $\text{Me}_4\text{Si}$  ([15]–[18] in Table V). Analogous results are found for cyclopropane which has unusually shielded  $^{13}\text{C}$  and  $^1\text{H}$  resonances (–2.6 and 0.222 ppm, respectively) compared with the higher homologues such as

TABLE V

Silacyclopropane silicon shieldings<sup>a</sup>

Compound	$\delta_{\text{Si}}$	Ref.
<div data-bbox="278 786 399 907"> </div>	–49.31	64
<div data-bbox="278 933 479 1055"> </div>	–51.78	62
<div data-bbox="278 1081 510 1203"> </div>	–53.21	62
<div data-bbox="278 1215 456 1319"> </div>	–59.8 <sup>b</sup>	65
<div data-bbox="278 1336 451 1440"> </div>	$\text{SiMe}_2$ –106.2 $\text{SiMe}_3$ –8.5	63

<sup>a</sup> In ppm relative to  $\text{Me}_4\text{Si}$ . Data converted from  $(\text{MeO})_4\text{Si}$  ( $\delta_{\text{Si}} = -78.5$ ) where necessary.

<sup>b</sup> Sample not isolated.

cyclopentane ( $\delta_C = 26.5$  ppm,  $\delta_H = 1.506$  ppm). (72) An extremely low frequency silicon resonance at  $-106.2$  ppm was found by Seyferth *et al.* (63) for the silacyclopropene [19] (Table V). This may be partly due to  $\pi$ -bonding with participation of the silicon d-orbitals.

Sufficient chemical shift information for various types of polysilanes is now available (32, 35, 57, 73, 74) to enable some trends in these systems to be determined. The data for several perhalogenated derivatives are shown in Table VI. (35, 57, 73) It is apparent from the chemical shift changes of the trichlorosilyl ( $\text{SiCl}_3$ ) groups that the increasing substitution of  $\text{SiCl}_3$  units at the other silicon has a progressively deshielding effect. The total chemical shift range of these groups is 11.5 ppm. Clearly the greatest changes occur for the silicon at which the substitution is taking place. Interestingly, a plot of  $\delta_{\text{Si}}$  vs.  $n$  for the series  $\text{Cl}_{4-n}\text{Si}^*(\text{SiCl}_3)_n$  shows the "sagging" pattern for progressive substitution of  $\text{SiCl}_3$  groups for Cl (increasing  $n$ ).

TABLE VI

<sup>29</sup>Si chemical shifts for some perhalogenated polysilanes<sup>a</sup>

Compound		$\delta_{\text{Si}}$	Ref.
$\text{F}_3\text{SiSiF}_3$		$-78.1^b$	35
$(\text{F}_3\text{Si})_2\text{SiF}_2$	$\text{SiF}_3$	$-80.1^b$	35
	$\text{SiF}_2$	$-17.9^b$	
$\text{Cl}_2\text{FSiSiCl}_3$	$\text{SiCl}_2\text{F}$	$-23.3^b$	35
	$\text{SiCl}_3$	$-7.1^b$	
$\text{Cl}_3\text{SiSiCl}_3$		$-8.0$	57
$(\text{Cl}_3\text{Si})_2\text{SiCl}_2$	$\text{SiCl}_3$	$-3.5$	73
	$\text{SiCl}_2$	$-7.2$	
$(\text{Cl}_3\text{Si})_3\text{SiCl}$	$\text{SiCl}_3$	$-2.3$	57
	$\text{SiCl}$	$-7.2$	
$(\text{Cl}_3\text{SiSiCl}_2)_2$	$\text{SiCl}_3$	$-6.1^c$	57
	$\text{SiCl}_2$	$-6.6^c$	
$(\text{Cl}_3\text{Si})_4\text{Si}$	$\text{SiCl}_3$	$+3.5$	73
	$\text{Si}$	$-80.0$	

<sup>a</sup> Chemical shifts in ppm from  $\text{Me}_4\text{Si}$ .

<sup>b</sup> Data converted to  $\text{Me}_4\text{Si}$  scale using

$\delta_{\text{Si}}(\text{SiF}_4) = -113.6$  ppm.

<sup>c</sup> May be reversed.

The situation is somewhat clearer for monosubstituted pentamethyl-disilanes. The chemical shift data for these compounds are shown in

Table VII along with the substituent effects ( $\Delta\delta$ ) relative to hexamethyldisilane ( $X = \text{Me}$ ) for  $\text{Si}^{\text{B}}$ :

$$\Delta\delta = \delta_{\text{Si}^{\text{B}}}(\text{Me}_3\text{Si}^{\text{A}}\text{Si}^{\text{B}}\text{Me}_2\text{X}) - \delta_{\text{Si}}(\text{Me}_6\text{Si}_2) \quad (6)$$

TABLE VII

<sup>29</sup>Si Chemical shifts for substituted disilanes  $\text{Me}_3\text{Si}^{\text{A}}\text{Si}^{\text{B}}\text{Me}_2\text{X}$  (73)<sup>a</sup>

X	$\delta_{\text{A}}$	$\delta_{\text{B}}$	$\Delta\delta^b$	$\delta_{\text{Si}}(\text{Me}_3\text{SiX})$ (ref. 42)
Me (ref. 42)	-19.8	-19.8	0	0
$\text{SiMe}_3$	-16.1	-48.7	-28.9	-19.8
H	-18.9	-39.1	-19.3	-16.3
Ph	-19.3	-21.7	-1.9	-4.4
Cl	-18.2	+22.8	+42.6	+30.3
$\text{NHSiMe}_2\text{SiMe}_3$	-22.0	-5.4	+14.4	+2.2 ( $X = \text{NHSiMe}_3$ )
F	-22.5	+34.0	+53.8	+32.0
$\text{OSiMe}_2\text{SiMe}_3$	-23.1	+5.2	+25.0	+6.8 ( $X = \text{OSiMe}_3$ )
CN (ref. 74)	-18.1	-32.3	-12.5	-11.6 (ref. 74)

<sup>a</sup> Chemical shifts in ppm relative to  $\text{Me}_4\text{Si}$ .

<sup>b</sup> See text for definition.

and the chemical shift of the corresponding trimethylsilyl derivatives. (42) In all cases except  $X = \text{Ph}$  the effect of replacing a methyl group with  $X$  is larger for the pentamethyldisilanyl derivatives than for the trimethylsilyl compounds. For some substituents (e.g.  $X = \text{F}$ ) the effect is quite a bit larger. The changes are unidirectional for the same substituent  $X$ ; if the substituent has a shielding effect in the trimethylsilyl series, it also effects a low frequency shift for  $\text{Si}^{\text{B}}$  in the pentamethyldisilanyl series. In both cases electronegative substituents cause high frequency shifts. As expected, the chemical shift changes for  $\text{Si}^{\text{A}}$  cover a much smaller range since the substituent is one bond further removed than it is for  $\text{Si}^{\text{B}}$ . It is interesting that in this series, for all cases except  $X = \text{Cl}$ , the chemical shift change in  $\text{Si}^{\text{A}}$  is the opposite of that observed for  $\text{Si}^{\text{B}}$ : if replacing a methyl group with  $X$  causes a low frequency shift in  $\text{Si}^{\text{B}}$ , then  $\text{Si}^{\text{A}}$  shifts to high frequency relative to hexamethyldisilane.

The substituent effects observed for tris(trimethylsiloxy)silanes  $(\text{Me}_3\text{Si}^{\text{A}}\text{O})_3\text{Si}^{\text{B}}\text{X}$  (75) are the opposite of those observed for the pentamethyldisilanyl and trimethylsilyl compounds. In this case electronegative substituents (such as  $-\text{CCl}_3$ ) at  $\text{Si}^{\text{B}}$  are found to have a shielding effect relative to  $X = \text{CH}_3$ . As is the case for the pentamethyldisilanes, the substituent effects are opposite for  $\text{Si}^{\text{A}}$  and  $\text{Si}^{\text{B}}$ . Although both  $\delta_{\text{Si}^{\text{A}}}$  and  $\delta_{\text{Si}^{\text{B}}}$  give linear correlations with Taft  $\sigma^*$  constants, the slopes have different signs. (75)

Finally, the effects of increasing chain length and chain branching in alkyl substituents are shown for  $\text{Ph}_3\text{SiSiMe}_2\text{R}$  in Table VIII. (74) The shieldings observed for  $\text{Si}^{\text{B}}$  are consistent with the trends observed for the trialkylsilanes with increasing chain length. (60) The similarity between the shifts for the *n*-propyl and *n*-octyl derivatives suggests that the major changes are caused by  $\alpha$ ,  $\beta$ , and  $\gamma$  effects and that  $\delta$  and  $\epsilon$  effects are small, as is the case for  $^{13}\text{C}$  shieldings of alkanes. (76) The deshielding effect of  $\beta$ -substitution is apparent for  $\text{Si}^{\text{B}}$  in the series  $^{\text{n}}\text{Pr} > ^{\text{i}}\text{Pr} > ^{\text{t}}\text{Bu}$ . The chemical shifts in this series also correlate with the Taft  $\sigma^*$  constants for R. The chemical shift of  $\text{Si}^{\text{A}}$  is quite insensitive to the changes at  $\text{Si}^{\text{B}}$  and virtually no chemical shift differences are observed for  $\text{Si}^{\text{A}}$ .

TABLE VIII

Effect of increasing chain length and branching in alkyl substituted disilanes (74)<sup>a</sup>

Compound	$\delta_{\text{A}}$	$\delta_{\text{B}}$
$\text{Ph}_3\text{Si}^{\text{A}}\text{Si}^{\text{B}}\text{Me}_3$	-20.4	-18.4
$\text{Ph}_3\text{Si}^{\text{A}}\text{Si}^{\text{B}}\text{Me}_2^{\text{n}}\text{Pr}$	-20.4	-17.0
$\text{Ph}_3\text{Si}^{\text{A}}\text{Si}^{\text{B}}\text{Me}_2^{\text{n}}\text{Oct}$	-20.4	-16.8
$\text{Ph}_3\text{Si}^{\text{A}}\text{Si}^{\text{B}}\text{Me}_2^{\text{i}}\text{Pr}$	-20.6	-11.9
$\text{Ph}_3\text{Si}^{\text{A}}\text{Si}^{\text{B}}\text{Me}_2^{\text{t}}\text{Bu}$	-20.4	-8.0

<sup>a</sup> Chemical shifts in ppm relative to internal  $\text{Me}_4\text{Si}$ .

## H. Organosilicones

In 1857 Wöhler suggested the term silicone to describe a class of compounds having the empirical formula  $\text{R}_2\text{SiO}$ , analogous to organic ketones ( $\text{R}_2\text{CO}$ ). Since the existence of  $\text{R}_2\text{Si}=\text{O}$  has not been demonstrated, the name silicone has evolved to encompass all organosilicon polymers and monomers. (77) For the purpose of this review, this section includes compounds of general structure  $(\text{R}_{3-n}\text{SiO}_n)_x$ , where  $n > 0$ ,  $x > 2$ , and R = alkyl, aryl, or H. Silicates and extravalent silicon compounds are treated in other sections.

The spectral dispersion for organosilicones may be considerable for certain families of compounds. This is reflected in the  $^{29}\text{Si}$  chemical shifts of siloxanes,  $-(\text{SiRR}'\text{O})_n-$ , an important class of compounds which includes resins, fluids, room-temperature vulcanized and heat-cured rubber consumer products. The first,  $^{29}\text{Si}$  NMR results (5, 78) reported on polydimethylsiloxanes showed that individual resonance

lines can be found for each different silicon nucleus up to a ten-unit oligomer, surpassing the structural resolution achieved by  $^{13}\text{C}$  and  $^1\text{H}$  NMR on the same materials (Table IX). The nomenclature used to define siloxane compounds incorporates the use of the letters M, D, T, and Q, which represent  $\text{R}_3\text{SiO}_{0.5}$ ,  $\text{R}_2\text{Si}(\text{O}_{0.5})_2$ ,  $\text{RSi}(\text{O}_{0.5})_3$ , and  $\text{Si}(\text{O}_{0.5})_4$  units respectively, and R which denotes aliphatic and/or aromatic substituents or H. Figure 14 shows a comparison of the  $^{13}\text{C}$  spectrum of  $\text{MD}_6\text{M}$  and the  $^{29}\text{Si}$  spectrum of  $\text{MD}_9\text{M}$  ( $\text{R} = \text{CH}_3$ ). In the  $^{13}\text{C}$  spectrum only the M methyls and outer D methyls ( $\text{D}^1$ ) are resolved, while in the longer chain oligomer the  $^{29}\text{Si}$  spectrum resolves the M silicon and each D unit from  $\text{D}^1$  to  $\text{D}^4$ . The central D unit ( $\text{D}^5$ ) is the only silicon unit not resolved. The chemical shift range for the nitrogen analogues of the siloxanes, the silazanes, is considerably smaller. (79)

TABLE IX

 $^{29}\text{Si}$  chemical shifts for some polydimethylsiloxanes (5)<sup>a</sup>

Compound	M	D <sup>1</sup>	D <sup>2</sup>	D <sup>3</sup>	D <sup>4</sup>	D <sup>5</sup>
MM	6.79					
MDM	6.70	-21.5				
MD <sub>2</sub> M	6.80	-22.0				
MD <sub>3</sub> M	6.90	-21.8	-22.6			
MD <sub>4</sub> M	7.0	-21.8	-23.4			
MD <sub>5</sub> M	7.0	-21.8	-22.4	-22.3		
MD <sub>6</sub> M	7.0	-21.8	-22.3	-22.2		
MD <sub>7</sub> M	7.0	-21.89	-22.49	-22.33	-22.29	
MD <sub>8</sub> M	6.93	-21.86	-22.45	-22.30	-22.20	
D <sub>3</sub> cyclic		-9.12				
D <sub>4</sub> cyclic		-19.51				
D <sub>5</sub> cyclic		-21.93				
D <sub>6</sub> cyclic		-22.48				

<sup>a</sup> Relative to internal  $\text{Me}_4\text{Si}$ . Accuracy of reported shifts better than 0.05 ppm (1 Hz). Solutions in acetone- $\text{d}_6$ .

The number of papers reporting  $^{29}\text{Si}$  NMR results on polymeric and oligomeric siloxanes has become quite significant (27, 30, 38, 39, 78–88). The increased structural resolution available in  $^{29}\text{Si}$  spectra relative to the  $^{13}\text{C}$  or  $^1\text{H}$  spectra makes it possible to study polymeric siloxanes in greater detail. Harris and Kimber (81a) have looked at end-group and tacticity effects in asymmetric polymeric siloxanes of average chain length 50 units ( $\text{MD}_n\text{M}$ ). In addition to the M unit ( $\text{Me}_3\text{SiO}_{0.5}$ )<sub>2</sub> they

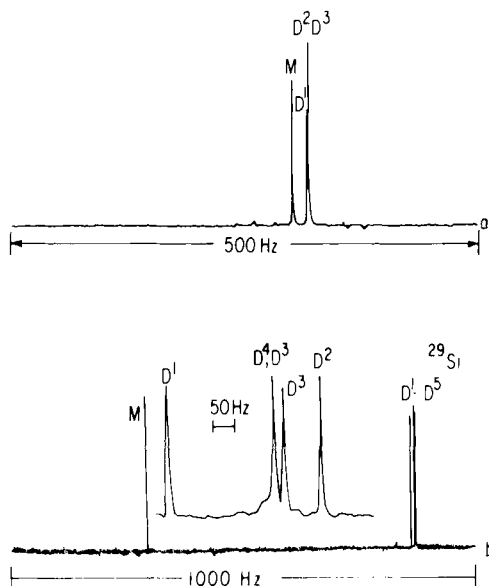


FIG. 14. (a)  $^{13}\text{C}$  spectrum of  $\text{MD}_6\text{M}$ . (b)  $^{29}\text{Si}$  spectrum of  $\text{MD}_9\text{M}$ . (5)

were able to resolve the  $\text{D}'$   $^{29}\text{Si}$  resonance  $[\text{MeHSi}(\text{O}_{0.5})_2]$  three units from each end of the chain. Using  $\text{MD}'_5\text{M}$  as a model they demonstrated the existence of both tacticity and end-group effects by interpreting the observed fine structure in the proton decoupled spectra as arising from asymmetric effects in the oligomer (Fig. 15). They assumed that, if only nearest-neighbour effects can influence adjacent nuclei, it is reasonable that the resonance consists of two lines since  $\text{D}'^2$

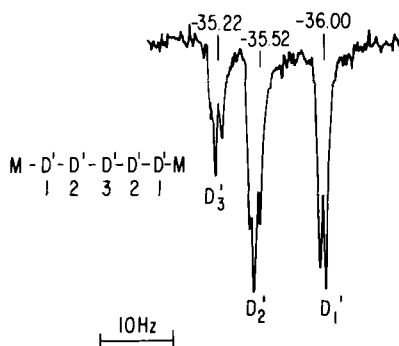


FIG. 15.  $\text{D}'$  region of the  $^{29}\text{Si}$  spectrum of  $\text{MD}'_3\text{M}$  where  $\text{D}' = [\text{MeHSi}(\text{O}_{0.5})_2]$ . (81a) Chemical shifts are in ppm relative to  $\text{Me}_4\text{Si}$ .

may be either *d* or *l* giving rise to two different environments for  $D'^1$ . Similarly, the  $D'^2$  and  $D'^3$  resonances will appear as three lines because each unit has two asymmetric neighbours. Thus, the sequence is  $ddd = lll$ ,  $ddl = ldd = lld = dll$ , and  $ldl = dld$ , which gives a 1:2:1 triplet. In the polymer of average composition  $MD'_{50}M$  the predominant feature is a 1:2:1 triplet centred at  $-34.88$  ppm from  $Me_4Si$  (Fig. 16). Harris and Kimber explain the triplet structure as resulting from either a totally atactic polymer, or that chains of different tacticities are produced in nearly equal amounts. Under higher amplification the  $D'^1$  and  $D'^2$  groups clearly appear as a doublet and triplet, respectively, analogous to the results obtained for  $MD'_5M$  (Fig. 15).

In a separate paper Harris and Kimber (30) examined mixed polymeric siloxanes of the type  $MD_xD'_yM$  where  $M = Me_3SiO_{0.5}$ ,  $D = Me_2Si(O_{0.5})_2$ , and  $D' = HMeSi(O_{0.5})_2$ . The  $^{29}Si$  spectrum of these polymers shows three distinct areas of resonance, M at  $+9.71$  to  $+7.07$  ppm, D from  $-18.81$  to  $-22.03$  ppm, and  $D'$  from  $-35.19$  to  $-37.35$  ppm. The resolution at 2.35 T is sufficient to show triad and pentad fine structure at the  $D'$  and D resonances, respectively, and chemical shift sensitivity at the M resonance to structural changes occurring up to six bonds away (Table X).

Triad structure in mixed dimethyl and phenyl methyl siloxanes has also been reported; multiple resonances are observed for M,  $M^{Ph}$ ,  $M^{Ph_2}$ , D,  $D^{Ph}$ , and  $D^{Ph_2}$  units, (79) where the superscripts denote any

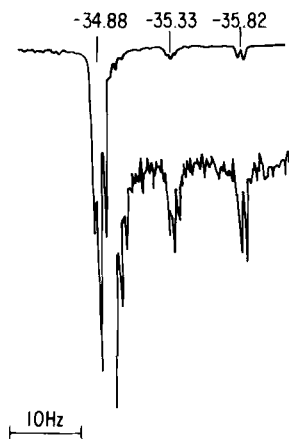


FIG. 16.  $D'$  region of the  $^{29}Si$  spectrum of  $MD'_{50}M$ . (81a) Chemical shifts are in ppm relative to  $Me_4Si$ .

TABLE X

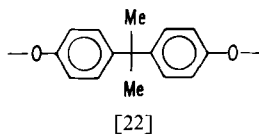
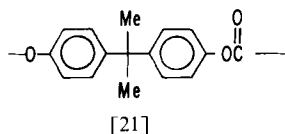
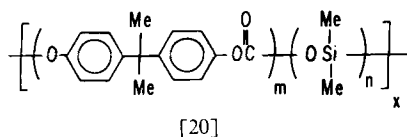
<sup>29</sup>Si chemical shifts for MD<sub>x</sub>D<sub>y</sub>M mixed polymers (30)<sup>a</sup>

Unit	δ <sub>Si</sub>	Unit	δ <sub>Si</sub>	Unit	δ <sub>Si</sub>
MD'D'D'	9.71	D'D'DD'D	-18.81	D'D'D'	-35.19
MD'D'D	9.61	DD'DD'D'	-19.02	DD'D'	-36.27
MD'DD'	9.33	DD'DD'D	-19.28	DD'D	-37.35
MD'DD	9.18	D'DDD'D'	-20.13		
MDD'D'	7.67	DDDD'D'	-20.41		
MDD'D	7.47	and D'DDD'D			
MDDD'	7.17	DDDD'D	-20.65		
MDDD	7.07	D'DDDD'	-21.46		
		D'DDDD	-21.76		
		DDDDD	-22.03		

<sup>a</sup> Data in ppm relative to Me<sub>4</sub>Si.

substitution at silicon other than methyl groups (e.g. D<sup>Ph</sup> represents a D unit with R<sup>1</sup> = CH<sub>3</sub>, R<sup>2</sup> = Ph).

<sup>29</sup>Si NMR of siloxane systems has been used in studying organosilicone containing block copolymers to determine block length and chemical redistribution during polymerization. (85) Block copolymers of bisphenol A polycarbonate (BPAP) and polydimethylsiloxane (PDMS) [20] were studied by both <sup>13</sup>C and <sup>29</sup>Si NMR to determine a variety of structural parameters.



In addition to the D units [Me<sub>2</sub>Si(O<sub>0.5</sub>)<sub>2</sub>] and bisphenol A (BPA) carbonate units [21], the nature of the polymer synthesis (85) gives rise to single BPA units [22] isolated between two silicone blocks. The <sup>29</sup>Si NMR spectrum of a sample polymer with average silicone block length  $\bar{n}_{\text{PDMS}} = 10$  is shown in Fig. 17. Peaks A and A' correspond to silicon atoms adjacent to polycarbonate blocks. The peak B corresponds to the second siloxane units in the silicone block and the rest of the



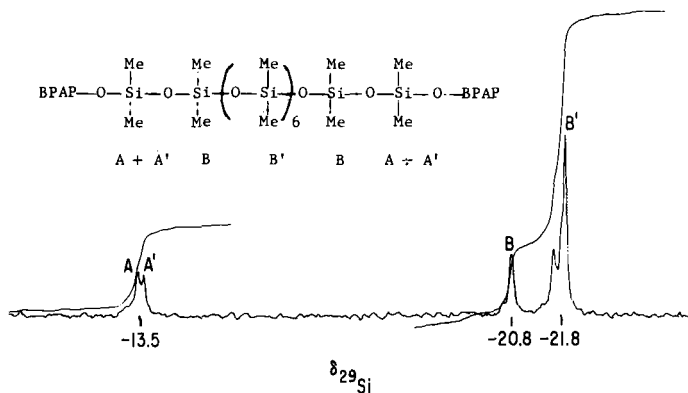


FIG. 17.  $^{29}\text{Si}$  NMR spectrum of a bisphenol A polycarbonate-polydimethylsiloxane block copolymer with average silicone block length  $\bar{n}_{\text{PDMS}} = 10$ . (85)

internal units appear under the bulk resonance line  $B'$ . The silicone block length can be calculated directly from:

$$\bar{n}_{\text{PDMS}} = 2[(B + B')/(A + A') + 1] \quad (7)$$

where  $A$ ,  $A'$ ,  $B$ , and  $B'$  correspond to the integrated areas under the respective peaks.

Although a considerable amount of information is obtained from the  $^{13}\text{C}$  spectra of these polymers (polycarbonate block length, number of isolated BPA units, and end-group effects), one very surprising result of the study is that isolated BPA units appear to be detectable in the  $^{29}\text{Si}$  spectrum as well. Closer examination of Fig. 17 reveals that the silicon atoms at the end of the silicone block separate into two closely spaced resonances  $A$  and  $A'$ . Although the resonances are not fully resolved, the addition of  $(\text{BPA-D}_{10})_n$ , which contains only isolated BPA units, clearly increases the intensity of peak  $A'$ . This suggests that the chemical shift of a silicone moiety adjacent to a polycarbonate block differs slightly from that adjacent to an isolated BPA unit. Although suitable model components must still be examined to prove that this chemical shift difference exists, the results are quite interesting since they indicate that silicon shieldings may be sensitive to structural changes over long distances.

In addition to silicone block length determinations,  $^{29}\text{Si}$  NMR has been used by LaRoche *et al.* (89) to determine molecular weights of silanol fluids by measuring average degree of polymerization ( $\bar{DP}$ ) of fluid mixtures,  $\text{HO}[(\text{CH}_3)_2\text{SiO}]_n\text{H}$ , where  $\bar{n} = 6-80$ . Several groups have investigated the flow behaviour of low molecular weight methyl-terminated polydimethylsiloxanes. Wilcock (90) and Hunter *et al.* (91)

determined the bulk viscosities ( $\eta$ ) of ten monodispersed polysiloxanes where  $n = 1-9$ . These viscosities are found to relate to molecular weight in agreement with the equation:

$$\log \eta = A + C \log M \quad (8)$$

where  $A$  and  $C$  are constants, and  $M$  can be either the viscosity molecular weight  $\bar{M}_v$  or the weight-average molecular weight  $\bar{M}_w$ . (92)

The use of NMR to determine sequence lengths in polymers is well established. Horn and Marsmann (23) previously demonstrated that  $^{29}\text{Si}$  NMR can resolve the terminal (A) and internal (B) silicon nuclei of low molecular weight disiloxanols. LaRochelle *et al.* (89) analysed a series of disiloxanols by  $^{29}\text{Si}$  NMR under quantitative conditions and determined the average degree of polymerization ( $\overline{\text{DP}}$ ) using:

$$\overline{\text{DP}} = 2(B/A) + 2 \quad (9)$$

where  $A$  and  $B$  are integrated areas under the respective peaks. The data are plotted against the bulk viscosity values previously measured (Fig. 18). The plot shows a linear relationship of bulk viscosity to chain length over a range of 6–80 dimethylsiloxy (D) units. This result is

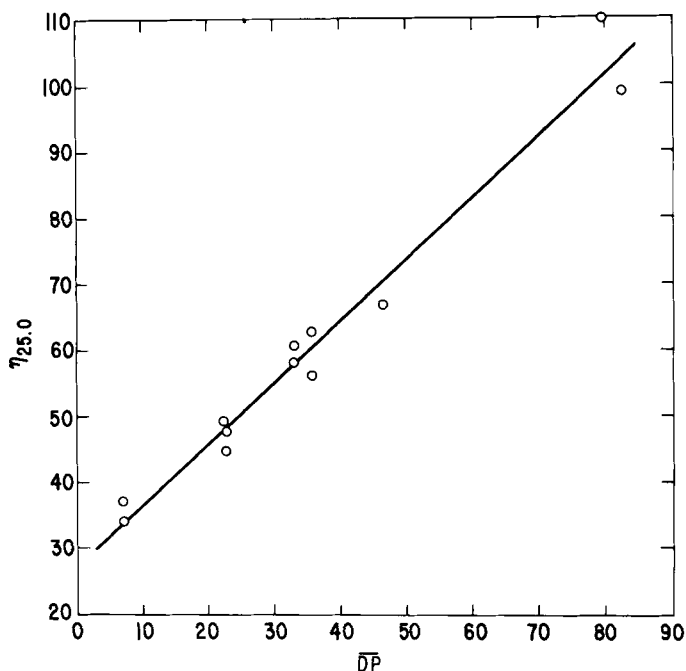


FIG. 18. Plot of bulk viscosity vs. average chain length (DP) as measured by  $^{29}\text{Si}$  NMR for hydroxy-terminated polydimethylsiloxanes. (89)

surprising since the  $\overline{DP}$  measured by  $^{29}\text{Si}$  NMR is directly convertible to  $\overline{M}_n$ . Classically, the flow of a polydispersed polymer fluid or melt correlates with  $\overline{M}_w$ , not  $\overline{M}_n$ . (92) Furthermore, the  $\overline{M}_w$  correlation with viscosity is linear only when plotted in a logarithmic fashion. Therefore it is probably fortuitous that a non-logarithmic linear relationship of disiloxanol viscosity to  $\overline{M}_n$  is found. Interestingly, the curve in Fig. 18 is of unit slope. This provides a convenient rule-of-thumb to convert disiloxanol viscosity into  $\overline{DP}$ :

$$\overline{DP} = \eta(25^\circ) \text{ (centistokes)} - 26 \quad (10)$$

There have been some very thorough structural studies conducted on MQ, (78, 86–88) MT, (78, 82) and DT (79) systems using  $^{29}\text{Si}$  NMR. Harris and Newman (87) have looked at the trimethylsilylation products of wollastonite, a form of anhydrous calcium metasilicate, and pseudo-wollastonite, a crystalline modification of that mineral. The chemical shifts of the four model compounds listed in Table XI were compared in order to determine the degree of spectral dispersion that would occur in the many polymeric structures formed from trimethylsilylation of the decomposed calcium silicate.

TABLE XI

$^{29}\text{Si}$  chemical shifts for some model trimethylsilyl esters of silicic acid (87)<sup>a</sup>

	M <sup>1</sup>	M <sup>2</sup>	Q <sup>0</sup>	Q <sup>1</sup>	Q <sup>2</sup>
M <sub>4</sub> Q	8.6		– 104.2		
M <sub>6</sub> Q <sub>2</sub>	9.3			– 106.5	
M <sub>8</sub> Q <sub>3</sub>	8.99	9.31		– 106.67	– 109.09
M <sub>8</sub> Q <sub>3</sub> cyclic	10.2			– 107.76	

<sup>a</sup> In ppm relative to Me<sub>4</sub>Si.

The greatest resolution occurs in the Q region of the spectrum which is therefore more useful for quantitative analysis of mixtures of MQ type compounds. Harris and Newman found an envelope of Q resonances spanning a region of 4.5 ppm with only a few discernible sharp peaks. Their explanation takes into account the large number of structural environments caused by crosslinking of the chains. A variety of cyclic structures and linear polymers must all contribute signals to form the broad envelope observed. A typical MQ spectrum is shown in Fig. 19. If special precautions to eliminate the signal contribution from the glass NMR tubes and receiver insert are taken, the M/Q ratio can

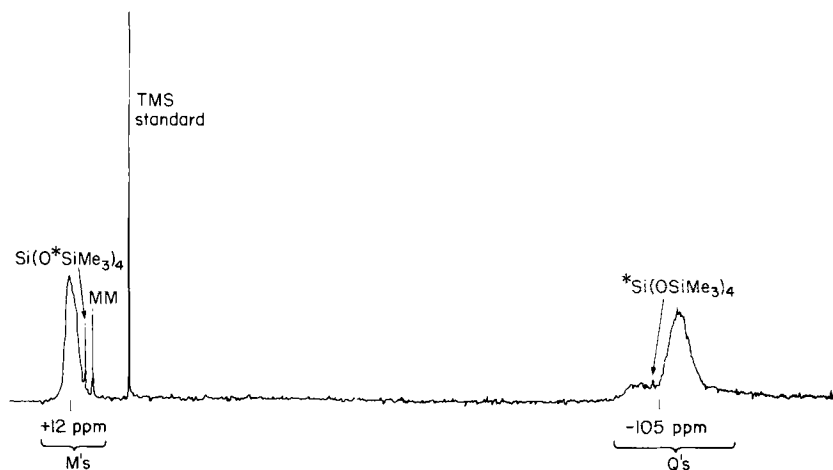
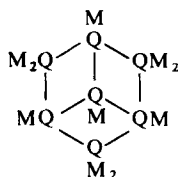


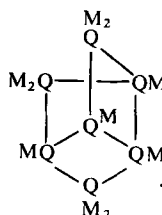
FIG. 19.  $^{29}\text{Si}$  NMR spectrum of an MQ resin. Chemical shifts are in ppm relative to  $\text{Me}_4\text{Si}$ .

be calculated, and can give a measure of the degree of trimethylsilylation.

Hoebbel *et al.* (88) have used  $^{29}\text{Si}$  NMR to investigate the structures of nine silicic acid trimethylsilyl esters. Their reported chemical shifts for  $\text{M}_4\text{Q}$ ,  $\text{M}_6\text{Q}_2$ ,  $\text{M}_8\text{Q}_3$ , and  $\text{M}_8\text{Q}_4$  (cyclic) differ by  $\sim 1$  ppm to lower frequency than the shifts reported by Harris and Newman (87) (see Table XII). Although both groups report their shifts relative to  $\text{Me}_4\text{Si} = 0$ , Harris and Newman found that in these systems  $\text{Me}_4\text{Si}$  is sensitive to medium effects and concentration. To avoid this problem they used  $\text{M}_4\text{Q}$ , which is much less sensitive to solution changes, as their standard and converted to the  $\text{Me}_4\text{Si}$  scale.



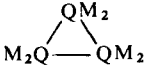
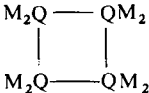
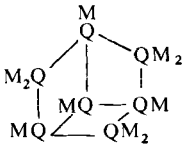
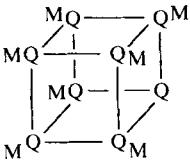
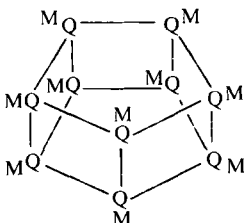
[23]



[24]

In their discussion of  $\text{M}_{10}\text{Q}_7$ , Hoebbel *et al.* noted the possibility of at least two isomeric structures, [23] and [24]. Since the  $^{29}\text{Si}$  NMR

TABLE XII  
<sup>29</sup>Si chemical shifts for some silicic acid trimethylsilyl esters(88)<sup>a</sup>

Compounds		M <sup>b</sup>	Q <sup>b</sup>
M <sub>4</sub> Q	M <sub>4</sub> Q	7.6(8.6)	-105.1(-104.2)
M <sub>6</sub> Q <sub>2</sub>	M <sub>3</sub> Q QM <sub>3</sub>	8.0(9.3)	-107.5(-106.5)
M <sub>8</sub> Q <sub>3</sub>	M <sub>3</sub> Q-M <sub>2</sub> Q-QM <sub>3</sub>	8.0(8.99) (M <sub>3</sub> Q)	-107.7(-106.7) (QM <sub>3</sub> )
		8.3(9.31) (M <sub>2</sub> Q)	-110.1(-109.1) (QM <sub>2</sub> )
M <sub>10</sub> Q <sub>4</sub>	M <sub>3</sub> Q-M <sub>2</sub> Q-M <sub>2</sub> Q-QM <sub>3</sub>	7.6 (M <sub>3</sub> Q)	-108.6 (QM <sub>3</sub> )
		7.7 (M <sub>2</sub> Q)	-110.04 (QM <sub>2</sub> )
M <sub>6</sub> Q <sub>3</sub>		6.4	-100.7
M <sub>8</sub> Q <sub>4</sub>		9.2(10.2)	-108.8(-107.8)
M <sub>10</sub> Q <sub>7</sub>		9.4 (M <sub>2</sub> Q)	-108.8 (QM <sub>2</sub> )
		10.0 (MQ)	-109.8 (QM)
M <sub>8</sub> Q <sub>8</sub>		11.7	-109.3
M <sub>10</sub> Q <sub>10</sub>		12.4	-110.2

<sup>a</sup> In ppm relative to Me<sub>4</sub>Si.<sup>b</sup> Values in parentheses are from ref. 87.

spectrum shows only four resonance lines only one structure appears possible (Table XII).

Any trisiloxane ring structure is eliminated because of the absence of a Q resonance at  $\sim -100$  ppm. Since structure [24] has QM<sub>2</sub> units in

TABLE XIII

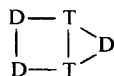
<sup>29</sup>Si chemical shifts of some polycyclic siloxanes  
(79)<sup>a</sup>

Compound	D	T
T <sub>2</sub> D <sub>3</sub>	-8.6	-55.2
	-19.4	
T <sub>2</sub> D <sub>4</sub>	-21.1	-65.8

<sup>a</sup> In ppm relative to Me<sub>4</sub>Si.

both a tetra- and a penta-siloxane ring configuration, more than two resonance lines are expected. However, the observed lines are sharp and unbroadened leading to the conclusion that only structure [23] is present in solution.

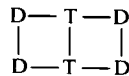
<sup>29</sup>Si NMR has been used by Jancke *et al.* (79) to identify isomeric structures in cyclic DT compounds. Gas chromatography shows that two structures for T<sub>2</sub>D<sub>3</sub> ([25], [26]) and four structures for T<sub>2</sub>D<sub>4</sub> ([27]–[30]) are possible.



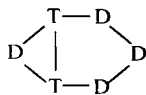
[25]



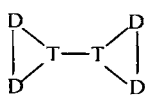
[26]



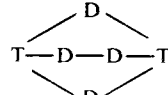
[27]



[28]



[29]



[30]

It is well known that D<sub>3</sub> cyclic has a <sup>29</sup>Si NMR signal at ~ -9 ppm, (5) and that higher oligomeric cyclic compounds (D<sub>4</sub> to D<sub>n</sub>) and linear dimethylsiloxy units appear between -19 and -22 ppm. When samples of T<sub>2</sub>D<sub>3</sub> and T<sub>2</sub>D<sub>4</sub> were examined by the Jancke group their results unequivocally identified structures [25] and [27] (chemical shifts in Table XIII).

Structure [26] is eliminated because two D resonances are found in the ratio 1:2 corresponding to a D unit in a trisiloxane ring and a D unit in a tetrasiloxane ring, respectively (Table XIII). For the T<sub>2</sub>D<sub>4</sub> compound, [28]–[30] are eliminated because no resonance line is

found corresponding to a D unit in a three-unit cyclic structure; only structure [27] fits the data.

Lippmaa *et al.* (86) have successfully studied solid state  $^{29}\text{Si}$  NMR of several trimethylsilyl silicate samples using proton-enhanced nuclear induction spectroscopy and magic angle spinning. They showed that the high resolution  $^{29}\text{Si}$  NMR of solids can be useful for structural studies of certain soluble and insoluble silicates, because many of these compounds with well defined molecular structures in the solid state tend to undergo very complicated rearrangements and condensation in solution. (93)

For cyclic dimethylsiloxanes there is an increase in  $^{29}\text{Si}$  shielding as ring size increases, approaching the chemical shifts for bulk D units (Table IX) in linear dimethylsiloxanes ( $\sim 22$  ppm). The deshielding in the smaller rings is particularly apparent for  $\text{D}_3$  cyclic which appears at  $-9\text{--}12$  ppm, whereas  $\text{D}_4$  and  $\text{D}_5$  occur at  $-19\text{--}51$  and  $-21\text{--}93$  ppm, respectively. (84) Harris *et al.* find that the same is true for  $\text{D}'_n$  cyclic compounds in rings where  $\text{D}'_n$  is  $(\text{MePhSiO})_n$  and  $(\text{MeHSiO})_n$ . The  $(\text{MePhSiO})_3$  compound has two peaks due to asymmetry with a 2:1 intensity ratio at  $-20\text{--}66$  and  $-20\text{--}69$  ppm from  $\text{Me}_4\text{Si}$ . The  $(\text{MePhSiO})_4$  resonance also appears as a multiplet between  $-30\text{--}11$  and  $-30\text{--}42$  ppm, about 10 ppm to low frequency of the  $\text{D}'_3$  compound. Again, this is due to the effect of asymmetry. The shift difference between  $\text{D}'_3$  and  $\text{D}'_4$  is about the same as that observed for the analogous cyclic dimethylsiloxanes. The large 10 ppm difference between the six-membered ring and larger rings is apparently due to steric interactions which occur upon ring contraction. (84)

Pestunovich *et al.* (94) recently reported  $^{29}\text{Si}$  data on a series of oligodiorganycyclosiloxanes  $\text{D}_n\text{F}_{m-n}$  ( $\text{D} = \text{Me}_2\text{SiO}$ ,  $\text{F} = \text{RMeSiO}$ ;  $\text{R} = {}^n\text{Pr}$ ,  $\text{ClCH}_2$ ,  $\text{NCCH}_2$ ,  $\text{CF}_3\text{CH}_2\text{CH}_2$ ,  $\text{Me}_2\text{FCCH}_2$ ,  $\text{CH}_2=\text{CH}$ ,  $\text{C}_6\text{H}_5$ ;  $m = 3$  to  $5$ ,  $n = 2$  to  $m$ ) to investigate the influence of the nature and ring positions of substituents on  $^{29}\text{Si}$  shielding. To estimate the substituent effects they calculated  $\Delta_1$ ,  $\Delta_2$ , and  $\Delta_3$ , where  $\Delta_1 = \delta_{\text{F}} - \delta_{\text{O}}$ ,  $\Delta_2 = \delta_{\text{D}_\alpha} - \delta_{\text{O}}$ ,  $\Delta_3 = \delta_{\text{D}_\beta} - \delta_{\text{O}}$ , and  $\delta_{\text{O}}$  represents the chemical shift of the non-substituted cyclosiloxanes,  $\delta_{\text{F}}$  is the shift of the F unit, and  $\delta_{\text{D}_\alpha}$  and  $\delta_{\text{D}_\beta}$  are the shifts of the D units  $\alpha$  and  $\beta$  to the F unit, respectively.

As expected, the largest shift difference occurs at the silicon to which the R group is attached. Fortuitously, with the substituents used in this study, all F units are to low frequency of the non-substituted compounds. With the exception of  $\text{R} = {}^n\text{Pr}$ ,  $\text{D}_\alpha$  and  $\text{D}_\beta$  shifts, where applicable; are all to high frequency in decreasing amounts relative to the non-substituted compounds (Table XIV). The magnitude of the shift change is found to be linearly related to the inductive properties of

TABLE XIV

<sup>29</sup>Si chemical shifts for a series of cyclosiloxanes (Me<sub>2</sub>SiO)<sub>m-1</sub>(RMeSiO)<sub>m</sub> (94)<sup>a</sup>

<i>m</i>	R	$\delta_{\text{Si}(\text{O})}^b$	$\delta_{\text{Si}(\text{F})}$	$\Delta_1$	$\Delta_2$	$\Delta_3$
3	CH <sub>3</sub>	-8.93				
3	CH <sub>3</sub> CH <sub>2</sub> CH <sub>2</sub>	-9.28	-9.91	-0.98	-0.35	
3	ClCH <sub>2</sub>	-7.31	-19.97	-11.04	+1.62	
3	CNCH <sub>2</sub> CH <sub>2</sub>	-7.79	-12.34	-3.41	+1.14	
3	CF <sub>3</sub> CH <sub>2</sub> CH <sub>2</sub>	-8.14	-11.61	-2.68	+0.79	
3	(CF <sub>3</sub> ) <sub>2</sub> FCCH <sub>2</sub> CH <sub>2</sub>	-8.14	-11.22	-2.29	+0.79	
3	CH <sub>2</sub> =CH	-8.69	-23.97	-15.04	+0.24	
3	C <sub>6</sub> H <sub>5</sub>	-8.23	-22.70	-13.77	+0.70	
4	CH <sub>3</sub>	-20.00				
4	ClCH <sub>2</sub>	-18.5( $\alpha$ ) -19.5( $\beta$ )	-30.6	-10.6	+1.5	+0.5
4	F <sub>3</sub> CCH <sub>2</sub> CH <sub>2</sub>	-18.27( $\alpha$ ) -18.58( $\beta$ )	-21.74	-2.10	+1.37	+1.06
4	C <sub>6</sub> H <sub>5</sub>	-18.29( $\alpha$ ) -18.81( $\beta$ )	-32.28	-12.64	+1.35	+0.83
5	CH <sub>3</sub>	-22.62				
5	F <sub>3</sub> CCH <sub>2</sub> CH <sub>2</sub>	-20.76( $\alpha$ ) -21.19( $\beta$ )	-24.10	-2.68	+1.26	+0.83

<sup>a</sup> In ppm relative to Me<sub>4</sub>Si.<sup>b</sup> See text for definition of the  $\alpha, \beta$  terminology.

the substituent R. The inductive influence of substituents on <sup>29</sup>Si shieldings had been observed previously (75,95) in other systems. Pestunovich *et al.* pointed out (94) that, along with an increase in substituent electronegativity at the F unit, there is an increase in the electron density on its silicon atom, and consequently an electron density decrease at the  $\alpha$  silicon atom (a general property of systems containing Si-O-Si groups). This accounts for the sign difference between  $\Delta_1$  and  $\Delta_2$  in Table XIV. In compounds of the type F<sub>2</sub>D<sub>2</sub>, F<sub>3</sub>D, F<sub>4</sub>, and F<sub>5</sub> these authors report peak multiplicity due to asymmetry. Attempts to calculate these shifts based on substituent effects prove to be more difficult, especially for the F<sub>4</sub> and F<sub>5</sub> compounds. Substituent effects are not the only factor affecting <sup>29</sup>Si shielding changes in cyclosiloxanes; steric interactions and other ring size effects must be considered. The correct choice of model compounds used to calculate substituent effects is critical in the cyclic systems as it also is in the linear siloxanes.



## I. Silicates

There are a number of papers which report the use of  $^{29}\text{Si}$  NMR in studies of the structures of various soluble silicates and alkali silicate glasses. (93, 97–103) Early workers concluded that in soluble sodium metasilicate solutions only simple monomeric silicate structures are present. (104) The presence of polymeric structures was subsequently identified using Raman spectroscopy (105–107) and trimethylsilylation experiments. (108) Marsmann (97) first reported the existence of dimer, linear trimer, tricyclic, and polymeric structures based on  $^{29}\text{Si}$  NMR

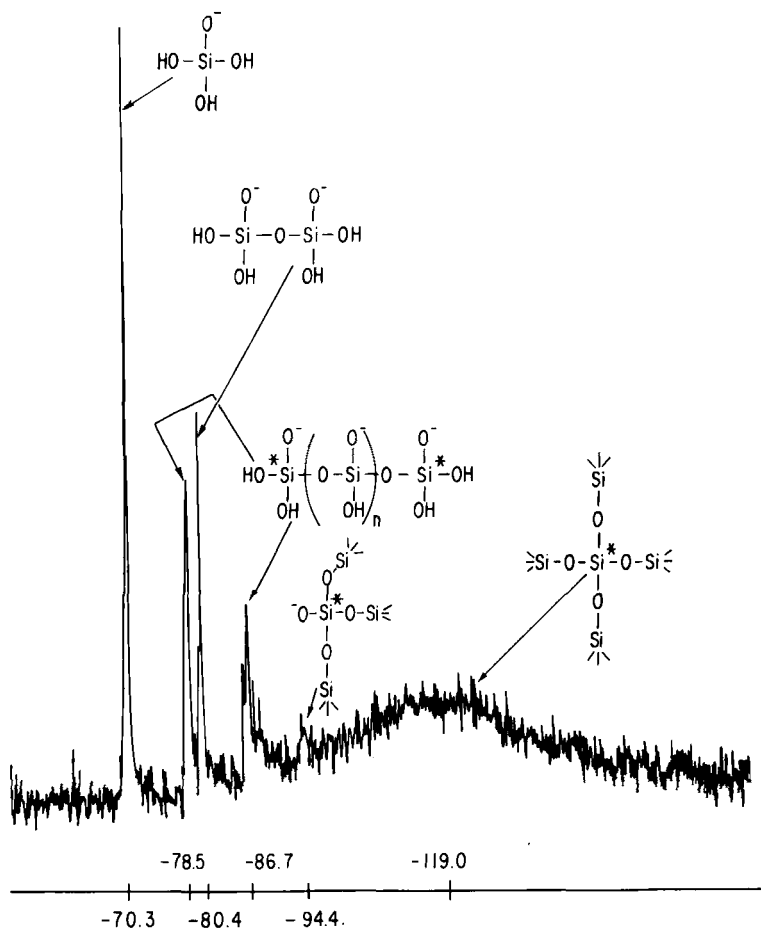


FIG. 20.  $^{29}\text{Si}$  NMR spectrum of sodium metasilicate. Chemical shifts are in ppm relative to  $\text{Me}_4\text{Si}$ .

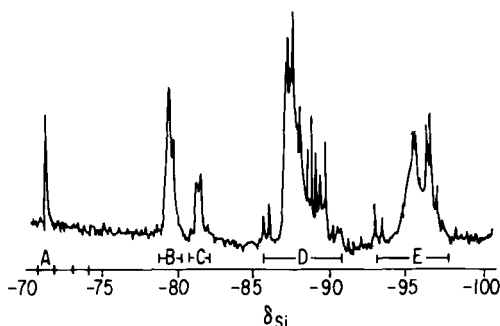


FIG. 21.  $^{29}\text{Si}$  NMR spectrum of a 4.1 M solution of sodium silicate with a 1:1 Na/Si ratio. (39) Chemical shifts are in ppm relative to  $\text{Me}_4\text{Si}$ .

results. Gould *et al.* (98) published similar  $^{29}\text{Si}$  NMR results at about the same time with the same results and conclusions. Their samples were prepared from recrystallized  $\text{NaSiO}_3 \cdot 9\text{H}_2\text{O}$  with precautions taken to filter out impurities and gases that would change pH and cause formation of colloidal silica. A typical sodium metasilicate solution  $^{29}\text{Si}$  NMR spectrum is shown in Fig. 20. At least six clear peaks can be seen including a broad resonance signal assigned to  $\text{Q}^4$  units, to which a large contribution comes from the glass sample tube and probe insert. Marsmann used Teflon sample tubes and a Teflon insert to record his  $^{29}\text{Si}$  spectra and was still able to observe a  $\text{Q}^4$  resonance which indicates that the polymeric structure is present. Engelhardt *et al.* (93) showed the effect of the Na/Si ratio on the  $^{29}\text{Si}$  spectrum of sodium silicate solutions. They were able to record very high resolution  $^{29}\text{Si}$  NMR spectra with more detail and fine structure than previous workers. A spectrum with Na/Si ratio of 1:1 is shown in Fig. 21. The spectrum clearly shows the presence of five building units (Table XV) with many observable signal splittings caused by neighbouring group

TABLE XV

Five silicate building units corresponding to Fig. 21 (93)

Signal	Unit	Branching
A	Monosilicate	$\text{Q}^0$
B	End group	$\text{Q}^1$
C and D	Middle group	$\text{Q}^2$
E	Branching group	$\text{Q}^3$
F (not in Fig. 21)	Crosslinking group	$\text{Q}^4$

effects. Figure 22 shows the effect on the spectrum when the Na/Si ratio is changed from 0.5 to 40. When the Na/Si ratio is small more polymeric silicon anions are present. As the ratio increases the polymeric structures decrease until only the monosilicate anion remains. Harris and Newman, (102) using dilute solutions to obtain narrow lines, performed a detailed structural analysis on carefully prepared samples of potassium and sodium metasilicates. Using monosilicate ( $Q^0$ ) as their standard and Engelhardt's (93, 103) notation for silicates, they assigned structures to seven distinct peaks in a spectrum of potassium silicate prepared with excess KOH to break down the more condensed silicate structures (Table XVI). Harris and

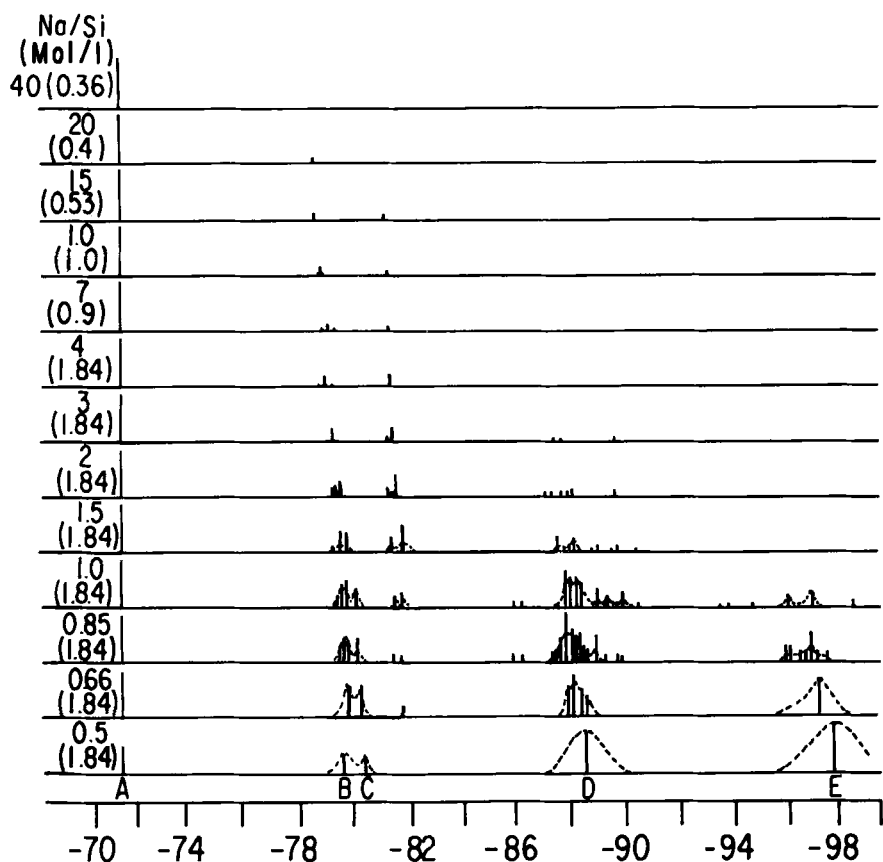


FIG. 22. Simulated  $^{29}\text{Si}$  NMR spectra for sodium silicate solutions with varying Na/Si ratios. Chemical shifts are in ppm relative to  $\text{Me}_4\text{Si}$ . (93)

TABLE XVI

Assignments of  $^{29}\text{Si}$  NMR resonance lines for  
potassium silicate solutions prepared with excess KOH  
(102)

Line	$\delta_{\text{Si}}^a$	Structure
1	0.00	$\text{Q}^0$ monosilicate
2	-7.30	$\text{Q}^1\text{Q}^2\text{Q}^1; \text{Q}^1\text{Q}^2\text{Q}^2\text{Q}^1$
3	-7.47	$\text{Q}^1\text{Q}^1; \text{Q}^1\overline{\text{Q}^3\text{Q}^2\text{Q}^2}$
4	-9.61	$\text{Q}^1\overline{\text{Q}^3\text{Q}^2\text{Q}^2}$
5	-9.81	$\overline{\text{Q}^2\text{Q}^2\text{Q}^2}$
6	-15.27	$\text{Q}^1\text{Q}^2\text{Q}^2\text{Q}^1$
7	-15.46	$\text{Q}^1\text{Q}^2\text{Q}^1$
8	-17.41	$\text{Q}^1\overline{\text{Q}^3\text{Q}^2\text{Q}^2}$

<sup>a</sup> In ppm relative to  $\text{Q}^0$ .

Newman interpreted the spectrum by including the presence of only five structural species as follows:

Mononuclear  $\text{Q}^0$

Dinuclear  $\text{Q}^1\text{Q}^1$

Cyclic trinuclear  $(\text{Q}^2)_3$

Substituted cyclic trinuclear  $\text{Q}^1\overline{\text{Q}^3\text{Q}^2\text{Q}^2}$

Linear trinuclear  $\text{Q}^1\text{Q}^2\text{Q}^1$

Linear tetranuclear  $\text{Q}^1\text{Q}^2\text{Q}^2\text{Q}^1$

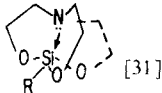
Because glass substitutes for NMR tubes and probe inserts are not yet commercially available, detailed studies of compounds with  $\text{Q}^4$  structures have not been extensive.  $^{29}\text{Si}$  NMR does seem to be an excellent tool with which to study silicates and glasses if this interference can be overcome.

## J. Silatranes

The silatranes [1-substituted-(2,2',2''-nitrilotriethoxy)silanes] are compounds with the unusual structure [31] (Table XVII) in which a coordinate bond  $\text{N} \rightarrow \text{Si}$  has been postulated to produce a pentacoordinate species. X-Ray data (109–111) confirm that the N–Si

TABLE XVII

<sup>29</sup>Si chemical shifts for some silatranes and the analogous triethoxysilanes<sup>a</sup> (112)

R		RSi(OEt) <sub>3</sub>
H	-83.6(-83.8) <sup>b</sup>	-59.5(-59.5) <sup>b</sup>
Me	-64.8	-44.2
Et	(-66.5)	(-45.4)
CH=CH <sub>2</sub>	-81.0(-82.3)	-59.5(-59.5)
Ph	-81.7(-81.4)	-58.4(-58.6)
PhC≡C	-94.7 (ref. 114)	-69.5 (ref. 114)

<sup>a</sup> Chemical shifts in ppm relative to Me<sub>4</sub>Si.<sup>b</sup> Data in parentheses from ref. 74.

distance is smaller than the sum of the van der Waals radii for nitrogen and silicon and show that the structure is approximately trigonal bipyramidal around silicon. Since these compounds are intermediate in nature between the "normal" tetracoordinate silanes and the penta- and hexa-coordinate silicon species, it is appropriate that they be discussed as a prelude to the latter.

Several workers (112-114) have examined a series of 1-substituted silatranes and the corresponding triethoxysilanes in order to determine the effects of the N → Si bond on the <sup>13</sup>C and <sup>29</sup>Si NMR data. The chemical shifts, which are in Table XVII, show a consistent shielding effect of approximately 20 ppm with silatrane formation. This effect is clearly associated with the silatrane structure since the model acyclic compounds MeSi(OCH<sub>2</sub>CH<sub>2</sub>NMe<sub>2</sub>)<sub>3</sub> (δ<sub>Si</sub> = -43.8) and MeSi(OCH<sub>2</sub>CH<sub>2</sub>NH<sub>2</sub>)<sub>3</sub> (δ<sub>Si</sub> = -41.5), (115) which have a nitrogen atom the same number of bonds from silicon, exhibit silicon resonances very close to MeSi(OEt)<sub>3</sub>. The shielding effect is in the direction expected on the basis of the shifts noted for penta- and hexa-coordinate compounds (see Section II.K). Recently the nitrogen analogue of 1-methylsilatrane (1-methylazasilatrane) was investigated and found to contain a stronger N → Si interaction. (116)

### K. Extracoordinate silicon compounds

The possibility of valence shell expansion is one reason for the often marked differences in chemical behaviour between silicon and carbon. This valency expansion for silicon leads to compounds (and suggested

reaction intermediates) in which the coordination number of silicon rises above 4. Stable extracoordinate silicon compounds result only when the silicon atom is bonded to highly electronegative atoms like fluorine, chlorine, oxygen, or nitrogen. A well known example of this is the fluorosilicate anion  $\text{SiF}_6^{2-}$  in which the fluorines are located in an octahedral array about silicon. Other negatively charged hexacoordinate and pentacoordinate complexes are known including the catecholates (117) and diolates. (118) Cationic and neutral complexes are also known in which silicon is penta- or hexa-coordinate. For example, tris(acetylacetonato)silicon(IV) chloride-hydrochloride was first prepared by Dilthey (119) in 1906. Since that time a number of structurally related cationic hexacoordinate tris-1,3-dicarbonyls and tropolonates have been prepared and characterized. (120, 121) Several pentacoordinate cationic silicon chelates have recently been described (122) as well as some neutral bis-1,3-dicarbonyl bis-aryl complexes. (123)

Characterization of these extracoordinate compounds has depended mostly on elemental analysis and differences in IR and UV spectra compared with typical tetravalent silicon compounds. (124)

$^{29}\text{Si}$  NMR offers a unique method for characterization of these complexes since their chemical shifts deviate greatly from the normal range found for most tetravalent silicon compounds. A number of different types of extracoordinate silicon complexes have been prepared and characterized (125) and their  $^{29}\text{Si}$  NMR chemical shifts determined. The chemical shift data are in Table XVIII.

TABLE XVIII

 $^{29}\text{Si}$  chemical shifts of extracoordinate silicon complexes (127)

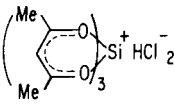
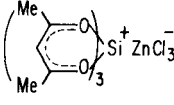
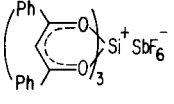
Compound	$\delta$ (ppm)	Solvent
<i>Cationic hexacoordinate</i>		
[32] 	-194.4 (ref. 128)	$\text{CHCl}_3$
[33] 	-193.7	DMSO
[34] 	-191.4	acetone

TABLE XVIII (continued)

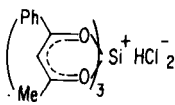
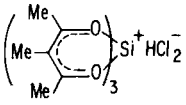
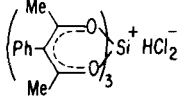
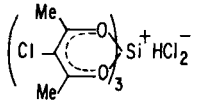
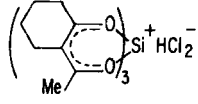
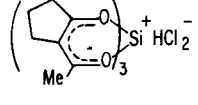
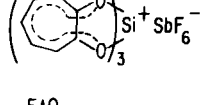
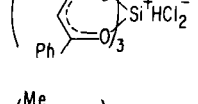
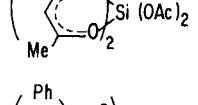
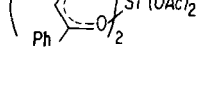
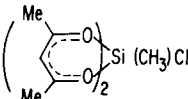
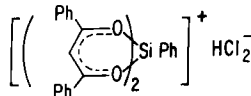
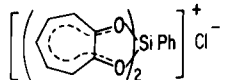
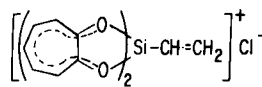
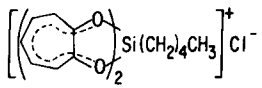
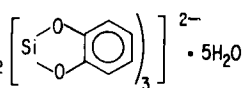
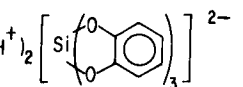
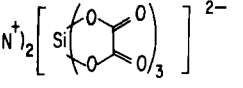
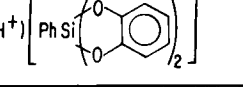
Compound	$\delta$ (ppm)	Solvent
[35] 	-192.4	DMSO
[36] 	-195.7	acetone
[37] 	-195.3	acetone
[38] 	-196.4	acetone
[39] 	-195.0	DMSO
[40] 	-191.2	acetone
[41] 	-139.4	CH <sub>3</sub> OH
[42] 	-187.9	acetone
<i>Neutral hexacoordinate</i>		
[43] 	-196.8	DMSO
[44] 	-195.4	DMSO

TABLE XVIII (continued)

Compound	$\delta$ (ppm)	Solvent
[45] 	-149.5	CHCl <sub>3</sub>
<i>Cationic pentacoordinate</i>		
[46] 	-175.8	DMSO
[47] 	-141.3	DMSO
[48] 	-141.8	DMSO
[49] 	-127.1	DMSO
<i>Anionic hexacoordinate</i>		
[50] Zn <sup>2+</sup> + SiF <sub>6</sub> <sup>2-</sup>	-185.3 (ref. 128)	H <sub>2</sub> O
[51] (NH <sub>4</sub> <sup>+</sup> ) <sub>2</sub>  • 5H <sub>2</sub> O	-135.3 (ref. 128)	DMSO
[52] (Et <sub>3</sub> NH <sup>+</sup> ) <sub>2</sub> 	-139.3	DMSO
[53] (n-Bu <sub>4</sub> N <sup>+</sup> ) <sub>2</sub> 	-173.3	C <sub>6</sub> F <sub>6</sub>
[54] (Et <sub>3</sub> NH <sup>+</sup> ) 	-87.1	acetone

Although there are too many gaps in structural types to permit any predictable correlation between structure and chemical shift, a number of trends are apparent, particularly among the cationic complexes. For example, hexacoordinate cationic and neutral complexes in which the



chelate ring is derived from a 1,3-diketone display nearly identical chemical shifts regardless of charge type or structure of the 1,3-dicarbonyl compound ([32]–[40], [43], [44]). The chelate derived from a keto-ester [42] is shifted to high frequency by nearly 50 ppm. Different chemical shifts are also observed for those complexes in which the chelate ring is five-membered ([41], [47]–[49], [51]–[54]).

In this series the "aromatic" ligands catechol and tropolone afford chelates whose chemical shift is a function of the number of oxygen atoms around silicon and the nature of the non-chelating group attached to silicon. Thus the cationic and anionic hexacoordinate complexes [41], [51], and [52] have essentially the same chemical shifts whether tropolone or catechol is the ligand.

It has been suggested (126) that similarity in chemical shift among the hexacoordinate complexes is due to the symmetry of distribution of the ligands in these compounds which effectively cancels any charge on the central atom. These symmetry effects disappear in the pentacoordinate complexes which should have a definite dipole moment. This appears to be the case since among the pentacoordinate chelates there are chemical shift differences between the anionic catechol and cationic tropolone derivatives ([47]–[49] and [54]). This may be due to a different effect of the aryl substituent depending on charge type.

For the cationic pentacoordinate tropolonates there appears to be an effect of the nature of the non-chelating group R on chemical shift. Those tropolone complexes in which the silicon atom is bonded to an  $sp^2$  hybridized carbon in R ([47] and [48]) exhibit a chemical shift of  $-141$  ppm compared with hexacoordinate  $T_3Si^+X^-$  ( $\delta = -139$  ppm). When the carbon atom attached to silicon is  $sp^3$  hybridized as in [48] a shift to  $-127$  ppm is observed. In these complexes the R group should affect the charge density around silicon thus causing the shift change.

The value of  $^{29}Si$  NMR in characterizing extracoordinate silicon complexes should be evident from the data in Table XVIII. Additionally this method can be used to establish whether a given ligand will form an extracoordinate complex with silicon or remain tetracoordinate. For example, a reaction mixture of  $SiCl_4$  and a bidentate ligand can be examined for resonances outside the normal Q region to determine whether an extracoordinate complex or a normal tetravalent compound is formed.

#### L. Solvent effects

Most studies of solvent effects on  $^{29}Si$  chemical shifts have been directed toward finding a suitable reference compound. (33, 129)

Indeed, the solvent effects are usually small ( $< 1$  ppm) compared with the changes arising from structural perturbations and are therefore generally not a problem in interpreting  $^{29}\text{Si}$  data. For cases in which specific solvent-solute interactions are possible, however, large solvent shifts can occur.

A series of silanol and silylamine chemical shifts were obtained in various solvents. (83) The silanols are found to be highly dependent ( $> 5$  ppm shifts) upon solvent basicity with the more basic solvents causing low frequency shifts. This shielding effect is found to give an excellent linear correlation with Gutmann's donor number (DN) (130) which is a measure of the electron pair donor ability of the solvent. Figure 23 shows the correlation for five of the compounds examined. It

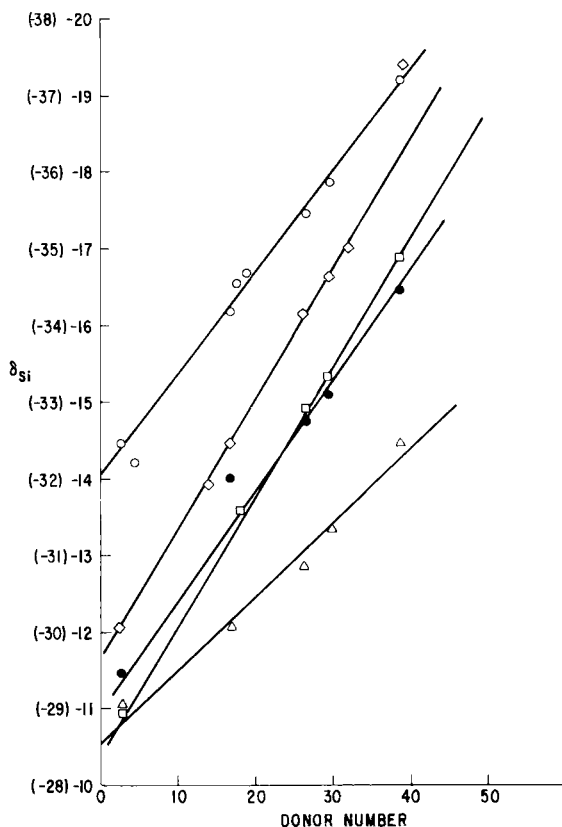


FIG. 23.  $^{29}\text{Si}$  chemical shifts vs. donor number of the solvent for  $\text{Ph}_3\text{SiOH}$  (○),  $\text{Ph}_2\text{Si(OH)}_2$  (◇),  $\text{(HOSiMe}_2)_2\text{O}$  (□),  $\text{HO(Me}_2\text{SiO)}_6\text{H}$  (●), and  $\text{(PhNH)}_2\text{SiMe}_2$  (△). (83) Chemical shifts are in ppm relative to  $\text{Me}_4\text{Si}$ . The scale in parentheses corresponds to  $\text{Ph}_2\text{Si(OH)}_2$ .

should be noted that of the four silylamines investigated only bis(phenylamino)dimethylsilane gives a good correlation with solvent donor number (see Fig. 23). In general the amines show much smaller solvent shifts than the silanols. It is interesting that for the hydroxy terminated siloxane  $\text{HO}(\text{SiMe}_2\text{O})_6\text{H}$  the shielding effect is transmitted down the chain (Fig. 24), with smaller chemical shift changes for  $\text{D}^2$  and  $\text{D}^3$  than for the terminal silicon ( $\text{D}^1$ ).

These solvent shifts have been attributed to an interaction of the type  $-\text{Si}-\text{O}-\text{H}\cdots\text{B}$ , which is consistent with  $^1\text{H}$  NMR data showing strong hydrogen bonding between silanols and dimethyl sulphoxide. (131) Although the relationship between electronic structure and  $^{29}\text{Si}$  chemical shift is not clear, the increase in screening due to a good donor solvent is consistent with repulsion of the  $\text{O}-\text{H}$  bonding electrons by the solvent electron pair, and a consequent increase in electron density at silicon. The extreme of this effect is anion formation; in the very basic solvent system sodium ethoxide-ethanol, in the presence of excess base, triphenylsilanol exists predominantly as the anion and has a chemical shift of  $-25.4$  ppm compared with triphenylsilanol in chloroform ( $-12.6$  ppm).

The strong solvent dependence of the chemical shifts does provide a ready means of detecting silanol resonances in complex mixtures. The sample can be examined in two solvents of widely varying donor ability (chloroform and acetone are sufficiently different to detect changes) or a small amount of a good donor solvent can be added to the sample. In the latter case small additions of the good donor solvent cause large shifts by preferential solvation. (83)

### M. Steric effects

The effects of crowding and steric interaction on  $^{29}\text{Si}$  chemical shifts have been considered by several authors. (32, 132-134) Each of these authors compared the  $^{29}\text{Si}$  NMR results with observed carbon shifts in analogous compounds and found that the steric effect on silicon shielding is roughly the same as on carbon. (32) Engelhardt and Schraml (132) have shown that a  $\gamma$  methyl group causes approximately a 3 ppm shielding effect in  $(\text{CH}_3)_3\text{SiOCH}_2\text{CH}_3$ . They estimated that polar contributions account for about 0.8 ppm, leaving the steric  $\gamma$  effect to account for a 2 ppm low frequency shift. Variations around this average value are interpreted as arising from differences in conformer populations. In trimethylsiloxy substituted benzenes,  $\text{C}_6\text{H}_4(\text{OSiMe}_3)_2$ , Schraml *et al.* (133) noted that crowding in the *ortho* derivative leads to a small but observable high frequency shift relative to trimethylphenoxysilane,  $\text{C}_6\text{H}_5\text{OSiMe}_3$ , of both the silicon and carbon

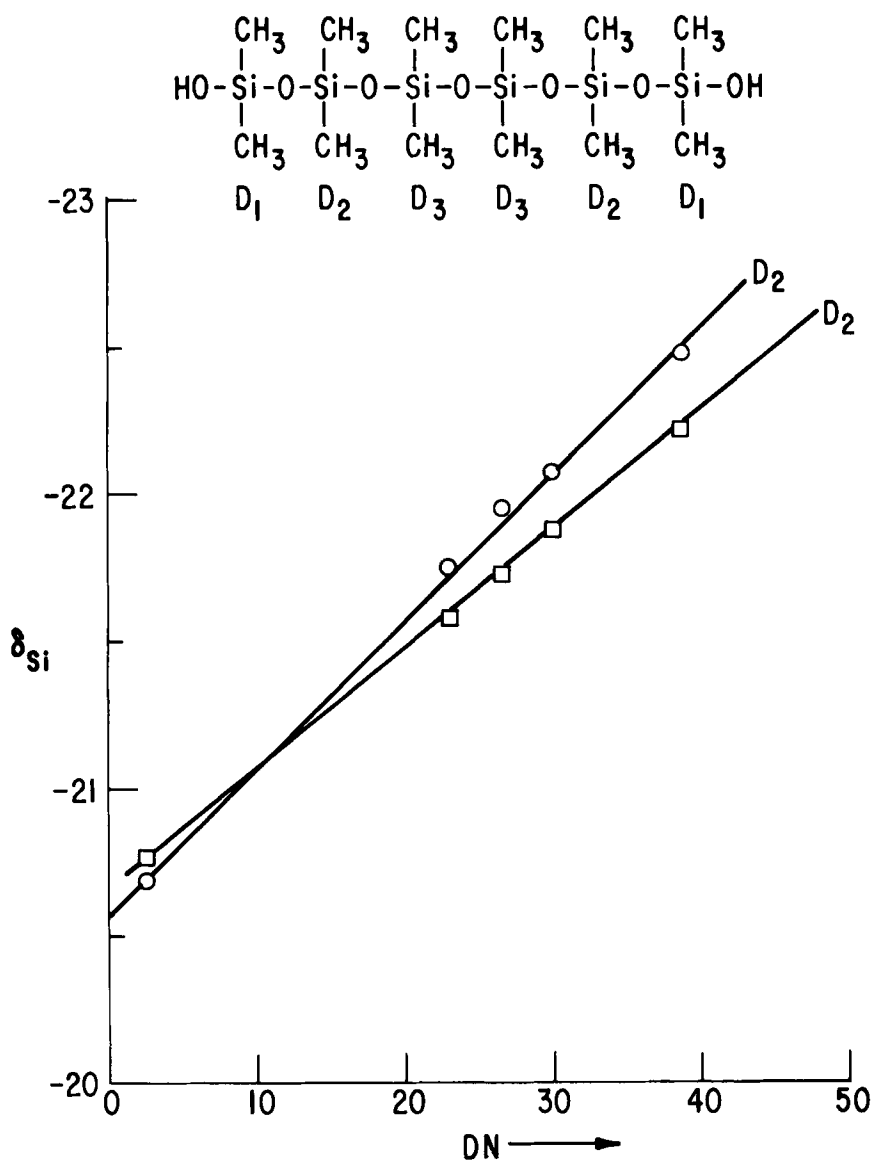


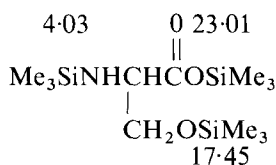
FIG. 24.  $^{29}\text{Si}$  chemical shifts in ppm relative to  $\text{Me}_4\text{Si}$  vs. donor number of the solvent for the internal silicon atoms ( $\text{D}^2$  and  $\text{D}^3$ ) of  $\text{HO}(\text{SiMe}_2\text{O})_6\text{H}$ . (83)

resonances of the trimethylsiloxy group. Upon comparison with analogous effects observed in trimethylsilylbenzenes,  $C_6H_4(SiMe_3)_2$ , the oxygen appears to increase the susceptibility of the silicon to the steric effect but to decrease that of the carbons. It is suggested (133) that the operative steric interaction may not be between the two terminal methyl groups but may involve the oxygen atom.

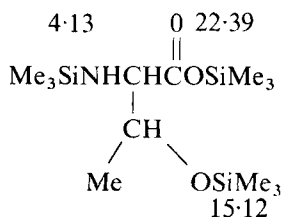
## N. Applications

The sensitivity of  $^{29}Si$  chemical shifts to structural changes and the technique of silylating compounds for more favourable analysis or synthesis have been combined by several researchers to produce a powerful structure elucidation technique for monofunctional or polyfunctional compounds. (135–141) Specifically, the trimethylsilyl derivatives of imidophosphoryl compounds, (141) sugars, (138–140) steroids, (140) amines, amides, and urethanes, (135, 136) and amino-, hydroxy-, and mercaptocarboxylic acids (137) have all been studied within the past three years.

Schraml *et al.* (137) found that the  $^{29}Si$  resonances of a series of silyl ester, alkoxy-silyl, and amino-silyl derivatives appear in different regions of the spectrum. On the basis of this information they suggested that  $^{29}Si$  NMR can be used for the structure elucidation of silylated hydroxy- or aminoacids. The silicon chemical shifts for DL-serine [55] and DL-threonine [56] are shown in ppm. The variation in the shielding for the alkoxy-silyl group demonstrates the previously noted sensitivity of  $^{29}Si$  NMR to the nature of R in  $Me_3SiOR$ . (140)



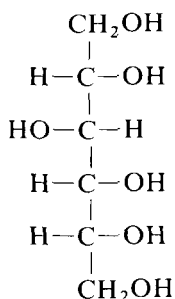
[55]



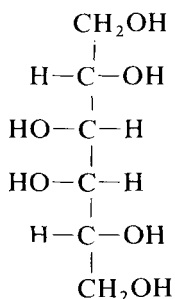
[56]

The utility of this technique is clearly demonstrated for sugars. (138, 140) The  $^{29}Si$  NMR spectrum of hexakis-*O*-trimethylsilyl-D-sorbitol (TMS derivative of 57) shows five resonances ( $\delta = 15.6$  to  $16.7$  ppm), one of which has twice the intensity of the others. This is consistent with the structure of [57]. The largest peak corresponds to trimethylsilylation at the two terminal hydroxymethyl groups. The corresponding compound with [58] also gives a  $^{29}Si$  NMR spectrum

consistent with its (symmetrical) structure; only three peaks of equal intensity are observed.



[57]



[58]

A variety of techniques including specific deuteration, selective proton decoupling, and lanthanide shift reagents (LSR),  $\text{Pr}(\text{dpm})_3$ , was used by Haines *et al.* (138) to assign completely the  $^1\text{H}$  and  $^{29}\text{Si}$  NMR spectra of methyl-2,3,4,6-tetra-*O*-trimethylsilyl- $\alpha$ -D-glucopyranoside. This paper also presents the first LSR study in  $^{29}\text{Si}$  NMR. It shows that the magnitudes of the LSR induced shifts in the  $^1\text{H}$  spectra are of the same order as those found for the  $^{29}\text{Si}$  resonances. (138)

$^{29}\text{Si}$  NMR has been used to study equilibria in *N*-silyl-amides and *N*-silyl-urethanes. (135) All the *N*-silyl-amides investigated are found to exist in an amide-imide equilibrium, with electron donating groups at N and lower temperatures favouring the amide form. In contrast, the silyl-urethanes are all in the amide form.

### III. COUPLING CONSTANTS

#### A. Theoretical considerations

The indirect coupling of nuclear spins through the bonding network is considered to be the sum of three terms. (142) The first term is due to the interaction of orbital electronic currents with nuclear moments. The second term arises from the dipole-dipole interaction between nuclear and electron magnetic moments. The third term is dependent upon the properties of the electrons at the nucleus (Fermi contact term) and is considered to be dominant in determining the coupling constant. Although the relative importance of the orbital and spin dipolar terms in determining  $^{29}\text{Si}$  coupling constants is not known, a number of highly successful calculations have been carried out using only the Fermi contact contribution. Indeed, recent calculations of  $^1J(\text{Si}-\text{C})$  by

Beer and Grinter (143) using the finite perturbation theory at the INDO level of approximation indicate that the combined orbital and spin-dipolar contributions are less than 1% of the observed coupling.

## B. Calculations of silicon coupling constants

Early workers attempted to explain  $^1J(\text{Si-H})$  using the same approach as the empirical linear additivity rule used for  $^1J(\text{C-H})$ . (144) Deviations were noted, however, with electronegative substituents (145–147) and it was noticed that the deviation increased with increasing substituent electronegativity. Substantial improvement was obtained using pairwise interaction terms (148, 149) with the coupling constant expressed as a sum of constants for each pair of substituents:

$$J(\text{XYZ}) = J'(\text{XY}) + J'(\text{XZ}) + J'(\text{YZ}) \quad (11)$$

where  $J'$  refers to a constant for each pair of substituents in the compound  $\text{SiHXYZ}$ , and  $J(\text{XYZ})$  is the one-bond Si-H coupling constant  $^1J(\text{Si-H})$ . Subsequently Jensen *et al.* (150) used the Pople-Santry method (151) of calculating coupling constants to explain these substituent effects. They concluded that the Fermi contact term is sufficient to explain the observations and that the important perturbation can be related to electronegativity of the substituent. Jensen (152) suggested a quadratic equation for  $^1J(\text{M-H})$ :

$$J(\text{MHXYZ}) = J(\text{MH}_4) + A(\alpha_X + \alpha_Y + \alpha_Z) + B(\alpha_X^2 + \alpha_Y^2 + \alpha_Z^2) + C(\alpha_X\alpha_Y + \alpha_Y\alpha_Z + \alpha_Z\alpha_X) \quad (12)$$

in which M can be either C or Si,  $\alpha_X$  is the Coulomb integral (or effective electronegativity) of the substituent X, and A, B, and C are constants. For silanes, the values of A, B, and C are determined to be 18.26 Hz/eV, 1.78 Hz/eV<sup>2</sup>, and -2.98 Hz/eV<sup>2</sup>, respectively. The effect of a  $\beta$ -substituent X on  $^1J(\text{Si-H})$  is evaluated (152) by means of:

$$\Delta\beta_X = K\alpha_X \quad (13)$$

where  $K = 3.9 \text{ Hz/eV}$ . If  $\Delta\beta_X$  is added to the calculated coupling constant, the results shown in Table XIX are obtained. Jensen's equation with the same values of A, B, and C is found to be useful for halogenated disilanes. (153) A further correlation is noted for  $^1J(\text{Si-H})$  of the silicon atom adjacent to the substituted silicon: (153)

$$^1J(\text{Si-H}) = ^1J(\text{Si-H})(\text{disilane}) + 2.25\alpha \quad (14)$$

TABLE XIX

Comparison of calculated and observed coupling constants  $^1J(\text{Si-H})$   
for some silanes (152)

Compound	$J_{\text{calc}}$ (Hz)	$J_{\text{obs}}$ (Hz)
$\text{ClCH}_2\text{SiH}_2\text{Me}$	-198.8	-198.5
$\text{Cl}_2\text{CHSiH}_2\text{Me}$	-208.6	-208.2
$\text{BrCH}_2\text{SiHMe}_2$	-192.9	-193.2
$\text{ICH}_2\text{SiHMe}_2$	-191.0	-191.4
$(\text{CH}_3\text{CH}_2)_3\text{SiH}$	-178.8	-179.2

Earlier, Yoshioka and MacDiarmid found the relationship:

$$^1J(\text{Si-H})(\text{H}_3\text{SiSiH}_2\text{X}) = ^1J(\text{Si-H})(\text{Si}_2\text{H}_6) + 0.75[^1J(\text{Si-H})(\text{SiH}_3\text{X}) - ^1J(\text{Si-H})(\text{SiH}_4)] \quad (15)$$

which gives good agreement with the experimental values for twelve disilanyl compounds. (163) All calculated values of  $J$  are in Hz.

An alternative approach for silanes was suggested by Ebsworth *et al.* (155) who noted that the difference between the value of  $J_A$  calculated from the additivity relationship and the experimentally observed  $J_{\text{obs}}$  is linearly proportional to the square of the electronegativity difference of the substituents from hydrogen. They suggested the following relationship for calculating  $J$  in dihalogenosilanes  $\text{SiH}_2\text{XY}$ :

$$J_B = J_A - 7.5(2\chi_H - \chi_X - \chi_Y)^2 \quad (16)$$

where  $J_A$  is given by:

$$J_A(\text{SiH}_2\text{XY}) = J(\text{SiH}_3\text{X}) + J(\text{SiH}_3\text{Y}) - J(\text{SiH}_4)$$

The value of  $J_B$  is found to be within experimental error of  $J_{\text{obs}}$  and is calculated using only one empirical parameter. (155)

Several workers have related the magnitude of  $^{29}\text{Si}$  couplings to the character in the bonding orbital to the coupled nucleus. (146, 154, 156-159) Rastelli and Pozzoli (154) find a simple relationship to be adequate:

$$^1J(\text{Si-H}) = 810\alpha_H^2 \quad (17)$$

where  $\alpha_H^2$  is the s character of the silicon orbital directed towards hydrogen as calculated by the Del Re method. Levy *et al.* (156) noted a rough proportionality between the magnitude of  $^1J(\text{Si-C})$  and the s



character of the carbon nucleus in several compounds containing only Si, C, and H. Kovacević and Maksić (158) reproduced this trend with calculations of  $^1J(\text{Si}-\text{C})$  based on the maximum overlap approximation method. Their calculations assume dominance of the Fermi contact term and include the average excitation energy approximation. A comparison between calculated and experimental values is presented in Table XX along with the s characters of the relevant atoms. The data show that the silicon atom remains very close to  $sp^3$  hybridization. A similar approach was used by Kovacević *et al.* to calculate  $^1J(\text{Si}-\text{H})$  in silanes. (159) Dreeskamp and Hildenbrand (157) examined tetra-vinylsilane as well as some vinyl- and chloro-silanes. They find the one-bond coupling constants  $^1J(\text{Si}-\text{C})$  to be proportional to the s character of the Si-C bond, whereas the two-bond couplings  $^2J(\text{Si}-\text{H})$  are dependent on the hybridization of both the silicon atom and the intervening carbon atom.

TABLE XX

Comparison of calculated and experimental coupling constants and the s characters of the atoms involved in the coupling (158)

Molecule	$S_{\text{Si-C}} (\%)$	$^1J(\text{Si}-\text{C})$ (Hz)	
		calc.	exp. (ref. 156)
$(\text{CH}_3)_4\text{Si}$	25.0	51.4	50.3
$(\text{CH}_3\text{CH}_2)_4\text{Si}$	25.0	52.2	50.2
$\text{PhSi}(\text{CH}_3)_3$	26.1	64.7	66.5
$(\text{CH}_2\text{CH})_2\text{Si}(\text{CH}_3)_2$	25.6	62.4	66.0
$(\text{CH}_2\text{CH})_3$	26.1	64.7	64.0
$\text{PhC}\equiv\text{CSi}(\text{CH}_3)_3$	25.4	85.2	83.6

Summerhays and Deprez have expressed caution, however, in extrapolating detailed hybridization information from experimental coupling constants. (160) These authors calculated  $^1J(\text{Si}-\text{C})$  using finite perturbation theory at the INDO level of approximation and including only the Fermi contact contribution. Good agreement with experimental values is obtained. Furthermore, linear correlations with the hybridization parameter  $P_{\text{SiSiC}}^2$  giving correlation coefficients of 0.98 and 0.96 are reported:

$$\text{Calculated: } ^1J(\text{Si}-\text{C}) = -1055.4P_{\text{SiSiC}}^2 + 15.9 \text{ Hz} \quad (18)$$

$$\text{Experimental: } ^1J(\text{Si}-\text{C}) = -1227.7P_{\text{SiSiC}}^2 + 26.0 \text{ Hz} \quad (19)$$

However, they pointed out that the sensitivity of  $^1J(\text{Si}-\text{C})$  to the valence bond equivalent of  $P_{\text{SiSiC}}^2$  in the compounds containing only Si, C, and H is substantially lower. (158) The authors suggest the possibility that this discrepancy arises from the assumption of a constant  $\Delta E$ . Correlations with charge density parameters reflecting electron deficiency of the Si-C bond and polarization in the sense  $\text{Si} \rightarrow \text{C}$  are also found. (160)

Beer and Grinter used finite perturbation theory to calculate  $^1J(\text{Si}-\text{H})$ ,  $^2J(\text{Si}-\text{H})$ , (161) and  $^1J(\text{Si}-\text{C})$  (143) as well as the analogous phosphorus couplings. The best results are obtained for  $^1J(\text{Si}-\text{C})$  (Table XXI) for which the correlation coefficient of the best fit of calculated to observed values is 0.985. The various calculated contributions to  $^1J(\text{Si}-\text{C})$  are in Table XXI. Clearly, the orbital and spin-dipolar terms, which are small and also of opposite sign, have little effect on the calculated value of  $J$ . It is concluded that the Fermi contact term is probably sufficient for the calculation of  $^1J(\text{Si}-\text{C})$  and that inclusion of silicon d orbitals is not required.

TABLE XXI

Calculated and observed values (Hz) of one-bond silicon-carbon couplings (143)

Molecule	FC <sup>a</sup>	OB <sup>a</sup>	SD <sup>a</sup>	Total	$J_{\text{obs}}$	Ref. ( $J_{\text{obs}}$ )
PhCCSiMe <sub>3</sub>	-86.8	0.7	-0.3	-86.4	83.6	156
(CH <sub>2</sub> CH) <sub>2</sub> Si	-69.0	0.8	-0.5	-68.7	70.0	156
(CH <sub>2</sub> CH) <sub>2</sub> SiMe <sub>2</sub>	-64.1	0.8	-0.6	-63.9	66.0	156
CH <sub>2</sub> CHSiMe <sub>3</sub>	-66.8	0.8	-0.6	-66.6	64.0	156
Ph*SiMe <sub>3</sub>	-63.1	0.9	-0.8	-63.0	66.5	156
MeSiHCl <sub>2</sub>	-63.9	1.0	-0.5	-63.4	-66.0	162
MeSiH <sub>2</sub> Cl	-57.1	1.0	-0.5	-56.6		
Me <sub>3</sub> SiF	-59.7	0.8	-0.5	-59.4	60.5	42
Me <sub>3</sub> SiCl	-55.7	0.8	-0.6	-55.5	57.7	42
PhSiMe <sub>3</sub>	-51.8	0.8	-0.6	-51.6	52.2	42
Me <sub>4</sub> Si	-51.2	0.8	-0.6	-51.0	-50.3	156
(MeCH <sub>2</sub> ) <sub>4</sub> Si	-52.8	0.8	-0.5	-52.5	50.2	156
Me <sub>3</sub> SiH	-52.4	0.9	-0.6	-52.1	50.8	42
MeSiH <sub>3</sub>	-52.9	1.1	-0.6	-52.4		
Me <sub>3</sub> SiSiMe <sub>2</sub> F	-44.4	0.8	-0.7	-44.3		
Me <sub>3</sub> SiSiMe <sub>2</sub> F	-48.6	0.9	-0.6	-48.3	47.9	73
Me <sub>3</sub> SiSiMe <sub>2</sub> Cl	-43.9	0.8	-0.7	-43.8	46.2	73
Me <sub>3</sub> SiSiMe <sub>2</sub> Cl	-46.1	0.9	-0.6	-45.8	45.9	73
Me <sub>3</sub> SiSiMe <sub>2</sub> H	-45.4	0.8	-0.6	-45.2	44.6	73
Me <sub>3</sub> SiSiMe <sub>2</sub> H	-44.8	0.9	-0.6	-44.5	43.8	73

<sup>a</sup> FC = Fermi contact contribution; OB = orbital contribution; SD = spin-dipolar contribution.

Several attempts to calculate the signs of silicon coupling constants have been made. (164–166) Cowley and White were able to reproduce the signs of several one- and two-bond couplings with a parameterized LCAO SCF method which includes overlap in the diagonalization of the secular equation. (165) The magnitude of  $^1J(\text{Si-F})$  calculated for  $\text{SiF}_4$  is quite close to the experimental value, but several of the other calculated values are too low. The experimental sign determinations that have been made are collected in Table XXII.

TABLE XXII

Signs of some  $^{29}\text{Si}$  coupling constants

$J$	Sign	References
$^1J(\text{Si-C})$	—	165–168
$^1J(\text{Si-F})$	+	165, 166, 169, 170
$^1J(\text{Si-H})$	—	165–167, 169–171
$^2J(\text{Si-CH})$	+	167, 172
$^3J(\text{Si-CCH})$	—	173

### C. One-bond coupling

Most of the one-bond couplings that have been determined are for  $^{29}\text{Si-H}$ . A wide variety of compounds have been investigated (4, 31–53, 113, 145, 174–202) and some general trends can be noted. Some representative values are shown in Table XXIII. The largest changes occur upon the introduction of an electronegative substituent, the absolute value of  $J$  increasing with substituent electronegativity. The replacement of one H with F in  $\text{FSiH}_3$ , for example, causes an increase in  $|^1J(\text{Si-H})|$  of 50 Hz. The changes within a series of alkylsilanes are much smaller, however. This can only be seen by considering the change in  $^1J(\text{Si-H})$  with progressive methyl substitution in the series  $\text{Me}_{4-n}\text{SiH}_n$  ( $n = 1$  to 4); the total change in coupling constant from  $\text{Me}_3\text{SiH}$  to  $\text{SiH}_4$  is less than 20 Hz.

Electron-rich substituents decrease the absolute magnitude of  $^1J(\text{Si-H})$ . Comparison of  $(\text{Me}_3\text{Si})_3\text{SiH}$  with  $\text{Me}_3\text{SiH}$  (Table XXIII) shows that the former has a lower  $|^1J(\text{Si-H})|$  by approximately 30 Hz. The effect of  $\beta$ -substitution is quite small. (181–185) The change in  $^1J(\text{Si-H})$  from  $\text{F}_2\text{SiH}_2$  to  $\text{F}_3\text{SiH}$  ( $\alpha$ -substitution of fluorine) is almost 100 Hz (145) whereas the analogous effect for substitution at a  $\beta$ -silicon  $\text{H}_3\text{SiSiHF}_2$  [ $^1J(\text{Si-H}_3) = 206.2 \text{ Hz}$ ] to  $\text{H}_3\text{SiSiF}_3$  [ $^1J(\text{Si-H}_3) = -212.0 \text{ Hz}$ ] is 5.8 Hz.

TABLE XXIII

Values of  $^1J(\text{Si-H})$  for some representative silanes

Compound	$^1J(\text{Si-H})$ (Hz)	Ref.	Compound	$^1J(\text{Si-H})$ (Hz)	Ref.
$\text{F}_3\text{SiH}$	-381.7	145	$\text{MeSiH}_3$	-194.0	177
$\text{Cl}_2\text{SiH}$	-353	174	$\text{Me}_2\text{SiH}_2$	-188.6	177
$\text{Br}_2\text{SiH}$	-349	174	$\text{Me}_3\text{SiH}$	-184.0	177
$(\text{AcO})_3\text{SiH}$	-344	176	$^i\text{Bu}_2\text{SiH}_2$	-182.1	177
$\text{F}_2\text{SiH}_2$	-282	145	$\text{Et}_3\text{SiH}$	-179.2	177
$\text{FSiH}_3$	-229.0	145	$(\text{Me}_3\text{Si})\text{Me}_2\text{SiH}$	-173	178
$\text{Sb}(\text{SiH}_3)_3$	-208.3	175	$(\text{Me}_3\text{Si})_3\text{SiH}$	-155	179
$\text{SiH}_4$	-202.5	145	$(\text{Et}_3\text{Si})_3\text{SiH}$	-147	180
$\text{Ph}_2\text{SiH}_2$	-198.2	177			

The changes caused by increasing halogen substitution are shown in Table XXIV. (4, 31) The greatest overall change occurs for the fluoro derivatives and the smallest for the iodo compounds. Chloro and bromo substituents cause almost identical increases in  $|J|$  with increasing substitution. It is interesting that  $^1J(\text{Si-H})$  for the silylcobalt carbonyls  $\text{H}_2\text{SiClCo}(\text{CO})_4$  and  $\text{HSiCl}_2\text{Co}(\text{CO})_4$  are -239 and -280 Hz, respectively, (186) which are quite similar to the corresponding mono- and di-chlorosilanes (Table XXIV). The transition metal is not electronegative and exhibits behaviour similar to that expected for an alkyl group. Similar results are obtained for dihydrides of manganese, rhenium, and iron. (187) The results obtained for silicon pentacoordination in silatrane are also revealing. They are quite consistent with the dependence of  $^1J(\text{Si-H})$  on the s character of the Si-H bond. (113) Whereas  $|^1J(\text{Si-H})|$  in triethoxysilane is 287.4 Hz, the value drops to 278.1 Hz in silatrane.

TABLE XXIV

Effect of halogen substitution on one-bond  $^{29}\text{Si}$ - $^1\text{H}$  coupling constants<sup>a</sup>

X	$\text{H}_3\text{SiX}$	$\text{H}_2\text{SiX}_2$	$\text{HSiX}_3$
F	-229.0	-282	-381.7
Cl	-238.1	-288.0	-362.9
Br	-240.5	-289.0	-360 (ref. 174)
I	-240.1	-280.5	-325 (ref. 174)

<sup>a</sup> Values in Hz. Data from ref. 145 unless noted otherwise.

There have been numerous correlations made between  $^1J(\text{Si-H})$  and various parameters of bonding and reactivity. A rough correlation has been drawn between  $^1J(\text{Si-H})$  and the Si-H force constant in  $\text{HSiX}_3$  compounds and with the Si-Si force constant in  $\text{Si}_2\text{X}_6$  compounds. (188) Good linear relationships between  $^1J(\text{Si-H})$  and Hammett  $\sigma$  constants have been demonstrated for benzyldimethylsilanes and phenyltetramethyldisilanes (189) and phenyl-, phenylmethyl-, and phenyldimethyl-silanes. (190) Similarly, Nagai *et al.* (190, 191) found an excellent correlation between  $^1J(\text{Si-H})$  and Taft polar substituent constants  $\sigma^*$  for compounds of the type  $\text{R}^1\text{R}^2\text{R}^3\text{SiH}$  where R = alkyl, phenyl, and hydrogen. The relationship:

$$^1J(\text{Si-H}) = -10.21\Sigma\sigma^* - 182.9 \quad (20)$$

was derived from the results for 30 silanes (correlation coefficient  $r = 0.994$ ). This is presented graphically in Fig. 25.

The relative reactivities of Si-H bonds towards the  $\cdot\text{CCl}_3$  radical are found to correlate well with  $^1J(\text{Si-H})$ . (192, 193) The results are rationalized on the basis of a change in the s character of the Si-H bond which indicates a change in electron density at hydrogen and thus its ease of removal by  $\cdot\text{CCl}_3$ .

The effect of substituents on the value of directly bound  $^{29}\text{Si}$ - $^{19}\text{F}$  couplings is much less straightforward than for  $^1J(\text{Si-H})$ . The values of  $J$  within the series  $\text{F}_n\text{SiH}_{4-n}$  ( $n = 1$  to 4), for example, are 281, 298, 275, (145) and 170 Hz. (203) Whereas in some cases increasing substituent electronegativity causes a decrease in  $J$ , in other cases  $J$  increases. For the  $\text{F}_3\text{SiX}$  compounds where  $\text{X} = \text{SiH}_3$  and  $\text{OMe}$ , the  $^1J(\text{Si-F})$  values are 356 (204) and 181 Hz (205) respectively. In contrast, the  $^1J(\text{Si-F})$

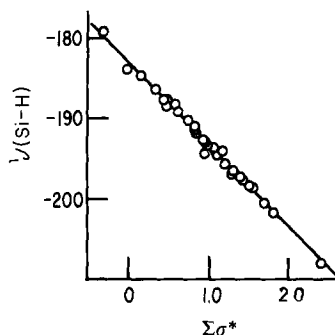


FIG. 25. Plot of one-bond silicon-hydrogen coupling constants vs. the sum of the Taft polar substituent constants for compounds of structure  $\text{R}^1\text{R}^2\text{R}^3\text{SiH}$ , where R = alkyl, phenyl, or hydrogen. (190, 191)

values for  $(\text{Me}_3\text{Si})_3\text{SiF}$  and  $\text{Br}_3\text{SiF}$  are 335 (206) and 368.7 Hz (207) respectively. Several values of  $^1J(\text{Si-F})$  are shown in Table XXV. (4, 26, 32, 59–63) Extreme values are reported for  $^1J(\text{Si-F})$  of 488 Hz (213) for [59] and  $\text{SiF}_6^{2-}$  (110 Hz, ref. 214; 108 Hz, ref. 215).

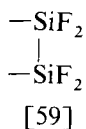


TABLE XXV

One-bond  $^{29}\text{Si}$ – $^{19}\text{F}$  coupling constants

Compound	$^1J(\text{Si-F})$ (Hz)	Ref.	Compound	$^1J(\text{Si-F})$ (Hz)	Ref.
$\text{SiFClI}_2$	401	208	$\text{SiF}_2\text{Ph}_2$	302.7	210
$\text{SiFClBrI}$	380	208	$\text{SiF}_3\text{I}$	296	176
$\text{SiFBr}_3$	368.7	207	$\text{SiFH}_2\text{Me}$	279.8	211
$(\text{F}_3\text{Si})_2\text{SiF}_2$	356.6 ( $\text{SiF}_2$ ) 344.4 ( $\text{SiF}_3$ )	169	$\text{SiF}_3\text{NMe}_2$	201.4	212
$\text{F}_3\text{SiSiF}_3$	321.8	209	$\text{SiF}_3\text{OSiMe}_3$	184.2	212
$\text{Me}_3\text{SiSiMe}_2\text{F}$	306.8	73	$\text{SiF}_3\text{OMe}$	181	205

The dependence of one-bond  $^{29}\text{Si}$ – $^{13}\text{C}$  coupling constants on the hybridization of the involved carbon has already been mentioned (Section III.B). In addition, Harris and Kimber find a linear dependence on substituent electronegativity for the trimethylsilyl derivatives  $\text{Me}_3\text{SiX}$ : (42)

$$^1J(\text{Si-C}) = 7.90\chi_X + 31.5 \quad (21)$$

(correlation coefficient  $r = 0.96$ ). They also established a linear correlation between  $^1K(\text{Si-C})$  and  $^1K(\text{C-C})$  for the analogous t-butyl derivatives, where  $^1K(\text{Si-C})$  and  $^1K(\text{C-C})$  are the reduced coupling constants:

$$|^1K(\text{Si-C})| = 1.72|^1K(\text{C-C})| + 0.80 \quad (22)$$

It is concluded that the Fermi contact mechanism is operative for both couplings. (42) The variation in  $^1J(\text{Si-C})$  for the series of ethoxysilanes  $\text{Me}_n\text{Si}(\text{OEt})_{4-n}$  was examined by the same authors (216) (values in Table XXVI). The changes are determined to be too large to be attributed solely to s character changes, although the Fermi contact model is still valid if substantial changes in effective nuclear charges at silicon are assumed. The variation in  $^1J(\text{Si-C})$  is found to be linearly

TABLE XXVI

One-bond  $^{29}\text{Si}$ - $^{13}\text{C}$  coupling constants

Compound	$^1J(\text{Si-C})$ (Hz)	Ref.	Compound	$^1J(\text{Si-C})$ (Hz)	Ref.
$\text{Me}_3\text{SiSiMe}_3$	-43.6	42	$\text{Me}_3\text{SiCHN}_2$	-62.2	220
$\text{Me}_3\text{SiSMe}$	-53.7	43	$\text{Me}_2\text{SiCl}_2$	-68.3	157
$(\text{Me}_3\text{Si})_2\text{NH}$	-56.2	42	$\text{Me}_2\text{Si}(\text{OEt})_2$	-73.0	221
$(\text{Me}_3\text{Si})_3\text{N}$	-56.8	219	$\text{MeSiCl}_3$	-86.6	157
$\text{Me}_3\text{SiC}(\text{N}_2)\text{CO}_2\text{Et}$	-58.4 (Me)	220	$\text{MeSi}(\text{OEt})_3$	-96.2	221
$\text{Me}_3\text{SiOEt}$	-59.0	42	$\text{ClCH}_2\text{SiCl}_3$	-97.6	157
$(\text{Me}_3\text{Si})_2\text{O}$	-60.0	42	$\text{CH}_2=\text{CHSiCl}_3$	-113	157
$\text{Me}_3\text{SiF}$	-60.5	—			

related to values of  $^1J(\text{Si-H})$  in the series  $\text{H}_n\text{Si}(\text{OMe})_{4-n}$  according to: (216)

$$|^1J(\text{Si-H})| = 2.20|^1J(\text{Si-C})| + 86.6 \quad (23)$$

Experimental values of  $^1J(\text{Si-C})$  are collected in Tables XX and XXI. Some additional values of  $^1J(\text{Si-C})$  are in Tables XXVI (42, 43, 157, 217, 221) and XXVII. (73)

The relationship established by Harris and Kimber (42) between  $^1J(\text{Si-C})$  and substituent electronegativity was extended to the coupling between directly bonded silicon atoms,  $^1J(\text{Si-Si})$ . (73) Sharp *et al.* examined a series of polysilanes and found a good linear correlation ( $r = 0.95$ ) between  $^1J(\text{Si-Si})$  (Table XXVII) and the sum of the substituent electronegativities on the coupled silicon atoms. This

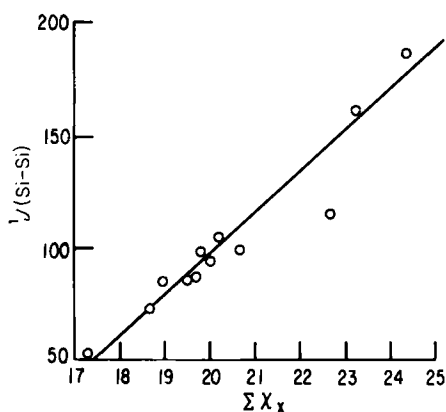


FIG. 26. Plot of the directly bonded silicon-silicon coupling constant *vs.* the sum of the substituent electronegativities on the coupled silicon atoms. (73)

TABLE XXVII

Some values of coupling constants (Hz) in polysilanes (73)

Compound	$^1J(\text{Si-Si})$	$^1J(\text{Si-C}^A)$	$^1J(\text{Si-C}^B)$
$(\text{Me}_3\text{Si}^A)_4\text{Si}^B$	52.5	-44.7	—
$(\text{Me}_3\text{Si}^A)_2\text{Si}^B\text{Me}_2$	73.2	-43.8	-37.0
$\text{Ph}_3\text{Si}^A\text{Si}^B\text{Me}_2^1\text{Bu}$	80.0 (ref. 74)	—	—
$\text{Me}_3\text{Si}^A\text{Si}^B\text{Me}_2\text{H}$	84.6	-44.6	-43.8
$\text{Me}_3\text{Si}^A\text{Si}^B\text{Me}_2\text{Ph}$	86.1	-44.1	-44.8
$\text{Me}_3\text{Si}^A\text{Si}^B\text{Ph}_3$	86.5	— <sup>a</sup>	— <sup>a</sup>
$\text{Me}_3\text{Si}^A\text{Si}^B\text{Me}_2\text{Cl}$	94.0	-46.2	-45.9
$(\text{Me}_3\text{Si}^A\text{Si}^B\text{Me}_2)_2\text{NH}$	96.0	-42 <sup>a</sup>	-46.6
$\text{Me}_3\text{Si}^A\text{Si}^B\text{Me}_2\text{F}$	98.7	— <sup>a</sup>	-47.9
$(\text{Me}_3\text{Si}^A\text{Si}^B\text{Me}_2)_2\text{O}$	103.4	-43.8	-48.0
$(\text{Cl}_3\text{Si}^A)_4\text{Si}^B$	110.5	—	—
$(\text{MeO})_3\text{Si}^A\text{Si}^B\text{Ph}_3$	160.0	—	— <sup>a</sup>
$(\text{EtO})_3\text{Si}^A\text{Si}^B\text{Ph}_3$	164.0 (ref. 74)	—	—
$(\text{Cl}_3\text{Si}^A)_2\text{Si}^B\text{Cl}_2$	186	—	—

<sup>a</sup> Assignments for  $^1J(\text{Si-C})$  not clear.

relationship is presented graphically in Fig. 26. Similarly, linear relationships have been established between  $^1J(\text{Si-Si})$  and  $^1J(\text{Si-C}^B)$  for the substituted silicon in seven pentamethyldisilanyl derivatives  $\text{Me}_3\text{Si}^A\text{Si}^B\text{Me}_2\text{X}$  (Table XXVII) and  $^1J(\text{Si-C}^B)$  and  $^1J(\text{Si-C})$  in the analogous trimethylsilyl derivatives. (73) Thus it appears that the same factors that determine  $^1J(\text{C-C})$  and  $^1J(\text{Si-C})$  couplings are also in effect for  $^1J(\text{Si-Si})$ . One-bond silicon couplings to some other nuclei are presented in Table XXVIII.

TABLE XXVIII

Some one-bond couplings of  $^{29}\text{Si}$ 

M	Compound	$^1J(\text{Si-M})$ (Hz)	Ref.
$^{199}\text{Hg}$	$\text{RHgSiMe}_3, \text{RHgSiEt}_3$	957-1357 <sup>a</sup>	217
$^{15}\text{N}$	$(\text{H}_3\text{Si})_3\text{N}$	+6	219
$^{31}\text{P}$	$\text{Me}_3\text{SiPH}_2$	+16.2	218
$^{31}\text{P}$	$\text{Me}_2\text{HSiPMe}_2$	+23.2	218
$^{31}\text{P}$	$(\text{H}_3\text{Si})_3\text{P}$	+42.2	175
$^{31}\text{P}$	$\text{Me}_3\text{SiPPh}_2$	+21.5	221
$^{195}\text{Pt}$	<i>trans</i> -[PtCl(SiH <sub>2</sub> Cl)(PEt) <sub>2</sub> ]	-1600	222
$^{77}\text{Se}$	$(\text{H}_3\text{Si})_2\text{Se}$	+110.6	171
$^{119}\text{Sn}$	$\text{Ph}_3\text{SiSnMe}_3$	+650	221

<sup>a</sup> Depending on nature of R.



### D. Longer range coupling

Trends that occur for one-bond coupling constants also appear for longer range couplings. The values of  $^2J(\text{Si-H})$ , for example, occur roughly in the region of 3–12 Hz with the larger values pertaining to silanes with more electronegative substituents. (49, 223) Likewise, in the three-bond couplings  $^3J(\text{Si-H})$  of the series  $\text{Cl}_n\text{Me}_{3-n}\text{SiOMe}$  and  $\text{Me}_{4-n}\text{Si(OMe)}_n$ , increasing the number of electronegative substituents (Cl or OMe) increased the magnitude of the coupling. (223) Some trends that do not fit into the expected pattern have been noted. Schmidbaur, for example, noted (224) that  $^2J(\text{Si-H})$  increases in the series  $\text{Me}_3\text{SiF} < \text{Me}_3\text{SiBr} < \text{Me}_3\text{SiI}$ , and in the series  $(\text{Me}_3\text{Si})_2\text{O} < (\text{Me}_3\text{Si})_2\text{S} < (\text{Me}_3\text{Si})_2\text{Se}$ , in contradiction to the expectations based on electronegativity. This was originally rationalized in terms of  $\pi$ -bonding (224) but other explanations have been offered. (157) A few of the many two- and three-bond coupling constants that have been reported are collected in Table XXIX. (74, 157, 169, 171, 173, 209, 223, 235–246) Other values can be found in ref. 6.

TABLE XXIX

Long range coupling constants involving  $^{29}\text{Si}$ 

Coupling	Compound	$J$ (Hz)	Ref.
$^2J(\text{Si-CH})$	$\text{Me}_4\text{Si}$	+6.75	235
	$\text{MeSiCl}_3$	+9.3	157
$^2J(\text{Si-CC})$	$\text{Me}_3\text{SiC}\equiv\text{CPh}$	16.1	236
$^2J(\text{Si-NSn})$	$[(\text{Me}_3\text{Si})_2\text{N}]_2\text{Sn}$	16.2	237
$^2J(\text{Si-OSi})$	$(\text{H}_3\text{Si})_2\text{O}$	+1.0	171
$^2J(\text{Si-SiF})$	$(\text{Me}_3\text{Si})_3\text{SiF}$	-16.8	238
	$(\text{F}_3\text{Si})_3\text{SiH}$	-41	239
	$\text{F}_3\text{SiSiF}_3$	-90.5	209
$^3J(\text{Si-CCH})$	$\text{Ph}_3\text{SiC}\equiv\text{CH}$	4.3	240
	$\text{Me}_3\text{SiC}(\text{Cl})=\text{CH}_2$	4.4( <i>cis</i> )	173
		-10.5( <i>trans</i> )	
$^3J(\text{Si-CSiH})$	$(\text{H}_2\text{SiCCl}_2)_3$	2.8	242
$^3J(\text{Si-NCH})$	$\text{Me}_3\text{SiNMe}_2$	3.7	241
	$(\text{H}_3\text{Si})_3\text{P}$	5.4	246
$^3J(\text{Si-OCH})$	$(\text{MeO})_3\text{SiH}$	4.2	74
	$\text{Cl}_3\text{SiOMe}$	6.0	223
$^3J(\text{Si-OSiF})$	$(\text{F}_3\text{Si})_2\text{O}$	2.5	209
$^3J(\text{Si-SeCH})$	$\text{Me}_3\text{SiSeMe}$	3.6	243
$^3J(\text{Si-SeSiH})$	$\text{H}_3\text{SiSeSiMe}_3$	2.1	244
$^3J(\text{Si-SiCH})$	$(\text{Me}_3\text{Si})_3\text{SiH}$	2.3	245
	$(\text{Me}_3\text{Si})_3\text{SiCl}$	3.20	238
$^3J(\text{Si-SiSiF})$	$(\text{F}_3\text{Si})_2\text{SiF}_2$	-15.7	169
$^3J(\text{Si-SSiH})$	$\text{H}_3\text{SiSSiMe}_3$	2.5	244

#### IV. RELAXATION PHENOMENA AND THE NUCLEAR OVERHAUSER EFFECT

$^{29}\text{Si}$  spin-lattice relaxation ( $T_1$ ) and  $^{29}\text{Si}$ - $^1\text{H}$  nuclear Overhauser effects (NOE) have been studied by several authors as probes for molecular dynamics and segmental motion in silicon-containing compounds. (5, 32, 38, 41, 43, 82, 102, 216, 225-228)

The four spin-lattice relaxation mechanisms that are usually considered for nuclei of spin  $\frac{1}{2}$  are: (i) dipole-dipole interactions (DD); (ii) spin-rotation interactions (SR); (iii) scalar coupling (SC); and (iv) chemical screening anisotropy (CSA). (5) In  $^{29}\text{Si}$  NMR SC is not generally considered, except in the rare cases when  $^{29}\text{Si}$  is spin-coupled to  $^{127}\text{I}$  or other nuclei with resonance frequencies close to that of  $^{29}\text{Si}$ . Table XXX compares the contribution of the three remaining mechanisms with  $^{29}\text{Si}$  relaxation times. Definitions of these relaxation mechanisms can be found in ref. 229. Since a theoretical discussion of  $^{29}\text{Si}$  relaxation and NOE is detailed elsewhere [(5) and references therein] only general observations are made in this section.

$^{29}\text{Si}$  spin-lattice relaxation times for organosilicon compounds are generally greater than 20s. Even in cases where there are directly attached protons which contribute to a very efficient DD mechanism in

TABLE XXX

Contribution of  $^{29}\text{Si}$  spin-lattice relaxation mechanisms<sup>a</sup> (5)

	DD	SR	CSA	DD (intermolecular)
<i>Very small molecules<sup>b</sup></i>				
Protonated	minor- appreciable <sup>c</sup>	appreciable- exclusive	negligible <sup>c</sup>	negligible- minor
Non-protonated	minor- appreciable	exclusive	negligible	negligible- minor
<i>Medium and large molecules</i>				
Protonated	appreciable- exclusive	negligible- exclusive	negligible	negligible- minor
Non-protonated	appreciable- exclusive	negligible- appreciable	minor- appreciable	minor- appreciable

<sup>a</sup> Relaxation near room temperature at 2.35 T;  $\text{O}_2$  excluded.

<sup>b</sup> Assumes no intermolecular association.

<sup>c</sup> Minor = 5-10 % contribution; negligible = 1-5 % contribution.

$^{13}\text{C}$  NMR resulting in short  $T_1$ , the  $^{29}\text{Si}$  relaxation times tend to be long. This results from a combination of two factors: a lower magnetogyric ratio for  $^{29}\text{Si}$  and a longer Si-H bond length (1.48 Å for a C-H bond), which when incorporated in equation (24) results in a tenfold lowering of the  $^{29}\text{Si}$  DD relaxation rate,  $R_1(\text{DD})$ , compared with  $^{13}\text{C}$ . In equation (24), which describes intramolecular DD relaxation for spin- $\frac{1}{2}$  nuclei:

$$1/T_1(\text{DD}) = R_1(\text{DD}) = \mu_0^2 \gamma_{\text{Si}}^2 \gamma_{\text{H}}^2 N \hbar^2 \tau_c (16\pi^2 r_{\text{Si-H}}^6)^{-1} \quad (24)$$

$N$  is the number of directly attached protons,  $\gamma_{\text{Si}}$  and  $\gamma_{\text{H}}$  are the magnetogyric ratios for  $^{29}\text{Si}$  and  $^1\text{H}$  respectively,  $r_{\text{Si-H}}$  is the distance between Si and H, and  $\tau_c$  is the molecular correlation time. This means that  $T_1(\text{DD})$  is longer for  $^{29}\text{Si}$  than it is for an analogous  $^{13}\text{C}$  nucleus. (5)

For  $^{29}\text{Si}-\{^1\text{H}\}$  experiments the maximum NOE is  $-2.52$ . (229) This occurs when the DD mechanism dominates the relaxation, and decreases when other relaxation mechanisms are prominent. In situations where the NOE is equal to  $-1$  no NMR is observed because, by definition, the signal is nulled into the baseline.

Levy *et al.* (38) have performed  $^{29}\text{Si}$   $T_1$  studies on a variety of organosilicon compounds. They observed that in linear polydimethylsiloxanes motional processes along the chain are quite different. They showed that in  $\text{MD}_n\text{M}$  systems the relaxation behaviour is not the same for M units and D units. M units are able to spin freely around their threefold axis of symmetry favouring an SR relaxation mechanism, while D units may rotate only through a restricted angle which favours the  $^{29}\text{Si}-^1\text{H}$  DD relaxation mechanism. Table XXXI shows the  $T_1$  and NOE data for six linear siloxanes. For the D silicons the spin-rotation

TABLE XXXI

$^{29}\text{Si}$  relaxation in linear polydimethylsiloxanes (38)

Compd. <sup>a</sup>	$T_1$ (s) <sup>b</sup>					NOE ( $-\eta$ ) <sup>b</sup>				
	M	D <sup>1</sup>	D <sup>2</sup>	D <sup>3</sup>	D <sup>4</sup>	M	D <sup>1</sup>	D <sup>2</sup>	D <sup>3</sup>	D <sup>4</sup>
MM	39.5					0.31				
MDM	35	54				0.36	0.55			
MD <sub>2</sub> M	38	78				0.53	1.2			
MD <sub>3</sub> M	46	82	77			0.57	1.1	1.2		
MD <sub>6</sub> M	42	64	55	59		0.7	1.6	1.9	1.9	
MD <sub>8</sub> M	44	67	60	55	55	0.7	1.5	1.8	2.0	2.0

<sup>a</sup> Samples: 90% siloxane, 10% acetone-d<sub>6</sub>; N<sub>2</sub> degassed.

<sup>b</sup>  $T_1$  at 38°; D units numbered from each end, e.g. MD<sup>1</sup>D<sup>2</sup>D<sup>1</sup>M.

mechanism is more strongly a function of molecular size and position of the D unit along the chain. Near the ends of the chain increased freedom of motion is evident resulting in a smaller NOE and longer DD spin-lattice relaxation. Engelhardt and Jancke (82) showed that, in phenyl substituted linear and branched siloxanes, SR relaxation at the ends of the chains decreases in importance because of steric interactions resulting in motional constraints, favouring a larger  $^{29}\text{Si-H}$  DD contribution to the  $T_1$ , and a larger NOE.

Scholl *et al.* (32) while reporting chemical shift information have noticed that for a large number of silicon compounds the NOE varies widely and is highly sensitive to subtle changes in molecular structure. It is their conclusion that the diversity of relaxations and NOE behaviour implies differences in molecular motion in solution and liquid state structure.

For compounds containing phenyl groups, Harris and Kimber (226, 234) compared  $^{29}\text{Si}$   $T_1$  and NOE data for six phenylsilanes (Table XXXII). Phenylsilane, diphenylsilane, and triphenylsilane are expected to have dipolar relaxation rates in a ratio of 3:2:1 corresponding to the number of directly attached protons on silicon. They found this not to be the case for phenylsilane because of internal rotation considerations and for diphenylsilane and triphenylsilane as is reflected by their NOE values (Table XXXII). The calculated dipolar relaxation rates are 200 s, 31 s, and 12.5 s for  $\text{PhSiH}_3$ ,  $\text{Ph}_2\text{SiH}_2$ , and  $\text{Ph}_3\text{SiH}$  respectively, far from the 3:2:1 ratio. For compounds with no directly attached protons the same authors (216) found that the DD mechanism is not an important consideration until the molecular size restricts motion to a point where Si-H long range dipolar interactions compete with SR making the DD relaxation mechanism important again. This is exemplified by the series  $(\text{EtO})_{4-n}\text{SiMe}_n$  which shows an increase in

TABLE XXXII

$^{29}\text{Si}\{-^1\text{H}\}$  nuclear magnetic relaxation data (226, 234)

Compound	$T_1$ (s)	NOE
Triphenylsilane	12.0	2.41
Diphenylsilane	26.5	-2.13
Diphenylsilane	26.0 (ref. 38)	-2.5 (ref. 38)
Phenylsilane	5.5	-0.07
Diphenylmethylsilane	35.4	-2.27
Phenyltrimethylsilane	42.0 (ref. 42)	-0.59 (ref. 42)
Diphenyldichlorosilane	126.2	-1.28

NOE as  $n$  is changed from 0 to 4. The slower moving molecules demonstrate an increased importance of the dipolar contribution. In diphenyldichlorosilane (234) DD and SR relaxation mechanisms contribute about equally to the  $^{29}\text{Si}$   $T_1$  value, providing a probable upper limit for a long range intermolecular contribution of dipolar relaxation from phenyl protons in phenylsilanes.

It is clear that NOE and  $T_1$  data can be used to study molecular motion in solution. It is also clear in cases of multisilicon compounds that these data can help in the interpretation of spectra. Even in cases of very complicated structures such as those found in soluble silicates,  $T_1$  and NOE have been used to help in the assignment of resonances (102, 228) by looking at paramagnetic coordination sites and line width changes in the resonance signals. It has been suggested (32) that more  $^{29}\text{Si}$  relaxation data will be needed if the molecular motions and structures of silicon-containing molecules are to be fully understood.

APPENDIX.  
SILICON-29 CHEMICAL SHIFTS<sup>a</sup>

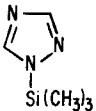
Empirical formula	Structure	$\delta$	Ref.
SiBrCl <sub>2</sub>	SiBrClH <sub>2</sub>	-181.9	57
SiBrCl <sub>2</sub> I	SiBrCl <sub>2</sub> I	-98.9	57
SiBrCl <sub>3</sub>	SiBrCl <sub>3</sub>	-34.3	57
SiBrF <sub>3</sub>	SiBrF <sub>3</sub>	-83.5	35
SiBrI <sub>3</sub>	SiBrI <sub>3</sub>	-280.1	57
SiBr <sub>2</sub> ClH	SiBr <sub>2</sub> ClH	-122.8	57
SiBr <sub>2</sub> Cl <sub>2</sub>	SiBr <sub>2</sub> Cl <sub>2</sub>	-50.7	57
SiBr <sub>2</sub> F <sub>2</sub>	SiBr <sub>2</sub> F <sub>2</sub>	-68.5	35
SiBr <sub>2</sub> I <sub>2</sub>	SiBr <sub>2</sub> I <sub>2</sub>	-212.3	57
SiBr <sub>3</sub> Cl	SiBr <sub>3</sub> Cl	-69.8	57
SiBr <sub>3</sub> F	SiBr <sub>3</sub> F	-68.1	35
SiBr <sub>3</sub> I	SiBr <sub>3</sub> I	-149.5	57
SiBr <sub>4</sub>	SiBr <sub>4</sub>	-92.7	57
		-93.6	13
SiClF <sub>3</sub>	SiClF <sub>3</sub>	-82.8	35
SiClH <sub>3</sub>	SiClH <sub>3</sub>	-245.9	57
SiCl <sub>2</sub> F <sub>2</sub>	SiCl <sub>2</sub> F <sub>2</sub>	-56.1	35
SiCl <sub>2</sub> I <sub>2</sub>	SiCl <sub>2</sub> I <sub>2</sub>	-151.5	57
SiCl <sub>3</sub> F	SiCl <sub>3</sub> F	-33.2	35
SiCl <sub>3</sub> I	SiCl <sub>3</sub> I	-75.4	57
SiCl <sub>4</sub>	SiCl <sub>4</sub>	-20.0	57
		-19.9	230
		-16.5	48

Empirical formula	Structure	$\delta$	Ref.
SiF <sub>4</sub>	SiF <sub>4</sub>	-110.1	35
		-117.4	22
		-109.0	13
SiF <sub>6</sub> <sup>2-</sup>	SiF <sub>6</sub> <sup>2-</sup>	-184.4	35
		-187.4	27
SiF <sub>6</sub> O	(SiF <sub>3</sub> ) <sub>2</sub> O	-109.5	35
SiI <sub>4</sub>	SiI <sub>4</sub>	-351.7	57
		-346.2	20
SiHCl <sub>3</sub>	HSiCl <sub>3</sub>	-9.6	230
SiH <sub>2</sub> Cl <sub>2</sub>	H <sub>2</sub> SiCl <sub>2</sub>	-11.0	230
SiH <sub>3</sub>	SiH <sub>3</sub> <sup>-</sup>	-165	249
SiH <sub>3</sub> Cl	H <sub>3</sub> SiCl	-36.1	230
SiH <sub>4</sub>	SiH <sub>4</sub>	-91.9	57
		-93.1	230
SiH <sub>4</sub> O <sub>4</sub>	Si(OH) <sub>4</sub>	-73.3	57
SiCH <sub>2</sub> ClF <sub>3</sub>	(CH <sub>2</sub> Cl)SiF <sub>3</sub>	-71.34	47
SiCH <sub>2</sub> Cl <sub>4</sub>	(CH <sub>2</sub> Cl)SiCl <sub>3</sub>	1.65	48
		0.08	31
SiCH <sub>3</sub> Br <sub>3</sub>	CH <sub>3</sub> SiBr <sub>3</sub>	-19.2	13
		-18.18	17
SiCH <sub>3</sub> Cl <sub>3</sub>	CH <sub>3</sub> SiCl <sub>3</sub>	12.47	29
		12.2	48
SiCH <sub>3</sub> F <sub>3</sub>	CH <sub>3</sub> SiF <sub>3</sub>	-51.8	13
SiCH <sub>3</sub> I <sub>3</sub>	CH <sub>3</sub> SiI <sub>3</sub>	-17.96	17
SiCH <sub>3</sub> Cl	H <sub>3</sub> SiCH <sub>2</sub> Cl	-56.5	250
SiCH <sub>6</sub>	H <sub>3</sub> SiCH <sub>3</sub>	-65.2	230
SiC <sub>2</sub> H <sub>3</sub> Cl <sub>3</sub>	CH <sub>2</sub> =C(H)SiCl <sub>3</sub>	-3.5	51
SiC <sub>2</sub> H <sub>4</sub> Cl <sub>3</sub> F	Cl <sub>3</sub> Si(CH <sub>2</sub> ) <sub>2</sub> F	9.64	50
SiC <sub>2</sub> H <sub>5</sub> ClF <sub>2</sub>	(CH <sub>3</sub> )(CH <sub>2</sub> Cl)SiF <sub>2</sub>	-9.03	48
SiC <sub>2</sub> H <sub>5</sub> Cl <sub>3</sub>	(CH <sub>3</sub> )(CH <sub>2</sub> Cl)SiCl <sub>2</sub>	21.48	48
		21.7	31

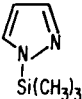
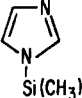
SiC <sub>2</sub> H <sub>6</sub> Br <sub>2</sub>	(CH <sub>3</sub> ) <sub>2</sub> SiBr <sub>2</sub>	19.2	13
		19.86	17
SiC <sub>2</sub> H <sub>6</sub> Cl <sub>2</sub>	(CH <sub>3</sub> ) <sub>2</sub> SiCl <sub>2</sub>	31.8	48
		32.17	17
SiC <sub>2</sub> H <sub>6</sub> F <sub>2</sub>	(CH <sub>3</sub> ) <sub>2</sub> SiF <sub>2</sub>	4.5	4
SiC <sub>2</sub> H <sub>6</sub> I <sub>2</sub>	(CH <sub>3</sub> ) <sub>2</sub> SiI <sub>2</sub>	-33.68	17
SiC <sub>2</sub> H <sub>6</sub> N <sub>6</sub>	(CH <sub>3</sub> ) <sub>2</sub> Si(N <sub>3</sub> ) <sub>2</sub>	0.06	13
SiC <sub>2</sub> H <sub>8</sub>	(CH <sub>3</sub> ) <sub>2</sub> SiH <sub>2</sub>	-41.5	247
		-37.3	230
SiC <sub>3</sub> H <sub>6</sub> Cl <sub>2</sub>	(CH <sub>3</sub> )Cl <sub>2</sub> SiCH=CH <sub>2</sub>	16.5	51
SiC <sub>3</sub> H <sub>6</sub> Cl <sub>3</sub> F	Cl <sub>3</sub> Si(CH <sub>2</sub> ) <sub>3</sub> F	13.34	50
SiC <sub>3</sub> H <sub>6</sub> F <sub>2</sub>	(CH <sub>3</sub> )F <sub>2</sub> SiCH=CH <sub>2</sub>	-13.4	51
SiC <sub>3</sub> H <sub>7</sub> Cl <sub>2</sub> F	(CH <sub>3</sub> ) <sub>2</sub> (CHCl <sub>2</sub> )SiF	19.7	13
SiC <sub>3</sub> H <sub>7</sub> Cl <sub>3</sub>	(CH <sub>3</sub> ) <sub>2</sub> (CHCl <sub>2</sub> )SiCl	22.8	13
SiC <sub>3</sub> H <sub>8</sub> BrCl	(CH <sub>3</sub> ) <sub>2</sub> Si(CH <sub>2</sub> Br)Cl	22.1	13
SiC <sub>3</sub> H <sub>8</sub> ClF	(CH <sub>3</sub> ) <sub>2</sub> (CH <sub>2</sub> Cl)SiF	24.6	13
		24.83	48
SiC <sub>3</sub> H <sub>8</sub> Cl <sub>2</sub>	(CH <sub>3</sub> ) <sub>2</sub> ClSiCH <sub>2</sub> Cl	23.08	48
		22.9	31
SiC <sub>3</sub> H <sub>9</sub> Br	(CH <sub>3</sub> ) <sub>3</sub> SiBr	26.41	29
SiC <sub>3</sub> H <sub>9</sub> Cl	(CH <sub>3</sub> ) <sub>3</sub> SiCl	30.21	29
		29.9	48
		32.5	44
SiC <sub>3</sub> H <sub>9</sub> Cl	(CH <sub>3</sub> ) <sub>2</sub> (CH <sub>2</sub> Cl)SiH	-12.29	32
SiC <sub>3</sub> H <sub>9</sub> ClO <sub>3</sub>	(CH <sub>3</sub> O) <sub>3</sub> SiCl	-66.7	74
SiC <sub>3</sub> H <sub>9</sub> ClO <sub>4</sub>	(CH <sub>3</sub> ) <sub>3</sub> SiClO <sub>4</sub>	43.4	44
SiC <sub>3</sub> H <sub>9</sub> F	(CH <sub>3</sub> ) <sub>3</sub> SiF	31.92	55
		30.5	44
SiC <sub>3</sub> H <sub>9</sub> I	(CH <sub>3</sub> ) <sub>3</sub> SiI	8.72	29
		8.6	44
SiC <sub>3</sub> H <sub>9</sub> N <sub>3</sub>	(CH <sub>3</sub> ) <sub>3</sub> SiN <sub>3</sub>	16.7	13
		15.3	44



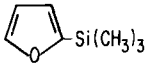
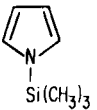
Empirical formula	Structure	$\delta$	Ref.
SiC <sub>3</sub> H <sub>10</sub>	(CH <sub>3</sub> ) <sub>3</sub> SiH	-16.34	42
		-15.5	230
SiC <sub>3</sub> H <sub>10</sub> O <sub>3</sub>	(CH <sub>3</sub> O) <sub>3</sub> SiH	-54.9	74
SiC <sub>4</sub> CoF <sub>3</sub> O <sub>4</sub>	SiF <sub>3</sub> Co(CO) <sub>4</sub>	-25.8	35
SiC <sub>4</sub> H <sub>6</sub> O <sub>6</sub>	CH <sub>3</sub> Si(OCOCH <sub>3</sub> ) <sub>3</sub>	-41.0	210
SiC <sub>4</sub> H <sub>7</sub> Cl <sub>2</sub> F <sub>3</sub>	Cl <sub>2</sub> Si(CH <sub>3</sub> )(CH <sub>2</sub> ) <sub>2</sub> CF <sub>3</sub>	31.2	47
SiC <sub>4</sub> H <sub>9</sub> Cl	(CH <sub>3</sub> ) <sub>2</sub> ClSiCH=CH <sub>2</sub>	16.7	51
SiC <sub>4</sub> H <sub>9</sub> F <sub>3</sub> O <sub>2</sub>	(CH <sub>3</sub> ) <sub>3</sub> SiOOCF <sub>3</sub>	34.3	44
SiC <sub>4</sub> H <sub>9</sub> F <sub>3</sub> O <sub>3</sub> S	(CH <sub>3</sub> ) <sub>3</sub> SiOSO <sub>2</sub> CF <sub>3</sub>	44.6	44
SiC <sub>4</sub> H <sub>9</sub> N	(CH <sub>3</sub> ) <sub>3</sub> SiCN	-12.3	22
		-12.2	44
SiC <sub>4</sub> H <sub>9</sub> NO	(CH <sub>3</sub> ) <sub>3</sub> SiNCO	7.4	22
		7.0	44
SiC <sub>4</sub> H <sub>9</sub> NO <sub>4</sub> S	(CH <sub>3</sub> ) <sub>3</sub> SiOSO <sub>2</sub> NCO	41.3	22
SiC <sub>4</sub> H <sub>9</sub> NS	(CH <sub>3</sub> ) <sub>3</sub> SiNCS	5.40	22
SiC <sub>4</sub> H <sub>10</sub> Cl <sub>2</sub>	(CH <sub>3</sub> ) <sub>3</sub> SiCHCl <sub>2</sub>	10.48	32
SiC <sub>4</sub> H <sub>10</sub> F <sub>2</sub>	(C <sub>2</sub> H <sub>5</sub> ) <sub>2</sub> SiF <sub>2</sub>	0.50	54
SiC <sub>4</sub> H <sub>10</sub> I <sub>2</sub>	(CH <sub>3</sub> ) <sub>2</sub> Si(CH <sub>2</sub> I) <sub>2</sub>	6.47	32
SiC <sub>4</sub> H <sub>10</sub> O <sub>2</sub>	(CH <sub>3</sub> ) <sub>3</sub> SiOCOH	25.2	210
SiC <sub>4</sub> H <sub>11</sub> Br	(CH <sub>3</sub> ) <sub>3</sub> SiCH <sub>2</sub> Br	3.12	32
SiC <sub>4</sub> H <sub>11</sub> Cl	(CH <sub>3</sub> ) <sub>3</sub> SiCH <sub>2</sub> Cl	2.79	48
SiC <sub>4</sub> H <sub>11</sub> F	(CH <sub>3</sub> ) <sub>3</sub> SiCH <sub>2</sub> F	-1.49	50
SiC <sub>4</sub> H <sub>12</sub>	(CH <sub>3</sub> ) <sub>4</sub> Si	0.0	—
SiC <sub>4</sub> H <sub>12</sub> O	(CH <sub>3</sub> ) <sub>3</sub> SiOCH <sub>3</sub>	17.2	132
		17.75	46
SiC <sub>4</sub> H <sub>12</sub> O <sub>2</sub>	(CH <sub>3</sub> ) <sub>2</sub> Si(OCH <sub>3</sub> ) <sub>2</sub>	-2.5	4
		-1.62	46
SiC <sub>4</sub> H <sub>12</sub> O <sub>2</sub>	(CH <sub>3</sub> ) <sub>3</sub> SiOOCH <sub>3</sub>	22.0	44
SiC <sub>4</sub> H <sub>12</sub> O <sub>3</sub>	CH <sub>3</sub> Si(OCH <sub>3</sub> ) <sub>3</sub>	-41.5	4
		-39.8	46

SiC <sub>4</sub> H <sub>12</sub> O <sub>4</sub>	Si(OCH <sub>3</sub> ) <sub>4</sub>	-79.15	46
SiC <sub>4</sub> H <sub>12</sub> S	(CH <sub>3</sub> ) <sub>3</sub> SiSCH <sub>3</sub>	15.92	43
		16.46	46
SiC <sub>4</sub> H <sub>12</sub> S <sub>2</sub>	(CH <sub>3</sub> ) <sub>2</sub> Si(SCH <sub>3</sub> ) <sub>2</sub>	28.14	46
SiC <sub>4</sub> H <sub>12</sub> S <sub>3</sub>	CH <sub>3</sub> Si(SCH <sub>3</sub> ) <sub>3</sub>	34.00	46
SiC <sub>4</sub> H <sub>12</sub> S <sub>4</sub>	Si(SCH <sub>3</sub> ) <sub>4</sub>	38.59	46
SiC <sub>4</sub> H <sub>13</sub> N	CH <sub>3</sub> NHSi(CH <sub>3</sub> ) <sub>3</sub>	3.99	136
SiC <sub>4</sub> H <sub>13</sub> N	(CH <sub>3</sub> ) <sub>3</sub> SiCH <sub>2</sub> NH <sub>2</sub>	0.5	52
SiC <sub>5</sub> H <sub>9</sub> Cl <sub>3</sub> O <sub>2</sub>	(CH <sub>3</sub> ) <sub>3</sub> SiOCOCCl <sub>3</sub>	32.50	210
SiC <sub>5</sub> H <sub>9</sub> F <sub>3</sub> O <sub>2</sub>	(CH <sub>3</sub> ) <sub>3</sub> SiOCOCF <sub>3</sub>	33.20	210
SiC <sub>5</sub> H <sub>10</sub> Cl <sub>2</sub> O <sub>2</sub>	(CH <sub>3</sub> ) <sub>3</sub> SiOCOCHCl <sub>2</sub>	30.20	210
SiC <sub>5</sub> H <sub>11</sub> BrO <sub>2</sub>	(CH <sub>3</sub> ) <sub>3</sub> SiOCOCH <sub>2</sub> Br	26.7	210
SiC <sub>5</sub> H <sub>11</sub> Cl	(CH <sub>3</sub> ) <sub>3</sub> SiCH=CHCl	-7.6	134
SiC <sub>5</sub> H <sub>11</sub> ClO <sub>2</sub>	(CH <sub>3</sub> ) <sub>3</sub> SiOCOCH <sub>2</sub> Cl	26.6	210
SiC <sub>5</sub> H <sub>11</sub> ClO <sub>2</sub>	(CH <sub>3</sub> ) <sub>2</sub> (CH <sub>2</sub> Cl)SiOCOCH <sub>3</sub>	14.9	31
SiC <sub>5</sub> H <sub>11</sub> FO <sub>2</sub>	(CH <sub>3</sub> ) <sub>3</sub> SiOCOCH <sub>2</sub> F	-40.9	210
SiC <sub>5</sub> H <sub>11</sub> N <sub>3</sub>		17.05	136
SiC <sub>5</sub> H <sub>12</sub>	(CH <sub>3</sub> ) <sub>3</sub> SiCH=CH <sub>2</sub>	-7.6	134
		-6.8	32
SiC <sub>5</sub> H <sub>12</sub>	(CH <sub>3</sub> ) <sub>2</sub> Si(CH <sub>2</sub> ) <sub>2</sub> CH <sub>2</sub>	18.90	32
SiC <sub>5</sub> H <sub>12</sub> Cl <sub>2</sub>	(CH <sub>3</sub> ) <sub>2</sub> (CH <sub>2</sub> Cl)SiCH(CH <sub>3</sub> )Cl	7.52	32
SiC <sub>5</sub> H <sub>13</sub> OS	(CH <sub>3</sub> ) <sub>3</sub> SiSC(O)CH <sub>3</sub>	22.42	137
SiC <sub>5</sub> H <sub>12</sub> O <sub>2</sub>	(CH <sub>3</sub> ) <sub>3</sub> SiOCOCH <sub>3</sub>	22.3	210
SiC <sub>5</sub> H <sub>13</sub> Cl	(CH <sub>3</sub> ) <sub>2</sub> (C <sub>2</sub> H <sub>5</sub> )SiCH <sub>2</sub> Cl	5.17	32
SiC <sub>5</sub> H <sub>13</sub> Cl	(CH <sub>3</sub> ) <sub>3</sub> SiCH(CH <sub>3</sub> )Cl	5.67	32
SiC <sub>5</sub> H <sub>13</sub> ClO	(CH <sub>3</sub> ) <sub>2</sub> (OC <sub>2</sub> H <sub>5</sub> )SiCH <sub>2</sub> Cl	8.9	31
SiC <sub>5</sub> H <sub>13</sub> ClO	(CH <sub>3</sub> ) <sub>3</sub> SiOCH <sub>2</sub> CH <sub>2</sub> Cl	18.3	52
SiC <sub>5</sub> H <sub>13</sub> Cl <sub>3</sub> NP	(C <sub>2</sub> H <sub>5</sub> ) <sub>2</sub> (CH <sub>3</sub> )PNSiCl <sub>3</sub>	-53.31	53
SiC <sub>5</sub> H <sub>13</sub> I	(CH <sub>3</sub> ) <sub>3</sub> SiCH(CH <sub>3</sub> )I	7.92	32

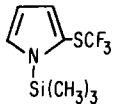
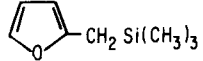
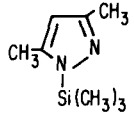
Empirical formula	Structure	$\delta$	Ref
SiC <sub>5</sub> H <sub>13</sub> NO	CH <sub>3</sub> CONHSi(CH <sub>3</sub> ) <sub>3</sub>	5.56 (NSi)	135
		17.55 (OSi)	135
SiC <sub>5</sub> H <sub>14</sub> O	(CH <sub>3</sub> ) <sub>3</sub> SiOC <sub>2</sub> H <sub>5</sub>	13.5	4
		14.53	132
SiC <sub>5</sub> H <sub>14</sub> O	(CH <sub>3</sub> ) <sub>3</sub> SiOC <sub>2</sub> H <sub>5</sub>	13.5	4
		14.53	132
SiC <sub>5</sub> H <sub>14</sub> O	(CH <sub>3</sub> ) <sub>3</sub> Si(CH <sub>2</sub> ) <sub>2</sub> OH	-0.30	32
SiC <sub>5</sub> H <sub>14</sub> O	(CH <sub>3</sub> ) <sub>3</sub> SiCH <sub>2</sub> OCH <sub>3</sub>	-1.55	32
SiC <sub>5</sub> H <sub>15</sub> I	(CH <sub>3</sub> ) <sub>3</sub> Si(CH <sub>2</sub> ) <sub>3</sub> I	1.76	32
SiC <sub>5</sub> H <sub>15</sub> N	(CH <sub>3</sub> ) <sub>3</sub> SiNHC <sub>2</sub> H <sub>5</sub>	4.02	133
SiC <sub>5</sub> H <sub>15</sub> N	(CH <sub>3</sub> ) <sub>3</sub> SiN(CH <sub>3</sub> ) <sub>2</sub>	6.50	133
		5.90	79
		6.52	46
SiC <sub>5</sub> H <sub>15</sub> N	(CH <sub>3</sub> ) <sub>3</sub> Si(CH <sub>2</sub> ) <sub>2</sub> NH <sub>2</sub>	-0.2	52
SiC <sub>5</sub> H <sub>15</sub> NO	C <sub>2</sub> H <sub>5</sub> O(CH <sub>3</sub> ) <sub>2</sub> SiCH <sub>2</sub> NH <sub>2</sub>	13.2	52
SiC <sub>5</sub> H <sub>15</sub> NO	(CH <sub>3</sub> ) <sub>3</sub> SiO(CH <sub>2</sub> ) <sub>2</sub> NH <sub>2</sub>	16.3	52
SiC <sub>5</sub> H <sub>15</sub> N <sub>4</sub> P	(CH <sub>3</sub> ) <sub>3</sub> PNSi(CH <sub>3</sub> ) <sub>2</sub> N <sub>3</sub>	-16.17	53
SiC <sub>6</sub> H <sub>4</sub> ClF <sub>3</sub>	<i>m</i> -ClC <sub>6</sub> H <sub>4</sub> SiF <sub>3</sub>	-74.19	54
SiC <sub>6</sub> H <sub>4</sub> ClF <sub>3</sub>	<i>p</i> -ClC <sub>6</sub> H <sub>4</sub> SiF <sub>3</sub>	-72.97	54
SiC <sub>6</sub> H <sub>4</sub> Cl <sub>4</sub>	<i>p</i> -ClC <sub>6</sub> H <sub>4</sub> SiCl <sub>3</sub>	-2.2	185
SiC <sub>6</sub> H <sub>4</sub> F <sub>4</sub>	<i>m</i> -FC <sub>6</sub> H <sub>4</sub> SiF <sub>3</sub>	-76.08	54
SiC <sub>6</sub> H <sub>4</sub> F <sub>4</sub>	<i>p</i> -FC <sub>6</sub> H <sub>4</sub> SiF <sub>3</sub>	-72.87	54
SiC <sub>6</sub> H <sub>5</sub> Cl <sub>3</sub>	C <sub>6</sub> H <sub>5</sub> SiCl <sub>3</sub>	-0.8	49
SiC <sub>6</sub> H <sub>5</sub> F <sub>3</sub>	C <sub>6</sub> H <sub>5</sub> SiF <sub>3</sub>	-73.2	49
		-72.71	7
		-76.2	22
SiC <sub>6</sub> H <sub>6</sub> Cl <sub>2</sub>	Cl <sub>2</sub> (C <sub>6</sub> H <sub>5</sub> )SiH	-2.10	74
SiC <sub>6</sub> H <sub>6</sub> F <sub>6</sub> O <sub>4</sub>	(CH <sub>3</sub> ) <sub>2</sub> Si(OCOCF <sub>3</sub> ) <sub>2</sub>	14.0	13
SiC <sub>6</sub> H <sub>8</sub>	C <sub>6</sub> H <sub>5</sub> SiH <sub>3</sub>	-61.5	4
		-59.9	49

$\text{SiC}_6\text{H}_{11}\text{Cl}$	$(\text{CH}_3)(\text{CH}_2\text{Cl})\text{Si}(\text{CH}=\text{CH}_2)_2$	-14.05	32
$\text{SiC}_6\text{H}_{11}\text{ClO}$	$(\text{CH}_3)_2(\text{CH}_2\text{Cl})\text{SiOCH}_3$	12.86	32
$\text{SiC}_6\text{H}_{11}\text{ClO}_4$	$(\text{CH}_3)(\text{OCOCH}_3)_2\text{SiCH}_2\text{Cl}$	-9.4	31
$\text{SiC}_6\text{H}_{12}$	$(\text{CH}_3)_2\text{Si}(\text{CH}=\text{CH}_2)_2$	-13.67	32
$\text{SiC}_6\text{H}_{12}\text{Cl}_4$	$[\text{Cl}(\text{CH}_2)_3]_2\text{SiCl}_2$	32.00	74
$\text{SiC}_6\text{H}_{12}\text{N}_2$		14.39	136
$\text{SiC}_6\text{H}_{12}\text{N}_2$		13.16	136
$\text{SiC}_6\text{H}_{12}\text{O}_4$	$(\text{CH}_3)_2\text{Si}(\text{OCOCH}_3)_2$	4.40	210
$\text{SiC}_6\text{H}_{13}\text{N}$	$(\text{CH}_3)_3\text{Si}(\text{CH}_2)_2\text{CN}$	2.95	32
$\text{SiC}_6\text{H}_{13}\text{NO}_3$	$\text{N}[\text{CH}_2\text{CH}_2\text{O}]_3\text{SiH}$	-83.6	112
$\text{SiC}_6\text{H}_{14}$	$(\text{CH}_3)_3\text{SiCH}_2\text{CH}=\text{CH}_2$	0.39	32
$\text{SiC}_6\text{H}_{14}$	$(\text{CH}_3)_2\text{Si}[(\text{CH}_2)_3]\text{CH}_2$	16.77	32
$\text{SiC}_6\text{H}_{14}$	$(\text{CH}_3)_2(\text{CH}_3\text{CH}_2)\text{SiCH}=\text{CH}_2$	-4.4	51
$\text{SiC}_6\text{H}_{14}\text{Cl}_2$	$\text{Cl}(\text{CH}_2)_4\text{Si}(\text{CH}_3)_2\text{Cl}$	31.4	74
$\text{SiC}_6\text{H}_{14}\text{Cl}_2\text{O}_2$	$(\text{CH}_3)_2\text{Si}(\text{OCH}_2\text{CH}_2\text{Cl})_2$	-1.6	52
$\text{SiC}_6\text{H}_{14}\text{O}$	$(\text{CH}_3)_2(\text{CH}_3\text{CH}_2\text{O})\text{SiCH}=\text{CH}_2$	2.7	51
$\text{SiC}_6\text{H}_{14}\text{O}_2$	$(\text{CH}_3)_3\text{Si}(\text{CH}_2\text{OCOCH}_3)$	0.30	47
$\text{SiC}_6\text{H}_{15}\text{Br}$	$(\text{CH}_3)_3\text{Si}(\text{CH}_2)_3\text{Br}$	2.00	32
$\text{SiC}_6\text{H}_{15}\text{Cl}$	$(\text{CH}_3)_3\text{Si}(\text{CH}_2)_3\text{Cl}$	2.05	32
$\text{SiC}_6\text{H}_{15}\text{Cl}$	$(\text{C}_2\text{H}_5)_3\text{SiCl}$	36.0	74
$\text{SiC}_6\text{H}_{15}\text{ClO}_2$	$(\text{CH}_3)(\text{OC}_2\text{H}_5)_2\text{SiCH}_2\text{Cl}$	-17.2	31
$\text{SiC}_6\text{H}_{15}\text{Cl}_3\text{NP}$	$(\text{C}_2\text{H}_5)_3\text{PNSiCl}_3$	-54.35	53
$\text{SiC}_6\text{H}_{15}\text{F}$	$(\text{CH}_3)_3\text{Si}(\text{CH}_2)_3\text{F}$	2.16	50
$\text{SiC}_6\text{H}_{15}\text{NO}$	$\text{CH}_3\text{CON}(\text{CH}_3)[\text{Si}(\text{CH}_3)_3]$	8.18	135
$\text{SiC}_6\text{H}_{16}$	$(\text{CH}_3)_2\text{Si}(\text{C}_2\text{H}_5)_2$	5.0	32

Empirical formula	Structure	$\delta$	Ref.
$\text{SiC}_6\text{H}_{16}$	$(\text{C}_2\text{H}_5)_3\text{SiH}$	0.15	60
$\text{SiC}_6\text{H}_{16}\text{Cl}_2\text{NP}$	$(\text{C}_2\text{H}_5)_2(\text{CH}_3)\text{PNSi}(\text{CH}_3)\text{Cl}_2$	-24.31	53
$\text{SiC}_6\text{H}_{16}\text{O}$	$(\text{CH}_3)_2\text{Si}(\text{C}_2\text{H}_5)[(\text{CH}_2)_2\text{OH}]$	2.04	32
$\text{SiC}_6\text{H}_{16}\text{O}$	$(\text{CH}_3)_3\text{Si}[\text{CH}_2\text{CH}(\text{CH}_3)\text{OH}]$	-0.02	32
$\text{SiC}_6\text{H}_{16}\text{O}$	$(\text{CH}_3)_3\text{Si}(\text{CH}_2)_2\text{OCH}_3$	0.45	32
$\text{SiC}_6\text{H}_{16}\text{O}$	$(\text{CH}_3)_3\text{SiOCH}(\text{CH}_3)_2$	12.12	132
$\text{SiC}_6\text{H}_{16}\text{O}_2$	$(\text{CH}_3)_2\text{Si}(\text{OC}_2\text{H}_5)_2$	-7.5	4
		-6.1	232
$\text{SiC}_6\text{H}_{16}\text{O}_3$	$(\text{C}_2\text{H}_5\text{O})_3\text{SiH}$	-59.5	112
$\text{SiC}_6\text{H}_{17}\text{N}$	$n\text{-C}_3\text{H}_7\text{NHSi}(\text{CH}_3)_3$	2.15	136
$\text{SiC}_6\text{H}_{17}\text{N}$	$(\text{CH}_3)_3\text{Si}(\text{CH}_2)_3\text{NH}_2$	1.6	52
$\text{SiC}_6\text{H}_{17}\text{NO}_2$	$(\text{C}_2\text{H}_5\text{O})_2(\text{CH}_3)\text{SiCH}_2\text{NH}_2$	-50.2	52
$\text{SiC}_6\text{H}_{18}\text{NP}$	$(\text{CH}_3)_3\text{PNSi}(\text{CH}_3)_3$	-13.75	53
$\text{SiC}_6\text{H}_{18}\text{N}_2$	$(\text{CH}_3)_2\text{Si}[\text{N}(\text{CH}_3)_2]_2$	-1.85	46
$\text{SiC}_6\text{H}_{18}\text{N}_2\text{O}_2$	$(\text{CH}_3)_2\text{Si}(\text{OCH}_2\text{CH}_2\text{NH}_2)_2$	-3.2	52
$\text{SiC}_7\text{H}_3\text{Cl}_9\text{O}_6$	$\text{CH}_3\text{Si}(\text{OCOCCl}_3)_3$	-37.7	210
$\text{SiC}_7\text{H}_3\text{F}_9\text{O}_6$	$\text{CH}_3\text{Si}(\text{OCOCF}_3)_3$	-38.5	210
$\text{SiC}_7\text{H}_4\text{F}_6$	$p\text{-CF}_3\text{C}_6\text{H}_4\text{SiF}_3$	-74.32	54
$\text{SiC}_7\text{H}_4\text{F}_6$	$m\text{-CF}_3\text{C}_6\text{H}_4\text{SiF}_3$	-74.31	54
$\text{SiC}_7\text{H}_6\text{Cl}_4$	$p\text{-ClC}_6\text{H}_4\text{CH}_2\text{SiCl}_3$	6.9	185
$\text{SiC}_7\text{H}_6\text{Cl}_6\text{O}_6$	$\text{CH}_3\text{Si}(\text{OCOCHCl}_2)_3$	-38.8	210
$\text{SiC}_7\text{H}_7\text{BrCl}_2$	$p\text{-BrC}_6\text{H}_4\text{Si}(\text{CH}_3)\text{Cl}_2$	18.2	185
$\text{SiC}_7\text{H}_7\text{Cl}_3$	$p\text{-CH}_3\text{C}_6\text{H}_4\text{SiCl}_3$	-2.1	185
$\text{SiC}_7\text{H}_7\text{Cl}_3$	$\text{C}_6\text{H}_5\text{CH}_2\text{SiCl}_3$	7.2	49
$\text{SiC}_7\text{H}_7\text{Cl}_3\text{O}$	$p\text{-CH}_3\text{OC}_6\text{H}_4\text{SiCl}_3$	-2.2	185
$\text{SiC}_7\text{H}_7\text{F}_3$	$p\text{-CH}_3\text{C}_6\text{H}_4\text{SiF}_3$	-72.02	54
$\text{SiC}_7\text{H}_7\text{F}_3$	$m\text{-CH}_3\text{C}_6\text{H}_4\text{SiF}_3$	-72.57	54
$\text{SiC}_7\text{H}_7\text{F}_3$	$\text{C}_6\text{H}_5\text{CH}_2\text{SiF}_3$	-64.2	49
$\text{SiC}_7\text{H}_7\text{F}_3\text{O}$	$p\text{-CH}_3\text{OC}_6\text{H}_4\text{SiF}_3$	71.49	54
$\text{SiC}_7\text{H}_7\text{F}_3\text{O}$	$m\text{-CH}_3\text{OC}_6\text{H}_4\text{SiF}_3$	73.03	54

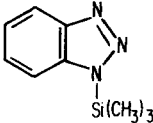
$\text{SiC}_7\text{H}_8\text{Cl}_2$	$\text{C}_6\text{H}_5\text{Si}(\text{CH}_3)\text{Cl}_2$	17.9	49
$\text{SiC}_7\text{H}_8\text{F}_2$	$\text{C}_6\text{H}_5\text{Si}(\text{CH}_3)\text{F}_2$	-12.4	49
$\text{SiC}_7\text{H}_9\text{Cl}_3\text{O}_6$	$\text{CH}_3\text{Si}(\text{OCOCH}_2\text{Cl})_3$	-41.2	210
$\text{SiC}_7\text{H}_{10}$	$\text{C}_6\text{H}_5\text{CH}_2\text{SiH}_3$	-56.0	49
$\text{SiC}_7\text{H}_{11}\text{ClO}_6$	$(\text{CH}_3\text{OCO})_3\text{SiCH}_2\text{Cl}$	-57.6	31
$\text{SiC}_7\text{H}_{12}$	$\text{CH}_3\text{Si}(\text{CH}=\text{CH}_2)_3$	-20.55	32
$\text{SiC}_7\text{H}_{12}\text{O}$		-11.5	96
$\text{SiC}_7\text{H}_{12}\text{O}_6$	$\text{CH}_3\text{Si}(\text{OCOCH}_3)_3$	-42.7	210
$\text{SiC}_7\text{H}_{13}\text{N}$		11.10	136
$\text{SiC}_7\text{H}_{13}\text{NO}_2$	$\text{OCCH}_2\text{CH}_2\text{CONSi}(\text{CH}_3)_3$	13.36	136
$\text{SiC}_7\text{H}_{14}\text{O}_2$	$(\text{CH}_3)_3\text{Si}(\text{OCOCH}=\text{CHCH}_3)$	22.3	210
$\text{SiC}_7\text{H}_{14}\text{O}_4$	$(\text{CH}_3)_2\text{Si}(\text{CH}_2\text{OCOCH}_3)(\text{OCOCH}_3)$	13.80	47
$\text{SiC}_7\text{H}_{15}\text{Cl}$	$\text{CH}_2(\text{CH}_2)_4\text{Si}(\text{CH}_3)(\text{CH}_2\text{Cl})$	-1.31	32
$\text{SiC}_7\text{H}_{15}\text{Cl}_3\text{O}_3$	$\text{CH}_3\text{Si}(\text{OCH}_2\text{CH}_2\text{Cl})_3$	41.9	52
$\text{SiC}_7\text{H}_{15}\text{NO}$	$\text{OC}(\text{CH}_2)_3\text{NSi}(\text{CH}_3)_3$	7.58	136
$\text{SiC}_7\text{H}_{15}\text{NO}_3$	$\text{N}[\text{CH}_2\text{CH}_2\text{O}]_3\text{SiCH}_3$	-44.2	112
$\text{SiC}_7\text{H}_{16}$	$(\text{CH}_3)(\text{CH}_3\text{CH}_2)\text{SiCH}=\text{CH}_2$	-2.3	51
$\text{SiC}_7\text{H}_{16}\text{O}$	$\text{CH}_2(\text{CH}_2)_3\text{Si}(\text{CH}_3)(\text{CH}_2)_2\text{OH}$	16.33	32
$\text{SiC}_7\text{H}_{16}\text{O}_2$	$(\text{CH}_3)_3\text{Si}(\text{CH}_2)_3\text{COOH}$	1.63	32
$\text{SiC}_7\text{H}_{16}\text{O}_2$	$(\text{CH}_3)_3\text{SiCH}_2\text{CH}(\text{CH}_3)\text{COOH}$	1.36	32
$\text{SiC}_7\text{H}_{16}\text{O}_2$	$(\text{CH}_3)_3\text{SiCH}_2\text{COOC}_2\text{H}_5$	2.81	32
$\text{SiC}_7\text{H}_{16}\text{O}_3$	$(\text{CH}_3)_2\text{Si}(\text{OC}_2\text{H}_5)(\text{CH}_2\text{OCOCH}_3)$	9.0	47
$\text{SiC}_7\text{H}_{16}\text{O}_3$	$(\text{CH}_3)_3\text{SiCH}_2\text{O}(\text{CH}_2)_2\text{COOH}$	-1.08	32
$\text{SiC}_7\text{H}_{17}\text{ClO}_3$	$(\text{C}_2\text{H}_5\text{O})_3\text{SiCH}_2\text{Cl}$	-59.7	31
$\text{SiC}_7\text{H}_{17}\text{F}$	$(\text{CH}_3)_2(\text{CH}_2\text{F})\text{Si}(\text{n-C}_4\text{H}_9)$	-0.53	32
$\text{SiC}_7\text{H}_{17}\text{I}$	$(\text{CH}_3)_2(\text{CH}_2\text{I})\text{Si}(\text{n-C}_4\text{H}_9)$	5.28	32

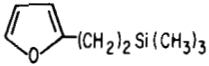
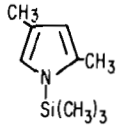
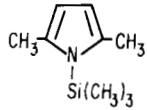
Empirical formula	Structure	$\delta$	Ref.
SiC <sub>7</sub> H <sub>18</sub> Cl <sub>2</sub> NP	(C <sub>2</sub> H <sub>5</sub> ) <sub>3</sub> PNSi(CH <sub>3</sub> )Cl <sub>2</sub>	- 25.29	53
SiC <sub>7</sub> H <sub>18</sub> O	(CH <sub>3</sub> )(C <sub>2</sub> H <sub>5</sub> ) <sub>2</sub> Si(CH <sub>2</sub> ) <sub>2</sub> OH	4.04	32
SiC <sub>7</sub> H <sub>18</sub> O	(CH <sub>3</sub> ) <sub>2</sub> Si(i-C <sub>3</sub> H <sub>7</sub> )(CH <sub>2</sub> ) <sub>2</sub> OH	4.16	32
SiC <sub>7</sub> H <sub>18</sub> O	(C <sub>2</sub> H <sub>5</sub> ) <sub>3</sub> SiOCH <sub>3</sub>	18.8	32
SiC <sub>7</sub> H <sub>18</sub> O	(CH <sub>3</sub> ) <sub>3</sub> SiOC(CH <sub>3</sub> ) <sub>3</sub>	6.20	132
SiC <sub>7</sub> H <sub>18</sub> O <sub>3</sub>	CH <sub>3</sub> Si(OC <sub>2</sub> H <sub>5</sub> ) <sub>3</sub>	- 45.5	4
		- 44.5	232
		- 44.2	112
SiC <sub>7</sub> H <sub>19</sub> ClNP	(C <sub>2</sub> H <sub>5</sub> ) <sub>2</sub> (CH <sub>3</sub> )PNSi(CH <sub>3</sub> ) <sub>2</sub> Cl	- 5.43	53
SiC <sub>7</sub> H <sub>19</sub> N	n-C <sub>4</sub> H <sub>9</sub> NHSi(CH <sub>3</sub> ) <sub>3</sub>	2.18	136
SiC <sub>7</sub> H <sub>19</sub> N	i-C <sub>4</sub> H <sub>9</sub> NHSi(CH <sub>3</sub> ) <sub>3</sub>	2.51	136
SiC <sub>7</sub> H <sub>19</sub> N	(C <sub>2</sub> H <sub>5</sub> ) <sub>2</sub> NSi(CH <sub>3</sub> ) <sub>3</sub>	3.74	136
SiC <sub>7</sub> H <sub>19</sub> N	(CH <sub>3</sub> ) <sub>3</sub> Si(CH <sub>2</sub> ) <sub>4</sub> NH <sub>2</sub>	1.4	52
SiC <sub>7</sub> H <sub>19</sub> NO	C <sub>2</sub> H <sub>5</sub> O(CH <sub>3</sub> ) <sub>2</sub> Si(CH <sub>2</sub> ) <sub>3</sub> NH <sub>2</sub>	15.8	52
SiC <sub>7</sub> H <sub>19</sub> NO <sub>3</sub>	(C <sub>2</sub> H <sub>5</sub> O) <sub>3</sub> SiCH <sub>2</sub> NH <sub>2</sub>	- 50.2	52
SiC <sub>7</sub> H <sub>21</sub> N <sub>3</sub>	CH <sub>3</sub> Si[N(CH <sub>3</sub> ) <sub>2</sub> ] <sub>3</sub>	- 17.5	79
		- 16.80	46
SiC <sub>7</sub> H <sub>21</sub> N <sub>3</sub> O <sub>3</sub>	CH <sub>3</sub> Si(OCH <sub>2</sub> CH <sub>2</sub> NH <sub>2</sub> ) <sub>3</sub>	- 41.5	52
SiC <sub>8</sub> H <sub>5</sub> Cl <sub>3</sub>	C <sub>6</sub> H <sub>5</sub> C≡CSiCl <sub>3</sub>	- 30.53	127
SiC <sub>8</sub> H <sub>10</sub> BrCl	<i>p</i> -BrC <sub>6</sub> H <sub>4</sub> Si(CH <sub>3</sub> ) <sub>2</sub> Cl	19.7	185
SiC <sub>8</sub> H <sub>10</sub> ClF	<i>p</i> -FC <sub>6</sub> H <sub>4</sub> Si(CH <sub>3</sub> ) <sub>2</sub> Cl	19.7	185
SiC <sub>8</sub> H <sub>10</sub> Cl <sub>2</sub>	<i>p</i> -ClC <sub>6</sub> H <sub>4</sub> Si(CH <sub>3</sub> ) <sub>2</sub> Cl	19.8	185
SiC <sub>8</sub> H <sub>10</sub> Cl <sub>2</sub>	<i>p</i> -CH <sub>3</sub> C <sub>6</sub> H <sub>4</sub> Si(CH <sub>3</sub> )Cl <sub>2</sub>	19.3	185
SiC <sub>8</sub> H <sub>10</sub> Cl <sub>2</sub>	C <sub>6</sub> H <sub>5</sub> CH <sub>2</sub> Si(CH <sub>3</sub> )Cl <sub>2</sub>	26.9	232
SiC <sub>8</sub> H <sub>10</sub> F <sub>2</sub>	<i>p</i> -CH <sub>3</sub> C <sub>6</sub> H <sub>4</sub> Si(CH <sub>3</sub> )F <sub>2</sub>	- 12.2	185
SiC <sub>8</sub> H <sub>10</sub> F <sub>2</sub>	C <sub>6</sub> H <sub>5</sub> CH <sub>2</sub> Si(CH <sub>3</sub> )F <sub>2</sub>	- 2.9	232
SiC <sub>8</sub> H <sub>11</sub> Cl	C <sub>6</sub> H <sub>5</sub> (CH <sub>3</sub> ) <sub>2</sub> SiCl	20.1	74
		19.9	49
SiC <sub>8</sub> H <sub>11</sub> F	(CH <sub>3</sub> ) <sub>2</sub> (C <sub>6</sub> H <sub>5</sub> )SiF	19.8	49
SiC <sub>8</sub> H <sub>12</sub>	Si(CH=CH <sub>2</sub> ) <sub>4</sub>	- 22.5	55

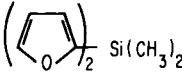
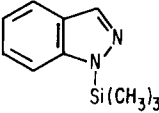
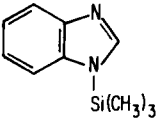
$\text{SiC}_8\text{H}_{12}$	$(\text{CH}_3)_2\text{SiH}(\text{C}_6\text{H}_5)$	-17.15	32
$\text{SiC}_8\text{H}_{12}\text{F}_3\text{NS}$		2.92	136
$\text{SiC}_8\text{H}_{12}\text{O}_8$	$\text{Si}(\text{OCOCH}_3)_4$	-74.5	4
$\text{SiC}_8\text{H}_{13}\text{N}$	$(\text{CH}_3)_3\text{Si}(2\text{-C}_5\text{H}_4\text{N})$	-5.79	32
$\text{SiC}_8\text{H}_{14}\text{O}$		1.2	96
$\text{SiC}_8\text{H}_{14}\text{O}_6$	$\text{CH}_3\text{Si}(\text{CH}_2\text{OCOCH}_3)(\text{OCOCH}_3)_2$	-18.1	47
$\text{SiC}_8\text{H}_{15}\text{NO}_3$	$\text{N}[\text{CH}_2\text{CH}_2\text{O}]_3\text{SiCH}=\text{CH}_2$	-81.6	112
$\text{SiC}_8\text{H}_{16}$	$(\text{CH}_3)_2\text{Si}(\text{CH}_2\text{CH}=\text{CH}_2)_2$	0.37	32
$\text{SiC}_8\text{H}_{16}\text{N}_2$		12.39	136
$\text{SiC}_8\text{H}_{17}\text{NO}_3$	$\text{N}(\text{CH}_2\text{CH}_2\text{O})_3\text{SiCH}_2\text{CH}_3$	-66.5	74
$\text{SiC}_8\text{H}_{18}$	$(\text{CH}_3)_2\text{CC}(\text{CH}_3)_2\text{Si}(\text{CH}_3)_2$	-49.31	64
$\text{SiC}_8\text{H}_{18}$	$(\text{CH}_3\text{CH}_2)_3\text{SiCH}=\text{CH}_2$	-1.7	51
$\text{SiC}_8\text{H}_{18}\text{O}$	$(\text{CH}_3)_2(\text{t-C}_4\text{H}_9\text{O})\text{SiCH}=\text{CH}_2$	-5.6	51
$\text{SiC}_8\text{H}_{18}\text{O}$	$\text{CH}_2(\text{CH}_2)_4\text{Si}(\text{CH}_3)[(\text{CH}_2)_2\text{OH}]$	-4.1	32
$\text{SiC}_8\text{H}_{18}\text{O}_2$	$(\text{CH}_3)_3\text{Si}(\text{CH}_2)_4\text{COOH}$	1.53	32
$\text{SiC}_8\text{H}_{18}\text{O}_2$	$(\text{CH}_3)_2\text{Si}(\text{C}_2\text{H}_5)(\text{CH}_2\text{COOC}_2\text{H}_5)$	5.17	32
$\text{SiC}_8\text{H}_{18}\text{O}_2$	$(\text{CH}_3)_3\text{Si}(\text{CH}_2)_2\text{COOC}_2\text{H}_5$	2.40	32
$\text{SiC}_8\text{H}_{18}\text{O}_2$	$(\text{CH}_3)_3\text{Si}(\text{OCO-t-C}_4\text{H}_9)$	22.6	210
$\text{SiC}_8\text{H}_{18}\text{O}_3$	$(\text{C}_2\text{H}_5\text{O})_3\text{SiCH}=\text{CH}_2$	-64.0	4
		-60.3	51
		-59.5	112

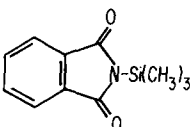
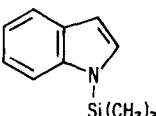


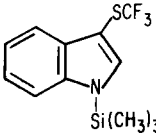
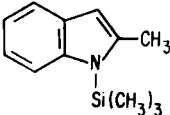
Empirical formula	Structure	$\delta$	Ref.
$\text{SiC}_8\text{H}_{18}\text{O}_4$	$(\text{CH}_3)(\text{C}_2\text{H}_5\text{O})_2\text{SiCH}_2\text{OCOCH}_3$	-16.0	47
$\text{SiC}_8\text{H}_{19}\text{F}$	$(\text{CH}_3)_3\text{Si}(\text{CH}_2)_5\text{F}$	1.45	50
$\text{SiC}_8\text{H}_{19}\text{N}$	$\text{CH}_2(\text{CH}_2)_3\text{CH}_2\text{NSi}(\text{CH}_3)_3$	3.43	136
$\text{SiC}_8\text{H}_{20}$	<i>trans</i> -( $\text{CH}_3$ ) <sub>3</sub> SiHC=CHSi( $\text{CH}_3$ ) <sub>3</sub>	-8.9	134
$\text{SiC}_8\text{H}_{20}$	<i>cis</i> -( $\text{CH}_3$ ) <sub>3</sub> SiHC=CHSi( $\text{CH}_3$ ) <sub>3</sub>	-11.8	134
$\text{SiC}_8\text{H}_{20}$	$[(\text{CH}_3)_3\text{Si}]_2\text{C}\equiv\text{CH}_2$	-3.11	134
$\text{SiC}_8\text{H}_{20}\text{O}$	$(\text{CH}_3)_3\text{Si}(\text{CH}_2)_2\text{C}(\text{CH}_3)_2\text{OH}$	2.41	32
$\text{SiC}_8\text{H}_{20}\text{O}$	$(\text{C}_2\text{H}_5)_3\text{Si}(\text{CH}_2)_2\text{OH}$	5.38	32
$\text{SiC}_8\text{H}_{20}\text{O}_4$	$(\text{C}_2\text{H}_5\text{O})_4\text{Si}$	-83.5	4
$\text{SiC}_8\text{H}_{21}\text{ClNP}$	$(\text{C}_2\text{H}_5)_3\text{PNSi}(\text{CH}_3)_2\text{Cl}$	-7.87	53
$\text{SiC}_8\text{H}_{21}\text{NO}_2$	$(\text{C}_2\text{H}_5\text{O})_2(\text{CH}_3)\text{Si}(\text{CH}_2)_3\text{NH}_2$	-5.7	52
$\text{SiC}_8\text{H}_{21}\text{NO}_3$	$(\text{C}_2\text{H}_5\text{O})_3\text{Si}(\text{CH}_2)_2\text{NH}_2$	-46.5	52
$\text{SiC}_8\text{H}_{22}\text{NOP}$	$(\text{C}_2\text{H}_5)_2(\text{CH}_3)\text{PNSi}(\text{CH}_3)_2\text{OCH}_3$	-16.47	53
$\text{SiC}_8\text{H}_{22}\text{NO}_2\text{P}$	$(\text{C}_2\text{H}_5)_2(\text{CH}_3)\text{PNSi}(\text{CH}_3)(\text{OCH}_3)_2$	-39.58	53
$\text{SiC}_8\text{H}_{22}\text{NO}_3\text{P}$	$(\text{C}_2\text{H}_5)_2\text{PNSi}(\text{OCH}_3)_3$	-69.56	53
$\text{SiC}_8\text{H}_{22}\text{NP}$	$(\text{C}_2\text{H}_5)_2(\text{CH}_3)\text{PNSi}(\text{CH}_3)_3$	-14.98	53
$\text{SiC}_8\text{H}_{24}\text{N}_2\text{P}_2$	$[(\text{CH}_3)_3\text{PN}]_2\text{Si}(\text{CH}_3)_2$	-31.76	53
$\text{SiC}_8\text{H}_{24}\text{N}_4$	$\text{Si}[\text{N}(\text{CH}_3)_2]_4$	-28.1	79
		-28.6	46
$\text{SiC}_9\text{H}_9\text{F}_5$	$(\text{CH}_3)_3\text{SiC}_6\text{F}_5$	0.00	13
$\text{SiC}_9\text{H}_{12}\text{Cl}_2$	$\text{C}_6\text{H}_5\text{CH}_2\text{CH}_2\text{Si}(\text{CH}_3)\text{Cl}_2$	31.6	49
$\text{SiC}_9\text{H}_{13}\text{Br}$	<i>p</i> -BrC <sub>6</sub> H <sub>4</sub> Si(CH <sub>3</sub> ) <sub>3</sub>	-4.1	185
$\text{SiC}_9\text{H}_{13}\text{BrO}$	<i>m</i> -BrC <sub>6</sub> H <sub>4</sub> OSi(CH <sub>3</sub> ) <sub>3</sub>	19.76	56
$\text{SiC}_9\text{H}_{13}\text{BrO}$	<i>p</i> -BrC <sub>6</sub> H <sub>4</sub> OSi(CH <sub>3</sub> ) <sub>3</sub>	19.49	56
$\text{SiC}_9\text{H}_{13}\text{Cl}$	<i>p</i> -ClC <sub>6</sub> H <sub>4</sub> Si(CH <sub>3</sub> ) <sub>3</sub>	-3.78	32
$\text{SiC}_9\text{H}_{13}\text{Cl}$	$(\text{CH}_3)_2(\text{CH}_2\text{Cl})\text{Si}(\text{C}_6\text{H}_5)$	-3.26	32
$\text{SiC}_9\text{H}_{13}\text{Cl}$	$\text{C}_6\text{H}_5\text{CH}_2\text{Si}(\text{CH}_3)_2\text{Cl}$	26.6	49
$\text{SiC}_9\text{H}_{13}\text{ClO}$	<i>p</i> -ClC <sub>6</sub> H <sub>4</sub> OSi(CH <sub>3</sub> ) <sub>3</sub>	19.85	32
		19.73	56

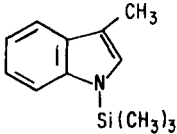
I	SiC <sub>9</sub> H <sub>13</sub> ClO	<i>m</i> -ClC <sub>6</sub> H <sub>4</sub> OSi(CH <sub>3</sub> ) <sub>3</sub>	20·67	32
			20·00	56
	SiC <sub>9</sub> H <sub>13</sub> ClO	<i>o</i> -ClC <sub>6</sub> H <sub>4</sub> OSi(CH <sub>3</sub> ) <sub>3</sub>	21·54	32
	SiC <sub>9</sub> H <sub>13</sub> ClO	<i>o</i> -CH <sub>3</sub> OC <sub>6</sub> H <sub>4</sub> Si(CH <sub>3</sub> ) <sub>2</sub> Cl	19·6	185
	SiC <sub>9</sub> H <sub>13</sub> F	<i>p</i> -FC <sub>6</sub> H <sub>4</sub> Si(CH <sub>3</sub> ) <sub>3</sub>	-4·01	32
	SiC <sub>9</sub> H <sub>13</sub> F	<i>m</i> -FC <sub>6</sub> H <sub>4</sub> Si(CH <sub>3</sub> ) <sub>3</sub>	-3·49	32
	SiC <sub>9</sub> H <sub>13</sub> F	<i>p</i> -CH <sub>3</sub> C <sub>6</sub> H <sub>4</sub> Si(CH <sub>3</sub> ) <sub>2</sub> F	19·8	185
	SiC <sub>9</sub> H <sub>13</sub> F	C <sub>6</sub> H <sub>5</sub> CH <sub>2</sub> Si(CH <sub>3</sub> ) <sub>2</sub> F	27·4	49
	SiC <sub>9</sub> H <sub>13</sub> FO	<i>p</i> -FC <sub>6</sub> H <sub>4</sub> OSi(CH <sub>3</sub> ) <sub>3</sub>	18·88	56
	SiC <sub>9</sub> H <sub>13</sub> IO	<i>p</i> -IC <sub>6</sub> H <sub>4</sub> OSi(CH <sub>3</sub> ) <sub>3</sub>	19·08	56
	SiC <sub>9</sub> H <sub>13</sub> NO <sub>2</sub>	<i>p</i> -NO <sub>2</sub> C <sub>6</sub> H <sub>4</sub> Si(CH <sub>3</sub> ) <sub>3</sub>	-2·47	32
	SiC <sub>9</sub> H <sub>13</sub> NO <sub>2</sub>	<i>m</i> -NO <sub>2</sub> C <sub>6</sub> H <sub>4</sub> Si(CH <sub>3</sub> ) <sub>3</sub>	-2·37	32
	SiC <sub>9</sub> H <sub>13</sub> NO <sub>2</sub>	<i>o</i> -NO <sub>2</sub> C <sub>6</sub> H <sub>4</sub> Si(CH <sub>3</sub> ) <sub>3</sub>	-2·33	32
	SiC <sub>9</sub> H <sub>13</sub> NO <sub>3</sub>	<i>m</i> -NO <sub>2</sub> C <sub>6</sub> H <sub>4</sub> OSi(CH <sub>3</sub> ) <sub>3</sub>	21·61	56
	SiC <sub>9</sub> H <sub>13</sub> NO <sub>3</sub>	<i>p</i> -NO <sub>2</sub> C <sub>6</sub> H <sub>4</sub> OSi(CH <sub>3</sub> ) <sub>3</sub>	22·11	56
II	SiC <sub>9</sub> H <sub>13</sub> N <sub>3</sub>		18·18	136
	SiC <sub>9</sub> H <sub>14</sub>	(CH <sub>3</sub> ) <sub>3</sub> SiC <sub>6</sub> H <sub>5</sub>	-4·50	55
III	SiC <sub>9</sub> H <sub>14</sub> O	(CH <sub>3</sub> ) <sub>3</sub> SiOC <sub>6</sub> H <sub>5</sub>	-5·1	49
			18·13	32
IV	SiC <sub>9</sub> H <sub>14</sub> O	(CH <sub>3</sub> ) <sub>2</sub> Si(CH <sub>2</sub> OH)(C <sub>6</sub> H <sub>5</sub> )	17·72	56
	SiC <sub>9</sub> H <sub>14</sub> O <sub>8</sub>	(CH <sub>2</sub> OCOCH <sub>3</sub> )Si(OCOCH <sub>3</sub> ) <sub>3</sub>	-6·14	32
V	SiC <sub>9</sub> H <sub>14</sub> S	(CH <sub>3</sub> ) <sub>3</sub> SiSC <sub>6</sub> H <sub>5</sub>	-82·5	47
	SiC <sub>9</sub> H <sub>15</sub> N	(CH <sub>3</sub> ) <sub>3</sub> SiCH <sub>2</sub> -2-C <sub>5</sub> H <sub>4</sub> N	15·3	44
VI	SiC <sub>9</sub> H <sub>15</sub> N	(CH <sub>3</sub> ) <sub>3</sub> SiCH <sub>2</sub> -2-C <sub>5</sub> H <sub>4</sub> N	2·17	32
	SiC <sub>9</sub> H <sub>15</sub> NO	<i>m</i> -NH <sub>2</sub> C <sub>6</sub> H <sub>4</sub> OSi(CH <sub>3</sub> ) <sub>3</sub>	17·90	56
VII	SiC <sub>9</sub> H <sub>15</sub> NO	<i>p</i> -NH <sub>2</sub> C <sub>6</sub> H <sub>4</sub> OSi(CH <sub>3</sub> ) <sub>3</sub>	17·40	56

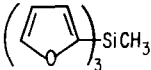
Empirical formula	Structure	$\delta$	Ref.
$\text{SiC}_9\text{H}_{16}\text{O}$		1.4	96
$\text{SiC}_9\text{H}_{17}\text{N}$		(2, 4) 8.55	136
$\text{SiC}_9\text{H}_{17}\text{N}$		(2, 5) 8.86	136
$\text{SiC}_9\text{H}_{18}$	$(\text{CH}_3)_3\text{SiC}=\text{CH}(\text{CH}_2)_3\text{CH}_2$	-6.08	32
$\text{SiC}_9\text{H}_{18}\text{O}_2$	$(\text{CH}_3)_3\text{Si}(\text{CH}_2)_2\text{COCH}_2\text{COCH}_3$	2.52	32
$\text{SiC}_9\text{H}_{18}\text{O}_5$	$(\text{CH}_3)_3\text{Si}(\text{O}-\text{t-C}_4\text{H}_9)(\text{OCOCH}_3)_2$	-51.1	74
$\text{SiC}_9\text{H}_{20}$	$(\text{CH}_3)_3\text{SiCH}(\text{CH}_2)_4\text{CH}_2$	2.40	32
$\text{SiC}_9\text{H}_{20}\text{O}$	$(\text{CH}_3)_3\text{Si}(\text{O}-\text{c-C}_6\text{H}_{11})$	12.7	32
$\text{SiC}_9\text{H}_{20}\text{O}_2$	$(\text{CH}_3)(\text{C}_2\text{H}_5)_2\text{SiCH}_2\text{COOC}_2\text{H}_5$	7.10	32
$\text{SiC}_9\text{H}_{20}\text{O}_5$	$(\text{C}_2\text{H}_5\text{O})_3\text{SiCH}_2\text{OCOCH}_3$	-58.2	47
$\text{SiC}_9\text{H}_{21}\text{Cl}_3\text{NP}$	$(\text{n-C}_3\text{H}_7)_3\text{PNSiCl}_3$	-54.61	53
$\text{SiC}_9\text{H}_{21}\text{F}$	$(\text{n-C}_3\text{H}_7)_3\text{SiF}$	28.8	13
$\text{SiC}_9\text{H}_{21}\text{N}$	$\text{CH}(\text{CH}_3)(\text{CH}_2)_4\text{NSi}(\text{CH}_3)_3$	2.20	136
$\text{SiC}_9\text{H}_{21}\text{N}$	$\text{CH}_2\text{CH}(\text{CH}_3)(\text{CH}_2)_3\text{NSi}(\text{CH}_3)_3$	3.58	136
$\text{SiC}_9\text{H}_{21}\text{N}$	$\text{CH}_2\text{CH}_2\text{CH}(\text{CH}_3)(\text{CH}_2)_2\text{NSi}(\text{CH}_3)_3$	3.58	136
$\text{SiC}_9\text{H}_{21}\text{N}$	$\text{CH}_2(\text{CH}_2)_5\text{NSi}(\text{CH}_3)_3$	3.63	136
$\text{SiC}_9\text{H}_{22}$	$(\text{n-C}_3\text{H}_7)_3\text{SiH}$	-8.50	13
		-8.11	60
$\text{SiC}_9\text{H}_{23}\text{N}$	$(\text{n-C}_3\text{H}_7)_2\text{NSi}(\text{CH}_3)_3$	4.20	136

$\text{SiC}_9\text{H}_{23}\text{NO}_2$	$(\text{C}_2\text{H}_5\text{O})_2\text{CH}_3\text{Si}(\text{CH}_2)_4\text{NH}_2$	-5.9	52
$\text{SiC}_9\text{H}_{23}\text{NO}_3$	$(\text{C}_2\text{H}_5\text{O})_3\text{Si}(\text{CH}_2)_3\text{NH}_2$	-45.3	52
$\text{SiC}_9\text{H}_{24}\text{NOP}$	$(\text{C}_2\text{H}_5)_3\text{PNSi}(\text{CH}_3)_2\text{OCH}_3$	-17.26	53
$\text{SiC}_9\text{H}_{24}\text{NO}_2\text{P}$	$(\text{C}_2\text{H}_5)_3\text{PNSiCH}_3(\text{OCH}_3)_2$	-40.07	53
$\text{SiC}_9\text{H}_{24}\text{NO}_3\text{P}$	$(\text{C}_2\text{H}_5)_3\text{PNSi}(\text{OCH}_3)_3$	-69.94	53
$\text{SiC}_9\text{H}_{24}\text{NP}$	$(t\text{-C}_4\text{H}_9)(\text{CH}_3)_2\text{PNSi}(\text{CH}_3)_3$	-15.23	53
$\text{SiC}_9\text{H}_{24}\text{NP}$	$(\text{C}_7\text{H}_8)_3\text{PNSi}(\text{CH}_3)_3$	-15.73	53
$\text{SiC}_{10}\text{H}_{12}\text{ClF}_3$	$m\text{-CF}_3\text{C}_6\text{H}_4\text{Si}(\text{CH}_3)_2\text{CH}_2\text{Cl}$	-2.31	32
$\text{SiC}_{10}\text{H}_{12}\text{O}_2$		-24.7	96
$\text{SiC}_{10}\text{H}_{14}\text{N}_2$		14.54	136
$\text{SiC}_{10}\text{H}_{14}\text{N}_2$		12.80	136
$\text{SiC}_{10}\text{H}_{14}\text{O}_2$	$(\text{CH}_3)_3\text{SiOCOC}_6\text{H}_5$	23.6	210
$\text{SiC}_{10}\text{H}_{15}\text{Cl}$	$(\text{CH}_3)_2(\text{CH}_2\text{Cl})\text{SiCH}_2\text{C}_6\text{H}_5$	2.94	32
$\text{SiC}_{10}\text{H}_{15}\text{Cl}$	$p\text{-ClC}_6\text{H}_4\text{CH}_2\text{Si}(\text{CH}_3)_3$	0.6	185
$\text{SiC}_{10}\text{H}_{15}\text{ClO}$	$p\text{-CH}_3\text{OC}_6\text{H}_4\text{Si}(\text{CH}_3)_2\text{CH}_2\text{Cl}$	-3.64	32
$\text{SiC}_{10}\text{H}_{15}\text{F}$	$p\text{-FC}_6\text{H}_4\text{CH}_2\text{Si}(\text{CH}_3)_3$	1.41	32
$\text{SiC}_{10}\text{H}_{15}\text{F}$	$m\text{-FC}_6\text{H}_4\text{CH}_2\text{Si}(\text{CH}_3)_3$	1.71	32
$\text{SiC}_{10}\text{H}_{16}$	$p\text{-CH}_3\text{C}_6\text{H}_4\text{Si}(\text{CH}_3)_3$	-4.76	32
$\text{SiC}_{10}\text{H}_{16}$	$o\text{-CH}_3\text{C}_6\text{H}_4\text{Si}(\text{CH}_3)_3$	-4.75	32
		-5.1	248

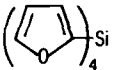
Empirical formula	Structure	$\delta$	Ref.
$\text{SiC}_{10}\text{H}_{16}$	$m\text{-CH}_3\text{C}_6\text{H}_4\text{Si}(\text{CH}_3)_3$	-4.63	32
		-4.9	248
$\text{SiC}_{10}\text{H}_{16}$	$\text{C}_6\text{H}_5\text{CH}_2\text{Si}(\text{CH}_3)_3$	0.4	49
$\text{SiC}_{10}\text{H}_{16}\text{O}$	$\text{C}_6\text{H}_5\text{Si}(\text{CH}_3)_2\text{OC}_2\text{H}_5$	5.1	49
$\text{SiC}_{10}\text{H}_{16}\text{O}$	$p\text{-CH}_3\text{OC}_6\text{H}_4\text{Si}(\text{CH}_3)_3$	-4.90	32
$\text{SiC}_{10}\text{H}_{16}\text{O}$	$p\text{-CH}_3\text{C}_6\text{H}_4\text{OSi}(\text{CH}_3)_3$	17.29	56
$\text{SiC}_{10}\text{H}_{16}\text{O}$	$m\text{-CH}_3\text{C}_6\text{H}_4\text{OSi}(\text{CH}_3)_3$	17.30	56
$\text{SiC}_{10}\text{H}_{16}\text{O}_2$	$p\text{-CH}_3\text{OC}_6\text{H}_4\text{OSi}(\text{CH}_3)_3$	17.73	56
$\text{SiC}_{10}\text{H}_{16}\text{O}_2$	$m\text{-CH}_3\text{OC}_6\text{H}_4\text{OSi}(\text{CH}_3)_3$	18.01	56
$\text{SiC}_{10}\text{H}_{17}\text{N}$	$(\text{CH}_3)_3\text{Si}(\text{CH}_2)_2\text{-2-C}_5\text{H}_4\text{N}$	1.84	32
$\text{SiC}_{10}\text{H}_{18}\text{O}_6$	$\text{CH}_3\text{Si}(\text{OCOC}_2\text{H}_5)_3$	-42.3	210
$\text{SiC}_{10}\text{H}_{18}\text{O}_7$	$t\text{-C}_4\text{H}_9\text{OSi}(\text{OCOCH}_3)_3$	-100.9	74
$\text{SiC}_{10}\text{H}_{20}\text{O}_2$	$\text{CH}_2(\text{CH}_2)_4\text{Si}(\text{CH}_3)\text{CH}_2\text{COOC}_2\text{H}_5$	1.25	32
$\text{SiC}_{10}\text{H}_{22}$	$(n\text{-C}_3\text{H}_7)\text{CHCH}(n\text{-C}_3\text{H}_7)\text{Si}(\text{CH}_3)_2$	-59.8	65
$\text{SiC}_{10}\text{H}_{24}$	$(\text{C}_2\text{H}_5)_3\text{Si}(s\text{-C}_4\text{H}_9)$	8.16	32
$\text{SiC}_{10}\text{H}_{24}$	$(\text{C}_2\text{H}_5)_3\text{Si}(n\text{-C}_4\text{H}_9)$	6.19	32
$\text{SiC}_{10}\text{H}_{24}$	$(\text{CH}_3)_3\text{Si}(n\text{-C}_7\text{H}_{15})$	1.41	32
$\text{SiC}_{10}\text{H}_{24}\text{Cl}_2\text{NP}$	$(n\text{-C}_3\text{H}_7)_3\text{PNSi}(\text{CH}_3)\text{Cl}_2$	-25.63	53
$\text{SiC}_{10}\text{H}_{24}\text{O}$	$(\text{CH}_3)_3\text{Si}(\text{CH}_2)_4\text{C}(\text{CH}_3)_2\text{OH}$	1.44	32
$\text{SiC}_{10}\text{H}_{25}\text{NO}_3$	$(\text{C}_2\text{H}_5\text{O})_3\text{Si}(\text{CH}_2)_4\text{NH}_2$	-45.6	52
$\text{SiC}_{11}\text{H}_{13}\text{NO}_2$		12.70	136
$\text{SiC}_{11}\text{H}_{15}\text{N}$		10.70	136

$\text{SiC}_{11}\text{H}_{16}$	$(\text{CH}_3)_3\text{Si}(\text{CH}=\text{CH})(\text{C}_6\text{H}_5)$	-6.49	32
$\text{SiC}_{11}\text{H}_{16}\text{ClNO}$	$\text{CH}_3\text{CON}[\text{p-ClC}_6\text{H}_4][\text{Si}(\text{CH}_3)_3]$	9.17 (NSi)	135
		20.29 (OSi)	135
$\text{SiC}_{11}\text{H}_{16}\text{O}_2$	$(\text{CH}_3)_3\text{SiOCOCH}_2\text{C}_6\text{H}_5$	24.0	210
$\text{SiC}_{11}\text{H}_{17}\text{NO}$	$\text{CH}_3\text{CON}(\text{C}_6\text{H}_5)[\text{Si}(\text{CH}_3)_3]$	8.66 (NSi)	135
		19.6 (OSi)	135
$\text{SiC}_{11}\text{H}_{18}$	$(\text{CH}_3)_3\text{SiCH}_2\text{CH}_2\text{C}_6\text{H}_5$	1.1	49
$\text{SiC}_{11}\text{H}_{18}$	$p\text{-C}_2\text{H}_5\text{C}_6\text{H}_4\text{Si}(\text{CH}_3)_3$	-5.0	185
$\text{SiC}_{11}\text{H}_{18}\text{O}$	$(\text{CH}_3)_2[(\text{CH}_2)_2\text{OH}]\text{SiCH}_2\text{C}_6\text{H}_5$	0.58	32
$\text{SiC}_{11}\text{H}_{18}\text{O}$	$\text{C}_6\text{H}_5\text{CH}_2\text{Si}(\text{CH}_3)_2(\text{OC}_2\text{H}_5)$	11.7	49
$\text{SiC}_{11}\text{H}_{20}\text{NP}$	$\text{C}_6\text{H}_5(\text{CH}_3)_2\text{PNSi}(\text{CH}_3)_3$	-12.72	53
$\text{SiC}_{11}\text{H}_{24}\text{O}_2$	$(\text{CH}_3)(\text{t-C}_4\text{H}_9\text{O})_2\text{SiCH}=\text{CH}_2$	-34.6	51
$\text{SiC}_{11}\text{H}_{26}$	$(\text{C}_2\text{H}_5)\text{Si}(\text{n-C}_3\text{H}_7)_3$	3.75	32
$\text{SiC}_{11}\text{H}_{17}\text{ClNP}$	$(\text{n-C}_3\text{H}_7)_3\text{PNSi}(\text{CH}_3)_2\text{Cl}$	-8.20	53
$\text{SiC}_{11}\text{H}_{27}\text{ClNP}$	$(\text{i-C}_3\text{H}_7)_3\text{PNSi}(\text{CH}_3)_2\text{Cl}$	-11.15	53
$\text{SiC}_{11}\text{H}_{27}\text{ClNP}$	$(\text{t-C}_4\text{H}_9)_2(\text{CH}_3)\text{PNSi}(\text{CH}_3)_2\text{Cl}$	-9.68	53
$\text{SiC}_{11}\text{H}_{27}\text{N}$	$(\text{n-C}_4\text{H}_9)_2\text{NSi}(\text{CH}_3)_3$	4.10	136
$\text{SiC}_{11}\text{H}_{27}\text{N}$	$(\text{i-C}_4\text{H}_9)_2\text{NSi}(\text{CH}_3)_3$	4.56	136
$\text{SiC}_{11}\text{H}_{33}\text{N}_5\text{O}_2\text{P}_2$	$[(\text{N}(\text{CH}_3)_2)_2\text{P}=\text{O}]_2\text{NSi}(\text{CH}_3)_3$	18.7	141
$\text{SiC}_{12}\text{H}_{10}\text{F}_2$	$(\text{C}_6\text{H}_5)_2\text{SiF}_2$	-30.5	247
$\text{SiC}_{12}\text{H}_{11}\text{Cl}$	$(\text{C}_6\text{H}_5)_2\text{Si}(\text{H})\text{Cl}$	-5.4	74
$\text{SiC}_{12}\text{H}_{12}$	$(\text{C}_6\text{H}_5)_2\text{SiH}_2$	-33.6	49
$\text{SiC}_{12}\text{H}_{12}\text{O}_2$	$(\text{C}_6\text{H}_5)_2\text{Si}(\text{OH})_2$	-32.4 (acetone)	83
$\text{SiC}_{12}\text{H}_{14}\text{F}_3\text{NS}$		14.18	136
$\text{SiC}_{12}\text{H}_{17}\text{N}$		9.88	136

Empirical formula	Structure	$\delta$	Ref.
$\text{SiC}_{12}\text{H}_{17}\text{N}$		9.73	136
$\text{SiC}_{12}\text{H}_{17}\text{NO}_3$	$\text{N}[\text{CH}_2\text{CH}_2\text{O}]_3\text{SiC}_6\text{H}_5$	-81.7	112
$\text{SiC}_{12}\text{H}_{19}\text{NO}$	$\text{CH}_3\text{CON}(p\text{-CH}_3\text{C}_6\text{H}_4)[\text{Si}(\text{CH}_3)_3]$	8.12 (NSi)	135
		18.92 (OSi)	135
$\text{SiC}_{12}\text{H}_{19}\text{NO}_2$	$\text{CH}_3\text{CON}(p\text{-CH}_3\text{OC}_6\text{H}_4)[\text{Si}(\text{CH}_3)_3]$	8.74 (NSi)	135
		9.19 (OSi)	135
$\text{SiC}_{12}\text{H}_{19}\text{NO}_2$	$\text{C}_2\text{H}_5\text{OCON}(\text{C}_6\text{H}_5)[\text{Si}(\text{CH}_3)_3]$	10.55	135
$\text{SiC}_{12}\text{H}_{19}\text{NO}_2$	$\text{C}_2\text{H}_5\text{OCON}(\text{CH}_3)[\text{Si}(\text{CH}_3)_2\text{C}_6\text{H}_5]$	2.58	135
$\text{SiC}_{12}\text{H}_{20}$	$\text{C}_6\text{H}_5(\text{CH}_2)_3\text{Si}(\text{CH}_3)_3$	1.1	49
$\text{SiC}_{12}\text{H}_{20}\text{O}$	$(\text{C}_2\text{H}_5)_3\text{Si}(\text{OC}_6\text{H}_5)$	19.71	32
$\text{SiC}_{12}\text{H}_{20}\text{O}_2$	$\text{C}_6\text{H}_5\text{CH}_2\text{Si}(\text{CH}_3)(\text{OC}_2\text{H}_5)_2$	-11.9	49
$\text{SiC}_{12}\text{H}_{20}\text{O}_3$	$\text{C}_6\text{H}_5\text{Si}(\text{OC}_2\text{H}_5)_3$	-59.4	49
		-60.50	4
$\text{SiC}_{12}\text{H}_{22}$	$[p\text{-(CH}_3)_3\text{Si}]\text{C}_6\text{H}_4\text{Si}(\text{CH}_3)_3$	-58.4	112
$\text{SiC}_{12}\text{H}_{22}$	[16] in text (Table V)	-4.2	185
$\text{SiC}_{12}\text{H}_{24}\text{O}_6$	$(\text{CH}_3\text{COO})_2\text{Si}(\text{O-t-C}_4\text{H}_9)_2$	-51.78	62
$\text{SiC}_{12}\text{H}_{27}\text{F}$	$(n\text{-C}_4\text{H}_9)_3\text{SiF}$	-102.9	74
$\text{SiC}_{12}\text{H}_{28}$	$(s\text{-C}_4\text{H}_9)_3\text{SiH}$	28.8	13
$\text{SiC}_{12}\text{H}_{28}$	$(n\text{-C}_4\text{H}_9)_3\text{SiH}$	-14.7	13
		-6.7	13
		-6.58	60
$\text{SiC}_{12}\text{H}_{30}\text{NOP}$	$(n\text{-C}_3\text{H}_7)_3\text{PNSi}(\text{CH}_3)_2\text{OCH}_3$	-17.38	53
$\text{SiC}_{12}\text{H}_{30}\text{NO}_2\text{P}$	$(n\text{-C}_3\text{H}_7)_3\text{PNSi}(\text{CH}_3)(\text{OCH}_3)_2$	-40.47	53
$\text{SiC}_{12}\text{H}_{30}\text{NO}_3\text{P}$	$(n\text{-C}_3\text{H}_7)_3\text{PNSi}(\text{OCH}_3)_3$	-70.06	53
$\text{SiC}_{12}\text{H}_{30}\text{NP}$	$(n\text{-C}_3\text{H}_7)_3\text{PNSi}(\text{CH}_3)_3$	-15.97	53

SiC <sub>12</sub> H <sub>30</sub> NP	(i-C <sub>3</sub> H <sub>7</sub> ) <sub>3</sub> PNSi(CH <sub>3</sub> ) <sub>3</sub>	- 18.12	53
SiC <sub>12</sub> H <sub>30</sub> NP	(t-C <sub>4</sub> H <sub>9</sub> ) <sub>2</sub> (CH <sub>3</sub> )PNSi(CH <sub>3</sub> ) <sub>3</sub>	- 16.49	53
SiC <sub>13</sub> H <sub>12</sub> O <sub>3</sub>		- 39.2	96
SiC <sub>13</sub> H <sub>13</sub> Cl	(CH <sub>3</sub> )(C <sub>6</sub> H <sub>5</sub> ) <sub>2</sub> SiCl	- 10.4	74
SiC <sub>13</sub> H <sub>13</sub> F	(CH <sub>3</sub> )(C <sub>6</sub> H <sub>5</sub> ) <sub>2</sub> SiF	7.7	13
SiC <sub>13</sub> H <sub>14</sub>	(CH <sub>3</sub> )(C <sub>6</sub> H <sub>5</sub> ) <sub>2</sub> SiH	- 19.5	74
SiC <sub>13</sub> H <sub>21</sub> ClO <sub>3</sub>	<i>p</i> -ClC <sub>6</sub> H <sub>4</sub> CH <sub>2</sub> Si(OC <sub>2</sub> H <sub>5</sub> ) <sub>3</sub>	- 53.4	185
SiC <sub>13</sub> H <sub>21</sub> NO <sub>2</sub>	C <sub>2</sub> H <sub>5</sub> OCON( <i>p</i> -CH <sub>3</sub> C <sub>6</sub> H <sub>4</sub> ) [Si(CH <sub>3</sub> ) <sub>3</sub> ]	10.32 (NSi)	135
SiC <sub>13</sub> H <sub>21</sub> NO <sub>2</sub>	C <sub>2</sub> H <sub>5</sub> OCON(CH <sub>3</sub> ) [Si(CH <sub>3</sub> ) <sub>2</sub> ( <i>p</i> -CH <sub>3</sub> C <sub>6</sub> H <sub>4</sub> )]	2.08 (NSi)	135
SiC <sub>13</sub> H <sub>21</sub> NO <sub>3</sub>	C <sub>2</sub> H <sub>5</sub> OCON(CH <sub>3</sub> ) [Si(CH <sub>3</sub> ) <sub>2</sub> ( <i>p</i> -CH <sub>3</sub> OC <sub>6</sub> H <sub>4</sub> )]	2.18 (NSi)	135
SiC <sub>13</sub> H <sub>22</sub>	C <sub>6</sub> H <sub>5</sub> (CH <sub>2</sub> ) <sub>4</sub> Si(CH <sub>3</sub> ) <sub>3</sub>	1.0	49
SiC <sub>13</sub> H <sub>22</sub> O	<i>p</i> -(t-C <sub>4</sub> H <sub>9</sub> )C <sub>6</sub> H <sub>4</sub> OSi(CH <sub>3</sub> ) <sub>3</sub>	12.5	4
SiC <sub>13</sub> H <sub>22</sub> O <sub>3</sub>	C <sub>6</sub> H <sub>5</sub> CH <sub>2</sub> Si(OC <sub>2</sub> H <sub>5</sub> ) <sub>3</sub>	- 52.7	49
SiC <sub>13</sub> H <sub>24</sub> O	(CH <sub>3</sub> ) <sub>3</sub> SiO-1-adamantyl	6.18	132
SiC <sub>13</sub> H <sub>24</sub> O	(CH <sub>3</sub> ) <sub>3</sub> SiO-2-adamantyl	12.58	132
SiC <sub>14</sub> H <sub>6</sub> F <sub>10</sub>	(CH <sub>3</sub> ) <sub>2</sub> Si(C <sub>6</sub> F <sub>5</sub> ) <sub>2</sub>	- 8.3	13
SiC <sub>14</sub> H <sub>14</sub> F <sub>2</sub>	( <i>p</i> -FC <sub>6</sub> H <sub>4</sub> ) <sub>2</sub> Si(CH <sub>3</sub> ) <sub>2</sub>	- 8.3	185
SiC <sub>14</sub> H <sub>16</sub>	(CH <sub>3</sub> ) <sub>2</sub> Si(C <sub>6</sub> H <sub>5</sub> ) <sub>2</sub>	- 8.19	74
SiC <sub>14</sub> H <sub>16</sub> O <sub>2</sub>	(CH <sub>3</sub> ) <sub>2</sub> Si(OC <sub>6</sub> H <sub>5</sub> ) <sub>2</sub>	- 6.1	13
SiC <sub>14</sub> H <sub>16</sub> O <sub>2</sub>	(CH <sub>3</sub> O) <sub>2</sub> Si(C <sub>6</sub> H <sub>5</sub> ) <sub>2</sub>	- 29.4	74
SiC <sub>14</sub> H <sub>30</sub> O <sub>3</sub>	(t-C <sub>4</sub> H <sub>9</sub> O) <sub>3</sub> SiCH=CH <sub>2</sub>	- 59.2	51
SiC <sub>14</sub> H <sub>33</sub> ClNP	(n-C <sub>4</sub> H <sub>9</sub> ) <sub>3</sub> PNSi(CH <sub>3</sub> ) <sub>2</sub> Cl	- 8.24	53
SiC <sub>14</sub> H <sub>33</sub> ClNP	(i-C <sub>4</sub> H <sub>9</sub> ) <sub>3</sub> PNSi(CH <sub>3</sub> ) <sub>2</sub> Cl	- 9.75	53
SiC <sub>14</sub> H <sub>36</sub> N <sub>2</sub> P <sub>2</sub>	[(C <sub>2</sub> H <sub>5</sub> ) <sub>3</sub> PN] <sub>2</sub> Si(CH <sub>3</sub> ) <sub>2</sub>	- 33.79	53
SiC <sub>14</sub> H <sub>36</sub> N <sub>2</sub> P <sub>2</sub>	[(t-C <sub>4</sub> H <sub>9</sub> )(CH <sub>3</sub> ) <sub>2</sub> PN] <sub>2</sub> Si(CH <sub>3</sub> ) <sub>2</sub>	- 32.63	53
SiC <sub>15</sub> H <sub>26</sub>	(CH <sub>3</sub> )(n-C <sub>4</sub> H <sub>9</sub> ) <sub>2</sub> SiC <sub>6</sub> H <sub>5</sub>	- 1.69	32
SiC <sub>15</sub> H <sub>36</sub> NP	(n-C <sub>4</sub> H <sub>9</sub> ) <sub>3</sub> PNSi(CH <sub>3</sub> ) <sub>3</sub>	- 16.08	53
SiC <sub>15</sub> H <sub>36</sub> NP	(i-C <sub>4</sub> H <sub>9</sub> ) <sub>3</sub> PNSi(CH <sub>3</sub> ) <sub>3</sub>	- 16.92	53
SiC <sub>15</sub> H <sub>36</sub> NP	(t-C <sub>4</sub> H <sub>9</sub> ) <sub>3</sub> PNSi(CH <sub>3</sub> ) <sub>3</sub>	- 19.70	53



Empirical formula	Structure	$\delta$	Ref
$\text{SiC}_{16}\text{H}_{12}\text{O}_4$		-56.0	96
$\text{SiC}_{16}\text{H}_{16}\text{O}_4$	$(\text{C}_6\text{H}_5)_2\text{Si}(\text{OCOCH}_3)_2$	29.9	74
$\text{SiC}_{16}\text{H}_{20}\text{O}_2$	$(\text{C}_2\text{H}_5\text{O})_2\text{Si}(\text{C}_6\text{H}_5)_2$	-34.5	4
$\text{SiC}_{16}\text{H}_{26}$	[17] in text (Table V)	-53.2	62
$\text{SiC}_{16}\text{H}_{30}\text{O}_6$	$\text{CH}_3\text{Si}(\text{OCO-t-C}_4\text{H}_9)_3$	-40.8	210
$\text{SiC}_{18}\text{H}_{15}\text{Cl}$	$(\text{C}_6\text{H}_5)_3\text{SiCl}$	1.23	74
$\text{SiC}_{18}\text{H}_{15}\text{F}$	$(\text{C}_6\text{H}_5)_3\text{SiF}$	-4.7	13
$\text{SiC}_{18}\text{H}_{15}\text{N}_3$	$(\text{C}_6\text{H}_5)_3\text{SiN}_3$	-6.5	22
$\text{SiC}_{18}\text{H}_{16}$	$(\text{C}_6\text{H}_5)_3\text{SiH}$	-17.8	74
$\text{SiC}_{18}\text{H}_{16}\text{S}$	$(\text{C}_6\text{H}_5)_3\text{SiSH}$	-3.18	74
$\text{SiC}_{18}\text{H}_{40}$	$(\text{n-C}_6\text{H}_{13})_3\text{SiH}$	-6.71	60
$\text{SiC}_{21}\text{H}_{24}\text{NP}$	$(\text{C}_6\text{H}_5)_3\text{PNSi}(\text{CH}_3)_3$	-11.29	53
$\text{SiC}_{24}\text{H}_{20}$	$(\text{C}_6\text{H}_5)_4\text{Si}$	-15.2	74
$\text{SiC}_{24}\text{H}_{20}\text{O}_4$	$(\text{C}_6\text{H}_5\text{O})_4\text{Si}$	-101.1	13
$\text{SiC}_{26}\text{H}_{60}\text{N}_2\text{P}_2$	$[(\text{n-C}_4\text{H}_9)_3\text{PN}]_2\text{Si}(\text{CH}_3)_2$	-33.96	53
$\text{SiC}_{26}\text{H}_{60}\text{N}_2\text{P}_2$	$[(\text{i-C}_4\text{H}_9)_3\text{PN}]_2\text{Si}(\text{CH}_3)_2$	-37.44	53

Empirical formula	Structure	$\delta_A$	$\delta_B$	$\delta_C$	Ref.
$\text{Si}_2\text{Cl}_5\text{F}$	$\text{Si}^A\text{FCl}_2\text{Si}^B\text{Cl}_3$	-19.8	-3.6		35
$\text{Si}_2\text{Cl}_6$	$(\text{SiCl}_3)_2$	-8.0			57
$\text{Si}_2\text{F}_6$	$(\text{SiF}_3)_2$	-74.6			35
$\text{Si}_2\text{H}_6$	$(\text{SiH}_3)_2$	-104.8			230
$\text{Si}_2\text{C}_4\text{H}_{14}\text{O}$	$[\text{H}(\text{CH}_3)_2\text{Si}]_2\text{O}$	-5.27			60
$\text{Si}_2\text{C}_5\text{H}_{15}\text{Cl}$	$(\text{CH}_3)_3\text{Si}^A\text{Si}^B(\text{CH}_3)_2\text{Cl}$	-18.2	22.8		73
$\text{Si}_2\text{C}_5\text{H}_{15}\text{F}$	$(\text{CH}_3)_3\text{Si}^A\text{Si}^B(\text{CH}_3)_2\text{F}$	-22.5	34.0		73
$\text{Si}_2\text{C}_5\text{H}_{16}$	$(\text{CH}_3)_3\text{Si}^A\text{Si}^B(\text{CH}_3)_2\text{H}$	-18.9	-39.1		73
$\text{Si}_2\text{C}_6\text{H}_{15}\text{N}$	$(\text{CH}_3)_3\text{Si}^A\text{Si}^B(\text{CH}_3)_2\text{CN}$	-18.1	-32.3		74
$\text{Si}_2\text{C}_6\text{H}_{16}$	$(\text{CH}_3)_2\text{Si}^A\text{CH}_2\text{Si}^B(\text{CH}_3)_2\text{CH}_2$	2.73			32
$\text{Si}_2\text{C}_6\text{H}_{16}\text{O}$	$(\text{CH}_3)_2\text{Si}^A\text{OSi}^B(\text{CH}_3)_2\text{CH}_2\text{CH}_2$	23.8			3a
$\text{Si}_2\text{C}_6\text{H}_{17}\text{ClO}$	$(\text{CH}_3)_3\text{Si}^A\text{OSi}^B(\text{CH}_3)_2\text{CH}_2\text{Cl}$	1.84	9.29		32
$\text{Si}_2\text{C}_6\text{H}_{18}$	$[(\text{CH}_3)_3\text{Si}]_2$	-19.58			32
		-19.78			42
$\text{Si}_2\text{C}_6\text{H}_{18}\text{O}$	$[(\text{CH}_3)_3\text{Si}]_2\text{O}$	6.97			5
$\text{Si}_2\text{C}_6\text{H}_{18}\text{O}_4$	$[(\text{CH}_3)(\text{OCH}_3)_2\text{Si}]_2$	-7.5			247
$\text{Si}_2\text{C}_6\text{H}_{18}\text{O}_4\text{S}$	$[(\text{CH}_3)_3\text{Si}]_2\text{SO}_4$	33.7			44
$\text{Si}_2\text{C}_6\text{H}_{18}\text{O}_6$	$[(\text{OCH}_3)_3\text{Si}]_2$	-5.25			247
$\text{Si}_2\text{C}_6\text{H}_{18}\text{S}$	$[(\text{CH}_3)_3\text{Si}]_2\text{S}$	12.8			44
$\text{Si}_2\text{C}_6\text{H}_{19}\text{N}$	$[(\text{CH}_3)_3\text{Si}]_2\text{NH}$	2.2			210
		2.22			42
$\text{Si}_2\text{C}_7\text{H}_{18}\text{N}_2$	$(\text{CH}_3)_3\text{SiN}=\text{C}=\text{NSi}(\text{CH}_3)_3$	-0.8			22
$\text{Si}_2\text{C}_7\text{H}_{18}\text{O}$	$(\text{CH}_3)_3\text{Si}^A\text{OSi}^B(\text{CH}_3)_2\text{CH}=\text{CH}_2$	7.4	-4.8		51
$\text{Si}_2\text{C}_7\text{H}_{19}\text{Cl}$	$(\text{CH}_3)_3\text{Si}^A\text{CH}_2\text{Si}^B(\text{CH}_3)_2\text{CH}_2\text{Cl}$	0.82	3.24		247
$\text{Si}_2\text{C}_7\text{H}_{21}\text{N}$	$[(\text{CH}_3)_3\text{Si}]_2\text{NCH}_3$	6.7			210
$\text{Si}_2\text{C}_7\text{H}_{21}\text{O}_3\text{P}$	$[(\text{CH}_3)_3\text{SiO}]_2\text{P}(\text{O})\text{CH}_3$	21.6			44
$\text{Si}_2\text{C}_7\text{H}_{23}\text{N}_3$	$[(\text{CH}_3)_2(\text{NHCH}_3)\text{Si}]_2\text{NCH}_3$	-3.1			79
$\text{Si}_2\text{C}_8\text{H}_{18}\text{F}_3\text{NO}$	$\text{CF}_3\text{C}[\text{OSi}^A(\text{CH}_3)_3]\text{NSi}^B(\text{CH}_3)_3$	24.48	-2.43		137
$\text{Si}_2\text{C}_8\text{H}_{18}\text{O}$	$[(\text{CH}_3)_2(\text{CH}=\text{CH}_2)\text{Si}]_2\text{O}$	-3.20			247
$\text{Si}_2\text{C}_8\text{H}_{20}\text{O}_2\text{S}$	$(\text{CH}_3)_3\text{Si}^A\text{SCH}_2\text{COOSi}^B(\text{CH}_3)_3$	25.29 <sup>b</sup>	25.39 <sup>b</sup>		137

Empirical formula	Structure	$\delta_A$	$\delta_B$	$\delta_C$	Ref.
$\text{Si}_2\text{C}_8\text{H}_{20}\text{O}_3$	$(\text{CH}_3)_3\text{Si}^{\text{A}}\text{OCH}_2\text{COOSi}^{\text{B}}(\text{CH}_3)_3$	19.66	24.14		137
$\text{Si}_2\text{C}_8\text{H}_{21}\text{NO}$	$\text{CH}_3\text{C}[\text{OSi}^{\text{A}}(\text{CH}_3)_3][\text{NSi}^{\text{B}}(\text{CH}_3)_3]$	16.41	5.74		135
$\text{Si}_2\text{C}_8\text{H}_{22}\text{O}$	$(\text{CH}_3)_3\text{Si}^{\text{A}}\text{CH}_2\text{Si}^{\text{B}}(\text{CH}_3)_2[(\text{CH}_2)_2\text{OH}]$	0.69	-0.06		32
$\text{Si}_2\text{C}_9\text{H}_{22}\text{O}_3$	$(\text{CH}_3)_3\text{Si}^{\text{A}}\text{OSi}^{\text{B}}(\text{CH}_3)_2(\text{CH}_2\text{COOC}_2\text{H}_5)$	—	8.89		247
$\text{Si}_2\text{C}_9\text{H}_{23}\text{NO}_2$	$(\text{CH}_3)_3\text{Si}^{\text{A}}\text{NHCH}(\text{CH}_3)\text{COOSi}^{\text{B}}(\text{CH}_3)_3$	3.02	23.14		137
$\text{Si}_2\text{C}_{10}\text{H}_{18}\text{O}_5$	$[\text{CH}_3\text{Si}(\text{OCOCH}_3)_2]_2\text{O}$	-51.0			247
$\text{Si}_2\text{C}_{10}\text{H}_{24}\text{O}_2$	$(\text{CH}_3)_3\text{Si}^{\text{A}}\text{CH}_2\text{Si}^{\text{B}}(\text{CH}_3)_2(\text{CH}_2\text{COOC}_2\text{H}_5)$	0.57	2.92		32
$\text{Si}_2\text{C}_{10}\text{H}_{26}$	$(\text{CH}_3)_3\text{Si}(\text{CH}_2)_4\text{Si}(\text{CH}_3)_3$	1.41			32
$\text{Si}_2\text{C}_{10}\text{H}_{28}\text{N}_2\text{O}$	$[(\text{CH}_3)_2(\text{NH}-i\text{-C}_3\text{H}_7)\text{Si}]_2\text{O}$	-15.2 to -16.7			74
$\text{Si}_2\text{C}_{10}\text{H}_{30}\text{N}_2\text{P}_2$	$[(\text{CH}_3)_3\text{PNSi}(\text{CH}_3)_2]_2$	-23.42			53
$\text{Si}_2\text{C}_{11}\text{H}_{20}$	$(\text{CH}_3)_3\text{Si}^{\text{A}}\text{Si}^{\text{B}}(\text{CH}_3)_2\text{C}_6\text{H}_5$	-19.3	-21.7		74
$\text{Si}_2\text{C}_{12}\text{H}_{22}$	1,2- $[\text{Si}(\text{CH}_3)_3]_2\text{C}_6\text{H}_4$	-4.1			248
$\text{Si}_2\text{C}_{12}\text{H}_{22}$	1,3- $[\text{Si}(\text{CH}_3)_3]_2\text{C}_6\text{H}_4$	-4.7			248
$\text{Si}_2\text{C}_{12}\text{H}_{22}$	1,4- $[\text{Si}(\text{CH}_3)_3]_2\text{C}_6\text{H}_4$	-4.7			248
$\text{Si}_2\text{C}_{12}\text{H}_{22}\text{O}_2$	1,2- $[\text{OSi}(\text{CH}_3)_3]_2\text{C}_6\text{H}_4$	18.10			133
$\text{Si}_2\text{C}_{13}\text{H}_{22}\text{O}_2$	1,3- $[\text{OSi}(\text{CH}_3)_3]_2\text{C}_6\text{H}_4$	17.87			133
$\text{Si}_2\text{C}_{12}\text{H}_{22}\text{O}_2$	1,4- $[\text{OSi}(\text{CH}_3)_3]_2\text{C}_6\text{H}_4$	17.25			133
$\text{Si}_2\text{C}_{12}\text{H}_{24}$	$(\text{CH}_3)_2\text{SiC}(\text{CH}_3)=\text{C}(\text{CH}_3)\text{Si}(\text{CH}_3)_2\text{C}(\text{CH}_3)=\text{C}(\text{CH}_3)$	-19.0			63
$\text{Si}_2\text{C}_{12}\text{H}_{26}\text{O}_3$	$[(\text{CH}_3)_3\text{Si}(\text{CH}_2)_2\text{CO}]_2\text{O}$	2.56			32
$\text{Si}_2\text{C}_{12}\text{H}_{30}\text{O}$	$[(\text{C}_2\text{H}_5)_3\text{Si}]_2\text{O}$	9.11			32
$\text{Si}_2\text{C}_{14}\text{H}_{26}$	1,4- $[\text{Si}(\text{CH}_3)_3]_2$ -2,5- $(\text{CH}_3)_2\text{C}_6\text{H}_2$	-5.4			248
$\text{Si}_2\text{C}_{14}\text{H}_{36}\text{NP}$	$(m\text{-C}_3\text{H}_7)_3\text{PNSi}^{\text{A}}(\text{CH}_3)_2\text{Si}^{\text{B}}(\text{CH}_3)_3$	-24.67	-23.43		53
$\text{Si}_2\text{C}_{14}\text{H}_{36}\text{NP}$	$(i\text{-C}_3\text{H}_7)_3\text{PNSi}^{\text{A}}(\text{CH}_3)_2\text{Si}^{\text{B}}(\text{CH}_3)_3$	-26.40	-23.06		53
$\text{Si}_2\text{C}_{15}\text{H}_{27}\text{NO}_2$	$(\text{CH}_3)_3\text{Si}^{\text{A}}\text{NHCH}(\text{CH}_2\text{C}_6\text{H}_5)\text{COOSi}^{\text{B}}(\text{CH}_3)_3$	3.68	23.13		137
$\text{Si}_2\text{C}_{16}\text{H}_{30}$	1 <sup>A</sup> ,4 <sup>B</sup> - $[\text{Si}(\text{CH}_3)_3]_2$ -2- $\text{CH}_3$ -5- $i\text{-C}_3\text{H}_7\text{C}_6\text{H}_2$	-5.0	-6.2		248
$\text{Si}_2\text{C}_{16}\text{H}_{42}\text{N}_2\text{P}_2$	$[(\text{C}_2\text{H}_5)_3\text{PNSi}(\text{CH}_3)_2]_2$	-25.18			53
$\text{Si}_2\text{C}_{16}\text{H}_{42}\text{N}_2\text{P}_2$	$[\text{t-C}_4\text{H}_9(\text{CH}_3)_2\text{PNSi}(\text{CH}_3)_2]_2$	-24.07			53
$\text{Si}_2\text{C}_{17}\text{H}_{42}\text{NP}$	$(i\text{-C}_4\text{H}_9)_3\text{PNSi}^{\text{A}}(\text{CH}_3)_2\text{Si}^{\text{B}}(\text{CH}_3)_3$	-25.64	-23.29		53
$\text{Si}_2\text{C}_{21}\text{H}_{24}$	$(\text{C}_6\text{H}_5)_3\text{Si}^{\text{A}}\text{Si}^{\text{B}}(\text{CH}_3)_3$	-20.4	-18.4		73

$\text{Si}_2\text{C}_{21}\text{H}_{24}\text{O}_3$	$(\text{CH}_3\text{O})_3\text{Si}^{\text{A}}\text{Si}^{\text{B}}(\text{C}_6\text{H}_5)_3$	-45.9	-29.2	73
$\text{Si}_2\text{C}_{22}\text{H}_{54}\text{N}_2\text{P}_2$	$[(n\text{-C}_3\text{H}_7)_3\text{PNSi}(\text{CH}_3)_2]_2$	-25.55		53
$\text{Si}_2\text{C}_{22}\text{H}_{54}\text{N}_2\text{P}_2$	$[(i\text{-C}_3\text{H}_7)_3\text{PNSi}(\text{CH}_3)_2]_2$	-27.33		53
$\text{Si}_2\text{C}_{22}\text{H}_{54}\text{N}_2\text{P}_2$	$[(t\text{-C}_4\text{H}_9)_2\text{CH}_3\text{PNSi}(\text{CH}_3)_2]_2$	-26.20		53
$\text{Si}_2\text{C}_{23}\text{H}_{28}$	$(\text{C}_6\text{H}_5)_3\text{Si}^{\text{A}}\text{Si}^{\text{B}}(\text{CH}_3)_2(n\text{-C}_3\text{H}_7)$	-20.6	-11.9	74
$\text{Si}_2\text{C}_{23}\text{H}_{28}$	$(\text{C}_6\text{H}_5)_3\text{Si}^{\text{A}}\text{Si}^{\text{B}}(\text{CH}_3)_2(i\text{-C}_3\text{H}_7)$	-20.4	-17.0	74
$\text{Si}_2\text{C}_{24}\text{H}_{30}$	$(\text{C}_6\text{H}_5)_3\text{Si}^{\text{A}}\text{Si}^{\text{B}}(\text{CH}_3)_2(t\text{-C}_4\text{H}_9)$	-20.4	-8.0	74
$\text{Si}_2\text{C}_{24}\text{H}_{30}\text{O}_3$	$(\text{C}_2\text{H}_5\text{O})_3\text{Si}^{\text{A}}\text{Si}^{\text{B}}(\text{C}_6\text{H}_5)_3$	-50.1	-29.0	74
$\text{Si}_2\text{C}_{26}\text{H}_{26}$	$(\text{C}_6\text{H}_5)_3\text{Si}^{\text{A}}\text{Si}^{\text{B}}(\text{C}_6\text{H}_5)(\text{CH}_3)_2$	-21.4	-21.8	74
$\text{Si}_2\text{C}_{27}\text{H}_{26}$	$(\text{C}_6\text{H}_5)_3\text{Si}^{\text{A}}\text{Si}^{\text{B}}(\text{C}_6\text{H}_5)(\text{CH}_3)(\text{CH}=\text{CH}_2)$	-22.5	-27.5	74
$\text{Si}_2\text{C}_{28}\text{H}_{38}$	$(\text{C}_6\text{H}_5)_3\text{Si}^{\text{A}}\text{Si}^{\text{B}}(\text{CH}_3)_2(n\text{-C}_8\text{H}_{17})$	-20.4	-16.8	74
$\text{Si}_2\text{C}_{28}\text{H}_{66}\text{N}_2\text{P}_2$	$[(n\text{-C}_4\text{H}_9)_3\text{PNSi}(\text{CH}_3)_2]_2$	-25.52		53
$\text{Si}_2\text{C}_{28}\text{H}_{66}\text{N}_2\text{P}_2$	$[(i\text{-C}_4\text{H}_9)_3\text{PNSi}(\text{CH}_3)_2]_2$	-26.54		53
$\text{Si}_3\text{Cl}_8$	$(\text{Cl}_3\text{Si}^{\text{A}})_2\text{Si}^{\text{B}}\text{Cl}_2$	-3.5	-7.2	73
$\text{Si}_3\text{F}_8$	$(\text{F}_3\text{Si}^{\text{A}})_2\text{Si}^{\text{B}}\text{F}_2$	-76.6	-14.4	35
$\text{Si}_3\text{H}_8$	$(\text{H}_3\text{Si}^{\text{A}})_2\text{Si}^{\text{B}}\text{H}_2$		-116.5	230
$\text{Si}_3\text{C}_3\text{Cl}_{12}$	$(\text{Cl}_2\text{SiCCl}_2)_3$	-1.01		68
$\text{Si}_3\text{C}_3\text{HCl}_{11}$	$\text{Si}^{\text{A}}\text{Cl}_2\text{CCl}_2\text{Si}^{\text{A}}\text{Cl}_2\text{CHClSi}^{\text{B}}\text{Cl}_2\text{CCl}_2$	3.29	-1.41	68
$\text{Si}_3\text{C}_3\text{H}_2\text{Cl}_{10}$	$\text{Si}^{\text{A}}\text{Cl}_2\text{CCl}_2\text{Si}^{\text{B}}\text{Cl}_2\text{CCl}_2\text{Si}^{\text{A}}\text{Cl}_2\text{CH}_2$	8.59	-0.91	68
$\text{Si}_3\text{C}_3\text{H}_4\text{Cl}_8$	$\text{Si}^{\text{A}}\text{Cl}_2\text{CH}_2\text{Si}^{\text{B}}\text{Cl}_2\text{CH}_2\text{Si}^{\text{A}}\text{Cl}_2\text{CCl}_2$	9.29	17.39	68
$\text{Si}_3\text{C}_3\text{H}_6\text{Cl}_6$	$(\text{Cl}_2\text{SiCH}_2)_3$	19.49		68
$\text{Si}_3\text{C}_3\text{H}_6\text{Cl}_6$	$(\text{H}_2\text{SiCCl}_2)_3$	-18.41		68
$\text{Si}_3\text{C}_3\text{H}_8\text{Cl}_4$	$\text{Si}^{\text{A}}\text{H}_2\text{CCl}_2\text{Si}^{\text{B}}\text{H}_2\text{CCl}_2\text{Si}^{\text{A}}\text{H}_2\text{CH}_2$	-16.91	-18.11	68
$\text{Si}_3\text{C}_3\text{H}_{10}\text{Cl}_2$	$\text{Si}^{\text{A}}\text{H}_2\text{CH}_2\text{Si}^{\text{B}}\text{H}_2\text{CH}_2\text{Si}^{\text{A}}\text{H}_2\text{CCl}_2$	-16.41	-31.01	68
$\text{Si}_3\text{C}_3\text{H}_{12}$	$(\text{H}_2\text{SiCH}_2)_3$	-39.11		68
$\text{Si}_3\text{C}_6\text{H}_{18}\text{O}_3$	$[(\text{CH}_3)_2\text{SiO}]_3$	-9.12		5
$\text{Si}_3\text{C}_6\text{H}_{21}\text{N}_3$	$[(\text{CH}_3)_2\text{SiNH}]_3$	-4.7		79
$\text{Si}_3\text{C}_6\text{H}_{33}\text{N}_3$	$[(\text{C}_2\text{H}_5)_2\text{SiNH}]_3$	-1.4		79
$\text{Si}_3\text{C}_8\text{H}_{24}$	$[(\text{CH}_3)_3\text{Si}^{\text{A}}]_2\text{Si}^{\text{B}}(\text{CH}_3)_2$	-15.93	-48.45	32
$\text{Si}_3\text{C}_8\text{H}_{24}\text{O}_2$	$[(\text{CH}_3)_3\text{Si}^{\text{A}}\text{O}]_2\text{Si}^{\text{B}}(\text{CH}_3)_2(\text{MDM})$	6.70	-21.50	5
$\text{Si}_3\text{C}_8\text{H}_{26}\text{N}_2$	$[(\text{CH}_3)_3\text{Si}^{\text{A}}\text{NH}]_2\text{Si}^{\text{B}}(\text{CH}_3)_2$	1.80	-6.80	79
$\text{Si}_3\text{C}_9\text{H}_{24}$	$[(\text{CH}_3)_2\text{SiCH}_2]_3$	0.29		68

Empirical formula	Structure	$\delta_A$	$\delta_B$	$\delta_C$	Ref.
$\text{Si}_3\text{C}_9\text{H}_{24}\text{O}_2$	$[(\text{CH}_3)_3\text{Si}^{\text{A}}\text{O}]_2\text{Si}^{\text{B}}(\text{CH}_3)(\text{CH}=\text{CH}_2)$		-35.1		51
$\text{Si}_3\text{C}_9\text{H}_{27}\text{BO}_3$	$[(\text{CH}_3)_3\text{SiO}]_3\text{B}$	12.3			44
$\text{Si}_3\text{C}_9\text{H}_{27}\text{N}$	$[(\text{CH}_3)_3\text{Si}]_3\text{N}$	2.37			43
$\text{Si}_3\text{C}_9\text{H}_{27}\text{N}_3$	$[(\text{CH}_3)(\text{C}_2\text{H}_5)\text{SiNH}]_3$	-14.4			79
$\text{Si}_3\text{C}_9\text{H}_{27}\text{O}_4\text{P}$	$[(\text{CH}_3)_3\text{SiO}]_3\text{P}=\text{O}$	20.0			44
$\text{Si}_3\text{C}_9\text{H}_{27}\text{P}$	$[(\text{CH}_3)_3\text{Si}]_3\text{P}$	0.4			22
$\text{Si}_3\text{C}_{10}\text{H}_{22}$	$(\text{CH}_3)_3\text{Si}^{\text{A}}\text{C}=\text{C}[\text{Si}^{\text{A}}(\text{CH}_3)_3]\text{Si}^{\text{B}}(\text{CH}_3)_2$	-8.5	-106.2		63
$\text{Si}_3\text{C}_{10}\text{H}_{28}$	$[(\text{CH}_3)_3\text{Si}^{\text{A}}\text{CH}_2]_2\text{Si}^{\text{B}}(\text{CH}_3)_2$	-0.83	0.35		32
$\text{Si}_3\text{C}_{10}\text{H}_{30}\text{N}_2$	$[(\text{CH}_3)_3\text{Si}^{\text{A}}\text{NH}]_2\text{Si}^{\text{B}}(\text{C}_2\text{H}_5)_2$	1.90	-3.50		79
$\text{Si}_3\text{C}_{11}\text{H}_{29}\text{NO}_2$	$[(\text{CH}_3)_3\text{Si}^{\text{A}}]_2\text{NCH}_2\text{COOSi}^{\text{B}}(\text{CH}_3)_3$	8.19	22.78		137
$\text{Si}_3\text{C}_{11}\text{H}_{30}\text{O}$	$[(\text{CH}_3)_3\text{Si}^{\text{A}}\text{CH}_2]_2\text{Si}^{\text{B}}(\text{CH}_3)(\text{C}_2\text{H}_4\text{OH})$	0.54	0.25		32
$\text{Si}_3\text{C}_{11}\text{H}_{32}\text{N}_2$	$[(\text{CH}_3)_3\text{Si}^{\text{A}}\text{NH}]_2\text{Si}^{\text{B}}(\text{CH}_3)(\text{C}_4\text{H}_9)$	1.3	-7.20		79
$\text{Si}_3\text{C}_{12}\text{H}_{31}\text{NO}_3$	$(\text{CH}_3)_3\text{Si}^{\text{A}}\text{NHCH}[\text{CH}_2\text{OSi}^{\text{B}}(\text{CH}_3)_3]\text{COOSi}^{\text{C}}(\text{CH}_3)_3$	4.03	17.45	23.01	137
$\text{Si}_3\text{C}_{13}\text{H}_{28}\text{N}_2$	$[(\text{CH}_3)_3\text{Si}^{\text{A}}\text{NH}]_2\text{Si}^{\text{B}}(\text{CH}_3)(\text{C}_6\text{H}_5)$	2.5	-15.0		79
$\text{Si}_3\text{C}_{13}\text{H}_{32}\text{O}_2$	$[(\text{CH}_3)_3\text{Si}^{\text{A}}\text{CH}_2]_2\text{Si}^{\text{B}}(\text{CH}_3)(\text{CH}_2\text{COOC}_2\text{H}_5)$	0.46	2.89		247
$\text{Si}_3\text{C}_{13}\text{H}_{33}\text{NO}_3$	$(\text{CH}_3)_3\text{Si}^{\text{A}}\text{NHCH}[\text{CH}(\text{CH}_3)\text{OSi}^{\text{B}}(\text{CH}_3)_3]\text{COOSi}^{\text{C}}(\text{CH}_3)_3$	4.13	15.12	22.39	137
$\text{Si}_3\text{C}_{15}\text{H}_{30}$	$1^{\text{A}}, 2^{\text{B}}, 4^{\text{C}} - [\text{Si}(\text{CH}_3)_3]_3\text{C}_6\text{H}_3$	3.6	4.1	4.6	248
$\text{Si}_3\text{C}_{18}\text{H}_{30}\text{N}_2$	$[(\text{CH}_3)_3\text{Si}^{\text{A}}\text{NH}]_2\text{Si}^{\text{B}}(\text{C}_6\text{H}_5)_2$	3.2	-24.2		79
$\text{Si}_3\text{C}_{36}\text{H}_{30}\text{O}_3$	$[(\text{C}_6\text{H}_5)_2\text{SiO}]_3$	-33.8			74
$\text{Si}_3\text{C}_{38}\text{H}_{36}$	$[(\text{C}_6\text{H}_5)_3\text{Si}^{\text{A}}]_2\text{Si}^{\text{B}}(\text{CH}_3)_2$	-17.0	-45.9		74
$\text{Si}_3\text{C}_{40}\text{H}_{38}$	$[(\text{C}_6\text{H}_5)_3\text{Si}^{\text{A}}]_2\text{Si}^{\text{B}}(\text{CH}_2)_3\text{CH}_2$	-16.8	-34.8		74
$\text{Si}_3\text{C}_{41}\text{H}_{40}$	$[(\text{C}_6\text{H}_5)_3\text{Si}^{\text{A}}]_2\text{Si}^{\text{B}}(\text{CH}_2)_4\text{CH}_2$	-18.4	-48.6		74
$\text{Si}_4\text{H}_{10}$	$(\text{Si}^{\text{A}}\text{H}_3)_3\text{Si}^{\text{B}}\text{H}$	—	-96.0		230
$\text{Si}_4\text{C}_8\text{H}_{24}\text{O}_4$	$[(\text{CH}_3)_2\text{SiO}]_4 (\text{D}_4)$	-19.51			5
$\text{Si}_4\text{C}_8\text{H}_{28}\text{N}_4$	$[(\text{CH}_3)_2\text{SiNH}]_4$	-8.2			79
$\text{Si}_4\text{C}_{10}\text{H}_{27}\text{Cl}_3\text{O}_3$	$[(\text{CH}_3)_3\text{Si}^{\text{A}}\text{O}]_3\text{Si}^{\text{B}}\text{CCl}_3$	12.67	-94.15		75
$\text{Si}_4\text{C}_{10}\text{H}_{28}\text{Cl}_2\text{O}_3$	$[(\text{CH}_3)_3\text{Si}^{\text{A}}\text{O}]_3\text{Si}^{\text{B}}\text{CHCl}_2$	11.41	-86.78		75

Si <sub>4</sub> C <sub>10</sub> H <sub>29</sub> ClO <sub>3</sub>	[(CH <sub>3</sub> ) <sub>3</sub> Si <sup>A</sup> O] <sub>3</sub> Si <sup>B</sup> CH <sub>2</sub> Cl	9·85	– 76·78		75
Si <sub>4</sub> C <sub>10</sub> H <sub>30</sub> O	[(CH <sub>3</sub> ) <sub>3</sub> Si <sup>A</sup> (CH <sub>3</sub> ) <sub>2</sub> Si <sup>B</sup> ] <sub>2</sub> O	– 23·1	5·2		75
Si <sub>4</sub> C <sub>10</sub> H <sub>30</sub> O <sub>3</sub>	[(CH <sub>3</sub> ) <sub>3</sub> Si <sup>A</sup> O] <sub>3</sub> Si <sup>B</sup> CH <sub>3</sub>	7·07	– 64·43		75
Si <sub>4</sub> C <sub>10</sub> H <sub>30</sub> O <sub>3</sub>	[(CH <sub>3</sub> ) <sub>3</sub> Si <sup>A</sup> O][(CH <sub>3</sub> ) <sub>2</sub> Si <sup>B</sup> O] <sub>2</sub> Si(CH <sub>3</sub> ) <sub>3</sub> (MD <sub>2</sub> M)	6·8	– 22·0		5
Si <sub>4</sub> C <sub>10</sub> H <sub>31</sub> N	[(CH <sub>3</sub> ) <sub>3</sub> Si <sup>A</sup> Si <sup>B</sup> (CH <sub>3</sub> ) <sub>2</sub> ] <sub>2</sub> NH	– 22·0	– 5·4		73
Si <sub>4</sub> C <sub>11</sub> H <sub>30</sub> O <sub>3</sub>	[(CH <sub>3</sub> ) <sub>3</sub> Si <sup>A</sup> O] <sub>3</sub> Si <sup>B</sup> CH=CH <sub>2</sub>	7·2	– 79·4		51
Si <sub>4</sub> C <sub>11</sub> H <sub>32</sub> O <sub>3</sub>	[(CH <sub>3</sub> ) <sub>3</sub> Si <sup>A</sup> O] <sub>3</sub> Si <sup>B</sup> CH <sub>2</sub> CH <sub>3</sub>	7·03	– 64·44		75
Si <sub>4</sub> C <sub>12</sub> H <sub>24</sub> O <sub>4</sub>	[(CH=CH <sub>2</sub> )(CH <sub>3</sub> SiO) <sub>4</sub>	– 32·48			5
Si <sub>4</sub> C <sub>12</sub> H <sub>33</sub> ClO <sub>3</sub>	[(CH <sub>3</sub> ) <sub>3</sub> Si <sup>A</sup> O] <sub>3</sub> Si <sup>B</sup> (CH <sub>2</sub> ) <sub>3</sub> Cl	7·85	– 66·38		75
Si <sub>4</sub> C <sub>12</sub> H <sub>36</sub> N <sub>4</sub>	[(CH <sub>3</sub> )(C <sub>2</sub> H <sub>5</sub> )SiNH] <sub>4</sub>	– 5·6			79
Si <sub>4</sub> C <sub>13</sub> H <sub>36</sub> O <sub>3</sub>	[(CH <sub>3</sub> ) <sub>3</sub> SiO] <sub>3</sub> SiC(CH <sub>3</sub> ) <sub>3</sub>	6·95	– 65·10		75
Si <sub>4</sub> C <sub>15</sub> H <sub>32</sub> O <sub>3</sub>	[(CH <sub>3</sub> ) <sub>3</sub> SiO] <sub>3</sub> SiC <sub>6</sub> H <sub>5</sub>	8·48	– 77·32		75
Si <sub>4</sub> C <sub>18</sub> H <sub>38</sub>	1,2,4,5- [Si(CH <sub>3</sub> ) <sub>3</sub> ] <sub>4</sub> C <sub>6</sub> H <sub>2</sub>	– 3·4			248
Si <sub>4</sub> C <sub>48</sub> H <sub>40</sub> O <sub>4</sub>	[(C <sub>6</sub> H <sub>5</sub> ) <sub>2</sub> SiO] <sub>4</sub> (D <sup>Ph</sup> <sub>4</sub> )	– 42·9			74
Si <sub>5</sub> Cl <sub>12</sub>	(Cl <sub>3</sub> Si <sup>A</sup> ) <sub>4</sub> Si <sup>B</sup>	3·5	– 80·0		73
Si <sub>5</sub> H <sub>12</sub>	(H <sub>3</sub> Si <sup>A</sup> ) <sub>4</sub> Si <sup>B</sup>		– 112·0		230
Si <sub>5</sub> C <sub>10</sub> H <sub>30</sub> O <sub>5</sub>	[(CH <sub>3</sub> ) <sub>2</sub> SiO] <sub>5</sub> (D <sub>5</sub> )	– 21·93			5
Si <sub>5</sub> C <sub>12</sub> H <sub>36</sub>	[(CH <sub>3</sub> ) <sub>3</sub> Si <sup>A</sup> ] <sub>4</sub> Si <sup>B</sup>	– 9·82	– 135·5		73
Si <sub>5</sub> C <sub>12</sub> H <sub>36</sub> O <sub>4</sub>	[(CH <sub>3</sub> ) <sub>3</sub> Si <sup>A</sup> O] <sub>4</sub> Si <sup>B</sup>	8·6	– 104·2		87
Si <sub>5</sub> C <sub>12</sub> H <sub>36</sub> O <sub>4</sub>	(CH <sub>3</sub> ) <sub>3</sub> SiO[(CH <sub>3</sub> ) <sub>2</sub> SiO] <sub>3</sub> Si(CH <sub>3</sub> ) <sub>3</sub> (MD <sub>3</sub> M)	6·9 (M)	– 21·8 (D <sup>1</sup> )	– 22·6 (D <sup>2</sup> )	5
Si <sub>6</sub> C <sub>12</sub> H <sub>36</sub> O <sub>6</sub>	[(CH <sub>3</sub> ) <sub>2</sub> SiO] <sub>6</sub> (D <sub>6</sub> )	– 22·48			5
Si <sub>6</sub> C <sub>14</sub> H <sub>42</sub> O <sub>5</sub>	(CH <sub>3</sub> ) <sub>3</sub> SiO[(CH <sub>3</sub> ) <sub>2</sub> SiO] <sub>4</sub> Si(CH <sub>3</sub> ) <sub>3</sub> (MD <sub>4</sub> M)	7·0 (M)	– 21·8 (D <sup>1</sup> )	– 23·4 (D <sup>2</sup> )	5
Si <sub>7</sub> C <sub>16</sub> H <sub>48</sub> O <sub>6</sub>	(CH <sub>3</sub> ) <sub>3</sub> SiO[(CH <sub>3</sub> ) <sub>2</sub> SiO] <sub>5</sub> Si(CH <sub>3</sub> ) <sub>3</sub> (MD <sub>5</sub> M)	7·0 (M)	– 21·8 (D <sup>1</sup> )	– 22·4 (D <sup>2</sup> )	5
Si <sub>8</sub> C <sub>18</sub> H <sub>54</sub> O <sub>7</sub>	(CH <sub>3</sub> ) <sub>3</sub> SiO[(CH <sub>3</sub> ) <sub>2</sub> SiO] <sub>6</sub> Si(CH <sub>3</sub> ) <sub>3</sub> (MD <sub>6</sub> M)	7·0 (M)	– 21·8 (D <sup>1</sup> )	– 22·3 (D <sup>3</sup> )	5

<sup>a</sup> Chemical shifts are given in ppm relative to Me<sub>4</sub>Si. Positive values to high frequency. Solvents were not specified except in a few cases where solvent shifts are known to be substantial.

<sup>b</sup> Values may be reversed.

<sup>c</sup> Peak to low frequency not observed.

### Acknowledgements

The authors thank Dr. J. Cella for providing the data used in the section on extracoordinate silicon compounds, and Dr. R. Grinter for providing the results of ref. 143 prior to publication. They also thank Ms. C. Joynson for collecting the data and references for the Appendix and placing the information in tabular form, and Dr. R. E. Joynson for writing the program to sort the data according to empirical formula. The authors also acknowledge the very helpful comments of Dr. J. Schraml.

### REFERENCES

1. R. R. Ernst and W. A. Anderson, *Rev. Sci. Instr.*, 1966, **37**, 93.
2. (a) R. Freeman, K. G. R. Pachler and G. N. LaMar, *J. Chem. Phys.*, 1971, **55**, 4586.  
(b) O. A. Gansow, A. R. Burke and W. D. Vernon, *J. Amer. Chem. Soc.*, 1972, **94**, 2550.
3. (a) P. C. Lauterbur, "Determination of Organic Structure by Physical Methods", Vol. 2, F. C. Nachod and W. D. Phillips (eds.), Academic Press, New York, 1970. (b) G. R. Holzman, P. C. Lauterbur, J. H. Anderson and W. Koth, *J. Chem. Phys.*, 1956, **25**, 172.
4. B. K. Hunter and L. W. Reeves, *Canad. J. Chem.*, 1968, **46**, 1399.
5. G. C. Levy and J. D. Cargioli,  $^{29}\text{Si}$  Fourier Transform NMR, in "Nuclear Magnetic Resonance Spectroscopy of Nuclei Other than Protons", T. Axenrod and G. A. Webb (eds.), Wiley, New York, 1974, p. 251.
6. J. Schraml and J. M. Bellama,  $^{29}\text{Si}$  Nuclear Magnetic Resonance, in "Determination of Organic Structure by Physical Methods", Vol. 6, F. C. Nachod, J. J. Zuckerman and E. W. Randall (eds.), Academic Press, New York, 1976, p. 203.
7. A. Saika and C. P. Slichter, *J. Chem. Phys.*, 1954, **22**, 26.
8. W. E. Lamb, Jr., *Phys. Rev.*, 1941, **60**, 817.
9. C. J. Jameson and H. S. Gutowsky, *J. Chem. Phys.*, 1964, **40**, 1714.
10. J. Mason, *J. Chem. Soc. (A)*, 1971, 1038.
11. C. R. Ernst, L. Spialter, G. R. Buell and D. L. Wilhite, *J. Amer. Chem. Soc.*, 1974, **96**, 5375.
12. J. H. Letcher and J. R. Van Wazer, *J. Chem. Phys.*, 1966, **44**, 815; 1966, **45**, 2916, 2926.
13. G. Engelhardt, R. Radeaglia, H. Jancke, E. Lippmaa and M. Mägi, *Org. Magn. Resonance*, 1973, **5**, 561.
14. R. Radeaglia and G. Engelhardt, *J. Organometal. Chem.*, 1974, **67**, C45.
15. R. Wolff and R. Radeaglia, *Z. Phys. Chem.*, (Leipzig), 1976, **257**, 181.
16. R. Wolff and R. Radeaglia, *Z. Phys. Chem.*, (Leipzig), 1977, **258**, 145.
17. E. V. van den Berghe and G. P. van der Kelen, *J. Organometal. Chem.*, 1973, **59**, 175.
18. R. Wolff and R. Radeaglia, *Org. Magn. Resonance*, 1977, **9**, 64.
19. V. S. Lyubimov and S. P. Ionov, *Russ. J. Phys. Chem.*, 1972, **46**, 486.
20. R. Radeaglia, *Z. Phys. Chem.*, (Leipzig), 1975, **256**, 453.
21. E. D. Becker, in "Nuclear Magnetic Resonance Spectroscopy of Nuclei Other than Protons", T. Axenrod and G. A. Webb (eds.), Wiley, New York, 1974, p. 1.
22. H. C. Marsmann, *Chem. Z.*, 1972, **96**, 5.
23. H. G. Horn and H. C. Marsmann, *Makromol. Chem.*, 1972, **162**, 255.
24. W. McFarlane and J. M. Seaby, *J. Chem. Soc., Perkin II*, 1972, 1561.
25. M. G. Gibby, A. Pines and J. S. Waugh, *J. Amer. Chem. Soc.*, 1972, **94**, 6231.
26. G. Engelhardt, R. Radeaglia, H. Janke, E. Lippmaa and M. Mägi, *Org. Magn. Resonance*, 1973, **5**, 561.
27. H. C. Marsmann, *Chem. Z.*, 1973, **97**, 128.

28. G. Engelhardt, M. Mägi and E. Lippmaa, *J. Organometal. Chem.*, 1973, **54**, 115.
29. E. V. van den Berghe and G. P. van der Kelen, *J. Organometal. Chem.*, 1973, **59**, 175.
30. R. K. Harris and B. J. Kimber, *J. Organometal. Chem.*, 1974, **70**, 43.
31. E. Lippmaa, M. Mägi, G. Engelhardt, H. Jancke V. Chvalovsky and J. Schraml, *Coll. Czech. Chem. Comm.*, 1974, **39**, 1041.
32. R. G. Scholl, G. E. Maciel and W. K. Musker, *J. Amer. Chem. Soc.*, 1972, **94**, 6376.
33. G. C. Levy, J. D. Cargioli, G. E. Maciel, J. J. Natterstad, E. B. Whipple and M. Ruta, *J. Magn. Resonance*, 1973, **11**, 352.
34. R. B. Johannesen, *J. Chem. Phys.*, 1967, **47**, 955.
35. R. B. Johannesen, F. E. Brinckman and T. D. Coyle, *J. Phys. Chem.*, 1968, **72**, 660.
36. M. Bacon, G. E. Maciel, W. K. Musker and R. Scholl, *J. Amer. Chem. Soc.*, 1971, **93**, 2537.
37. G. C. Levy and J. D. Cargioli, *J. Magn. Resonance*, 1972, **6**, 143.
38. G. C. Levy, J. D. Cargioli, P. C. Juliano and T. D. Mitchell, *J. Amer. Chem. Soc.*, 1973, **95**, 3445.
39. G. C. Levy, J. D. Cargioli, P. C. Juliano and T. D. Mitchell, *J. Magn. Resonance*, 1972, **8**, 399.
40. G. C. Levy and J. D. Cargioli, *J. Magn. Resonance*, 1973, **10**, 231.
41. G. C. Levy, *J. Amer. Chem. Soc.*, 1972, **94**, 4793.
42. R. K. Harris and B. J. Kimber, *J. Magn. Resonance*, 1975, **17**, 174.
43. R. K. Harris and B. Lemarié, *J. Magn. Resonance*, 1976, **23**, 371.
44. H. C. Marsmann and H. G. Horn, *Z. Naturforsch.*, 1972, **27b**, 1448.
45. C. G. Pitt, *J. Organometal. Chem.*, 1973, **61**, 49.
46. E. V. van den Berghe and G. P. van der Kelen, *J. Organometal. Chem.*, 1976, **122**, 329.
47. J. Schraml, J. Pola, V. Chvalovský, M. Mägi and E. Lippmaa, *J. Organometal. Chem.*, 1973, **49**, C19.
48. J. Schraml, J. Včelák, and V. Chvalovský, *Coll. Czech Chem. Comm.*, 1974, **39**, 267.
49. N. D. Chuy, V. Chvalovský, J. Schraml, M. Mägi and E. Lippmaa, *Coll. Czech. Chem. Comm.*, 1975, **40**, 875.
50. J. Schraml, J. Včelák, G. Engelhardt and V. Chvalovský, *Coll. Czech. Chem. Comm.*, 1976, **41**, 3758.
51. J. Schraml, V. Chvalovský, M. Mägi and E. Lippmaa, *Coll. Czech. Chem. Comm.*, 1977, **42**, 306.
52. J. Schraml, N. D. Chuy, V. Chvalovský, M. Mägi and E. Lippmaa, *Org. Magn. Resonance*, 1975, **7**, 379.
53. W. Buchner and W. Wolfsberger, *Z. Naturforsch.*, 1977, **32b**, 967.
54. C. R. Ernst, L. Spialter, G. R. Buell and D. L. Wilhite, *J. Organometal. Chem.*, 1973, **59**, C13.
55. C. R. Ernst, L. Spialter, G. R. Buell and D. L. Wilhite, *J. Amer. Chem. Soc.*, 1974, **96**, 5375.
56. J. Schraml, P. Koehler, K. Licht and G. Engelhardt, *J. Organometal. Chem.*, 1976, **121**, C1.
57. U. Niemann and H. C. Marsmann, *Z. Naturforsch.*, 1975, **30b**, 202.
58. H. C. Marsmann and H. G. Horn, *Chem. Z.*, 1972, **96**, 456.
59. G. C. Levy and G. L. Nelson, "Carbon-13 Nuclear Magnetic Resonance for Organic Chemists", Wiley-Interscience, New York, 1972, p. 52.
60. R. K. Harris and B. J. Kimber, *Adv. Mol. Relax. Proc.*, 1976, **8**, 15.
61. D. M. Grant and E. G. Paul, *J. Amer. Chem. Soc.*, 1964, **86**, 2984.
62. R. L. Lambert, Jr. and D. Seyferth, *J. Amer. Chem. Soc.*, 1972, **94**, 9246.
63. D. Seyferth, D. C. Annarelli and S. C. Vick, *J. Amer. Chem. Soc.*, 1976, **98**, 6382.
64. D. Seyferth and D. C. Annarelli, *J. Amer. Chem. Soc.*, 1975, **97**, 2273.
65. D. Seyferth and D. C. Annarelli, *J. Organometal. Chem.*, 1976, **117**, C51.
66. F. Duboudin, G. Bourgeois, A. Faucher and P. Mazerolles, *J. Organometal. Chem.*, 1977, **133**, 29.
67. G. Fritz and P. Böttinger, *Z. Anorg. Allg. Chem.*, 1973, **395**, 159.



68. G. Fritz and N. Braunagel, *Z. Anorg. Allg. Chem.*, 1973, **399**, 280.
69. G. Fritz, H. Fröhlich and D. Kummer, *Z. Anorg. Allg. Chem.*, 1967, **353**, 34.
70. G. Fritz and M. Hähnke, *Z. Anorg. Allg. Chem.*, 1972, **390**, 137, 157.
71. M. L. Filleux-Blanchard, N. Dinh-An and G. Manuel, *Org. Magn. Resonance*, 1978, **11**, 150.
72. J. J. Burke and P. C. Lauterbur, *J. Amer. Chem. Soc.*, 1964, **86**, 1870.
73. K. G. Sharp, P. A. Sutor, E. A. Williams, J. D. Cargioli, T. C. Farrar and K. Ishibitsu, *J. Amer. Chem. Soc.*, 1976, **98**, 1977.
74. E. A. Williams and J. D. Cargioli, unpublished results, 1978.
75. G. Engelhardt, H. Jancke, R. Radeaglia, H. Kriegsmann, M. F. Larin, V. A. Pestunovich, E. I. Dubinskaja and M. Voronkov, *Z. Chem.*, 1977, **17**, 376.
76. J. B. Stothers, "Carbon-13 NMR Spectroscopy", Academic Press, New York, 1972, pp. 55-58.
77. A. L. Smith, "Analysis of Silicones", Wiley-Interscience, New York, 1974, p. 4.
78. G. Engelhardt, H. Jancke, M. Mägi, T. J. Pehk and E. Lippmaa, *J. Organometal. Chem.*, 1971, **28**, 293.
79. H. Jancke, G. Engelhardt, M. Mägi and E. Lippmaa, *Z. Chem.*, 1973, **13**, 435.
80. H. Jancke, G. Engelhardt, M. Mägi and E. Lippmaa, *Z. Chem.*, 1973, **13**, 392.
81. R. K. Harris and B. J. Kimber, (a) *Chem. Comm.*; (b) *Appl. Spectroscopy Rev.*, 1975, **10**, 117.
82. G. Engelhardt and H. Jancke, *Z. Chem.*, 1974, **14**, 206.
83. E. A. Williams, J. D. Cargioli and R. W. LaRochelle, *J. Organometal. Chem.*, 1976, **108**, 153.
84. R. K. Harris, B. J. Kimber, M. D. Wood and A. Holt, *J. Organometal. Chem.*, 1976, **116**, 291.
85. E. A. Williams, J. D. Cargioli and S. Y. Hobbs, *Macromolecules*, 1977, **10**, 782.
86. E. Lippmaa, M. A. Alla, T. J. Pehk and G. Engelhardt, *J. Amer. Chem. Soc.*, 1978, **100**, 1929.
87. R. K. Harris and R. H. Newman, *Org. Magn. Resonance*, 1977, **9**, 426.
88. D. Hoebbel, G. Garzo, G. Engelhardt, H. Jancke, P. Franke and W. Wiekler, *Z. Anorg. Allg. Chem.*, 1976, **424**, 115.
89. R. W. LaRochelle, J. D. Cargioli and E. A. Williams, *Macromolecules*, 1976, **9**, 85.
90. D. F. Wilcock, *J. Amer. Chem. Soc.*, 1946, **68**, 691.
91. M. J. Hunter, E. L. Warrick, J. F. Hyde and C. C. Currie, *J. Amer. Chem. Soc.*, 1946, **68**, 2284.
92. T. G. Fox and P. J. Flory, (a) *J. Phys. Chem.*, 1951, **55**, 221; (b) *J. Polymer Sci.*, 1954, **14**, 315.
93. G. Engelhardt, D. Zeigan, H. Jancke, D. Hoebbel and W. Wiekler, *Z. Anorg. Allg. Chem.*, 1975, **418**, 17.
94. V. A. Pestunovich, M. F. Larin, M. G. Voronkov, G. Engelhardt, H. Jancke, V. P. Mileshekevich and Y. A. Yuzhelevski, *Zh. Strukt. Khim.*, 1977, **18**, 578.
95. V. P. Mileshekevich, V. O. Reikhsfeld, A. I. Suprunenko, V. A. Pestunovich, M. F. Larin and M. G. Voronkov, *Dokl. Akad. Nauk SSSR*, 1976, **231**, 1134.
96. M. Mägi, E. Lippmaa, E. Lukevics and N. P. Ercak, *Org. Magn. Resonance*, 1977, **9**, 297.
97. H. C. Marsmann, *Z. Naturforsch.*, 1974, **29b**, 495.
98. R. O. Gould, B. M. Lowe and N. A. MacGilp, *Chem. Comm.*, 1974, 720.
99. G. Engelhardt, W. Altenburg, D. Hoebbel and W. Wiekler, *Z. Anorg. Allg. Chem.*, 1977, **428**, 43.
100. G. Engelhardt, W. Altenburg, D. Hoebbel and W. Wiekler, *Z. Anorg. Allg. Chem.*, 1977, **437**, 249.
101. B. D. Mosel, W. Muller-Warmuth and H. Dutz, *Phys. Chem. Glasses*, 1974, **15**, 154.
102. R. K. Harris and R. H. Newman, *J. Chem. Soc., Faraday*, 1977, **73**, 9, 1204.
103. G. Engelhardt, H. Jancke, D. Hoebbel and W. Wiekler, *Z. Chem.*, 1974, **14**, 109.
104. R. K. Iler, "The Colloid Chemistry of Silica and Silicates", **26**, Cornell University Press, Ithaca, New York, 1955.
105. D. Fortnum and J. O. Edwards, *J. Inorg. Nuclear Chem.*, 1956, **2**, 264.
106. J. E. Earley, D. Fortnum, A. Wojcicki and J. O. Edwards, *J. Amer. Chem. Soc.*, 1959, **81**, 1295.
107. E. Freund, *Bull. Soc. Chim. France*, 1973, 2238.
108. C. W. Lentz, *Inorg. Chem.*, 1964, **3**, 574.

109. J. W. Turley and F. B. Boer, *J. Amer. Chem. Soc.*, 1968, **90**, 4026.
110. L. Párkányi, K. Simon and J. Nagy, *Acta Cryst. (B)*, 1974, **30**, 2328.
111. L. Párkányi, J. Nagy and K. Simon, *J. Organometal. Chem.*, 1975, **101**, 11.
112. R. K. Harris, J. Jones and S. Ng, *J. Magn. Resonance*, 1978, **30**, 521.
113. V. A. Pestunovich, S. N. Tandura, M. G. Voronkov, V. P. Baryshok, G. I. Zelchan, V. I. Glukhikh, G. Engelhardt and M. Witanowski, *Spectros. Lett.*, 1978, **11**, 339.
114. V. A. Pestunovich, S. N. Tandura, M. G. Voronkov, G. Engelhardt, E. Lippmaa, T. Pehk, V. F. Sidorkin, G. I. Zelchan, V. P. Baryshok, *Dokl. Akad. Nauk SSSR*, 1978, **240**, 914.
115. T. Pehk, E. Lippmaa, E. Lukevics and L. I. Simchenko, *J. Gen. Chem. (U.S.S.R.)*, 1976, **46**, 600.
116. S. N. Tandura, V. A. Pestunovich, M. G. Voronkov, G. Zelchan, I. I. Solomennikova and E. Lukevics, *Khim. Geterotsikl. Soedin.*, 1977, 1063.
117. C. L. Frye, *J. Amer. Chem. Soc.*, 1964, **86**, 3170.
118. British Pat. 1,208,908, October 1970.
119. W. Diltthey, *Annalen*, 1906, 344, 300.
120. G. Schott, H. U. Kibbel and W. Hildebrandt, *Z. Anorg. Allg. Chem.*, 1969, **371**, 81.
121. E. L. Muetterties and C. M. Wright, *J. Amer. Chem. Soc.*, 1964, **86**, 5132.
122. G. Schott and K. Golz, *Z. Anorg. Allg. Chem.*, 1971, **383**, 314.
123. R. M. Pike and R. R. Luongo, *J. Amer. Chem. Soc.*, 1965, **87**, 1403.
124. L. H. Sommer, "Stereochemistry, Mechanism and Silicon", McGraw-Hill, 1965, Ch. 1, pp. 4-24.
125. J. A. Cella, unpublished results, 1978.
126. R. K. Harris, private communication.
127. J. A. Cella and J. D. Cargioli, unpublished results, 1978.
128. H. C. Marsmann and R. Löwer, *Chem. Z.*, 1973, **97**, 660.
129. M. R. Bacon and G. E. Maciel, *J. Amer. Chem. Soc.*, 1973, **95**, 2413.
130. V. Gutmann, *Chem. Brit.*, 1971, 7, 102.
131. J. F. Hampton, C. W. Lacefield and J. F. Hyde, *Inorg. Chem.*, 1965, **4**, 1659.
132. G. Engelhardt and J. Schraml, *Org. Magn. Resonance*, 1977, **9**, 239.
133. J. Schraml, V. Chvalovský, H. Jancke and G. Engelhardt, *Org. Magn. Resonance*, 1977, **9**, 237.
134. E. Lippmaa, M. Mägi, V. Chvalovský and J. Schraml, *Coll. Czech. Chem. Comm.*, 1977, **42**, 318.
135. H. Jancke, G. Engelhardt, S. Wagner, W. Dirnens, G. Herzog, E. Thieme and K. Ruhlmann, *J. Organometal. Chem.*, 1977, **134**, 21.
136. B. Heinz, H. C. Marsmann and U. Niemann, *Z. Naturforsch.*, 1977, **32b**, 163.
137. J. Schraml, J. Pola, V. Chvalovský, H. C. Marsmann and K. Bláha, *Coll. Czech. Chem. Comm.*, 1977, **42**, 1165 and references therein.
138. A. H. Haines, R. K. Harris and R. C. Rao, *Org. Magn. Resonance*, 1977, **9**, 432.
139. D. J. Gale, A. H. Haines and R. K. Harris, *Org. Magn. Resonance*, 1975, **7**, 635.
140. J. Schraml, J. Pola, H. Jancke, G. Engelhardt, M. Černý and V. Chvalovský, *Coll. Czech. Chem. Comm.*, 1976, **41**, 360.
141. L. Riesel, A. Clausnitzer and C. Ruby, *Z. Anorg. Allg. Chem.*, 1977, **433**, 200.
142. N. F. Ramsey and E. M. Purcell, *Phys. Rev.*, 1952, **85**, 143.
143. M. D. Beer and R. Grinter, *J. Magn. Resonance*, 1978, **31**, 187.
144. E. R. Malinowski, *J. Amer. Chem. Soc.*, 1961, **83**, 4479.
145. E. A. V. Ebsworth and J. J. Turner, *J. Chem. Phys.*, 1962, **36**, 2628.
146. C. Juan and H. S. Gutowsky, *J. Chem. Phys.*, 1962, **37**, 2198.
147. H. J. Campbell-Ferguson, E. A. V. Ebsworth, A. G. MacDiarmid and T. Yoshioka, *J. Phys. Chem.*, 1967, **71**, 723.
148. E. O. Bishop and M. A. Jensen, *Chem. Comm.*, 1966, 922.

149. E. P. Malinowski and T. Vladimiroff, *J. Amer. Chem. Soc.*, 1969, **86**, 3575.
150. R. Ditchfield, M. A. Jensen and J. N. Murrell, *J. Chem. Soc. (A)*, 1967, 1674.
151. J. A. Pople and D. P. Santry, *Mol. Phys.*, 1964, **8**, 1; 1965, **9**, 311.
152. M. A. Jensen, *J. Organometal. Chem.*, 1968, **11**, 423.
153. J. E. Drake and N. Goddard, *J. Chem. Soc. (A)*, 1970, 2587.
154. A. Rastelli and S. A. Pozzoli, *J. Mol. Struct.*, 1973, **18**, 463.
155. E. A. V. Ebsworth, A. G. Lee, and G. M. Sheldrick, *J. Chem. Soc. (A)*, 1968, 2294.
156. G. C. Levy, D. M. White and J. D. Cargioli, *J. Magn. Resonance*, 1972, **8**, 280.
157. H. Dreeskamp and K. Hildenbrand, *Annalen*, 1975, 712.
158. K. Kovacević and Z. B. Maksić, *J. Mol. Struct.*, 1973, **17**, 203.
159. K. Kovacević, K. Krmpotić and Z. B. Maksić, *Inorg. Chem.*, 1977, **16**, 1421.
160. K. D. Summerhays and D. A. Deprez, *J. Organometal. Chem.*, 1976, **118**, 19.
161. M. D. Beer and R. Grinter, *J. Magn. Resonance*, 1977, **26**, 421.
162. W. McFarlane, *J. Chem. Soc. (A)*, 1967, 1275.
163. T. Yoshioka and A. C. MacDiamid, *J. Mol. Spectros.*, 1966, **21**, 103.
164. A. H. Cowley, W. D. White and S. L. Manatt, *J. Amer. Chem. Soc.*, 1967, **89**, 6433.
165. A. H. Cowley and W. D. White, *J. Amer. Chem. Soc.*, 1969, **91**, 1913, 1917.
166. C. J. Jameson and H. S. Gutowsky, *J. Chem. Phys.*, 1969, **51**, 2790.
167. W. McFarlane, *J. Chem. Soc. (A)*, 1967, 1275.
168. R. R. Dean and W. McFarlane, *Mol. Phys.*, 1967, **12**, 289, 364.
169. R. B. Johannesen, *J. Chem. Phys.*, 1967, **47**, 955.
170. S. S. Danyluk, *J. Amer. Chem. Soc.*, 1964, **86**, 4504.
171. G. Pfisterer and H. Dreeskamp, *Ber. Bunsenges. Phys. Chem.*, 1969, **73**, 654.
172. S. A. Linde, H. J. Jakobsen and B. J. Kimber, *J. Amer. Chem. Soc.*, 1975, **97**, 3219.
173. S. Danyluk, *J. Amer. Chem. Soc.*, 1965, **87**, 2300.
174. E. Hengge and F. Hofler, *Z. Naturforsch.*, 1971, **26a**, 768.
175. E. A. V. Ebsworth and G. M. Sheldrick, *Trans. Faraday Soc.*, 1966, **62**, 3282.
176. J. L. Margrave, K. G. Sharp and P. W. Wilson, *J. Inorg. Nuclear Chem.*, 1970, **32**, 1813.
177. C. Schumann and H. Dreeskamp, *J. Magn. Resonance*, 1970, **3**, 204.
178. J. V. Urenovitch and R. West, *J. Organometal. Chem.*, 1965, **3**, 138.
179. H. Bürger and W. K. Kilian, *J. Organometal. Chem.*, 1969, **18**, 299.
180. H. Bürger and W. Kilian, *J. Organometal. Chem.*, 1971, **26**, 47.
181. C. H. Van Dyke and A. G. MacDiarmid, *Inorg. Chem.*, 1964, **3**, 1071.
182. J. E. Drake and N. P. C. Westwood, *J. Chem. Soc. (A)*, 1971, 3300.
183. C. H. Van Dyke, E. W. Kiefer and G. A. Gibbon, *Inorg. Chem.*, 1972, **11**, 408.
184. E. A. V. Ebsworth, H. J. Emeléus and N. Welcman, *J. Chem. Soc.*, 1962, 2290.
185. J. Schraml, V. Chvalovský, M. Mägi and E. Lippmaa, *Coll. Czech. Chem. Comm.*, 1975, **40**, 897.
186. K. M. Abraham and G. Urry, *Inorg. Chem.*, 1973, **12**, 2850.
187. B. J. Aylett and H. M. Colquhoun, *J. Chem. Res. (Symposiums)*, 1977, 148.
188. E. Hengge, *Monatsh. Chem.*, 1971, **102**, 734.
189. F. K. Cartledge and K. H. Riedel, *J. Organometal. Chem.*, 1972, **34**, 11.
190. Y. Nagai, M. Ohtsuki, T. Nakano and H. Watanabe, *J. Organometal. Chem.*, 1972, **37**, 81.
191. Y. Nagai, H. Matsumoto, T. Nakano and H. Watanabe, *Bull. Chem. Soc. Japan*, 1972, **45**, 2560.
192. Y. Nagai, S. Inaba, H. Matsumoto and H. Watanabe, *Bull. Chem. Soc. Japan*, 1972, **45**, 3224.
193. Y. Nagai, H. Matsumoto, M. Hayashi, E. Tajima and H. Watanabe, *Bull. Chem. Soc. Japan*, 1971, **44**, 3113.
194. F. Feher, P. Hadicke and H. Frings, *Inorg. Nuclear Chem. Lett.*, 1973, **9**, 931.
195. G. Fritz and P. Bottinger, *Z. Anorg. Allg. Chem.*, 1973, **395**, 159.

196. G. Fritz, G. Becker and D. Kummer, *Z. Anorg. Allg. Chem.*, 1970, **372**, 171.
197. G. Fritz, J. Grobe and D. Kummer, *Adv. Inorg. Chem. Radiochem.*, 1965, **7**, 400.
198. W. E. Newton and E. G. Rochow, *Inorg. Chim. Acta*, 1970, **4**, 133.
199. E. Hengge and H. Markatz, *Monatsh. Chem.*, 1970, **101**, 528.
200. C. Glidewell and D. W. H. Rankin, *J. Chem. Soc. (A)*, 1970, 279.
201. C. Glidewell, *J. Chem. Soc. (A)*, 1971, 823.
202. G. K. Barker, J. E. Drake and R. T. Hemmings, *J. Chem. Soc., Dalton*, 1974, 450.
203. S. G. Frankiss, *J. Phys. Chem.*, 1963, **67**, 752.
204. J. E. Drake and N. P. C. Westwood, *J. Chem. Soc. (A)*, 1971, 3300.
205. W. Airey and G. M. Sheldrick, *J. Inorg. Nuclear Chem.*, 1970, **32**, 1827.
206. H. Bürger and W. Kilian, *J. Organometal. Chem.*, 1971, **26**, 47.
207. E. Hengge, *Monatsh. Chem.*, 1971, **102**, 734.
208. F. Höfler and W. Veigl, *Angew. Chem.*, 1971, **83**, 977; *Internat. Edn.*, 1971, **10**, 977.
209. R. B. Johannesen, T. C. Farrar, F. E. Brinckman and T. D. Coyle, *J. Phys. Chem.*, 1966, **44**, 962.
210. H. C. Marsmann, *Chem. Z.*, 1972, **96**, 288.
211. E. A. V. Ebsworth and S. G. Frankiss, *Trans. Faraday Soc.*, 1963, **59**, 1518.
212. J. J. Moscony and A. G. MacDiarmid, *Chem. Comm.*, 1965, 307.
213. J. C. Thompson and J. L. Margrave, *Chem. Comm.*, 1966, 566.
214. E. L. Muetterties and W. D. Phillips, *J. Amer. Chem. Soc.*, 1959, **81**, 1084.
215. R. J. Gillespie and J. W. Quail, *J. Chem. Phys.*, 1963, **39**, 2555.
216. R. K. Harris and B. J. Kimber, *Org. Magn. Resonance*, 1975, **7**, 460.
217. T. N. Mitchell and H. C. Marsmann, *J. Organometal. Chem.*, 1978, **150**, 171.
218. G. Fritz and H. Schafer, *Z. Anorg. Allg. Chem.*, 1974, **409**, 137.
219. D. W. W. Anderson, J. E. Bentham and D. W. H. Rankin, *J. Chem. Soc., Dalton*, 1973, 1215.
220. R. Gruning, P. Krommes and J. Lorberth, *J. Organometal. Chem.*, 1977, **127**, 167.
221. H. Elser and H. Dreeskamp, *Ber. Bunsenges. Phys. Chem.*, 1969, **73**, 619.
222. D. W. W. Anderson, E. A. V. Ebsworth and D. W. H. Rankin, *J. Chem. Soc., Dalton*, 1973, 2370.
223. H. A. Brune, *Chem. Ber.*, 1964, **97**, 2848.
224. H. Schmidbaur, *J. Amer. Chem. Soc.*, 1963, **85**, 2336.
225. G. C. Levy and J. D. Cargioli, *Proc. NATO Advanced Study Inst., Italy*, 1972.
226. R. K. Harris and B. J. Kimber, *Chem. Comm.*, 1973, 255.
227. B. J. Kimber and R. K. Harris, *J. Magn. Resonance*, 1974, **18**, 354.
228. G. Engelhardt, *Z. Chem.*, 1975, **15**, 495.
229. J. H. Noggle and R. E. Schirmer, "The Nuclear Overhauser Effect", Academic Press, New York, 1971.
230. R. Löwer, M. Vongehr and H. C. Marsmann, *Chem. Z.*, 1975, **99**, 33.
231. H. C. Marsmann, *Chem. Z.*, 1972, **96**, 288.
232. J. Schraml, N. D. Chuy, V. Chvalovský, M. Mägi, and E. Lippmaa, *J. Organometal. Chem.*, 1973, **51**, C-5.
233. D. W. W. Anderson, J. E. Bentham and D. W. H. Rankin, *J. Chem. Soc., Dalton*, 1973, 1215.
234. R. K. Harris and B. J. Kimber, *Adv. Mol. Relax. Proc.*, 1976, **8**, 23.
235. R. West, F. A. Kramer, E. Carberry, M. Kumada and M. Ishikawa, *J. Organometal. Chem.*, 1967, **8**, 79.
236. D. M. White and G. C. Levy, *Macromolecules*, 1972, **5**, 526.
237. C. D. Schaeffer, Jr. and J. J. Zuckerman, *J. Amer. Chem. Soc.*, 1974, **96**, 7160.
238. H. Bürger, W. Kilian and K. Burczyk, *J. Organometal. Chem.*, 1970, **21**, 291.
239. D. Solan and A. B. Burg, *Inorg. Chem.*, 1972, **11**, 1253.
240. M. P. Simonnin, *J. Organometal. Chem.*, 1966, **5**, 155.

- 241. M. Fukui, K. Itoh and Y. Ishii, *J. Chem. Soc. Perkin II*, 1972, 1043.
- 242. G. Fritz, H. Frohlich and D. Kummer, *Z. Anorg. Allg. Chem.*, 1967, **353**, 34.
- 243. J. W. Anderson, G. K. Barker, J. E. Drake, and M. Rodger, *J. Chem. Soc., Dalton*, 1973, 1716.
- 244. S. Craddock, E. A. V. Ebsworth and H. F. Jessep, *J. Chem. Soc., Dalton*, 1972, 359.
- 245. E. Carberry, R. West and G. E. Glass, *J. Amer. Chem. Soc.*, 1969, **91**, 5446.
- 246. E. A. V. Ebsworth and G. M. Sheldrick, *Trans. Faraday Soc.*, 1966, **62**, 3282.
- 247. G. C. Levy and J. D. Cargioli, unpublished results.
- 248. J. Schraml, V. Chvalovský, M. Magi, E. Lippmaa, R. Calas, J. Dunoguès and P. Bourgeois, *J. Organometal. Chem.*, 1976, **120**, 41.
- 249. H. Bürger, R. Eujen and H. C. Marsmann, *Z. Naturforsch.*, 1974, **29b**, 149.
- 250. H. Schmidbaur, B. Zimmer, F. H. Köhler and W. Buchner, *Z. Naturforsch.*, 1977, **32b**, 481.
- 251. M. Vongehr and H. C. Marsmann, *Z. Naturforsch.*, 1976, **31b**, 1423.
- 252. V. A. Pestunovich, M. F. Larin, E. I. Dubinskaya and M. G. Voronkov, *Dokl. Akad. Nauk. SSSR*, 1977, **233**, 378.

# Magnetic Multiple Resonance

W. McFARLANE

*Department of Chemistry, City of London Polytechnic,  
Jewry Street, London EC3N 2EY*

AND

D. S. RYCROFT

*Department of Chemistry, University of Glasgow,  
Glasgow G12 8QQ*

I. Introduction . . . . .	320
II. Theoretical aspects . . . . .	322
III. Instrumentation . . . . .	325
IV. Techniques . . . . .	329
A. INDOR spectra . . . . .	329
B. Spin population transfer . . . . .	333
C. Spin-echo and two-dimensional spectra . . . . .	338
D. Triple resonance . . . . .	356
E. The assignment of $^{13}\text{C}$ spectra . . . . .	358
V. The nuclear Overhauser effect (NOE) . . . . .	365
A. Homonuclear systems . . . . .	367
B. Heteronuclear systems . . . . .	370
C. The $^{13}\text{C}$ - $\{^1\text{H}\}$ NOE . . . . .	372
D. The NOE for other pairs of nuclei . . . . .	375
E. CIDNP and the NOE . . . . .	377
VI. Chemical exchange . . . . .	377
VII. Chemical applications . . . . .	379
A. The determination of chemical shifts . . . . .	379
B. The determination of the signs and magnitudes of coupling constants . . . . .	385
1. Simple spin systems . . . . .	385
2. Complex spin systems . . . . .	389
C. General applications: simplification and assignment . . . . .	390
1. $^1\text{H}$ - $\{\text{X}\}$ experiments . . . . .	390
2. $^{13}\text{C}$ - $\{\text{X}\}$ experiments . . . . .	392
3. Other experiments . . . . .	397
D. Oriented molecules . . . . .	400

Acknowledgement . . . . .	401
References . . . . .	401

## I. INTRODUCTION

In the previous article (1) on heteronuclear double resonance in this series it was suggested that such experiments would soon vie for importance with homonuclear ones. In fact, there has been an almost total eclipse; partly as a result of the use of proton decoupling in all  $^{13}\text{C}$  work, partly because of improved methods of frequency generation and control which have made experimental distinctions between the two types of experiment much less important. The present review therefore deals with both homo- and hetero-nuclear experiments and includes multiple resonance work also. The seven years up to mid-1978 are covered, although it has been impossible to mention every experiment. Emphasis is laid upon new ideas and developments of technique, with some preference for the more recent work. The Chemical Society specialist reports on NMR spectroscopy have included regular articles on multiple resonance (2, 3) and a number of reviews deal with various aspects of the subject. (4–19) It has been decided to omit work on the solid state.

The most important development in high resolution NMR during the past decade has been the application of pulsed FT methods to proton and especially  $^{13}\text{C}$  spectra and subsequently to other nuclei. Initially, only CW decoupling was used but then the advantages of various gating schemes to separate the decoupling and nuclear Overhauser effects became apparent, (20, 21) and when allied to selective excitation (22, 23) these provide extremely powerful assignment techniques for  $^{13}\text{C}$  spectroscopy. More recently experiments have been reported in which both the observing and irradiating RF fields are pulsed to yield spin-echoes which when subject to double Fourier transformation yield two-dimensional spectra in which the different chemical shifts and/or coupling constants can be displayed along different axes. (14, 24–26) Already, manufacturers are making it possible to perform experiments of this kind (routinely?) on their instruments, and for complex molecules in particular an attractive range of possibilities is opening up.

## II. THEORETICAL ASPECTS

The way in which strong rf fields (which may or may not be modulated by “noise” or otherwise) can achieve spin decoupling is well

understood. However, there have been a few theoretical developments during our period.

One effect of using noise modulation in the decoupling of one nucleus from another is to make available an additional mechanism of transverse relaxation for the observed nucleus. That is, there is another contribution to  $T_2^*$ , and in  $^{13}\text{C}-\{^1\text{H}\}$  experiments, for example, it is not possible to achieve  $^{13}\text{C}$  line-widths that are less than the line-widths of the coupled protons unless  $B_2$  is large enough. (27) This behaviour is especially important in spin-echo work, and attempts to use  $90^\circ-\tau-180^\circ$  pulses to generate  $^{13}\text{C}$  spin-echoes from  $^{13}\text{C}$ -enriched methyl iodide failed when simultaneous noise-modulated proton irradiation was used (28) but were successful in the presence of coherent irradiation or none at all. Effectively, the noise modulation causes a dephasing of the precessing transverse  $^{13}\text{C}$  magnetization which is not refocussed by the second pulse. Similarly, measurements of  $T_{1\rho}$  by pulse techniques must be conducted without noise modulation, although this need not be a serious problem provided that  $\gamma B_2/2\pi$  is large enough (27) (say  $>4000$  Hz for  $^{13}\text{C}-\{^1\text{H}\}$  experiments in a 1.4 T field).

$^{13}\text{C}$   $T_1$  measurements are now routinely conducted under conditions of complete proton decoupling, it generally being assumed that this has a negligible effect upon the results. Initially, this seemed to be supported by saturation recovery determinations of  $T_1(^1\text{H})$  for the methyl group of methanol. Values of  $0.62 \pm 0.02$  and  $0.64 \pm 0.02$  s were obtained when coupling to the OH proton was removed by double resonance and by acid-catalysed exchange respectively. However, detailed theoretical analysis (29–31) shows that following a spin-population inversion there is not an exactly exponential recovery of the  $^{13}\text{C}$  longitudinal magnetization unless the protons are decoupled completely. In the absence of proton decoupling it is necessary to consider the proton relaxation probabilities, and the apparent  $^{13}\text{C}$  relaxation times obtained may differ significantly from those found with full proton decoupling. Tests on benzene (31) using both adiabatic fast passage and pulsed methods to determine  $T_1(^{13}\text{C})$  as well as formic acid (29) and the protons of cytidine (29) indicate that, in the absence of decoupling, errors in  $T_1$  of up to 10 % may occur. Even with full decoupling there may be errors in  $T_1$  determinations since although cross-relaxation effects are eliminated the cross-correlation ones remain. This is especially important in degenerate spin systems. Thus the decay of  $^{13}\text{C}$  magnetization in inversion-recovery experiments with  $\text{CH}_2$  and  $\text{CH}_3$  groups is in general bi-exponential when the protons are decoupled, and the most serious errors are likely to arise under conditions of anisotropic molecular motion. (32)



Molecules dissolved in liquid crystal solvents give rise to spectra covering a very wide range which can cause problems if decoupling is required. This is especially the case if partial deuterium substitution is used to simplify the spectrum given by the remaining protons, since then the nuclear quadrupole moment of  $^2\text{D}$  generates widths of several kHz. It has been shown theoretically that in these circumstances efficient decoupling is brought about by using a strong rf field centred on the double quantum transition which lies at the centre of the deuterium spectrum. (33) The early work of Anderson and Nelson (34) leads one to expect that coherent phase modulation of the irradiating rf field will improve the efficiency of decoupling in oriented molecules. An extension (35) of the general equations (36) for double resonance supports this in the cases of the oriented  $A_n-\{X\}$ ,  $A-\{X_n\}$ , and  $A_3-\{X_2\}$  ( $I_A = I_X = \frac{1}{2}$ ) and  $A-\{X\}$  and  $A_3-\{X\}$  ( $I_A = \frac{1}{2}$ ,  $I_X = 1$ ) spin systems. Some support for this is obtained from  $^1\text{H}-\{^2\text{D}\}$  experiments (35, 37) on  $\text{CH}_3\text{OD}$ ,  $\text{CHD}_2\text{OH}$ ,  $\text{CH}_3\text{CD}_2\text{OH}$ , and  $\text{C}_6\text{D}_5\text{COCH}_3$  in a number of different nematic solvents. One should perhaps note that Anderson and Nelson's (34) calculations lead to a modulation frequency equal to or a little larger than  $\gamma(X)B_2/2\pi$ , whereas in practice the frequencies used were of many kHz, corresponding to the deuterium quadrupole splittings in the oriented samples.

The use of gated and pulsed experiments to achieve spin decoupling has been examined theoretically. The simplest approach is to assume that for sufficiently fast pulses the effect is that of an average perturbing  $\langle B_2 \rangle$  given by  $B_2\tau_p/T_p$ , where  $\tau_p$  is the pulse length and  $T_p$  its repetition period. (38) Although this description can be successful in certain cases it is fundamentally incorrect since it ignores the fact that the gating or pulsing generates a series of modulation sidebands whose interaction with the spin system must be taken into account. Treatment of a number of homo- and hetero-nuclear examples confirms the necessity for the more exact approach. (39)

Most earlier theoretical work on multiple resonance used either the Bloch equations or the spin-Hamiltonian. That is, relaxation is considered separately from other effects. The tendency in recent years has been to adopt the density-matrix approach but on some occasions simpler methods have still been appropriate. In the interpretation of multiple resonance experiments it is often necessary to consider the labelling of the energy level diagram in detail.

This can give rise to difficulties in tightly coupled spin systems when there may be virtually complete mixing of some pairs of wave functions. (40) Most of the problems can be avoided, however, by an appropriate new choice of wave functions (41) and this approach should always be

borne in mind. Of course it is always possible to avoid contact with such problems simply by comparing experimental spectra with those calculated by computer. Several more programs have been made available for this purpose (42, 43) including one for the calculation of INDOR spectra which can assist in the interpretation of double resonance experiments aimed at giving the relative signs of coupling constants. (44) The spin-Hamiltonian approach has also been used in the calculation of the two-dimensional spectra given by some representative spin systems, and more details are given in Section IV.C. (45, 46) The results of triple resonance experiments have also been predicted and the occurrence of line splittings and combination signals has been verified experimentally for AX and AMX spin systems. (47)

Meakin and Jesson (48) used the Bloch equations in part of their work on the computer simulation of multiple-pulse experiments. They find that this approach is efficient for the effect upon the magnetization vector of any sequence of pulses and delays in weakly coupled spin systems. However, relaxation processes and tightly coupled spin systems cannot be dealt with satisfactorily in this way and require the use of the density matrix.

Many workers have in fact used density matrix methods for the calculation of line shapes and intensities in multiple resonance experiments, and two excellent reviews of the background theory are available. (49, 50) In addition there is also a "simple" guide (51) to the actual use of the method which is capable of predicting the results of quite elaborate experiments. Major applications have included: the calculation of the *complete* double resonance spectrum from an AX spin system which gives 12 transitions in all; (52) an extremely detailed study of the relaxation behaviour of the AX<sub>2</sub> systems provided by 1,1,2-trichloroethane and 2,2-dichloroethanol; (53) the effects of gating and of selective and non-selective pulses on AB and AX spin systems and the importance of the time evolution of the off-diagonal elements of the density matrix in repetitively pulsed FT NMR and spin-echo work; (54) the use of double resonance to sort out relaxation mechanisms and transient responses; (55) the calculation of general multiple resonance spectra; (56) and triple resonance studies of relaxation in AB and AX spin systems. (57)

Many apparent anomalies in the spectra produced by double resonance experiments can be resolved by a density matrix treatment. Thus in A- $\{X_n\}$  experiments with a reduced amplitude of the irradiated field the normal effect of the NOE upon the intensities of the transitions may be severely modified and both emission and absorption may be observed. (58) It turns out that the overall behaviour depends upon

two factors: (a) the "tilt" effect which is due to the effective field in the rotating frame not lying along an axis, and (b) the relaxation effect. The second affects only the intensities while the first can lead to additional lines in the spectrum. Detailed calculations using density matrix theory on  $^{13}\text{CH}_3\text{I}$  with  $\gamma(^1\text{H})B_2/2\pi = 0.06J(^{13}\text{C}-^1\text{H})$  predict that the  $^{13}\text{C}$  spectrum will contain sixteen lines (six in emission, nine in absorption, and one of almost zero intensity), and this has been confirmed by experiment. (58) Other systems under similar conditions of double irradiation also give rise to time-dependent modulations of the transition intensities following a standard inversion-recovery  $^{13}\text{C}$  sequence. (59) These appear to be due to the mixing-in of the off-diagonal elements of the relaxation matrix by the proton irradiating field, (59) an interpretation which can account for abnormal spectra obtained in  $^1\text{H}-\{^{14}\text{N}\}$  experiments on ammonia. (60)

The density matrix approach is also important or even essential for the proper treatment of double resonance experiments on systems undergoing chemical exchange, although straightforward saturation transfer experiments may of course be interpreted more simply. A treatment of the exchanging AB spin system when subject simultaneously to a weak and a strong rf field has been presented. (61) From the detailed band-shape calculations it appears that the use of double resonance experiments can extend the time scale at the slow exchange limit by a factor of up to 100. This of course was known already in a qualitative way from the early work of Hoffman and Forsén. (62) Other systems that have been studied in detail include 2,2,2-trichloroethanol (an  $\text{AB}_2$  case) (63) and 1,2-dibromo-1,1-dichloro-2,2-difluoroethane (AB exchanging with C-2). (64)

Bucci and his coworkers (65, 66) treated double resonance by means of a second quantization of the rf fields to avoid the use of the rotating frame. The total Hamiltonian  $\mathcal{H}_T$  is then given by equation (1) in which  $\mathcal{H}_S$  is the normal Hamiltonian of the isolated spin system in the absence of radiation but in the magnetic field,  $\mathcal{H}_R$  is the radiation Hamiltonian, and  $\mathcal{H}_I$  represents the interaction between the spins and the radiation field(s).

$$\mathcal{H}_T = \mathcal{H}_S + \mathcal{H}_R + \mathcal{H}_I \quad (1)$$

This approach accurately predicts the behaviour of a single spin and the AB system under normal double resonance conditions, and has the advantage of being applicable when the rf power is very high and/or many rf fields are used.

Other examples of the use of multiple resonance to study relaxation include: a demonstration of the advantages of steady state selective

saturation rather than transient methods in coupled spin systems; (67) a detailed study of the structure and dynamics of  $\text{CH}_2\text{I}_2$  in solution by  $^{13}\text{C}$  and  $^1\text{H}$  experiments; (68) the use of a liquid crystal solvent to remove the singlet-triplet degeneracy in  $^{13}\text{CH}_2\text{I}_2$  so as to permit detailed study of differences in relaxation behaviour; (69) a measurement of  $^2J(^{35}\text{Cl}-^1\text{H}) = 9.3 \pm 0.3 \text{ Hz}$  in  $\text{HSiCl}_3$  from  $T_{1\rho}$  and  $^1\text{H}-\{^{35}\text{Cl}\}$  line sharpening experiments; (70) the effect of rapid  $^{13}\text{C}$  relaxation in  $\text{CHBr}_3$  in producing perturbation of an *unconnected* proton transition in a  $^1\text{H}-\{^{13}\text{C}\}$  experiment; (71) and a comparison of gated homonuclear (proton-proton) double resonance experiments performed under CW and FT conditions. (72) In this last work several AB and ABC spin-systems were examined with the selective irradiating field gated so as to retain the NOE and it was found that for small flip angles the FT results are very similar to the CW ones but for flip angles near  $90^\circ$  there are marked discrepancies. (72) The detailed behaviour depends on the particular relaxation mechanism involved and upon the relative signs of the coupling constants; it was analysed satisfactorily using the general theory of Shaublin, Höhener, and Ernst. (73)

### III. INSTRUMENTATION

Most manufacturers now provide highly versatile instruments for high resolution work, so there is much less need for the experimenter to build his own electronics for multiple resonance. Similarly, modifications to software are generally straightforward, although at least one maker remains remarkably uncooperative over this.

A modern  $^{13}\text{C}$  or multinuclear pulse FT spectrometer will be equipped with proton decoupling coils in the probe, and it is generally convenient to adapt these to accept an additional radio frequency if it is desired to perform  $^{13}\text{C}-\{^1\text{H}, \text{X}\}$  or similar triple resonance experiments. There are then two possibilities: (i) Insert a proton frequency trap circuit and tune also to the X resonance frequency in a manner similar to that used in an early modification (74) of the Varian HA-100 spectrometer; (75) (ii) Reconstruct the proton matching circuit so that it is double tuned to the proton and a *particular* X frequency. Method (i) has the advantage of versatility in that a wide range of nuclei can be accommodated with a single modification (although for some frequencies the X rf field at the sample may be rather small) but has the disadvantage that about half of the proton power is lost in the trap circuit which therefore gets quite hot. Method (ii) achieves the maximum rf field at the sample but in general a separate unit is required for each nucleus X. Figure 1 shows a circuit using method (ii) for the

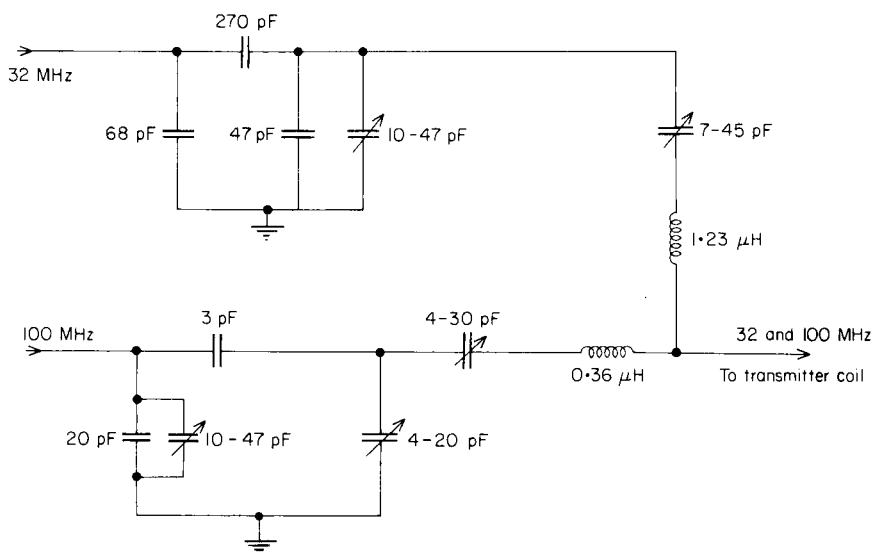


FIG. 1. Electronic circuit for adapting the  $^{13}\text{C}$  probe of the Varian XL-100-15 spectrometer for simultaneous  $^1\text{H}$  and  $^{11}\text{B}$  decoupling at 100 and 32 MHz respectively. By altering the component values other frequencies can be accommodated. From ref. 76.

simultaneous decoupling of  $^1\text{H}$  at 100 MHz and  $^{11}\text{B}$  at 32 MHz from  $^{13}\text{C}$  in a Varian XL-100-15 spectrometer, the rf fields generated being  $\gamma B_2/2\pi = 1700$  and 340 Hz respectively. (76) The decoupling of  $^{19}\text{F}$  from  $^{13}\text{C}$  presents special problems owing to the large frequency spread of  $^{19}\text{F}$  spectra.

Several manufacturers have the problem in hand as Fig. 2 shows. (77) In addition a modification of a Bruker spectrometer for  $^{13}\text{C}-\{^{19}\text{F}\}$  experiments has been described (78) and circuits for  $^1\text{H}-\{\text{X}\}$ , (79, 80)  $^1\text{H}-\{^{19}\text{F}\}$ , (81)  $^{19}\text{F}-\{^1\text{H}\}$ , (81)  $^1\text{H}-\{^1\text{H}, ^{14}\text{N}\}$ , (82)  $^{19}\text{F}-\{^{19}\text{F}, ^{14}\text{N}\}$ , (83) and other (84-86) experiments are available. A number of descriptions of "home-built" and modified spectrometers have also referred to the methods used to conduct double resonance experiments (87-91) including two designed for experiments on solids. (92)

In a modern NMR spectrometer with facilities for homo- and hetero-nuclear multiple resonance the dangers of interference among the various radio frequencies present are quite high. However, they can be avoided by gating at rates high compared with any spectral splittings. Details are available of electronic circuits for this purpose. (90, 89, 54)

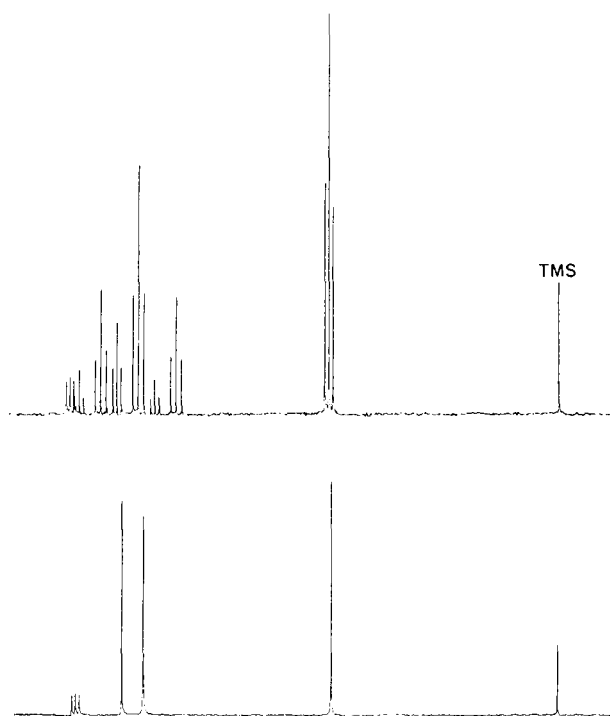


FIG. 2. Simultaneous decoupling of protons and  $^{19}\text{F}$  from  $^{13}\text{C}$ . Upper trace: normal fully coupled  $^{13}\text{C}$  spectrum at 25 MHz of 2,2,3,3-tetrafluoropropanol,  $\text{CHF}_2\text{CF}_2\text{CH}_2\text{OH}$ . Lower trace: with wide-band  $^1\text{H}$ ,  $^{19}\text{F}$  decoupling. The total spectral width is 4000 Hz. By courtesy of JEOL (U.K.) Limited.

Another way of avoiding interference in homonuclear experiments is by means of phase-splitting circuitry in which half of the modulation signal, used to produce the decoupling sideband, is fed to the receiver phase-sensitive detector where it cancels out the beat signal. (93) It is well known that for A- $\{\text{X}\}$  decoupling experiments it is best to modulate the X radio frequency with noise if the spread of the X resonances arises from chemical shift differences, but with coherent audio frequency if very large spin-spin splittings are involved. (94, 95) To some extent one can have the best of both worlds by using square-wave modulation (96) or better still by using a versatile broadband modulator capable of operating in several modes. (97) Nowadays of course a modern frequency synthesizer will generally have very versatile modulation facilities, although it is worth remarking that there is nothing to beat adequate total decoupling power.

Undoubtedly the best way of generating the extra radio frequencies needed for heteronuclear triple resonance experiments is to use two frequency synthesizers but this is rather expensive. A more economical alternative is to use only one synthesizer and to generate the third rf by means of a crystal-controlled oscillator. Frequency variation of the output of this can be achieved by modulation with a known audio frequency (98) or by "pulling" the crystal with a series capacitor and using the frequency synthesizer for calibration (99) if a suitable rf counter is not available. Figure 3 shows a simple oscillator circuit which in a non-air-conditioned laboratory environment has a stability of better than 0.1 ppm/h. This can be used for heteronuclear double resonance experiments without any frequency synthesizer at all. (100)

Other instrumental developments of relevance to double resonance have been reported and are worth noting briefly. A TTL-IC sequence controller has been described in considerable detail (101) and can provide both digital and analogue trigger sequences that should be of value in quite complex multiple resonance experiments, and circuits are available (102) for a two-channel analogue pulse generator that is particularly easy to construct. When double resonance experiments are performed in the field sweep mode this can give rise to difficulties of interpretation which can be avoided if the irradiating rf is swept in step with the magnetic field sweep. A circuit based upon an operational

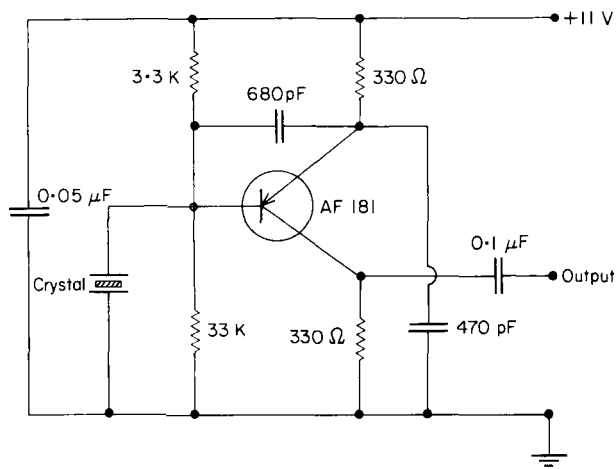


FIG. 3. Simple oscillator circuit for generating stable radio frequencies up to 15 MHz. The output exceeds 0.1 volt RMS, and under normal laboratory conditions the frequency stability is better than  $10^{-7}$ /h.

amplifier has been reported (103) which makes it possible to do this for homonuclear experiments on the Varian HR-220 spectrometer. A number of JEOL instruments possess this as a built-in feature.

## IV. TECHNIQUES

### A. INDOR spectra

Although the term INDOR can be applied to any double resonance experiment it is generally reserved for ones involving continuous monitoring (normally of a transition) at a particular frequency in the spectrum of one nucleus whilst  $\nu_2$  is swept through an appropriate range so that the excursions of the recorder pen correspond to the transitions in the spectrum of the irradiated nucleus. (104) These excursions may arise as a consequence of spin population transfers (in which case there will be positive and negative responses), or spin tickling effects (all the responses will be of the same sign), or a combination of both (which may lead to confusion). The main applications of proton homonuclear INDOR have been to the detection of hidden resonances in the spectra of complex organic molecules (105, 106) such as a thermal dimerization product from the compound 11,13-dioxo-12-methyl-12-aza[4,4,3]propellane (107) and to sorting out energy level diagrams for relatively simple spin systems. A guide to this last application has been published. (108) Heteronuclear INDOR is especially valuable for the presentation of the "spectra" of insensitive nuclei. Although the growth of multinuclear FT spectrometers is steadily eroding its value it still has considerable advantages for such nuclei as  $^{57}\text{Fe}$ ,  $^{103}\text{Rh}$ ,  $^{107/109}\text{Ag}$ , and  $^{183}\text{W}$  which have very low magnetogyric ratios. It is also possible to use triple resonance experiments to record heteronuclear INDOR spectra, as in the MINDOR and TINDOR experiments (109) (see p. 356), or to use a reasonably sensitive nucleus such as  $^{31}\text{P}$  rather than the proton for detection.

A major instrumental problem with the conventional A-{X} INDOR experiment is that the need to monitor a particular observed transition places extremely stringent demands upon the frequency stability of the spectrometer if spurious responses are to be avoided. This is particularly serious under conditions of poor signal-to-noise ratio when it is desired to use signal averaging, and an alternative approach has been described which greatly alleviates the difficulty. (110) In many situations of interest one is dealing effectively with an  $A_nX$  spin system with  $A = ^1\text{H}$ , so the proton spectrum is simply a doublet which can be collapsed to a single line at  $\nu(^1\text{H})$  by irradiation at



$\nu(X)$ . Thus, by monitoring at the frequency  $\nu(^1\text{H})$  (where there is normally no signal) and sweeping  $\nu(X)$  through the appropriate range, a response is obtained as the centre of the X resonance is traversed. The advantages of this method are that an instability of up to  $J(\text{AX})/10$  in the monitoring frequency can be tolerated, since most of the time no response at all is present, unlike the situation with normal INDOR. The monitoring rf field can be set at considerably higher amplitude than normal so as to give a better signal-to-noise ratio. Figure 4 illustrates the application (110) of this technique to the determination of  $^1J(^{119}\text{Sn}-\text{Sn})$  in the species  $(\text{Me}_3\text{Sn})_3\text{Sn}^-\text{Li}^+\cdot 3\text{THF}$  by observation of the methyl protons and irradiation of the  $^{119}\text{Sn}^-$  resonance, the response being due to collapse of  $^3J(^{119}\text{Sn}\cdots ^1\text{H}) = 2\text{ Hz}$ . This technique is also useful for studying quadrupolar nuclei, especially when quadrupolar relaxation is so fast that there is only a small residual broadening of the proton signal produced by modulation of  $J(\text{HX})$ . The monitoring point is then the top of this broadened

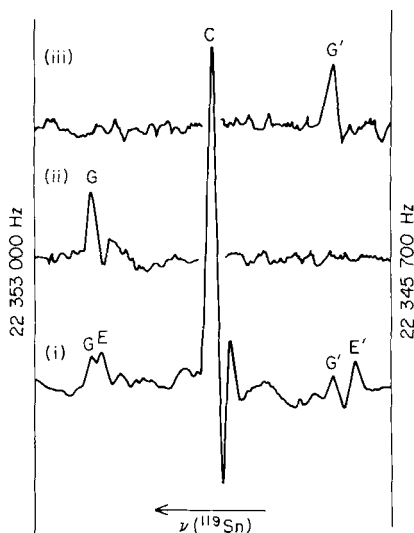


FIG. 4.  $^1\text{H}-\{^{119}\text{Sn}\}$  accumulated INDOR spectra (32 scans) of  $(\text{Me}_3\text{Sn})_3\text{Sn}^-\text{Li}^+\cdot 3\text{THF}$  obtained by collapsing the 2 Hz coupling  $^3J(^{119}\text{Sn}\cdots ^1\text{H})$ . Trace (i): top of main methyl resonance monitored. Trace (ii): top of high frequency ( $^2J$ )  $^{117}\text{Sn}$  satellite of methyl resonance monitored. Trace (iii): top of low frequency ( $^2J$ )  $^{117}\text{Sn}$  satellite of methyl resonance monitored. G and G' arise from species containing one  $^{119}\text{Sn}$  and  $^{117}\text{Sn}$  nucleus, E and E' from species containing two  $^{119}\text{Sn}$ . The asymmetry arises from second-order features since  $^1J(^{119}\text{Sn}-^{119}\text{Sn})/\delta(\text{Sn}, \text{Sn}) \approx 0.22$ . From ref. 110.

resonance. The method has also been applied to  $^{14}\text{N}$  studies of pyrimidines (111) and to the production of  $^{17}\text{O}$  INDOR spectra of enriched methanol (112) (Fig. 5) and some organophosphorus compounds. (113) This technique is quite closely related to some experiments by Ziessow (114) whereby transient nutations (Torrey oscillations) of the monitored nucleus are induced by an adiabatic fast passage through the X-spectrum, together with signal averaging to attain a satisfactory signal-to-noise ratio.

The foregoing INDOR experiments have all been CW ones, with continuous monitoring of a position in the observed spectrum. In view of the considerable sensitivity advantages of FT NMR efforts have been made to devise a pulsed FT equivalent of INDOR. The basic idea has been to subtract a pair of spectra, one with and the other without irradiation of the second nucleus. This is of course quite straightforward on a modern FT spectrometer in which the data are stored in digital form in a computer and either the FIDs or the transformed spectra may be subtracted, with essentially the same results, although it should be noted that the use of a subtraction technique will degrade the signal-to-noise ratio by a factor of  $\sqrt{2}$  since the noise components of the two spectra will be added. The first example of this approach was by Feeney and Partington (115)

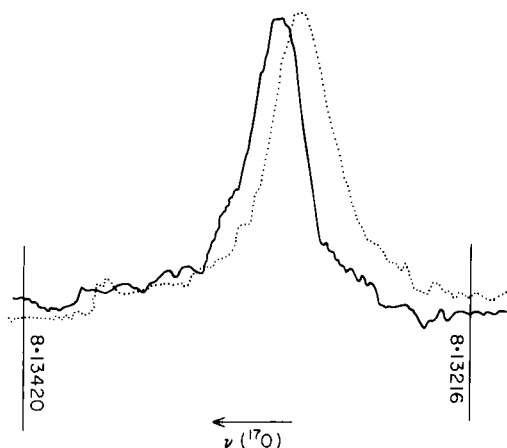
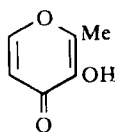


FIG. 5. Oxygen-17 INDOR spectra of methanol enriched to 10 mol %, obtained by monitoring the Me resonance in the proton spectrum. The frequency markers are in MHz and each trace is the result of 64 scans. Full line: high frequency component of doublet monitored; broken line: low frequency component monitored. From ref. 112.

who subtracted a normal FT spectrum from one obtained with simultaneous saturating irradiation of a particular transition. This led to cancellation of most of the signals, the residual responses corresponding to the frequencies of the transitions connected in the energy level diagram with the irradiated one, so that the result closely resembled a conventional INDOR spectrum. The loss of signal-to-noise ratio mentioned above can be avoided in this type of experiment by applying a selective  $180^\circ$  pulse to the transition immediately prior to collection of the FID so as to invert rather than merely equalize the populations of the energy levels. (116) In homonuclear experiments of this type the non-selective detecting pulse perturbs all of the spin system, including the saturated or inverted transition, and this can cause difficulties. These can be mitigated (117) by using a non-selective pulse of less than  $90^\circ$ , values of *ca.*  $30^\circ$  being found to give a good compromise between the conflicting interests of retention of the spin-population transfer effect and the attainment of a satisfactory signal-to-noise ratio. It has been claimed (117) that this kind (116, 118) of experiment is markedly superior to the earlier form of pseudo-INDOR (115) and to certain saturation experiments. (119) This is probably true but it should be noted that rather more sophisticated equipment is needed. More recently Hall and his coworkers (120) have used weak  $180^\circ$  pulses to achieve selective inversion and so produce FT INDOR spectra which assisted the determination of the conformation of a disaccharide. (121) Other examples of homonuclear INDOR include the detection of hidden resonances in the high field proton spectra of the basic pancreatic trypsin inhibitor (122) and some studies of maltol [1]. (123)



[1]

In heteronuclear FT INDOR there is no danger of unwanted perturbation by the detecting pulse, and in  $A-\{X\}$  experiments with  $|\gamma_X| > |\gamma_A|$  large intensity changes can be obtained so that the INDOR spectra have a good signal-to-noise ratio, although not as good as direct X spectra themselves. A case in point is the  $^{13}\text{C}-\{^1\text{H}\}$  system where selective experiments were used to give spectra which yield the relative signs of coupling constants in 2,3-dibromothiophen. (119) In all these experiments it is essential that there is no drift in the frequency

dimension between the spectra to be subtracted, otherwise serious apparent phase anomalies and "spikes" appear. One difficulty is that most subtraction routines do not permit one to compensate for drifts that do not correspond to an integral number of data points in the transformed spectrum, but details of a sophisticated program are now available which makes it possible to correct for such factors as drift of  $B_0$  or  $\nu_1$  and variations in spectral amplitude,  $B_0$  homogeneity, rf phase, and spinning sidebands prior to subtraction. (124) A simpler way of dealing with many of the problems is to ensure that there are enough data points over each peak; this can be achieved either by using a sufficiently narrow spectral width or by confining attention to samples with broad lines, such as liquid crystal samples. In this way it is possible to determine the  $^{15}\text{N}$ -H and  $^{13}\text{C}$ -H splittings in partly oriented *s*-triazine containing the isotopes  $^{15}\text{N}$  and  $^{13}\text{C}$  in natural abundance. (125) In the case of alumichrome it proved convenient to degrade the resolution somewhat to get a  $^{15}\text{N}$  spectrum. (126)

Some of the two-dimensional experiments described in Section IV.D are also capable of yielding FT INDOR spectra but it is important to appreciate that all the pulse-detection methods so far used depend upon transfer of magnetization (either transverse or longitudinal) and not upon spin tickling or decoupling behaviour. An important consequence of this is that the gains in signal intensity are of the order of the ratio of the magnetic moments of the two nuclear species involved, whereas in CW INDOR using spin tickling or decoupling effects the gain depends upon the cube of this ratio.

## B. Spin population transfer

This is sometimes referred to as the generalized Nuclear Overhauser Effect but we consider this usage to be inappropriate. The ability of pulsed FT spectrometers to sample magnetization immediately after a selective perturbation of the spin system has been utilized in a variety of ingenious experiments. Many of these have been of the type  $^{13}\text{C}\{-^1\text{H}\}$  because although there is a loss of sensitivity compared with the corresponding  $^1\text{H}\{-^{13}\text{C}\}$  experiment there are no problems associated with a strong signal from molecules containing the isotope  $^{12}\text{C}$ . The main use of this type of experiment has been to establish the connectivity of the energy level diagram in order to determine the relative signs of coupling constants. The reasoning involved is independent of the precise way in which this is done. That is, the interpretation of the experiments is fundamentally the same as that of the analogous spin tickling experiments used in earlier CW work. The general procedure is similar to that used for the production of FT

pseudo-INDOR spectra; a weak selective pulse or saturation is applied to a proton transition and the effect upon the  $^{13}\text{C}$  spectrum is measured. This is illustrated in Fig. 6 for MeNC in experiments (127) which give the relative signs of  $^1J(^{14}\text{N}\equiv^{13}\text{C})$  and  $^2J(^{14}\text{N}\cdots\text{H})$  (128) in this molecule. In this particular set of experiments the proton transition is selectively saturated so that the affected spin populations are equalized, rather than inverted. It is claimed that this is the best technique for this system owing to the effects of the  $^{14}\text{N}$  nuclear quadrupole moment. (127) However, this has been questioned by other workers (129) who suggest on theoretical grounds that a  $180^\circ$  selective pulse should always be better since it will lead to double the intensity changes in the observed spectrum. This view is supported by the results of density matrix calculations. (130) The first of the techniques ( $90^\circ$

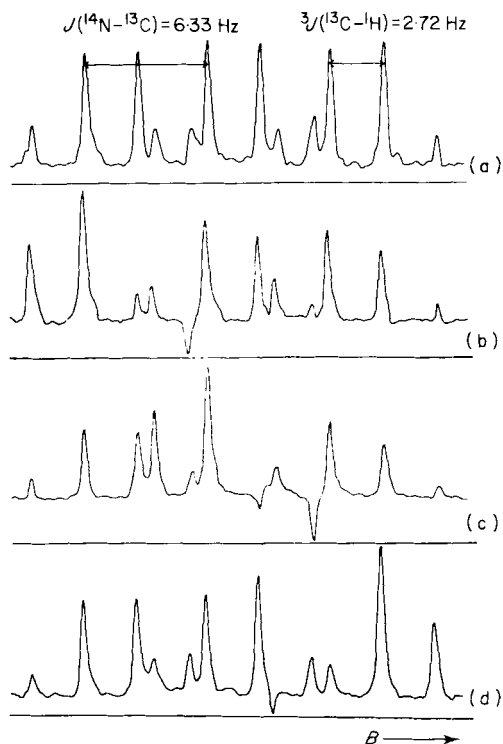


FIG. 6. Selective population transfer experiments.  $^{13}\text{C}$  FT spectra of  $-\text{NC}$  region of  $\text{CH}_3\text{NC}$ . (A) Normal fully coupled spectrum. (B) With continuous weak saturating irradiation of  $^{13}\text{C}$  satellite at lowest frequency in proton spectrum. (C) With irradiation of satellite at next lowest frequency. (D) With irradiation of satellite at highest frequency. From ref. 127.

pulse, or saturation) is termed SPT (Selective Population Transfer) and the second SPI (Selective Population Inversion). It is to be deplored that recently the letters SPT have also been used (131) to designate Soft Pulse Transfer.

There has been some discussion (127, 129, 132) of the relative merits of such techniques as pseudo-INDOR, SPT, SPI, spectral analysis, and spin tickling for the determination of the relative signs of coupling constants. It appears to the present writers that much depends upon the particular circumstances, namely, the nature of the spin system (including the relative values of relaxation times), the available instrumentation, and the abilities of the spectroscopist. Certainly, when  $\gamma_X > \gamma_A$  (e.g. for  $^{13}\text{C}-\{^1\text{H}\}$ ) the effects of simultaneous spin population transfer can make the interpretation of spin tickling effects very tricky.

As mentioned earlier, when  $\gamma_X < \gamma_A$  the effects of spin population transfers in  $A-\{X\}$  experiments are markedly reduced but can be sufficiently augmented in systems with degeneracies to lead to useful observable effects. This was established long ago in connection with CW work on transitory selective irradiation (TSI) (133) and has been rediscovered with the aid of FT instrumentation (129) in  $^{13}\text{C}-\{^{14}\text{N}\}$  experiments on methyl isocyanide in which the electric field gradient at nitrogen is small enough for quadrupolar effects to be unimportant. The ratio  $\gamma(^{14}\text{N})/\gamma(^{13}\text{C})$  is only 0.3 but changes of up to 50% in the intensities of carbon transitions are recorded following 180° selective pulses to a nitrogen spin. This effect arises partly because of degeneracies of the transitions of the methyl group protons. (129)

Such effects can also be of great value even when  $\gamma_X > \gamma_A$  since the sensitivity of the A spin will then be lower. They have been examined in some detail with  $^{13}\text{C}-\{^1\text{H}\}$  experiments in mind for the  $\text{AX}_n$  spin system, and it appears that it is often possible to realize very substantial gains in sensitivity. (134) One of the most effective experiments is to apply a selective 180° pulse to *one* of the components of the X (i.e.  $^1\text{H}$ ) doublet (note that each component of the doublet consists of  $2^{n-1}$  degenerate transitions) prior to the normal 90° exciting pulse and acquisition of the A spectrum. For  $n = 0$  to 6 and  $A = ^{13}\text{C}$ ,  $X = ^1\text{H}$  (i.e.  $\gamma_A/\gamma_X = 0.25$ ) the calculated population transfer enhancements of the lines of the A multiplet are then given by Fig. 7(a) and the resulting intensities by Fig. 7(b). A comparison of Fig. 7(b) with the usual Pascal's triangle shows that very substantial gains in signal height can be brought about in this way, e.g. a factor of 5 for one of the inner peaks of the quartet of an  $\text{AX}_3$  system and more than 10 in other cases. It must be stressed that the entries in Fig. 7(a) add up to zero, so there is no *net* gain in intensity in this experiment. This is because there is no net

0								1							
-4				4				-3				5			
-8		0		8				-7		2		9			
-12		-12		12		12		-11		-9		15		13	
-16		-32		0		32		16		-15		-28		6	
-20		-60		-40		40		60		20		-19		-55	
-24		-96		-120		0		120		96		24		-25	
(a)								(b)							

FIG. 7. Calculated SPT enhancements (a) and resulting intensities (b) in the lines of the A spectrum of an  $AX_n$  spin system with  $A = {}^1\text{H}$ ,  $X = {}^{13}\text{C}$ , and complete inversion of the populations of one set of degenerate X transitions. From ref. 134.

transfer of longitudinal magnetization, a fact that has important consequences for the production of certain types of two-dimensional spectrum (see p. 351). Samples of  ${}^{13}\text{CH}_3\text{I}$  ( $AX_3$ ) and  $(\text{CH}_3)_2{}^{13}\text{CO}$  were examined (134) to confirm the correctness of the predictions of Fig. 7.

Intensity gains of the foregoing kind can also facilitate the detection by subtraction methods (difference spectroscopy) of hidden transitions. This is typically a serious problem in the measurement of  ${}^{13}\text{C}$ – ${}^{13}\text{C}$  coupling constants in samples containing  ${}^{13}\text{C}$  in natural abundance. In an artificial 16:1 mixture of  $(\text{CD}_3)_2\text{CO}$  and  $(\text{CH}_3)_2\text{CO}$  enhancement of certain resonances in the  ${}^{13}\text{CO}$  spectrum of the latter molecule was effected by means of a selective  $180^\circ$  pulse to one of the (hidden)  ${}^{13}\text{CO}$  satellites in the proton spectrum, and alternate addition and subtraction of successive FIDs obtained with and without the proton pulse then gave a transformed spectrum containing no signals from the dominant deuteriated species. (135)

An especially ingenious use of SPI has been suggested for improving the signal-to-noise ratio from quaternary carbons in  ${}^{13}\text{C}$ – $\{{}^1\text{H}\}$  experiments. (136) It is well known that this is unfavourable owing to the absence of the NOE and to long relaxation times  $T_1({}^{13}\text{C})$ , which necessitate long pulse intervals. In fact, if the pulse interval  $t$  is sufficiently long the  ${}^{13}\text{C}$  intensity of quaternary carbons is proportional to  $\gamma({}^{13}\text{C})$  but as  $t$  becomes shorter than  $T_1({}^{13}\text{C})$  then the signal intensity tends to zero. However, it is common for there to be some long range coupling of a few Hz from at least one proton to the quaternary carbon, and the application of a selective  $180^\circ$  pulse to one of the associated proton transitions prior to acquisition of the  ${}^{13}\text{C}$  FID leads to enhancements of  $\pm\gamma({}^1\text{H})$  [ $= \pm 4\gamma({}^{13}\text{C})$ ] for the two  ${}^{13}\text{C}$  transitions in the case of an  $AX$  system (see Fig. 7) provided that

$t \gg T_1(^1\text{H})$ . Indeed, the dual condition  $T_1(^{13}\text{C}) \gg t \gg T_1(^1\text{H})$  can often be satisfied, and it is possible to realize a gain in sensitivity of  $\gamma(^1\text{H})/\gamma(^{13}\text{C}) = 4$ . This gain is augmented by a saving in time since the maximum pulse repetition rate is now governed by  $T_1(^1\text{H})$  rather than by  $T_1(^{13}\text{C})$  which may be over 50 s for a quaternary carbon. In practice (136) a gain in signal-to-noise ratio of 12.4 is achieved for C-1 of 1,1,2-trichloroethylene, and this corresponds to a time-saving factor of *ca.* 160, this being made up of  $4^2 \times 10$ . It is clear that for simple molecules this should be a useful technique, although if the proton spectrum is complicated it may be difficult to apply. Furthermore, there is again no *net* gain in sensitivity since positive and negative enhancements will cancel and, for small  $J(^{13}\text{C}-^1\text{H})$  values it may be necessary to adopt various artifices to circumvent this (see p 351).

Another class of experiments which really involve spin population transfer are those aimed at the suppression of a solvent or other strong resonance which otherwise creates problems associated with the dynamic range of the analogue-to-digital converter and possibly the word length of FT spectrometers. These are especially important in studies of biologically important materials which often must be examined at such extreme dilution that residual HDO in heavy water can be troublesome. Some of the available solutions do not involve double resonance, e.g. "tailored excitation" (137) and adaptations of selective excitation, (138) but others do. In a detailed study Hoult (139) has concluded that straightforward saturation (140) by a second rf field is probably best. However, it must be borne in mind that under certain conditions of chemical exchange some of the spin saturation could be transferred to sites in the molecule being studied, which would obviously affect the interpretation of the results. An experimental obstacle can be the appearance of a "spike" in the spectrum as a result of inadequate gating. A simple way (141) of avoiding this is to ensure that the saturating rf is not synchronized with the reference rf. If possible a large number of FIDs should be acquired prior to Fourier transformation, even if this is not necessary on the grounds of sensitivity, so that the effectively random phases of any irradiating rf which breaks through will cancel out to a large extent. Alternatively, advantage can be taken of the generally longer proton relaxation time of HDO compared with many samples, and a  $(180^\circ - \tau - 90^\circ - T)_n$  pulse sequence (142) such as is normally available for  $T_1$  measurements can be used to saturate selectively (143) the HDO resonance by a suitable choice of  $\tau$ . Some further improvement may be attainable by using a homogeneity spoiling pulse in addition, to destroy transverse magnetization in each cycle. (144)



### C. Spin-echo and two-dimensional spectra

The use of spin-echoes to study the solid state is almost as old as NMR itself. More recently there have been applications in high resolution work on liquid samples. A review that provides an excellent introduction to this area of work is available (145) and in addition there is a brief survey of the two-dimensional technique (146) which incidentally is the subject of a German patent. (147) The relevance of spin-echo experiments to the present review is that during the period of echo formation it is possible to bring about changes in the conditions of multiple resonance and thereby gain considerable experimental control over the spin-Hamiltonian. Thus not only can the effects of magnetic field inhomogeneity be eliminated, as is usual in a spin-echo experiment, but it is also possible to isolate the effects either of spin coupling or of chemical shift differences in a completely controllable manner. At present the benefits of this are only just beginning to be realized, and there have been only a few applications to actual chemical problems. This situation can be expected to change soon.

Consider an AX system with the A spins observed, X a different nuclear species, and  $J(AX) \neq 0$ . Figure 8(a) shows the behaviour of the transverse magnetization in the rotating frame in a normal  $90^\circ - \tau - 180^\circ$  pulse sequence for the generation of a spin echo. At time  $\tau$  the  $-$  and  $+$  isochromats corresponding to opposite spin states of X are reflected in the y-axis but continue to precess in the *same direction* so that at time  $2\tau$  complete refocusing has occurred and the echo shows no effects due to the spin coupling or magnetic field inhomogeneity. Consider now the

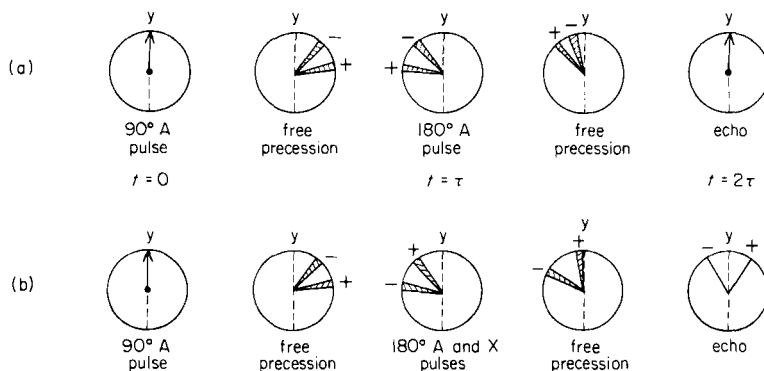


FIG. 8. View of the transverse magnetization projected on to the xy-plane in the rotating frame for a heteronuclear AX spin system. The pulse at time  $t = 0$  is applied along the x-direction to tip the magnetization from the z- to the y-axis, and the pulses at time  $t = \tau$  are applied along the y-direction. (a) Formation of unmodulated spin-echo. (b) Formation of modulated spin-echo. Adapted from ref. 145.

same experiment but with a  $180^\circ$  pulse applied to the X spins also at time  $\tau$ . Then, as shown in Fig. 8(b), the + and - isochromats are interchanged at time  $\tau$  but since each continues to precess at its original rate they are not aligned along the y-direction at time  $2\tau$  when the echo is formed. The extent to which the + and - isochromats deviate from the y-direction when the echo is formed will of course depend upon  $\tau$ , so the echoes are phase modulated as a function of  $\tau$ . Note that since the dephasing and rephasing periods are always equal in length the elimination of the effects of magnetic field inhomogeneity still take place, and so it is possible to detect the existence of a very small coupling  $J(AX)$  by its effect of modulation of the echoes. In fact, this kind of  $J$  modulation was first recorded for homonuclear systems in which one  $180^\circ$  pulse at time  $t = \tau$  both induces echo formation and exchanges the nuclear spin states. Figure 9 illustrates this behaviour for the  $A_2X$  spin system of 1,1,2-trichloroethane in which  $J(AX) = 5.9$  Hz and is readily resolvable, and Fig. 10 for 2,4,5-trichloronitrobenzene in which  $J(AX) = 0.4$  Hz and is normally unresolvable under the conditions of the experiment. Each trace in these figures was obtained by conventional Fourier transformation of the second half of the spin-echo generated by a different value of  $\tau$ . It is striking in Fig. 10 that whilst  $J(AX)$  is not resolved in any individual trace its effect is readily apparent when a succession of traces is considered. In this case the phase modulation of the echoes as a function of  $\tau$  is converted by the instrumental line-width into an amplitude modulation because the + x and - x components of the echoes cancel.

The next step in this process is clearly to perform the Fourier transformation as a function of  $\tau$ . When this is done using the

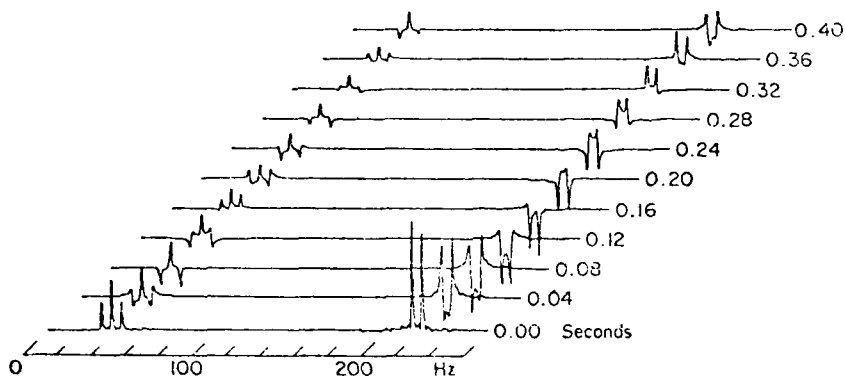


FIG. 9. Phase modulation in proton spectra of 1,1,2-trichloroethane obtained by Fourier transformation of the last half of a spin-echo obtained with  $2\tau = 20$  milliseconds. The time scale represents the duration of the Carr-Purcell sequence. From ref. 145.

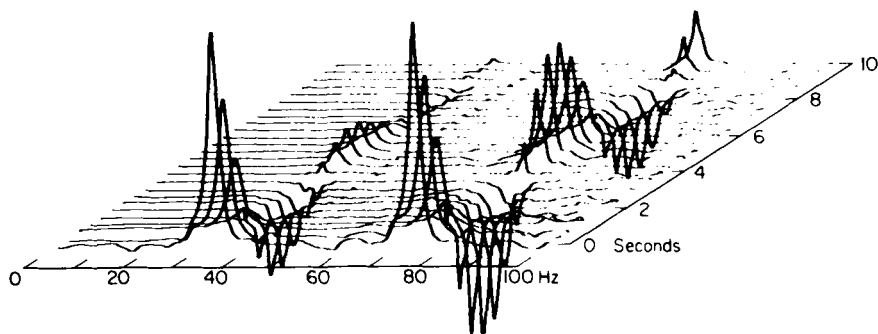


FIG. 10. Amplitude modulation of spectra obtained by Fourier transformation of the last half of a spin-echo when there is a small unresolved homonuclear spin-spin coupling constant. The spectra are from the protons in 2,4,5-trichloronitrobenzene which has a *para* coupling of 0.4 Hz. From ref. 145.

amplitude of the echo at time  $2\tau$ , a so-called *J*-spectrum results, which has extremely high resolution. Since no isolation of the individual frequencies of precession has been undertaken prior to this transformation the *J*-spectrum will contain responses from all detected nuclei, each centred about zero frequency because chemical shift effects have been eliminated. Figure 11 shows the high frequency half (the low frequency portion is its mirror image) of the *J*-spectrum obtained by transforming the spin-echo envelope from 1,1,2-trichloroethane as a function of  $\tau$ . It can be seen that there are two signals, one at 2.97 Hz

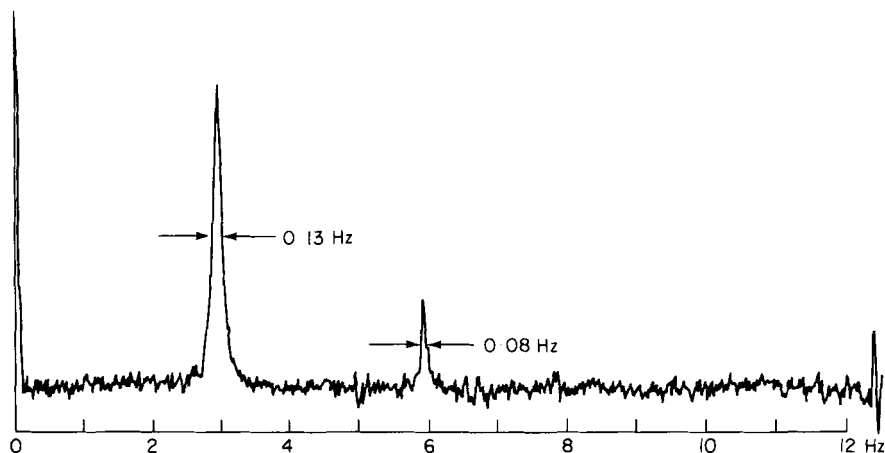


FIG. 11. *J*-spectrum obtained by Fourier transformation of the spin-echo envelope from the protons of 1,1,2-trichloroethane. The interval between echoes is  $2\tau = 40$  milliseconds and echoes have been sampled for 30 seconds. Responses are observed at 0 Hz, 2.97 Hz, and 5.94 Hz. From ref. 145.

( $= J/2$ ) from the  $\text{CH}_2$  protons and the other at 5.94 Hz from the CH proton whose resonance in a normal spectrum is a 1:2:1 triplet with outer components which precess at twice the rate of the components of the  $\text{CH}_2$  doublet. (148) In fact each spin-echo normally contains a number of different frequency components which can be separated by electronic filtration or by Fourier transformation to yield a set of  $J$ -spectra which can then be conveniently displayed in a two-dimensional plot. In practice the second approach is normally used, and thus the set of spin-echoes is subjected to a double Fourier transformation according to equation (2) in which care must be taken to combine correctly the real and imaginary transforms. (26)

$$S(\omega_1, \omega_2) = \int_0^\infty dt_1 e^{-i\omega_1 t_1} \int_0^\infty dt_2 (e^{-i\omega_2 t_2}) s(t_1, t_2) \quad (2)$$

In equation (2)  $t_1$  corresponds to the period of echo formation while  $t_2$  corresponds to the time during which the echo is sampled;  $\omega_1$  and  $\omega_2$  correspond to the dispersion within individual  $J$ -spectra and to the normal spectral spread respectively. The resulting two-dimensional spectrum  $S(\omega_1, \omega_2)$  is of course made up of real and imaginary parts according (26) to equation (3) where terms such as  $S^{cc}(\omega_1, \omega_2)$  are defined by equation (4), the superscripts s and c referring to sine and cosine respectively.

$$S(\omega_1, \omega_2) = S^{cc}(\omega_1, \omega_2) - S^{ss}(\omega_1, \omega_2) - iS^{cs}(\omega_1, \omega_2) - iS^{sc}(\omega_1, \omega_2) \quad (3)$$

$$S^{cc}(\omega_1, \omega_2) = \int_0^\infty dt_1 \cos(\omega_1 t_1) \int_0^\infty dt_2 [\cos(\omega_2 t_2)] s(t_1, t_2) \quad (4)$$

It is therefore possible to display either one of the four real components  $S^{cc}(\omega_1, \omega_2)$  etc., or to plot an absolute value spectrum  $|S|(\omega_1, \omega_2)$  defined by:

$$|S|(\omega_1, \omega_2) = [S^{cc}(\omega_1, \omega_2)^2 + S^{cs}(\omega_1, \omega_2)^2 + S^{sc}(\omega_1, \omega_2)^2 + S^{ss}(\omega_1, \omega_2)^2]^{1/4} \quad (5)$$

It should be clear from the foregoing that the two-dimensional  $J$ -spectrum of a homonuclear AX spin system subject to a non-selective  $180^\circ$  refocussing pulse should consist of four lines arranged in a  $2 \times 4$  grid. Their coordinates  $(\omega_1, \omega_2)$  are:  $J/2, \delta_A + J/2$ ;  $-J/2, \delta_A - J/2$ ;  $J/2, \delta_X + J/2$ ; and  $-J/2, \delta_X - J/2$ . For systems with second-order features there is mixing between various states and this leads to additional transitions in the two-dimensional spectrum, and diagonalization of the appropriate spin-Hamiltonian must be undertaken to determine (26) their frequencies and intensities. This has

been done by Kumar (45) and also by Freeman and his coworkers, (149) so analytic expressions are available for the AB, AB<sub>2</sub>, and ABX systems. Table I lists the frequencies and intensities of the lines of the AB system following a non-selective 180° pulse (149) and Fig. 12 shows an experimental spectrum. (149) Equation (6) gives the contribution of the magnetization component  $M_{jk}(t_1, t_2)$  to the absolute value

TABLE I

Frequencies and intensities of the lines in the two-dimensional  $J$ -spectrum of an AB spin system when both spins experience the same 180 non-selective inverting pulse (45)

Line number	$\omega_2$	$\omega_1$	Intensity
1	$\frac{1}{2}(M + J - D)$	$\frac{1}{2}(J - D)$	$(1 + \sin t) \sin t$
2	$\frac{1}{2}(M + J - D)$	$\frac{1}{2}J$	$\cos^2 t$
3	$\frac{1}{2}(M + J + D)$	$\frac{1}{2}J$	$\cos^2 t$
4	$\frac{1}{2}(M + J + D)$	$\frac{1}{2}(J + D)$	$-(1 - \sin t) \sin t$
5	$\frac{1}{2}(M - J + D)$	$-\frac{1}{2}(J - D)$	$(1 + \sin t) \sin t$
6	$\frac{1}{2}(M - J + D)$	$-\frac{1}{2}J$	$\cos^2 t$
7	$\frac{1}{2}(M - J - D)$	$-\frac{1}{2}J$	$\cos^2 t$
8	$\frac{1}{2}(M - J - D)$	$-\frac{1}{2}(J + D)$	$-(1 - \sin t) \sin t$

$$M = \delta_A + \delta_B; D = [J^2 + (\delta_A - \delta_B)^2]^{\frac{1}{2}}; J = J(\text{AB}); \cos t = (\delta_A - \delta_B)/D; \sin t = J/D$$

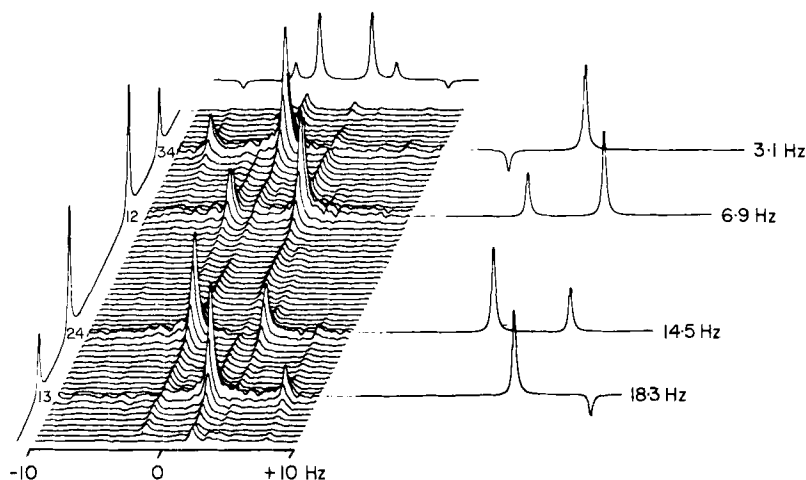


FIG. 12. Experimental absolute-value display of the two-dimensional  $J$ -spectrum of the AB spin system provided by methyl 5-nitrofur-2-carboxylate in  $(\text{CD}_3)_2\text{CO}$ . The four traces on the right are theoretical simulations with Lorentzian line-shapes. From ref. 149.

$|S|(\omega_1, \omega_2)$  of the two-dimensional spectrum for  $\omega_2 \geq 0$ .

$$|S|_{jk}(\omega_1, \omega_2) = \frac{1}{2} M_{jk}(0, 0) [1/T_{2jk}^2 + (\omega_1 - \nu_{jk})^2]^{-\frac{1}{2}} \times [1/T_{2jk}^{*2} + (\omega_2 - \omega_{jk})^2]^{-\frac{1}{2}} \quad (6)$$

where  $\omega_{jk} = \nu_j + \nu_{jk}$  and  $\nu_{jk} = 2\pi \sum_l J_{jl} m_{lk}$ . The subscripts  $k$  and  $j$  refer to the  $k$ th line of the multiplet belonging to the  $j$ th set of equivalent nuclei, and  $m_{jk}$  is the magnetic quantum number of the  $l$ th nucleus of the  $j$ th set. Evidently, responses appear in the absolute value two-dimensional spectrum only when  $(\omega_1 - \nu_{jk})$  and  $(\omega_2 - \omega_{jk}) \approx 0$  such that each multiplet line in the normal one-dimensional spectrum gives *one* line in the absolute value two-dimensional spectrum. In the case of the homonuclear AX spin system the four lines are in the positions shown in Fig. 13, and it is immediately obvious that, by projecting the spectrum on to the  $\omega_2$  axis along the direction p-q, *one* resonance is obtained for the A spin and one for the X. Consideration of equation (6) shows that this is possible for any first-order spin system in which the line separations within individual multiplets are all multiples of various coupling constants. That is, the spread along the  $\omega_1$  axis is always such that a single direction is available so that in the projected spectrum the various couplings are "masked out" (151) and the resulting spectrum has the same appearance as one produced by broadband homonuclear decoupling. This is illustrated (150) in Fig. 14 for the proton spectrum

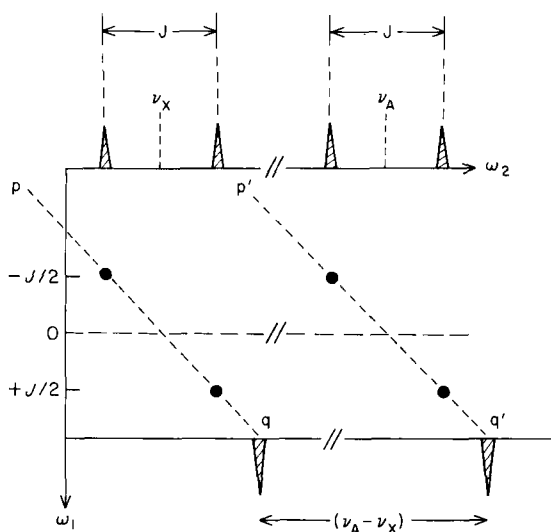


FIG. 13. Schematic illustration of the method of projecting a two-dimensional spectrum along a direction at  $45^\circ$  to the axes to achieve a simulation of broadband homonuclear decoupling.

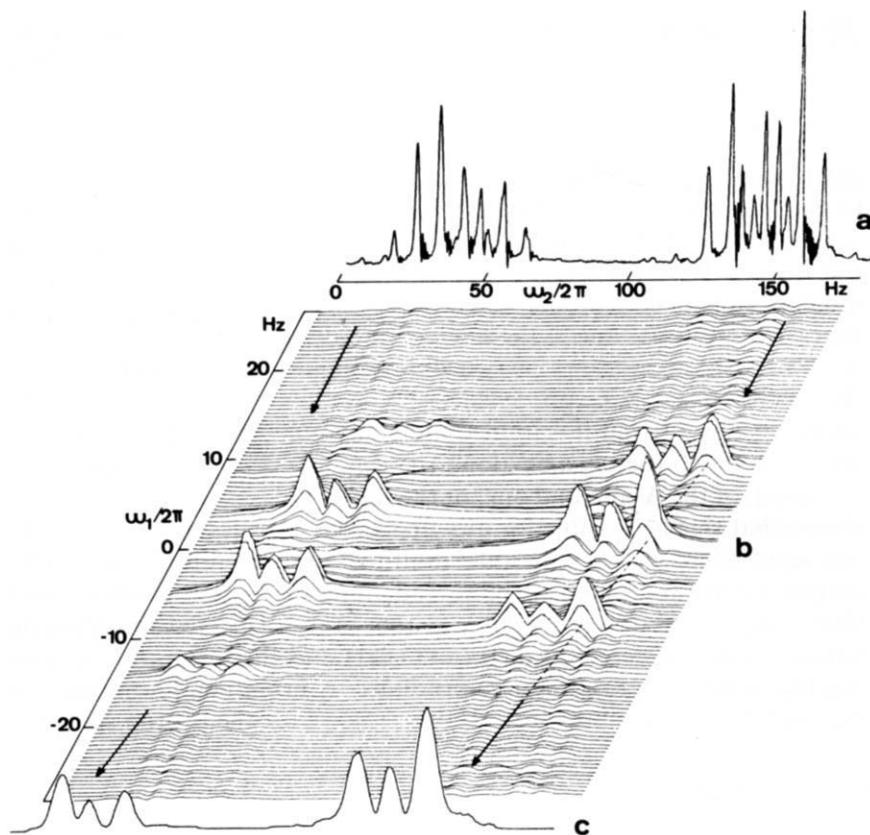


FIG. 14. Example of a two-dimensional  $J$ -resolved proton spectrum. (a) 60 MHz spectrum of a mixture of 45 vol%,  $\text{CH}_3\text{CH}_2\text{Cl}$ , 25 vol%,  $\text{CH}_3\text{CH}_2\text{Br}$ , and 30 vol%,  $\text{CH}_3\text{CH}_2\text{I}$ . (b) Two-dimensional  $J$ -resolved spectrum computed from 64 single echoes represented by 64 sample values. (c) Broad-band decoupled spectrum obtained by projecting the two-dimensional  $J$ -resolved spectrum on to the  $\omega_2$  axis. From ref. 150.

of a mixture of ethyl chloride, bromide, and iodide. It can be seen that the projected spectrum in the foreground shows peaks only at the chemical shift positions of the three kinds of  $\text{CH}_2$  and  $\text{CH}_3$  groups. Of course in this experiment the various multiplet components are really still precessing at the same rates as in an undecoupled spectrum, but the technique offers very real advantages for the study of large molecules at high fields where the one-dimensional proton spectrum is often first-order but is complicated by much overlapping. (152)

Most demonstrations of  $J$ -resolved two-dimensional spectroscopy have been heteronuclear, using  $^{13}\text{C}-\{^1\text{H}\}$  experiments, and the methods, including computer programming, by which such spectra can

be obtained have been expounded in some detail. (22) Figure 15 shows schematically a routine for the treatment of the raw data. (22) Actually, two different techniques have been used to produce the spin-echoes in heteronuclear  $J$ -resolved two-dimensional spectra, namely the experiment outlined at the beginning of this section, generally termed the "proton flip" method, which causes phase modulation of the echoes at a frequency of  $J/2$ , and the "gated decoupler" method. In this latter experiment the proton decoupler is on during the defocusing period  $t = 0 - \tau$  of the spin-echo sequence and is gated off immediately after the 180° pulse during the period  $t = \tau - 2\tau$ . (24, 26) In consequence of this at the echo maximum ( $t = 2\tau$ ) each component of the carbon multiplet

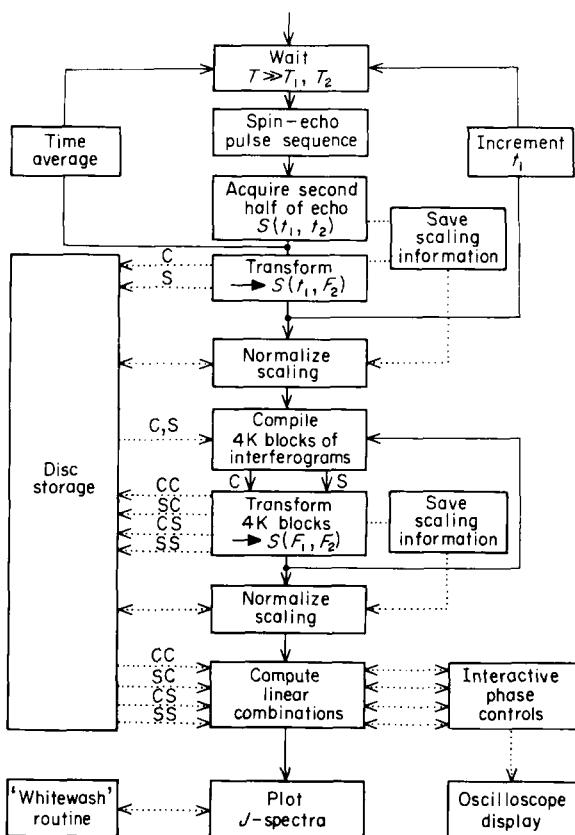


FIG. 15. A schematic diagram of the operation of a double Fourier transformation program for obtaining two-dimensional spectra. Sine and cosine transforms are represented by S and C, and the corresponding double transforms by CC, SC, CS, and SS. Operations in the sequence are represented by solid lines and information transfer by dotted lines. From ref. 22.



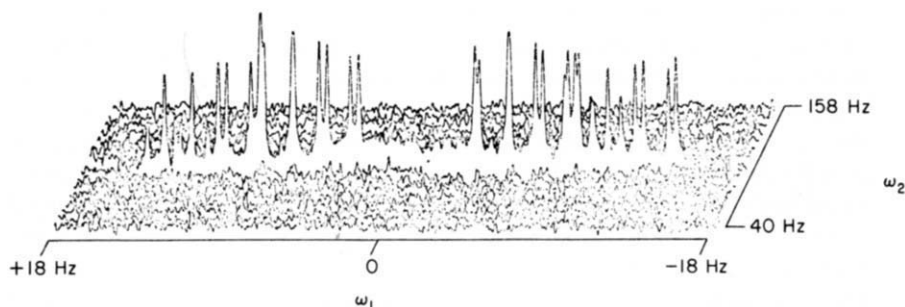


FIG. 16. A portion of the two-dimensional  $J$ -spectrum of pyridine corresponding to the C site, obtained by the "gated decoupler" method. Aliasing caused by the low sampling rate has drawn the two halves of the spectrum together by 72 Hz. From ref. 153.

has accumulated a different phase angle and the echo components are phase modulated at a frequency  $J/4$ . For systems in which the proton spectrum is first-order the two-dimensional Fourier transformation then leads to spectra that are identical for the two methods except for a scaling factor of 2 in the  $\omega_1$  dimension. However, if the proton spectrum has second-order features, the two-dimensional spectra produced by the two methods differ in a fundamental way. That produced by gated decoupling consists of multiplets which are of the same form (153) as those from conventional NMR, whereas when the proton flip method is used there are extra lines and each of the multiplets is symmetrical. In addition some lines are of negative intensity. (154) Figure 16 shows the two-dimensional  $J$ -resolved  $^{13}\text{C}$  spectrum of pyridine, obtained by the gated decoupler method, and Fig. 17 that obtained by the proton flip;

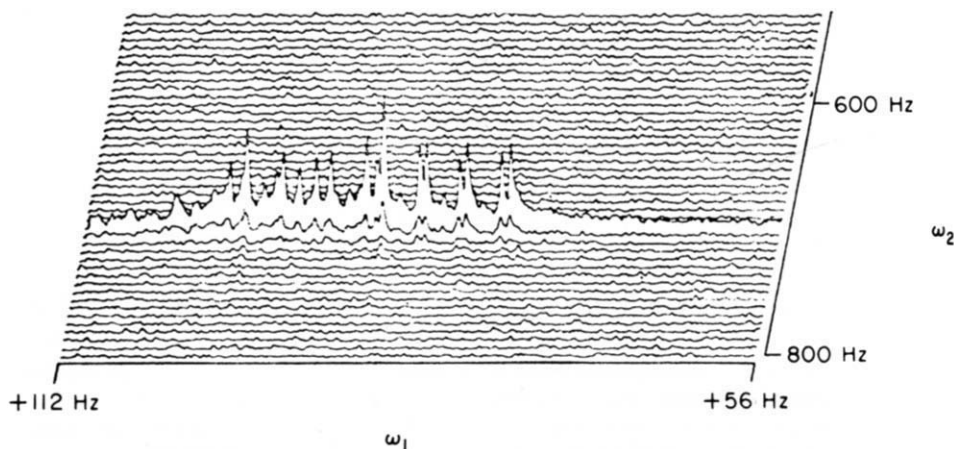


FIG. 17. Similar spectrum to that shown in Fig. 16 but obtained by the proton flip method and using different offset frequencies. From ref. 154.

the differences are quite striking. It proved to be possible to use a modified version of LAOCOON III to calculate the ABCDEX spectrum of Fig. 17 and excellent agreement is obtained. Furthermore, it is possible to use iteration to match the calculated and experimental spectra and so get values for the various  $^{13}\text{C}$ - $^1\text{H}$  coupling constants virtually identical with those already obtained from the one-dimensional spectrum. (154) In the same paper (154) analytic expressions are presented for the X part of the two-dimensional spectrum of an ABX system subject to a  $180^\circ$  AB-flip. In another demonstration of this type of experiment the "gated decoupler"  $^{13}\text{C}$ - $\{^1\text{H}\}$  two-dimensional spectrum of methyl iodide is presented; (155) a "normal" 1:3:3:1 quartet appears along one axis and responses at  $J(^{13}\text{C}-^1\text{H})/4$  and  $3J(^{13}\text{C}-^1\text{H})/4$  along the other. Another interesting feature of heteronuclear spin-echoes is that if the spectrum of the unobserved nuclear species has second-order features then it is not necessary to perturb it in order to achieve modulation of the spin-echo. (156)

The types of experiment described above are only examples of many possibilities for two-dimensional NMR spectroscopy. Ernst has

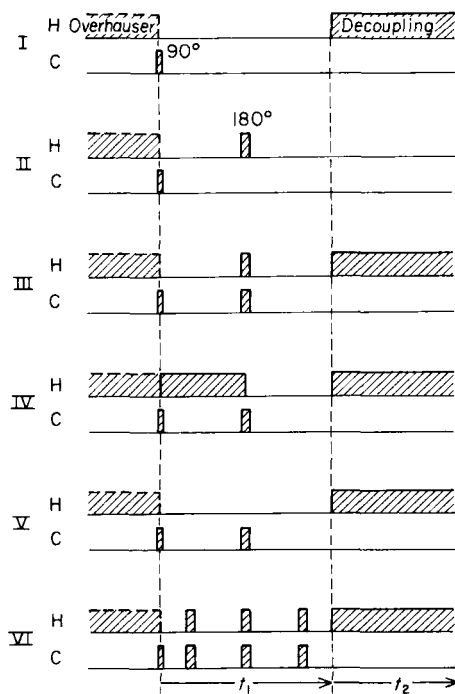


FIG. 18. Schemes for two-dimensional heteronuclear ( $^{13}\text{C}$ - $\{^1\text{H}\}$ ) spectroscopy described in the text.  $t_1$  is the time variable in the evolution period,  $t_2$  that in the detection period. From ref. 156.

presented a thorough treatment in general terms of the whole field. (26) In addition, he has surveyed some of the ways in which heteronuclear two-dimensional spectra, with particular reference to  $^{13}\text{C}-\{^1\text{H}\}$ , can be produced. (156) Figure 18 summarizes his results. The first experiment is the original two dimensional one and does not involve spin-echo formation. In it the  $^{13}\text{C}$  magnetization precesses under the influence of the complete spin Hamiltonian during the period  $t_1$  and with proton decoupling during the period  $t_2$ , as shown in Fig. 19. Thus, after double Fourier transformation with respect to  $t_1$  and  $t_2$ , responses in the  $\omega_2$  dimension are obtained only at the positions corresponding to lines in the decoupled spectrum. However, in the  $\omega_1$  dimension the full multiplet structure is displayed. This is illustrated in Fig. 20 for n-hexane (note the interchange of the  $\omega_1$  and  $\omega_2$  axes compared with Fig. 14) and is clearly an experiment of considerable potential for the organic chemist. It is possible to achieve the result of Fig. 20 in a number of other ways which do not require double Fourier transformation; these include selective excitation (23) or selective saturation. (202) Both are allied to gated decoupling and are discussed on pages 364 and 365.

In experiment II (Fig. 18) a  $180^\circ$  proton pulse is applied in the middle of the  $t_1$  period and in consequence the components of a particular  $^{13}\text{C}$  multiplet are rephased along the y-direction at a particular time  $t_1$ ; dispersal of the chemical shifts is achieved along the  $\omega_1$  axis whilst the dispersal along  $\omega_2$  depends upon the full spin-Hamiltonian including effects due to  $J(^{13}\text{C}-^1\text{H})$ . Experiment III is really the one described at the beginning of this section on two-dimensional spectra, with the addition of proton decoupling during the period of acquisition of the FID. It achieves a complete separation of chemical shifts and heteronuclear couplings in the two dimensions, provided that the

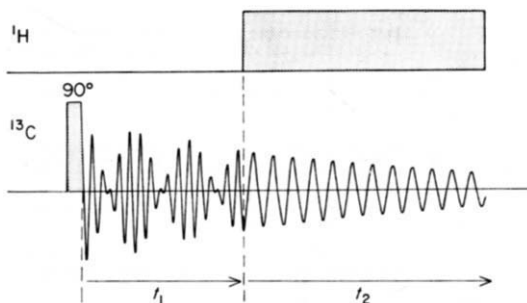


FIG. 19. Schematic representation of a simple (non-spin echo) form of two-dimensional spectroscopy.  $t_1$  is the evolution,  $t_2$  the detection period. From ref. 157.

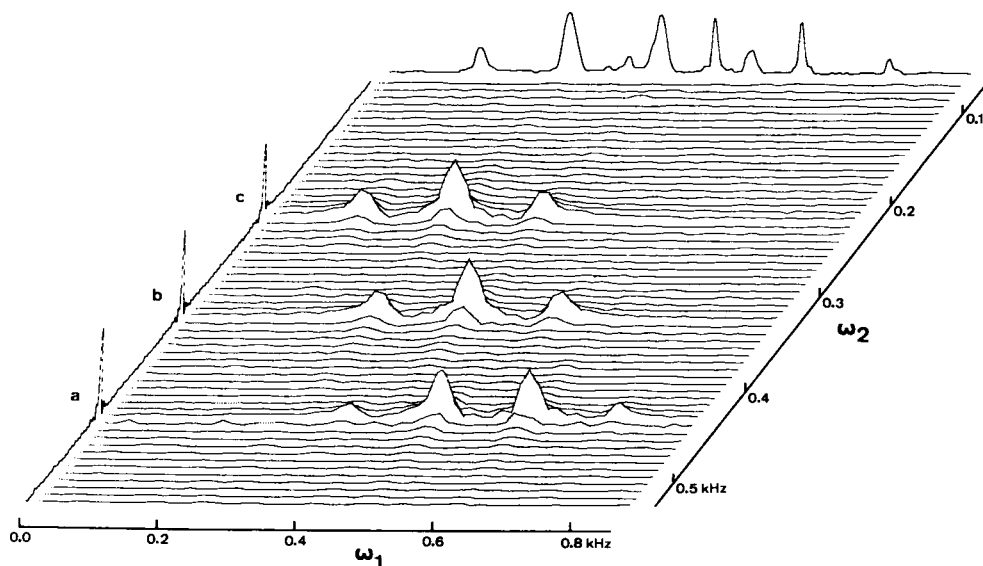


FIG. 20. Two-dimensional resolved  $^{13}\text{C}$  spectrum of n-hexane recorded with the technique indicated in Fig. 19. Twenty-two experiments were co-added for each of the 64 values of  $t_1$  between 0 and 35 ms. Resolution is severely limited by the  $64 \times 64$  data matrix used to represent the two-dimensional Fourier transform. The absolute values of the Fourier coefficients are plotted. The uncoupled one-dimensional spectrum is indicated along the  $\omega_1$  axis, and the proton-decoupled spectrum is shown along the  $\omega_2$  axis. From ref. 157.

interproton interactions are weak, i.e. provided that the proton spectrum is first-order. The same result is attained by experiment IV except that in this case the separation of coupling constants and chemical shifts occurs even if the proton spectrum is tightly coupled. Finally, experiment V permits the effects of heteronuclear echo modulation to be observed, and VI is an echo-train experiment (i.e. a form of Carr–Purcell sequence) in which diffusion effects are substantially eliminated and extremely high resolution can be achieved along the  $\omega_1$  direction. Indeed, it should be mentioned that most of the experiments treated in this section can be performed either in an echo-train mode, or in the simpler manner already described.

It will have been noticed [equations (3) and (5)] that although the absolute value mode is often used to display two-dimensional spectra it should in principle be possible also to get pure absorption mode spectra by a suitable combination of the individual computed sine and cosine transforms. This is of course highly desirable because the absolute value mode spectra can suffer from much line broadening especially at the base of the peaks. However, in the absence of any

mixing pulse which separates the two time periods—the evolution ( $t_1$ ) and the detection ( $t_2$ )—of the normal two-dimensional experiment the particular phase component of the signal which is actually observed depends upon the setting of the phase-sensitive detector of the spectrometer used. It is not generally possible to calculate the coefficients of the sine and cosine functions needed to give a pure absorption spectrum. This problem has been solved in two different ways, both of which yield signals containing the necessary phase information. (158) The first of these has been termed Phase Separation by Reversed Precession and involves the application of a suitable  $180^\circ$  mixing pulse to the carbon spins which is  $90^\circ$  out of phase with the initial  $90^\circ$  exciting pulse. This mixing pulse is applied at time  $t = t_1$  (i.e. at the beginning of collection of the FID) and it is necessary to collect data from a “normal” (i.e. without the mixing pulse) experiment as well. The two responses  $S(t_1, t_2)$  normal and  $\bar{S}(t_1, t_2)$  “reversed” are then linearly combined and transformed according to equation (7) to produce the phase-corrected two-dimensional spectrum, which may be of the  $J$ -resolved or the  $\delta$ -resolved type according to the nature of the pulsing scheme.

$$\begin{aligned} \tilde{S}(\omega_1 > 0, \omega_2 > 0) \\ &= \frac{1}{4} [\mathcal{F}_{cc}\{S(t_1, t_2) + \bar{S}(t_1, t_2)\} - \mathcal{F}_{ss}\{S(t_1, t_2) - \bar{S}(t_1, t_2)\}] \\ \tilde{S}(\omega_1 < 0, \omega_2 > 0) \\ &= \frac{1}{4} [\mathcal{F}_{cc}\{S(t_1, t_2) + \bar{S}(t_1, t_2)\} + \mathcal{F}_{ss}\{S(t_1, t_2) - \bar{S}(t_1, t_2)\}] \end{aligned} \quad (7)$$

where  $\mathcal{F}_{cc}$  and  $\mathcal{F}_{ss}$  represent cosine and sine Fourier transformations respectively.

In the second method for phase separation it is necessary to apply  $90^\circ$  phase-shifted phase selection pulses between the evolution and detection periods and to measure the two quadrature components which evolve after the application of these pulses. The normal  $[S(t_1, t_2)]$  and “shifted”  $[\bar{S}(t_1, t_2)]$  responses are then combined according to equation (8) to give the pure absorption two-dimensional spectrum. It will be noticed that the main computational difference between the two methods is that in the first the normal and changed signals are combined prior to transformation, whereas in the second the combination is done after transformation. It seems likely that techniques of this type will become widely used for the production of high quality two-dimensional spectra in molecules of real chemical interest.

$$\begin{aligned}\tilde{S}(\omega_1 > 0, \omega_2 > 0) &= \frac{1}{2}\{S^{cc}(\omega_1, \omega_2) + \bar{S}^{ss}(\omega_1, \omega_2)\} \\ \tilde{S}(\omega_1 < 0, \omega_2 > 0) &= \frac{1}{2}\{S^{cc}(\omega_1, \omega_2) - \bar{S}^{ss}(\omega_1, \omega_2)\}\end{aligned}\quad (8)$$

It is mentioned several times in this review that many of the pulsing schemes used to effect population transfer and produce two-dimensional spectra lead to a transfer of *transverse* magnetization but not of *net* longitudinal magnetization. In other words, the various lines of a spin multiplet become polarized with opposite signs and so the total integrated signal intensity is zero, as exemplified by Fig. 7. This is very important, because it prevents the production of two-dimensional spectra that are completely decoupled in both dimensions. The problem has been solved by Ernst and his coworkers (159) who have devised heteronuclear pulsing schemes which perturb simultaneously the *I* and the *S* spins during the mixing period of the experiment. The method, which requires the least critical adjustment of the experimental conditions, is to apply 90° pulses to the *I* and *S* spins during the mixing period. This produces a *net* transfer of magnetization and gives either *S* or *I* spin decoupling according to the timing. Furthermore, by presaturation of one set of spins it is possible to achieve decoupling in both dimensions, so that  $^{13}\text{CH}_3\text{I}$  for example then gives a two-dimensional spectrum consisting of a single line (Fig. 21). This is clearly of immense value for the correlation of proton and carbon chemical shifts in complex molecules. A disadvantage of this method is that it does not yield pure absorption spectra. It is possible to get these by having an overlap of the *S* and *I* spin decoupling times during the mixing period. It is then important to adjust the amplitudes of the two rf fields so that the Hartmann–Hahn condition  $\gamma_s B_s = \gamma_I B_I$  is satisfied. If this is done precisely, transient oscillations lead to a *net* transfer of magnetization in the rotating frame.

Bodenhausen and Freeman (160) have managed to avoid the complications of some of the above experiments but have obtained similar results by adopting various artifices. If the decoupling power is deliberately inadequate during the decoupling period, the multiplet components of opposite sign are close together but do not cancel. By a suitable choice of digitization interval it is then possible to plot a transformed two-dimensional spectrum in which the residual splittings are not resolved so that the absolute value spectrum has the appearance of a decoupled one obtained at rather poor resolution. Alternatively one may adapt the process of *J*-scaling (161) and adjust the timing of the pulses so that the refocussing of precessing vectors associated with different spin states is not exact. There is again a residual splitting in the spectrum which prevents the cancellation of the multiplet components

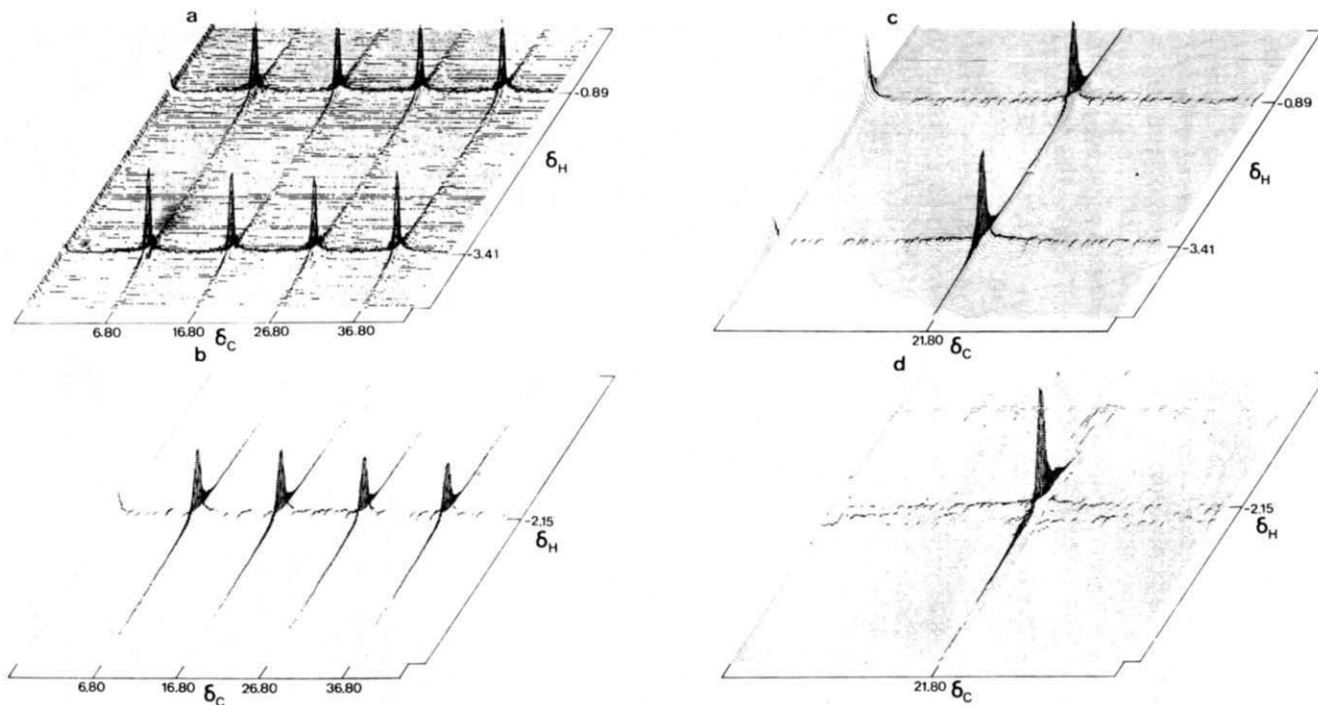


FIG. 21. Heteronuclear two-dimensional spectra of  $^{13}\text{C}$  methyl iodide cross-correlating proton and carbon spectra by direct observation of proton resonance and magnetization transfer by pulse-interrupted free precession. (a) No decoupling. (b) With carbon decoupling (frequency-modulated decoupling field). (c) With proton decoupling (CW decoupling). (d) With simultaneous proton and carbon decoupling. Line positions are indicated in parts per million from TMS (negative shifts are to high frequency). From ref. 159.

of opposite sign. Suitable adjustment of the digitization prevents any splitting from being visible in the final spectrum.

A spin-echo is produced when an exciting pulse is followed by a refocusing one, and these two pulses are usually applied at the same frequency. However, if the pulses are applied at different frequencies, magnetic order may be transferred from one transition to another to generate a "coherence transfer echo". (162) If the transfer is from a multiple quantum transition, a "multiple quantum transfer echo" is formed. This may be a good way of detecting (forbidden) multiple quantum transitions. Of more immediate relevance to the present review is the possibility of getting a "heteronuclear transfer echo". This has been achieved (162) in some experiments on  $^{13}\text{C}$ -enriched methyl iodide. The echo is generated at time  $4\tau$  [in general  $\tau\gamma(\text{X})/\gamma(\text{A})$ ] by applying simultaneous  $90^\circ$  proton and carbon pulses at time  $\tau$  following a  $90^\circ$  carbon pulse. The  $^{13}\text{C}$  echoes are modulated as a function of  $\tau$ , and the two-dimensional transformed spectrum has high resolution along a direction which is a function of  $\gamma(\text{A})/\gamma(\text{X})$  instead of along the  $\omega_1$  axis.

As is to be expected in any new technique there are a number of instrumental difficulties associated with two-dimensional NMR spectroscopy which must be solved before the method becomes routine. Some of these have been looked at carefully by Freeman and his coworkers (163) and a four-part sequence involving alternations of the phases of the receiver reference and the refocusing pulses has been devised for eliminating the effects of imprecise setting of the  $90^\circ$  and  $180^\circ$  spin-flip angles and of spatial inhomogeneity of the rf fields. These effects usually lead to spurious responses which are termed "ghosts" and "phantoms" according to their origin; the sequence for eliminating them is called the "exorcycle". It has been applied to the two-dimensional spectrum of methyl iodide. (163)

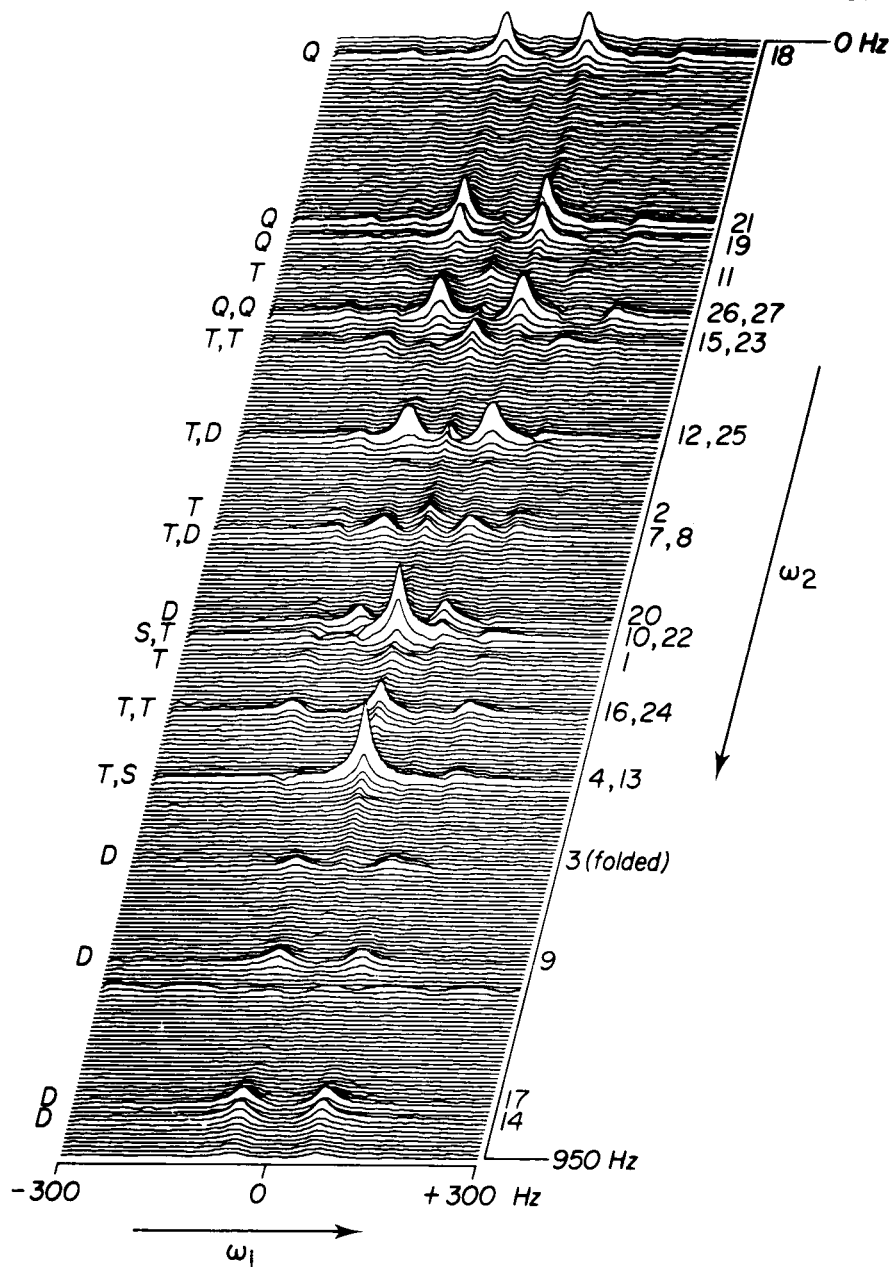
It is important to realize that double Fourier transformation is not an essential part of two-dimensional NMR spectroscopy. This was made clear by Ernst in his early article (26) and when the spin system is simple there may be no particular advantage in using it. This approach was adopted in studies of  $^{13}\text{C}$ -enriched methyl formate in which various selective  $^1\text{H}$  and/or  $^{13}\text{C}$  pulses were applied to individual transitions and it was found possible to deduce an accurate value for  $\nu(^{13}\text{C})$  and draw conclusions about relaxation behaviour. (164–166) Detailed analysis (167) also shows that the sensitivity of two-dimensional Fourier transform spectroscopy can be as good as half that achieved in ordinary one-dimensional experiments. In this connection we should note that the time-saving gain of Fourier transformation



really applies only to the  $t_2/\omega_2$  dimension since it is still necessary to perform a set of individual experiments to achieve the spread along the  $t_1/\omega_1$  axis.

Although it is early days yet, there have been a few applications of spin-echo and two-dimensional experiments to systems of chemical interest, and it is convenient to deal with these here. One of the problems in very complex proton spectra is that of establishing pairs of coupled resonances. Several of the available double resonance methods make it difficult to be clear about the multiplicity of particular resonances, even when difference spectroscopy is used. (168) An ingenious way (169) of dealing with this is to use the fact that for  $\tau = 1/J$  in a standard  $90^\circ\text{--}\tau\text{--}180^\circ$  spin-echo experiment first-order doublets have inverted phase while singlets and the central components of triplets have normal phase. If selective decoupling is then applied up to the time when data acquisition begins and a difference spectrum is recorded, it contains only the resonances affected by the double resonance experiment but does not suffer from having the spikes and other spurious responses which can easily arise if the homonuclear decoupling field is on during data acquisition.

A particularly impressive application of  $J$ -resolved spectroscopy is the presentation of the two-dimensional  $^{13}\text{C}$  spectrum of cholesterol. (170) Even though this was obtained at only 20 MHz the overlapping of resonances was almost completely avoided and the one-bond  $^{13}\text{C}\text{--}^1\text{H}$  splitting patterns of quartet, triplet, doublet, or singlet were clearly displayed along the  $\omega_1$  axis. In this work 800 echoes were recorded for each of 64 values of  $t_1$  to yield a  $64 \times 512$  data matrix in 16 hours. This spectrum is shown in Fig. 22, and the relatively coarse digitization along the  $\omega_1$  axis prevents any confusion from the longer range  $^{13}\text{C}\text{--}^1\text{H}$  splittings. Proton and carbon chemical shifts were correlated in menthone and in camphor by recording the two-dimensional  $^{13}\text{C}\text{--}\{^1\text{H}\}$  spectra (171) in which responses arise as a result of both the one-bond and longer range couplings. A number of complex molecules including proteins and amino-acids have been studied at high field where two-dimensional techniques seem to be particularly appropriate. (152, 172) Finally, the high resolution in the  $\omega_1$  dimension, due to the elimination of the effects of magnetic field inhomogeneity, has been utilized for the determination of  $^{13}\text{C}\text{--}^{13}\text{C}$  coupling constants in enriched samples. (173) Under conditions of complete proton decoupling the homonuclear spin-echoes generated by a  $90^\circ\text{--}\tau\text{--}180^\circ$  pulse sequence are modulated by  $J(^{13}\text{C}\text{--}^{13}\text{C})$  and so the two-dimensional spectrum exhibits these splittings along the  $\omega_1$  dimension. Benzyl alcohol and alanine have been studied and couplings as small as 0.8 Hz resolved.



#### D. Triple resonance

Experiments of this type range from straightforward simultaneous decoupling by irradiating at two different radio frequencies to ones in which both irradiating fields are of a magnitude to produce only spin-tickling or population transfer effects. They can be wholly homonuclear, mixed homo-heteronuclear, or wholly heteronuclear, and are usually designated by  $A-\{M, X\}$ . The commonest experiments are of course those in which at least one of the irradiating rf fields is of decoupling magnitude. These are mentioned in the appropriate part of Section VII. Their interpretation is usually the same as for normal double resonance experiments, although some of the possible ramifications of the nuclear Overhauser effect in this kind of work do not appear to have been exploited yet. When both irradiating rf fields are applied selectively the interpretation becomes more complicated. Such experiments can then be used to get otherwise inaccessible information, for example from incomplete spin systems in which certain coupling constants are zero. In  $A_p M_q X_r$  and related spin systems with  $J(AM) \neq 0$ ,  $J(MX) \neq 0$ , and  $J(AX) = 0$  it is not possible to perturb the A spectrum by irradiating at the resonant frequency of X. This makes it impossible to use  $A-\{X\}$  double resonance experiments to determine the chemical shift of X or to get the relative signs of  $J(AM)$  and  $J(MX)$ . However, irradiation of X transitions affects the M spectrum, and these effects are transmitted to the A spectrum by simultaneous irradiation at the M resonant frequency which can thus be determined. The simplest experiment is to adjust  $\nu(M)$  and  $\gamma(M)B_2$  until partial collapse of the splitting due to  $J(AM)$  is achieved in the A spectrum.  $\nu(X)$  can then be varied through an appropriate range until the M spectrum is perturbed, and since this destroys the previously established M resonance condition the effect is noticed in the A spectrum. This method was first applied (174, 98) to the measurement of  $^{77}\text{Se}$  chemical shifts in organophosphorus selenides in which  $J(^{77}\text{Se}-^1\text{H}) = 0$  and has since been used to determine  $^{183}\text{W}$ ,  $^{14}\text{N}$ ,  $^{63/65}\text{Cu}$ , and  $^2\text{D}$  shieldings in like circumstances. (99, 175, 109, 176) A variety of ways can be envisaged displaying the results of such experiments, and two kinds of triple resonance INDOR have been described. (109) The MINDOR (Modified INDOR) spectrum is obtained by recording an  $A-\{M\}$  INDOR spectrum under some particular steady-state conditions of simultaneous irradiation in the X spectrum; it generally shows additional splittings. The TINDOR (Transferred INDOR) spectrum is obtained by monitoring a chosen point in the A spectrum under conditions of steady-state simultaneous irradiation in the M spectrum and sweeping  $\nu(X)$ ; it resembles the  $M-\{X\}$  INDOR spectrum. Examples of both types of spectrum have

been obtained (109) from the  $[(\text{MeO})_3\text{P}]_4\text{Cu}^+$  ion ( $A = {}^1\text{H}$ ,  $M = {}^{31}\text{P}$ ,  $X = {}^{63}\text{Cu}$ ) in which tetrahedral symmetry at copper largely eliminates the effects of quadrupolar relaxation. The TINDOR spectrum is shown in Fig. 23.

The other reported applications of fully selective triple resonance are to the determination of the relative signs of  $J(\text{AM})$  and  $J(\text{MX})$  in the  $A_pM_qX_r$  spin system with  $J(\text{AX}) = 0$ . This experiment is based on exactly the same principles as the homonuclear one first described (177) in 1963, and the only differences, when it is applied to the fully heteronuclear case, are ones of technique although it may be pointed out that in this case measurement at a lower field strength would not introduce the second-order features which make possible the relative sign determination. The basic difficulty is that transitions in the A spectrum associated with different spin states of X are degenerate, but this degeneracy may be lifted by weak (spin-tickling) irradiation of *one* of the non-degenerate M transitions. The  $A-\{X\}$  experiment then succeeds and can be interpreted in the usual way; that is, it is determined which A and X transitions are associated with a particular spin state of M, which immediately gives the relative signs of  $J(\text{AM})$  and  $J(\text{MX})$ . The first completely heteronuclear system to which this method was applied was  $(\text{CH}_3\text{O})_3\text{PBH}_3$ , in which  ${}^4J({}^{11}\text{B}-{}^1\text{H})$  is vanishingly small. (178) Although there are complications due to the  ${}^{11}\text{B}$  nuclear quadrupole moment and the splitting due to  ${}^1J({}^{11}\text{B}-{}^1\text{H}) = \text{ca. } 100 \text{ Hz}$ , (179) it proved possible by selective  ${}^{31}\text{P}$  irradiation to remove the degeneracy of the methyl proton transitions associated with different spin states of  ${}^{11}\text{B}$  and so use the effects of  ${}^{11}\text{B}$

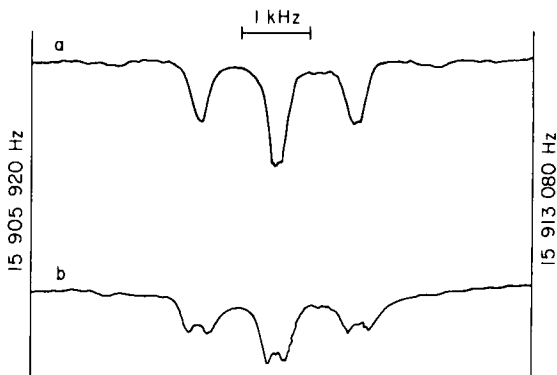


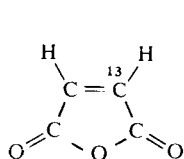
FIG. 23. Copper-63 TINDOR spectra of  $[(\text{CH}_3\text{O})_3\text{P}]_4\text{Cu}^+$  obtained by monitoring the proton spectrum with continuous irradiation of a component of the  ${}^{31}\text{P}$  spectrum. (a) Inner component irradiated. (b) Outer component irradiated. From ref. 109.

irradiation to compare the signs of  $^3J(^{31}\text{P}-^1\text{H})$  and  $^1J(^{31}\text{P}-^{11}\text{B})$ . Other systems studied in this way include:  $(\text{MeO})_3\text{PSe}$  [ $\text{A} = ^1\text{H}$ ,  $\text{M} = ^{31}\text{P}$ ,  $\text{X} = ^{77}\text{Se}$ ] to get the relative signs of  $^3J(^{31}\text{P}\cdots^1\text{H})$  and  $^1J(^{77}\text{Se}-^{31}\text{P})$ ; (100)  $\text{CF}_3\text{AuPMePh}_2$  [ $\text{A} = ^1\text{H}$ ,  $\text{M} = ^{31}\text{P}$ ,  $\text{X} = ^{19}\text{F}$ ] to get the relative signs of  $^2J(^{31}\text{P}\cdots^1\text{H})$  and  $^3J(^{31}\text{P}\cdots^{19}\text{F})$ ; (180) and the homo/hetero system  $[p\text{-MeC}_6\text{H}_4\text{CH}_2\text{PPh}_3]^+\text{Br}^-$  [ $\text{A} = ^1\text{H}$ ,  $\text{M} = ^{31}\text{P}$ ,  $\text{X} = ^1\text{H}$ ] to get the relative signs of  $^2J(^{31}\text{P}\cdots^1\text{H})$  and  $^7J(^{31}\text{P}\cdots^1\text{H})$ . (181)

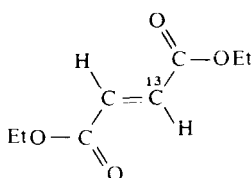
### E. The assignment of $^{13}\text{C}$ spectra

To the organic chemist this is a very important area, and considerable effort has gone into the development of double resonance techniques which can aid  $^{13}\text{C}$  assignments in the spectra of complex molecules. The very simplicity that is introduced by complete proton decoupling is itself an obstacle to assignment in many cases since it represents a serious (deliberate) loss of information. The earliest approach to this problem was to use off-resonance noise decoupling so that only carbons without any attached protons give sharp singlets which are readily identified. (182) It was soon realized that the loss in intensity from carbons bearing at least one proton was due partly to transfer of noise from the proton irradiating field by off-resonance effects; thus, if coherent CW off-resonance irradiation is used each carbon appears as a singlet, doublet, triplet, or quartet according to whether it has zero, one, two, or three protons. In addition all splittings are reduced to a few per cent of these normal values so that the longer range proton-carbon couplings are unresolved. (183, 184) These experiments actually suffer from a variety of disadvantages including the production of abnormal intensity patterns (especially for the triplets arising from the carbons of  $\text{CH}_2$  groups where the outer components are often abnormally weak) and residual splittings whose size depends upon the degree of offset. A particularly serious situation arises when the  $\text{CH}_2$  group has inequivalent protons. Then the  $^{13}\text{C}$  is the X part of an ABX spin system and under conditions of poor signal-to-noise ratio its residual splitting may be mistaken for a doublet. This has been looked into in some detail (185) and the effects of different degrees of off-resonance decoupling of the AB protons have been examined. Experimental confirmation of the main conclusions was obtained (185) and the AA'X spin systems provided by [2] and [3] were studied. (186) It is thus shown to be possible to obtain the relative signs of  $J(\text{AX})$  and  $J(\text{A}'\text{X})$  from  $^{13}\text{C}-\{^1\text{H}\}$  off-resonance experiments. It has even been suggested that this kind of experiment could be used to "fingerprint" complex molecules. (187) This kind of behaviour is really an example of deceptive simplicity arising when the residual splitting is

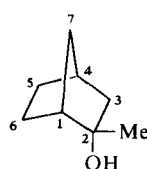
comparable to the interproton couplings and is strictly analogous to the “phenomenon” of virtual coupling. It has also been observed in 1,2-dichloroethane, (188) poly-(*cis*-butadiene), (188) and 2-methylnorbornan-2-ol [4]. (189) Indeed in the last molecule it is put to good use since it makes possible the assignment of the different types of methylene group. It is found that the  $^{13}\text{C}$  residual triplet is well resolved if the two  $^1J(^{13}\text{C}-^1\text{H})$  couplings are of similar magnitude (and sign!) but is considerably broadened if the neighbouring protons are strongly coupled to the directly bound ones. In fact, C-3 and C-4 give sharp triplets while C-5 and C-6 provide only broad poorly resolved multiplets. (189)



[2]

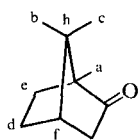


[3]



[4]

More recently an elegant solution to the problem of getting well defined multiplets in  $^{13}\text{C}$  NMR spectra, under conditions of partial proton decoupling, has been devised. (161) This is known as “*J*-scaling” and leads to spectra in which all multiplet components have their normal intensities but all the splittings are reduced by any desired factor which is the same for each carbon. Typically a scaling factor of 30 is found convenient since then the residual one-bond  $^{13}\text{C}$ – $^1\text{H}$  splittings are reduced to 4–7 Hz and the longer range ones to <0.5 Hz when they are not resolved. The  $^{13}\text{C}$  magnetization prior to data collection is allowed to precess for part of the time with and part of the time without proton decoupling. The scaling factor is then controlled by the relative lengths of these two periods. It will be appreciated that no double Fourier transformation is required to present the resulting spectrum, although it is necessary to apply a sequence of refocusing  $180^\circ$  carbon pulses with suitable gating of the receiver to get a complete interferogram in a reasonable period of time. Figure 24 shows the excellent spectrum obtained in this way from camphor [5] using a



[5]

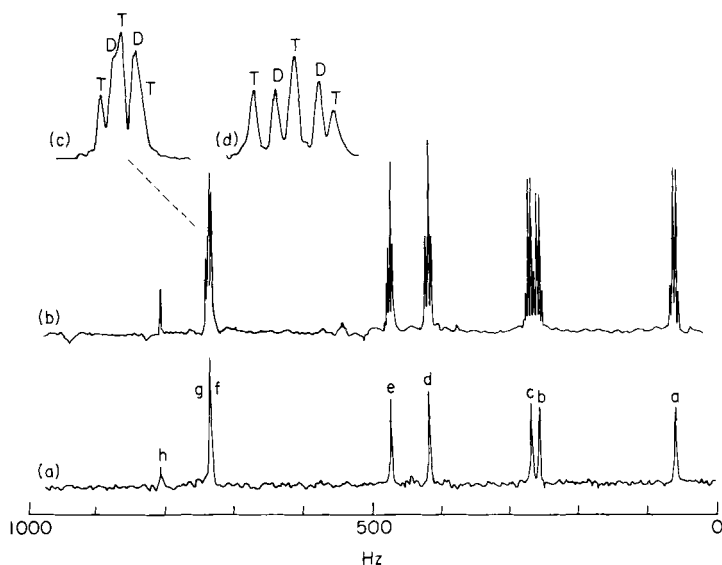


FIG. 24. Part of the carbon-13 spectrum of camphor. (a) Noise decoupled. (b) With the proton splittings scaled down by a factor of 30. Inset (c) shows the detail of an overlapping doublet and triplet, while inset (d) shows the same region with the splittings scaled down 15 times in order to identify the doublet (D) and triplet (T) components. From ref. 161.

scaling factor of 30. An alternative way of producing the same result is to use a refocusing  $180^\circ$  proton pulse close to, but not exactly at, the mid-point of the period between the initial  $^{13}\text{C}$   $90^\circ$  pulse and data collection. The degree of mistiming of the proton pulse then determines the scaling factor. (161)

In an off-resonance  $^{13}\text{C}-\{^1\text{H}\}$  decoupling experiment the residual splitting,  $J_R$ , is related to the original splitting,  $J_O$ , by Ernst's (190) equation:

$$J_R = [(\Delta\nu - \frac{1}{2}J_O)^2 + (\gamma B_2/2\pi)^2]^{\frac{1}{2}} - [(\Delta\nu + \frac{1}{2}J_O)^2 + (\gamma B_2/2\pi)^2]^{\frac{1}{2}} \quad (9)$$

in which  $\Delta\nu$  is the proton frequency offset from exact resonance and  $\gamma B_2/2\pi$  is the amplitude of the proton irradiating field in frequency units. If the condition  $\gamma B_2/2\pi \gg |\Delta\nu|$  is fulfilled then equation (9) simplifies to equation (10). This is of course a linear relationship which can be used to correlate proton and carbon chemical shifts in quite complex molecules. (191)

$$\Delta\nu = \gamma B_2 J_R / 2\pi J_O \quad (10)$$

This is illustrated in Fig. 25 which shows a  $^{13}\text{C}-\{^1\text{H}\}$  study of nicotinamide adenine dinucleotide. A particular value of  $\gamma B_2/2\pi$  is

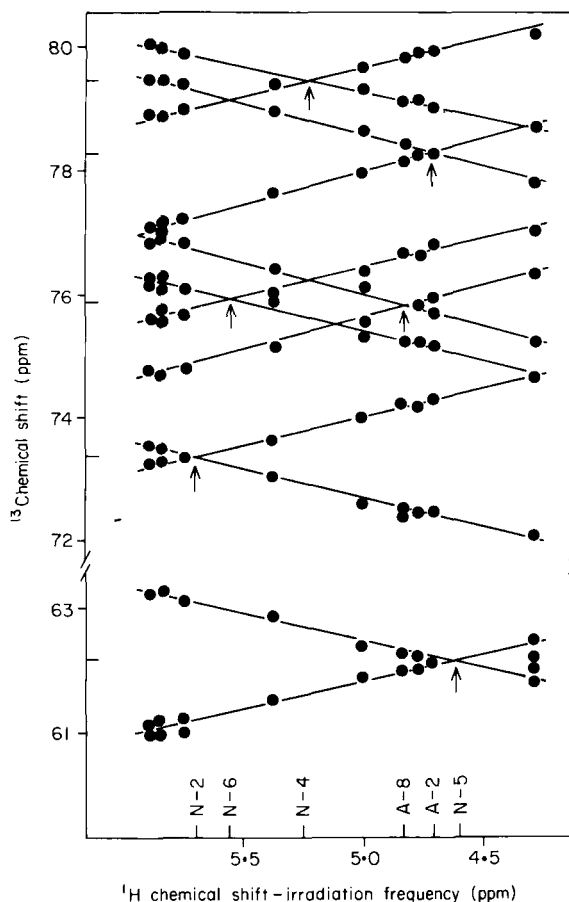


FIG. 25. Plot of peak frequencies in the  $^1\text{H}$  off-resonance selectively decoupled  $^{13}\text{C}$  spectra of  $\text{NAD}^+$  as a function of position of irradiation in the  $^1\text{H}$  spectrum, expressed in ppm to high frequency of internal dioxan. The positions of the peaks in the  $^1\text{H}$  noise-decoupled  $^{13}\text{C}$  spectrum are shown by lines on the ordinate, and the positions of the proton peaks by lines on the abscissa. The arrows indicate the point of collapse of the  $^{13}\text{C}$  doublet and the connection between a given  $^{13}\text{C}$  peak and the assigned proton peak. The errors in the position measurements of the  $^{13}\text{C}$  peaks are indicated by the size of the points, except near the cross-over positions where the errors are larger ( $\pm 0.15$  ppm). Small doublet splittings are observed on some of the signals from long-range (C-H) spin-coupling interactions. From ref. 191.

chosen and the irradiating frequency is then moved through the proton spectrum, the positions of the  $^{13}\text{C}$  resonances being plotted for each setting of  $\Delta\nu$ . It is then possible to connect the points on the graph by a series of straight lines of slope proportional to  $\pm B_2$  and from their intersections to deduce the proton chemical shifts associated with the decoupled  $^{13}\text{C}$  resonances. (191)



Although this method is very satisfactory when the range of proton chemical shifts is small, the deviations from linearity of equation (10), which occur when this is not so soon becomes serious. It is however possible to rearrange Ernst's equation in a number of different ways which avoid this difficulty. One of the most widely used methods is Pachler's (192) in which equation (11) is used. This requires the less stringent condition,  $\gamma B_2/2\pi \gg \frac{1}{2}|J_O - J_R|$ .

$$\Delta v = \gamma B_2 J_R / 2\pi (J_O^2 - J_R^2)^{\frac{1}{2}} \quad (11)$$

Thus by plotting  $\Delta v$  against  $J_R/(J_O^2 - J_R^2)^{\frac{1}{2}}$  a straight line is obtained for a wide range of values of  $\Delta v$ . It is possible simply to obtain a single off-resonance spectrum and use this in conjunction with equation (11) provided that accurate values of  $J_O$  are available. (193) Another way of looking (194) at this situation is to rearrange equation (9) to give equation (12). Equation (11) then approximates to this provided that  $\gamma B_2/2\pi \gg \frac{1}{2}(J_O^2 - J_R^2)^{\frac{1}{2}}$ . Since  $(J_O^2 - J_R^2)^{\frac{1}{2}} > (J_O - J_R)$  this is a more restrictive condition than that suggested by Pachler (192) and implies that his method is rather less general than originally supposed. It is further possible to rearrange:

$$\Delta v = J_R [(\gamma B_2/2\pi)^2 + \frac{1}{4}(J_O^2 - J_R^2)]^{\frac{1}{2}} / (J_O^2 - J_R^2)^{\frac{1}{2}} \quad (12)$$

to give

$$\Delta v [1 - J_R^2/(2\Delta v)^2]^{\frac{1}{2}} = \gamma B_2 J_R / 2\pi (J_O^2 - J_R^2)^{\frac{1}{2}} \quad (13)$$

which evidently approximates to equation (11) under the condition  $|\Delta v| \gg \frac{1}{2}|J_R|$ . This last condition contains only the actual observables of the experiment, hence the circumstances under which it is permissible to use equation (11) are more readily appreciated. (194)

In many cases one finds that considerably more off-resonance experiments are performed than are strictly necessary. This is clearly a considerable waste of spectrometer time when weak samples are involved. In fact two separate coherent experiments will always suffice (195) provided that the decoupler power is known with precision. It is then necessary to solve a quartic equation. Since this will probably be done by iteration it may be helpful to perform one or two additional off-resonance experiments so that spurious solutions can be rejected.

In off-resonance decoupling experiments of this type difficulties may arise for certain levels of the decoupling power, since then the combined effects of spin-tickling and spin population transfer may lead to certain important lines having very low intensity. It has therefore been suggested (196) that the amplitude of the irradiating rf field used should

be  $\gamma B_2/2\pi \approx 3J_O$ . At higher power levels the sensitivity to changes in  $\Delta\nu$  is rather small, and at lower levels unduly complex spectra may be produced.

All the foregoing experiments depend upon having a means of setting the proton offset frequency with sufficient precision, say  $\pm 10$  Hz or better. On certain "low-cost" spectrometers this may not be possible. It is then convenient to use (197) equation (14) to relate the residual splitting to  $\gamma B_2/2\pi$ .

$$J_R/(J_O^2 - J_R^2)^{\frac{1}{2}} = 2\pi \Delta\nu/\gamma B_2 \quad (14)$$

This equation is valid provided that  $\gamma B_2/2\pi \gg \frac{1}{2}|J_O - J_R|$ , and its advantage is that by plotting  $J_R/(J_O^2 - J_R^2)^{\frac{1}{2}}$  against  $2\pi/\gamma B_2$  at constant  $\Delta\nu$  a straight line of slope  $\Delta\nu$  is obtained which can be used to deduce the exact resonance frequency in the proton spectrum. (197)

In all of the foregoing it has been tacitly assumed that the Bloch-Siegert frequency shift will have no appreciable effect upon the proton chemical shifts determined. This has in fact been confirmed, (198) and it is also known that in homonuclear proton double and triple resonance experiments the irradiating fields of  $\gamma B_2/2\pi$  of a few tens of Hz have small effects which can be allowed for easily or ignored. In a  $^{13}\text{C}-\{^1\text{H}, ^1\text{H}\}$  triple resonance experiment, however, in which one of the proton rf fields is of decoupling intensity the Bloch-Siegert shift of the proton lines which are to be selectively irradiated by the third rf field, may be as much as 1000 Hz which must be allowed for. (199) When a single spin with resonance frequency  $\nu_A$  is exposed to a strong rf field of amplitude  $B_2$  and frequency  $\nu_2$ , a strong (s) and a weak (w) line are obtained whose Bloch-Siegert frequency shifts  $S$  are given by equations (15).

$$S^s = (\nu_A - \nu_2)([(\gamma B_2/2\pi)^2/(\nu_A - \nu_2)^2 + 1]^{\frac{1}{2}} - 1) \quad (15a)$$

$$S^w = -(\nu_A - \nu_2)([(\gamma B_2/2\pi)^2/(\nu_A - \nu_2)^2 + 1]^{\frac{1}{2}} + 1) \quad (15b)$$

In practice one will be dealing with a more complex spin system but it is easy to extend these equations to the AX and AMX cases and hence calculate the frequencies at which the selective proton rf field,  $B_3$ , must be applied to perturb the Bloch-Siegert shifted transitions. (199)

The most complete information about the proton-carbon interactions is of course contained in the fully proton-coupled  $^{13}\text{C}$  spectrum. Unfortunately for molecules of any complexity there may be so much overlapping that complete interpretation is not possible. One of Ernst's two-dimensional experiments (Fig. 20) provides a solution by displaying the fully coupled  $^{13}\text{C}$  resonances from different sites

separately. However, this method requires considerable computer storage capacity. (157) An alternative is to use selective excitation (22, 23) allied to gated proton decoupling. That is, the  $^{13}\text{C}$  resonance from a single site is excited selectively under proton-decoupled conditions, and the FID is collected with the decoupling power turned off. The resulting spectrum then contains only the response from the chosen carbon site. Since the spectrum is acquired without proton decoupling it shows all the splitting due to the long and the short range proton couplings. In principle the selective excitation can be achieved by using a long weak pulse at the appropriate frequency but there are problems associated with relaxation occurring while the pulse is being applied if this is done. The method actually adopted is to apply a train of short mini-pulses of medium power for a time comparable to the reciprocal of the selectivity required. The only resonance then excited by the end of the train is the one separated from the carrier by a frequency equal to the rate of application of the mini-pulses, and a selectivity of  $\pm 1$  Hz is said to be attainable. (200) Figure 26 illustrates the application of this technique to the  $^{13}\text{C}$  spectrum of 1-dimethylamino-2-methylpropene, and it has also been used to study

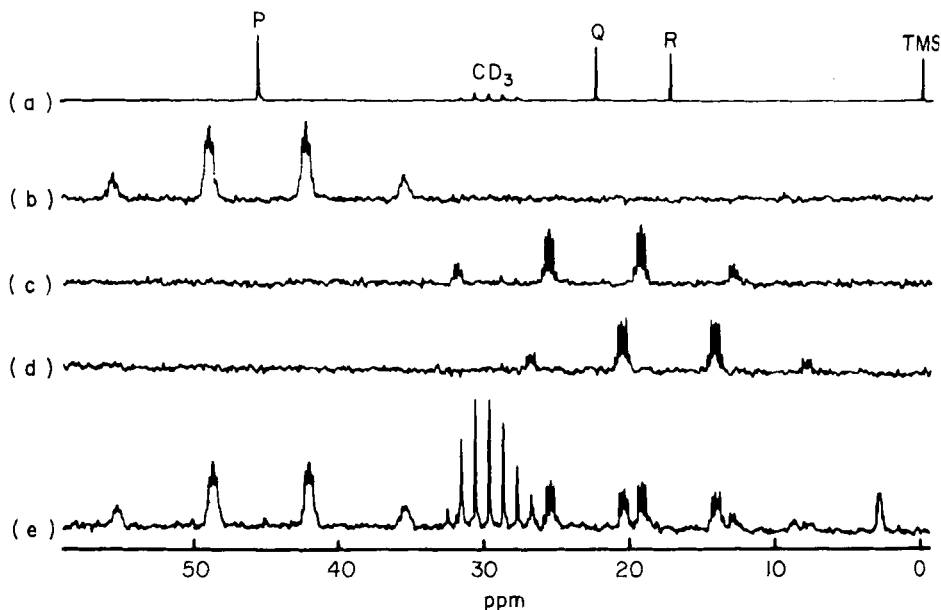
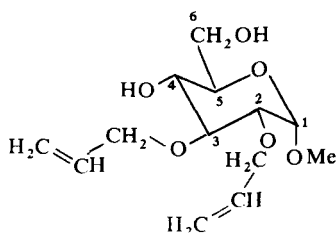


FIG. 26. The high-field regions of spectra of 1-dimethylamino-2-methylpropene. (a) Proton-decoupled spectrum. (b)–(d) Multiplet sub-spectra corresponding to the three methyl resonances P, Q, and R respectively. (e) Full proton-coupled spectrum, showing overlapping and interference from acetone- $\text{d}_6$  and tetramethylsilane. From ref. 23.

menthone. (201) The train of mini-pulses is known as the DANTE (Delays Alternating with Nutations for Tailored Excitation) sequence. (201) It is also possible to conceive (157) of performing the experiment by using broadband tailored excitation to saturate all but the chosen decoupled  $^{13}\text{C}$  resonance. (137)

Another way of getting substantially the same result is based upon a homonuclear  $^{13}\text{C}$  experiment to saturate selectively the chosen resonance under proton decoupled conditions. (202) The spectrum is again acquired under fully coupled conditions and thus is a complete coupled  $^{13}\text{C}$  spectrum except that the multiplet from the saturated  $^{13}\text{C}$  site is absent. This spectrum is subtracted from a normal fully coupled one to yield a trace that contains only the multiplet from the desired carbon. Full fine structure is displayed. Figure 27 shows the application of this method to the  $^{13}\text{C}$  spectrum of the monosaccharide derivative



[6]

[6] and it is clear that each of the thirteen carbon sites gives its own fully coupled spectrum free from any overlapping of resonances from other carbons. This is known as the CASS (Carbon Assignment by Selective Saturation) technique. Despite certain minor disadvantages associated with difference spectroscopy it can achieve a degree of selectivity and sensitivity that is comparable to that of the selective excitation method. (202)

Finally in this section it should be noted that many of these off-resonance decoupling techniques are applicable to other nuclei and indeed have been used in some  $^{15}\text{N}\{-^1\text{H}\}$  studies of molecules with several nitrogen sites, although of course here the problems are generally not so serious. (203)

## V. THE NUCLEAR OVERHAUSER EFFECT (NOE)

The book by Noggle and Schirmer (6) gives a comprehensive account of the NOE together with applications up to 1971. Almost all of the work described is proton homonuclear, and much of it is aimed at

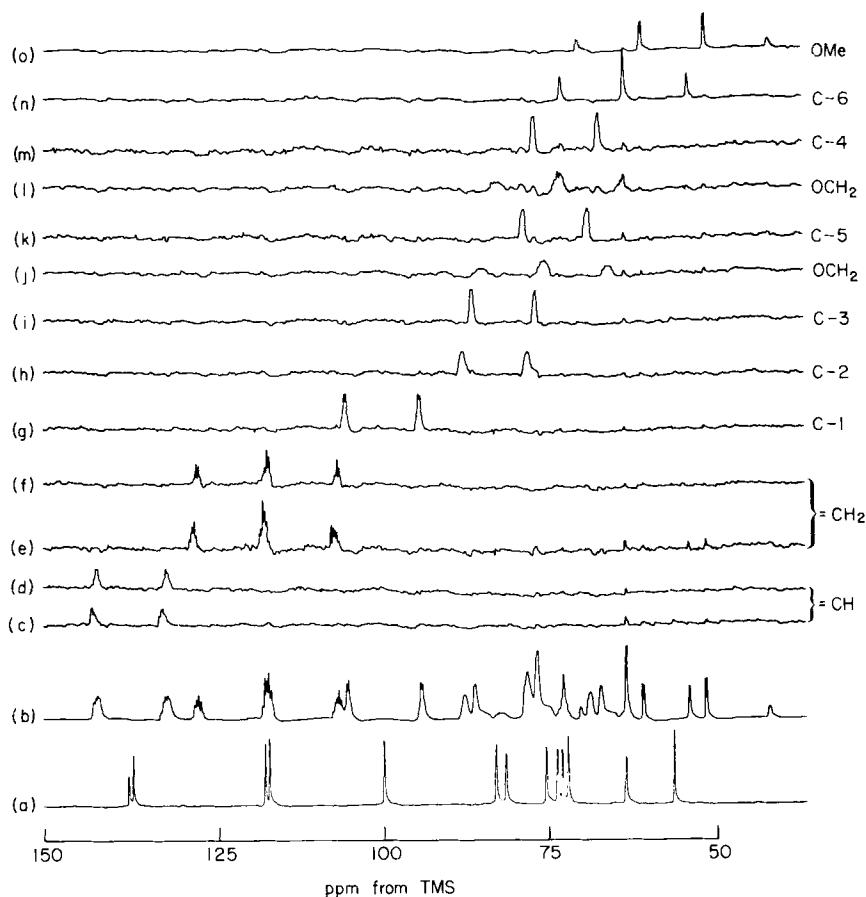


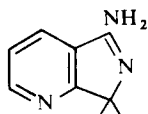
FIG. 27. CASS experiments on the carbohydrate derivative [6]. (a) Proton-decoupled  $^{13}\text{C}$  spectrum. (b) Proton-coupled  $^{13}\text{C}$  spectrum. (c)–(o) Selectively saturated and subtracted spectra from each of the carbon sites indicated on the right of the traces. From ref. 202.

establishing molecular configuration by providing reliable estimates of interproton distances. In recent years the emphasis has changed to homonuclear studies of molecular motion and to work on heteronuclear systems.

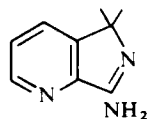
The NOE is the change of integrated intensity in the signal from one nucleus when all the transitions of another are saturated. It is due to the direct dipole–dipole interaction between the two nuclei. The saturation is generally brought about by sufficiently high power irradiation to guarantee an adequate frequency spread. It can also be accomplished by using a set of weak saturating frequencies (produced perhaps by audio modulation), one centred on each individual transition.

### A. Homonuclear systems

It is the dependence of the size of the dipole–dipole interaction upon the inverse sixth power of the internuclear separation that makes it possible to use the NOE for geometrical purposes, although it must always be remembered that in the absence of any other sizeable relaxation mechanism the NOE may still be quite large even though the nuclei involved are not particularly close together. Typical of this kind of application of the proton–proton NOE are: studies of the conformation in solution of cycloguanosines; (204) studies of the internal rotation in dimethylformamide; (205) studies of the orientation of the *N*-methyl group in tetrahydro-3,3,4,6-tetramethyl-1,3-oxazine; (206) the assignment of the spectra of the E and C nigabillactones; (207) the determination of the stereochemistry of 1,3,5,7-tetramethyltricyclo[5.1.0.0]octane; (208) assignments of the two methoxy resonances in 1,2-dimethoxy-4-hydroxy-5-nitrobenzene; (209) and an identification of an enamine as [7] rather than [8]. (210)



[7]



[8]

We emphasize that these are only a selection from the many examples in the literature. The problem of achieving saturation of all resonances of one type of nucleus without perturbing nearby signals was solved (211) in a study of pyranose derivatives by using a tailored exciting rf field of predetermined spectral density. (137) Selective NOE experiments have also been used to study relaxation processes and conformational effects in ABX (vinyl bromide) and A<sub>2</sub>X (1,1,2-trichloroethane) spin systems, (212) and it has been pointed out (213) that useful augmentations of the intensity changes can be brought about by using a 180° inverting pulse rather than saturation.

The time scale of the build-up and decay of the NOE is often such that it can be used to study processes that proceed appreciably more slowly than those accessible to band-shape studies. This has been used in studies of: restricted rotation in amides; (205,214) the *cis-trans* equilibrium of 4-bromo-2-formyl-1-methylpyrrole; (215) exchange in water solution of the system 1-(1'-pyrazolyl)ethanol–acetaldehyde; (216) and the *cis-trans* equilibrium in 4-bromo-2-formylfuran. (217)

In more complex molecules it may be difficult to measure the NOE in the presence of overlapping peaks. One solution which may be

satisfactory if only qualitative results are required is to use an INDOR technique. This has been employed (218) in connection with the assignment of methyl resonances in the proton spectra of some triterpenes. However, if this approach is adopted it is necessary to remember that at least part of the observed intensity change may be due to spin tickling and/or decoupling effects, since an INDOR experiment will not readily distinguish these from the NOE. A probably more general solution of this problem is to use NOE difference spectra. These offer the added advantage that it is possible to observe individual multiplets in the proton spectra of, for example, biologically interesting macromolecules. The method (219) is to subtract a normal spectrum from one in which the intensities of chosen resonances have been altered by a selective NOE experiment. This eliminates the background signal resulting from the presence of many similar protons, and impressive spectra for the protein BPTI have been presented. (219)

This NOE difference technique was used in studies of the binding of the hapten *O*-carboxymethyl-4-methylumbelliferone to its specific antibody; irradiation of the resonances of aliphatic protons in the antibody gives *negative* enhancements of the intensity of certain proton resonances in the hapten, which make it possible to produce a detailed model of the binding site. (220) Peptide NH protons have also been studied with the aid of the  $^1\text{H}-\{^1\text{H}\}$  NOE. (221)

The occurrence of a negative NOE when both nuclei have magnetogyric ratios of the same sign can be attributed to a breakdown of the extreme narrowing condition so that equation (16) is no longer valid. (222–227)

$$\eta = \gamma(\text{X})f_d/2\gamma(\text{A}) \quad (16)$$

In this equation  $f_d$  is the fractional contribution to relaxation made by the dipolar mechanism, and  $\eta$  is defined by equation (17) where  $S_o$  and  $S_e$  are the original and enhanced intensities respectively.

$$S_e = S_o(1 + \eta) \quad (17)$$

Thus when  $(\omega_A + \omega_X)\tau_r$  is not much less than 1, where  $\tau_r$  is the molecular rotational correlation time, the potential maximum enhancement is not attained and it is not possible directly to use the size of the observed NOE to deduce the relative contribution of the dipole–dipole mechanism to the overall longitudinal relaxation of the observed nucleus. (228) The extreme narrowing condition is more stringent at higher measuring fields, but even for protons at say 300 MHz it is easily fulfilled (229) by small molecules for which  $\tau_r \approx 10^{-12}$ – $10^{-10}$  s. However, with large molecules such as globular

protons  $\tau_r$  may be relatively long and in these circumstances equation (18) must be used for the homonuclear enhancement. (230)

$$\eta = \frac{5 + \omega^2\tau_r^2 - 4\omega^4\tau_r^4}{10 + 23\omega^2\tau_r^2 + 4\omega^4\tau_r^4} \quad (18)$$

This equation becomes identical to equation (16) provided that  $\omega^2\tau_r^2 \ll 1$  and hence yields  $\eta = 0.5$  for the maximum enhancements but gives  $\eta = -1$  at the other extreme of  $\omega^2\tau_r^2 \gg 1$ . "Enhancements" (i.e. zero signal) of this order have indeed been observed in the case of small molecules reversibly binding to a specific site on a large one. (231) This is of course really a manifestation of the *inter*-molecular NOE. Other observations of negative interproton NOE have already been referred to (220) and in addition are found (232) for the H-2 resonance of ADP in the creatine-kinase-ADP complex upon irradiation of the resonances at  $\delta = 0.9$  and  $1.7$  ppm of the  $\beta$  and  $\gamma$  methylene protons of an arginyl residue of the enzyme as well as in some studies (233) of hen egg-white lysozyme. In this last piece of work, performed at 270 MHz, intensity changes of  $\eta = -0.45$  to  $-0.55$  are obtained by irradiating resonances in a tryptophan residue and yield  $\tau_r = 1.5 \times 10^{-9}$  s which is in good agreement with a value deduced from measurements of relaxation times. (233)

The *inter*-molecular NOE is mentioned above briefly. It is of course this which makes it desirable to use samples in a solvent without nuclei of high  $\gamma$  for these experiments. There have, however, been few detailed studies of this effect. (234) A density matrix description (235) has been successfully applied to the effect upon the solute (1,1,2-trichloroethane) protons of irradiating the solvent ( $\text{Me}_4\text{Si}$ ) resonance (235) and differential effects upon the resonances of the  $[\text{AB}]_2$  spin system provided by the protons of *o*-dichlorobenzene have been used to aid the assignment. (236)

Since the observed NOE depends upon the relative contributions made by the dipole-dipole interaction and other mechanisms to  $T_1$ , anything that affects  $T_1$  may also affect the NOE. Indeed, it has been found (237) that even when a vacuum technique is used to remove dissolved oxygen the paramagnetism of what remains may be enough to reduce  $T_1$  and hence alter the NOE significantly. This difficulty can be overcome by distilling the sample from a mixture of the complex  $[\text{Co}^{\text{II}}\text{bipy}_3](\text{ClO}_4)_2$  and  $\text{NaBH}_4$  prior to examination. (237) This effect of paramagnetic species will obviously be important if a lanthanide shift reagent has been used to spread out the spectrum prior to performing the NOE experiments. It has been shown that there are concentrations of shift reagent that give useful spectral spread without



excessive reduction of the NOE. This has been used in assignments of the 100 MHz proton spectra of some ten-membered-ring sesquiterpene lactones. (238) Furthermore, a paramagnetic species will interact differentially with the nuclei of a complex molecule, those near the periphery experiencing preferential reduction of the NOE. This can be used as a delicate means of probing ligand binding sites. (239)

## B. Heteronuclear systems

With the advent of FT  $^{13}\text{C}$  NMR and subsequently multinuclear spectrometers broadband proton decoupling has become widespread and is usually accompanied by a NOE which is often substantial [equation (16)] and can provide a useful gain in sensitivity. However, the dependence upon the competition between dipole-dipole and other relaxation mechanisms means that the NOE can vary from one site to another which militates against reliable intensity measurements. In these circumstances it is desirable to be able to quench the NOE, and this may also be necessary for nuclei with a negative magnetogyric ratio for which a really unfortunate combination of relaxation times can lead to zero signal intensity.

As indicated in Section V.A, addition of a paramagnetic species usually reduces or even eliminates the NOE. (240–242) It has been found that paramagnetic transition metal ions are better than free radicals for this purpose. (240, 241) One of the most popular species is  $[\text{Cr}^{\text{III}}\text{acac}_3]$  since this is soluble in commonly used NMR solvents such as  $\text{CDCl}_3$ . Theoretical analysis (242) of the mode of action of a paramagnetic species shows that at suitable concentrations the NOE can be quenched effectively with very little line broadening, and further that  $\text{Cr}^{3+}$  produces little or no contact shift of the observed resonances. (243) The addition of a paramagnetic species has the added advantage that it decreases  $T_1$  and thus makes it possible to pulse more rapidly, a feature that is especially valuable for nuclei that otherwise have rather large values of  $T_1$  (e.g. quaternary  $^{13}\text{C}$  and  $^{15}\text{N}$ ). (244) Addition of the paramagnetic ion  $[\text{Mn}(\text{EDTA})]^{2-}$  has been used to aid  $^{13}\text{C}$  assignments in the spectra of some thallium(I) complexes by producing selective quenching of the  $^{13}\text{C}-\{^1\text{H}\}$  NOE. (246)

As an alternative to the above method for eliminating the NOE an instrumental technique is available. This depends upon the realization (247) that the time-dependent behaviour of the NOE and of spin decoupling are different. Thus the NOE takes a time comparable for  $T_1$  to build up or to decay after application or removal of a rf field, whereas spin decoupling effects appear or disappear almost instantaneously. Consequently if the proton decoupler is gated off immediately prior to

acquisition of the FID a fully coupled spectrum *with* NOE is obtained. Conversely if the decoupler is off prior to the period of data acquisition, but is on during it, a decoupled spectrum *without* NOE is obtained. The first demonstration of this was conducted manually (247) on a CW spectrometer but the twin techniques are of course ideally suited to FT instruments, (248, 249) and suitable facilities are now provided as standard equipment. (248–251) The timing schemes and behaviour of the transverse magnetization of the observed nuclei (i.e. the signal) are shown schematically in Fig. 28. (248, 249)

The gated method for suppressing the NOE but retaining spin decoupling provides a convenient way of getting quantitative measurements of the NOE; one simply compares the intensities in the decoupled spectra obtained with and without the NOE being operative. (252) It is important to realize, however, that one must wait sufficiently long with the decoupler off between pulses to ensure that all residual magnetization has decayed if accurate results are to be obtained. It is often recommended that this waiting period should be at least  $5T_1(A)$  in an A- $\{X\}$  experiment. In fact (253) this may be too short

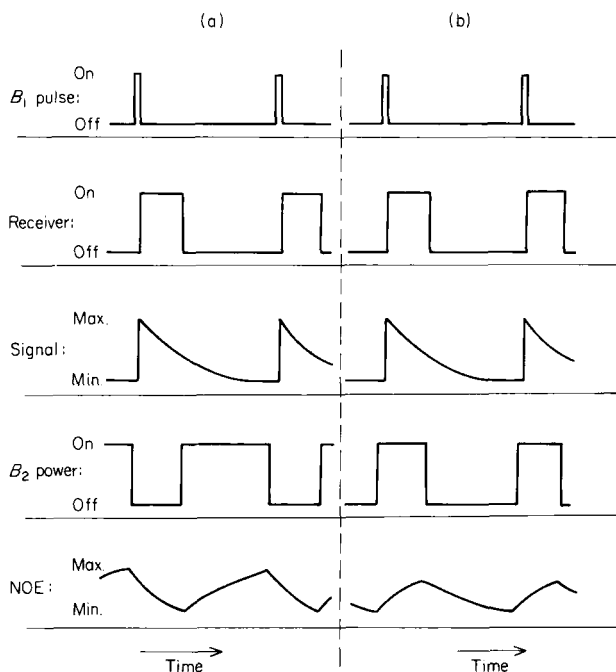


FIG. 28. Pulsing schemes for controlling the NOE. (a) With retention of the NOE and no spin decoupling. (b) Decoupled with NOE suppressed. From ref. 248.

a time unless  $T_1(X) \ll T_1(A)$  or  $|\eta|$  is well below its possible maximum value. A fairly general treatment (254) of this problem shows that in a sequence of the form [decoupler on–90°–FID–decoupler off– $T$ ] $_n$ , in which  $T$  is the waiting period intended to permit the system to regain equilibrium, there are really two delay periods, i.e. with and without the decoupler on. It is only when the decoupler is off that  $T_1(X)$  need be considered.

### C. The $^{13}\text{C}$ – $\{^1\text{H}\}$ NOE

This is by far the commonest use of the heteronuclear NOE experiment and has been the subject of many theoretical investigations. When the extreme narrowing condition is fulfilled the maximum value of  $\eta$  is 1.998 (say 2) which is independent of the number of protons involved. (228) In practice it is only when the carbon atom has directly attached protons that the dipole–dipole mechanism dominates the  $^{13}\text{C}$  relaxation to the extent that  $\eta$  approaches 2. As the molecular motion becomes significantly anisotropic there may be differences for  $\rightarrow\text{CH}$ ,  $\rightarrow\text{CH}_2$ , and  $-\text{CH}_3$  groups. These conclusions have been confirmed by studies of adamantane (228) and formic acid. (255) For larger molecules with  $\tau_c \approx 10^{-9}$ – $10^{-8}$  s the enhancement may fall, becoming  $\eta = 0.153$  when  $\omega_c\tau_c \gg 1$ . It then turns out that the gain in signal-to-noise ratio, which otherwise arises as a result of increasing the measuring field strength, may be much less than that expected. (256)

Internal rotations, e.g. of a methyl group, can also affect the  $^{13}\text{C}$ – $\{^1\text{H}\}$  NOE. It has been predicted (257) that cross-correlation effects should lead to different values for a methyl group according to whether the protons are in a doublet or a quartet state. In more extended work Wigner rotation matrices have been used to show that, except within a comparatively narrow range of internal diffusion coefficients, cross-correlations in chains of methylene carbons where multiple rotations have to be considered have little influence upon the  $^{13}\text{C}$ – $\{^1\text{H}\}$  NOE. (258) However, anomalies do occur when the  $^{13}\text{C}$  spin–lattice relaxation is non-exponential. Experimental confirmation of these conclusions was obtained by studying  $^{13}\text{C}$ -labelled galactolipids. (258) The results should be of general interest (259) in a number of biological systems.

Frequently measurements of the  $^{13}\text{C}$ – $\{^1\text{H}\}$  NOE have been made in connection with detailed studies of relaxation behaviour, often with the aim of getting a clearer understanding of molecular dynamics. This was done in studies of: neat liquid pyrimidine and pyridazine; (260) methyl substituted long-chain alkanes; (261) chloroplast membranes;

(262) the diamagnetic complexes  $[\text{Co}(\text{acac})_3]$  and  $[\text{Pd}(\text{acac})_2]$ ; (263) the basic pancreatic trypsin inhibitor; (264) organosilicon compounds; (265) *p,p'*-azoxyanisole as an isotropic liquid; (266) hindered methyl groups; (267) chloroform partly oriented in a nematic solvent; (268) aqueous solutions of acetamide and *N,N*-dimethylacetamide; (269) labelled sodium acetate; (270) substituted purines; (271) indazole; (272) *N,N*-dimethylformamide; (273) 10-methylnonadecane; (274) adenosine and guanosine 5'-monophosphate; (275) some trimethylsilyl compounds; (276) and other molecules. (277, 278)

Fairly recently it has been pointed out that, even when the extreme narrowing condition is satisfied, equation (16) may not be correct if cross-correlation of the  $^1\text{H}$  and  $^{13}\text{C}$  relaxation processes is at all important. Consequently equation (19) should be used instead (cf. refs. 257 and 258):

$$\eta = \frac{1}{2} \left( \frac{\gamma_{\text{H}}}{\gamma_{\text{C}}} \right) \left( \frac{f_{\text{dd}} - \Omega}{1 - \Omega} \right) \quad (19)$$

where  $\Omega$  is defined by equation (20) in which  $r$  is the proton- $^{13}\text{C}$  internuclear distance,  $\theta$  is the angle between the internuclear vector and the axis of internal reorientation, and  $X$  depends upon random field interactions in the proton frame. (279)

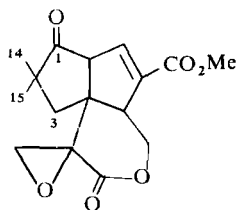
$$\Omega = \left( \frac{\gamma_{\text{H}}^2 \gamma_{\text{C}}^2 \hbar^2}{2r^6} \right)^2 \left( \frac{(3 \cos^2 \theta - 1)^4 \tau_r^2}{T_1(^{13}\text{C})^{-1} (T_1(^{13}\text{C}) + 2X)} \right) \quad (20)$$

These equations were used in a study of the peptide tetragastrin. (279) This kind of behaviour will usually be accompanied by irregularities of the  $^{13}\text{C}$  relaxation which under conditions of proton decoupling is not exponential for  $-\text{CH}_3$  and  $-\text{CH}_2-$  groups (280, 281) (or more generally  $\text{AX}_3$  and  $\text{AX}_2$  systems). Relaxation of A is exponential for  $\text{A}-\{\text{X}, \text{Y}, \text{Z}, \dots\}$  experiments, provided that there is no symmetry or equivalence in the  $\text{XYZ} \dots$  spin system and that all of X, Y, Z, ... are strongly irradiated. This has been detected experimentally in studies of  $^{13}\text{C}$ -enriched methyl mercury compounds. (282)

For large molecules the main point of interest is whether a NOE of less than the theoretical maximum ( $\eta = 2$ ) arises because of non-dipolar contributions to the  $^{13}\text{C}$  relaxation or as a result of a breakdown of the extreme narrowing condition. (283) By measuring  $T_1$  for both  $^{13}\text{C}$  and  $^1\text{H}$  it is possible to distinguish between these two possibilities, since a *single* derived correlation time for a particular group (say  $-\text{CH}_3$ ) indicates that dipolar relaxation is dominant and any reduction in the NOE indicates a breakdown of the extreme narrowing condition. (284) The results of this kind of work give a good

deal of information about the chain dynamics and mobility in solution of polymers, and the following have been studied in some detail: branched polyethylenes; (285) poly(vinylidene fluoride); (286) poly(methyl methacrylate); (284, 286–288) poly(alkyl methacrylate); (289) poly(but-1-ene); (290) long-chain alkanes; (261) and crosslinked gels. (291)

In connection with techniques a comparison (292) of gated decoupling and the use of a paramagnetic reagent for the suppression of the  $^{13}\text{C}-\{^1\text{H}\}$  NOE in quantitative work has suggested that the former is preferable, although rather time-consuming. The use of a pulse modulated scheme of wideband decoupling has also been described. (293) The suppression of the NOE for quantitative analysis has been reviewed (294) although it has been shown (295) that it is possible in certain circumstances to get good results without NOE suppression. Selective  $^{13}\text{C}-\{^1\text{H}\}$  NOE have been obtained for quaternary carbons (296) and used (297) to aid the assignment of [9], a 50% enhancement of the C-1 resonance being observed upon irradiation of the C-3 methylene *or* the C-14,15 methylene protons.



[9]

It is sometimes necessary to eliminate or take into account the effect of other magnetic nuclei in the system when studying the NOE. Thus  $^2\text{D}$  decoupling was used in  $^{13}\text{C}$  studies of deuteriated bromomethanes (298) and  $^{14}\text{N}$  quadrupolar relaxation was found (275) to be important in species with a direct C–N bond, although  $^{19}\text{F}$  decoupling was not used in a relaxation study (299) of  $\text{CFBr}_3$ . In species enriched in  $^{13}\text{C}$  interactions between pairs of  $^{13}\text{C}$  nuclei must also be considered. It has been shown (300) that under conditions of broadband proton decoupling these can contribute significantly to  $^{13}\text{C}$  relaxation and hence alter the  $^{13}\text{C}-\{^1\text{H}\}$  NOE. (301, 302) Enhancement factors of 1.51 and 1.80 are obtained for the  $^{13}\text{C}-\{^1\text{H}\}$  NOE of the carboxyl carbon of 6-phosphogluconate with and without an adjacent  $^{13}\text{C}$  nucleus. It is clear that this behaviour has important implications in biochemical work using  $^{13}\text{C}$ -enriched samples.

As an alternative to measuring the  $^{13}\text{C}-\{^1\text{H}\}$  NOE directly it has been suggested (303) that values of  $T_1(^1\text{H})$  in molecules with and without  $^{13}\text{C}$  should be compared to determine the  $^{13}\text{C}$  dipolar contribution to the proton relaxation. A measurement of  $T_1(^{13}\text{C})$  then makes it possible to calculate the  $^{13}\text{C}-\{^1\text{H}\}$  NOE, and some results have been presented for  $^{13}\text{C}$ -labelled amino-sugars. (303) This may well save some time. However, it would have been nice to have had an experimental comparison with the direct method.

A claim (304) to have detected a negative intermolecular  $^{13}\text{C}-\{^1\text{H}\}$  NOE between  $\text{CS}_2$  and  $\text{CHCl}_3$  has been questioned (305) and it has been pointed out (306) that some results (307) for the  $^{13}\text{C}$  relaxation time of  $\text{CHCl}_3$  may be incorrect because the intermolecular  $^1\text{H}-\{^1\text{H}\}$  NOE is not considered in evaluating the results of relevant  $^1\text{H}-\{^{13}\text{C}\}$  experiments.

#### D. The NOE for other pairs of nuclei

$^2\text{H}-\{^1\text{H}\}$  This has been reported (308) to be small because the deuterium relaxation is dominated by its quadrupole moment.

$^3\text{H}-\{^1\text{H}\}$  Initial claims (309) that this is normally absent have been withdrawn, (310) and values ranging from  $\eta = 0$  to 0.44 have been reported. (310–312) The theoretical maximum is  $\eta = 0.47$ .

$^{13}\text{C}-\{^{19}\text{F}\}$  No effect is observed (313) in studies of fluorophosphoranes.

$^{15}\text{N}-\{^1\text{H}\}$  This effect is very important in natural abundance  $^{15}\text{N}$  NMR, and owing to the negative magnetogyric ratio of  $^{15}\text{N}$   $\eta$  can range from 0 to  $-4.93$  according to conditions. For aqueous solutions of species with N–H bonds the effect is often pH-dependent (314) and in the wrong circumstances the value of  $\eta$  can be  $-1$  so that the signal vanishes, e.g. in 1,4-diaminobutane. (314) The elimination of the effect by the use of a paramagnetic reagent (315, 316) or gated decoupling is therefore important. It must of course be recognized that a decoupled signal intensity close to zero can also be due to a number of other factors. These include: the use of inadequate decoupling power and/or an unsuitable decoupling frequency, NOE averaging as a result of fast exchange between different sites, and a breakdown of the extreme narrowing condition. Some experiments on gramicidin S were used to demonstrate (317) the importance of the last of these.

The following  $^{15}\text{N}-\{^1\text{H}\}$  NOE have also been reported: in a variety of simple molecules (317a) in which it varied from  $\eta = -5$  to 0; in nucleosides and nucleotides (318) ( $\eta = -2$  to  $-1$ ); in zinc tetraphenylporphyrin (319) ( $\eta = 0$ ); in acetamide and *N,N*-dimethylacetamide; (269) in aniline, the anilinium ion, and aminobenzoic

acids (320) ( $\eta = -3$  to  $-5$ ); alumichrome in DMSO solution; (321) in aqueous histidine; (322) and in whole cells as part of a probe of their dynamic structure. (323)

$^{19}\text{F}-\{^1\text{H}\}$  For small freely tumbling molecules the theoretical maximum is  $\eta = 0.53$  and values up to  $0.33$  are obtained from studies (324) of some derivatives of 2,3,5,6-tetrafluorophenylhydrazine, from which it appeared that experiments of this type provide effective means of establishing the proximity or otherwise of hydrogen and fluorine atoms. The dipolar contribution to  $^{19}\text{F}$  relaxation in a bilayer system containing the lipid 1-palmitoyl-2-(8,8-difluoropalmitoyl)-*sn*-glycero-3-phosphorylcholine was assessed from measurements of the  $^{19}\text{F}-\{^1\text{H}\}$  NOE over a range of temperatures (325) and the effect upon geometries deduced from the NOE of slow molecular reorientation has been calculated for *p*-fluorophenyl residues in macromolecules. (283, 326)

$^{29}\text{Si}-\{^1\text{H}\}$  As with  $^{15}\text{N}$  the negative magnetogyric ratio of  $^{29}\text{Si}$  ( $\eta$  can vary from  $-2.52$  to  $0$ ) makes it important to be able to suppress the NOE, and this has been done both by using paramagnetic reagents (327–329) and by gating the decoupling field. (254, 330, 331) Most of the molecules on which the NOE has been measured so far are relatively simple ones:  $\text{Ph}_3\text{SiH}$  and  $\text{PhSiH}_3$  ( $\eta = -2.4$  and  $-0.07$  respectively) (332) and species with  $\text{Me}_3\text{Si}$ ,  $\text{Me}_2\text{Si}$ , and  $\text{MeSi}$  units. (262, 330, 331) If  $\eta$  is close to  $-1$  it is difficult to measure because the observed signal is so weak, but in  $\text{MeSi}(\text{OEt})_3$  this problem is circumvented by switching on the decoupler some time  $t$  prior to collecting the FID. The NOE then builds up according to equation (21) in which  $S_t$  and  $S_x$  are the intensities at times  $t$  and  $t_x$  ( $\gg T_1$ ). (333)

$$S_x - S_t = (S_x - S_0)e^{t/T_1} \quad (21)$$

$^{31}\text{P}-\{^1\text{H}\}$  Enhancements up to the theoretical maximum of  $\eta = 1.24$  have been reported for a range of species (334–336) including some biphosphines and their disulphides (337) and di- $\lambda^5$ -phosphathianes. (338) It appears that care must be taken if decoupled  $^{31}\text{P}$  spectra are to be used for quantitative analysis. The frequency dependence of the  $^{31}\text{P}-\{^1\text{H}\}$  NOE was measured to determine the predominant orientation of the phosphorylcholine polar head group in phospholipid bilayers. (339)

Surprisingly large intermolecular NOE up to  $\eta = 1.24$  are reported for inorganic orthophosphate upon irradiation of the solvent water resonance. (340) These are attributed to  $\text{P}-\text{O} \cdots \text{H}$  hydrogen bonding.

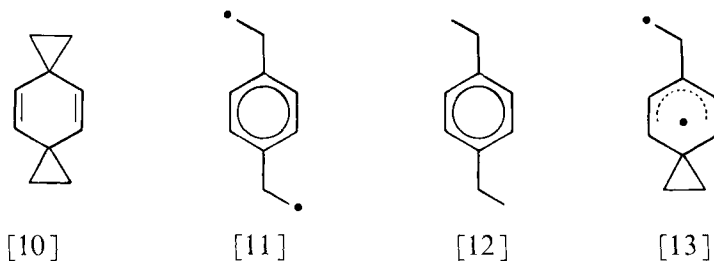
$^{113}\text{Cd}-\{^1\text{H}\}$  Both magnetic isotopes of cadmium have a negative magnetogyric ratio but inverted signals are not obtained in proton-decoupled  $^{113}\text{Cd}$  spectra. (341)

$^{119}\text{Sn}-\{^1\text{H}\}$   $\gamma(^{119}\text{Sn})$  is negative and therefore  $[\text{Cr}(\text{acac})_3]$  has been used to avoid difficulties. (342) In fact for small molecules the NOE appears to be quite small, and with larger ones raising the temperature can help. (342)

$^{199}\text{Hg}-\{^1\text{H}\}$  The theoretical maximum is  $\eta = 2.79$  but experimentally  $\eta = 0$  in work done so far. (343)

### E. CIDNP and the NOE

In CIDNP studies the pattern of nuclear spin polarizations is used to deduce the structures of free radical intermediates, and if there is a simultaneous NOE this can affect the conclusions drawn. (344) In the photolysis of [10] to yield [12] the biradical intermediate [11] should not cause significant polarization of the olefinic protons of [10] but in fact these are observed to have weak emission. This raises the possibility that the intermediate is really the biradical [13], but a homonuclear double resonance experiment which destroyed the cyclopropyl spin polarization of [10] eliminated the olefinic emission which was evidently solely due to the NOE. Thus it is confirmed that [11] is indeed the intermediate in the reaction. (344)



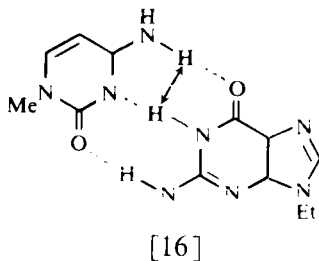
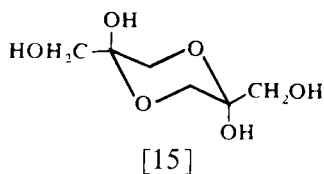
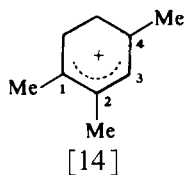
The  $^{13}\text{C}-\{^1\text{H}\}$  NOE is suppressed by gated decoupling to avoid complications in studies of the  $^{13}\text{C}$  CIDNP of photolysed perfluorobenzoyl peroxide in the presence of chlorobenzene. (345)

## VI. CHEMICAL EXCHANGE

The more theoretical aspects of double resonance experiments in systems undergoing chemical exchange are referred to in Section II. Here we deal with the use of the Hoffman-Forsén saturation transfer method for the study of slow rates of exchange. The basis of this method (62) is simply that since  $T_1$  is often longer than  $T_2^*$  an experiment that relates the exchange rate to the longitudinal relaxation time is more suitable for studying slow processes than one (e.g. band-shape analysis)



that depends upon the transverse relaxation time. Such an experiment is one in which the resonance associated with one site is saturated and the change in signal intensity at another site is observed. Its application to proton NMR is well established, as for example in a study of the rearrangement of the cyclohexenyl cation [14]. (346) At  $-24^\circ$  saturation of the resonance of the C-4 proton diminishes the C-3 proton resonance. At  $-4^\circ$  saturation of the C-4 methyl affects the C-1 methyl and it is possible to account for the results in terms of *two* rearrangement processes occurring at rates of *ca.*  $0.1$  and  $10\text{ s}^{-1}$ . Improvements to the straightforward technique of CW saturation and swept observation have included continuous monitoring of one resonance (i.e. an INDOR experiment) in studies of the exchange of the OH protons in [15] (347) and the use of selective pulses to achieve saturation in a study of the conformational flipping of [2,2]-2,5-pyrrolloparacyclophane. (348) Experiments of this kind have been used to study biological systems (349) including: the inversion of the seven-membered benzodiazepine ring of valium; (349) exchange of the NH ring proton of tryptophan in water solution; (350) the demonstration of the occurrence of proton exchange in the system [16] (351) in which the double-headed arrow indicates the exchanging protons; the demonstration of hemiacetal formation between the active site thiol of the proteolytic enzyme papain and the inhibitor *N*-benzoylaminoacetaldehyde (352) and between  $\alpha$ -chymotrypsin and the inhibitor hydrocinnamaldehyde; (353) the assignment of the individual heme c methyl resonances in ferricytochrome c; (354) and the details of the kinetics of the adenylate kinase-catalysed AMP-ADP conversion in a  $^{31}\text{P}$ - $\{^{31}\text{P}\}$  experiment. (355, 356)



Of late, such studies have been conducted using  $^{13}\text{C}$  NMR under conditions of complete proton decoupling, the main protagonist of the method being Mann who has reviewed the subject. (357) He studied the relatively slow inversion of *cis*-decalin by measuring the change in  $^{13}\text{C}$  signal intensity from one site upon saturation of the resonance of the other site (358) and has examined *N,N*-dimethylformamide in detail. (359) In this work it is necessary to determine an apparent  $T_1(^{13}\text{C})$  at one site with rf saturation at the other site, since a conventional  $(180^\circ - \tau - 90^\circ)_n$  pulse sequence cannot be used to determine the true values of  $T_1$  in the presence of the exchange. Results (359) obtained at temperatures as high as  $160^\circ$  agree with those from earlier proton work. (360, 361)

Similar  $^{13}\text{C}$ - $\{^{13}\text{C}\}$  experiments were used at low temperatures to get accurate thermodynamic parameters for the ring inversion of dimethylcyclohexanes (362) and in a study of the Cope rearrangement of barbaralane. (363) It seems likely that these experiments will be especially useful in connection with fluxional organometallic compounds, and two recent reports confirm this. Thus  $\eta^4\text{-C}_7\text{H}_8\text{Fe}(\text{CO})_3$  begins to decompose below temperatures at which single resonance  $^{13}\text{C}$  NMR could demonstrate fluxionality, and this behaviour was clearly established by  $^{13}\text{C}$  spin saturation transfer experiments. (364) In the other report the four-site exchange problem presented by the fluxionality of  $\eta^6\text{-C}_8\text{H}_8\text{Fe}(\text{CO})_3$  was studied and 1,3-shifts were found to predominate. (365)

So far, the Hoffman-Forsén method has been confined almost entirely to proton and  $^{13}\text{C}$  NMR but there can be no doubt that in the near future similar studies will appear using many other nuclei.

## VII. CHEMICAL APPLICATIONS

### A. The determination of chemical shifts

As described in previous reports, (1-3) all multiple resonance experiments (without noise modulation) can be used to determine chemical shifts indirectly even if the primary objective is spectral simplification, assignment, or a study of coupling constants. It must be remembered that the different applications of multiple resonance cannot necessarily be pursued independently and that in chemical shift determinations care must be taken, especially in complex spin systems, to ensure that the centre of the total spectrum and not of a sub-spectrum is found.

The question of suitable reference compounds for many of the less commonly studied nuclei is a vexed one; ideally the reference should be

TABLE II

Resonance frequencies of nuclei in a polarizing magnetic field of strength corresponding to a proton resonance in TMS of exactly 100 MHz

Nucleus (X)	Compound	$\Xi(X)$ (Hz) <sup>a</sup>	Ref.
<sup>1</sup> H	Me <sub>4</sub> Si	100 000 000.0	1
<sup>2</sup> H	(CD <sub>3</sub> )(CD <sub>2</sub> H)SO	15 350 650	10
<sup>7</sup> Li	(MeLi) <sub>4</sub>	38 863 887	371
<sup>10</sup> B	BH <sub>4</sub> <sup>-</sup>	10 743 230	372
<sup>11</sup> B	BH <sub>4</sub> <sup>-</sup>	32 082 695	372
<sup>13</sup> C	Me <sub>4</sub> Si	25 145 005	10
<sup>14</sup> N	(NH <sub>4</sub> <sup>+</sup> ) <sub>2</sub> SO <sub>4</sub> <sup>-</sup>	7 223 750	10
<sup>15</sup> N	(Me <sub>4</sub> N <sup>+</sup> )I <sup>-</sup>	10 133 351	568
<sup>17</sup> O	MeOH	13 555 900	112
<sup>19</sup> F	C <sub>6</sub> F <sub>6</sub>	94 078 500	10
<sup>29</sup> Si	Me <sub>4</sub> Si	19 867 185	10
<sup>31</sup> P	(MeO) <sub>3</sub> P	40 486 455	10
<sup>63</sup> Cu	[(MeO) <sub>3</sub> P] <sub>4</sub> Cu <sup>+</sup>	26 517 635	109
<sup>77</sup> Se	Me <sub>2</sub> Se	19 071 520	10
<sup>95</sup> Mo	(MeO) <sub>3</sub> PMo(CO) <sub>5</sub>	6 504 805	409
<sup>103</sup> Rh	<i>mer</i> -(Me <sub>2</sub> S) <sub>3</sub> RhCl <sub>3</sub>	3 172 310	410
<sup>107</sup> Ag	[(EtO) <sub>3</sub> P] <sub>4</sub> Ag <sup>+</sup> NO <sub>3</sub> <sup>-</sup>	4 053 256	569
<sup>109</sup> Ag	[(EtO) <sub>3</sub> P] <sub>4</sub> Ag <sup>+</sup> NO <sub>3</sub> <sup>-</sup>	4 659 786	569
<sup>111</sup> Cd	Me <sub>2</sub> Cd	21 215 478	416
<sup>113</sup> Cd	Me <sub>2</sub> Cd	22 193 173	416
<sup>117</sup> Sn	Me <sub>4</sub> Sn	35 632 294	570
<sup>119</sup> Sn	Me <sub>4</sub> Sn	37 290 665	10
<sup>125</sup> Te	Me <sub>2</sub> Te	31 549 802	418
<sup>183</sup> W	WF <sub>6</sub>	4 161 780	10
<sup>195</sup> Pt	<i>cis</i> -(Me <sub>2</sub> S) <sub>2</sub> PtCl <sub>2</sub>	21 420 980	423
<sup>199</sup> Hg	Me <sub>2</sub> Hg	17 910 780	433
<sup>205</sup> Tl	Me <sub>2</sub> Tl <sup>+</sup>	57 893 970	10
<sup>207</sup> Pb	Me <sub>4</sub> Pb	20 920 597	439

<sup>a</sup> In certain cases the values differ from those previously quoted (1, 10); this can be attributed to changes in the conditions of measurement.

suites to study by both direct and indirect (double resonance) methods, and of course should be readily available. Table II lists resonance frequencies for some 28 nuclei as determined by double resonance experiments, but we stress that we do not necessarily recommend the particular species quoted as the ideal reference material.

The compilation in the following sub-sections of chemical shifts of various nuclei determined by multiple resonance supplements that provided earlier (1) but is not intended to be exhaustive, particularly in the cases of the most popular nuclei.

$^1\text{H}$  Most double resonance measurements of proton shifts have been homonuclear studies of hidden and unresolved lines (e.g. refs. 107 and 366). However, in  $^{13}\text{C}$  NMR, measurements of proton shifts using the correlation of  $^{13}\text{C}$  and  $^1\text{H}$  spectra by off-resonance  $^{13}\text{C}-\{^1\text{H}\}$  decoupling is common. While the aim is usually to assign the  $^{13}\text{C}$  signals, it can also be to assign proton signals, as in the case of the *N*-methylene protons of amides (367) and the methyl signals of valine. (368)  $^1\text{H}$  shifts derived from similar experiments can be used as trial parameters for the iterative analysis of complex  $^1\text{H}$  spectra; this technique was demonstrated for [1,1,3- $^2\text{H}_3$ ]indene. (369)

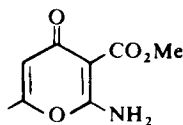
$^2\text{H}$   $^1\text{H}-\{^{31}\text{P}, ^2\text{H}\}$  selective triple resonance experiments were used in isotope effect studies of *P*-deuterio dimethyl phosphite, (176) where  $^4J(^1\text{H}\cdots^2\text{H})$  is effectively zero. The measurement of the  $^2\text{H}$  frequency enabled a very precise value for  $\gamma(^1\text{H})/\gamma(^2\text{H})$  to be obtained.  $^1\text{H}-\{^2\text{H}\}$  INDOR spectra with linewidths as small as 0.5 Hz have been obtained (370) from the monoprotonated impurities in commercial perdeuterated solvents.

$^7\text{Li}$  The only shift obtained by double resonance is that in the methyl-lithium tetramer. (371)

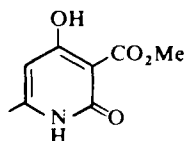
$^{10,11}\text{B}$  Tickling experiments on  $^{10}\text{B}$  and  $^{11}\text{B}$  in  $\text{BH}_4^-$  and  $\text{BF}_4^-$  have been reported. (372) They show that the primary isotope effect upon the boron chemical shift is only  $0.11 \pm 0.03$  ppm, which is negligible for most practical purposes.

$^{13}\text{C}$  Double resonance measurements of  $^{13}\text{C}$  shifts for their own sake are now extremely rare because of the use of pulsed FT methods but some are still reported where they are obtained as part of a wider investigation. (371, 373–376)

$^{14,15}\text{N}$   $^{14}\text{N}$  shifts have been measured in compounds both with and without direct N–H bonds. (111, 377, 378) The measurement accuracy of *ca.* 1 ppm is sufficient for studies of hydrogen-bonding and solvent effects in some N-heterocycles. (378)  $^1\text{H}-\{^{14}\text{N}\}$  INDOR was used (379) to measure characteristic  $^{14}\text{N}$  shifts of  $\gamma$ -pyrones and  $\alpha$ -pyridones such as [17] and [18].



[17]



[18]

This method of distinguishing the isomeric compounds is found to be quicker than the alternative of measuring  $^2J(\text{C}-6, \text{H}-5)$ . The  $^{14}\text{N}$  shifts

of the N-bonded isomers of  $[\text{Pt}(\text{CNS})_2(\text{SMe}_2)_2]$  were measured (175) using  $^1\text{H}-\{^{195}\text{Pt}, ^{14}\text{N}\}$  selective triple resonance and found to be similar to those characteristic of known N-bonded thiocyanates. Values of  $\delta(^{14}\text{N})$  in several methyl isocyanide complexes have also been reported. (380)

$^{15}\text{N}$  with  $I = \frac{1}{2}$  is more amenable to double resonance. (381–385) In the *trans* isomer of  $[\text{Co}^{\text{III}}(\text{glycinato})_3]$  all three chelate rings are different and give rise to three NH proton signals in  $\text{D}_2\text{SO}_4$ ; the corresponding  $^{14}\text{N}$  signals are broad and unresolved whereas three  $^{15}\text{N}$  signals can be seen for the  $^{15}\text{N}$ -enriched compound. (386) AISEFT (Abundant Isotope Signal Elimination FT) spectra have been used to measure  $^{15}\text{N}$  shifts of some amides with  $^{15}\text{N}$  in natural abundance. (387) A series of spectra with  $\nu(^{15}\text{N})$  varied away from resonance enables the residual N–H splittings to be related to the degree of off-resonance. Similar methods were used to measure the natural abundance  $^{15}\text{N}$  spectrum of the cyclohexapeptide alumichrome; (126) difference spectra were not required for the fully  $^{15}\text{N}$ -labelled compound.

$^{17}\text{O}$  Time-averaged  $^1\text{H}-\{^{17}\text{O}\}$  INDOR spectra have given  $^{17}\text{O}$  chemical shifts in  $\text{MeOH}$ ,  $(\text{MeO})_3\text{P}$ , and  $(\text{MeO})_2\text{PHO}$ . (112, 113) Even with  $^{17}\text{O}$  ( $I = \frac{5}{2}$ ) enriched to 10%, effects due to decoupling of  $^2J(^{17}\text{O} \cdots ^1\text{H})$  are too small to be detected in a single scan thus making spectral accumulation necessary.

$^{29}\text{Si}$  The multiplicities observed in  $^1\text{H}-\{^{29}\text{Si}\}$  INDOR spectra of methylsilicon halides enabled (388)  $\text{Me}_3\text{Si}$ ,  $\text{Me}_2\text{Si}$ , and  $\text{MeSi}$  species to be readily distinguished. However, in other derivatives only broad INDOR signals were observed. (389)  $\delta(^{29}\text{Si})$  values in  $\text{Si}-\text{N}$  (381, 384) and  $\text{Si}-\text{Pt}$  (390, 391) compounds have been measured.

$^{31}\text{P}$  The usual method of obtaining phosphorus chemical shifts now is from pulsed FT  $^{31}\text{P}-\{^1\text{H}\}$  spectra. However, the  $^1\text{H}-\{^{31}\text{P}\}$  technique is still widely used by preparative phosphorus chemists as an interpretative aid. Some studies still use double resonance specifically to measure  $\delta(^{31}\text{P})$ . This is probably due as much to instrument availability as to the suitability of the method. The microstructure of organophosphorus polymers has been studied in this way because direct detection is difficult. (392) Milligram quantities of substituted methylphosphonic acids (such as *N*-phosphonomethylglycine) have been studied as a function of pH. (393)  $^1\text{H}-\{^{31}\text{P}\}$  experiments were used for  $\delta(^{31}\text{P})/\text{pH}$  titrations of biogenic amine–organic phosphate mixtures. (394) The solvent dependence of  $\delta(^{31}\text{P})$  in paramagnetic complexes  $[\text{Ln}^{\text{III}}\text{L}_3]$  ( $\text{Ln} = \text{Pr}, \text{Nd}, \text{Eu}$ ;  $\text{L} = \text{Me}_2\text{PS}_2^-$ ) was also investigated indirectly. (395)

<sup>57</sup>Fe The magnetogyric ratio of <sup>57</sup>Fe ( $I = \frac{1}{2}$ , natural abundance 2.2%) is very small and direct detection of its resonance is difficult. Labelling with <sup>57</sup>Fe has enabled shifts of ferrocene derivatives to be determined from <sup>13</sup>C- $\{^1\text{H}_{\text{noise}}, ^{57}\text{Fe}\}$  experiments. (396) <sup>13</sup>C and <sup>57</sup>Fe labelled haemoproteins, e.g. sperm whale carbonyl myoglobin, have been prepared with a view to performing similar experiments (397) but these have not yet been reported.

<sup>63</sup>Cu Copper has two naturally occurring isotopes both with spin  $I = \frac{3}{2}$ . Of these, <sup>63</sup>Cu is the more abundant. Selective triple resonance <sup>1</sup>H- $\{^{31}\text{P}, ^{63}\text{Cu}\}$  TINDOR spectra (109) were used to study  $\delta(^{63}\text{Cu})$  in  $[(\text{MeO})_3\text{P}]_4\text{Cu}^+$ . The lines observed are split into three in an analogous way to the doublet splitting observed when  $I = 1$ , as in <sup>1</sup>H- $\{^{14}\text{N}\}$  INDOR spectra (398) (ref. 1).

<sup>75</sup>As The quadrupole moment of <sup>75</sup>As prevents double resonance measurements even in quaternary arsonium salts but the <sup>19</sup>F- $\{^{75}\text{As}\}$  INDOR spectrum of  $\text{AsF}_6^-$  has been measured and found to be a septet. (399)

<sup>77</sup>Se Double resonance has been used to measure  $\delta(^{77}\text{Se})$  in Sn-Se (375, 400-402) and P-Se compounds (403, 404), silyl and germyl selenides, (404) and secondary phosphine selenides. (98, 174, 405) <sup>1</sup>H- $\{^{31}\text{P}, ^{77}\text{Se}\}$  selective triple resonance was used (98, 174) for organophosphorus selenides where  $J(^1\text{H} \cdots ^{77}\text{Se})$  is effectively zero. Recently <sup>31</sup>P- $\{^1\text{H}_{\text{noise}}, ^{77}\text{Se}\}$  pulsed FT experiments have been performed to measure  $\delta(^{77}\text{Se})$  in  $[\text{MePhP}(\text{Se})]_2\text{CH}_2$  (406) and several cyclodiphosphazane selenides. (407)

<sup>95</sup>Mo Phosphine complexes of molybdenum(0) show satellites which are attributed (408) to coupling to both <sup>95</sup>Mo and <sup>97</sup>Mo. <sup>31</sup>P- $\{^1\text{H}_{\text{noise}}, ^{95}\text{Mo}\}$  decoupling experiments have shown (409) that the satellites arise solely from <sup>95</sup>Mo. The much larger quadrupole moment of <sup>97</sup>Mo compared with <sup>95</sup>Mo broadens the <sup>97</sup>Mo satellites to such an extent that they are not observed.

<sup>103</sup>Rh Shifts in several extensive series of rhodium complexes have now been reported from <sup>1</sup>H- $\{^{103}\text{Rh}\}$  experiments. Thirty-five octahedral rhodium(III) complexes with chalcogen and phosphorus ligands included mixed species and configurational isomers which are only observed in solution. (410) Two other reports (411, 412) include 20 complexes containing tertiary phosphine, carbonyl, and halide ligands. <sup>1</sup>H- $\{^{103}\text{Rh}\}$  INDOR was one technique used to study proton scrambling in  $[\text{Rh}_{13}(\text{CO})_{24}\text{H}_{5-n}]^{n-}$  ( $n = 2$  and  $3$ ); the metal cluster is hexagonally close-packed and the inner Rh is deshielded by 3000-4000 ppm relative to the outer Rh nuclei. (413)

<sup>111,113</sup>Cd <sup>1</sup>H- $\{^{113}\text{Cd}\}$  experiments have given  $\delta(^{113}\text{Cd})$  values for

a series of dialkylcadmium compounds. (414) Two earlier pulsed FT measurements (415) are found to be in error. It is shown that the methyl substitution effect on the metal chemical shift is similar in  $R_2Cd$  and  $R_2Hg$ . A series of methylcadmium alkoxides and alkanethiolates, where the shifts are useful as a probe of solution properties (as in tin analogues), have also been studied. (416) For  $Me_2Cd$ ,  $MeCdO^iBu$ , and  $MeCdOPh$ ,  $^1H-\{^{111}Cd\}$  and  $^1H-\{^{113}Cd\}$  experiments were used to show that there is no significant primary isotope effect. The value obtained for  $\gamma(^{113}Cd)/\gamma(^{111}Cd)$  is ten times more precise than the existing literature figure.

$^{117,119}Sn$  The rich chemistry of tin has led to extensive studies of tin chemical shifts. Most of the results of three published compilations (417) were obtained by double resonance and it is only recently that pulsed FT methods have been used. As with phosphorus, double resonance correlation is a very useful tool for the experimental tin chemist.

$^{125}Te$  Shifts obtained by double resonance have been reported. (400, 401, 418, 419) The range observed shows that a plot of  $^{125}Te$  vs.  $^{77}Se$  shifts is linear. (418)

$^{183}W$  Tungsten carbonyl derivatives have been studied by multiple resonance. With tertiary phosphine or cyclopentadienyl ligands  $^1H-\{^{183}W\}$  experiments sufficed. However, the effectively zero tungsten-proton coupling with ligands such as  $(MeO)_3P$  necessitated  $^1H-\{^{31}P, ^{183}W\}$  selective triple resonance experiments. (99, 374) The shifts of some methylimidotungsten(vi) fluorides have also been reported. (420)

$^{195}Pt$  Platinum is another nucleus which has been extensively studied by double resonance, so much so that recent pulsed FT work has been concentrated on systems where indirect methods cannot be applied. Several large lists of shifts have appeared. (390, 421–423) One group (422) found it possible to derive substituent parameters. Platinum shifts have been very useful in structural studies and for characterization of reaction products in solution. (424, 425) The mode of bonding of thiocyanate (379, 426) and cyanate (427) has a characteristic effect on the platinum shift. Numerous other data have been published (175, 391, 412, 428–432) including a study of temperature effects. (432)

$^{199}Hg$  Organomercury compounds have been studied by double resonance (433, 433a) and  $^1H-\{^{199}Hg\}$  INDOR spectra were used in studies of the fluxional behaviour of two cyclopentadienylmercury derivatives. (434) The solvent and concentration dependence of  $\delta(^{199}Hg)$  in  $[(MeO)_2P(O)]_2Hg$  has been investigated. (435)

<sup>205</sup>Tl Shifts of some dimethylthallium compounds have been reported. (436)

<sup>207</sup>Pb Lead chemical shifts have been measured in organolead compounds by double resonance (437–439) and comparisons made with analogous tin compounds. (439) The trends are usually similar although the lead shielding is three times more sensitive than that of tin to changes in chemical environment.

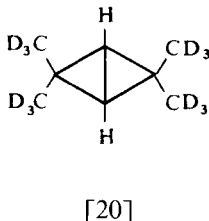
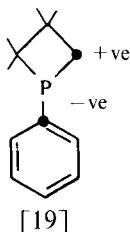
## B. The determination of the signs and magnitudes of coupling constants

Selective double resonance experiments of various kinds can be used to determine relative signs of coupling constants. It is the signs of the *reduced* couplings  $K$  ( $K_{AB} = J_{AB}4\pi^2/h\gamma_A\gamma_B$ ) that are actually compared. This fact must be taken into consideration if a nucleus with a negative magnetogyric ratio is irradiated or observed. The surprising negative signs reported (440) for  ${}^2K(P\cdots H)$  and  ${}^2K(P\cdots F)$  in  $H_2NP(CF_3)_2$  probably arise (381) because the negative magnetogyric ratio of  ${}^{15}N$  was not properly considered when the  ${}^{31}P\text{--}\{{}^{15}N\}$  double resonance experiments were interpreted.

### 1. Simple spin systems

The work in this category hinges on the identification of the various sub-spectra associated with different nuclear spin states, and no explicit consideration of the energy level diagrams is normally necessary.

The signs of many more one-bond couplings, in a greater variety of bonding situations, are now available and have necessitated the revision of some generalizations made earlier on the basis of more limited data. For example,  ${}^1K(Sn\text{--}C)$ , which is normally positive, is negative in  $Me_3SnLi$  (441) and  ${}^1K(Sn\text{--}Sn)$ , also normally positive, is negative in  $LiSn(SnMe_3)_3 \cdot 3THF$ . (110) One-bond couplings to a central atom of atoms in the same oxidation state can have different signs, e.g. the two  ${}^1K(W\text{--}F)$  couplings in  $XWF_5^-$  ( $X = O, NMe$ ) are of opposite sign, (420, 441, 442) as are  ${}^1K(P\text{--}C)$  in [19]. (444) Coupling between the bridgehead carbons of bicyclobutanes such as [20] is





negative, (445) in agreement with theoretical predictions. The discovery (127) of  $^1K(C-N)$  positive in  $MeNC$  contradicted an earlier theoretical calculation but agrees with the most recent one. (446)

Another reduced coupling involving the proton has been shown to be positive, namely  $^1K(O-H)$ . (112)  $^1K(Se-C)$  is negative in  $Se(II)$ ,  $Se(IV)$ , and  $Se(VI)$  compounds, (447) although a parallel with  $^1K(P-C)$  is maintained in that there is a large positive change in going from  $Se(II, IV)$  to  $Se(VI)$ . Similarly, all signs of  $^1K(Sn-P)$  measured to date are negative (448) but for trimethylstannylphosphines the coupling is much more positive in metal complexes than in the free ligand.  $^1K(Sn-X)$  (375, 400, 401) and  $^1K(Pb-X)$  (438) data have been compared (438) for a range of  $X$ ; a similar comparison has been made for  $^1K(Sn-X)$  and  $^1K(C-X)$ . (400)  $^1K(Pt-Se)$  and  $^1K(Pt-Te)$  are found to be usually positive, but variable in magnitude, in a range of complexes; (449) the exception is  $[PtI_5(SeMe_2)]^-$  with a negative  $^1K(Pt-Se)$ . Other signs determined involving metals are for  $^1K(C-Li)$ , (371)  $^1K(W-P)$ , (374)  $^1K(Hg-P)$ , (435) and  $^1K(Pt-Si)$ . (390) All are positive.  $^1K(P=Se)$ , (98, 174, 405)  $^1K(P-O)$ , and  $^1K(P=O)$  (113) are all negative.  $^1K(P-N)$  is usually negative (381–383, 440) but is reported to be positive in  $F_3P(NH_2)_2$  relative to a negative value of  $^1K(P-F)$ ; the experiments reported could not give this comparison, although they would have given a comparison with the positive  $^1K(N-H)$ .  $^1K(P-N)$  is also positive in  $F_2HP(NH_2)_2$ . (450)

$^1K(P-C)$  in aryl phosphines has been shown to be negative by means of  $^{13}C-\{^1H\}$  off-resonance proton decoupling. (451–454) When this technique is applied to systems where, say,  $^{31}P$  also couples, the degree of off-resonance is different for proton lines associated with the

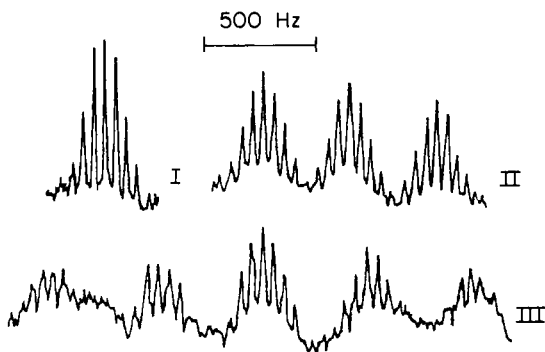


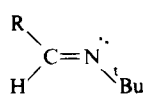
FIG. 29.  $^1H-\{^{195}Pt\}$  INDOOR spectra of isomers of thiocyanate complexes of platinum(II). (I)  $trans-[Pt(SCN)_2(SMe_2)_2]$ ; (II)  $trans-[Pt(SCN)(NCS)(SMe_2)_2]$ ; (III)  $trans-[Pt(NCS)_2(SMe_2)_2]$ . From ref. 175.

different phosphorus spin orientations; this results in different residual couplings for the associated carbon resonances and enables the relative assignment of phosphorus spin states, hence the sign comparison, to be made. In favourable cases the signs of several pairs of couplings can be compared from a single off-resonance decoupled spectrum. (451)

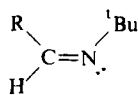
$^1K(P-C)$  in acetylenic compounds behaves "normally", being negative in P(III) and positive in P(V) derivatives. (455)  $^{13}C-\{^1H\}$  selective proton decoupling was used to show that the rather small value of  $^1K(Pt-C)$  in  $[Pt(C_2H_4)Cl_3]^-$  is positive. (456) Off-resonance decoupled  $^{13}C-\{^1H\}$  spectra of  $[^{15}N]$ pyridine and derivatives require simulation to be interpreted (because of the second-order character of the spectra) and show that  $^1K(C-N)$  can be either positive or negative. (457) The first demonstration of a negative  $^1K(C-N)$  was reported earlier. (458)  $^1K(B-C)$  is positive. (400, 459)

Platinum-nitrogen couplings have been observed in  $^1H-\{^{195}Pt\}$  INDOR spectra of several complexes with N-donors such as thiocyanate and amines (Fig. 29). (175, 426, 427)

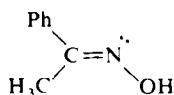
In much of the preceding work the signs of longer range coupling constants were also necessarily determined. Many cases are now known where not only the magnitude but the sign of couplings can have diagnostic use. Thus in both methylplatinum-(II) (428) and -(IV) (460) complexes containing tertiary phosphines *cis*- and *trans*- $^3J(PPtCH)$  are positive and negative respectively. In similar trifluoromethyl compounds  $^3J(PPtCF)$  is always positive but much larger for *trans* than *cis*. (180) Geminal coupling in imines and oximes has been studied.  $^2J(^1H-C=^{15}N)$  is positive in [21] and negative in [22] ( $R = 9$ -anthryl). (461) Similarly  $^2J(^{13}C-C=^{15}N)$  is positive in [23] and negative in [24]. (462)



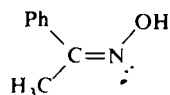
[21]



[22]



[23]



[24]

Following interest in  $^1J(P-P)$  there have been many multiple resonance studies of geminal P-P coupling, especially  $^2J(PNP)$ . (463, 464) The conformational sign-dependence of  $^2J(PNC)$  has also been studied. (465) Off-resonance  $^{13}C-\{^1H\}$  decoupling was used to relate signs, and Fig. 30 shows how for  $MeN(PF_2)_2$  a single spectrum can be used to determine the signs of  $^2J(CNP)/^3J(PNCH)$  and of  $^3J(CNPF)/^4J(FPNCH)$ . Knowledge of the signs of even longer range couplings can be important.  $^4J(PP)$  in phosphazenylicyclophos-

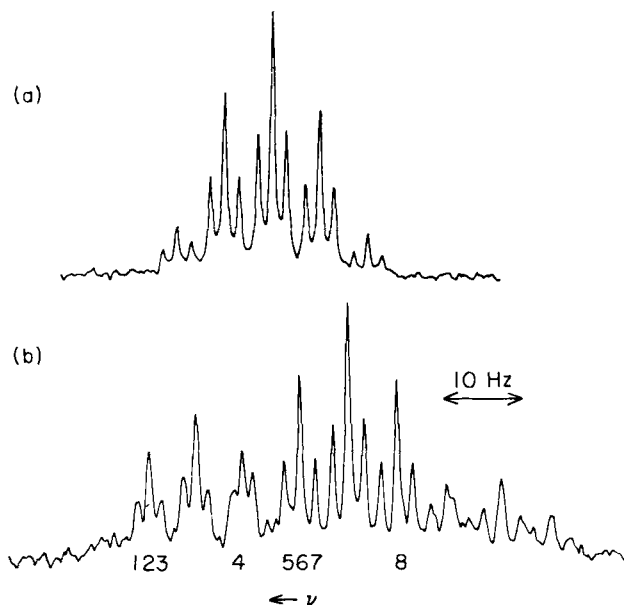
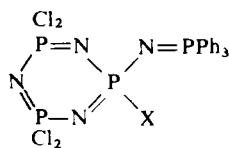
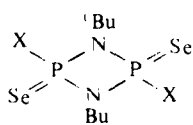


FIG. 30.  $^{13}\text{C}$  spectra of  $\text{F}_2\text{PN}(\text{Me})\text{PF}_2$ . (a) With proton noise decoupling. (b) With CW proton irradiation to high frequency of *N*-methyl signals. The relationships of the residual splittings (1–5) < (3–7) and (2–6) < (4–8) show that  $^2J(\text{CNP})/^3J(\text{PNCH})$  and  $^3J(\text{CNPF})/^4J(\text{FPNCH})$  are both positive. From ref. 465.

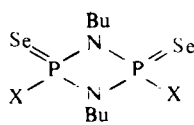
phazenes [25] was found to be related to the conformation of the exocyclic phosphazeny group when it was shown that the sign can change from positive to negative as X is varied. (466)  $^3J(\text{PSe})$  in a series of cyclodiphosphazane diselenides [26] can be positive or negative but is always more positive in the *cis* than in the *trans* isomer. (467)



[25]



*trans* [26]



*cis* [26]

As part of a study of the stereochemical dependence of geminal C–H coupling, the sign of  $^2J(\text{C–H})$  in the OCCCH fragment of carbohydrates was determined from  $^{13}\text{C}\{-^1\text{H}\}$  SPT experiments. (468) The relative signs of  $^2J(\text{PtNC})$  and  $^3J(\text{PtNCH})$  in  $^{13}\text{C}$ -labelled  $[\text{Pt}(\text{gly})\text{Cl}_2]^-$  and  $[\text{Pt}(\text{gly})(\text{NH}_3)_3]^+$  were measured by  $^1\text{H}\{-^{13}\text{C}\}$  tickling in an attempt to understand the importance of two- and three-bond coupling paths in the five-membered chelate rings. (469) The signs of tin–carbon couplings have been determined in work on stannacycloalkanes, and the relative contributions of the two- and three-bond Sn–C coupling paths in 1,1-diphenylstannacyclopentane have been considered. (470)

## 2. Complex spin systems

Double resonance in the  $A_nA'_nXX'$  spin system with  $J(\text{AA}') = 0$  is mentioned briefly in the previous report. (1) Subsequently the use (435) of  $A\{-X\}$  experiments to measure  $J(\text{XX}')$  by locating weak lines in the X spectrum has found many applications.  $^{31}\text{P}\text{--}^{31}\text{P}$  coupling in metal complexes and biphosphines was studied initially. (435, 471) Other groups have presented the results in the form of asymmetric INDOR spectra (472) which make it easier to measure smaller  $^{31}\text{P}\text{--}^{31}\text{P}$  couplings. P–N–P couplings have also been studied this way. (464, 473) The method is sensitive enough to measure the lead–lead coupling in hexamethyldilead with  $^{207}\text{Pb}$  in natural abundance. (474)

A development of the method in order to study  $A_nA'_nXX'M$  systems, where it is not convenient to observe A, has been reported. (475) In this situation the M resonance is a triplet, because of coupling to the two X nuclei, and the outer lines have energy levels in common with one or other of the groups of weak outer lines at a distance  $J(\text{XX}')$  from the centre of the X spectrum. Hence when  $M\{-X\}$  experiments are used to locate the outer lines the signs of  $J(\text{MX})$  and  $J(\text{XX}')$  are compared. Compounds such as  $(\text{Ph}_2\text{P})_2\text{CMe}_2$  were studied in this way. (475)

These methods do not work when  $J(\text{XX}')$  is very small. The problem (476) of tetramethylbiphosphine disulphide has been finally solved by means of  $^{13}\text{C}\{-^1\text{H}_{\text{noise}}, ^{31}\text{P}\}$  experiments. (75) Tickling of X transitions in the  $\text{AXX}'$  spin system enables the signs of  $[J(\text{AX}) + J(\text{AX}')]$  and  $J(\text{XX}')$  to be compared and hence show that  $^1J(\text{PP})$  is  $-18.8$  Hz.

Difficult analyses of complex spin systems can be eased by use of double resonance. An example is the planar  $[\text{AX}_9]_4$  spin system present in  $[\text{Pt}(\text{PMe}_3)_4]^{2+}$ .  $^1\text{H}\{-^{195}\text{Pt}\}$  INDOR experiments were used to break down the broad proton resonance into contributions from molecules with different total phosphorus spin quantum number. (477) The analysis of the tetrahedral  $[\text{AX}]_4$  systems given by

$ML_4$  [where  $M = Ni, Pt$ ;  $L = \overline{FPOC_6H_4O}$ ,  $FP(OPh)_2$ ] was also simplified by means of  $^{19}F-\{^{31}P\}$  INDOR experiments. (431)

The use of selective triple resonance experiments to determine the signs of coupling constants is mentioned on p. 357. In addition, an example has been published of the measurement of the *magnitude* of a coupling constant by means of a selective triple resonance experiment. (99) In a series of zerovalent tungsten carbonyl complexes,  $^1H-\{^{31}P\}$  selective decoupling experiments were used to measure  $^1J(^{31}P-^{183}W)$ . For the compound  $[PhP(SnMe_3)_2W(CO)_5]$  these experiments were unsuccessful owing to the similarity of  $^1J(^{31}P-^{117,119}Sn)$  and  $^1J(^{31}P-^{183}W)$  and the relatively high  $^{31}P$  power needed.  $^1J(^{31}P-^{183}W)$  can however be obtained from the  $^1H-\{^{31}P, ^{183}W\}$  selective triple resonance experiments which are used to measure the tungsten spectrum. This normally shows two lines, separated by  $^1J(^{31}P-^{183}W)$ , each of which is split by the phosphorus irradiation field into doublets with a separation of  $\gamma(^{31}P)B_2$ . In the experiment actually performed  $\gamma(^{31}P)B_2$  was of the same order of magnitude as  $^1J(^{31}P-^{183}W)$  and the four lines show pseudo-AB character with  $\gamma(^{31}P)B_2$  behaving as  $J(AB)$  and  $^1J(^{31}P-^{183}W)$  as  $\Delta\nu(A-B)$ . A straightforward calculation gives the value of  $^1J(^{31}P-^{183}W)$ . (99)

### C. General applications: simplification and assignment

Although placed towards the end, this section deals with the double resonance experiments that are probably applied most routinely. None of the principles involved is peculiar to a particular nuclear species but it is convenient to consider the possibilities of double resonance by dealing with specific nuclei and situations commonly met by practising chemists. Two important areas are the simplification of  $^1H$  spectra and the assignment of resonances in  $^{13}C$  spectra.

#### 1. $^1H-\{X\}$ experiments

$^1H-\{^2H\}$  Deuterium labelling combined with deuterium decoupling is well known as a method in spectral analysis and in stereochemical and conformational studies. The deuterium-decoupled proton spectra of XCHD, CHDY compounds produced during mechanistic studies are useful for determining the stereochemical course of reactions such as the methoxymercuration of ethylene, (478) the conversion of tyramine into tyrosol, (479) the non-catalytic addition of deuterium molecules to cyclopentadiene, (480) and alkyl transfer and olefin elimination in 2-phenyl-1,2-dideuterioethyl transition metal compounds. (481) The proton spectra of  $[^2H_4]$ - and  $[^2H_6]$ -t-butylcyclohexanes were

completely analysed with the help of deuterium decoupling. (482) Among other conformational studies (483, 484) the problem of 1,4-dioxan was tackled by looking at the  $^{13}\text{C}$  satellites in the  $^1\text{H}\{-^2\text{H}\}$  spectrum of a  $[\text{}^2\text{H}_4]$ -species. (484) Most deuteriated solvents show residual proton signals which can be broadened by means of  $^1\text{H}\{-^2\text{H}\}$  off-resonance noise-decoupling if signals of interest are obscured. (485) The sensitivity of the method was demonstrated by observing a signal from 0.002 vol % acetone present in hexadeuterioacetone (99.5 % D).

$^1\text{H}\{-^{11}\text{B}\}$  Proton spectra of boron compounds are often broad because the  $^{11}\text{B}$  quadrupole causes partial relaxation of  $^{11}\text{B}\cdots^1\text{H}$  coupling, and boron decoupling is usually a necessary preliminary before the power of  $^1\text{H}$  NMR reveals itself in borane chemistry. In the case of some small *closo*-carboranes decoupling revealed fine structure arising from long-range proton-proton coupling. (486)  $^1\text{H}\{-^{11}\text{B}\}$  and  $^1\text{H}\{-^{27}\text{Al}\}$  decoupling was used to study solutions of aluminium borohydride complexes. (487) More recently the structures of several metallocentaborane derivatives were confirmed by double resonance, including  $^1\text{H}\{-^{11}\text{B}\}$  experiments. (488)

$^1\text{H}\{-^{13}\text{C}\}$  Exchange of oleic acid residues between phospholipids produced by *E. coli* has been studied by means of a novel form of double-labelling and  $^1\text{H}\{-^{13}\text{C}\}$  difference spectra. (489) The cells were first grown in a medium containing  $[2\text{-}^2\text{H}]$ glycerol and  $[1\text{-}^{13}\text{C}]$ oleate, and then in a medium with unlabelled precursors. The only way that the 2-H proton of the diglycerides from the phospholipids produced can have enriched  $^{13}\text{C}$  satellites is due to oleate exchange during synthesis. By subtracting a normal proton spectrum from one with  $^{13}\text{C}$  decoupled it is found that the  $^{13}\text{C}$  satellites arise from naturally occurring  $^{13}\text{C}$  only and hence that exchange has not occurred.

$^1\text{H}\{-^{14}\text{N}\}$  The quadrupole of  $^{14}\text{N}$  also causes line-width problems, and  $^{14}\text{N}$  decoupling is often used to sharpen spectra. This is necessary in the case of  $[\text{PdX}_2(\text{CNMe})_2]$  ( $\text{X} = \text{Cl}, \text{Br}$ ) in order to see signals from *cis* and *trans* isomers. (380) It is also useful in kinetic studies of barriers to C-N bond rotation where line-shapes have to be measured. (490) Removal of line-broadening by decoupling is an unequivocal way of establishing the origin of the line-broadening. This was used to settle a controversy (491) as to whether the broadness of the hydride resonances of the N-bonded isomer of *trans*- $[\text{PtH}(\text{NCS})\text{L}_2]$  ( $\text{L} = \text{Et}_3\text{As}, \text{R}_3\text{P}$ ) is due to the  $^{14}\text{N}$  quadrupole or to phosphine exchange.  $^{14}\text{N}$ -decoupling removes the broadening. (492) In addition, simultaneous  $^{14}\text{N}$  and  $^{31}\text{P}$  decoupling has shown that phosphine exchange makes no additional contribution to the width of the peaks. (100)  $^{14}\text{N}$  decoupling was used to sharpen  $^{31}\text{P}$  spectra of some fluorinated cyclotriphosphazatrienes

prior to analysis. (493) The nitrogen methyl protons of  $\text{WF}_4(\text{NMe})(\text{NCMe})$  resonate as a complex multiplet;  $^1\text{H}-\{^{14}\text{N}\}$  and  $^1\text{H}-\{^{19}\text{F}\}$  experiments confirm the presence of both  $^{14}\text{N}$  and  $^{19}\text{F}$  coupling, enabling accurate values of  $^2J(^{14}\text{N} \cdots ^1\text{H})$  and  $^4J(^{19}\text{F} \cdots ^1\text{H})$  to be obtained. (494)

$^1\text{H}-\{^{31}\text{P}\}$  In addition to measurements of chemical shifts and coupling constants,  $^{31}\text{P}$  decoupling is often used to simplify spin systems so that the parameters obtained from a partial analysis can be used in a full analysis including  $^{31}\text{P}$ . Examples of applications of this approach are 1,3,2-diazaphosphorinans, (495) 1,3,2-oxazaphosphorinans, (496) 1,3,2-dithiaphospholans (497) phosphonates and hydroxyphosphonates, (498) and triphenylphosphine. (499) The correlation of resonances in  $^1\text{H}$  and  $^{31}\text{P}$  spectra is probably the most useful application of selective  $^1\text{H}-\{^{31}\text{P}\}$  experiments. An example of a chemical phenomenon studied in this way is the intermolecular association of biphosphines. (500) The methyl signals of certain biphosphines in dichloromethane solution are found to be broad. Double resonance experiments on a mixture of  $\text{Me}_4\text{P}_2$  and  $\text{Ph}_4\text{P}_2$  in  $\text{CH}_2\text{Cl}_2$  show that the methyl signal is coupled to two distinct regions in the phosphorus spectrum, corresponding closely to those of the individual biphosphines. Only after several days does the spectrum change to that of the ultimate product  $\text{Me}_2\text{PPPh}_2$ .

## 2. $^{13}\text{C}-\{X\}$ experiments

$^{13}\text{C}-\{^1\text{H}\}$  The number of variations that have been written on the theme of  $^{13}\text{C}-\{^1\text{H}\}$  double resonance reflects both the difficulty and importance of correct assignment in  $^{13}\text{C}$  NMR. Section IV.E deals mostly with the more technical aspects of this problem; the present section adopts a more applied approach.

The first step in the assignment process after considering the chemical shifts themselves is to obtain one or more off-resonance decoupled spectra to determine the number of protons attached to the carbons and to correlate the carbon and proton resonances. (191, 192) [It remains to be seen whether or not the two-dimensional FT technique of producing chemical shift correlation maps directly (159, 501) will supersede the more conventional methods.] Only then should more sophisticated experiments be contemplated. Many of the papers concerned with  $^{13}\text{C}-^1\text{H}$  correlation have concentrated on deriving accurate proton shifts. This can be unnecessary since often all that is required are the relative positions of the proton signals. These can be obtained easily by interpolation from two off-resonance decoupled

spectra without knowledge of the decoupler power even when equation (10) is not strictly valid.

The deceptive simplicity observed in off-resonance decoupling experiments on ABX systems where A and B are protons that are not attached to the same carbon is discussed in Section IV.E. This type of second-order effect has been used to assign aromatic and olefinic carbon signals of indan- and benzocyclo-alkenes (502) and of eight pterocarpanes. (503) French workers have also simulated spectra of this type of system as a function of  $J_{AB}$  and  $\Delta\nu/\gamma B_2$ . (504) In addition to these systems, Hagaman (505) has considered the ABX system present in the  $^{13}\text{CH}_A\text{H}_B$  unit. In an off-resonance decoupled spectrum where equation (10) applies, if  $J(\text{CH}_A) = J(\text{CH}_B)$  and  $\text{H}_A$  and  $\text{H}_B$  are weakly coupled then the  $^{13}\text{C}$  resonance is a doublet of doublets where the separation of the centre two lines is independent of the frequency of  $B_2$ . This property could if necessary be used to distinguish the observed spectrum from that given by a CH doublet. The  $^{13}\text{C}$  splitting in an off-resonance decoupled ABX spectrum obtained under the conditions

$$\gamma(^1\text{H})B_2 \gg |\nu_2 - \nu_A| \gg J_{AX}, J_{BX}, |\nu_A - \nu_B|$$

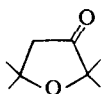
has been shown by Radeaglia (506) to be calculable without explicit consideration of the strength of the decoupler field. The spectrum can be simulated as a simple ABX system with  $J_{AX}$ ,  $J_{BX}$ , and  $|\nu_A - \nu_B|$  reduced by the common factor  $J_R/J_0 = |\nu_2 - \nu_A|/\gamma(^1\text{H})B_2$ . By plotting line positions in the  $\text{X}(^{13}\text{C})$  spectrum for different decoupler powers, it is possible to use the straight line obtained to calculate the ABX parameters without observing the  $\text{AB}(^1\text{H})$  spectrum.

Noise-modulated experiments can be useful for assignment. Low-power on-resonance noise-decoupling (507) as well as higher power off-resonance noise-decoupling (182, 508) can be used to identify quaternary carbons, although caution must be exercised since the central component of the triplet of a  $\text{CH}_2$  group with magnetically equivalent protons also remains sharp under these conditions. (190, 509) This fact was used (510) to distinguish methylene and methine carbons in polymers; in both low molecular weight liquid and high molecular weight solid poly(propylene oxide) the signal that remains sharp as the power of  $B_2$  is varied was assigned to the methylene carbons. When the protons of a  $\text{CH}_2$  group are not magnetically equivalent, the residual linewidth is proportional to the proton chemical shift difference and can be used as the basis of a correlation method; (509) the behaviour of X in AX and  $\text{A}_3\text{X}$  spin systems in the

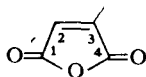


presence of off-resonance noise-decoupling of A was also examined in this work.

Selective decoupling can also be used in assignment, although achievement of selectivity requires careful setting of both decoupler frequency and power. It is possible to decouple one-bond and/or longer range coupling selectively. Selective decoupling experiments are performed for various reasons. They may be used to remove one-bond couplings for correlation purposes as a supplement to off-resonance experiments, (511) or to remove long range coupling in order to correlate groups further removed in a molecule. The pairs of methyl groups in [27] were assigned by means of low power selective decoupling of the vicinal  $^{13}\text{C}\text{CCH}$  couplings between the methyl groups. (512) Selective decoupling can also be used to reveal long range coupling. (513, 514) For example, decoupling of the aromatic protons of some alkylbenzenes simplifies the aromatic carbon signals so that long range coupling to the alkyl protons can be observed. (513) Another variation is to combine selective decoupling of long range CH couplings with deuterium exchange of hydroxyl protons (giving an isotope shift and removing OH coupling) in order to assign quaternary carbons. (515) The quaternary carbons of  $^{13}\text{C}$ -labelled chlorophyll-a were assigned (516) by accumulating  $^1\text{H}\{-^{13}\text{C}\}$  INDOR spectra in a manner similar to that (110) described on p. 330; the centres of resonances of protons two or three bonds away from the quaternary carbons are monitored so that responses are observed when the long range CH couplings collapse.



[27]

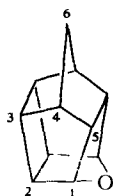


[28]

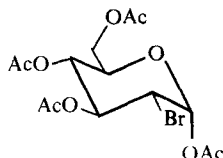
Selective  $^{13}\text{C}\{-^1\text{H}\}$  NOE of quaternary carbons have been observed in selective decoupling experiments. (296, 297) However, a study (517) of the frequency dependence of the NOE in [28] shows that, although differential NOE are observed for C-1 and C-3 when H-2 is irradiated with a field of strength  $\gamma B_2/2\pi \approx 20$  Hz, the frequency selectivity is not very good. The utility of the experiment as an assignment technique may therefore be somewhat restricted if the protons responsible for the selective NOE cannot be identified.

Spin population transfer experiments also need selective irradiation. As well as being used (136) to increase the intensity of quaternary carbon signals (p. 336), they have value for assignment by virtue of the

long range proton couplings which are exploited to produce the intensity changes. (518) A novel example (519) of the use of the selective intensity enhancements given by SPI is provided by [29]; the signals from C-4 and C-2 overlap and fine structure from long range couplings is not observed clearly. However, SPI experiments on the  $^{13}\text{C}$  satellites of H-4 enhance the C-4 signal so that a doublet arising from a long-range CH coupling becomes visible. SPI was also used to locate the  $^{13}\text{C}$  satellites of the H-6 proton signals of [29]. Similar selective population transfer experiments have been called "gated spin tickling" (GASP) and were used to assign the C-2 and C-5 carbon signals of 3-substituted furans. (520) SPT can be used in exactly the same way as conventional tickling experiments to establish connectivity of transitions for spectral analysis; in the analysis of the proton-coupled  $^{13}\text{C}$  spectrum of the  $[2\text{-}^{13}\text{C}]$ -isotopomer of butadieneiron tricarbonyl, eight solutions with reasonable RMS errors were obtained, but SPT experiments were used to eliminate seven of them. (521)



[29]



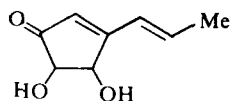
[30]

Population transfer effects in selective irradiation experiments are useful so long as they can be interpreted. When they arise in selective decoupling experiments on complicated molecules they tend to be regarded as undesirable intensity anomalies. A method of overcoming them has therefore been suggested. (522) In addition to the low power selective proton irradiation which is applied continuously, a high power noise-modulated proton decoupling field is applied during a delay before the sampling pulse and the acquisition of the FID. This procedure creates the maximum NOE for all the peaks and retains the selective decoupling. The method was illustrated with the pyranose derivative [30].

$^{13}\text{C}\{-^2\text{H}\}$  Polydeuteration followed by measurement of deuterium-decoupled  $^{13}\text{C}$  spectra has been suggested as a method of obtaining  $^{13}\text{C}\text{-}^1\text{H}$  coupling constants. By replacing all protons but one with deuterium, coupling of the remaining proton can then be observed in a first-order manner to  $^{13}\text{C}$  nuclei throughout the molecule.  $[^2\text{H}_{11}]$ Cyclohexane (at both ambient and low temperatures), (523) the

three isomers of  $[^2\text{H}_4]$ pyridine, (524) and the two isomers of  $[^2\text{H}_7]$ naphthalene (525) have been examined in this way.

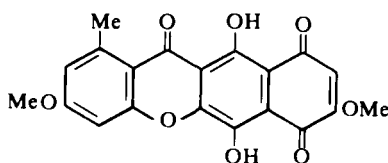
$^{13}\text{C}-\{^2\text{H}\}$  decoupling has also been used in biosynthetic work. Results concerning the incorporation of [*methyl*- $^{13}\text{C}^2\text{H}_3$ ]methionine during the biosynthesis of vitamin  $\text{B}_{12}$  were published simultaneously by three groups in 1976. Two of the groups (526, 527) used deuterium-noise-decoupled  $^{13}\text{C}$  spectra to show that the  $^{13}\text{C}^2\text{H}_3$  unit was incorporated intact into vitamin  $\text{B}_{12}$ , while the third group (528) used the complementary technique of  $^1\text{H}-\{^{13}\text{C}\}$  difference spectroscopy to reach the same conclusion by showing that the  $^{13}\text{C}$  satellites of the appropriate methyl protons arise from naturally abundant  $^{13}\text{C}$  only and hence that the  $^{13}\text{C}$  label has not acquired any protons during biosynthesis. The methyl group of terrein [31] obtained from the labelled biosynthetic precursor methyl[ $^{13}\text{C}^2\text{H}_3$ ] acetate is found to contain  $^{13}\text{C}^2\text{H}_3$  on decoupling the carbon signals from deuterium; (529) this result shows that the methyl group is a chain starter unit.



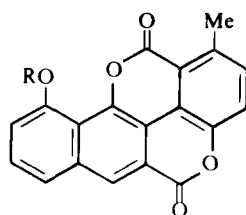
[31]

Metabolism of deuterium-labelled ethanol in rats has been investigated; (530, 531) low levels of deuterium incorporation into bile acids are observed in difference spectra obtained by subtracting  $^{13}\text{C}-\{^1\text{H}\}$  from  $^{13}\text{C}-\{^1\text{H}, ^2\text{H}\}$  spectra. The difference spectra contain only signals from  $^{13}\text{C}$  coupled to  $^2\text{H}$  and as little as 20 nmol of  $^{13}\text{C}-^2\text{H}$  is reported to be observable in this way. (531)

$^{13}\text{C}-\{^{13}\text{C}\}$   $^{13}\text{C}-\{^1\text{H}_{\text{noise}}, ^{13}\text{C}\}$  decoupling has been applied to biosynthetic studies. The method of biosynthetically labelling molecules with  $^{13}\text{C}_2$  units, usually from  $[1,2-^{13}\text{C}_2]$ acetate, is now very widely used; often the variation in the values of  $^1J(\text{C}-\text{C})$  is sufficient to identify the appropriate pairs and can be a valuable aid in assigning the signals. Sometimes ambiguity remains, especially in polyaromatic systems such as bikaverin [32] (532) and chartreusin [33]. (533) In the case of [32] the difficulties are compounded by low incorporation of  $^{13}\text{C}$  and poor solubility, necessitating the use of  $\text{CF}_3\text{CO}_2\text{D}-\text{CDCl}_3$  as solvent. These problems are overcome by means of homonuclear  $^{13}\text{C}$  decoupling with  $\gamma(^{13}\text{C})B_2/2\pi \approx 70$  Hz, which enables all the pairs of  $^{13}\text{C}$  satellites to be correlated. The instrumental arrangement used has been described briefly. (533)



[32]



R = D-digalose-D-fucose

[33]

A homonuclear  $^{13}\text{C}$  irradiation experiment has been described (534) which can involve observation of the natural abundance  $^{13}\text{C}$  satellites of  $^{13}\text{C}$  signals. Adiabatic rapid passage ( $40\text{ Hz s}^{-1}$ ) irradiation (89) of one  $^{13}\text{C}$  satellite perturbs the populations of energy levels so that, when a sampling pulse is applied to obtain a FT spectrum, the intensities of the coupled  $^{13}\text{C}$  satellites are also perturbed, one being enhanced and the other diminished. Adjacent carbons can therefore be identified. Even when the  $^{13}\text{C}$  satellites are not clear initially, the enhancement produced by the double irradiation can make the experiment successful. As well as a demonstration with  $[^{13}\text{C}_2]\text{ethyl acetate}$ , the technique was used to assign the methylene carbons of  $\text{MeOC}(\text{CH}_2\text{CH}_2)_3\text{CMe}$  by correlating them with the bridgehead carbons.

$^{13}\text{C}\{-^{19}\text{F}\}$  The power requirements for broad-band decoupling of fluorine from carbon are exceptional because of the large frequency spread of  $^{19}\text{F}$  spectra but can be provided. (77, 78)  $^{13}\text{C}$  shielding in several perfluorinated organic compounds was studied using a 50 W decoupler system generating  $\gamma(^{19}\text{F})B_2 = 13\text{ kHz}$  and a noise bandwidth of 7 kHz. (78)

### 3. Other experiments

Proton decoupling is usually used routinely for direct observation of "other" nuclei coupled to protons. As well as increasing the sensitivity (although negative NOE arising from negative magnetogyric ratios can cause problems) and simplifying the spectra, it can be essential where accurate line-shapes are required. This is the case in a  $^7\text{Li}$  study (535) of exchange processes in alkyl-lithium-tetra-alkylaluminates systems and in the measurement of  $^{17}\text{O}$  quadrupole coupling constants from  $^{17}\text{O}$  spectra. (536)

$^{29}\text{Si}$  NMR has been used to study some polytrimethylsilylated sugars. (537, 538) Selective decoupling, gated to remove the negative

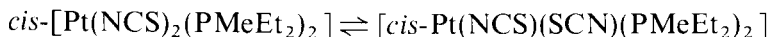
NOE, of  $\text{Me}_3\text{Si}$  proton signals enabled residual couplings from  $\text{Me}_3\text{SiOCH}_n$  protons to be observed. (537) Doublets and triplets distinguished between fragments with  $n = 1$  and  $n = 2$ .  $^{29}\text{Si}-\{^1\text{H}\}$  experiments have been used to correlate  $^{29}\text{Si}$  and  $^1\text{H}$  signals of  $\text{Me}_3\text{Si}$  groups; (538) it is necessary to add  $\text{Pr}(\text{dpm})_3$  in order to spread out the proton signals. The use of lanthanide shift reagents in  $^{13}\text{C}-\{^1\text{H}\}$  shift correlation experiments is well established. (539)

Measurement of a proton shift by means of selective  $^{31}\text{P}-\{^1\text{H}\}$  decoupling shows (540) that the shift of the protons coupled to the phosphate group covalently bound at the active site of phosphoglucosomutase is similar to that of the analogous protons in phosphoserine.

The multiplicities observed in  $^1\text{H}-\{\text{X}\}$  INDOR spectra are useful for assigning structures to parts of molecules, as for example in some work (541) involving  $^{29}\text{Si}$ ,  $^{31}\text{P}$ , and  $^{77}\text{Se}$ . However, it is always important when proton lines are monitored to ensure that the intensities in the INDOR spectra are correct. This problem was not adequately considered in work (542) that used  $^1\text{H}-\{^{119}\text{Sn}\}$  INDOR spectra to identify  $\text{Me}_3\text{Sn}$ ,  $\text{Me}_2\text{Sn}$ , and  $\text{MeSn}$  moieties; it has since been shown (543) by comparison of the tin chemical shifts that a compound described (542) as  $\text{MeSn}(\text{OEt})_3$  is in fact  $\text{Me}_2\text{Sn}(\text{OEt})_2$ .

A very "applied" example of double resonance has appeared as a U.S.S.R. patent. (544) It is suggested that the boron isotopic compositions of boric acid and boron oxide can be determined by dissolving the materials in HF and then recording the  $^{10}\text{B}$ -decoupled  $^{19}\text{F}$  spectra. In this way the  $^{10}\text{BF}_4^-$  signal appears (10) as a singlet instead of seven lines, and the time required to compare the intensities of the signals from  $^{10}\text{BF}_4^-$  and  $^{11}\text{BF}_4^-$  is reduced.

The different time-scales that are effective in the NMR spectra of different nuclei and their effects in double resonance experiments are illustrated in  $^1\text{H}-\{^{195}\text{Pt}\}$  INDOR spectra of the thiocyanate complexes present in the equilibrium: (427)



The rate of interconversion of the two complexes is such that exchange is fast with respect to the chemical shift between the  $\text{MeP}$  proton signals but slow with respect to the difference between the  $^{195}\text{Pt}$  signals. As a result two sets of  $^{195}\text{Pt}$  INDOR responses are obtained by monitoring a single  $\text{MeP}$  proton resonance.

When double resonance experiments are used to determine relative signs of coupling constants a set of unequivocally correlated couplings can be obtained. In the case of  $\text{Me}_6\text{Pb}_2$  a suggestion, (545) based on

arguments of analogy, to reverse the double resonance assignment of the one- and two-bond lead-carbon couplings did not take into account the necessary reversal of the assignment of the related two- and three-bond lead-proton couplings that this would entail. A repeat (546) of the double resonance experiments shows the original assignment to be correct.

The interpretation of INDOR experiments on nuclei with  $I > \frac{1}{2}$  is not necessarily straightforward. However, in the case of two coupled  $^{11}\text{B}$  nuclei ( $I = \frac{3}{2}$ ) it has been shown by deriving the energy level diagram that, when spin population effects predominate, intensity changes are apparent only when the outer lines of the multiplets are observed and irradiated. The interpretation of such experiments can therefore be relatively easy. This homonuclear  $^{11}\text{B}-\{^{11}\text{B}\}$  INDOR approach was used to assign the  $^{11}\text{B}$  spectrum of 6-methyldecaborane, where there is extensive coupling between the boron nuclei. (547, 548) Boron-boron couplings were measured from the  $^{11}\text{B}$  spectra of  $\text{B}_4\text{H}_{10}$  and  $\text{CB}_5\text{H}_9$  after the proton-coupling was removed by noise-decoupling. (549) A previously reported value (550) for  $^1J(^{11}\text{B}_1-^{11}\text{B}_3)$  in  $\text{B}_4\text{H}_{10}$  has been revised on the basis of the observation of the corresponding  $^{10}\text{B}-^{11}\text{B}$  coupling. Homonuclear  $^{31}\text{P}-\{^{19}\text{F}_{\text{noise}}, ^{31}\text{P}\}$  tickling experiments are used to correlate transitions during the analysis of the phosphorus spectrum of the cyclopentaphosphine  $(\text{CF}_3\text{P})_5$ . (551)

A Carr-Purcell pulse sequence has been used to demonstrate through-space spin coupling in an enzyme. (552) Two of the signals in the proton-noise-decoupled fluorine spectrum of a complex of dihydrofolate reductase (from *L. casei*) containing 6-fluoro labelled tryptophans appear as doublets. The splitting was thought to arise from a spin coupling since it was the same in spectra obtained at two different field strengths. It was not possible to decouple protons and fluorine simultaneously on the instruments available but the use of a  $(90^\circ-\tau-180^\circ-\tau)$  pre-acquisition pulse sequence has confirmed that the cause of the splitting is a spin coupling. In these experiments doublets arising from  $J$  are inverted and singlets appear with normal phase when  $2\tau = 1/J$ . (553) Since no other magnetic nuclei that could have caused the coupling were thought to be present the splitting is attributed to a fluorine-fluorine coupling (the advantage of homonuclear decoupling is that *proof* of fluorine-fluorine coupling could have been obtained). None of the tryptophans is near another in the primary amino-acid sequence of the enzyme, so the coupling must arise from a close through-space interaction in the three-dimensional folded structure. (552)

### D. Oriented molecules

When a molecule is partly oriented by dissolution in a liquid crystal solvent it is necessary to consider direct dipolar splittings, nuclear screening anisotropies, and possibly also very large quadrupolar splittings, in order to account for the spectrum. The ways in which this can affect multiple resonance experiments have been considered already. (33, 35–37, 46) In this section we discuss some applications. Naturally, proton decoupling is often used to simplify  $^{13}\text{C}$  spectra of oriented molecules, although it is desirable to avoid complete decoupling of the solvent protons.

The problem of achieving decoupling of deuterium in oriented species was overcome to the extent that satisfactory proton spectra were obtained of oriented  $\text{CH}_3\text{OD}$ ,  $\text{CF}_3\text{CH}_2\text{OH}$ ,  $\text{CHD}_2\text{OH}$ ,  $\text{CH}_3\text{CD}_2\text{OH}$ , and  $\text{C}_6\text{D}_5\text{COCH}_3$  in various nematic phases. (33, 35, 37) Selective irradiation has also been used in this type of work to confirm relative signs of coupling constants and to measure the deuterium quadrupolar splitting. (554–556) Proton decoupling (an easier proposition) was used to simplify the deuterium spectrum of  $[1,1\text{-}^2\text{H}_2]\text{-n-propanol}$ , (557)  $^{31}\text{P}$  decoupling was used in a study of oriented triethynylphosphine, (558) and  $^{19}\text{F}$  decoupling simplified the  $^{19}\text{F}$  spectra of oriented phosphazenes. (559)

An early report (560) mentions the use of homonuclear spin tickling to aid the assignment of the lines of an AB spectrum from an oriented molecule. The method has been applied to the 4-proton spectrum from ethylene oxide in EBBA (561) and to the detection and assignment of weak transitions in the proton spectrum of oriented *o*-dichlorobenzene. (562)

$^1\text{H}\text{-}\{\text{X}\}$  experiments offer the following advantages for the study of chemical shift anisotropies: high sensitivity; relative signs of direct and indirect spin couplings are obtained to simplify the analysis; an internal reference (e.g. TMS) can be used; splittings in X and  $^1\text{H}$  spectra can be measured contemporaneously. Examples of this approach, however, are few but some data have been measured in this way:  $^{13}\text{C}$  and  $^{15}\text{N}$  anisotropies in enriched methyl cyanide; (563) the  $^{31}\text{P}$  anisotropy in  $\text{Me}_3\text{P}$ ,  $\text{Me}_3\text{PO}$ , and  $\text{Me}_3\text{PS}$ ; (564) the  $^{111/113}\text{Cd}$  anisotropy in dimethylcadmium; (565) and the  $^{199}\text{Hg}$  anisotropy in  $\text{Me}_2\text{Hg}$  and  $\text{MeHgX}$  ( $\text{X} = \text{Cl}, \text{Br}, \text{I}$ ). (433, 566) In a study of oriented  $\text{MeN}(\text{PCl}_2)_2$ , enriched in  $^{13}\text{C}$  or  $^{15}\text{N}$ ,  $^1\text{H}\text{-}\{^{13}\text{C}\}$ ,  $^1\text{H}\text{-}\{^{15}\text{N}\}$ , and  $^1\text{H}\text{-}\{^{31}\text{P}\}$  experiments were used to give heteronuclear dipolar couplings and their signs and so deduce the PNP interbond angle. (567) This work also gives the  $^{13}\text{C}$ ,  $^{15}\text{N}$ , and  $^{31}\text{P}$  nuclear screening anisotropies. (567)

## Acknowledgement

We are most grateful to Mrs. J. Fronek for her speedy and efficient typing of the manuscript.

## REFERENCES

1. W. McFarlane, in *Ann. Reports NMR Spectroscopy*, E. F. Mooney (ed.), 1972, **5A**, 353.
2. D. Shaw, in *NMR Specialist Per. Reports* (The Chemical Society, London), 1972, **1**, 257; 1973, **2**, 269.
3. W. McFarlane and D. S. Rycroft, in *NMR Specialist Per. Reports* (The Chemical Society, London), 1975, **4**, 174; 1977, **6**, 67; 1978, **7**, 125; in press.
4. W. von Philipsborn, *Angew. Chem. Internat. Edn.*, 1971, **10**, 472.
5. R. B. Johannesen and T. D. Coyle, *Endeavour*, 1972, **31**, 10.
6. J. H. Noggle and R. E. Schirmer, "The Nuclear Overhauser Effect: Chemical Applications", Academic Press, New York, 1971.
7. G. E. Backers and T. Schaefer, *Chem. Rev.*, 1971, **71**, 617.
8. R. L. Miehler, *Magn. Resonance Rev.*, 1972, **1**, 225.
9. L. R. Dalton, *Magn. Resonance Rev.*, 1972, **1**, 301.
10. W. McFarlane, in "Nuclear Magnetic Resonance Spectroscopy of Nuclei Other than Protons", T. Axenrod and G. A. Webb (eds.), Academic Press, New York, 1974, p. 31.
11. L. R. Dalton and L. A. Dalton, *Magn. Resonance Rev.*, 1973, **2**, 361.
12. L. D. Hall, *Adv. Carbohydrate Chem. Biochem.*, 1974, **29**, 11.
13. K. Möbius, *Ber. Bunsenges. Phys. Chem.*, 1974, **78**, 1116.
14. R. R. Ernst, *Chimia*, 1975, **29**, 179.
15. J. D. Memory, *Magn. Resonance Rev.*, 1972, **1**, 91, 185, 333.
16. D. Shaw, *J. Phys. (E)*, 1974, **7**, 689.
17. G. W. Gray, *Analyt. Chem.*, 1975, **47**, 546A.
18. I. P. Biryukov, B. E. Alekseev and U. Ulmanis, *Radiats. Fiz.*, 1975, **8**, 124.
19. L. G. Werbelow and D. M. Grant, in *Adv. Magn. Resonance*, J. Waugh (ed.) 1977, **9**, 189.
20. R. Freeman and H. D. W. Hill, *J. Magn. Resonance*, 1971, **5**, 278.
21. R. Freeman, H. D. W. Hill and R. Kaptein, *J. Magn. Resonance*, 1972, **7**, 327.
22. G. Bodenhausen, R. Freeman, R. Niedermeyer and D. L. Turner, *J. Magn. Resonance*, 1977, **26**, 133.
23. G. Bodenhausen, R. Freeman and G. A. Morris, *J. Magn. Resonance*, 1976, **23**, 171.
24. J. Jeener, Ampère International Summer School II, Basko Polje, 1971; 2nd European Experimental N.M.R. Conference, Enschede, Holland, 1975.
25. G. Bodenhausen, R. Freeman, R. Niedermeyer and D. L. Turner, *J. Magn. Resonance*, 1976, **24**, 291.
26. W. P. Aue, E. Bartholdi and R. R. Ernst, *J. Chem. Phys.*, 1976, **64**, 2229.
27. R. Freeman and H. D. W. Hill, *J. Chem. Phys.*, 1971, **54**, 3367.
28. M. J. Gerace and K. F. Kuhlmann, *J. Phys. Chem.*, 1972, **76**, 1152.
29. I. D. Campbell and R. Freeman, *J. Magn. Resonance*, 1973, **11**, 143.
30. W. Buchner, *J. Magn. Resonance*, 1973, **12**, 82.
31. T. D. Alger, R. Freeman and D. M. Grant, *J. Chem. Phys.*, 1972, **57**, 2168.
32. L. G. Werbelow and D. M. Grant, *J. Chem. Phys.*, 1975, **63**, 4742.
33. L. C. Snyder and S. Meiboom, *J. Chem. Phys.*, 1973, **58**, 5096; R. C. Hewitt, S. Meiboom and L. C. Snyder, *ibid*, p. 5089.
34. W. A. Anderson and F. A. Nelson, *J. Chem. Phys.*, 1965, **42**, 1199.



35. J. W. Emsley, J. C. Lindon and J. M. Tabony, *J. Chem. Soc., Faraday II*, 1973, **69**, 10.
36. R. Freeman and W. A. Anderson, *J. Chem. Phys.*, 1962, **37**, 85.
37. J. W. Emsley, J. C. Lindon, J. M. Tabony and T. H. Wilmshurst, *Chem. Comm.*, 1971, 1277.
38. J. P. Jesson, P. Meakin and G. Kneissel, *J. Amer. Chem. Soc.*, 1973, **95**, 618.
39. A. Pines and J. D. Ellet, Jr., *J. Amer. Chem. Soc.*, 1973, **95**, 4437.
40. R. A. Hoffman and S. Forsén, in *Progr. NMR Spectroscopy*, J. Emsley, J. Feeney and L. H. Sutcliffe (eds.), 1966, **1**, 15.
41. T. J. Batterham and C. J. Bigum, *Org. Magn. Resonance*, 1972, **4**, 67.
42. H. Fukui and J. Sohma, *Hokkaido Daigaku Kogakuba Kenkyu Hokoku*, 1974, **72**, 103.
43. P. Anstey and R. K. Harris, *S.R.C. NMR Computer Program Library*, 1975, Bulletin 9.
44. V. I. Mstislavskii, *Zh. Fiz. Khim.*, 1976, **50**, 2446.
45. A. Kumar, *J. Magn. Resonance*, 1978, **30**, 227.
46. A. Kumar and C. L. Khetrpal, *J. Magn. Resonance*, 1978, **30**, 137.
47. V. F. Bystrov, *J. Magn. Resonance*, 1970, **3**, 350.
48. P. Meakin and J. P. Jesson, *J. Magn. Resonance*, 1973, **10**, 290.
49. R. M. Lynden-Bell, in *Progr. NMR Spectroscopy*, J. Emsley, J. Feeney and L. H. Sutcliffe (eds.), 1967, **2**, 163.
50. B. D. Nageswara Rao, in *Adv. Magn. Resonance*, J. Waugh (ed.), 1970, **5**, 271.
51. P. D. Buckley, K. W. Jolley and D. N. Pinder, in *Progr. NMR Spectroscopy*, J. Emsley, J. Feeney and L. H. Sutcliffe (eds.), 1975, **10**, 1.
52. B. Gestblom, O. Hartmann and J. M. Anderson, *J. Magn. Resonance*, 1971, **5**, 174.
53. N. R. Krishna and B. D. Nageswara Rao, *Mol. Phys.*, 1972, **23**, 1013.
54. P. Meakin and J. P. Jesson, *J. Magn. Resonance*, 1973, **11**, 182; 1974, **13**, 354; 1976, **18**, 411.
55. B. W. Goodwin and R. Wallace, *J. Magn. Resonance*, 1973, **12**, 60.
56. B. W. Goodwin and R. Wallace, *J. Magn. Resonance*, 1972, **8**, 41.
57. J.-C. Duplan, A. Briguët and J. Delmau, *J. Magn. Resonance*, 1973, **12**, 270; J.-C. Duplan, C. Chapelet-Barbier and J. Delmau, *Mol. Phys.*, 1972, **23**, 609.
58. A. D. Bain, R. M. Lynden-Bell, W. M. Litchman and E. W. Randall, *J. Magn. Resonance*, 1977, **25**, 315.
59. G. E. Hawkes, S. Paget and E. W. Randall, *J. Magn. Resonance*, 1978, **30**, 393.
60. M. A. Dugan and J. M. Anderson, *J. Magn. Resonance*, 1977, **27**, 133.
61. J. I. Kaplan, P. P. Yang and G. Fraenkel, *J. Amer. Chem. Soc.*, 1975, **97**, 3881.
62. S. Forsén and R. A. Hoffman, *J. Chem. Phys.*, 1964, **40**, 1189.
63. P. P. Young and S. L. Gordon, *J. Chem. Phys.*, 1971, **54**, 1779.
64. B. M. Fung and P. M. Olympia, *Mol. Phys.*, 1970, **19**, 685.
65. P. Bucci, M. Martinelli and S. Santucci, *J. Chem. Phys.*, 1970, **53**, 4524.
66. P. Bucci, M. Martinelli, S. Santucci and A. M. Serra, *J. Magn. Resonance*, 1972, **6**, 281.
67. P. E. Fagerness, D. M. Grant and R. B. Parry, *J. Magn. Resonance*, 1977, **26**, 267.
68. C. L. Mayne, D. M. Grant and D. W. Alderman, *J. Chem. Phys.*, 1976, **65**, 1684.
69. J. Courtieu, P. E. Fagerness and D. M. Grant, *J. Chem. Phys.*, 1976, **65**, 1202.
70. A. Briguët, J.-C. Duplan, D. Graveron-Demilly and J. Delmau, *Mol. Phys.*, 1974, **28**, 177.
71. A. Briguët, J.-C. Duplan, D. Graveron-Demilly and J. Delmau, *Phys. Letters (A)*, 1974, **49**, 106.
72. R. E. D. McClung and N. R. Krishna, *J. Magn. Resonance*, 1978, **29**, 573.
73. S. Shaublin, A. Höhener and R. R. Ernst, *J. Magn. Resonance*, 1974, **13**, 196.
74. A. Charles and W. McFarlane, *Mol. Phys.*, 1968, **14**, 299.
75. I. J. Colquhoun and W. McFarlane, *J. Magn. Resonance*, 1978, **31**, 63.
76. M. Mazurek, T. M. Mallard and P. A. J. Gorin, *Org. Magn. Resonance*, 1977, **9**, 193.
77. Anonymous, *JEOL Newsletter*, 1977, A203.
78. D. W. Overall and J. J. Chang, *J. Magn. Resonance*, 1977, **25**, 361.

79. H. J. C. Yeh, R. G. Tschudin, D. N. Lincoln and E. Lustig, *J. Magn. Resonance*, 1973, **10**, 237.
80. R. Burton, L. D. Hall and P. R. Steiner, *Canad. J. Chem.*, 1971, **49**, 588.
81. G. Matson, *J. Magn. Resonance*, 1977, **25**, 481.
82. V. Barboiu and V. Petrescu, *Org. Magn. Resonance*, 1973, **5**, 43.
83. V. Barboiu, J. W. Emsley and J. C. Lindon, *J. Chem. Soc., Faraday II*, 1972, **68**, 241.
84. O. Dahl and S. A. Laursen, *Org. Magn. Resonance*, 1976, **8**, 1.
85. V. Barboiu, *Mol. Phys.*, 1974, **28**, 707.
86. R. K. Harris, M. I. M. Wazeer, O. Schluk and R. Schmutzler, *J. Chem. Soc., Dalton*, 1974, 1912.
87. A. G. Marshall, L. D. Hall, M. Hatton and J. Sallos, *J. Magn. Resonance*, 1974, **13**, 392.
88. A. Sügis and M. Alla, *Izvest. Akad. Nauk Est. S.S.R., Ser. Tekh. i Fiz.-mat. Nauk*, 1973, **22**, 65.
89. H. C. Born, S. J. Uurtamo and G. E. Maciel, *Rev. Sci. Instr.*, 1973, **44**, 128.
90. A. G. Redfield and R. K. Gupta, *Adv. Magn. Resonance*, 1971, **5**, 81.
91. D. M. Wilson, R. W. Olsen and A. L. Burlingame, *Rev. Sci. Instr.*, 1974, **45**, 1095.
92. J. D. Ellett, Jr., M. G. Gibby, V. Haeberlen, A. Pines and J. S. Waugh, *Adv. Magn. Resonance*, 1971, **5**, 117.
93. P. Bucci, P. A. Rolla and C. A. Veracini, *Rev. Sci. Instr.*, 1973, **44**, 1423.
94. W. A. Anderson and F. A. Nelson, *J. Chem. Phys.*, 1963, **39**, 183.
95. R. Freeman and W. A. Anderson, *J. Chem. Phys.*, 1965, **42**, 1199.
96. J. B. Grutzner and R. E. Santini, *J. Magn. Resonance*, 1974, **19**, 173.
97. G. C. Levy, I. R. Peat, R. Rosanske and S. Parks, *J. Magn. Resonance*, 1975, **8**, 205.
98. W. McFarlane and D. S. Rycroft, *J. Chem. Soc., Dalton*, 1973, 2162.
99. H. C. E. McFarlane, W. McFarlane and D. S. Rycroft, *J. Chem. Soc., Dalton*, 1976, 1616.
100. W. McFarlane and D. S. Rycroft, unpublished observations.
101. Y. Takarada, *Kyoto Sangyo Daigaku Ronshu*, 1975, **5**, 82 (*Chem. Abs.*, **87**, 93408g).
102. T. W. Orth and L. J. Burnett, *J. Magn. Resonance*, 1978, **29**, 39.
103. R. C. Ferguson and H. M. Records, *J. Magn. Resonance*, 1973, **11**, 266.
104. E. B. Baker, *J. Chem. Phys.*, 1962, **37**, 911.
105. D. H. R. Barton, P. N. Jenkins, R. Letcher and O. A. Widdowson, *Chem. Comm.*, 1970, 391.
106. R. Burton, L. D. Hall and P. R. Steiner, *Canad. J. Chem.*, 1970, **48**, 2679.
107. Q. Sciacovelli, W. von Philipsborn, C. Amith and D. Ginsburg, *Tetrahedron*, 1970, **26**, 4589.
108. F. W. van Deursen, *Org. Magn. Resonance*, 1971, **3**, 221.
109. W. McFarlane and D. S. Rycroft, *J. Magn. Resonance*, 1976, **24**, 95.
110. J. D. Kennedy and W. McFarlane, *J. Chem. Soc., Dalton*, 1976, 1219.
111. W. McFarlane and C. J. Turner, *Bull. Soc. Chim. Belg.*, 1978, **87**, 271.
112. W. B. Jenkins and W. McFarlane, *Chem. Comm.*, 1977, 922.
113. H. C. E. McFarlane and W. McFarlane, *Chem. Comm.*, 1978, 531.
114. D. Ziessow, *J. Chem. Phys.*, 1971, **55**, 984; *Chem. Comm.*, 1971, 463; D. Ziessow and E. Lippert, *Ber. Bunsenges. Phys. Chem.*, 1970, **74**, 568.
115. J. Feeney and P. Partington, *Chem. Comm.*, 1973, 611.
116. K. G. R. Pachler and P. L. Wessels, *J. Magn. Resonance*, 1973, **12**, 337.
117. K. G. R. Pachler and P. L. Wessels, *Chem. Comm.*, 1974, 1038.
118. S. Sørensen, R. Hansen and H. J. Jakobsen, *J. Magn. Resonance*, 1974, **14**, 243.
119. A. A. Chalmers, K. G. R. Pachler and P. L. Wessels, *J. Magn. Resonance*, 1974, **15**, 415.
120. K. Bock, R. Burton and L. D. Hall, *Canad. J. Chem.*, 1976, **54**, 3526; 1977, **55**, 1045.
121. L. D. Hall, K. F. Wang and W. Schittenhelm, *Amer. Chem. Soc. Symp. Ser.*, 1977, **41** (Sacrochem. Symp. 1977, 1976), 22.
122. G. Wagner and K. Wüthrich, *J. Magn. Resonance*, 1975, **20**, 435; G. Wagner, A. de Marco and K. Wüthrich, *ibid.*, p. 565.
123. K. Kushida, K. Aoki and S. Sutoh, *J. Amer. Chem. Soc.*, 1975, **97**, 443.
124. J. M. Wouters and G. A. Petersson, *J. Magn. Resonance*, 1977, **28**, 81, 93.

125. J. P. Marchal and D. Canet, *J. Chem. Phys.*, 1977, **66**, 2566.
126. M. Llinas, W. J. Horsley and M. P. Klein, *J. Amer. Chem. Soc.*, 1976, **98**, 7554.
127. N. J. Koole, D. Krol and M. J. A. de Bie, *J. Magn. Resonance*, 1976, **21**, 499.
128. W. McFarlane, *J. Chem. Soc. (A)*, 1967, 1660.
129. H. J. Jakobsen and H. Bildsøe, *J. Magn. Resonance*, 1976, **26**, 183.
130. H. Bildsøe, *J. Magn. Resonance*, 1977, **27**, 393.
131. J. R. Alger and J. A. Prestegard, *J. Magn. Resonance*, 1977, **27**, 137.
132. N. J. Koole and M. J. A. de Bie, *J. Magn. Resonance*, 1976, **23**, 9.
133. R. A. Hoffman, B. Gestblom and S. Forsen, *J. Chem. Phys.*, 1964, **40**, 3734; 1963, **39**, 468; *J. Mol. Spectroscopy*, 1964, **13**, 221.
134. H. J. Jakobsen, S. A. Linde and S. Sørensen, *J. Magn. Resonance*, 1974, **15**, 385.
135. T. Bundgaard and H. J. Jakobsen, *J. Magn. Resonance*, 1975, **18**, 209.
136. K. G. R. Pachler and P. L. Wessels, *J. Magn. Resonance*, 1977, **28**, 53; *Org. Magn. Resonance*, 1977, **9**, 557.
137. B. L. Tomlinson and H. D. W. Hill, *J. Chem. Phys.*, 1973, **59**, 1775.
138. R. K. Harris, R. H. Newman and A. Okruszek, *Org. Magn. Resonance*, 1977, **9**, 58.
139. D. I. Hoult, *J. Magn. Resonance*, 1976, **21**, 337.
140. H. E. Bleich and J. A. Glasel, *J. Magn. Resonance*, 1975, **18**, 401.
141. N. R. Krishna, *J. Magn. Resonance*, 1976, **22**, 555.
142. S. L. Patt and B. D. Sykes, *J. Chem. Phys.*, 1972, **56**, 3182.
143. E. S. Mooberry and T. R. Krugh, *J. Magn. Resonance*, 1975, **17**, 128.
144. F. W. Benz, J. Feeney and G. C. K. Roberts, *J. Magn. Resonance*, 1972, **8**, 114.
145. R. Freeman and H. D. W. Hill, in "Dynamic Nuclear Magnetic Resonance Spectroscopy", L. M. Jackman and F. A. Cotton (eds.), Academic Press, New York, 1975, p. 131.
146. R. R. Ernst, W. P. Aue, P. Bachmann, J. Karhan, A. Kumar and L. Müller, *Magn. Resonance Condens. Matter—Recent Dev.*, Proc. Ampère Internat. Summer School 4th, 1976, p. 89.
147. R. R. Ernst, Ger. Pat. 2,656,166 (*Chem. Abs.*, **88**, 200956v).
148. R. Freeman and H. D. W. Hill, *J. Chem. Phys.*, 1971, **54**, 301.
149. G. Bodenhausen, R. Freeman, G. A. Morris and D. L. Turner, *J. Magn. Resonance*, 1978, **31**, 75.
150. W. P. Aue, J. Karhan and R. R. Ernst, *J. Chem. Phys.*, 1976, **64**, 4226.
151. J. F. Collins, personal communication.
152. K. Nagayama, K. Wüthrich, P. Bachmann and R. R. Ernst, *Naturwiss.*, 1977, **64**, 581.
153. R. Freeman, G. A. Morris and D. L. Turner, *J. Magn. Resonance*, 1977, **26**, 373.
154. G. Bodenhausen, R. Freeman, G. A. Morris and D. L. Turner, *J. Magn. Resonance*, 1977, **28**, 17.
155. G. Bodenhausen, R. Freeman and D. L. Turner, *J. Chem. Phys.*, 1976, **65**, 839.
156. R. R. Ernst and A. Kumar, *J. Magn. Resonance*, 1977, **25**, 384.
157. L. Müller, A. Kumar and R. R. Ernst, *J. Chem. Phys.*, 1975, **63**, 5490.
158. P. Bachmann, W. P. Aue, L. Müller and R. R. Ernst, *J. Magn. Resonance*, 1977, **28**, 29.
159. A. A. Maudsley, L. Müller and R. R. Ernst, *J. Magn. Resonance*, 1977, **28**, 463.
160. G. Bodenhausen and R. Freeman, *J. Magn. Resonance*, 1977, **28**, 471.
161. R. Freeman and G. A. Morris, *J. Magn. Resonance*, 1978, **29**, 173.
162. A. A. Maudsley, A. Wokaun and R. R. Ernst, *Chem. Phys. Lett.*, 1978, **55**, 9; A. A. Maudsley and R. R. Ernst, *ibid.*, 1977, **50**, 368; A. Wokaun and R. R. Ernst, *ibid.*, 1977, **52**, 407.
163. G. Bodenhausen, R. Freeman and D. L. Turner, *J. Magn. Resonance*, 1977, **27**, 511.
164. M. E. Stoll, A. J. Vega and R. W. Vaughan, *J. Chem. Phys.*, 1977, **67**, 2029.
165. P. M. Henrichs and L. J. Schwartz, *J. Magn. Resonance*, 1977, **28**, 477.
166. N. Zumbulyadis, P. M. Henrichs and L. J. Schwartz, *J. Chem. Phys.*, 1977, **67**, 1780.
167. W. P. Aue, P. Bachmann, A. Wokaun and R. R. Ernst, *J. Magn. Resonance*, 1978, **29**, 523.

168. I. D. Campbell, C. M. Dobson and R. J. P. Williams, *Proc. Roy. Soc. (B)*, 1975, **189**, 503.
169. I. D. Campbell and C. M. Dobson, *Chem. Comm.*, 1975, 750.
170. D. L. Turner and R. Freeman, *J. Magn. Resonance*, 1978, **29**, 587.
171. G. Bodenhausen and R. Freeman, *J. Amer. Chem. Soc.*, 1978, **100**, 320.
172. K. Nagayama, K. Wüthrich, P. Bachmann and R. R. Ernst, *Biochem. Biophys. Res. Commun.*, 1977, **78**, 99.
173. R. Niedermeyer and R. Freeman, *J. Magn. Resonance*, 1978, **30**, 617.
174. W. McFarlane and D. S. Rycroft, *Chem. Comm.*, 1972, 902.
175. S. J. Anderson and R. J. Goodfellow, *Chem. Comm.*, 1975, 443.
176. W. McFarlane and D. S. Rycroft, *Mol. Phys.*, 1972, **24**, 893.
177. A. D. Cohen, R. Freeman, K. A. McLaughlan and D. H. Whiffen, *Mol. Phys.*, 1963, **7**, 45.
178. H. C. E. McFarlane, W. McFarlane and D. S. Rycroft, *J. Chem. Soc., Faraday II*, 1972, **68**, 1300.
179. W. G. Henderson and E. F. Mooney, in *Ann. Reports NMR Spectroscopy*, E. F. Mooney (ed.), 1969, **2**, 219.
180. J. D. Kennedy, W. McFarlane and R. J. Puddephatt, *J. Chem. Soc., Dalton*, 1976, 745.
181. W. McFarlane, *Org. Magn. Resonance*, 1969, **1**, 3.
182. E. Wenkert, A. O. Clouse, D. W. Cochran and D. Doddrell, *J. Amer. Chem. Soc.*, 1969, **91**, 6879.
183. H. J. Reich, M. Jautelat, M. T. Messe, F. J. Weigert and J. D. Roberts, *J. Amer. Chem. Soc.*, 1969, **91**, 7445.
184. P. S. Pregosin and E. W. Randall, *Det. Org. Struct. Phys. Meth.*, 1971, **4**, 263.
185. H. Fritz and H. Sauter, *J. Magn. Resonance*, 1975, **18**, 527.
186. H. Fritz and H. Sauter, *J. Magn. Resonance*, 1974, **15**, 177.
187. G. Jikeli, W. Herrig and H. Günther, *J. Amer. Chem. Soc.*, 1974, **96**, 323.
188. R. A. Newmark and J. R. Hill, *J. Amer. Chem. Soc.*, 1973, **95**, 4435.
189. J. B. Grutzner, *Chem. Comm.*, 1974, 64.
190. R. R. Ernst, *J. Chem. Phys.*, 1966, **45**, 3845.
191. B. Birdsall, N. J. M. Birdsall and J. Feeney, *Chem. Comm.*, 1972, 316.
192. K. G. R. Pachler, *J. Magn. Resonance*, 1972, **7**, 442.
193. P. H. McCabe and C. R. Nelson, *J. Magn. Resonance*, 1976, **22**, 183.
194. D. S. Rycroft, unpublished results.
195. J. C. McDonald and M. Mazurek, *J. Magn. Resonance*, 1977, **28**, 181.
196. J. C. McDonald and M. Mazurek, *J. Magn. Resonance*, 1975, **19**, 51.
197. K. Roth, H. Bauer and D. Rewicki, *J. Magn. Resonance*, 1976, **26**, 219.
198. J. C. McDonald and M. Mazurek, *J. Magn. Resonance*, 1976, **24**, 367.
199. H. J. Jakobsen, T. Liptaj, T. Bundgaard and S. Sørensen, *J. Magn. Resonance*, 1977, **26**, 71.
200. R. Freeman, G. A. Morris and M. J. T. Robinson, *Chem. Comm.*, 1976, 754.
201. G. A. Morris and R. Freeman, *J. Magn. Resonance*, 1978, **29**, 433.
202. G. T. Andrews, I. J. Colquhoun, B. R. Doggett, W. McFarlane, B. E. Stacey and M. R. Taylor, *Chem. Comm.*, 1979, 89.
203. G. E. Hawkes, E. W. Randall and W. E. Hull, *J. Chem. Soc., Perkin II*, 1977, 1268.
204. R. E. Schirmer, J. H. Noggle, J. P. Davis and P. A. Hart, *J. Amer. Chem. Soc.*, 1970, **92**, 3266.
205. J. K. Saunders and R. A. Bell, *Canad. J. Chem.*, 1970, **48**, 1114, 512.
206. H. Booth and R. U. Lemieux, *Canad. J. Chem.*, 1971, **49**, 777.
207. T. Murae, T. Ikoda, T. Tsuyki, T. Nishihama and T. Takahoshi, *Tetrahedron Lett.*, 1971, 3897.
208. M. Gordon, W. C. Howell, C. H. Jackson and J. B. Stothers, *Canad. J. Chem.*, 1971, **49**, 143.
209. J. Dedina and J. Schraml, *Coll. Czech. Chem. Comm.*, 1975, **40**, 1538.
210. V. Skala, J. Kuthan, J. Dedina and J. Schraml, *Coll. Czech. Chem. Comm.*, 1974, **39**, 834.

211. R. Freeman, H. D. W. Hill, B. L. Tomlinson and L. D. Hall, *J. Chem. Phys.*, 1974, **61**, 4466.
212. N. R. Krishna, P. P. Yang and S. L. Gordon, *J. Chem. Phys.*, 1973, **58**, 2906.
213. I. D. Campbell and R. Freeman, *J. Chem. Phys.*, 1973, **58**, 2666.
214. A. H. Lewin and M. Frucht, *Org. Magn. Resonance*, 1975, **7**, 206.
215. B. Roques, C. Jaureguiberry, M. C. Fournie-Zaluski and S. Combrisson, *Tetrahedron Lett.*, 1971, 2693.
216. J. M. Lawlor and J. P. Warren, *J. Magn. Resonance*, 1972, **7**, 319.
217. S. Combrisson, B. Roques, P. Rigny and J. J. Basselier, *Canad. J. Chem.*, 1971, **49**, 904.
218. T. Kikuchi, T. Yokoi, M. Niwa and T. Shingu, *Chem. Pharm. Bull.*, 1977, **25**, 2078.
219. R. Richarz and K. Wüthrich, *J. Magn. Resonance*, 1978, **30**, 147.
220. B. M. Harina, A. A. Bothner-By and T. J. Gill, *Biochemistry*, 1977, **16**, 4504.
221. D. W. Urry, M. A. Khaled, V. Renugopalakrishnan and R. S. Rapaka, *J. Amer. Chem. Soc.*, 1978, **100**, 696.
222. Ref. 50, p. 278.
223. A. Abragam, "Principles of Nuclear Magnetism", Oxford University Press, London and New York, 1961.
224. N. Bloembergen, E. M. Purcell and R. V. Pound, *Phys. Rev.*, 1948, **73**, 679.
225. L. D. Hall and H. D. W. Hill, *J. Amer. Chem. Soc.*, 1976, **98**, 1269.
226. A. J. Vega and D. Fiat, *J. Chem. Phys.*, 1974, **60**, 579.
227. A. J. Vega and D. Fiat, *J. Magn. Resonance*, 1975, **19**, 21.
228. K. F. Kuhlmann, D. M. Grant and R. K. Harris, *J. Chem. Phys.*, 1970, **52**, 3439.
229. J. R. Scrivens and F. Heatley, *J. Chem. Soc., Faraday II*, 1976, 2164.
230. P. Balaram, A. A. Bothner-By and J. Dadok, *J. Amer. Chem. Soc.*, 1972, **94**, 4015.
231. P. Balaram, A. A. Bothner-By and J. Dadok, *J. Amer. Chem. Soc.*, 1972, **94**, 4017.
232. T. L. James, *Biochemistry*, 1976, **15**, 4724.
233. I. D. Campbell, C. M. Dobson and R. J. P. Williams, *J. Chem. Soc., Chem. Comm.*, 1974, 888.
234. R. Kaiser, *J. Chem. Phys.*, 1965, **2**, 1838.
235. N. R. Krishna and S. L. Gordon, *J. Chem. Phys.*, 1973, **58**, 5687.
236. N. R. Krishna and S. L. Gordon, *J. Chem. Phys.*, 1973, **59**, 4569.
237. J. Homer, A. R. Dudley and W. R. McWhinnie, *Chem. Comm.*, 1973, 893.
238. K. Tori, I. Horibe, Y. Tamura and H. Tada, *Chem. Comm.*, 1973, 620.
239. H. S. Gutowsky and D. F. S. Natusch, *J. Chem. Phys.*, 1972, **57**, 1203.
240. G. N. La Mar, *Chem. Phys. Lett.*, 1971, **10**, 230.
241. G. N. La Mar, *J. Amer. Chem. Soc.*, 1971, **93**, 1040.
242. D. F. S. Natusch, *J. Amer. Chem. Soc.*, 1971, **93**, 2566.
243. R. Freeman, K. G. R. Pachler and G. N. La Mar, *J. Chem. Phys.*, 1971, **55**, 4586.
244. O. A. Gansow, A. R. Burke and G. N. La Mar, *Chem. Comm.*, 1972, 456.
245. S. Bariza and N. Engstrom, *J. Amer. Chem. Soc.*, 1972, **94**, 1762.
246. O. W. Howarth, P. Moore and N. Winterton, *Chem. Comm.*, 1974, 665.
247. J. Feeney, D. Shaw and P. J. S. Pauwells, *Chem. Comm.*, 1970, 554.
248. R. Freeman and H. D. W. Hill, *J. Magn. Resonance*, 1971, **5**, 278.
249. R. Freeman, H. D. W. Hill and R. Kaptein, *J. Magn. Resonance*, 1972, **7**, 327.
250. O. A. Gansow and W. Schittenhelm, *J. Amer. Chem. Soc.*, 1971, **93**, 4296.
251. O. A. Gansow, M. R. Willcott and R. E. Lenkinski, *J. Amer. Chem. Soc.*, 1971, **93**, 4295.
252. S. J. Opella, D. J. Nelson and O. Jardetzky, *J. Chem. Phys.*, 1976, **64**, 2533.
253. D. Canet, *J. Magn. Resonance*, 1976, **23**, 361.
254. R. K. Harris and R. H. Newman, *J. Magn. Resonance*, 1976, **24**, 449.
255. T. D. Alger, S. W. Collins and D. M. Grant, *J. Chem. Phys.*, 1971, **54**, 2820.
256. D. M. Doddrell, V. Glushko and A. Allerhand, *J. Chem. Phys.*, 1972, **56**, 3683.
257. W. Buchner, *J. Magn. Resonance*, 1975, **17**, 229.

258. W. E. London and J. Avitabile, *J. Chem. Phys.*, 1976, **65**, 2443.
259. D. W. Wilson, private communication.
260. E. J. Pedersen, R. R. Vold and R. L. Vold, *Mol. Phys.*, 1978, **35**, 997.
261. R. C. Long, J. H. Goldstein and C. J. Carman, *Macromolecules*, 1978, **11**, 574.
262. S. R. Johns, D. R. Leslie, R. I. Willing and D. G. Bishop, *Austral. J. Chem.*, 1977, **30**, 813, 823.
263. D. M. Doddrell, M. R. Bendall, A. J. O'Connor and D. T. Pegg, *Austral. J. Chem.*, 1977, **30**, 943.
264. K. Wüthrich and R. Baumann, *Org. Magn. Resonance*, 1976, **8**, 532.
265. R. K. Harris and B. Lemarie, *J. Magn. Resonance*, 1976, **23**, 371.
266. K. Hayamizu and O. Yamamoto, *Bull. Chem. Soc. Japan*, 1977, **50**, 1295.
267. D. E. Axelson and C. E. Holloway, *Canad. J. Chem.*, 1976, **54**, 2820.
268. J. M. Courtieu, C. L. Mayne and D. M. Grant, *J. Chem. Phys.*, 1977, **66**, 2669.
269. D. D. Giannini, I. M. Armitage, H. Pearson, D. M. Grant and J. D. Roberts, *J. Amer. Chem. Soc.*, 1975, **97**, 3416.
270. K. T. Suzuki, L. W. Cary and K. F. Kuhlmann, *J. Magn. Resonance*, 1975, **18**, 390.
271. M. C. Thorpe, W. C. Coburn and J. A. Montgomery, *J. Magn. Resonance*, 1974, **15**, 98.
272. J. Elguero, A. Fruchier and M. del C. Pardo, *Canad. J. Chem.*, 1976, **54**, 1329.
273. H. Nakanishi and O. Yamamoto, *Chem. Phys. Lett.*, 1975, **35**, 407.
274. J. R. Lyerla and T. T. Horikawa, *J. Phys. Chem.*, 1976, **80**, 1106.
275. R. S. Norton and A. Allerhand, *J. Amer. Chem. Soc.*, 1976, **98**, 1007.
276. R. K. Harris and B. J. Kimber, *J. Magn. Resonance*, 1975, **17**, 174.
277. G. A. Gray and S. E. Cremer, *J. Magn. Resonance*, 1973, **12**, 5.
278. G. C. Levy, J. D. Cargioli and F. A. L. Anet, *J. Amer. Chem. Soc.*, 1973, **95**, 1527.
279. J. D. Cutnell and J. A. Glasel, *J. Amer. Chem. Soc.*, 1976, **98**, 7542.
280. L. G. Werbelow and D. M. Grant, *J. Chem. Phys.*, 1975, **63**, 544.
281. D. M. Grant, K. F. Kuhlmann, C. L. Mayne and R. B. Parry, *J. Chem. Phys.*, 1975, **63**, 2524.
282. A. J. Brown, O. W. Howarth, P. Moore and A. D. Bain, *J. Magn. Resonance*, 1977, **28**, 317.
283. W. E. Hull and B. D. Sykes, *J. Mol. Biol.*, 1975, **98**, 121.
284. J. D. Cutnell and J. A. Glasel, *J. Amer. Chem. Soc.*, 1977, **99**, 42.
285. D. E. Axelson, L. Mandelkern and G. C. Levy, *Macromolecules*, 1977, **10**, 557.
286. F. A. Bovey, F. C. Schilling, T. K. Kwei and H. L. Frisch, *Macromolecules*, 1977, **10**, 559.
287. J. Spevacek and B. Schneider, *Polymer*, 1978, **19**, 63.
288. J. R. Lyerla, T. T. Horikawa and D. E. Johnson, *J. Amer. Chem. Soc.*, 1977, **99**, 2463.
289. Y. Hirai, T. Ito and Y. Imamura, *Bull. Chem. Soc. Japan*, 1978, **51**, 677.
290. F. C. Schilling and F. A. Bovey, *Macromolecules*, 1978, **11**, 325.
291. K. Yokota, A. Abe, S. Hosaka, I. Sakai and H. Saito, *Macromolecules*, 1978, **11**, 95.
292. B. Thiault and M. Mersseman, *Org. Magn. Resonance*, 1976, **8**, 28.
293. G. C. Levy and I. R. Peat, *J. Magn. Resonance*, 1975, **18**, 500.
294. J. N. Shoolery, in *Progr. NMR Spectroscopy*, J. Emsley, J. Feeney and L. H. Sutcliffe (eds.), 1977, **11**, 79.
295. T. H. Mareci and K. N. Scott, *Analyt. Chem.*, 1977, **49**, 2130.
296. S. Takeuchi, J. Uzawa, H. Seto and H. Yonehara, *Tetrahedron Lett.*, 1977, 2943.
297. H. Seto, T. Sasaki, H. Yonehara and J. Uzawa, *Tetrahedron Lett.*, 1978, 923.
298. O. Yamamoto and M. Yanagisawa, *J. Chem. Phys.*, 1977, **67**, 3803.
299. S.-G. Huang and M. T. Rogers, *J. Chem. Phys.*, 1978, **78**, 5601.
300. C. G. Moreland and F. I. Carroll, *J. Magn. Resonance*, 1974, **15**, 596.
301. K. T. Suzuki, L. W. Cary and K. F. Kuhlmann, *J. Magn. Resonance*, 1975, **18**, 390.
302. R. E. London, W. A. Matwiyoff, V. H. Kollman and D. D. Mueller, *J. Magn. Resonance*, 1975, **18**, 555.

303. R. E. London, T. E. Walker, V. M. Kollman and W. A. Matwiyoff, *J. Magn. Resonance*, 1977, **26**, 213.
304. D. P. Miller, B. Ternai and G. E. Maciel, *J. Amer. Chem. Soc.*, 1973, **95**, 1336.
305. J. C. Vandenbosch, D. Zimmermann and J. Reisse, *Org. Magn. Resonance*, 1976, **8**, 436.
306. A. Briguet, J.-C. Duplan and J. Delmau, *J. Chem. Phys.*, 1974, **60**, 719.
307. H. Ozawa, Y. Arata and S. Fujiwara, *J. Chem. Phys.*, 1972, **57**, 1613.
308. J. M. Briggs, L. F. Farrell and E. W. Randall, *Chem. Comm.*, 1973, 70.
309. J. M. A. Al-Rawi, J. P. Bloxidge, J. A. Elvidge, J. R. Jones, V. E. M. Chambers, V. M. A. Chambers and E. A. Evans, *Steroids*, 1976, **28**, 359.
310. J. P. Bloxidge, J. A. Elvidge, J. R. Jones and R. B. Mare, *J. Chem. Research (S)*, 1977, 258.
311. L. J. Altman and N. Silberman, *Steroids*, 1977, **29**, 557.
312. L. J. Altman and N. Silberman, *Analyt. Biochem.*, 1977, **79**, 302.
313. J. A. Gibson and G.-V. Röschenthaler, *J. Chem. Soc., Dalton*, 1976, 1440.
314. R. L. Lichter and J. D. Roberts, *J. Amer. Chem. Soc.*, 1971, **93**, 3200.
315. L. F. Farrell, E. W. Randall and A. T. White, *Chem. Comm.*, 1972, 1159.
316. J. P. Warren and J. D. Roberts, *J. Phys. Chem.*, 1974, **78**, 2507.
317. G. E. Hawkes, W. M. Litchman and E. W. Randall, *J. Magn. Resonance*, 1975, **19**, 255.
- 317a. G. C. Levy, C. E. Holloway, R. C. Rosanke, J. M. Hewitt and C. H. Bradley, *Org. Magn. Resonance*, 1976, **8**, 643.
318. V. Markowski, G. R. Sullivan and J. D. Roberts, *J. Amer. Chem. Soc.*, 1977, **99**, 714.
319. D. Gast and J. D. Roberts, *J. Amer. Chem. Soc.*, 1977, **99**, 3637.
320. G. C. Levy, A. D. Godwin, J. M. Hewitt and C. Sutcliffe, *J. Magn. Resonance*, 1978, **29**, 553.
321. M. Llinas and K. Wüthrich, *Biochem. Biophys. Acta*, 1978, **532**, 29.
322. F. Blomberg, W. Maurer and H. Rüterjans, *J. Amer. Chem. Soc.*, 1977, **99**, 8149.
323. A. Lapidot and C. S. Irving, *Proc. Nat. Acad. Sci. USA*, 1977, **74**, 1988.
324. A. J. Elliot and M. S. Gibson, *Canad. J. Chem.*, 1975, **53**, 2534.
325. M. P. N. Gent, I. M. Armitage and J. H. Prestegard, *J. Amer. Chem. Soc.*, 1976, **98**, 3749.
326. J. T. Gerig, *J. Amer. Chem. Soc.*, 1977, **99**, 1721.
327. R. K. Harris and B. J. Kimber, *J. Organometal. Chem.*, 1974, **70**, 43.
328. G. C. Levy, J. D. Cargioli and T. D. Mitchell, *J. Amer. Chem. Soc.*, 1973, **95**, 3445.
329. C. R. Ernst, L. Spialter, G. R. Buell and D. C. Wilhite, *J. Organometal. Chem.*, 1973, **59**, C13.
330. R. K. Harris and B. Kimber, *J. Magn. Resonance*, 1975, **17**, 174.
331. G. Engelhardt and H. Jancke, *Z. Chem.*, 1974, **14**, 206.
332. R. K. Harris and B. J. Kimber, *Chem. Comm.*, 1973, 255.
333. B. J. Kimber and R. K. Harris, *J. Magn. Resonance*, 1974, **16**, 354.
334. H. Beierbeck, R. Martino, J. K. Saunders and C. Benzra, *Canad. J. Chem.*, 1976, **54**, 1918.
335. P. L. Yeagle, W. C. Hutton and R. B. Martin, *J. Amer. Chem. Soc.*, 1975, **97**, 7175.
336. N. J. Koole, A. J. de Konig and M. J. A. de Bie, *J. Magn. Resonance*, 1977, **25**, 371.
337. R. K. Harris and E. M. McVicker, *J. Chem. Soc., Faraday II*, 1976, 2291.
338. R. K. Harris, E. M. McVicker and G. Hägele, *J. Chem. Soc., Dalton*, 1978, 9.
339. P. L. Yeagle, W. C. Hutton, C.-H. Huang and R. B. Martin, *Biochemistry*, 1977, **16**, 4344.
340. T. Glonek, *J. Amer. Chem. Soc.*, 1976, **98**, 7090.
341. G. E. Maciel and M. Borzo, *Chem. Comm.*, 1973, 394.
342. T. N. Mitchell and G. Walter, *J. Chem. Soc., Perkin II*, 1977, 1842.
343. M. A. Sens, N. K. Wilson, P. D. Ellis and J. D. Odom, *J. Magn. Resonance*, 1975, **19**, 323.
344. G. L. Closs and M. S. Czeropski, *Chem. Phys. Lett.*, 1977, **45**, 115.
345. R. Kaptein, R. Freeman, H. D. W. Hill and J. Bargon, *Chem. Comm.*, 1973, 953.
346. R. Cone, R. P. Haseltine, P. Kazmeier and T. S. Sørensen, *Canad. J. Chem.*, 1974, **52**, 3320.
347. Y. Kuroda, *Bull. Chem. Soc. Japan*, 1977, **50**, 3118.
348. F. W. Dahlquist, K. J. Longmuir and R. B. du Vernet, *J. Magn. Resonance*, 1975, **17**, 406.

349. I. D. Campbell, C. M. Dobson, R. G. Ratcliffe and R. J. P. Williams, *J. Magn. Resonance*, 1978, **29**, 397.
350. I. D. Campbell, C. M. Dobson and R. G. Ratcliffe, *J. Magn. Resonance*, 1977, **27**, 455.
351. H. Iwahashi and C. Y. Kyogoku, *Nature*, 1978, **271**, 277.
352. P. I. Clark, G. Lowe and D. Nurse, *Chem. Comm.*, 1977, 451.
353. G. Lowe and D. Nurse, *Chem. Comm.*, 1977, 815.
354. R. M. Keller and K. Wüthrich, *Biochim. Biophys. Acta*, 1978, **533**, 195.
355. T. R. Brown and S. Ogawa, *Proc. Nat. Acad. Sci. USA*, 1977, **74**, 3627.
356. T. R. Brown and S. Ogawa, *Biomol. Struct. Funct. (Symp. 1977)*, 1978, 369.
357. B. E. Mann, in *Progr. NMR Spectroscopy*, J. Emsley, J. Feeney and L. H. Sutcliffe (eds.), 1977, **11**, 95.
358. B. E. Mann, *J. Magn. Resonance*, 1976, **21**, 17.
359. B. E. Mann, *J. Magn. Resonance*, 1977, **25**, 91.
360. M. Rabinovitz and A. Pines, *J. Amer. Chem. Soc.*, 1969, **91**, 1585.
361. H. S. Gutowsky and H. N. Cheng, *J. Chem. Phys.*, 1975, **63**, 2439.
362. B. E. Mann, *J. Chem. Soc., Perkin II*, 1977, 84.
363. P. Ahlberg, *Chem. Scripta*, 1976, **9**, 47.
364. B. E. Mann, *J. Magn. Resonance*, 1977, **141**, C33.
365. B. E. Mann, *Chem. Comm.*, 1977, 626.
366. L. Radics and J. Kardos, *Org. Magn. Resonance*, 1973, **5**, 251; M. Attimonelli and O. Sciacovelli, *ibid.*, 1977, **9**, 601.
367. C. Piccini-Leopardi, O. Fabre, D. Zimmermann, J. Reisse, F. Cornea and C. Fulea, *Org. Magn. Resonance*, 1976, **8**, 536.
368. J. G. Batchelor and J. Feeney, *Chem. Comm.*, 1975, 503.
369. Yu. N. Luzikov, N. M. Sergeyev and Yu. A. Ustynyuk, *J. Magn. Resonance*, 1975, **18**, 406.
370. J. R. Campbell, L. D. Hall and P. R. Steiner, *Canad. J. Chem.*, 1972, **50**, 504.
371. W. McFarlane and D. S. Rycroft, *J. Organometal. Chem.*, 1974, **64**, 303.
372. W. McFarlane, *J. Magn. Resonance*, 1973, **10**, 98.
373. R. Burton, L. D. Hall and P. R. Steiner, *Canad. J. Chem.*, 1971, **49**, 588.
374. W. McFarlane and D. S. Rycroft, *Chem. Comm.*, 1973, 336.
375. J. D. Kennedy and W. McFarlane, *J. Chem. Soc., Dalton*, 1973, 2134.
376. J. D. Kennedy and W. McFarlane, *J. Chem. Soc., Perkin II*, 1974, 146.
377. H. Sioito and K. Nurada, *J. Amer. Chem. Soc.*, 1971, **93**, 1072, 1077; P. Hampson, A. Mathias and R. Westhead, *J. Chem. Soc. (B)*, 1971, 397; F. W. Wehrli, W. Giger and W. Simon, *Helv. Chim. Acta*, 1971, **54**, 229.
378. H. Saito, Y. Tanaka and S. Nagata, *J. Amer. Chem. Soc.*, 1973, **95**, 324.
379. F. Cavagna and H. Pietsch, *Org. Magn. Resonance*, 1978, **11**, 204.
380. J. Browning, P. L. Goggin and R. J. Goodfellow, *J. Chem. Research (S)*, 1978, 328; (M), 4201.
381. D. W. Anderson, J. E. Bentham and D. W. H. Rankin, *J. Chem. Soc., Dalton*, 1973, 1215.
382. W. McFarlane and B. Wrackmeyer, *Inorg. Nuclear Chem. Lett.*, 1975, **11**, 719; *J. Chem. Soc., Dalton*, 1976, 2351.
383. D. E. J. Arnold and D. W. H. Rankin, *J. Chem. Soc., Dalton*, 1975, 889.
384. S. Craddock, E. A. V. Ebsworth and N. Hosmane, *J. Chem. Soc., Dalton*, 1975, 1624.
385. E. A. V. Ebsworth, D. W. H. Rankin and J. G. Wright, *J. Chem. Soc., Dalton*, 1977, 2348.
386. B. M. Fung, S. C. Wei, T. H. Martin and I. Wei, *Inorg. Chem.*, 1973, **12**, 1203.
387. J.-P. Marchal and D. Canet, *J. Amer. Chem. Soc.*, 1975, **97**, 6581.
388. E. V. van den Berghe and G. P. van der Kelen, *J. Organometal. Chem.*, 1973, **59**, 175.
389. E. V. van den Berghe and G. P. van der Kelen, *J. Organometal. Chem.*, 1976, **122**, 329.
390. D. W. W. Anderson, E. A. V. Ebsworth and D. W. H. Rankin, *J. Chem. Soc., Dalton*, 1973, 2370.



391. E. A. V. Ebsworth, J. M. Edward and D. W. H. Rankin, *J. Chem. Soc., Dalton*, 1976, 1667.
392. L. N. Mashlyakovskii, A. V. Dogadina and B. I. Ionin, *J. Gen. Chem. (U.S.S.R.)*, 1974, **44**, 1171.
393. M. L. Rueppel and J. T. Marvel, *Org. Magn. Resonance*, 1976, **8**, 19.
394. R. Katz, H. J. C. Yeh and D. F. Johnson, *Mol. Pharmacol.*, 1977, **13**, 615.
395. G. Hägele, W. Kuchen and P. N. Mohan Das, *Indian J. Chem.*, 1977, **15A**, 147.
396. A. A. Koridze, P. V. Petrovskii, S. P. Gubin and E. I. Fedin, *J. Organometal. Chem.*, 1975, **93**, C26.
397. G. N. La Mar, D. B. Viscio, D. L. Budd and K. Gersonde, *Biochem. Biophys. Res. Comm.*, 1978, **82**, 19.
398. W. McFarlane and D. H. Whiffen, *Mol. Phys.*, 1969, **17**, 603.
399. R. Keat, unpublished results.
400. J. D. Kennedy, W. McFarlane, G. S. Pyne and B. Wrackmeyer, *J. Chem. Soc., Dalton*, 1975, 386.
401. J. D. Kennedy and W. McFarlane, *J. Organometal. Chem.*, 1975, **94**, 7.
402. J. D. Kennedy, W. McFarlane, G. S. Pyne, P. L. Clarke and J. L. Wardell, *J. Chem. Soc., Perkin II*, 1975, 1234.
403. W. McFarlane and J. A. Nash, *Chem. Comm.*, 1969, 913.
404. D. E. J. Arnold, J. S. Dryburgh, E. A. V. Ebsworth and D. W. H. Rankin, *J. Chem. Soc., Dalton*, 1972, 2518.
405. D. W. W. Anderson, E. A. V. Ebsworth, G. D. Meikle and D. W. H. Rankin, *Mol. Phys.*, 1973, **25**, 381.
406. I. J. Colquhoun and W. McFarlane, *J. Chem. Research (S)*, 1978, 368.
407. R. Keat, D. S. Rycroft and D. G. Thompson, *Org. Magn. Resonance*, in press.
408. D. S. Milbrath, J. G. Verkade and R. J. Clark, *Inorg. Nuclear Chem. Lett.*, 1976, **12**, 921.
409. G. T. Andrews and W. McFarlane, *Inorg. Nuclear Chem. Lett.*, 1978, **14**, 215.
410. H. C. E. McFarlane, W. McFarlane and R. J. Wood, *Bull. Soc. Chim. Belg.*, 1976, **85**, 864.
411. E. M. Hyde, J. D. Kennedy, B. L. Shaw and W. McFarlane, *J. Chem. Soc., Dalton*, 1977, 1571.
412. J. Browning, P. L. Goggin, R. J. Goodfellow, M. G. Norton, A. J. M. Rattray, B. F. Taylor and J. Mink, *J. Chem. Soc., Dalton*, 1977, 2061.
413. S. Martinego, B. T. Heaton, R. J. Goodfellow and P. Chini, *Chem. Comm.*, 1977, 39.
414. C. J. Turner and R. F. M. White, *J. Magn. Resonance*, 1977, **26**, 1.
415. G. E. Maciel and M. Borzo, *Chem. Comm.*, 1973, 394; A. D. Cardin, P. D. Ellis, J. D. Odom and J. W. Howard, *J. Amer. Chem. Soc.*, 1975, **97**, 1672.
416. J. D. Kennedy and W. McFarlane, *J. Chem. Soc., Perkin II*, 1977, 1187.
417. P. J. Smith and L. Smith, *Inorg. Chim. Acta Rev.*, 1973, **7**, 11; J. D. Kennedy and W. McFarlane, *Rev. Silicon, Germanium, Tin and Lead Chem.*, 1974, **1**, 235; P. J. Smith and A. P. Tupčiauskas, in *Ann. Reports NMR Spectroscopy*, G. A' Webb (ed), 1978, **8**, 291.
418. H. C. E. McFarlane and W. McFarlane, *J. Chem. Soc., Dalton*, 1973, 2416.
419. W. McFarlane, F. J. Berry and B. C. Smith, *J. Organometal. Chem.*, 1976, **113**, 139.
420. O. R. Chambers, M. E. Harman, D. S. Rycroft, D. W. A. Sharp and J. M. Winfield, *J. Chem. Research (S)*, 1977, 150; (*M*), 1849.
421. W. McFarlane, *J. Chem. Soc., Dalton*, 1974, 324.
422. P. L. Goggin, R. J. Goodfellow, S. R. Haddock and B. F. Taylor, *J. Chem. Soc., Dalton*, 1976, 459.
423. J. D. Kennedy, W. McFarlane, R. J. Puddephatt and P. J. Thompson, *J. Chem. Soc., Dalton*, 1976, 874.
424. D. W. W. Anderson, E. A. V. Ebsworth and D. W. H. Rankin, *J. Chem. Soc., Dalton*, 1973, 854.

425. P. L. Goggin, R. J. Goodfellow and F. J. S. Reed, *J. Chem. Soc., Dalton*, 1974, 576.
426. S. J. Anderson and R. J. Goodfellow, *J. Chem. Soc., Dalton*, 1977, 1683.
427. S. J. Anderson, P. L. Goggin and R. J. Goodfellow, *J. Chem. Soc., Dalton*, 1976, 1959.
428. M. A. Bennett, R. Bramley and I. B. Tomkins, *J. Chem. Soc., Dalton*, 1973, 166.
429. P. W. Hall, R. J. Puddephatt and C. F. H. Tipper, *J. Organometal. Chem.*, 1974, **71**, 145.
430. E. A. V. Ebsworth, J. M. Edward and D. W. H. Rankin, *J. Chem. Soc., Dalton*, 1976, 1673.
431. C. Crocker and R. J. Goodfellow, *J. Chem. Soc., Dalton*, 1977, 1687.
432. S. M. Cohen and T. H. Brown, *J. Chem. Phys.*, 1974, **61**, 2985.
433. A. P. Tupčiauskas, N. M. Sergeyev, Yu. A. Ustynyuk and A. N. Kashin, *J. Magn. Resonance*, 1972, **7**, 124.
434. R. J. Goodfellow and S. R. Stobart, *J. Magn. Resonance*, 1977, **27**, 143.
435. W. McFarlane and D. S. Rycroft, *J. Chem. Soc., Faraday II*, 1974, **70**, 377.
436. G. M. Sheldrick and J. P. Yesinowski, *J. Chem. Soc., Dalton*, 1975, 870.
437. M. J. Cooper, A. K. Holliday, P. H. Makin, R. J. Puddephatt and P. J. Smith, *J. Organometal. Chem.*, 1974, **65**, 377.
438. J. D. Kennedy, W. McFarlane and B. Wrackmeyer, *Inorg. Chem.*, 1976, **15**, 1299.
439. J. D. Kennedy, W. McFarlane and G. S. Pyne, *J. Chem. Soc., Dalton*, 1977, 2332.
440. A. H. Cowley, J. R. Schweiger and S. L. Manatt, *Chem. Comm.*, 1970, 1491.
441. J. D. Kennedy and W. McFarlane, *Chem. Comm.*, 1975, 983.
442. W. McFarlane, A. Noble and J. M. Winfield, *Chem. Phys. Lett.*, 1970, **6**, 547; *J. Chem. Soc. (A)*, 1971, 948.
443. O. R. Chambers, D. S. Rycroft, D. W. A. Sharp and J. M. Winfield, *Inorg. Nuclear Chem. Lett.*, 1976, **12**, 559.
444. G. A. Gray and S. E. Cremer, *Chem. Comm.*, 1974, 451; 1975, 304.
445. M. Pomerantz, R. Fink and G. A. Gray, *J. Amer. Chem. Soc.*, 1976, **98**, 291; H. Finkelmeier and W. Lüttke, *ibid.*, 1978, **100**, 6261.
446. T. Khin and G. A. Webb, *Org. Magn. Resonance*, 1978, **11**, 487.
447. W. McFarlane and D. S. Rycroft, *Chem. Comm.*, 1973, 10; W. McFarlane, D. S. Rycroft and C. J. Turner, *Bull. Soc. Chim. Belg.*, 1977, **86**, 457.
448. W. McFarlane and D. S. Rycroft, *J. Chem. Soc., Dalton*, 1974, 1977.
449. P. L. Goggin, R. J. Goodfellow and S. R. Haddock, *Chem. Comm.*, 1975, 176.
450. D. E. J. Arnold and D. W. H. Rankin, *J. Chem. Soc., Dalton*, 1976, 1130.
451. H. J. Jakobsen, T. Bundgaard and R. S. Hansen, *Mol. Phys.*, 1972, **23**, 197.
452. T. Bundgaard and H. J. Jakobsen, *Acta Chem. Scand.*, 1972, **26**, 2548.
453. S. Sørensen, R. S. Hansen and H. J. Jakobsen, *J. Amer. Chem. Soc.*, 1973, **95**, 5080.
454. S. Sørensen, R. S. Hansen and H. J. Jakobsen, *J. Amer. Chem. Soc.*, 1972, **94**, 5900.
455. R.-M. Lequan, M.-J. Pouet and M.-P. Simonnin, *Chem. Comm.*, 1974, 475; *Org. Magn. Resonance*, 1975, **7**, 392.
456. T. Iwayanagi and Y. Saito, *Chem. Lett.*, 1976, 1193.
457. T. Bundgaard and H. J. Jakobsen, *Tetrahedron Lett.*, 1976, 1621.
458. W. B. Jennings, D. R. Boyd, C. G. Watson, E. D. Becker, R. B. Bradley and D. M. Jerina, *J. Amer. Chem. Soc.*, 1972, **94**, 8501.
459. V. V. Negrebitskii, V. S. Bogdanov, A. V. Kessenikh, P. V. Petrovskii, Yu. N. Bubnov and B. M. Mikhailov, *J. Gen. Chem. (U.S.S.R.)*, 1974, **44**, 1849; B. M. Mikhailov, V. V. Negrebitskii, V. S. Bogdanov, A. V. Kessenikh, Yu. N. Bubnov, T. K. Baryshnikova and V. N. Smirnov, *ibid.*, p. 1844; W. McFarlane, B. Wrackmeyer and H. Nöth, *Chem. Ber.*, 1975, **108**, 3831.
460. R. Bramley, J. R. Hall, G. A. Swile and I. B. Tomkins, *Austral. J. Chem.*, 1974, **27**, 2491.
461. H. J. C. Yeh, H. Ziffer, D. M. Jerina and D. R. Boyd, *J. Amer. Chem. Soc.*, 1973, **95**, 2741.
462. G. W. Buchanan and B. A. Dawson, *Canad. J. Chem.*, 1977, **55**, 1437.

463. G. Hägele, R. K. Harris, M. I. M. Wazeer and R. Keat, *J. Chem. Soc., Dalton*, 1974, 1985; R. K. Harris, M. I. M. Wazeer, O. Schluk and R. Schmutzler, *ibid.*, 1974, 1912; R. K. Harris, M. Lewellyn, M. I. M. Wazeer, J. R. Woplin, R. E. Dunmur, M. J. C. Hewson and R. Schmutzler, *ibid.*, 1975, 61; R. K. Harris, M. I. M. Wazeer, O. Schlak and R. Schmutzler, *ibid.*, 1976, 17, 306; R. K. Harris and M. I. M. Wazeer, *ibid.*, 1976, 302; I. J. Colquhoun and W. McFarlane, *ibid.*, 1977, 1674.
464. R. Keat and D. G. Thompson, *J. Chem. Soc., Dalton*, 1978, 634.
465. G. Bulloch, R. Keat and D. S. Rycroft, *J. Chem. Soc., Dalton*, 1978, 764.
466. M. Biddlestone, R. Keat, H. Rose, D. S. Rycroft and R. A. Shaw, *Z. Naturforsch.*, 1976, **31b**, 1001.
467. I. J. Colquhoun, R. Keat, H. C. E. McFarlane, W. McFarlane, J. A. Nash, D. S. Rycroft and D. G. Thompson, *Org. Magn. Resonance*, in press.
468. N. Cyr, G. K. Hamer and A. S. Perlin, *Canad. J. Chem.*, 1978, **56**, 297.
469. L. E. Erickson, J. E. Sarneski and C. N. Reilley, *Inorg. Chem.*, 1978, **17**, 1701.
470. A. G. Davies, M.-W. Tse, J. D. Kennedy, W. McFarlane, G. S. Pyne, M. F. C. Ladd and D. C. Povey, *Chem. Comm.*, 1978, 791.
471. H. C. E. McFarlane and W. McFarlane, *Chem. Comm.*, 1975, 582.
472. R. J. Goodfellow and B. F. Taylor, *J. Chem. Soc., Dalton*, 1974, 1676.
473. R. J. Cross, T. H. Green and R. Keat, *J. Chem. Soc., Dalton*, 1976, 1424; R. Keat, R. A. Shaw, and M. Woods, *ibid.*, p. 1582.
474. J. D. Kennedy and W. McFarlane, *J. Organometal. Chem.*, 1974, **80**, C47.
475. I. J. Colquhoun, J. D. Kennedy, W. McFarlane and R. J. Puddephatt, *Chem. Comm.*, 1975, 638.
476. R. K. Harris and R. G. Hayter, *Canad. J. Chem.*, 1964, **42**, 2282.
477. P. L. Goggin, R. J. Goodfellow, J. R. Knight, M. G. Norton and B. F. Taylor, *J. Chem. Soc., Dalton*, 1973, 2220.
478. T. Ibusuki and Y. Saito, *J. Organometal. Chem.*, 1973, **56**, 103.
479. C. Fuganti, D. Ghiringhelli, P. Grasselli and A. Santopietro-Amisano, *Chem. Comm.*, 1973, 862.
480. F. A. L. Anet and F. Leyendecker, *J. Amer. Chem. Soc.*, 1973, **95**, 156.
481. D. Slack and M. C. Baird, *Chem. Comm.*, 1974, 701; J. Z. Chrzastowski, C. J. Cooksey, M. D. Johnson, B. L. Lockman and P. N. Steggles, *J. Amer. Chem. Soc.*, 1975, **97**, 932.
482. V. R. Haddon and L. M. Jackman, *Org. Magn. Resonance*, 1973, **5**, 333.
483. J.-P. Aycard, R. Geiss, J. Berger and H. Bodot, *Org. Magn. Resonance*, 1973, **5**, 473.
484. F. R. Jensen and R. A. Neese, *J. Amer. Chem. Soc.*, 1975, **97**, 4345.
485. K. Roth, *Org. Magn. Resonance*, 1977, **9**, 414.
486. T. Onak and E. Wan, *J. Chem. Soc., Dalton*, 1974, 665.
487. G. N. Boiko, Yu. I. Malov and K. N. Semenenko, *Izvest. Akad. Nauk S.S.S.R., Ser. khim.*, 1973, 1143.
488. N. N. Greenwood, J. D. Kennedy and J. Staves, *J. Chem. Soc., Dalton*, 1978, 1146.
489. J. E. Cronan, Jr. and J. H. Prestegard, *Biochemistry*, 1977, **16**, 4738.
490. W. Walter, E. Schaumann and H. Rose, *Tetrahedron*, 1972, **28**, 333; *Org. Magn. Resonance*, 1973, **5**, 191.
491. A. Pidcock, *Chem. Comm.*, 1973, 249; M. W. Adlard and G. Socrates, *ibid.*, 1972, 17; *J. Chem. Soc., Dalton*, 1972, 797; *J. Inorg. Nuclear Chem.*, 1972, **34**, 2339; J. Powell and B. L. Shaw, *J. Chem. Soc.*, 1965, 3879.
492. B. E. Mann, B. L. Shaw and A. J. Stringer, *J. Organometal. Chem.*, 1974, **73**, 129.
493. P. Clare, D. B. Sowerby, R. K. Harris and M. I. M. Wazeer, *J. Chem. Soc., Dalton*, 1975, 625.
494. M. Harman, D. W. A. Sharp and J. M. Winfield, *Inorg. Nuclear Chem. Lett.*, 1974, **10**, 183.
495. R. O. Hutchins, B. E. Maryanoff, J.-P. Albrand, A. Cogne, D. Gagnaire and J.-B. Robert, *J. Amer. Chem. Soc.*, 1972, **94**, 9151.

496. J. Durrieu, R. Kraemer and J. Navech, *Org. Magn. Resonance*, 1972, **4**, 709.
497. J.-P. Albrand, D. Gagnaire, J. Martin and J.-B. Robert, *Org. Magn. Resonance*, 1973, **5**, 33.
498. L. Evelyn, L. D. Hall, P. R. Steiner and D. H. Stokes, *Org. Magn. Resonance*, 1973, **5**, 141.
499. L. Radics, E. Baitz-Gačs and A. Neszmélyi, *Org. Magn. Resonance*, 1974, **6**, 60.
500. H. C. E. McFarlane and W. McFarlane, *Chem. Comm.*, 1972, 1189.
501. R. Freeman and G. A. Morris, *Chem. Comm.*, 1978, 684.
502. H. Günther, G. Jikeli and H. Schmickler, *Angew. Chem. Internat. Edn.*, 1973, **12**, 762.
503. A. A. Chalmers, G. J. H. Rall and M. E. Oberholzer, *Tetrahedron*, 1977, **33**, 1735.
504. T. Prange and J.-Y. Lallemand, *Compt. rend., C*, 1976, **282**, 61.
505. E. W. Hagaman, *Org. Magn. Resonance*, 1976, **8**, 389.
506. R. Radeglia, *Org. Magn. Resonance*, 1977, **9**, 164.
507. I. H. Sadler, *Chem. Comm.*, 1973, 809.
508. A. Allerhand, R. F. Childers and E. Oldfield, *Biochemistry*, 1973, **12**, 1335.
509. K. Roth, *Org. Magn. Resonance*, 1977, **10**, 56.
510. J. Schaefer, *Macromolecules*, 1972, **5**, 590.
511. R. Rowan and B. D. Sykes, *J. Amer. Chem. Soc.*, 1974, **96**, 7000.
512. P. M. Burke, W. F. Reynolds, J. C. L. Tam and P. Yates, *Can. J. Chem.* 1976, **54**, 1449.
513. S. Sørensen, M. Hansen and H. J. Jakobsen, *J. Magn. Resonance*, 1973, **12**, 340.
514. W. von Philipsborn, *Pure Appl. Chem.*, 1974, **40**, 159; U. Vogeli and W. von Philipsborn, *Org. Magn. Resonance*, 1975, **7**, 617.
515. D. H. O'Brien and R. D. Stipanovic, *J. Org. Chem.*, 1978, **43**, 1105.
516. S. G. Boxer, G. L. Closs and J. J. Katz, *J. Amer. Chem. Soc.*, 1974, **96**, 7058.
517. J. Uzawa and S. Takeuchi, *Org. Magn. Resonance*, 1978, **10**, 502.
518. P. S. Steyn, R. Vleggaar, P. L. Wessels and D. B. Scott, *Chem. Comm.*, 1975, 193.
519. T. G. Dekker, K. G. R. Pachler and P. L. Wessels, *Org. Magn. Resonance*, 1976, **8**, 530.
520. J. Runsink, J. de Wit and W. D. Weringa, *Tetrahedron Lett.*, 1974, 55.
521. K. Bachmann and W. von Philipsborn, *Org. Magn. Resonance*, 1976, **8**, 530.
522. K. Bock and C. Pedersen, *J. Magn. Resonance*, 1977, **25**, 227.
523. V. A. Chertkov and N. M. Sergeev, *J. Amer. Chem. Soc.*, 1977, **99**, 6750.
524. H. Günther, H. Seel and H. Schickler, *J. Magn. Resonance*, 1977, **28**, 145.
525. W. Seel, R. Aydin and H. Günther, *Z. Naturforsch.*, 1978, **33b**, 353.
526. M. Imfeld, C. A. Townsend and D. Arigoni, *Chem. Comm.*, 1976, 541.
527. A. Battersby, R. Hollenstein, E. McDonald and D. C. Williams, *Chem. Comm.*, 1976, 543.
528. A. I. Scott, M. Kajiwar, T. Takahashi, I. M. Armitage, P. Demon and D. Petrocine, *Chem. Comm.*, 1976, 544.
529. M. J. Garson, R. A. Hill and J. Staunton, *Chem. Comm.*, 1977, 921.
530. D. M. Wilson, A. L. Burlingame, T. Cronholm and J. Sjövall, *Biochem. Biophys. Res. Comm.*, 1974, **56**, 828.
531. D. M. Wilson, A. L. Burlingame, T. Cronholm and J. Sjövall, *Proc. Int. Conf. Stable Isot.*, 2nd, 1975, 1976, 485.
532. A. G. McInnes, D. G. Smith, J. A. Walter, L. C. Vining and J. L. C. Wright, *Chem. Comm.*, 1975, 66; A. G. McInnes, J. A. Walter, D. G. Smith, J. L. C. Wright and L. C. Vining, *J. Antibiot.*, 1976, **29**, 1050.
533. P. L. Canham, L. C. Vining, A. G. McInnes, J. A. Walter, and J. L. C. Wright *Canad. J. Chem.*, 1977, **55**, 2450.
534. H. C. Dorn and G. E. Maciel, *J. Phys. Chem.*, 1972, **76**, 2972.
535. R. L. Kieft and T. L. Brown, *J. Organometal. Chem.*, 1974, **77**, 289.
536. W. L. Earl and W. Niederberger, *J. Magn. Resonance*, 1977, **27**, 351.
537. D. J. Gale, A. H. Haines and R. K. Harris, *Org. Magn. Resonance*, 1975, **7**, 635.
538. A. H. Haines, R. K. Harris and R. C. Rao, *Org. Magn. Resonance*, 1977, **9**, 432.

539. B. Birdsall, J. Feeney, J. A. Glasel, R. J. P. Williams and A. V. Xavier, *Chem. Comm.*, 1971, 1473.
540. W. J. Ray, Jr., A. S. Mildvan and J. B. Grutzner, *Arch. Biochem. Biophys.*, 1977, **184**, 453.
541. S. Craddock, E. A. V. Ebsworth, H. Morets, D. W. H. Rankin and W. J. Savage, *Angew. Chem. Internat. Edn.*, 1973, **12**, 317.
542. E. V. van den Bergh and G. P. van der Kelen, *J. Mol. Struct.*, 1974, **20**, 147.
543. J. D. Kennedy, *J. Mol. Struct.*, 1976, **31**, 207.
544. A. G. Kucheryaev and V. A. Lebedev, U.S.S.R. 591,755 (1978), from *Otkrytiya, Izobret., Prom. Obraztsy, Tovarnye Znaki*, 1978, **55**, 147 (*Chem. Abs.*, 1978, **88**, 182040).
545. G. Singh, *J. Organometal. Chem.*, 1975, **99**, 251.
546. W. McFarlane, *J. Organometal. Chem.*, 1976, **116**, 315.
547. R. F. Sprecher and J. C. Carter, *J. Amer. Chem. Soc.*, 1973, **95**, 2369.
548. R. F. Sprecher, B. E. Aufderheide, G. W. Luther and J. C. Carter, *J. Amer. Chem. Soc.*, 1974, **96**, 4404.
549. T. Onak, J. B. Leach, S. Anderson, M. J. Frisch and D. Marynick, *J. Magn. Resonance*, 1976, **23**, 237.
550. R. C. Hopkins, J. D. Baldeschwieler, R. Schaeffer, F. N. Tebbe and A. Norman, *J. Chem. Phys.*, 1965, **43**, 975.
551. J. P. Albrand and J. B. Robert, *Chem. Comm.*, 1974, 645.
552. B. J. Kimber, J. Feeney, G. C. K. Roberts, B. Birdsall, D. V. Griffiths, A. S. V. Burgen and B. D. Sykes, *Nature*, 1978, **271**, 184.
553. I. D. Campbell, C. M. Dobson, R. J. P. Williams and P. E. Wright, *FEBS Letters*, 1975, **57**, 96.
554. J. W. Emsley, J. C. Lindon and J. Tabony, *Mol. Phys.*, 1973, **26**, 1485; 1973, **26**, 1499; 1976, **31**, 1617.
555. R. Ader and A. Loewenstein, *Mol. Phys.*, 1974, **27**, 113; 1975, **30**, 199.
556. J. W. Emsley, J. C. Lindon and J. Tabony, *J. Chem. Soc., Faraday II*, 1975, **71**, 579, 586.
557. P. Diehl and W. Niederberger, *J. Magn. Resonance*, 1974, **15**, 391.
558. W. McFarlane and B. Wrackmeyer, *J. Mol. Struct.*, 1976, **30**, 125.
559. N. Zumbulyadis and B. P. Dailey, *J. Magn. Resonance*, 1974, **13**, 189.
560. P. Diehl and H. P. Kellerhals, unpublished result quoted by P. Diehl and C. L. Khetrapal, in "NMR—Basic Principles and Progress", P. Diehl, E. Fluck and R. Kosfeld (eds.), 1969, **1**, 1.
561. J. Degelean, E. Arte and J. M. Dereppe, *J. Chem. Phys.*, 1974, **61**, 5295.
562. E. Arte, J. Degelean and J. M. Dereppe, *J. Chem. Phys.*, 1975, **63**, 3171.
563. J. D. Kennedy and W. McFarlane, *Mol. Phys.*, 1975, **29**, 593.
564. J. D. Kennedy and W. McFarlane, *Chem. Comm.*, 1976, 666.
565. J. Dalton, J. D. Kennedy, W. McFarlane and J. R. Wedge, *Mol. Phys.*, 1977, **34**, 215.
566. J. D. Kennedy and W. McFarlane, *Chem. Comm.*, 1974, 595.
567. I. J. Colquhoun and W. McFarlane, *J. Chem. Soc., Faraday II*, 1977, **73**, 722.
568. E. D. Becker, R. B. Bradley and T. Axenrod, *J. Magn. Resonance*, 1971, **4**, 136.
569. I. J. Colquhoun and W. McFarlane, to be published.
570. H. C. E. McFarlane, W. McFarlane and C. J. Turner, *Mol. Phys.*, in press.

## SUBJECT INDEX

*The numbers in **bold** indicate the pages on which the topic is discussed in detail*

### A

- Acetaldehyde, *N*-benzoylamino-, reaction with papain, 378
- Acetamide  
 $^{13}\text{C}$ -( $^1\text{H}$ ) NMR, 373  
 $^{15}\text{N}$ -( $^1\text{H}$ ) NOE, 375  
*N,N*-dimethyl- $^{13}\text{C}$ -( $^1\text{H}$ ) NMR, 373  
 $^{15}\text{N}$ -( $^1\text{H}$ ) NOE, 375
- Acetates, exchange reactions in paramagnetic transition metal complexes, 63
- Acetic acid, transition metal complexes, 31  
benzene-1,2-dioxy-, conformation, lanthanide shift reagents and, 73  
diethylenetriaminopenta-, transition metal complexes, 33  
ethylenediamine-*N,N'*-di-, transition metal complexes, 53.  
ethylenediaminetetra-, paramagnetic complexes, 62  
iminodi-, transition metal complexes, 31  
nitrilotri-, lanthanide complexes, 36
- Acetoacetic acid, trifluoro-, ethyl ester, lanthanide complexes, 36
- Acetonitrile, exchange reactions in paramagnetic transition metal complexes, 62
- Acetylacetone  
complexes, temperature and, 10  
ethylene di-imine cobalt complexes, 16  
transition metal complexes, 23–25
- Acetylene compounds, INDOR spectra, 387
- Actinides, complexes, 35–37
- Adamantane,  $^{13}\text{C}$ -( $^1\text{H}$ ) NMR, 372
- Adenosine,  $^{13}\text{C}$ -( $^1\text{H}$ ) NMR, 373
- Adenosine-5'-monophosphate  
conversion to adenosine diphosphate, 378  
metal binding properties, 101
- 3',5'-Adenosine monophosphate, cyclic, metal binding properties, 101
- Alanine  
lanthanide complexes, 36  
two dimensional  $^{13}\text{C}$  spectrum, 354
- Alcohols  
exchange, paramagnetic metal complexes, 61  
transition metal complexes, 31
- Aldehydes, conformation, lanthanide shift reagents and, 73
- Alkali metals  
anions, 148  
covalent compounds, 149–153  
ions, complexation, 142–149  
quadrupolar relaxation, 134–137  
solvation, 137–142  
NMR, 130–135  
nuclear properties, 130–132  
relaxation rates, 132
- Alkaline earths  
covalent compounds, structural studies, 159–161  
ions, relaxation in aqueous solution, 154  
NMR, 153–161  
nuclear properties, 153, 154
- Alkanes  
 $^{13}\text{C}$ -( $^1\text{H}$ ) NMR, 372  
long-chain,  $^{13}\text{C}$ -( $^1\text{H}$ ) NMR, 374
- Alumichrome,  $^{15}\text{N}$ -( $^1\text{H}$ ) NOE, 376
- Aluminium  
cations, solvation, 164  
hydrated ions, quadrupole relaxation, 162  
ions, solvation, 167
- Aluminium compounds, trialkyl, NMR, 174
- Aluminium halides, adducts, 175
- Aluminium salts, hydrolysis, 165
- Amides  
restricted rotation, 367  
trimethylsilyl derivatives,  $^{29}\text{Si}$  chemical shifts, 270

Amines  
 transition metal complexes, 27  
 trimethylsilyl derivatives,  $^{29}\text{Si}$  chemical shifts, 270  
 Aminium cation radicals, triaryl-, 49  
 Amino acids  
 alkali metal ion complexation, 143  
 conformation, 87–90  
 lanthanide shift reagents and, 75  
 trimethylsilyl derivatives,  $^{29}\text{Si}$  chemical shifts, 270  
 Ammonium, tetra-alkyl-, ion pairs with tri-bromo(triphenyl phosphine) cobalt (II), 56  
 Aniline,  $^{15}\text{N}$ -( $^1\text{H}$ ) NOE, 375  
 Anilinium,  $^{15}\text{N}$ -( $^1\text{H}$ ), NOE, 375  
 Anisole, *p,p'*-azoxy-,  $^{13}\text{C}$ -( $^1\text{H}$ ) NMR, 373  
 Antimony-121, NMR, 179–180  
 Antimony-123, NMR, 180  
 Arsenic-75  
 chemical shift determination in magnetic multiple resonance, 383  
 NMR, 177–179  
 12-Aza [4,4,3] propellane, 11,13-dioxo-12-methyl-, dimer, INDOR spectra, 329

## B

Bacitracin, conformation, lanthanide shift reagents and, 84  
 Barbaralone, Cope rearrangement, 379  
 Benzene, *o*-dichloro-, intermolecular NOE, 369  
 1,2-dimethoxy-4-hydroxy-5-nitro-, methoxy resonance, 367  
 2,4,5-trichloronitro-, spin echo spectra, 340  
 trimethylsilyl-,  $^{29}\text{Si}$  chemical shift, steric effects and, 270  
 Benzenedithiol, cobalt complexes, 15  
 Benzoic acid, amino,  $^{15}\text{N}$ -( $^1\text{H}$ ) NOE, 375  
 Benzoyl peroxide, perfluoro-,  $^{13}\text{C}$  CIDNP, 377  
 Benzyl alcohol, two dimensional  $^{13}\text{C}$  spectrum, 354  
 Benzyl radicals, electron distribution and bonding, 49  
 Bicyclobutanes, coupling constant sign and magnitude, 385  
 Binding sites in peptides, 87

Biological applications, NMR, 84–105  
 Biphenyl radicals, electron distribution and bonding, 41  
 4,4'-Bipyridylum radicals, 49  
 Bismuth-209, NMR, 180, 181  
 Bloch equations 322  
 Bloch-Siegert frequency shift, 363  
 Bonding in paramagnetic species, 14, 15  
 Borane, (trimethoxyphosphinyl)-, triple resonance, 357  
 Borneols, conformation, lanthanide shift reagents and, 73  
 Boron-10, chemical shift determination in magnetic multiple resonance, 381  
 Boron-11, chemical shift determination in magnetic multiple resonance, 381  
 Boron trichloride as shift reagent, 83

## C

Cadmium-111, chemical shift determination in magnetic multiple resonance, 383  
 Cadmium-113, chemical shift determination in magnetic multiple resonance, 383  
 Cadmium (II) complexes, flavoquinone, 32  
 Caesium-133  
 chemical shift, solvation shield and, 140  
 ions, relaxation rate in glycerol, 136  
 solvation, 137  
 Camphor  
 $^{13}\text{C}$  spectrum, 360  
 assignment, 359  
 Carbamic acid, dithio-, transition metal complexes, 28, 54  
 Carbon-13  
 assignment, double resonance techniques, 358–365  
 chemical shift determination in magnetic multiple resonance, 381  
 proton decoupling, 321  
 relaxation time, 321  
 Carboxylates, conformation, lanthanide shift reagents and, 73  
 Carboxylic acids, mercapto-, trimethylsilyl derivatives,  $^{29}\text{Si}$  chemical shifts, 270  
 Carr-Purcell pulse sequence, 399  
 CASS technique, 365

- Catechol  
 fluorosilicates,  $^{29}\text{Si}$  chemical shifts, 263  
 silicon derivatives,  $^{29}\text{Si}$  chemical shifts, 266  
 Cerium fluoride,  $^{19}\text{F}$  hyperfine interactions, 68  
 Chemical shifts  
 determination in multiple resonance experiments, 379–385  
 $^{29}\text{Si}$ , 287–311  
 theory, 223–226  
 Chiral shift reagents, 82  
 Chloroform,  $^{13}\text{C}$ -( $^1\text{H}$ ) NMR, 373  
 Chlorophyll-a, radical cation, 50  
 Chloroplast membranes  
 $^{13}\text{C}$ -( $^1\text{H}$ ) NMR, 372  
 NMR, 105  
 Cholesterol, two dimensional  $^{13}\text{C}$  spectrum, 354, 355  
 Chromium-53, NMR, 196  
 Chromium (II) complexes, 34  
 Chromium (III) complexes  
 acetylacetonate, 27  
 spin lattice relaxation pathway enhancement, 65  
 $\alpha$ -Chymotrypsin, reaction with hydrocinnamaldehyde, 378  
 CIDNP, NOE and, 377  
 Cobalamines, conformation, 89  
 Cobalt, tris(acetylacetonate),  $^{13}\text{C}$ -( $^1\text{H}$ ) NMR, 373  
 Cobalt-59, NMR, 201–208  
 Cobalt (II) complexes  
 acetylacetonatedipyridyl, 23  
 alcohols, 31  
 aminocarboxylates, 22  
 benzoyltrifluoroacetate, 25  
 bis(di-*p*-tolyl-dithiophosphinato)-, 22  
 4-coordinate, electron distribution and bonding in, 14  
 dithiophosphates, 28  
 electron distribution and bonding, 15, 16  
 flavoquinone, 32  
 imidazole, 29  
 1,8-naphthyridine, 30  
*N,N'* - 1,1 - dimethylethylene - bis(salicylideneiminato)-, pyridine adduct, 22  
 octahedral, 23  
 pseudotetrahedral, 16  
 pyridine, 30  
 pyridine-*N*-oxide, 30  
 tetragonal high-spin, psuedocontact shifts, calculation, 7  
 tetrahydrocorins, 33  
 thyroxine, 22  
 tribromo(triphenyl phosphine), 56  
 Cobalt (III) complexes, 4-coordinate, electron distribution and bonding in, 15  
 Cobaltocenes, paramagnetic, 38  
 Cobinamides, conformation, 89  
 Coherence transfer echo, 353  
 Complexation, 156  
 alkali metal ions, 142–149  
 Group III metals, 164–174  
 Concanavalin A, conformation, 89  
 Conformation  
 amino acids, 87  
 oxygen donor substrates, lanthanide shift reagents and, 73  
 Coordination complexes, structure, lanthanide shift reagents and, 74  
 Copper-63  
 chemical shift determination in magnetic multiple resonance, 383  
 NMR, 209  
 (trimethoxyphosphinyl)-,  $^{63}\text{Cu}$  TINDOR spectra, 357  
 Copper-65, NMR, 209  
 Copper (I) complexes, flavoquinone, 32  
 Copper (II) complexes  
 acetyl acetate, 23  
 nuclear spin relaxation time, 10  
 bis(*N*-alkylsalicylaldiminato)-, 17  
 bis(diazoaminobenzene)-, dimer, 18  
 exchange and relaxation studies, 64  
 pseudo-octahedral, 16  
 pseudotetrahedral, 16  
 Corin, tetrahydro-, 1,19-disubstituted, transition metal complexes, 33  
 Corrinoids, conformation, 89  
 Coupling constants  
 determination of sign and magnitude in magnetic multiple resonance, 385–390  
 $^{29}\text{Si}$ , calculations, 272–276  
 $^{29}\text{Si}$ , theory of, 271–272  
 Crown ethers  
 alkali metal ion complexation by, 143  
 complexation, 145  
 Cryptands, alkali metal ion complexation by, 143  
 Cycloguanosines, conformation, 367



Cyclohexane, dimethyl-, ring inversion, 379  
 Cyclohexanones, conformation, lanthanide shift reagents and, 73  
 Cyclohexenyl cations, rearrangement, 378  
 Cyclophosphazane diselenides, coupling constants, 388  
 Cyclophosphazine, phosphazenyl-, INDOR spectra, 387  
 Cyclosiloxanes, oligodiorganyl-,  $^{29}\text{Si}$  chemical shift, 256  
 Cyclotetrasiloxane, octamethyl-, as reference NMR, 228  
 Cytidine-5'-monophosphate, cyclic, metal binding properties, 102  
 Cytochrome B<sub>2</sub>, conformation, 94  
 Cytochrome B<sub>5</sub>, conformation, 94  
 Cytochrome c, conformation, 93  
 Cytochrome c-557, conformation, 94

## D

DANTE sequence, 365  
 Decaborane, 6-methyl-, 11B spectrum, 399  
*cis*-Decalin, inversion, 379  
 Density matrix methods in multiple resonance experiments, 323  
 Deuterium  
   chemical shift determination in magnetic multiple resonance, 381  
   decoupling, 400  
 Dihydrofolate reductase, spin coupling in, 399  
 $\beta$ -Diketones, lanthanide complexes, 36  
 Dilead, hexamethyl-, complex spin systems, 389  
 Dimethylsiloxanes, cyclic,  $^{29}\text{Si}$  chemical shifts, 256  
 Dimethyl sulphoxide, paramagnetic complexes, solvation parameters, 61  
 Diols, fluorosilicates,  $^{29}\text{Si}$  chemical shifts, 263  
 1,3,2-Dioxaphosphorinanes, conformation, lanthanide shift reagents and, 75  
 Dipolar relaxation, theory, 9  
 Disiloxane, hexamethyl-, as NMR reference, 228  
 Disiloxanols, sequence lengths, 251  
 Double resonance experiments, 390  
   calculation, 323

$^{13}\text{C}$ -( $^1\text{H}$ ) NMR, 392–395  
 $^{13}\text{C}$ -( $^{13}\text{C}$ ) NMR, 396  
 $^{13}\text{C}$ -( $^{19}\text{F}$ ) NMR, 397  
 $^{13}\text{C}$ -( $^2\text{H}$ ) NMR, 395, 396  
 $^1\text{H}$ -( $^{13}\text{C}$ ) NMR, 391  
 $^1\text{H}$ -( $^{11}\text{D}$ ) NMR, 391  
 $^1\text{H}$ -( $^2\text{H}$ ) NMR, 390  
 $^1\text{H}$ -( $^{14}\text{N}$ ) NMR, 391  
 $^1\text{H}$ -( $^{31}\text{P}$ ) NMR, 392  
 Drugs, alkali metal ion complexation by, 143

## E

EHMO calculations, 12  
 Electron distribution in paramagnetic species, 14, 15  
 Electron spin relaxation, theory, 9  
 Electron transfer, paramagnetic transition metal complexes, 63  
 Electronic equilibria, paramagnetic species, 54, 55  
 Electronic structure, theory, 11–13  
 Enzymes, active site, 90  
 Esters, conformation, lanthanide shift reagents and, 73  
 Ethane, 1,2-dichloro-,  $^{13}\text{C}$  spectra assignment, 359  
   1,2-dichloro-2,2-difluoro-, double resonance experiments, exchange reactions and, 324  
   1,1,2-trichloro-  
     conformation, 367  
     intermolecular nuclear Overhauser effect, 369  
     multiple resonance spectrum, 323  
     proton spectra, phase modulation in, 339, 340  
 Ethanol 1,2-dichloro-, multiple resonance spectrum, 323  
   1-(1-pyrazolyl)-, acetaldehyde system, exchange, 367  
   2,2,2-trichloro-, double resonance experiments, exchange reactions and, 324  
 Ethylenediamine, lanthanide complexes, 36  
 Ethyl radical, isotropic  $\beta$ -proton hyperfine coupling constant, delocalisation and polarisation contributions, 13  
 Etioporphyrins I, paramagnetic, 93  
 Europium,  $^{19}\text{F}$  hyperfine interactions, 68

Exchange reactions  
 double resonance experiments, 324  
 magnetic multiple resonance and, 377–379  
 paramagnetic metal complexes, 59–64

## F

Fermi contact shift, 5  
 Ferredoxin, NMR, 100  
 Ferricenium hexafluorophosphate, 37  
 Ferricytochrome c, exchange reactions, 378  
 Ferrimyoglobin, cyano-, conformation, 95  
 Flavoquinone, transition metal complexes, 32  
 Fluorenone radicals, electron distribution and bonding, 41  
 Fluorine-19, decoupling, 400  
 Fluorosilicates,  $^{29}\text{Si}$  chemical shifts, 263  
 Formamide, *N,N*-dimethyl-  
 $^{13}\text{C}$ -( $^1\text{H}$ ) NMR, 373  
 exchange reactions, 379  
 internal rotation, 367  
 Formation, paramagnetic metal complexes, 59–64  
 Formic acid,  $^{13}\text{C}$ -( $^1\text{H}$ ) NMR, 372  
 Free radicals, electron distribution and bonding, 40–50  
 Frequency synthesizer, 128  
 in magnetic multiple resonance, 328  
 Furan, 4-bromo-2-formyl-, *cis-trans* equilibrium, 367  
 2-Furancarboxylic acid, 5-nitro-, methyl ester, two-dimensional spectrum, 342

## G

Gadolinium,  $^{19}\text{F}$  hyperfine interactions, 68  
 Galactolipids,  $^{13}\text{C}$ -( $^1\text{H}$ ) NMR, 372  
 Gallium  
 cations, solvation, 164  
 hydrated ions quadrupole relaxation, 162  
 organophosphorus complexes, 172  
 Gallium halides, solution properties, 166  
 Gated decoupling, 374  
 Gated experiments, spin decoupling by, 322  
 Gels, cross-linked,  $^{13}\text{C}$ -( $^1\text{H}$ ) NMR, 374  
 $^{73}\text{Ge}$ , NMR, 176

$\alpha$ -D-Glucopyranoside, 2,3,4,6-tetra-*O*-tri-methylsilyl-methyl,  $^{29}\text{Si}$  chemical shift, 271

Glycine, lanthanide complexes, 36  
 Gold, (trifluoromethyl)(methyldiphenylphosphinyl)-, triple resonance spectrum, 358

Group III metals

NMR, 161–177

nuclear properties, 161

Group IV metals, nuclear properties, 162

Guanosine 5'-monophosphate,  $^{13}\text{C}$ -( $^1\text{H}$ ) NMR, 373

## H

Hamiltonian operator, 322  
 total spin, 2  
 Hartree-Fock calculations, 12  
 Heme proteins  
 conformation, 95  
 paramagnetic, 90–99  
 Hemocyanin, conformation, 89  
 Hemoglobin  
 cooperative oxygen binding in, 97  
 NMR, 95  
 Heteronuclear double resonance, 320  
 Heteronuclear transfer echo, 353  
 n-Hexane,  $^{13}\text{C}$  spectrum, two dimensional, 349  
 Hoffmann-Forsen saturation transfer method for slow rates of exchange, 377  
 Hydration, paramagnetic metal complexes, 60  
 Hydroxy acids, trimethylsilyl derivatives,  $^{29}\text{Si}$  chemical shifts, 270  
 Hydrazyl radicals, electron distribution and bonding, 49  
 Hydrocinnamaldehyde, reaction with  $\alpha$ -chymotrypsin, 378  
 $^1\text{H}$ , chemical shift determination by magnetic multiple resonance, 381

## I

Imidazole, transition metal complexes, 29  
 Iminonitroxide radicals, electron distribution and bonding, 43

Immunoglobulins, conformation, lanthanide shift reagents and, 84

Indazole,  $^{13}\text{C}$ -( $^1\text{H}$ ) NMR, 373

Indium

cations, solvation, 164

organophosphorus complexes, 172

$^{113}\text{In}$ , NMR, 172

INDO calculations, 12

INDOR spectra, 329–333

calculation, 323

triple resonance, 356

INDOR technique, 368

Ionophores, alkali metal ion complexation by, 143

Ion pairing, metal complexes, 55–59

Iron-57

chemical shift determination in magnetic multiple resonance, 383

INDOR spectra, 329

Iron, troponyltricarbonyl-, conformation, lanthanide shift reagents and, 73

Iron complexes

nitrosyl, 19

salicylideneiminato, 19

Iron porphyrins, NMR, 90

Iron (II) complexes

flavoquinone, 32

imidazole, 29

pyridine, 30

Iron (III) complexes, 34

dithiocarbamates, 28, 54

halogenobis(*N*-dialkylthiocarbamato)-, 20

nuclear spin relaxation time, 10

Iron (III) iodide, bis(*N,N*-diethyldithiocarbamato), nuclear spin relaxation times, 10

Iron (III) perchlorate, second solvation sphere, 58

Isopropyl group, rotation, 84

Isoquinoline, conformation, lanthanide shift reagents and, 74

## K

Ketones, conformation, lanthanide shift reagents and, 73

Kurland-McGarvey treatment, 2

## L

Lactones, cyclic, alkali metal ion complexation by, 143

Lanthanate (III) complexes

hexa-nitrato, 55

penta-nitrato, 55

Lanthanides, complexes, 35–37

Lanthanide induced shifts, 71

Lanthanide shift reagents, 67–84

origin of shifts, 67–73

solution equilibria, 76–82

substrate structure determinations, 73

$^{139}\text{La}$ , NMR, 185

Lead-207, chemical shift determination in magnetic multiple resonance, 385

Leghemoglobins, conformation, 95

Line intensities in multiple resonance experiments, calculations, 323

Line shapes in multiple resonance experiments, calculations, 323

Liquid crystal solvents

magnetic multiple resonance in, 322, 400

paramagnetic shifts, theory, 7

Lithium-6, quadrupole relaxation, 133

Lithium-7

chemical shift determination in magnetic multiple resonance, 381

ions, relaxation rate in glycerol, 136

proton decoupling and, 397

Lithium cryptates, solvation, 144

Lysozyme, conformation, 89

## M

Magnetic multiple resonance, 319–414

instrumentation, 325–329

techniques, 329–365

theory, 320–325

Manganese (II) complexes

acetylacetonate, 23

inner sphere, 59

outer sphere, 59

Manganese (III) complexes, dithiocarbamates, 28

$^{55}\text{Mn}$ , NMR, 198

Manganocene

electronic equilibria, 55

paramagnetic, 38

1,1'-dimethyl-, paramagnetic, 38

Membranes, NMR, 103–105  
 Menthone,  $^{13}\text{C}$  spectrum, 364  
 Mercury-199, chemical shift determination in  
   magnetic multiple resonance, 384  
 Mesoporphyrins IX, paramagnetic, 93  
 Metallocarboranes, paramagnetic, 39  
 Metallocenes, paramagnetic, 37  
 Metalloporphyrin  
   cation radicals, 50  
   NMR, 90  
 Methane, bromodeutero-,  $^{13}\text{C}$ -( $^2\text{D}$ ) NOE,  
   374  
 Methanol, INDOOR spectra, 331  
 Metmyoglobin, conformation, 95  
 MINDOR spectra, triple resonance, 356  
 Molybdenum-95  
   chemical shift determination in magnetic  
     multiple resonance, 383  
   NMR, 197  
 Molybdenum (II) complexes, 34  
 Multinuclear spectrometers, 128  
 Multiple quantum transfer echo, 353  
 Myoglobin, conformation, 94  
   deoxy-, conformation, 94

## N

Naphthylamine, conformation, lanthanide  
   shift reagents and, 74  
 1,8-Naphthyridine, transition metal com-  
   plexes, 30  
 Nickel (II) complexes, 30  
   acetates, 31  
   acetylacetonate, 23  
   amines, 27  
   alcohols, 31  
   benzoyltrifluoroacetate, 25  
   bis(alkylxanthato)-, 29  
   bis(di-*p*-tolyl-dithiophosphinato)-, 22  
   *N,N'*-bis(2-pyridylmethylene)-1,3-diamino  
     propane, 27  
   4-coordinate, electron distribution and  
     bonding in, 14  
     square-planar-tetrahedral equilibrium,  
       50  
   dihalogenobis(tertiary phosphine), 50  
   dithiophosphates, 28  
   ethylenediamine-*N,N'*-diacetic acid, 53  
   flavoquinone, 32

*N*-hydroxypropylsalicylaldehydes, 28  
 imidazole, 29  
 iminodiacetates, 31  
 1,8-naphthyridine, 30  
 octahedral, 23  
 pseudo-octahedral, 16, 52  
 pseudotetrahedral, 16  
 pyridine, 30  
 tetrahydrocorins, 33  
 triazine-1-oxide, 30  
 tris(ethylenediamine)-, 27  
 Nickelocenes, paramagnetic, 38  
 Nicotinamide adenine dinucleotide,  $^{13}\text{C}$  spec-  
   tra, 360, 361  
 Nigabliactones, NOE, 367  
 $^{93}\text{Nb}$ , NMR, 188  
 Nitriles, conformation, lanthanide shift  
   reagents and, 74  
 Nitrogen-14, chemical shift determination in  
   magnetic multiple resonance, 381  
 Nitrogen-15, chemical shift determination in  
   magnetic multiple resonance, 381  
 Nitrosyl complexes, transition metal, 19  
 Nitroxide radicals, electron distribution and  
   bonding, 41  
 Noise modulation in spin decoupling, 321  
 Nonadecane, 10-methyl-,  $^{13}\text{C}$ -( $^1\text{H}$ ) NMR, 373  
 Norbornan-2-ol, 2-methyl-,  $^{13}\text{C}$  spectra  
   assignment, 359  
 7-Norbornenyl-type radicals, electron distri-  
   bution and bonding, 49  
 Nuclear Overhauser Effect, 365–377  
    $^{13}\text{C}$ -( $^{19}\text{F}$ ), 375  
    $^{13}\text{C}$ -( $^1\text{H}$ ), 372–375  
    $^{113}\text{Cd}$ -( $^1\text{H}$ ), 376  
 CIDNP and, 377  
   difference spectra, 368  
    $^{19}\text{F}$ -( $^1\text{H}$ ), 376  
   generalized—*See* Spin population transfer  
    $^2\text{H}$ -( $^1\text{H}$ ), 375  
    $^3\text{H}$ -( $^1\text{H}$ ), 375  
   heteronuclear systems, 370–372  
    $^{199}\text{Hg}$ -( $^1\text{H}$ ), 377  
   homonuclear systems, 367  
   intermolecular, 369  
    $^{15}\text{N}$ -( $^1\text{H}$ ), 375  
    $^{31}\text{P}$ -( $^1\text{H}$ ), 376  
    $^{29}\text{Si}$ - $^1\text{H}$ , 283–286  
    $^{29}\text{Si}$ -( $^1\text{H}$ ), 376  
    $^{119}\text{Sn}$ -( $^1\text{H}$ ), 377

suppression, gated techniques, 371  
 Nucleic acids, conformation, 104,  
 Nucleosides alkali metal ion complexation  
   by, 143  
   conformation, 104  
    $^{15}\text{N}$ -( $^1\text{H}$ ) NOE, 375  
 Nucleotides  
   alkali metal ion complexation by, 143  
   conformation, 104  
    $^{15}\text{N}$ -( $^1\text{H}$ ) NOE, 375

## O

One-bond coupling,  $^{29}\text{Si}$  NMR, 276–281  
 Organic acids, alkali metal ion complexation  
   by, 143  
 Organoberyllium compounds, NMR, 159  
 Organolithium compounds NMR, 149  
   relaxation, 133  
 Organometallic compounds, paramagnetic,  
   37–40  
 Organophosphorus compounds conforma-  
   tion, lanthanide shift reagents, 75  
   Group III metal complexes, 172  
   INDOR spectra, 331  
 Organosilicone compounds  
    $^{13}\text{C}$ -( $^1\text{H}$ ) NMR, 373  
    $^{29}\text{Si}$  chemical shifts, 245–257  
 1,3-Oxazine, tetrahydro-3,3,4,6-tetramethyl-,  
   *N*-methyl group orientation, 367  
 Oxygen-17, chemical shift determination by  
   magnetic multiple resonance, 382

## P

Palladium, bis(acetylacetonate),  $^{13}\text{C}$ -( $^1\text{H}$ )  
   NMR, 373  
 Pancreatic trypsin inhibitor,  $^{13}\text{C}$ -( $^1\text{H}$ ) NMR,  
   373  
 Papain, reaction with *N*-benzoylacetalde-  
   hyde, 378  
 Paramagnetic linewidth, theory, 8–11  
 Paramagnetic shift, theory, 2–7  
 Paramagnetic species, NMR, 1–124  
 Paramagnetic susceptibilities, measurement,  
   65  
 Penicillins, conformation, lanthanide shift  
   reagents and, 84

Pentasiloxane,  $^{29}\text{Si}$  chemical shifts, 255  
 Peptides  
   conformation, 87–90  
   cyclic, alkali metal ion complexation by,  
     143  
   NH protons, NOE, 368  
 Phosphates, paramagnetic vanadium com-  
   plexes, 63  
 Phosphines, aryl, coupling constants, 386  
 Phosphinimine, *N*-silylated triorgano,  $^{29}\text{Si}$   
   NMR, 235  
 Phosphinium, (*p*-methylbenzyl)triphenyl-,  
   bromide, triple resonance spectrum,  
   358  
 Phospholipids in membranes, NMR, 104  
 Phosphorus-31  
   chemical shift determination in magnetic  
     multiple resonance, 382  
   decoupling, 400  
 Phosphoryl compounds, trimethylsilylimido  
   derivatives,  $^{29}\text{Si}$  chemical shifts, 270  
 Picoline  
   actinide complexes, 35  
   *N*-oxide, lanthanide complexes, 35  
 Piperidines, conformation, lanthanide shift  
   reagents and, 74  
   nitroso-, conformation, lanthanide shift  
   reagents and, 73  
 Plastocyanins, conformation, 89  
 Platinum  
   nitrogen complexes, INDOR spectra, 387  
   thiocyanate complexes, INDOR spectra,  
     386  
 Platinum-195, chemical shift determination  
   in magnetic multiple resonance, 384  
 Poly(alkyl methacrylate),  $^{13}\text{C}$ -( $^1\text{H}$ ) NMR,  
   374  
 Poly(but-1-ene),  $^{13}\text{C}$ -( $^1\text{H}$ ) NMR, 374  
 Poly(*cis*-butadiene),  $^{13}\text{C}$  spectra assignment,  
   359  
 Polydimethylsiloxane  
   as reference NMR, 228  
   flow behaviour, 250  
    $^{29}\text{Si}$  chemical shift, 246  
    $^{29}\text{Si}$  relaxation in, 284  
 Polyethylene,  $^{13}\text{C}$ -( $^1\text{H}$ ) NMR, 374  
 Poly(methyl methacrylate),  $^{13}\text{C}$ -( $^1\text{H}$ ) NMR,  
   374  
 Polysilanes  
   coupling constants, 281  
    $^{29}\text{Si}$  chemical shift, 240–245

Polysiloxanes, bulk viscosity, 251  
 Poly(vinylidene fluoride),  $^{13}\text{C}$ -( $^1\text{H}$ ) NMR, 374  
 Porphyrins  
   lanthanide complexes, 76  
   paramagnetic, 90–99  
 Potassium-39, ions, solvation, 137  
 Potassium silicate,  $^{29}\text{Si}$  chemical shift, 261  
 Propene, (1-dimethylamino)-2-methyl-,  $^{13}\text{C}$  spectrum, 364  
 Proteins  
   conformation, 87–90  
   iron-sulphur, NMR, 99–101  
   solution conformation, 85  
 Proton decoupling in double resonance experiments, 397  
 Proton flip in two dimensional spectra, 246  
 Pseudocontact shifts, calculation, 5  
 Pulsed experiments, spin decoupling by, 322  
 Pulsed Fourier transform NMR, 222  
 Pulse FT spectrometers, multinuclear, 325  
 Purines,  $^{13}\text{C}$ -( $^1\text{H}$ ) NMR, 373  
 Pyridazine,  $^{13}\text{C}$ -( $^1\text{H}$ ) NMR, 372  
 Pyridine  
   conformation, lanthanide shift reagents and, 74  
   *N*-oxide, transition metal complexes, 30  
   transition metal complexes, 30  
 Pyrimidine  
    $^{13}\text{C}$ -( $^1\text{H}$ ) NMR, 372  
 INDOR spectra, 331  
 Pyrroles, conformation, lanthanide shift reagents and, 74  
   4-bromo-2-formyl-1-methyl-, *cis-trans* equilibrium, 367

## Q

Quadrupolar nuclei  
   instrumental requirement for NMR, 128–130  
   less common, NMR, 125–219  
 Quadrupole relaxation, Group III metals, 162  
 Quaternary carbon atoms, selective population inversion and, 336  
 Quinoline, conformation, lanthanide shift reagents and, 74

## R

Relaxation  
   alkali metal nuclei, 132–134  
    $^{29}\text{Si}$  NMR, 283–286  
 Relaxation perturbation probes, biological applications, 84  
 $^{185}\text{Re}$ , NMR, 200  
 $^{187}\text{Re}$ , NMR, 200  
 Rhenium (III) complexes, 34  
 Rhodium-103  
   chemical shift determination in magnetic multiple resonance, 383  
   INDOR spectra, 329  
 tRNA, structure, 103  
 Ruthenium (III) complexes  
   acetylacetonate, nuclear spin relaxation times, 10  
   amino, 34  
   tetra-ammine, nuclear spin relaxation times, 11

## S

Salicylic acid, trimethyl silyl derivatives,  $^{29}\text{Si}$  NMR, 256  
 Salicylaldimine, *N*-hydroxypropyl-, ethyl complexes, 28  
 J-Scaling, 359  
 $^{45}\text{Sc}$ , NMR, 183  
 Selective population inversion, 335  
 Selective population transfer, 335  
 Selenium-77, chemical shift determination in magnetic multiple resonance, 383  
 Selenium, (trimethoxyphosphinyl)-, triple resonance spectrum, 358  
 Sesquiterpenes, lactones, NOE, 370  
 Shielding range, alkali metal nuclei, 131  
 Shift perturbation probes, biological applications, 84  
 Sick cell hemoglobin, conformation, 99  
 Silacyclopropane,  $^{29}\text{Si}$  chemical shift, 242  
 Silacyclopentene,  $^{29}\text{Si}$  chemical shift, 243  
 Silanes  
   aryl,  $^{29}\text{Si}$  chemical shift, 225, 238–240  
   coupling constants calculations, 273  
   cyclic,  $^{29}\text{Si}$  chemical shift, 240–245  
   halogeno,  $^{29}\text{Si}$  chemical shift, 237, 238

- methyl derivatives,  $^{29}\text{Si}$  chemical shift, 229–236  
 one-bond coupling, 277  
 $^{29}\text{Si}$  chemical shift, 226  
 ethoxytrimethyl-,  $^{29}\text{Si}$  chemical shifts, steric effects and, 268  
 2,2',2''-nitrilotriethoxy-,  $^{29}\text{Si}$  chemical shifts, 261  
 phenoxytrimethyl-,  $^{29}\text{Si}$  chemical shift, 236  
 phenyl-, NOE, 285  
 phenylenedioxybis(trimethyl-,  $^{29}\text{Si}$  chemical shift, and steric effects, 268  
 phenyltrimethyl-,  $^{29}\text{Si}$  chemical shift, 236  
 tetraethoxy-, as reference NMR, 228  
 tetrafluoro-, as reference NMR, 228  
 tetramethoxy-, as reference NMR, 228  
 tetramethyl-, as reference NMR, 228  
 triethoxy-,  $^{29}\text{Si}$  chemical shifts, 262  
 trimethylphenoxy-,  $^{29}\text{Si}$  chemical shifts, steric effect and, 268  
**Silanols**  
   fluids, molecular weight, 250  
    $^{29}\text{Si}$  chemical shifts, solvent effect, 267  
**Silatranes**,  $^{29}\text{Si}$  chemical shifts, 261–262  
**Silazanes**,  $^{29}\text{Si}$  chemical shift, 246  
**Silicates**,  $^{29}\text{Si}$  chemical shifts, 258–261  
**Silicic acid**, trimethyl silyl esters, structure, 253, 254  
**Silicone**, organo-,  $^{29}\text{Si}$  chemical shift, 245–257  
**Silicon-29**  
   chemical shift determination in magnetic multiple resonance, 382  
   NMR, 221–318  
     long range coupling, 282  
     polytrimethylsilylated sugars, proton decoupling in, 397  
     reference compounds, 227–229  
**Silicon compounds**, extracoordinate,  $^{29}\text{Si}$  chemical shift, 262–266  
**Silicon(IV) compounds**, trisacetylacetonato,  $^{29}\text{Si}$  chemical shift, 263  
**Silicon hydrides**,  $^{29}\text{Si}$  chemical shifts, 238–240  
**Siloxane**  
   polycyclic,  $^{29}\text{Si}$  chemical shifts, 255  
   polymeric,  $^{29}\text{Si}$  chemical shift, 248  
**Silver-107**, INDOR spectra, 329  
**Silver-109**, INDOR spectra, 329  
**Silver (I) complexes**, flavoquinone, 32  
**Silylamine**,  $^{29}\text{Si}$  chemical shifts, solvent effect, 267  
**Sodium**, anions, 148  
**Sodium-23**, chemical shifts, 137  
**Sodium acetate**,  $^{13}\text{C}$ -( $^1\text{H}$ ) NMR, 373  
**Sodium cryptates**, decomplexation, 144  
**Sodium metasilicate**,  $^{29}\text{Si}$  chemical shift, 258  
**Sodium silicate**,  $^{29}\text{Si}$  chemical shift, 260  
**Solvation**  
   alkali metal ions, 137–142  
   Group III metals, 164–174  
   metal complexes, 55–59  
**Solvent effects**,  $^{29}\text{Si}$  chemical shifts and, 266–268  
**Spin decoupling**, 320  
**Spin delocalisation**, theory, 11–13  
**Spin echo spectra**, 338–355  
**Spin population transfer** in magnetic multiple resonance, 333–337  
**Stannic tetrachloride** as shift reagents, 83  
**Stereochemistry**, paramagnetic species, 50–55  
**Steric effects**,  $^{29}\text{Si}$  chemical shifts and, 268–270  
**Steroids**, trimethylsilyl derivatives,  $^{29}\text{Si}$  chemical shifts, 270  
**Structure**, paramagnetic species, 50–55  
**Sugars**  
   alkali metal ion complexation by, 143  
   conformation, lanthanide shift reagents and, 75  
   polytrimethylsilylated,  $^{29}\text{Si}$  NMR, proton decoupling in, 397  
   trimethylsilyl derivatives,  $^{29}\text{Si}$  chemical shifts, 270  
 $^{33}\text{S}$ , NMR, 181, 182  
**Susceptibility field**, 9

## T

- Tellurium-125**, chemical shift determination in magnetic multiple resonance, 384  
**Temperature**, metal acetylacetonate complexes and, 10  
**Tetracycline**, conformation, lanthanide shift reagents and, 84  
**Tetrasiloxane**,  $^{29}\text{Si}$  chemical shifts, 255  
**Thallium-205**, chemical shift determination in magnetic multiple resonance, 385  
**Thiophosphoric acid**, transition metal complexes, 28

- Thulium fluorides,  $^{19}\text{F}$  hyperfine interactions, 67
- Thyroxine, copper complexes, 22
- Tin, trimethylstanyl-, lithium salt, tetrahydrofuran adduct, INDOR spectra, 330
- Tin-117, chemical shift determination in magnetic multiple resonance, 384
- Tin-119, chemical shift determination in magnetic multiple resonance, 384
- TINDOR spectra, triple resonance, 356
- $^{47}\text{Ti}$ , NMR, 187
- $^{49}\text{Ti}$ , NMR, 187
- Titanium tetrachloride as shift reagents, 83
- Toluene-dithiol, cobalt complexes, 15
- Transition metal complexes
- acetylacetonates, 25
  - bis(benzoyltrifluoroacetato)-, 24
  - 4-coordinate, electron distribution and bonding in, 14–20
  - 5-coordinate, electron distribution and bonding in, 20–22
  - 6-coordinate, electron distribution and bonding in, 23–35
  - flavoquinone, 32
  - tris(acetylacetonato), 57
  - tris(dithiocarbamato), 51
- Transition metals, NMR, 182–212
- Triazine, 1-oxide, transition metal complexes, 30
- Tricyclo [5.1.0.0] octane, 1,3,5,7-tetramethyl-, stereochemistry, 367
- Trimethylsilyl compounds
- $^{13}\text{C}$ -( $^1\text{H}$ ) NMR, 373
  - $^{29}\text{Si}$  NMR, 229
- Triple resonance in magnetic multiple resonance, 356–358
- Trisiloxane,  $^{29}\text{Si}$  NMR, 254
- Triterpenes, INDOR technique, 368
- Tropolene, silicon derivatives,  $^{29}\text{Si}$  chemical shifts, 266
- Tryptophan, exchange reactions, 378
- TTL-IC sequence controller, 328
- Tungsten-183
- chemical shift determination in magnetic multiple resonance, 384
  - INDOR spectra, 329
- Tungsten carbonyl complexes, complex spin systems, 390
- Tungsten (IV) complexes, 35
- Two-dimensional spectra, 338–355
- U**
- Umbelliferone, *O*-carboxymethyl-4-methyl-, binding to antibodies, 368
- Urethanes, trimethylsilyl derivatives,  $^{29}\text{Si}$  chemical shifts, 270
- Uranium,
- tetrakis (tetraethylammonium) octa-thio-cyanato-, 36
- Uranium (IV) complexes, 36
- tetra-allyl, 37
  - triscyclopentadienyl, 37
- Urea, thio-, transition metal complexes, 29
- V**
- Valium, inversion in, 378
- Vanadium, bis( $h^5$ -t-butylcyclopentadienyl)-, paramagnetic, 37
- Vanadium-51, NMR, 188
- Vanadium (IV) complexes
- acetylacetonate, 25
  - oxo, 20
  - ligand exchange, 62
- Vancomycin, conformation, lanthanide shift reagents and, 84
- Vinyl bromide, relaxation processes, 367
- Vitamin B12, conformation, 89
- Vitamin D, conformation, lanthanide shift reagents and, 84
- W**
- Water exchange reactions, paramagnetic metal complexes, 60
- Woolstenite, trimethylsilyl derivatives,  $^{29}\text{Si}$  NMR, 252
- X**
- Xanthene, 9,9-dialkylthio-, cation radicals, 49



**Y**

Ytterbium,  $^{19}\text{F}$  hyperfine interactions, 68  
Ytterbium fluorides,  $^{19}\text{F}$  hyperfine interactions, 67

**Z**

Zeolites complexation of molecular hydrogen on, 67  
    synthetic, molecular motion in, 67  
 $^{67}\text{Zn}$ , NMR, 210  
Zinc (II) complexes, flavoquinone, 32  
Zinc tetraphenylporphyrin,  $^{15}\text{N}$ -( $^1\text{H}$ ) NOE, 375